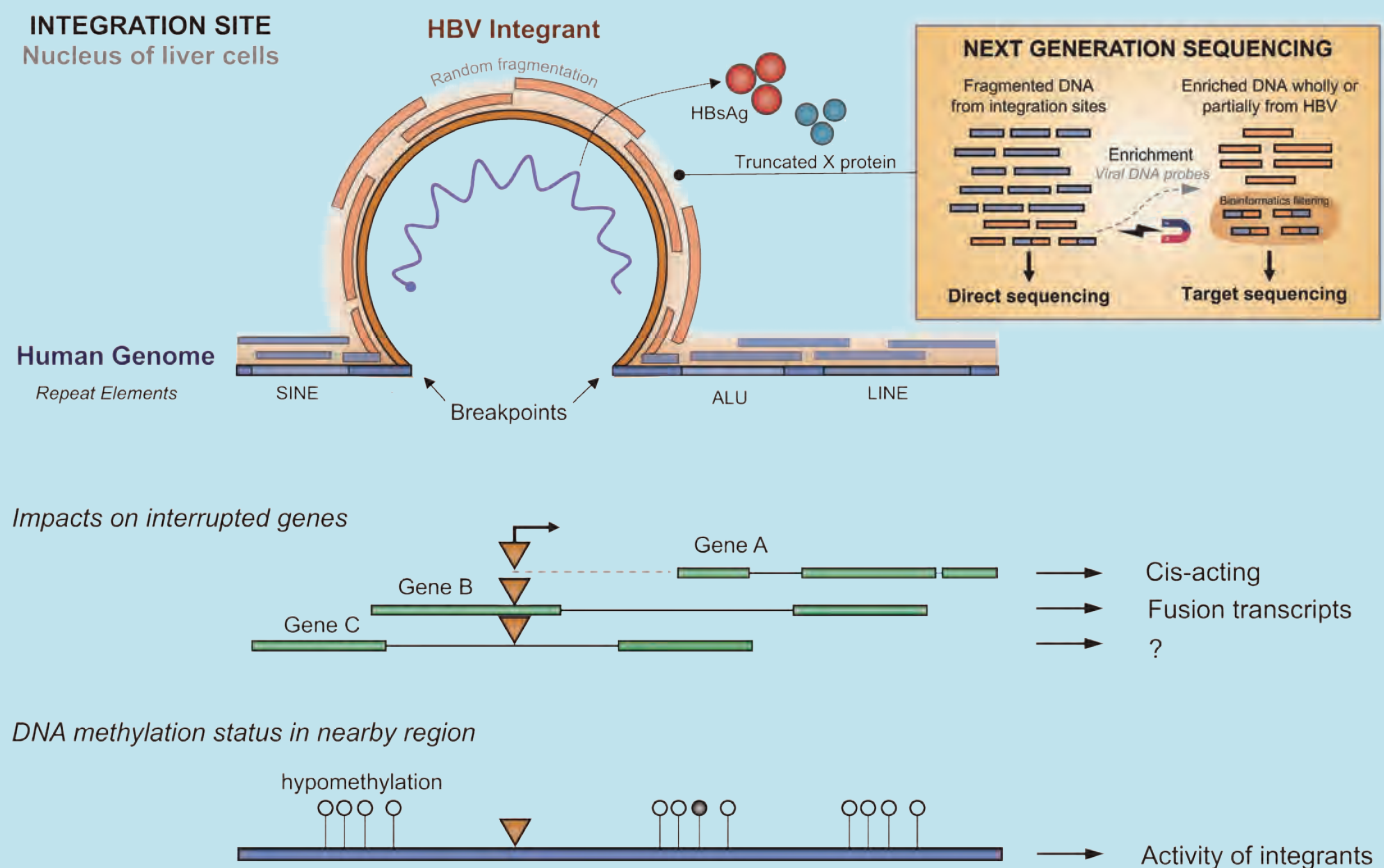


**2021**

Volume 9 Issue 3

May / June

# Journal of Clinical and Translational Hepatology



## Editors-in-Chief

### Prof. Hong Ren

General Editor-in-Chief

The Second Affiliated Hospital of  
Chongqing  
Medical University, China

### Prof. George Y. Wu

Comprehensive Editor-in-Chief

University of Connecticut Health Center, USA

### Dr. Harry Hua-Xiang Xia

Editor-in-Chief

Guangdong Pharmaceutical University, China

## Managing Editors

### Huaidong Hu

Chongqing, China

### Zhi Peng

Chongqing, China

### Sandeep Kumar Karn

Chongqing, China

## Executive Editor

### Hua He

Houston, USA

## Technical Editor

### Huili Zhang

Wuhan, China

## Contact Information

### Editorial Office

**Managing Editors:** Dr. Huaidong Hu  
Dr. Zhi Peng  
Dr. Sandeep Kumar Karn

**Telephone:** +86-23-6370 1383

**Fax:** +86-23-6370 1383

**E-mail:** jcth@xiahepublishing.com

**Postal Address:** 74 Linjiang Road, Yuzhong  
District, 400010 Chongqing,  
CHINA

### Publisher

Xia & He Publishing Inc.

**Website:** www.xiahepublishing.com

**E-mail:** service@xiahepublishing.com

**Postal Address:** 14090 Southwest Freeway,  
Suite 300, Sugar Land, Texas,  
77478, USA

## Current Issue: Volume 9, Issue 3

Publication date: June 28, 2021

## Aims and Scope

*Journal of Clinical and Translational Hepatology (JCTH, J Clin Transl Hepatol)* publishes high quality, peer-reviewed studies in the clinical and basic human health sciences of liver diseases. *JCTH* welcomes submissions of articles within its topical scope including: novel discoveries in clinical and basic hepatology; liver disease mechanisms; novel techniques in research and management of liver diseases; epidemiological/environmental factors of liver diseases; role of immune system function in liver diseases; acute and chronic hepatitis; cirrhosis; genetic and metabolic liver diseases and their complications; hepatobiliary diseases; liver cancer; drug metabolism; biliary disease; peritoneal tuberculosis. *JCTH* publishes various types of articles, including original article, review, short communication, systematic review, meta-analysis, case report, methodology article, letter to the editor, and editorial.

## Indexing & Abstracting

*JCTH* is now indexed in Science Citation Index Expanded (SCIE); PubMed; PubMed Central; Scopus; Baidu Scholar; CNKI Scholar; Dimensions; EBSCOhost; Google Scholar; Microsoft Academic; SafetyLit; ScienceOpen; Scilit; Semantic Scholar; Wanfang Data; Web of Science; WorldCat Discovery Services; Zetoc.

## Open Access

*JCTH* adopts open access publishing model, and all articles are distributed under the terms of the CC BY-NC 4.0 license (<http://creativecommons.org/licenses/by-nc/4.0/>). Under this license, anyone may copy, distribute, or reuse these articles for non-commercial purposes, provided the original work is properly cited. Manuscripts submitted for publication in an open access journal are subject to the same rigorous peer-review and quality control as in scholarly subscription journals.

## Disclaimer

All articles published in Xia & He journals represent the views and opinions of their authors, and not the views, opinions, or policies of the publisher, except where explicitly indicated. Xia & He Publishing shall not be held responsible for the use of views and opinions expressed in the articles; use of any information in the articles shall not be considered an endorsement by Xia & He Publishing of the products advertised.

## Links

Journal Home: <https://www.xiahepublishing.com/journal/jcth>

Editorial Board: <https://www.xiahepublishing.com/journal/jcth/editors>

Archive: <https://www.xiahepublishing.com/journal/jcth/archive>

Instructions for Authors: <https://www.xiahepublishing.com/journal/jcth/instruction>

Online Submission System: <https://www.editorialmanager.com/jcth/default.aspx>

## Associate Editors



### **Viral Hepatitis, Cirrhosis and Liver Failure**

#### **Mohamed A Daw**

Faculty of Medicine, University of Tripoli  
Tripoli, Libya

#### **Xiao-Guang Dou**

Department of Infectious Diseases, Shengjing Hospital of China Medical University  
Shenyang, China

#### **Jin-Lin Hou**

Hepatology Unit and Department of Infectious Diseases, Nanfang Hospital, Southern Medical University  
Guangzhou, China

#### **Jun-Qi Niu**

Department of Hepatology, The First Hospital of Jilin University  
Changchun, China

#### **Nikolaos T. Pyrsopoulos**

Division of Gastroenterology and Hepatology, Rutgers New Jersey Medical School University Hospital  
Newark, USA

#### **Arielle Rosenberg**

University Paris Descartes  
Paris, France

#### **Qing-Feng Sun**

Department of Infectious Diseases, The Third Affiliated Hospital to Wenzhou Medical College  
Wenzhou, China

#### **Fu-Sheng Wang**

The Institute of Translational Hepatology, 302 Military Hospital of China  
Beijing, China

#### **Da-Zhi Zhang**

Department of Infectious Diseases, The Second Affiliated Hospital of Chongqing Medical University  
Chongqing, China

### **Alcohol and Nonalcoholic Fatty Liver Disease**

#### **Gyorgy Baffy**

Department of Gastroenterology, VA Boston Healthcare System, Harvard Medical School  
Boston, USA

#### **Marko Duvnjak**

Department of Gastroenterology and Hepatology, Clinic of Internal medicine, Clinical Hospital Centre "Sestre milosrdnice"  
Zagreb, Croatia

#### **Yu-Chen Fan**

Department of Hepatology, Qilu Hospital of Shandong University  
Jinan, China

#### **Kittichai Promrat**

Alpert Medical School of Brown University  
Providence, USA

#### **Ashwani Singal**

Division of Gastroenterology and Hepatology, University of South Dakota, Avera McKennan University Health Center and Transplant Institute  
Sioux Falls, USA

#### **Lai Wei**

Hepatopancreatobiliary Center, Beijing Tsinghua Changgung Hospital, School of Clinical Medicine, Tsinghua University  
Beijing, China

#### **Ming-Hua Zheng**

NAFLD Research Center, Department of Hepatology, the First Affiliated Hospital of Wenzhou Medical University  
Wenzhou, China

### **Autoimmune and Cholestatic Liver Disease, DILI, Immunology**

#### **John W. Birk**

UCONN Health, Division of Gastroenterology and Hepatology  
Farmington, USA

#### **Timothy Billiar**

Department of Surgery, University of Pittsburgh School of Medicine  
Pittsburgh, USA

#### **Aziz A. Chentoufi**

Immunology/HLA Department, National Reference Laboratory, Mohammed VI University of Health Sciences  
Casablanca, Morocco

#### **Ji-Dong Jia**

Liver Research Center, Beijing Friendship Hospital, Capital Medical University  
Beijing, China

#### **Lun-Gen Lu**

Department of Gastroenterology, Shanghai General Hospital, Shanghai Jiao Tong University School of Medicine  
Shanghai, China

#### **Farzin Roohvand**

Molecular Virology Department, Pasteur Institute of Iran

Tehran, Iran

#### **Xue-Feng Xia**

Key Laboratory for Reproduction and Genetics of Guangdong Higher Education Institutes, Key Laboratory for Major Obstetric Diseases of Guangdong Province, Third Affiliated Hospital of Guangzhou Medical University; Department of Reproductive Medicine, Third Affiliated Hospital of Guangzhou Medical University  
Guangzhou, China

### **Surgery and Transplantation**

#### **Michael Schilsky**

Yale New Haven Transplantation Center, Yale University School of Medicine  
New Haven, USA

### **Radiology**

#### **Li-Min Chen**

Institute of Blood Transfusion, Chinese Academy of Medical Sciences, and Peking Union Medical College  
Chengdu, China

### **Pathology**

#### **Wendy Cao**

New York University Langone Health  
New York, USA

#### **Lan-Jing Zhang**

Department of Pathology, Princeton Medical Center  
Plainsboro, USA

### **Liver Cancer and Oncology**

#### **Douglas LaBrecque**

Department of Internal Medicine, University of Iowa  
Iowa City, USA

#### **Joseph Lim**

Section of Digestive Diseases/Yale Liver Center, Yale University School of Medicine  
New Haven, USA

#### **Tawesak Tanwandee**

Division of Gastroenterology, Department of Medicine, Faculty of Medicine Siriraj Hospital, Mahidol University  
Bangkok, Thailand

#### **Man-Fung Yuen**

Department of Medicine, The University of Hong Kong; Division of Gastroenterology and Hepatology, Department of Medicine, Queen Mary Hospital  
Hong Kong

## Editorial Board Members



**Avin Aggarwal**  
Las Vegas, USA  
**Gianfranco D. Alpin**  
Temple, USA  
**Leon D. Averbukh**  
Farmington, USA  
**Mostafa El Awady**  
Giza, Egypt  
**Sina Aziz**  
Karachi, Pakistan  
**Mahmoud Mohamed Bahgat**  
Cairo, Egypt  
**Fernando Bessone**  
Rosario, Argentina  
**Peter Buch**  
Farmington, USA  
**Chalermrat Bunchornta-vakul**  
Bangkok, Thailand  
**Phunchai Charatcharoen-witthaya**  
Bangkok, Thailand  
**En-Qiang Chen**  
Chengdu, China  
**Po-Hung Chen**  
Baltimore, USA  
**Li Chen**  
Shanghai, China  
**Ashok Kumar Choudhury**  
New Delhi, India  
**Jian-Qiang Ding**  
Foshan, China  
**Qiong-Zhu Dong**  
Shanghai, China  
**Maysaa El Sayed Zaki**  
Cairo, Egypt  
**Jian-Gao Fan**  
Shanghai, China  
**Heather L Francis**  
Bryan, USA  
**Catherine Frenette**  
La Jolla, USA  
**Artin Galoosian**  
San Francisco, USA  
**Yan-Hang Gao**  
Changchun, China  
**George Boon-Bee Goh**  
Singapore, Singapore  
**Chang-Cun Guo**  
Xi'an, China  
**Ahmet Gurakar**  
Baltimore, USA  
**Steven-Huy Bui Han**  
Los Angeles, USA

**Ying Han**  
Xi'an, China  
**Amr Shaaban Hanafy**  
Zagazig, Egypt  
**Kazuhiko Hayashi**  
Nagoya, Japan  
**Peng Hu**  
Chongqing, China  
**Jing Hua**  
Shanghai, China  
**Yue-Hua Huang**  
Guangzhou, China  
**Trana Hussaini**  
Vancouver, Canada  
**Hartmut Jaeschke**  
Kansas City, USA  
**Wasim Jafri**  
Karachi, Pakistan  
**Tatsuo Kanda**  
Tokyo, Japan  
**Ruhail Kohli**  
Baltimore, USA  
**John Koskinas**  
Athens, Greece  
**Anastasios Koulaouzidis**  
Edinburgh, UK  
**Anand V Kulkarni**  
Hyderabad, India  
**Ashish Kumar**  
New Delhi, India  
**Manoj Kumar**  
New Delhi, India  
**Xiang-Ming Lao**  
Guangzhou, China  
**Kin Wah Lee**  
Hong Kong, China  
**Jun Li**  
Hangzhou, China  
**Jie Li**  
Jinan, China  
**Su Lin**  
Fuzhou, China  
**Wen-Yu Lin**  
Boston, USA  
**Chao-Hong Liu**  
Wuhan, China  
**Cheng-Hai Liu**  
Shanghai, China  
**Man-Qing Liu**  
Wuhan, China  
**Feng-Min Lu**  
Beijing, China  
**Ming-Qin Lu**  
Wenzhou, China

**Alessandro Mantovani**  
Verona, Italy  
**Qing Mao**  
Chongqing, China  
**Matthew McMillin**  
Austin, USA  
**Nahum Mendez-Sanchez**  
Mexico City, Mexico  
**Fan-Yin Meng**  
Temple, USA  
**Ahmed Mesalam**  
Cairo, Egypt  
**Albert D. Min**  
New York, USA  
**Paul Naylor**  
Detroit, USA  
**James S. Park**  
New York, USA  
**María Teresa Pérez-Gracia**  
Valencia, Spain  
**Cyriac Abby Philips**  
Kochi, India  
**Atoosa Rabiee**  
Washington, USA  
**Alok Ranjan**  
Washington, USA  
**Sahaj Rath**  
Vancouver, Canada  
**Sammy Saab**  
Los Angeles, USA  
**Behnam Saberi**  
Baltimore, USA  
**Ke-Qing Shi**  
Wenzhou, China  
**Chao Sun**  
Tianjin, China  
**Gamal Shiha**  
Mansoura, Egypt  
**Surajit Sinha**  
Bethesda, USA  
**Coleman Smith**  
Washington, USA  
**Martina Smolic**  
Osijek, Croatia  
**Robert Smolic**  
Osijek, Croatia  
**Jonathan G. Stine**  
Charlottesville, USA  
**Giovanni Targher**  
Verona, Italy  
**Rolf Teschke**  
Frankfurt, Germany  
**Claudio Tiribelli**  
Trieste, Italy

**Sombat Treeprasertsuk**  
Bangkok, Thailand  
**George Tsoulfas**  
Thessaloniki, Greece  
**Vladimir Maximovich Tsykunov**  
Grodno, Belarus  
**Kang-Sheng Tu**  
Xi'an, China  
**David Victor**  
New York, USA  
**Gen-Shu Wang**  
Guangzhou, China  
**Le-Yi Wang**  
Urbana, USA  
**Yu Jun Wong**  
Singapore  
**Yong-Ning Xin**  
Qingdao, China  
**Ming Yan**  
Jinan, China  
**Dong-Liang Yang**  
Wuhan, China  
**Li Yang**  
Cincinnati, USA  
**Tian Yang**  
Xi'an, China  
**Eric M. Yoshida**  
Vancouver, Canada  
**Hong You**  
Beijing, China  
**Samar Samir Youssef**  
Cairo, Egypt  
**Jia Yu**  
Wuhan, China  
**Yu-Feng Yuan**  
Wuhan, China  
**Xin-Xin Zhang**  
Shanghai, China  
**Xu-Chen Zhang**  
New Haven, USA  
**Yuan-Yuan Zhang**  
Chengdu, China  
**Xin Zheng**  
Wuhan, China  
**Yu-Bao Zheng**  
Guangzhou, China  
**Hong Zhou**  
Nanjing, China  
**Hui-Ping Zhou**  
Richmond, USA  
**Yu Zhou**  
Wuhan, China  
**Jian-Hong Zhong**  
Nanning, China



# JOURNAL OF CLINICAL AND TRANSLATIONAL HEPATOLOGY

---

## CONTENTS

2021 9(3):279–451

### Editorials

#### **Ariadne's Thread in the Network of Hepatocellular Carcinoma Immunobiology**

John Koskinas and Athanasios Armakolas . . . . . 279

#### **Prediction and Prevention of Post-hepatectomy Liver Failure: Where Do We Stand?**

Amr Shaaban Hanafy . . . . . 281

### Original Articles

#### **PD-1 Involvement in Peripheral Blood CD8<sup>+</sup> T Lymphocyte Dysfunction in Patients with Acute-on-chronic Liver Failure**

Xiaoshuang Zhou, Yidong Li, Yaqiu Ji, Tian Liu, Ninghui Zhao, Jiefeng He and Jia Yao . . . . . 283

#### **Development and Validation of a Nomogram Based on Perioperative Factors to Predict Post-hepatectomy Liver Failure**

Bin Xu, Xiao-Long Li, Feng Ye, Xiao-Dong Zhu, Ying-Hao Shen, Cheng Huang, Jian Zhou, Jia Fan, Yong-Jun Chen and Hui-Chuan Sun . . . . . 291

#### **Integrative Characterization of Immune-relevant Genes in Hepatocellular Carcinoma**

Wei-Feng Hong, Yu-Jun Gu, Na Wang, Jie Xia, Heng-Yu Zhou, Ke Zhan, Ming-Xiang Cheng and Ying Cai . . . 301

#### **Differentiation of Hepatocellular Carcinoma from Hepatic Hemangioma and Focal Nodular Hyperplasia using Computed Tomographic Spectral Imaging**

Weixia Li, Ruokun Li, Xiangtian Zhao, Xiaozhu Lin, Yixing Yu, Jing Zhang, Kemin Chen, Weimin Chai and Fuhua Yan . . . . . 315

#### **3-year Treatment of Tenofovir Alafenamide *vs.* Tenofovir Disoproxil Fumarate for Chronic HBV Infection in China**

Jinlin Hou, Qin Ning, Zhongping Duan, You Chen, Qing Xie, Fu-Sheng Wang, Lunli Zhang, Shanming Wu, Hong Tang, Jun Li, Feng Lin, Yongfeng Yang, Guozhong Gong, John F. Flaherty, Anuj Gaggar, Shuyuan Mo, Cong Cheng, Gregory Camus, Chengwei Chen, Yan Huang, Jidong Jia, Mingxiang Zhang and GS-US-320-0110 and GS-US-320-0108 China Investigators . . . . . 324

#### **Tenofovir Alafenamide Fumarate, Tenofovir Disoproxil Fumarate and Entecavir: Which is the Most Effective Drug for Chronic Hepatitis B? A Systematic Review and Meta-analysis**

Xuefeng Ma, Shousheng Liu, Mengke Wang, Yifen Wang, Shuixian Du, Yongning Xin and Shiyang Xuan . . . 335

#### **Validation of the Nanjing Criteria for Diagnosing Pyrrolizidine Alkaloids-induced Hepatic Sinusoidal Obstruction Syndrome**

Wei Zhang, Lu Liu, Ming Zhang, Feng Zhang, Chunyan Peng, Bin Zhang, Jun Chen, Lin Li, Jian He,

Jiangqiang Xiao, Yanhong Feng, Xunjiang Wang, Aizhen Xiong, Li Yang, Xiaoping Zou, Yuecheng Yu and Yuzheng Zhuge . . . . . 345

**Efficacy of Intra-gastric Balloons in the Markers of Metabolic Dysfunction-associated Fatty Liver Disease: Results from Meta-analyses**

Zi-Yuan Zou, Jing Zeng, Tian-Yi Ren, Yi-Wen Shi, Rui-Xu Yang and Jian-Gao Fan . . . . . 353

**Roles of SET7/9 and LSD1 in the Pathogenesis of Arsenic-induced Hepatocyte Apoptosis**

Bing Han, Yi Yang, Lei Tang, Rujia Xie and Qin Yang. . . . . 364

**Icaritin Attenuates Lipid Accumulation by Increasing Energy Expenditure and Autophagy Regulated by Phosphorylating AMPK**

Yue Wu, Ying Yang, Fang Li, Jie Zou, Yu-Hao Wang, Meng-Xia Xu, Yong-Lun Wang, Rui-Xi Li, Yu-Ting Sun, Shun Lu, Yuan-Yuan Zhang and Xiao-Dong Sun . . . . . 373

**Predictive Value of Inflammation Biomarkers in Patients with Portal Vein Thrombosis**

Jian-Bo Han, Qing-Hua Shu, Yu-Feng Zhang and Yong-Xiang Yi . . . . . 384

**Characteristics and Inpatient Outcomes of Primary Biliary Cholangitis and Autoimmune Hepatitis Overlap Syndrome**

Yi Jiang, Bing-Hong Xu, Brandon Rodgers and Nikolaos Pyrsopoulos . . . . . 392

**Review Articles**

**HBV Integration Induces Complex Interactions between Host and Viral Genomic Functions at the Insertion Site**

Dake Zhang, Ke Zhang, Urike Protzer and Changqing Zeng . . . . . 399

**A Review of Hepatitis B Virus and Hepatitis C Virus Immunopathogenesis**

Corey Saraceni and John Birk . . . . . 409

**Direct-acting Antiviral Regimens for Patients with Chronic Infection of Hepatitis C Virus Genotype 3 in China**

Xiaozhong Wang and Lai Wei. . . . . 419

**Nonalcoholic Fatty Liver Disease after Liver Transplant**

Akshay Shetty, Fanny Giron, Mukul K. Divatia, Muhammad I. Ahmad, Sudha Kodali and David Victor . . . . . 428

**Current and New Drugs for COVID-19 Treatment and Its Effects on the Liver**

Sandeep Satsangi, Nitin Gupta and Parul Kodan . . . . . 436

**Case Report**

**Acute-on-chronic Liver Failure in a Patient with *Candida Endophthalmitis*: A Case Report**

Ying Cao, Ying Fan, Yanbin Wang, Xiyao Liu and Wen Xie . . . . . 447



## Editorial

# Ariadne's Thread in the Network of Hepatocellular Carcinoma Immunobiology

John Koskinas\* and Athanasios Armakolas

2<sup>nd</sup> Academic Department of Medicine, National and Kapodistrian University of Athens, Medical School Hippokration General Hospital, Athens, Greece

Received: 13 April 2021 | Revised: 5 May 2021 | Accepted: 21 May 2021 | Published: 7 June 2021

**Citation of this article:** Koskinas J, Armakolas A. Ariadne's thread in the network of hepatocellular carcinoma immunobiology. *J Clin Transl Hepatol* 2021;9(3):279–280. doi: 10.14218/JCTH.2021.00140.

Hepatocellular carcinoma (HCC) accounts for approximately 90% of primary liver cancers and represents a major global health problem. The main risk factors responsible for the development of HCC are chronic viral infections, non-alcoholic fatty liver disease, and alcohol-related liver disease, with wide geographical distribution.<sup>1</sup> HCC development and growth involve multiple factors and pathways that lead to changes in gene expression, immune interactions and changes in the tumor microenvironment. In recent years, much progress has been made in understanding the mechanisms underlying tumor-immune system interactions and immunotherapy has been successfully applied to many tumors. Moreover, cancer-specific immune prognostic signatures have been evaluated in order to predict prognosis and response.<sup>2</sup>

Immune reconstitution and restoration of immune cell function against the tumor is the optimal target of immunotherapy. The factors that play a critical role are complex. HCC is a very heterogeneous tumor, with low/moderate mutation burden and microsatellite instability affecting antigenicity.<sup>1,3</sup> Etiology of the underlying liver disease, i.e. chronic hepatitis C virus/hepatitis B virus (HCV/HBV) infection vs. non-alcoholic fatty liver, may also have an impact on the immune system function and the constitution of liver microenvironment, resulting in immune tolerance and development of HCC.<sup>3</sup>

Current immunotherapy for advanced HCC is based on the utility of immune checkpoint inhibitors, namely programmed cell death 1 receptor (PD-1), programmed cell death-ligand 1 (PD-L1), and cytotoxic T-lymphocyte-associated antigen 4 (CTLA-4), administered as monotherapy or combination therapy and having an up to 35% objective response rate.<sup>4</sup> However, response to treatment is not related to PD-L1 expression, suggesting that more complex

mechanisms are involved in immune intervention. In fact, tumor heterogeneity, new tumor antigen formation and alterations in the immune response and microenvironment make selection of patients and type of immunotherapy a very hard task. Furthermore, immune markers for identification of immunologically “hot” HCC and evaluation of treatment response in clinical practice are lacking.

In the past decade there has been an explosion of health-care-related data with digitalization of medical records and utilization of new sophisticated molecular testing for analysis of various genetic, cellular and tissue biological parameters (“omics”).

Big data, by nature, are infinitely versatile and powerful. Extensive analysis and combination of various datasets give a great ability to create powerful algorithms for robust immune-related gene signatures and open a new avenue towards personalized therapy in HCC.

Targeted immunotherapy is actively investigated, with the aim of inhibiting aberrant oncogenic pathways and remodeling the immune microenvironment so as to improve prognosis.

In this issue, Hong *et al.*<sup>5</sup> gives a bird's-eye view of the incredible depth and scale of big data prior to the determination of possible targets for immunotherapy in HCC microenvironment.

The authors systematically integrated genomic profiling to illustrate a global portrait of the HCC immune microenvironment, in order to identify immune-related genetic changes. Key immune-relevant genes (KIRGs) were obtained through integration of the differentially-expressed genes of The Cancer Genome Atlas (TCGA), immune genes from the Immunology Database and Analysis Portal ([www.ImmPort.org](http://www.ImmPort.org)), and immune differentially-expressed genes determined by single-sample gene set enrichment analysis (ssGSEA) scores.

They found that among the 21 KIRGs involved in the pathogenesis and progression of HCC, four genes (IKBKE, IL2RG, EDNRA, IGHA1) seem to be equally or more important to PD-L1. This theory was verified through analysis of tissue expression in HCC samples. The fact that the most significant immune-related molecules obtained by this analysis are major effectors of many oncogenic pathways, promoting transformation in many cancers, renders them possible candidates for HCC treatment. To further investigate the possible regulation mechanism and identify a regulatory network for the involved genes, they studied their relative transcription factors and the long non-coding (lnc) RNAs. They found that the IKBKE gene was mainly related to lncRNA AC127024.5, with NRF1 being its most relevant transcription factor. This axis was found to be involved in

**Abbreviations:** CTLA-4, cytotoxic T-lymphocyte-associated antigen 4; HBV, hepatitis B virus; HCC, hepatocellular carcinoma; HCV, hepatitis C virus; ISG, interferon-stimulated gene; KIRG, key immune-relevant gene; lncRNA, long non-coding RNA; PD-1, programmed cell death 1 receptor; PD-L1, programmed cell death-ligand 1; ssGSEA, single-sample gene set enrichment analysis; TCGA, The Cancer Genome Atlas.

\*Correspondence to: John Koskinas, 2<sup>nd</sup> Academic Department of Medicine, National and Kapodistrian University of Athens, Medical School Hippokration General Hospital, Athens, Greece. E-mail: [koskinasj@yahoo.gr](mailto:koskinasj@yahoo.gr)

many biological pathways of HCC and could therefore be a potential therapeutic target.

In previous studies, IKBKE has been found to be over-expressed in various kinds of tumors, including HCC. Apart from its tumorigenic function, exerted through various signaling pathways, it also regulates the secretion of inflammatory cytokines and thus affects the tumor microenvironment.<sup>6</sup>

Finally in the current study, a risk score model, based on the KIRGs-lncRNA network, was created and evaluated in the testing cohort of patients. It showed good correlation with immune check point genes and infiltration of the microenvironment with CD4, macrophages and neutrophils.

Data from other studies have shown aberrant biogenesis of distinct lncRNAs in HCC. Their role is still elusive, but by binding with DNA, RNA or proteins they modulate oncogenesis and the tumor microenvironment.<sup>7</sup> Furthermore, recent evidence suggests that HCV upregulates the level of a series of lncRNAs that inhibit the expression of IFN-stimulated genes (ISGs), leading to immune suppression and chronic inflammation, both of which are associated with the development and progression of HCC.<sup>8</sup>

Moreover, studies that have explored and analyzed immune multi-omics databases have shown: 1) a significant overexpression of checkpoint genes (PDCD1, CD274, PD-CD1LG2, CTLA4, CD86, CD80) in a subtype of HCC characterized by increased immune cell infiltration score (including tumor matrix, immunity, purity);<sup>9</sup> and, 2) a molecular signature based on 10 immune genes with prognostic role.<sup>10</sup>

In line with the aforementioned findings, the evidence analyzed in the study being discussed herein unveils new associations between tumor and immune interface and provides new insights into the mechanisms of the disease and possible treatment. Furthermore, these results provide additional information that can be incorporated along with other algorithms obtained by bioinformatics into the selec-

tion and management of patients with advanced HCC.

Although identification of immune genes renders a very useful set of targets for the development of novel targeted therapies, the steps towards clinical practice must be taken with great caution. The exploration journey towards new immunotherapy agents needs to be fully traveled. Along this route, it will be important to identify and prioritize patients who could benefit from such therapies.

## References

- [1] Llovet JM, Kelley RK, Villanueva A, Singal AG, Pikarsky E, Roayaie S, *et al*. Hepatocellular carcinoma. Nat Rev Dis Primers 2021;7(1):6. doi:10.1038/s41572-020-00240-3.
- [2] Das S, Camphausen K, Shankavaram U. Cancer-specific immune prognostic signature in solid tumors and its relation to immune checkpoint therapies. Cancers (Basel) 2020;12(9):2476. doi:10.3390/cancers12092476.
- [3] Giraud J, Chalopin D, Blanc JF, Saleh M. Hepatocellular carcinoma immune landscape and the potential of immunotherapies. Front Immunol 2021;12:655697. doi:10.3389/fimmu.2021.655697.
- [4] Ghavimi S, Apfel T, Azimi H, Persaud A, Pysopoulos NT. Management and treatment of hepatocellular carcinoma with immunotherapy: a review of current and future options. J Clin Transl Hepatol 2020;8(2):168–176. doi:10.14218/JCTH.2020.00001.
- [5] Hong WF, Gu YJ, Wang N, Xia J, Zhou HY, Zhan K, *et al*. Integrative characterization of immune-relevant genes in hepatocellular carcinoma. J Clin Transl Hepatol 2021;9(3):301–314. doi:10.14218/JCTH.2020.00132.
- [6] Yin M, Wang X, Lu J. Advances in IKBKE as a potential target for cancer therapy. Cancer Med 2020;9(1):247–258. doi:10.1002/cam4.2678.
- [7] Huang Z, Zhou JK, Peng Y, He W, Huang C. The role of long noncoding RNAs in hepatocellular carcinoma. Mol Cancer 2020;19(1):77. doi:10.1186/s12943-020-01188-4.
- [8] Liu X, Duan X, Holmes JA, Li W, Lee SH, Tu Z, *et al*. A long noncoding RNA regulates hepatitis C virus infection through interferon alpha-inducible protein 6. Hepatology 2019;69(3):1004–1019. doi:10.1002/hep.30266.
- [9] Li W, Wang H, Ma Z, Zhang J, Ou-Yang W, Qi Y, *et al*. Multi-omics analysis of microenvironment characteristics and immune escape mechanisms of hepatocellular carcinoma. Front Oncol 2019;9:1019. doi:10.3389/fonc.2019.01019.
- [10] Zhao K, Xu L, Li F, Ao J, Jiang G, Shi R, *et al*. Identification of hepatocellular carcinoma prognostic markers based on 10-immune gene signature. Biosci Rep 2020;40(8):BSR20200894. doi:10.1042/BSR20200894.



## Editorial

# Prediction and Prevention of Post-hepatectomy Liver Failure: Where Do We Stand?

Amr Shaaban Hanafy\* 

Internal Medicine - Gastroenterology and Hepatology Department, Zagazig University, Ash Sharqia Governorate, Egypt

Received: 17 April 2021 | Revised: 4 June 2021 | Accepted: 7 June 2021 | Published: 18 June 2021

**Citation of this article:** Hanafy AS. Prediction and prevention of post-hepatectomy liver failure: where do we stand? J Clin Transl Hepatol 2021;9(3):281–282. doi: 10.14218/JCTH.2021.00144.

No standardized description or definition of post-hepatectomy liver failure has been introduced. Definitions based on the degree of rise in serum total bilirubin or prolongation of prothrombin time postoperatively were predictive of short-term mortality. Due to lack of universal definition, however, its prevalence is variable but may reach up to 12% post-hepatectomy, according to the definition by International Study Group of Liver Surgery, and or 34%, as in some reports.<sup>1</sup>

The normal liver starts to regenerate within 2 weeks, and is completed mostly after 3 months; the process is initiated by increased production of endothelial nitric oxide in liver sinusoids, secondary to the shear stress on vascular endothelium caused by sudden increase in portal flow after partial hepatectomy and augmented by increased expression of transcription factors, such as c-fos and c-myc.<sup>2</sup> The therapeutic behavior after partial hepatectomy should be directed towards protection of residual hepatocyte function and microvascular functional organization, rather than restoration of liver volume.

Post-hepatectomy liver failure can be defined as post-operative failed ability of the liver to maintain the synthetic, excretory and detoxifying functions with coagulopathy and hyperbilirubinemia on the 5th post-operative day, in addition to the development of clinical symptoms, such as encephalopathy and ascites, in combination with results from liver function tests. Balzan *et al.*<sup>3</sup> established a definition using 50-50 criteria, by which PT <50% and serum bilirubin >50 µmol/L on the 5th day of surgery was associated with >50% risk of early post-operative mortality. Another study found that a peak serum bilirubin concentration of >7 mg/dL strongly predicted liver-related death and worse postoperative outcomes after hepatectomy.<sup>4</sup> Schindl *et al.*<sup>5</sup> provided a classification for the severity of post-hepatectomy liver failure into four grades and included four parameters (i.e. total serum bilirubin concentration, prothrombin time, serum lactate concentration, and grade of encephalopathy).

The International Study Group of Liver Surgery had postulated a definition of post-hepatectomy liver failure<sup>6</sup> in which a postoperatively acquired deterioration in the ability

of the liver to maintain its synthetic, excretory, and detoxifying functions, characterized by an increased international normalized ratio (or need of clotting factors to maintain normal international normalized ratio) and hyperbilirubinemia on or after the fifth postoperative day. Other obvious causes for the biliary obstruction should be excluded. As such, Grade A represents abnormal laboratory parameters requiring no change in the clinical management of the patient, Grade B results in a clinical management but without invasive treatment, and Grade C results in a clinical management requiring invasive treatment.

A risk score was developed to define post-hepatectomy liver failure after evaluation of 1,269 patients, and was able to identify the extent of surgery and pre-operative bilirubin, international normalized ratio, and creatinine as predictors of post-hepatectomy liver failure.<sup>7</sup> Risk factors of liability to post-hepatectomy liver failure are patient related as increasing age above 65 years; however, other studies found no actual relation of age with operative outcomes, the presence of malnutrition was associated with higher incidence of post-hepatectomy liver failure and that higher body mass index was associated with higher risk of hepatic dysfunction. Furthermore, sepsis and associated endotoxemia was found to impair the ability of Kupffer cells to produce and transfer regenerative cytokines. Renal and cardiopulmonary impairment and preoperative thrombocytopenia have also been linked to high risk of post-hepatectomy liver failure, as platelet-derived serotonin is important for hepatic regeneration and tissue repair after hepatectomy and any medications that reduce intraplatelet serotonin should be avoided.<sup>8</sup> Liver-related risk factors, such as fatty liver disease, have been associated with inflammation, due to higher risk of ischemia-reperfusion injury in the steatotic liver, severity of cirrhosis with the presence of ascites, hyperbilirubinemia and the harmful effects of preoperative chemotherapy of colorectal cancer on the occurrence of post-hepatectomy liver failure as irinotecan and oxaliplatin-based chemotherapies which induce fatty infiltration, sinusoidal dilation and biliary complications.

Additional operation-related risk factors are intraoperative blood loss of more than 1,000–1,200 mL, which may stimulate bacterial translocation, systemic inflammatory response and coagulopathy, and technical-related factors including vascular resections or repair, or injury to tissues around the portal triad and hepatoduodenal ligament. The future liver remnant volume/standardized liver volume ratio should exceed 20%. In line with this, the body weight ratio of liver volume cutoff value of 0.5 is highly predictive of post-hepatectomy liver failure.

A major hepatic resection is defined as resection of three or more segments. The remnant liver volume is an impor-

\*Correspondence to: Amr Shaaban Hanafy, Internal Medicine - Gastroenterology and Hepatology Department, Zagazig University, Al-Sharkia 44519, Egypt. ORCID: <https://orcid.org/0000-0003-2901-2614>. Tel: +20-1100061861, Fax: +20-552377179, E-mail: [amrhanafy@zu.edu.eg](mailto:amrhanafy@zu.edu.eg)



tant parameter, and another is the small-for-size syndrome, if the graft recipient weight ratio is less than 0.8–1.0 or less than half of standard/estimated liver volumes.<sup>9</sup>

Reduced functional liver volume increases the portal pressure suddenly, with an increase in the intra-sinusoidal pressures and endothelial shear stress. Patients with a small future liver remnant are at a higher risk for post-operative failure. The future liver remnant is calculated as the ratio of the remnant liver volume and the total functioning liver volume, with the latter being calculated by subtracting the tumor volume from the total liver. At least, the future liver remnant should be 20% of normal livers and 40% of cirrhotic liver.

Assessment of patients can be achieved qualitatively by Child-Turcotte-Pugh scoring. Patients with Child's B or C are not candidates for liver resection, an additional scoring system, the model for end stage liver disease is useful, with a score >10 having a higher mortality risk ( $p < 0.001$ ). Metabolic excretion tests, such as indocyanine green retention rate, are also used and a cut-off value of 14% can triage patients liable for significant morbidity. Other metabolic tests, mainly the LiMax breathe test (methacetin injection), can predict postoperative liver function.

Prevention of post-hepatectomy liver failure can be achieved by modulating the porto-splenic circulation and thereby impacting the remnant liver volume. The portal vein can be embolized to stimulate the production of nitric oxide in patients with cirrhosis and expected future liver remnant of <40. The sluggish portal flow after embolization will enhance arterial flow in the embolized segments (i.e. hepatic arterial buffer response). Hepatic venous outflow reconstruction can ensure an adequate venous outflow; minimizing the venous kinks and congestion (on the surgical table) is essential for preventing post-hepatectomy liver failure.

In situ hypothermic liver perfusion decreases the cellular activity via hypothermia and minimizes ischemia-reperfusion injury. Splenectomy may be a feasible procedure, as the spleen shares 25–30% of the portal flow, reaching nearly 50% in cases of splenomegaly, due to portal hypertension; thus, splenectomy lessens the stress on endothelial lining and hepatocytes with an increase in hepatic arterial buffer response.

In the current research by Xu *et al.*<sup>10</sup> a total of 492 patients who had undergone hepatectomy from July 2015 to June 2018 were retrospectively analyzed. Multivariate analysis identified three preoperative variables, including total bilirubin ( $p = 0.001$ ), international normalized ratio ( $p < 0.001$ ) and platelet count ( $p = 0.004$ ), and two intra-operative variables, including extent of resection ( $p = 0.002$ ) and blood loss ( $p = 0.004$ ) as independent predictors of post-hepatectomy liver failure. The area under the receiver operating characteristic curve of the postulated score was 0.838, with an advantage over the model for end-stage liver disease score and albumin-bilirubin and platelet-albumin-bilirubin scores (0.723, 0.695 and 0.663, respectively;  $p < 0.001$ ). That report also provided a new nomogram to predict post-hepatectomy liver failure, composed of peri-

operative factors, but other intra-operative variables may affect the outcome, such as the extent of resection and the amount of blood loss. The score was easy to calculate based on readily available pre-operative and intra-operative data and helps to identify patients at higher risk.

That study had involved patients either with benign or malignant lesions, so that tumor number, size and associated biomarkers were not analyzed; yet, inadequate future liver remnant volume can lead to post-hepatectomy liver failure. Measuring future liver remnant volume and function should have been studied; however, utilizing simple and readily available variables may significantly contribute to the postoperative work-up of these patients for better outcome.

## Funding

None to declare.

## Conflict of interest

The author has no conflict of interests related to this publication.

## References

- [1] Søreide JA, Deshpande R. Post hepatectomy liver failure (PHLF) - Recent advances in prevention and clinical management. *Eur J Surg Oncol* 2021; 47(2): 216–224. doi: 10.1016/j.ejso.2020.09.001.
- [2] Tu Z, Bozorgzadeh A, Pierce RH, Kurtis J, Crispe IN, Orloff MS. TLR-dependent cross talk between human Kupffer cells and NK cells. *J Exp Med* 2008; 205: 233–244. doi: 10.1084/jem.20072195.
- [3] Balzan S, Belghiti J, Farges O. The “50-50 criteria” on postoperative day 5: an accurate predictor of liver failure and death after hepatectomy. *Ann Surg* 2005; 242: 824–828. doi: 10.1097/01.sla.0000189131.90876.9e.
- [4] Mullen JT, Ribero D, Reddy SK, Donadon M, Zorzi D, Gau-tam S, *et al.* Hepatic insufficiency and mortality in 1,059 noncirrhotic patients undergoing major hepatectomy. *J Am Coll Surg* 2007; 204: 854–862. doi: 10.1016/j.jamcollsurg.2006.12.032.
- [5] Schindl MJ, Redhead DN, Fearon KC, Garden OJ, Wigmore SJ. The value of residual liver volume as a predictor of hepatic dysfunction and infection after major liver resection. *Gut* 2005; 54: 289–296. doi: 10.1136/gut.2004.046524.
- [6] Rahbari NN, Garden OJ, Padbury R, Brooke-Smith M, Crawford M, Adam R, *et al.* Posthepatectomy liver failure: a definition and grading by the International Study Group of Liver Surgery (ISGLS). *Surgery* 2011; 149(5): 713–724. doi: 10.1016/j.surg.2010.10.001.
- [7] Dasari BVM, Hodson J, Roberts KJ, Sutcliffe RP, Marudanayagam R, Mirza DF, *et al.* Developing and validating a pre-operative risk score to predict post-hepatectomy liver failure. *HPB (Oxford)* 2019; 21(5): 539–546. doi: 10.1016/j.hpb.2018.09.011.
- [8] Starlinger P, Pereyra D, Hackl H, Ortmayr G, Braunwarth E, Santol J, *et al.* Consequences of perioperative serotonin reuptake inhibitor treatment during hepatic surgery. *Hepatology* 2021; 73(5): 1956–1966. doi: 10.1002/hep.31601.
- [9] Guglielmi A, Ruzzenente A, Conci S, Valdegamberi A, Iacono C. How much remnant is enough in liver resection? *Dig Surg* 2012; 29(1): 6–17. doi: 10.1159/000335713.
- [10] Xu B, Li XL, Ye F, Zhu XD, Shen YH, Huang C, *et al.* Development and validation of a nomogram based on perioperative factors to predict post-hepatectomy liver failure. *J Clin Transl Hepatol* 2021; 9(3): 291–300. doi: 10.14218/JCTH.2021.00013.



Original Article

# PD-1 Involvement in Peripheral Blood CD8<sup>+</sup> T Lymphocyte Dysfunction in Patients with Acute-on-chronic Liver Failure

Xiaoshuang Zhou<sup>1</sup>, Yidong Li<sup>2</sup>, Yaqiu Ji<sup>2</sup>, Tian Liu<sup>2</sup>, Ninghui Zhao<sup>2\*</sup>, Jiefeng He<sup>3\*</sup> and Jia Yao<sup>2,4\*</sup>

<sup>1</sup>Department of Nephrology, Shanxi Provincial People's Hospital, Shanxi Medical University, Taiyuan, Shanxi, China; <sup>2</sup>Department of Gastroenterology, Shanxi Bethune Hospital, Shanxi Medical University, Taiyuan, Shanxi, China; <sup>3</sup>Department of Hepatobiliary Surgery, Shanxi Bethune Hospital, Shanxi Medical University, Taiyuan, Shanxi, China; <sup>4</sup>Institute of Liver Disease and Organ Transplantation, Shanxi Medical University, Taiyuan, Shanxi, China

Received: 30 November 2020 | Revised: 9 January 2021 | Accepted: 7 March 2021 | Published: 31 March 2021

## Abstract

**Background and Aims:** Programmed cell death-1 (PD-1) plays an important role in downregulating T lymphocytes but the mechanisms are still poorly understood. This study aimed to explore the role of PD-1 in CD8<sup>+</sup> T lymphocyte dysfunction in hepatitis B virus (HBV)-related acute-on-chronic liver failure (ACLF). **Methods:** Thirty patients with HBV-ACLF and 30 healthy controls (HCs) were recruited. The differences in the numbers and functions of CD8<sup>+</sup> T lymphocytes, PD-1 and glucose transporter-1 (Glut1) expression from the peripheral blood of patients with HBV-ACLF and HCs were analyzed. *In vitro*, the CD8<sup>+</sup> T lymphocytes from HCs were cultured (HC group) and the CD8<sup>+</sup> T lymphocytes from ACLF patients were cultured with PD-L1-IgG (ACLF+PD-1 group) or IgG (ACLF group). The numbers and functions of CD8<sup>+</sup> T lymphocytes, PD-1 expression, glycogen uptake capacity, and Glut1, hexokinase-2 (HK2), and pyruvate kinase (PKM2) expression were analyzed among the HC group, ACLF group and ACLF+PD-1 group. **Results:** The absolute numbers of CD8<sup>+</sup> T lymphocytes in the peripheral blood from patients with HBV-ACLF were lower than in the HCs ( $p<0.001$ ). The expression of PD-1 in peripheral blood CD8<sup>+</sup> T lymphocytes was lower in HCs than in patients with HBV-ACLF ( $p=0.021$ ). Compared with HCs, PD-1 expression was increased ( $p=0.021$ ) and Glut1 expression was decreased ( $p=0.016$ ) in CD8<sup>+</sup> T lymphocytes from the HBV-ACLF group. *In vitro*, glycogen uptake and functions of ACLF CD8<sup>+</sup> T lymphocytes were significantly lower than that in HCs ( $p=0.017$ ; all  $p<0.001$ ). When PD-1/PD-L1 was activated, the glycogen uptake rate and expression levels of Glut1, HK2, and PKM2 showed a decreasing trend (ACLF+PD-1 group compared to ACLF group

, all  $p<0.05$ ). The functions of CD8<sup>+</sup> T lymphocytes in the ACLF+PD-1 group [using biomarkers of Ki67, CD69, IL-2, interferon-gamma, and tumor necrosis factor- $\alpha$ ] were lower than in the ACLF group (all  $p<0.05$ ). **Conclusions:** CD8<sup>+</sup> T lymphocyte dysfunction is observed in patients with HBV-ACLF. PD-1-induced T lymphocyte dysfunction might involve glycolysis inhibition.

**Citation of this article:** Zhou X, Li Y, Ji Y, Liu T, Zhao N, He J, *et al.* PD-1 involvement in peripheral blood CD8<sup>+</sup> T lymphocyte dysfunction in patients with acute-on-chronic liver failure. J Clin Transl Hepatol 2021;9(3):283–290. doi: 10.14218/JCTH.2020.00142.

## Introduction

Hepatitis B virus (HBV) infection-induced acute-on-chronic liver failure (ACLF) (i.e. HBV-ACLF) is a common clinical condition of critical liver diseases, with rapid progression and 28- and 90-day transplantation-free mortality rates of 32.8% and 51.2%, respectively.<sup>1</sup> The pathophysiology of ACLF is related to an initial widespread immune activation, systematic inflammatory response syndrome, and secondary sepsis due to immune dysfunction.<sup>2</sup> ACLF increases the risk of secondary infection and infection-related death.<sup>3–6</sup> ACLF is an important cause of hepatic encephalopathy, hepatorenal syndrome, ascites, hyponatremia, and infectious shock.<sup>7</sup> The exact mechanisms involved in the immune dysfunction of patients with HBV-ACLF are poorly understood.

Wasmuth *et al.*<sup>8</sup> proposed that the pathogenesis of ACLF is similar to that of sepsis-like immune paralysis, manifesting by reduced expression of human leukocyte antigen-DR molecules on the surface of monocytes in peripheral blood, inactivation of immune function, and reduced production of tumor necrosis factor- $\alpha$  (TNF- $\alpha$ ). T lymphocyte dysfunction (manifested by increased apoptosis, weakened proliferative ability, and decreased reactivity or non-reactivity of T lymphocytes in ACLF)<sup>9</sup> is observed in ACLF. Similar to sepsis, ACLF leads to decreased numbers of CD4<sup>+</sup> and CD8<sup>+</sup> T lymphocytes in peripheral blood,<sup>10</sup> as well as low activation of CD8<sup>+</sup> T lymphocytes in patients with ACLF.<sup>11</sup> The production of T lymphocyte-related cytokines in peripheral blood is also decreased.<sup>12</sup> Therefore, T lymphocyte dysfunction plays an important role in the immune suppression of patients with ACLF, but the specific mechanisms are still unknown.<sup>1</sup>

**Keywords:** Acute and chronic liver failure; Programmed cell death 1; Immune function; Glycolysis; Glut1.

**Abbreviations:** ACLF, acute-on-chronic liver failure; Glut1, glucose transporter 1; HBsAg, hepatitis B surface antigen; HBV, hepatitis B virus; HC, healthy control; HK2, hexokinase-2; IFN- $\gamma$ , interferon-gamma; MFI, mean fluorescence intensity; PBMC, prepared peripheral blood mononuclear cell; PBS, phosphate-buffered saline; PD-1, programmed cell death-1; PD-L1/2, programmed cell death 1-ligand 1/2; PKM2, pyruvate kinase; TNF- $\alpha$ , tumor necrosis factor- $\alpha$ .

**\*Correspondence to:** Jia Yao and Ninghui Zhao, Department of Gastroenterology, Shanxi Baijiu Hospital, Shanxi Medical University, No. 99 Longcheng Street, Taiyuan, Shanxi 030001, China. ORCID: <https://orcid.org/0000-0003-2210-7717> (JY), <https://orcid.org/0000-0002-9715-9303> (NZ). Tel/Fax: +86-199-3491-1619, E-mail: [yaojia2006@163.com](mailto:yaojia2006@163.com) (JY) and [ZHAONINGHUIHUI@163.com](mailto:ZHAONINGHUIHUI@163.com) (NZ); Jiefeng He, Department of Hepatobiliary Surgery, Shanxi Bethune Hospital, Shanxi Medical University, Taiyuan, Shanxi 030001, China. ORCID: <https://orcid.org/0000-0003-2958-0232>. E-mail: [hejiefeng2008@163.com](mailto:hejiefeng2008@163.com)

**Table 1. Characteristics of the ACLF patients and HCs at the time of hospital admission**

Indicator	ACLF patients, <i>n</i> =30	HCs, <i>n</i> =30	<i>p</i> <sup>a</sup>
Age in years	53.2±9.2	50.5±11.2	0.595
Female, <i>n</i> (%)	12 (40.0)	13 (43.3)	0.962
BMI in kg/m <sup>2</sup>	23.6±3.6	25.6±2.9	0.496
ALT in U/L	121.4±90.8	33.3±11.1	<0.001*
AST in U/L	129.6±41.7	24.3±6.3	<0.001*
TBIL in μmol/L	410.4±143.7	17.7±5.8	<0.001*
PTA, %	28.5±4.2	120.0±5.1	<0.001*
INR	2.1±0.3	0.9±0.2	<0.001*
Albumin in g/L	29.1±3.5	39.5±1.6	<0.001*
Urea in mmol/L	5.2±1.4	5.4±1.1	0.474
Creatinine in μmol/L	70.3±6.3	67.1±3.1	0.133
MELD score	23.5±5.5	—	—

\**p*<0.05. <sup>a</sup>*p*-values were acquired by chi-square test or *t*-test. ACLF, acute-on-chronic liver failure; ALT, alanine aminotransferase; AST, aspartate aminotransferase; BMI, body mass index; HCs, healthy controls; INR, international normalized ratio; MELD, model for end-stage liver disease; PTA, prothrombin activity; TBIL, total bilirubin.

ATP provided by glycolysis and the electron transport chain is the fuel for the activity and function of any cell.<sup>13,14</sup> The activation of T lymphocytes is accompanied by changes in glucose metabolism. Naïve T lymphocytes are dependent on oxidative phosphorylation for energy, but once stimulated, they differentiate into effector T lymphocytes, with the reprogramming of metabolic patterns, increasing the expression of glucose transporter 1 (Glut1) on the cell membrane, promoting glycogen uptake and using it as the main energy supply, and reducing oxidative phosphorylation.<sup>15</sup> Glycolysis levels affect T lymphocyte proliferation, activation, and immune function.<sup>16,17</sup>

Programmed death-1 (PD-1) is mainly expressed in activated CD8<sup>+</sup> T lymphocytes, and its ligands are programmed cell death 1-ligand 1 and 2 (PD-L1 and PD-L2).<sup>18</sup> The PD-1/PD-L1/2 co-stimulatory signaling pathway plays an important negative regulatory role in T lymphocyte activation, proliferation, and cytokine secretion.<sup>19</sup> In chronic lymphocytic leukemia, PD-1 inhibits key glycolytic enzymes [hexokinase-2 (HK2) and pyruvate kinase (PKM2)] in monocytes, and blocking PD-1 can restore their glycolytic levels.<sup>20</sup> *In vitro*, PD-1 inhibits the uptake and use of glycogen in T lymphocytes and affects the differentiation of T lymphocytes.<sup>21</sup> Whether PD-1 mediates its negative function by regulating the glycolysis of T lymphocytes is currently unknown. Therefore, this study explored how PD-1 mediates T lymphocyte dysfunction in ACLF by regulating the glycolytic pathway. This study provides insights into the immune dysfunction observed in ACLF.

## Methods

### Subjects

Thirty patients with HBV-ACLF from the Gastroenterology Department of Shanxi Baijiu Hospital were screened from June 2018 to June 2019, and 30 healthy controls (HCs) were recruited during the same period from among healthy volunteers. The study protocol was approved by the Ethics Committee of Shanxi Baijiu Hospital, Taiyuan (No. 2017LL039), China. The study was conducted in accordance with the Declaration of Helsinki. All patients and healthy volunteers pro-

vided written informed consent prior to study inclusion.

For patients with HBV-ACLF, the inclusion criteria were: 1) ACLF with positivity for hepatitis B surface antigen (HBsAg) or positivity for HBV DNA; and 2) meeting the diagnostic criteria for ACLF by the Asian Pacific Association for the Study of the Liver:<sup>22</sup> total bilirubin ≥85 μmol/L, international normalized ratio ≥1.5, or prothrombin activity ≤40%. For the HCs, the inclusion criteria were: 1) normal liver function; and 2) negative HBsAg.

The exclusion criteria for all the subjects were: 1) alcoholic, drug-induced, or other viral hepatitis; 2) cancer; or 3) other diseases involving the immune system.

The clinical data of the subjects are shown in Table 1.

### Detection of the expression levels of CD8<sup>+</sup> T lymphocyte subsets

EDTA-K<sub>2</sub> anticoagulation tubes were used to collect the peripheral blood samples to detect the absolute number of CD8<sup>+</sup> T lymphocytes. Whole blood (100 μL) was added to a test tube with standard microspheres and 10 μL of CD3-PC5- and CD8-PE-labeled monoclonal antibodies (BD Biosciences, Franklin Lakes, NJ, USA). The suspension was mixed thoroughly and incubated at room temperature for 20–30 min. Then, 2 mL of erythrocyte solution was added, mixed thoroughly, and incubated at room temperature for 10 min. The tubes were centrifuged at 1,500 rpm for 5 min, and the supernatant was discarded. Normal saline (2 mL) was added, the sample centrifuged at 1,500 rpm for 5 min, and the supernatant was discarded. Then, normal saline (1 mL) was added to resuspend the cells, and the sample subjected to flow cytometric analysis using a FACS Calibur system (BD Diagnostics, Sparks, MD, USA). Data analysis was performed using FlowJo software (Tree Star Inc., Ashland, OR, USA).

### Detection of CD8<sup>+</sup> T lymphocytes

The peripheral blood mononuclear cells (PBMCs) were sorted using Miltenyi cell sorting magnetic beads (Miltenyi Biotec GmbH, Bergisch Gladbach, Germany). Positive selection was applied. CD8<sup>+</sup> T lymphocytes magnetic bead antibody (20 μL; Miltenyi Biotec GmbH) was added, incubated for 15

m at 4°C, and 500 µL of magnetic bead buffer was added. After being washed three times, the cell suspension was passed through a magnetic column. The CD8<sup>+</sup> T lymphocytes were retained in the column and subsequently eluted. The whole process was performed under sterile conditions. The cells were washed twice to remove the magnetic beads. After cells were added to the CD8-FITC-labeled antibodies (BD Biosciences), the purity of the sorted CD8<sup>+</sup> T lymphocytes was detected by flow cytometry. Purity >99% was required for the subsequent experiments.

### Evaluation of PD-1 and Glut1 expression levels

The sorted CD8<sup>+</sup> T lymphocytes were resuspended in 2% phosphate-buffered saline (PBS) and stained with FITC-conjugated anti-PD-1 antibody (R&D Systems, Minneapolis, MN, USA) and FITC-conjugated anti-Glut1 antibody (Biolegend, San Diego, CA, USA). Mouse IgG2b (BD Biosciences) was used as an isotype control. The cells were incubated on ice for 30 m, washed twice with 2% PBS, and analyzed for PD-1 and Glut1 by flow cytometry.

### Cell culture

According to a previous study,<sup>23</sup> the cells were purified using a CD8<sup>+</sup> T lymphocyte purification column and cultured for 48 h. The CD8<sup>+</sup> T lymphocytes sorted from HCs were immunized with anti-human CD28 (0.5 µg/mL) and anti-human CD3 (20 U/mL) antibodies (HC group). For the CD8<sup>+</sup> T lymphocytes sorted from patients with HBV-ACLF, two groups were divided out. One group was cultured with anti-human CD28 (0.5 µg/mL) and anti-human CD3 (20 U/mL)+PD-L1-IgG fusion protein (Cat. No. 16-9989-82, at 10 µg/mL; eBioscience, San Diego, CA, USA) (ACLF+PD-1 group); the other group was added with anti-human CD28 (0.5 µg/mL) and anti-human CD3 (20 U/mL) + IgG (Cat. No. 16-4714-82; eBioscience) (ACLF group).

### Detection of CD8<sup>+</sup> T lymphocyte proliferative ability (Ki67), cell viability (CD69), and cytokine production [IL-2, interferon-gamma (IFN-γ), and TNF-α]

The CD8<sup>+</sup> T lymphocytes were treated with CD3/CD28 and IL-12 stimulation *in vitro* for the detection of proliferative ability (Ki67) and cell viability (CD69). First, the cells were resuspended with 2% PBS, added with Ki67 (Cat. No. 558616; BD Biosciences) and CD69 (Cat. No. 310904; Biolegend) antibodies, incubated on ice for 30 m, washed twice with 2% PBS, and detected by flow cytometry. For the detection of IL-2 (Cat. No. 500310; Biolegend), IFN-γ (Cat. No. 502515; Biolegend), and TNF-α (Cat. No. 559321; BD Biosciences), phorbol myristate acetate (Enzo Life Sciences, Inc., Farmingdale, NY, USA) and ionomycin (Enzo Life Sciences, Inc.) were added, and the cells were cultured for 5 h. In the third hour of cultivation, the protein transport inhibitor Monensin 3 µM (BD Biosciences) was added. After centrifugation and washing, the cells were treated with fixation and membrane-breaking agents. The fluorescence-labeled antibodies were added and incubated for 30 m and detected by flow cytometry. The results were expressed as mean fluorescence intensity (MFI).

### Detection of glucose uptake

At total of  $1 \times 10^6$  cells of CD8<sup>+</sup> T lymphocytes were taken and

cultured at room temperature for 2 h in PBS, washed with PBS, added with 1 µCi/ml of 2-deoxy-D-[<sup>3</sup>H]-labeled glucose, and incubated for 20 m. The cells were rinsed three times with pre-chilled PBS to stop the reaction. All operations were performed according to the instructions of the glucose uptake assay kit (Cat. No. ab136955; Abcam, Cambridge, UK). The glucose levels were quantified using the FLUOstar Omega plate reader (BMG LABTECH GmbH, Ortenberg, Germany). The results were expressed as the average of three tests.

### Western blotting

The total cell proteins were extracted from the HC, ACLF, and ACLF+PD-1 groups, respectively. The protein concentration was determined by the bicinchoninic acid method, and the proteins (35 µg per sample) were separated using 12% sodium dodecyl sulfate-polyacrylamide gel electrophoresis. After electrotransferring the proteins to polyvinylidene fluoride membranes, the membranes were cut into strips and incubated with the corresponding antibody solution (anti-β-actin mouse monoclonal antibody, anti-HK2 mouse monoclonal antibody, and anti-PKM2 mouse monoclonal antibody) (Millipore Corp., Billerica, MA, USA) in 5% nonfat-dried milk at 4°C, with gentle agitation, overnight. After washing with Tris-buffered saline three times (30 m each time), the membranes were incubated with the secondary antibody, with gentle agitation, at room temperature, for 1 h. Finally, the membranes were washed three times with Tris-buffered saline, developed with a chemiluminescence solution, and photographed.

### Statistical analysis

All statistical analyses were performed using SPSS 19.0 software (IBM Corp., Armonk, NY, USA). According to the Kolmogorov-Smirnov test, if the data fit the normal distribution pattern, continuous data were presented as mean ± standard deviation, and if the data did not fit the normal distribution pattern, median was presented. The clinical characteristic variables were analyzed using the independent-samples *t*-test and Pearson's chi-square test between ACLF patients and HCs. The numbers and functions of CD8<sup>+</sup> T lymphocytes, PD-1 expression, glycogen uptake capacity, and Glut1, HK2 and PKM2 expression were analyzed using independent-samples *t*-test between the two groups. Two-sided (except for the chi-square test) *p*-values <0.05 were considered statistically significant.

## Results

### Absolute numbers of CD8<sup>+</sup> T lymphocytes and the expression of PD-1 in the peripheral blood from HCs and patients with HBV-ACLF

The absolute numbers of CD8<sup>+</sup> T lymphocytes in the peripheral blood from patients with HBV-ACLF were lower than in the HCs ( $333.88 \pm 147.74$  vs.  $872.50 \pm 206.64$ ,  $p < 0.001$ ) (Fig. 1). The expression of PD-1 in peripheral blood CD8<sup>+</sup> T lymphocytes was lower in HCs ( $7.02 \pm 2.12\%$ ) than in patients with HBV-ACLF ( $13.33 \pm 2.52\%$ ) ( $p = 0.021$ ) (Fig. 2).

### Glycolysis and immune function analysis of CD8<sup>+</sup> T lymphocytes in peripheral blood from HCs and patients with HBV-ACLF

The expression of Glut1 in CD8<sup>+</sup> T lymphocytes in the pe-



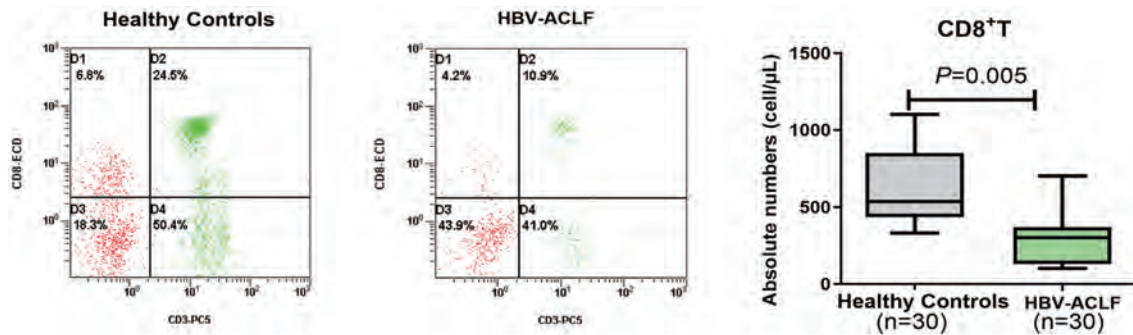


**Fig. 1.** Proportion and absolute numbers of peripheral CD8<sup>+</sup> T cells in patients with HBV-ACLF and HCs. HBV-ACLF, hepatitis B virus infection-induced acute-on-chronic liver failure; HCs, healthy controls.

peripheral blood of patients with ACLF was lower than that in HCs ( $13.33 \pm 1.40\%$  vs.  $19.27 \pm 2.05\%$ ,  $p=0.016$ ) (Fig. 3). *In vitro*, the glycogen uptake capacity of CD8<sup>+</sup> T lymphocytes from patients with HBV-ACLF was significantly lower than that from HCs ( $2.8 \pm 0.11$  vs.  $3.6 \pm 0.14$  pmol/cell,  $p=0.017$ ) (Fig. 4). The expressions of Glut1, HK2, and PKM2 in CD8<sup>+</sup> T lymphocytes in patients with HBV-ACLF were significantly lower than those in HCs (all  $p<0.001$ ) (Fig. 5).

Compared with HCs, the peripheral blood CD8<sup>+</sup> T lymphocytes from patients with HBV-ACLF were in an immune

paralysis state. The cell viability (CD69) of ACLF CD8<sup>+</sup> T lymphocytes was weaker than that of HCs (MFI:  $1,722.9 \pm 142.5$  vs.  $3,017.4 \pm 132.1$ ,  $p<0.001$ ). The proliferative ability (Ki67) of ACLF CD8<sup>+</sup> T lymphocytes was weaker than that of HCs (MFI:  $1,737.2 \pm 139.3$  vs.  $2,603.4 \pm 172.8$ ,  $p<0.001$ ). The productive levels cytokines of ACLF CD8<sup>+</sup> T lymphocytes were lower than in HCs [IL-2 (MFI:  $330,067.2 \pm 10,033.3$  vs.  $150,586.9 \pm 9,157.2$ ,  $p<0.001$ ), IFN- $\gamma$  (MFI:  $2,423.2 \pm 115.6$  vs.  $1,737.4 \pm 161.2$ ,  $p<0.001$ ), and TNF- $\alpha$  (MFI:  $10,947.5 \pm 819.3$  vs.  $4,049.6 \pm 241.5$ ,  $p<0.001$ )] (Fig. 6).

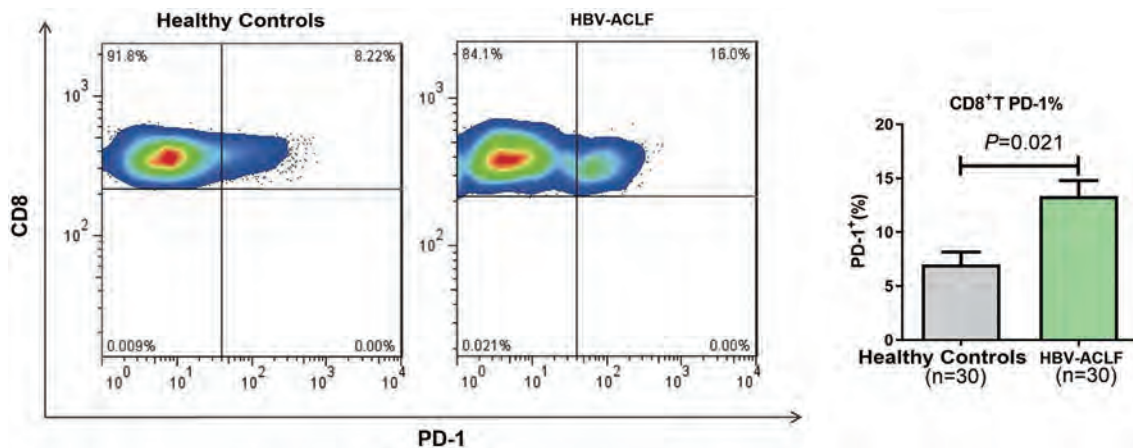


**Fig. 2.** Expression of PD-1 in peripheral CD8<sup>+</sup> T cells of patients with HBV-ACLF and HCs. HBV-ACLF, hepatitis B virus infection-induced acute-on-chronic liver failure; HCs, healthy controls; PD-1, programmed cell death-1.

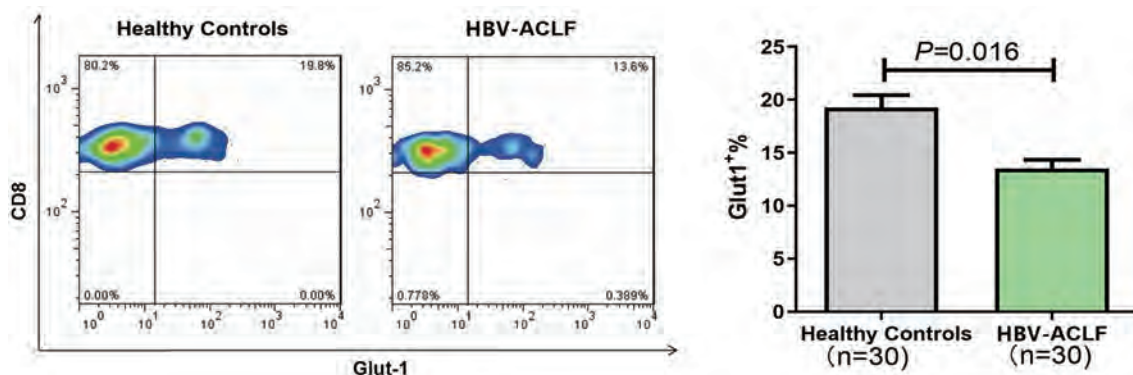


**Fig. 3.** Expression of Glut1 in peripheral CD8<sup>+</sup> T cells of patients with HBV-ACLF and HCs. HBV-ACLF, hepatitis B virus infection-induced acute-on-chronic liver failure; HCs, healthy controls.



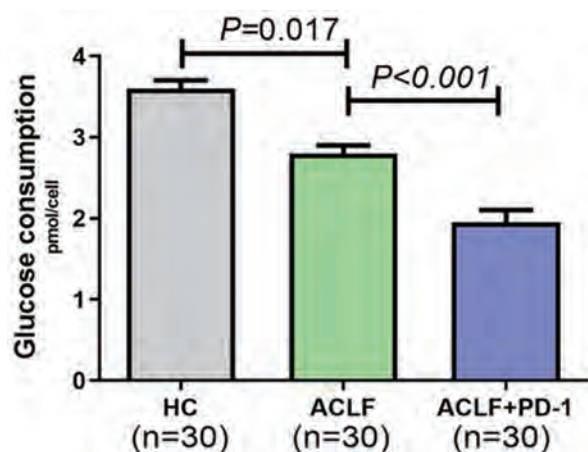


Fig. 4. Glycogen uptake capacity of CD8<sup>+</sup> T lymphocytes from the Healthy controls (HCs), Acute-on-chronic liver failure (ACLF), and ACLF+PD-1 groups. ACLF, acute-on-chronic liver failure; HCs, healthy controls; PD-1, programmed cell death-1.

#### Effects of PD-1 on glycolysis and immune functions of CD8<sup>+</sup> T lymphocytes in vitro

When PD-1/PD-L1 was activated, the expressions of Glut1, HK2, and PKM2 in CD8<sup>+</sup> T lymphocytes in the ACLF+PD-1 group were lower than in the ACLF group (all  $p < 0.001$ ) (Fig. 5). At the same time, the glycogen uptake in patients in the ACLF+PD-1 group was lower than in the ACLF group ( $2.0 \pm 0.21$  vs.  $2.8 \pm 0.11$  pmol/cell,  $p < 0.001$ ) (Fig. 4).

With regard to the immune function of CD8<sup>+</sup> T lymphocytes in the PD-1/PD-L1 activated state, the cell viability (CD69) (MFI:  $916.7 \pm 43.3$  vs.  $1,722.9 \pm 142.5$ ,  $p < 0.001$ ) and proliferative ability (Ki67) (MFI:  $940.3 \pm 71.3$  vs.  $1,737.2 \pm 139.3$ ,  $p < 0.001$ ) of CD8<sup>+</sup> T lymphocytes in the ACLF+PD-1 group were lower than in the ACLF group. The levels of secreted IL-2 (MFI:  $64,267.1 \pm 3,643.7$  vs.  $150,586.9 \pm 9,157.2$ ,  $p < 0.001$ ), IFN- $\gamma$  (MFI:  $1,307.1 \pm 95.6$  vs.  $1,737.4 \pm 161.2$ ,  $p = 0.031$ ), and TNF- $\alpha$  (MFI:  $2,099.5 \pm 119.3$  vs.  $4,049.6 \pm 241.5$ ,  $p < 0.001$ ) were lower than in the ACLF group (Fig. 7).

#### Discussion

Patients with HBV-ACLF often show immune dysfunction

and are prone to secondary infection, related complications, and mortality.<sup>3–6</sup> T lymphocyte dysfunction is an important mechanism of ACLF immune suppression.<sup>10,11</sup> The results of this study showed that PD-1 regulates CD8<sup>+</sup> T lymphocyte dysfunction in patients with ACLF and that the immune dysfunction possibly involves the glycolytic pathway.

The pathogenesis of immune depletion in ACLF is similar to that observed in sepsis. The dysfunction or depletion of CD8<sup>+</sup> T lymphocytes manifests as decreases in cell proliferation and secretion of effector cytokines (IL-2, IFN- $\gamma$ , and TNF- $\alpha$ ).<sup>24</sup> This study showed that the absolute number, viability, proliferative ability, and cytokine secretion of CD8<sup>+</sup> T lymphocytes in the peripheral blood of patients with ACLF were lower than that of HCs. In addition, PD-1 expression was increased in CD8<sup>+</sup> T lymphocytes in the peripheral blood of patients with HBV-ACLF. In order to explore the role of PD-1/PD-L1 signaling in the function of CD8<sup>+</sup> T lymphocytes, PD-L1 was added to the culture medium to activate PD-1/PD-L1 signaling, and the viability, proliferation, and cytokines secretion abilities of the CD8<sup>+</sup> T lymphocytes were weakened. The upregulation of PD-1 expression is an important mechanism involved in T lymphocyte immune dysfunction in cancer<sup>25</sup> and other conditions.<sup>26</sup> In the early stage of acute HBV infection, the upregulation of PD-1 expression on CD8<sup>+</sup> T lymphocytes in peripheral blood helps reduce the damage to the liver by CD8<sup>+</sup> T lymphocytes,<sup>27</sup> but this immune suppression participates in secondary infections. HBV-ACLF is often associated with immune depletion. The number of immune cells with upregulated PD-1 expression in liver tissues of patients with HBV-ACLF is higher than that of patients with chronic hepatitis B and HCs.<sup>28</sup> Similarly, Liu *et al.*<sup>29</sup> found that PD-1 expression is upregulated in CD8<sup>+</sup> T lymphocytes in the peripheral blood of patients with HBV-ACLF and is directly proportional to the severity of the disease. Therefore, those results suggest that the PD-1/PD-L1 signaling pathway is involved in CD8<sup>+</sup> T lymphocyte dysfunction or depletion in patients with HBV-ACLF.

The expression levels of Glut1 and the key glycolytic enzymes HK2 and PKM2 in the CD8<sup>+</sup> T lymphocytes in the peripheral blood of patients with HBV-ACLF were decreased. The glycogen uptake rate of CD8<sup>+</sup> T lymphocytes in peripheral blood of patients with HBV-ACLF was lower than that of HCs, and the glycogen metabolism provides ATP to the immune cells for their activities and functions.<sup>13</sup> Once exposed to external stimuli, naïve T lymphocytes differentiate into effector T lymphocytes, a process accompanied by reprogramming of the metabolic patterns that involves increased Glut1 expression on the cell membrane and increased glycogen uptake.<sup>30–32</sup> In contrast, when Glut1 expression is decreased, the glycogen uptake and aerobic glycolysis of T

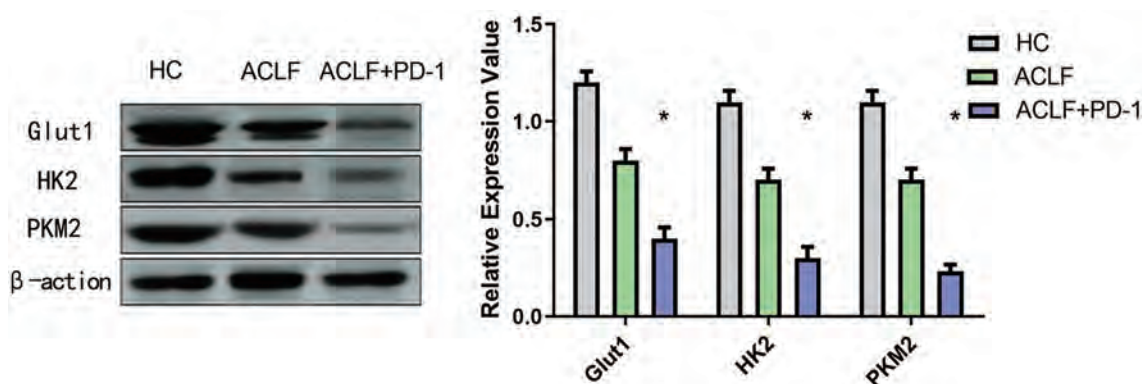
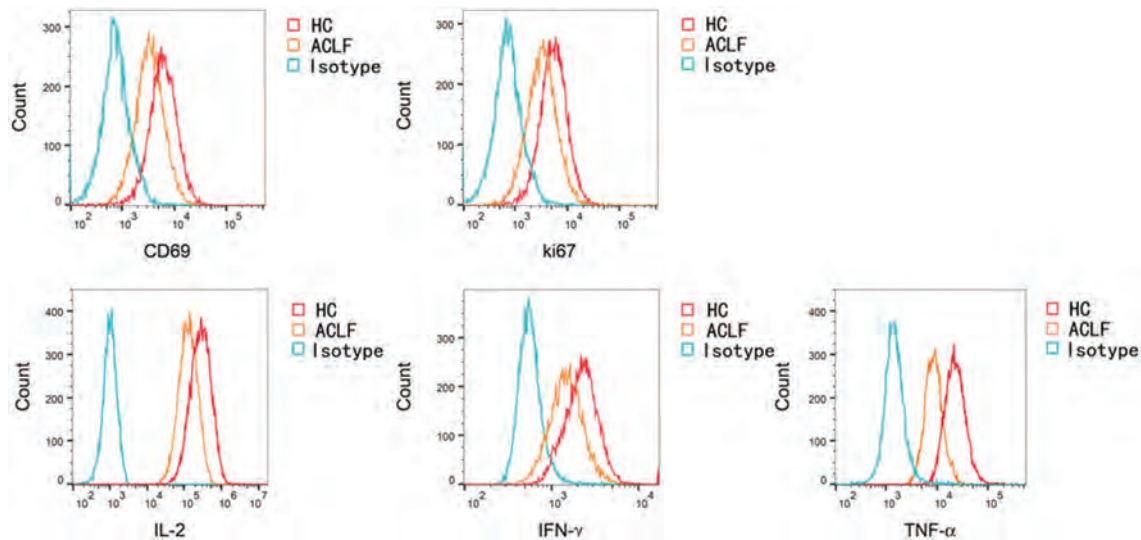


Fig. 5. Expression of Glut1 and key glycolytic enzymes (HK2 and PKM2) in the HCs, ACLF, and ACLF+PD-1 groups. \*ACLF vs. ACLF+PD-1,  $p < 0.05$ ,  $n = 3$  experiments. ACLF, acute-on-chronic liver failure; Glut1, glucose transporter 1; HCs, healthy controls; HK2, hexokinase-2; PD-1, programmed cell death-1; PKM2, pyruvate kinase.



**Fig. 6.** Compared with HCs, the CD8<sup>+</sup> T lymphocytes in peripheral blood from patients with HBV- ACLF were in an immune paralysis state. The cell viability (CD69) of ACLF patients (MFI: 1,723±143) was weaker than that of HCs (MFI: 3,017±132,  $p<0.001$ ). The proliferative ability (Ki67) of ACLF (MFI: 1,737±139) was weakened compared with that of HCs (MFI: 2,603±173,  $p<0.001$ ). Compared with HCs, the levels of secreted IL-2 (MFI: 330,067±10,033 vs. 150,587±9,157,  $p<0.001$ ), IFN- $\gamma$  (MFI: 2,423±116 vs. 1,737±161,  $p<0.001$ ) and TNF- $\alpha$  (MFI: 10,948 ±819 vs. 4,050±242,  $p<0.001$ ) were decreased in the ACLF group. ACLF, acute-on-chronic liver failure; HBV- ACLF, hepatitis B virus infection-induced acute-on-chronic liver failure; HCs, healthy controls; IFN- $\gamma$ , interferon-gamma; MFI, mean fluorescence intensity; TNF- $\alpha$ , tumor necrosis factor-alpha.

lymphocytes are reduced, thereby reducing the proliferation and differentiation capacity of T lymphocytes, especially of the effector T lymphocytes.<sup>16</sup> In the present study, PD-L1 was added to the culture medium of CD8<sup>+</sup> T lymphocytes from patients with HBV-ACLF to activate PD-1/PD-L1 signaling, and the expression levels of Glut1, HK2, and PKM2 were found to be significantly decreased, as was the glycolysis uptake capacity. Similarly, in chronic lymphocytic leukemia, PD-1 inhibits the glycolytic pathway of monocytes and blocking PD-1 can restore their glycolytic level, indicating that PD-1 can affect the regulation of T lymphocyte glycolysis.<sup>20</sup> The expression of Glut1 is under control of the

PI3K pathway, which can be interfered by PD-1.<sup>23</sup> The restoration of PI3K when blocking PD-1 is probably involved in Glut1 expression and the restored glycolysis.<sup>33</sup>

A previous study involving non-small lung cancer indicated that blocking the PD-1/PD-L1 axis produces more effects on the function of CD8<sup>+</sup> T cells than blocking the PD-1/PD-L2 axis.<sup>25</sup> This differential effect of PD-L1 and PD-L2 should be explored in ACLF CD8<sup>+</sup> T cells in future studies. In addition, in cancer-associated CD8<sup>+</sup> T cell dysfunction, blocking PD-1 only results in a partial restoration of the CD8<sup>+</sup> T cell functions, indicating that other pathways are involved.<sup>25,34</sup> Therefore, pathways like that regulated by lymphocyte-ac-

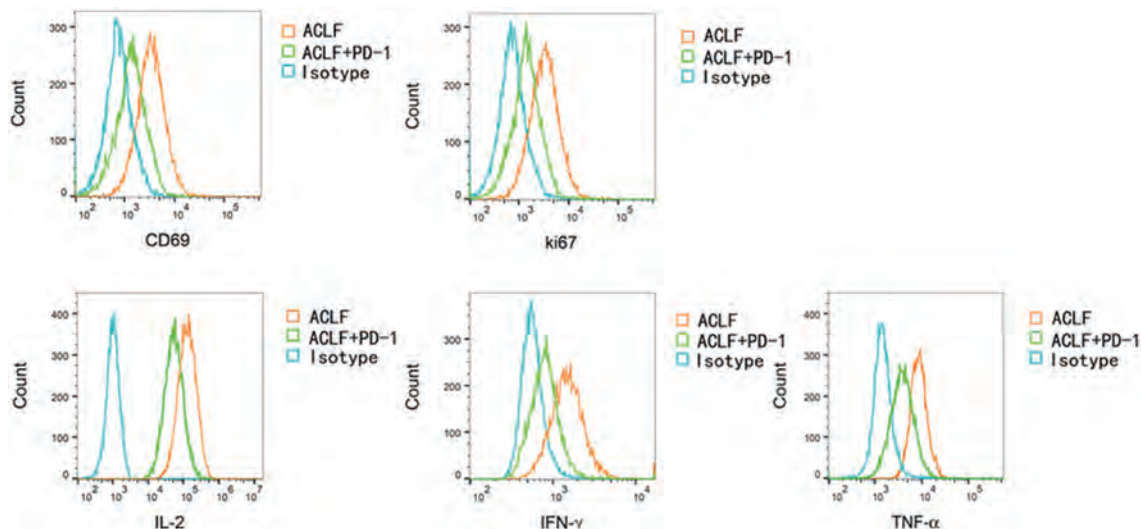


**Fig. 7.** When PD-1/PD-L1 was activated, the cell viability (CD69) (MFI: 917±43 vs. 1,723±143,  $p<0.001$ ) and proliferative ability (Ki67) (MFI: 940±71 vs. 1,737±139,  $p<0.001$ ) of CD8<sup>+</sup> T lymphocytes in patients in the ACLF+PD-1 group were lower than those in the ACLF group. The levels of IL-2 (MFI: 64,267±3,644 vs. 150,587±9,157,  $p<0.001$ ), IFN- $\gamma$  (MFI: 1,307±96 vs. 1,737±161,  $p=0.031$ ), TNF- $\alpha$  (MFI: 2,100±119 vs. 4,050±242,  $p<0.001$ ) were lower than those in the ACLF group. ACLF, acute-on-chronic liver failure; IFN- $\gamma$ , interferon-gamma; MFI, mean fluorescence intensity; PD-1, programmed cell death-1; PD-L1/2, programmed cell death 1-ligand 1/2; TNF- $\alpha$ , tumor necrosis factor-alpha.

tivation gene-3 could also be involved in CD8<sup>+</sup> T cell dysfunction,<sup>35</sup> and the related impact on energy metabolism of immune cells should be explored in ACLF. Dysfunctional T cells and T cells with activated PD-1 pathway are prone to apoptosis,<sup>36–38</sup> and whether the dysfunctional energy metabolism contributes to apoptosis in CD8<sup>+</sup> T cells in ACLF should be explored in the future.

In cancer, blocking the PD-1 axis shows benefits through the abrogation of immune tolerance toward the tumor.<sup>39</sup> In the present study, activating the PD-1 axis resulted in lower expression of IL-2, IFN- $\gamma$ , and TNF- $\alpha$ . Decreased IL-2 expression will contribute to CD8<sup>+</sup> T cell dysfunction,<sup>40</sup> and a decreased IFN- $\gamma$  and TNF- $\alpha$  production will contribute to the onset of secondary infection.<sup>41,42</sup> Whether blocking the PD-1 axis could be beneficial in patients hospitalized for ACLF remains to be examined, but the findings from the present study indirectly suggest that blocking PD-1 in such patients might have therapeutic value by restoring the activity of CD8<sup>+</sup> T cells, which could decrease the occurrence of secondary infections. This is of importance since another study showed that the expression of PD-L1 and PD-L2 in the liver of patients with ACLF is higher than in patients with chronic hepatitis B without ACLF.<sup>28</sup> A recent review summarized the theoretical basis for the use of immune checkpoint inhibitors in patients with cirrhosis and ACLF,<sup>43</sup> but this theoretical topic will still have to be examined in future trials.

This study has limitations. It only brushed on the surface of the relationship between PD-1 and glycolysis, and additional studies are necessary to determine the exact relationships between the two. In addition, molecular studies are necessary to determine the exact genes and proteins that are regulated in this process.

In summary, the findings from this study suggest that PD-1 induces CD8<sup>+</sup> T lymphocyte dysfunction in patients with HBV-ACLF, possibly by regulating the glycolytic pathway. The results of this study, thus, help clarify the role of PD-1 in the occurrence of immune suppression in ACLF, providing a new potential effective target molecule for the prevention and treatment of immune dysfunction in patients with ACLF as well as a new theoretical basis for disease prevention and treatment.

## Acknowledgments

The authors acknowledge the help of the Shanxi Province 136 Revitalization Medical Project.

## Funding

This study was funded by the National Natural Science Foundation of China (81700562), the Shanxi Outstanding Youth Fund Project (201801D211009), and the Shanxi Province Key Program Project (201903D321125), and the Shanxi Province 136 Revitalization Medical Project (General Surgery Department), International Cooperation in Key R&D Projects of Shanxi Province (No. 201903D421026).

## Conflict of interest

The authors have no conflict of interests related to this publication.

## Author contributions

Conception and design (JY), administrative support (JH),

provision of study materials or patients (YL), collection and assembly of data (NZ, TL), data analysis and interpretation (XZ), manuscript writing and final approval of the manuscript (all authors).

## Data sharing statement

No additional data are available.

## References

- [1] Arroyo V, Moreau R, Jalan R. Acute-on-chronic liver failure. *N Engl J Med* 2020;382(22):2137–2145. doi:10.1056/NEJMra1914900.
- [2] Sarin SK, Choudhury A. Acute-on-chronic liver failure: terminology, mechanisms and management. *Nat Rev Gastroenterol Hepatol* 2016;13(3):131–149. doi:10.1038/nrgastro.2015.219.
- [3] Bernsmeier C, Pop OT, Singanayagam A, Triantafyllou E, Patel VC, Weston CJ, *et al*. Patients with acute-on-chronic liver failure have increased numbers of regulatory immune cells expressing the receptor tyrosine kinase MERTK. *Gastroenterology* 2015;148(3):603–615, e614. doi:10.1053/j.gastro.2014.11.045.
- [4] Bernsmeier C, Singanayagam A, Patel VC, Wendon J, Antoniadou CG. Immunotherapy in the treatment and prevention of infection in acute-on-chronic liver failure. *Immunotherapy* 2015;7(6):641–654. doi:10.2217/imt.15.27.
- [5] Grimaldi D, Litjens JF, Pene F. Post-infectious immune suppression: a new paradigm of severe infections. *Med Mal Infect* 2014;44(10):455–463. doi:10.1016/j.medmal.2014.07.017.
- [6] Conway Morris A, Anderson N, Brittan M, Wilkinson TS, McAuley DF, Antonelli J, *et al*. Combined dysfunctions of immune cells predict nosocomial infection in critically ill patients. *Br J Anaesth* 2013;111(5):778–787. doi:10.1093/bja/aet205.
- [7] Sarin SK, Kedarisetty CK, Abbas Z, Amarapurkar D, Bihari C, Chan AC, *et al*. Acute-on-chronic liver failure: consensus recommendations of the Asian Pacific association for the study of the liver (APASL) 2014. *Hepatol Int* 2014;8(4):453–471. doi:10.1007/s12072-014-9580-2.
- [8] Wasmuth HE, Kunz D, Yagmur E, Timmer-Stranghoner A, Vidacek D, Siewert E, *et al*. Patients with acute on chronic liver failure display “sepsis-like” immune paralysis. *J Hepatol* 2005;42(2):195–201. doi:10.1016/j.jhep.2004.10.019.
- [9] Albillos A, Lario M, Alvarez-Mon M. Cirrhosis-associated immune dysfunction: distinctive features and clinical relevance. *J Hepatol* 2014;61(6):1385–1396. doi:10.1016/j.jhep.2014.08.010.
- [10] Dong X, Gong Y, Zeng H, Hao Y, Wang X, Hou J, *et al*. Imbalance between circulating CD4<sup>+</sup> regulatory T and conventional T lymphocytes in patients with HBV-related acute-on-chronic liver failure. *Liver Int* 2013;33(10):1517–1526. doi:10.1111/liv.12248.
- [11] Ye Y, Liu J, Lai Q, Zhao Q, Peng L, Xie C, *et al*. Decreases in activated CD8<sup>+</sup> T cells in patients with severe hepatitis B are related to outcomes. *Dig Dis Sci* 2015;60(1):136–145. doi:10.1007/s10620-014-3297-x.
- [12] Dirchwolf M, Podhorzer A, Marino M, Shulman C, Cartier M, Zunino M, *et al*. Immune dysfunction in cirrhosis: distinct cytokines phenotypes according to cirrhosis severity. *Cytokine* 2016;77:14–25. doi:10.1016/j.cyt.2015.10.006.
- [13] Gaber T, Strehl C, Sawitzki B, Hoff P, Buttgeriet F. Cellular energy metabolism in T-lymphocytes. *Int Rev Immunol* 2015;34(1):34–49. doi:10.3109/08830185.2014.956358.
- [14] Loftus RM, Finlay DK. Immunometabolism: cellular metabolism turns immune regulator. *J Biol Chem* 2016;291(1):1–10. doi:10.1074/jbc.R115.693903.
- [15] Pearce EL, Poffenberger MC, Chang CH, Jones RG. Fueling immunity: insights into metabolism and lymphocyte function. *Science* 2013;342(6155):1242454. doi:10.1126/science.1242454.
- [16] Macintyre AN, Gerriets VA, Nichols AG, Michalek RD, Rudolph MC, Deoliveira D, *et al*. The glucose transporter Glut1 is selectively essential for CD4 T cell activation and effector function. *Cell Metab* 2014;20(1):61–72. doi:10.1016/j.cmet.2014.05.004.
- [17] Chang CH, Pearce EL. Emerging concepts of T cell metabolism as a target of immunotherapy. *Nat Immunol* 2016;17(4):364–368. doi:10.1038/ni.3415.
- [18] Schonrich G, Raftery MJ. The PD-1/PD-L1 axis and virus infections: a delicate balance. *Front Cell Infect Microbiol* 2019;9:207. doi:10.3389/fcimb.2019.00207.
- [19] Kuol N, Stojanovska L, Nurgali K, Apostolopoulos V. PD-1/PD-L1 in disease. *Immunotherapy* 2018;10(2):149–160. doi:10.2217/imt-2017-0120.
- [20] Qorraj M, Bruns H, Bottcher M, Weigand L, Saul D, Mackensen A, *et al*. The PD-1/PD-L1 axis contributes to immune metabolic dysfunctions of monocytes in chronic lymphocytic leukemia. *Leukemia* 2017;31(2):470–478. doi:10.1038/leu.2016.214.
- [21] Michalek RD, Rathmell JC. The metabolic life and times of a T-cell. *Immunol Rev* 2010;236:190–202. doi:10.1111/j.1600-065X.2010.00911.x.
- [22] Sarin SK, Choudhury A, Sharma MK, Maiwall R, Al Mahtab M, Rahman S, *et al*. Acute-on-chronic liver failure: consensus recommendations of the Asian Pacific association for the study of the liver (APASL): an update. *Hepatol Int* 2019;13(4):353–390. doi:10.1007/s12072-019-09946-3.

- [23] Patsoukis N, Bardhan K, Chatterjee P, Sari D, Liu B, Bell LN, *et al*. PD-1 alters T-cell metabolic reprogramming by inhibiting glycolysis and promoting lipolysis and fatty acid oxidation. *Nat Commun* 2015; 6:6692. doi:10.1038/ncomms7692.
- [24] Wang X, He Q, Shen H, Xia A, Tian W, Yu W, *et al*. TOX promotes the exhaustion of antitumor CD8(+) T cells by preventing PD1 degradation in hepatocellular carcinoma. *J Hepatol* 2019; 71(4): 731–741. doi:10.1016/j.jhep.2019.05.015.
- [25] Zhang Y, Huang S, Gong D, Qin Y, Shen Q. Programmed death-1 upregulation is correlated with dysfunction of tumor-infiltrating CD8+ T lymphocytes in human non-small cell lung cancer. *Cell Mol Immunol* 2010; 7(5):389–395. doi:10.1038/cmi.2010.28.
- [26] Qin W, Hu L, Zhang X, Jiang S, Li J, Zhang Z, *et al*. The diverse function of PD-1/PD-L pathway beyond cancer. *Front Immunol* 2019; 10:2298. doi:10.3389/fimmu.2019.02298.
- [27] Zhang Z, Zhang JY, Wherry EJ, Jin B, Xu B, Zou ZS, *et al*. Dynamic programmed death 1 expression by virus-specific CD8 T cells correlates with the outcome of acute hepatitis B. *Gastroenterology* 2008; 134(7):1938–1949. doi:10.1053/j.gastro.2008.03.037.
- [28] Cao D, Xu H, Guo G, Ruan Z, Fei L, Xie Z, *et al*. Intrahepatic expression of programmed death-1 and its ligands in patients with HBV-related acute-on-chronic liver failure. *Inflammation* 2013; 36(1):110–120. doi:10.1007/s10753-012-9525-7.
- [29] Liu XY, Shi F, Zhao H, Wang HF. Research of PD-1 expression in CD8+ T cell of peripheral blood with HBV-associated acute-on-chronic liver failure. *Zhonghua Shi Yan He Lin Chuang Bing Du Xue Za Zhi* 2010; 24(2):125–127.
- [30] Cheng SC, Quintin J, Cramer RA, Shepardson KM, Saeed S, Kumar V, *et al*. mTOR- and HIF-1 $\alpha$ -mediated aerobic glycolysis as metabolic basis for trained immunity. *Science* 2014; 345(6204):1250684. doi:10.1126/science.1250684.
- [31] Palmer CS, Anzinger JJ, Zhou J, Gouillou M, Landay A, Jaworowski A, *et al*. Glucose transporter 1-expressing proinflammatory monocytes are elevated in combination antiretroviral therapy-treated and untreated HIV+ subjects. *J Immunol* 2014; 193(11):5595–5603. doi:10.4049/jimmunol.1303092.
- [32] Izquierdo E, Cuevas VD, Fernandez-Arroyo S, Riera-Borrull M, Orta-Zavalza E, Joven J, *et al*. Reshaping of human macrophage polarization through modulation of glucose catabolic pathways. *J Immunol* 2015; 195(5):2442–2451. doi:10.4049/jimmunol.1403045.
- [33] McClanahan F, Hanna B, Miller S, Clear AJ, Lichter P, Gribben JG, *et al*. PD-L1 checkpoint blockade prevents immune dysfunction and leukemia development in a mouse model of chronic lymphocytic leukemia. *Blood* 2015; 126(2):203–211. doi:10.1182/blood-2015-01-622936.
- [34] Barber DL, Wherry EJ, Masopust D, Zhu B, Allison JP, Sharpe AH, *et al*. Restoring function in exhausted CD8 T cells during chronic viral infection. *Nature* 2006; 439(7077):682–687. doi:10.1038/nature04444.
- [35] Blackburn SD, Shin H, Haining WN, Zou T, Workman CJ, Polley A, *et al*. Coregulation of CD8+ T cell exhaustion by multiple inhibitory receptors during chronic viral infection. *Nat Immunol* 2009; 10(1):29–37. doi:10.1038/ni.1679.
- [36] Dong H, Strome SE, Salomao DR, Tamura H, Hirano F, Flies DB, *et al*. Tumor-associated B7-H1 promotes T-cell apoptosis: a potential mechanism of immune evasion. *Nat Med* 2002; 8(8):793–800. doi:10.1038/nm730.
- [37] Muhlbauer M, Fleck M, Schutz C, Weiss T, Froh M, Blank C, *et al*. PD-L1 is induced in hepatocytes by viral infection and by interferon-alpha and -gamma and mediates T cell apoptosis. *J Hepatol* 2006; 45(4):520–528. doi:10.1016/j.jhep.2006.05.007.
- [38] Zhang P, Su DM, Liang M, Fu J. Chemopreventive agents induce programmed death-1-ligand 1 (PD-L1) surface expression in breast cancer cells and promote PD-L1-mediated T cell apoptosis. *Mol Immunol* 2008; 45(5):1470–1476. doi:10.1016/j.molimm.2007.08.013.
- [39] Han Y, Liu D, Li L. PD-1/PD-L1 pathway: current researches in cancer. *Am J Cancer Res* 2020; 10(3):727–742.
- [40] Carter L, Fouser LA, Jussif J, Fitz L, Deng B, Wood CR, *et al*. PD-1:PD-L inhibitory pathway affects both CD4(+) and CD8(+) T cells and is overcome by IL-2. *Eur J Immunol* 2002; 32(3):634–643. doi:10.1002/1521-4141(200203)32:3<634::AID-IMMU634>3.0.CO;2-9.
- [41] Day CL, Kaufmann DE, Kiepiela P, Brown JA, Moodley ES, Reddy S, *et al*. PD-1 expression on HIV-specific T cells is associated with T-cell exhaustion and disease progression. *Nature* 2006; 443(7109):350–354. doi:10.1038/nature05115.
- [42] Wherry EJ, Blattman JN, Murali-Krishna K, van der Most R, Ahmed R. Viral persistence alters CD8 T-cell immunodominance and tissue distribution and results in distinct stages of functional impairment. *J Virol* 2003; 77(8):4911–4927. doi:10.1128/jvi.77.8.4911-4927.2003.
- [43] Riva A, Mehta G. Regulation of monocyte-macrophage responses in cirrhosis-role of innate immune programming and checkpoint receptors. *Front Immunol* 2019; 10:167. doi:10.3389/fimmu.2019.00167.





Original Article

# Development and Validation of a Nomogram Based on Perioperative Factors to Predict Post-hepatectomy Liver Failure

Bin Xu<sup>1,2#</sup>, Xiao-Long Li<sup>1,2#</sup>, Feng Ye<sup>3#</sup>, Xiao-Dong Zhu<sup>1,2</sup>, Ying-Hao Shen<sup>1,2</sup>, Cheng Huang<sup>1,2</sup>, Jian Zhou<sup>1,2</sup>, Jia Fan<sup>1,2</sup>, Yong-Jun Chen<sup>3\*</sup> and Hui-Chuan Sun<sup>1,2\*</sup>

<sup>1</sup>Department of Liver Surgery and Transplantation, Liver Cancer Institute, Zhongshan Hospital, Fudan University, Shanghai, China; <sup>2</sup>Key Laboratory of Carcinogenesis and Cancer Invasion of Ministry of Education, Shanghai, China; <sup>3</sup>Department of Hepatobiliary Surgery, Ruijin Hospital, Shanghai Jiao Tong University School of Medicine, Shanghai, China

Received: 5 January 2021 | Revised: 11 February 2021 | Accepted: 17 February 2021 | Published: 15 March 2021

## Abstract

**Background and Aims:** Post-hepatectomy liver failure (PHLF) is a severe complication and main cause of death in patients undergoing hepatectomy. The aim of this study was to build a predictive model of PHLF in patients undergoing hepatectomy. **Methods:** We retrospectively analyzed patients undergoing hepatectomy at Zhongshan Hospital, Fudan University from July 2015 to June 2018, and randomly divided them into development and internal validation cohorts. External validation was performed in an independent cohort. Least absolute shrinkage and selection operator (commonly referred to as LASSO) logistic regression was applied to identify predictors of PHLF, and multivariate binary logistic regression analysis was performed to establish the predictive model, which was visualized with a nomogram. **Results:** A total of 492 eligible patients were analyzed. LASSO and multivariate analysis identified three preoperative variables, total bilirubin ( $p=0.001$ ), international normalized ratio ( $p<0.001$ ) and platelet count ( $p=0.004$ ), and two intraoperative variables, extent of resection ( $p=0.002$ ) and blood loss ( $p=0.004$ ), as independent predictors of PHLF. The area under receiver operating characteristic curve (referred to as AUROC) of the predictive model was 0.838 and

outperformed the model for end-stage liver disease score, albumin-bilirubin score and platelet-albumin-bilirubin score (AUROCs: 0.723, 0.695 and 0.663, respectively;  $p<0.001$  for all). The optimal cut-off value of the predictive model was 14.7. External validation showed the model could predict PHLF accurately and distinguish high-risk patients. **Conclusions:** PHLF can be accurately predicted by this model in patients undergoing hepatectomy, which may significantly contribute to the postoperative care of these patients.

**Citation of this article:** Xu B, Li XL, Ye F, Zhu XD, Shen YH, Huang C, et al. Development and validation of a nomogram based on perioperative factors to predict post-hepatectomy liver failure. J Clin Transl Hepatol 2021;9(3):291–300. doi: 10.14218/JCTH.2021.00013.

## Introduction

Hepatectomy is the main treatment for patients with benign or malignant liver lesions. However, patients undergoing liver resection are at increased risk for peri- and postoperative complications. Among these, post-hepatectomy liver failure (PHLF), defined as the impaired ability of the liver to maintain its synthetic, excretory and detoxifying functions, is one of the worst complications after hepatectomy and one of the major causes of perioperative mortality.<sup>1,2</sup> Despite improvements in operative techniques, perioperative management and understanding of liver regeneration have improved the safety of liver resection over years, PHLF remains a challenge for patients undergoing hepatectomy and a concern of hepatic surgeons.<sup>3</sup>

Various assessment tools for liver function assessment and prediction of PHLF prior to surgery have been developed to reduce the incidence of PHLF and postoperative mortality. Indocyanine green retention rate at 15 min (ICG-R15) can measure the global liver function, and has been widely adopted in Eastern centers, whereas it is rarely used in Western countries due to its expensive cost and time-consuming requirement for performance.<sup>4</sup> Clinic-biological scores like the model for end-stage liver disease (MELD) score, albumin-bilirubin (ALBI) score and platelet-albumin-bilirubin (PALBI) score are also adopted to evaluate the functional liver reserve,<sup>5–7</sup> and are reported to accurately predict PHLF following hepatectomy.<sup>8–10</sup> Volume and func-

**Keywords:** Hepatectomy; Post-hepatectomy liver failure; LASSO; Nomogram.

**Abbreviations:** ALB, albumin; ALBI, albumin-bilirubin; ALT, alanine aminotransferase; AUROC, area under receiver operating characteristic curve; CI, confidence interval; CT, computed tomography; DCA, decision curve analysis; FLR, future liver remnant; GGT,  $\gamma$ -glutamyl transpeptidase; HA, hyaluronic acid; Hb, hemoglobin; HBeAg, hepatitis B e antigen; HBsAg, hepatitis B surface antigen; HBV DNA, HBV DNA copy number; ICG-K, indocyanine green clearance rate constant; ICG-R15, indocyanine green retention rate at 15 min; INR, international normalized ratio; IQR, interquartile range; ISGLS, International Study Group of Liver Surgery; IV-col, type IV collagen; LASSO, least absolute shrinkage and selection operator; LN, laminin; LS, liver stiffness; MELD, model for end-stage liver disease; OR, odds ratio; PIIINP, procollagen III N-terminal peptide; P-ALB, pre-albumin; PALBI, platelet-albumin-bilirubin; PHLF, post-hepatectomy liver failure; PLT, platelet count; PPV, positive predictive value; ROC, receiver operating characteristics curve; TB, total bilirubin; WBC, white blood cell.

\*These authors contributed equally to this work.

**\*Correspondence to:** Hui-Chuan Sun, Liver Cancer Institute and Zhongshan Hospital, Fudan University, 180 Fenglin Road, Shanghai 200032, China. ORCID: <https://orcid.org/0000-0003-3761-7058>. Tel: +86-21-3115-1990, Fax: +86-21-6403-7181, E-mail: [sun.huichuan@zs-hospital.sh.cn](mailto:sun.huichuan@zs-hospital.sh.cn); Yong-Jun Chen, Department of Hepatobiliary Surgery and Ruijin Hospital, Shanghai Jiao Tong University School of Medicine, 197 Second Ruijin Road, Shanghai 200025, China. ORCID: <https://orcid.org/0000-0002-6486-2000>. Tel: +86-21-6431-4781, Fax: +86-21-6431-4781, E-mail: [yongjunchen@yahoo.com](mailto:yongjunchen@yahoo.com)



tion of the future liver remnant (FLR), as assessed by different imaging modalities, also have a superior ability to predict PHLF, but they could delay the time to surgery and also have financial constraints.<sup>11,12</sup>

Intraoperative events can also influence the risk of PHLF.<sup>13</sup> However, none of the models mentioned above include surgery-related factors, such as blood loss, extent of hepatectomy and intraoperative transfusions, to predict the probability of PHLF immediately after surgery.

The aim of this study was, therefore, to determine predictors of PHLF, including preoperative and intraoperative variables, and to build predictive models of PHLF in patients undergoing hepatectomy.

## Methods

### Study population

Five hundred and five consecutive patients who underwent hepatectomy at Zhongshan Hospital, Fudan University (Zhongshan cohort, from July 2015 to June 2018), and 167 consecutive patients at Ruijin Hospital, Shanghai Jiao Tong University School of Medicine (Ruijin cohort, from January 2018 to October 2019) were included in this study. Thirteen (2.6%) of the total patients in the Zhongshan cohort were excluded because of incomplete data. The remaining 492 patients in the Zhongshan cohort were randomly divided into a development cohort ( $n=344$ ) and an internal validation cohort ( $n=148$ ) using simple random sampling, with a random number seed of 2,017,0307. All patients in the Ruijin cohort were used as an external validation cohort ( $n=167$ ) (Fig. 1).

The inclusion criteria were as follows: (i) patients who received hepatectomy; (ii) patients who received contrast-enhanced computed tomography (CT) scans or magnetic resonance imaging (MRI) conducted 1 week before resection; and (iii) patients who received blood routine test, biochemical test, coagulation function test, hepatitis B serologic test, liver fibrosis test<sup>14</sup> and liver stiffness (LS)<sup>15</sup> assessed by shear wave elastography conducted within 1 week before surgery.

This study was approved by the Institutional Ethics Committee of the two hospitals and was conducted in accordance with the Declaration of Helsinki (as revised in 2013). Informed consent was obtained from all patients.

### Data collection and definition

Clinical characteristics, including 22 preoperative variables, 3 intraoperative variables and 2 clinical outcomes, were recorded (Table 1). In addition, the MELD, ALBI and PALBI scores were calculated as reported,<sup>5–7</sup> to compare with the model established in this study. No missing data were found for any patient in any of the study cohorts.

PHLF was defined as postoperative deterioration of liver function with an increase in the international normalized ratio (INR) and concomitant hyperbilirubinemia on or after postoperative day 5, as proposed by the International Study Group of Liver Surgery (commonly known as the ISGLS).<sup>1</sup>

Presence of gastroesophageal varices and splenomegaly were confirmed by CT scans or MRI report.<sup>16–22</sup> The extent of resection was defined by number of Couinaud's segments. Extent of resection  $\geq 3$  Couinaud's segments was defined as major resection, otherwise it was minor resection. The extent of resection was characterized as an intraoperative variable because the extent of resection planned preoperatively could differ from the actual extent during the surgery. Hospital stay was calculated from the date of surgery to date of discharge.

## Statistical analysis

Categorical variables were expressed as counts and percentages, and were compared using Pearson's  $\chi^2$  analysis, Fisher's exact test or Mann-Whitney  $U$  test, as appropriate. Continuous variables were expressed as mean ( $\pm$  standard deviation) or median (interquartile range [IQR]) and were compared using Student's  $t$ -test, Mann-Whitney  $U$  test or Kruskal-Wallis test, as appropriate. The  $p$ -values were adjusted by Holm's method for multiple comparisons.

The least absolute shrinkage and selection operator (LASSO) logistic regression model with 10-fold cross-validation was performed to select perioperative variables associated with PHLF. As the group of variables selected by LASSO is not completely consistent every time due to randomness of cross-validation,<sup>23</sup> we repeated the same LASSO algorithm with the same candidate variables 1,000 times, and the most frequent group of selected variables was accepted as significant variables.

A multivariate binary logistic regression model was then produced to identify significant independent predictors of PHLF, with a removal significance level of 0.05. No evidence of non-log-linear relationship was found for all continuous variables. All significant variables were reserved in the final model because multicollinearity was not found.

Predictive performance was assessed using the receiver operating characteristic (ROC) curve and compared by DeLong's test. The optimal cut-off value of the logistic model was determined using ROC by maximizing the Youden index (sensitivity plus specificity minus 1). Calibration curves were plotted to assess the calibration of the model. Decision curve analysis (DCA) was conducted to determine the clinical utility of the model.<sup>24</sup> A nomogram was established based on the predictive model for the development cohort.

Statistical testing was carried out at the 2-sided tailed  $\alpha$  level of 0.05. Data were analyzed using R version 3.6.2 (Vienna, Austria). Variable selection with LASSO was performed by the *cv.glmnet* function in the *glmnet* package. Binary logistic regression modeling was performed by the *glm* function. The nomogram was plotted by the *nomogram* function in the *rms* package. Delong's test was produced by the *roc.test* function in the *pROC* package. Calibration curves and DCA were analyzed by the *calibrate* function in the *rms* package and the *decision\_curve* function in the *rmda* package, respectively.

## Results

### Clinical characteristics

The clinical characteristics of patients in the Zhongshan cohort are listed in Table 1. The comparison of clinical characteristics between the Zhongshan cohort and the Ruijin cohort is shown in Supplementary Table 1. The clinical characteristics were similar between the development and internal validation cohorts.

In the Zhongshan cohort, hospital stay of patients without PHLF (median [IQR]: 8 [7–10] days) was shorter than that of grade A (10 [8–13] days), grade B (10 [8–13] days) and grade C (16.5 [10–29] days) PHLF patients ( $p<0.001$  for all).

### Establishment of the predictive model in the development cohort

All variables listed in Table 1 were analyzed. The result of variable selection by LASSO is shown in Supplementary Ta-

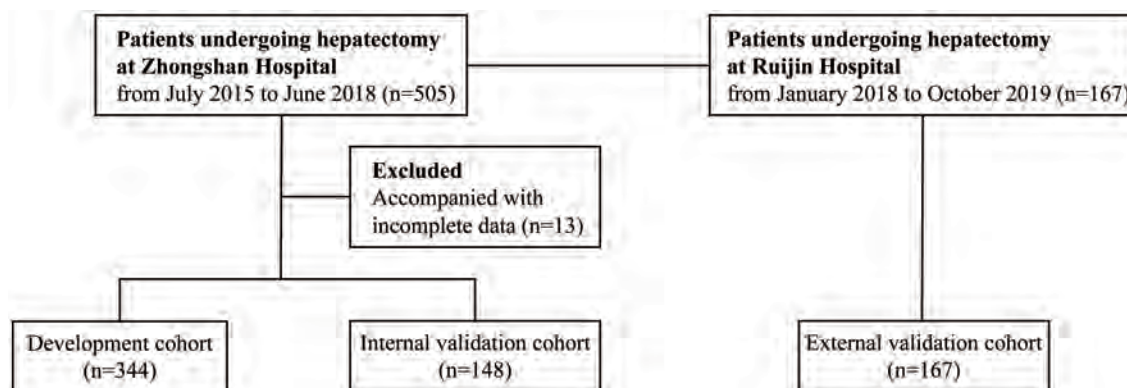


Fig. 1. Flowchart of this study's design.

ble 2, which identified type IV collagen, total bilirubin (referred to as TB), albumin (ALB), INR, platelet count, extent of resection and blood loss as the most significantly related factors to PHLF.

The result of multivariate logistic regression analysis is shown in Table 2. These independent predictors were used to establish a predictive model, which was designated as the PHLF score, and visualized with a nomogram (Fig. 2).

#### **Predictive accuracy and calibration of the PHLF score compared to other scores in the development cohort**

The area under the ROC curve (AUROC) [95% confidence interval (CI)] of the PHLF score was 0.838 (0.790–0.885), which has better accuracy in predicting PHLF than the other three scores ( $p<0.001$  for all, compared by Delong's test): MELD score, 0.723 (0.664–0.782); ALBI score, 0.695 (0.630–0.758) and PALBI score, 0.663 (0.600–0.726), respectively (Fig. 3A). Calibration curves showed good agreement between prediction and observation (Fig. 4A). DCA revealed that the PHLF score provided superior net benefit over the other three scores (Fig. 3D).

#### **Risk stratification based on the PHLF score in the development cohort**

The optimal cut-off value of the PHLF score was determined to be 14.7 using ROC by maximizing the Youden index. The sensitivity, specificity, positive predictive value (referred to as PPV) and negative predictive value in predicting PHLF were 76.9%, 78.3%, 56.0%, and 90.4%, respectively.

Patients with PHLF score  $\geq 14.7$  were defined as the high-risk group, otherwise the patients were classified as the low-risk group. The incidence (55.6% vs. 9.6%,  $p<0.001$ ) and severity ( $p<0.001$ ) of PHLF were significantly different between the two groups (Table 3 and Fig. 5A).

#### **Validation of the PHLF score in two independent cohorts**

In the internal validation cohort, the AUROC of the PHLF score was 0.788 (0.693–0.884), which outperformed the other three scores in predicting PHLF (compared by Delong's test): MELD score ( $p=0.006$ ), ALBI score ( $p=0.010$ ) and PALBI score ( $p=0.002$ ), respectively (Fig. 3B). PHLF score showed good agreement between prediction and observation in calibration curve (Fig. 4B) and provided supe-

rior net benefit over other scores in the DCA curve (Fig. 3E). The incidence (42.6% vs. 12.9%,  $p<0.001$ ) and severity ( $p<0.001$ ) of PHLF were significantly different between high-risk and low-risk groups (Table 3 and Fig. 5B).

In the external validation cohort, the AUROC of the PHLF score was 0.750 (0.632–0.868), which was marginally superior to other three scores in predicting PHLF (compared by Delong's test): MELD score ( $p=0.103$ ), ALBI score ( $p=0.535$ ) and PALBI score ( $p=0.100$ ), respectively (Fig. 3C). PHLF score also provided superior net benefit over other scores in DCA analysis (Fig. 3F). The incidence (16.9% vs. 5.2%,  $p=0.013$ ) and severity ( $p=0.015$ ) of PHLF were also significantly different between the high-risk and low-risk groups (Table 3 and Fig. 5C).

## **Discussion**

In this study, PHLF in patients undergoing hepatectomy could be accurately predicted immediately after surgery using routinely available variables, including three preoperative (TB, INR and platelet count) and two intraoperative (extent of resection and blood loss) factors. In addition, patients could be properly stratified in terms of the risk of PHLF, with a cut-off value of 14.7.

This study suggested that hepatic surgeons can take the optimized measures to prevent or manage PHLF perioperatively. On the basis that patients reserve good liver function, surgeons can calculate the maximum of intraoperative blood loss they can tolerate to prevent PHLF, because the extent of resection can be estimated by preoperative imaging data, and blood loss was the only unknown variable. This could remind surgeons to be more careful during surgery to reduce blood loss in order to prevent PHLF. Furthermore, surgeons could better inform patients and their families of the risk of PHLF after surgery. When the risk of PHLF is highly predicted, surgeons may suggest patients take medications to improve liver function and/or take systemic therapy to shrink the tumor as the best choice at that time, rather than surgery. Then, when the liver function or the tumor regression reaches a certain extent, surgery can be performed. If patients insist on performance of the surgery, surgeons can determine the appropriate level of postoperative care and extend the length of hospital stay, in addition performing a more careful operation.

The aim of this study was to establish a model to predict PHLF in patients undergoing hepatectomy. Many useful criteria and scores were demonstrated to predict the incidence of PHLF. One of the most classic models was "Makuuchi's criteria", representing a decision tree for selection of operative procedures in patients with impaired liver function

**Table 1. Comparison of clinical characteristics between development and internal validation cohorts**

Variables	Development cohort, <i>n</i> =344	Internal validation cohort, <i>n</i> =148	<i>p</i> -value
Age in years	56.4±11.2	57.0±10.9	0.625
Sex			0.714
Male	298 (86.6%)	130 (87.8%)	
Female	46 (13.4%)	18 (12.2%)	
Diabetes			0.878
No	291 (84.6%)	126 (85.1%)	
Yes	53 (15.4%)	22 (14.9%)	
HBsAg			0.078
–	56 (16.3%)	34 (23.0%)	
+	288 (83.7%)	114 (77.0%)	
HBeAg			0.763
–	282 (82.0%)	123 (83.1%)	
+	62 (18.0%)	25 (16.9%)	
HBV DNA			0.275
≤10 <sup>3</sup> /mL	198 (57.6%)	93 (62.8%)	
>10 <sup>3</sup> /mL	146 (42.4%)	55 (37.2%)	
Hb in g/L	143.0 (127.0–153.0)	142.0 (133.0–150.3)	0.948
WBC as ×10 <sup>9</sup> /L	5.3 (4.2–6.5)	5.3 (4.5–6.3)	0.587
PLT as ×10 <sup>9</sup> /L	148.0 (106.0–207.0)	162.5 (114–195.3)	0.400
TB in μmol/L	11.9 (8.8–15.9)	11.7 (9.2–16.5)	0.886
ALB in g/L	42.0 (39.0–45.0)	42.0 (39.0–45.0)	0.708
P-ALB in g/L	0.22 (0.17–0.26)	0.22 (0.18–0.26)	0.590
ALT in U/L	29.0 (20.0–43.0)	29.0 (20.8–42.3)	0.717
GGT in U/L	56.5 (33.0–108.0)	63.0 (34.8–115.5)	0.734
INR	1.01 (0.96–1.07)	1.03 (0.97–0.106)	0.345
HA in ng/mL	87.3 (64.2–135.2)	85.5 (60.0–135.4)	0.486
LN in ng/mL	50.0 (50.0–67.0)	50.0 (50.0–64.8)	0.536
PIIINP in ng/mL	6.5 (5.3–8.4)	6.7 (5.4–8.4)	0.829
IV-col in ng/mL	51.8 (50.0–83.9)	54.6 (50.0–79.6)	0.807
LS in kPa	12.0 (9.2–15.2)	11.4 (8.5–15.0)	0.240
Gastroesophageal varices			0.634
No	309 (89.8%)	135 (91.2%)	
Yes	35 (10.2%)	13 (8.8%)	
Splenomegaly			0.285
No	90 (26.2%)	32 (21.6%)	
Yes	254 (73.8%)	116 (78.4%)	
Extent of resection			0.395
Minor, <3 Couinaud's segments	250 (72.7%)	113 (76.4%)	
Major, ≥3 Couinaud's segments	94 (27.3%)	35 (23.6%)	
Hilar occlusion in min	15.0 (0.0–18.0)	14.5 (0.0–18.3)	0.740
Intraoperative blood loss in mL	200.0 (100.0–300.0)	200.0 (100.0–300.0)	0.816
Causes of hepatectomy			1
Malignant tumor	343 (99.7%)	148 (100%)	

(continued)

**Table 1.** (continued)

Variables	Development cohort, n=344	Internal validation cohort, n=148	p-value
Benign tumor	1 (0.3%)	0 (0%)	
<i>Clinical outcomes</i>			
PHLF <sup>†</sup>			0.330
No	253 (73.5%)	115 (77.7%)	
Yes	91 (26.5%)	33 (22.3%)	
PHLF grade <sup>‡</sup>			0.300
0	253 (73.5%)	115 (77.7%)	
A	63 (18.3%)	24 (16.2%)	
B	19 (5.5%)	8 (5.4%)	
C	9 (2.6%)	1 (0.7%)	
Hospital stay as median (IQR) in days	8 (7–11)	8.5 (7–11)	0.863

<sup>†</sup>PHLF was defined as postoperative deterioration of liver function with an increase in the INR and concomitant hyperbilirubinemia on or after postoperative day 5, as proposed by the ISGLS. <sup>‡</sup>Following the ISGLS definition of PHLF grade. ALT, alanine aminotransferase; Hb, hemoglobin; HBeAg, hepatitis B e antigen; HBsAg, hepatitis B surface antigen; HBV DNA, hepatitis B virus DNA; HA, hyaluronic acid; IV-col, type IV collagen; LN, laminin; LS, liver stiffness; P-ALB, pre-albumin; PIIINP, procollagen III N-terminal peptide; PLT, platelet count; WBC, white blood cell; GGT, γ-glutamyl transpeptidase.

**Table 2.** Independent predictors of PHLF after multivariate logistic analysis

Variables	β	OR	95% CI	p-value
Intercept	−15.585			
TB in μmol/L	0.074	1.077	1.029–1.128	0.001
INR <sup>†</sup> , per 0.1 increase	1.332	3.788	2.531–5.867	<0.001
PLT, per 10 <sup>9</sup> /L increase	−0.007	0.993	0.989–0.998	0.004
Extent of resection				
Minor, <3 segments		1		
Major, ≥3 segments	1.059	2.883	1.471–5.716	0.002
Blood loss <sup>‡</sup> , per 100 mL increase	0.132	1.141	1.043–1.251	0.004

<sup>†</sup>INR was multiplied by 10 and put into the multivariate binary logistic regression model. <sup>‡</sup>Blood loss was divided by 100 and put into the multivariate binary logistic regression model. The score and predicted probability of PHLF can be calculated using the following formulas: PHLF score:  $0.074 \times \text{TB} + 1.332 \times \text{INR (multiplied by 10)} - 0.007 \times \text{PLT (per } 10^9/\text{L)} + 1.059 \times \text{extent of resection (major=1; minor=0)} + 0.132 \times \text{blood loss (divided by 100)}$ . The predicted probability of PHLF =  $1/(1 + \exp(-\text{PHLF score} + 15.585))$ . CI, confidence interval; OR, odds ratio.

reserve, which included three determining factors: ascites, serum TB value, and ICG-R15.<sup>25</sup> Imamura *et al.*<sup>26</sup> reported

zero-mortality after hepatectomy and only one patient developed PHLF from among nine hundred and fifteen con-

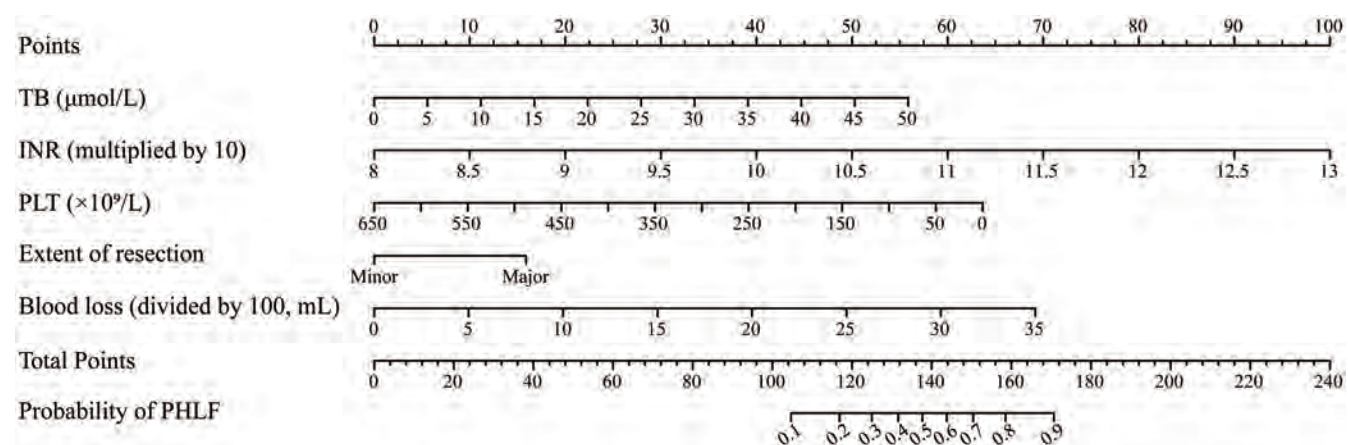


**Fig. 2.** Nomogram for the prediction of PHLF. The nomogram was established based on the development cohort. PHLF, post-hepatectomy liver failure.



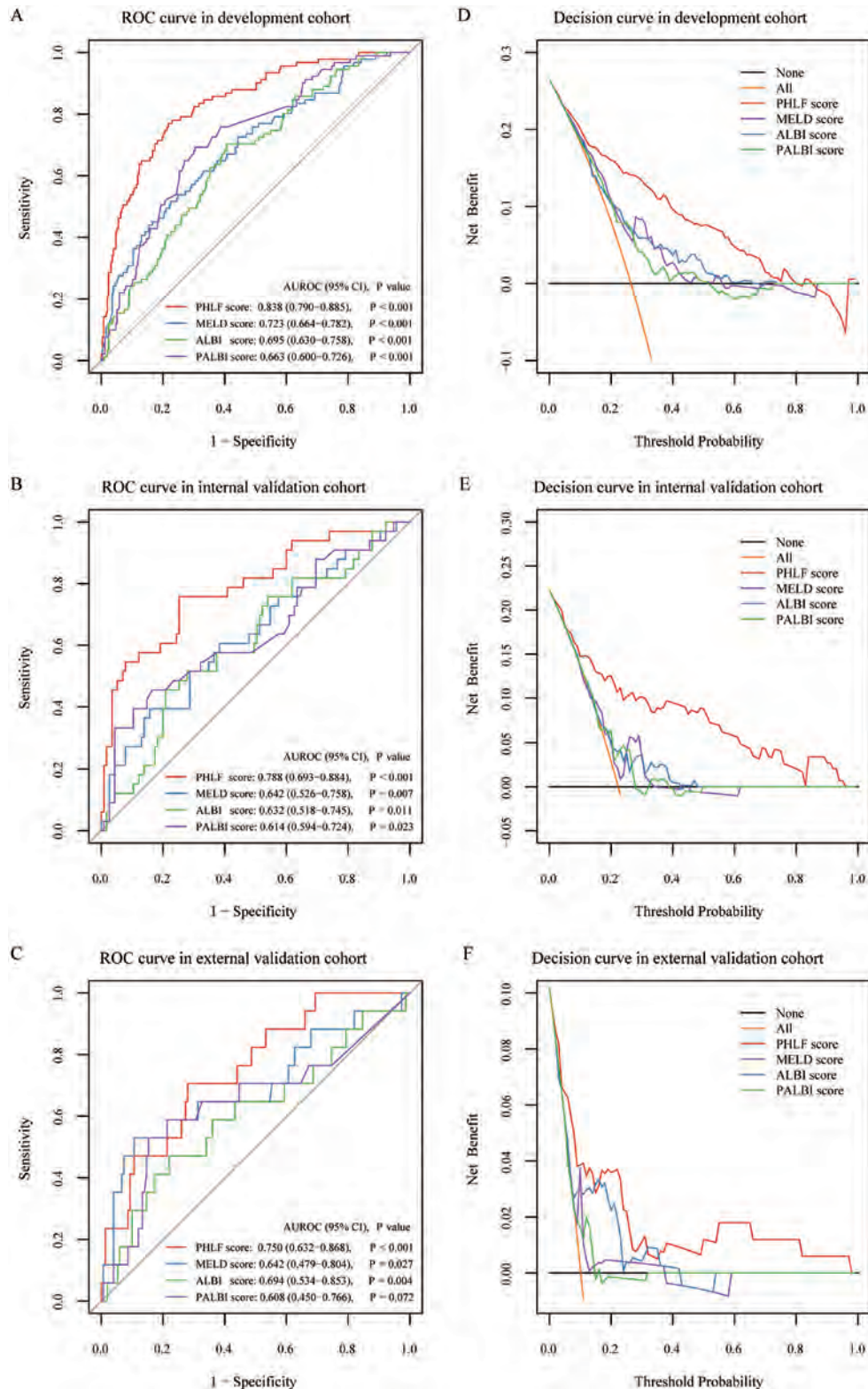


**Fig. 3. ROC curves and decision curves for the prediction of PHLF.** ROC curves of PHLF score, MELD score, ALBI score and PALBI score in the (A) development cohort, (B) internal validation cohort and (C) external validation cohort. Decision curves of PHLF score, MELD score, ALBI score and PALBI score in the (D) development cohort, (E) internal validation cohort and (F) external validation cohort. The orange line indicates the net benefit of assuming that all patients have PHLF. The black line indicates the net benefit of assuming no patients have PHLF. ALBI, albumin-bilirubin; MELD, model for end-stage liver disease; PALBI, platelet-albumin-bilirubin; PHLF, post-hepatectomy liver failure; ROC, receiver operating characteristics curve.



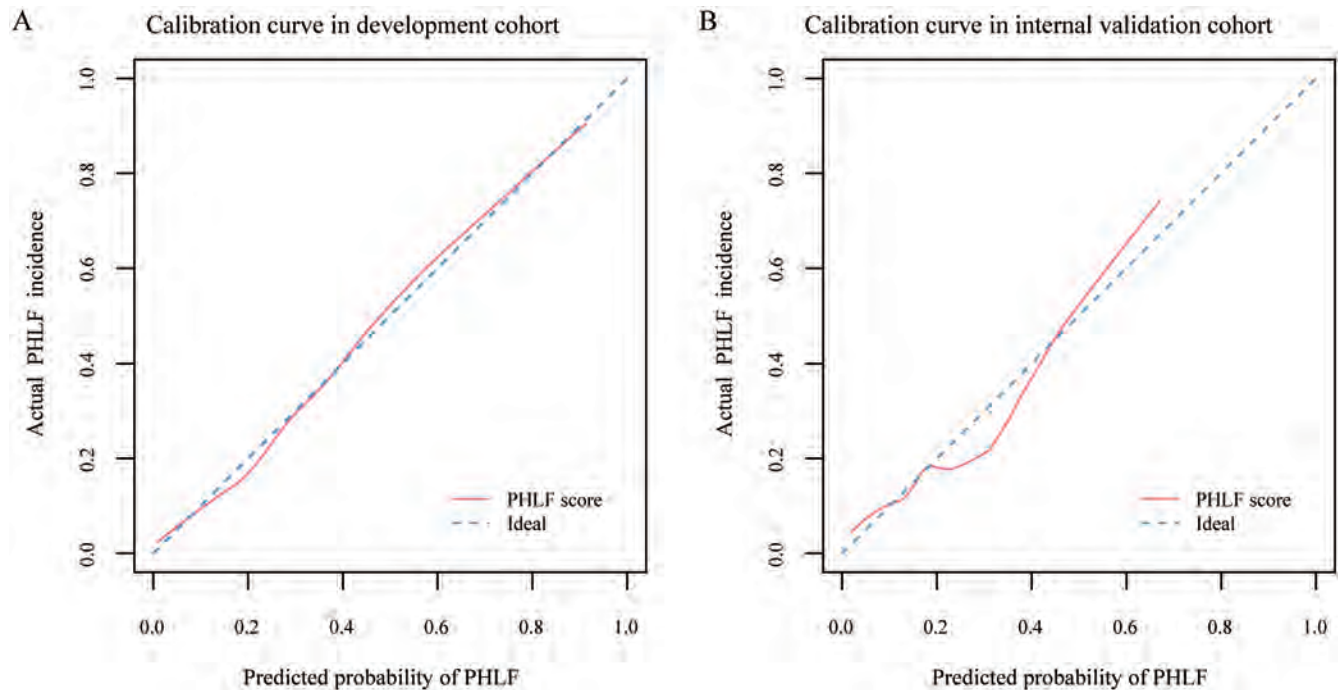


**Fig. 4. Calibration curves for the prediction of PHLF.** Calibration curves of the PHLF score in (A) development cohort and (B) internal validation cohort. The diagonal blue dashed line represents a perfect prediction by an ideal model. The pink solid line represents the performance of the predictive model, of which a closer fit to the diagonal blue dashed line represents a better prediction. PHLF, post-hepatectomy liver failure.

secutive patients within the criteria. However, within each category of Makuuchi's criteria, there is a relatively wide range of hepatic function reserve and it does not take into account the individual variation in the FLR volume.<sup>27</sup>

MELD,<sup>8</sup> ALBI<sup>10,28</sup> and PALBI<sup>29</sup> scores were previously reported to be accurate for the prediction of PHLF in patients with hepatocellular carcinoma. However, the ALBI score and PALBI score were based on a relatively low proportion of 727 (28.0%) patients undergoing hepatectomy.<sup>6,7</sup> A study showed neither ALBI nor PALBI could predict survival of patients following transjugular intrahepatic portosystemic shunt creation,<sup>30</sup> which may suggest that they were not the

most suitable to predict PHLF for patients undergoing surgery. All patients in the current study underwent hepatectomy and their indications of surgery did not only include hepatocellular carcinoma, but all had reasoned hepatectomy. Our model may be more suitable for this target population and perform better in such.

Furthermore, ALB, which was included in both the ALBI and PALBI scores, was not included in our model. ALBI and PALBI scores were determined patients with data of ALB level, reported as median (IQR) of 35 (31–39) g/L, but the ALB level of patients in this study was 42 (39–45) g/L. Hence, the ability of ALB to predict PHLF was not as impor-

**Table 3. Incidences of PHLF of high-risk and low-risk groups with a cut-off value of 14.7 by the PHLF score in development and two validation cohorts**

Development cohort, <i>n</i> =344			Internal validation co- hort, <i>n</i> =148			External validation cohort, <i>n</i> =167			
	High-risk group, <i>n</i> =126	Low-risk group, <i>n</i> =218	<i>p</i> - value	High-risk group, <i>n</i> =47	Low-risk group, <i>n</i> =101	<i>p</i> - value	High-risk group, <i>n</i> =71	Low-risk group, <i>n</i> =96	<i>p</i> -value
PHLF†			<0.001			<0.001			0.013
No	56 (44.4%)	197 (90.4%)		27 (57.4%)	88 (87.1%)		59 (83.1%)	91 (94.8%)	
Yes	70 (55.6%)	21 (9.6%)		20 (42.6%)	13 (12.9%)		12 (16.9%)	5 (5.2%)	
PHLF grade†			<0.001			<0.001			0.015
0	56 (44.4%)	197 (90.4%)		27 (57.4%)	88 (87.1%)		59 (83.1%)	91 (94.8%)	
A	48 (38.1%)	15 (6.9%)		12 (25.5%)	12 (11.9%)		9 (12.7%)	3 (3.1%)	
B	15 (11.9%)	4 (1.8%)		7 (14.9%)	1 (1.0%)		1 (1.4%)	2 (2.1%)	
C	7 (5.6%)	2 (0.9%)		1 (2.1%)	0 (0%)		2 (2.8%)	0 (0%)	

<sup>†</sup>PHLF was defined as postoperative deterioration of liver function with an increase in the INR and concomitant hyperbilirubinemia on or after postoperative day 5 as proposed by the ISGLS. <sup>‡</sup>Following the ISGLS definition of PHLF grade.

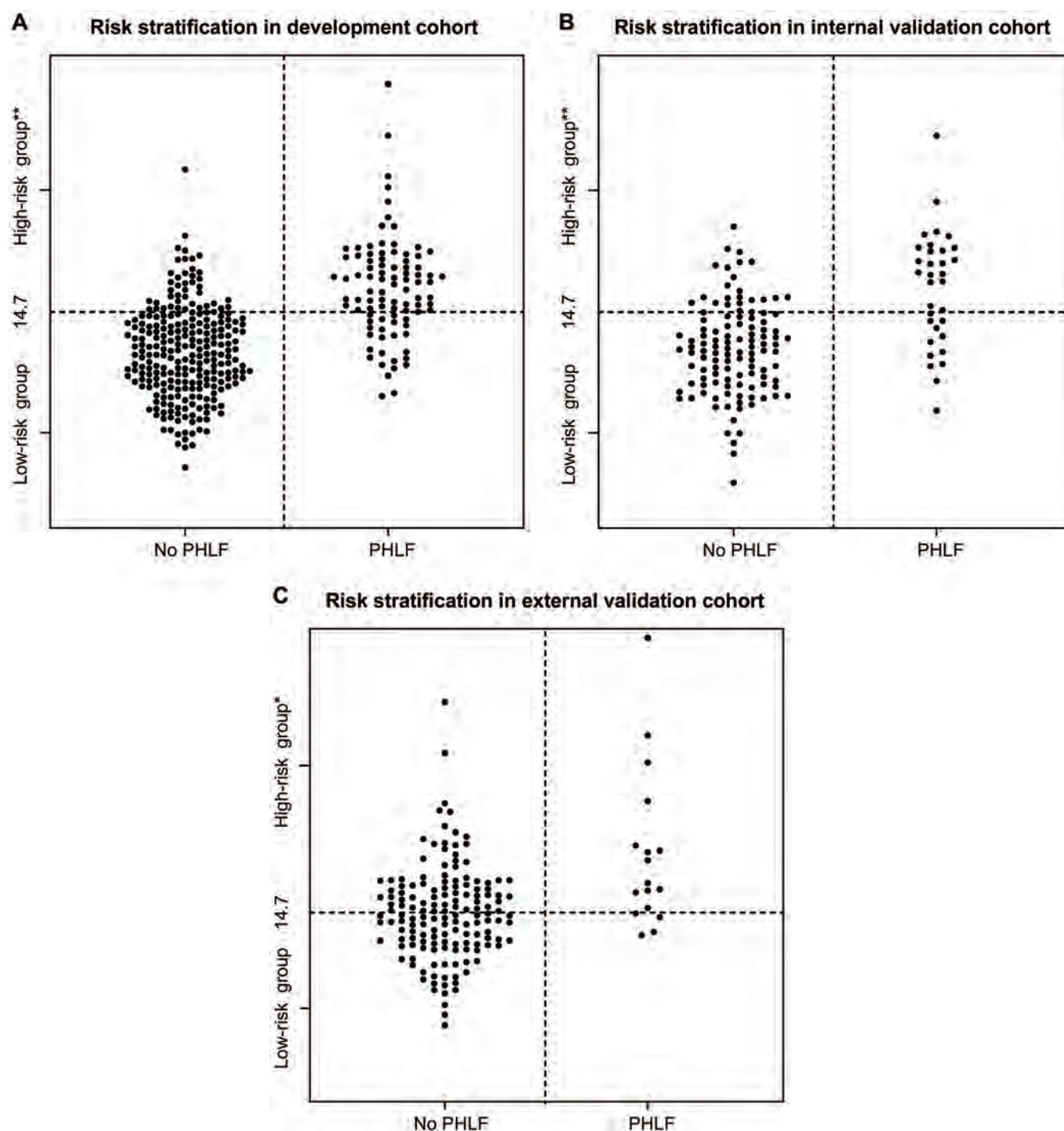


**Fig. 5.** Relationship between the value of the PHLF score and occurrence of PHLF in (A) development cohort, (B) internal validation cohort and (C) external validation cohort. The horizontal dotted line indicates the cut-off value of the PHLF score (14.7) for the prediction of PHLF. Patients with PHLF score  $\geq 14.7$  belong to the high-risk group, otherwise patients were classified in the low-risk group. \* $p < 0.05$ , \*\* $p < 0.001$ , in comparison with the low-risk group. PHLF, post-hepatectomy liver failure.

tant as in patients with advanced diseases.

The indocyanine green clearance rate constant (referred to as ICG-K) and ICG-R15 have been widely adopted in Eastern centers to measure liver function, but neither of them is a routine test in our center. Hwang *et al.*<sup>31</sup> established a quantified model combined with ICG-K and FLR to predict PHLF,

which was similar to our model, both containing factors representing liver function and resected liver volume. However, surgery-related factors were not included in the model by Hwang *et al.*<sup>31</sup> and in none of the models mentioned above. As PHLF could be influenced by surgery-related factors like blood loss, extent of hepatectomy,<sup>13,32</sup> our model with intra-

operative variables could predict PHLF more accurately.

This study included almost all indicators of laboratory tests, important clinical signs available before surgery, and three intraoperative factors. To develop a predictive model based on as many as 25 candidate variables, we employed LASSO, which has been developed to overcome the limitations when too many predictors are needing to be analyzed, to guarantee the objectivity of variables included in the model.<sup>33</sup> In addition, DCA was performed to compare the clinical utility of different models, visualizing the clinical consequences of a diagnostic strategy.<sup>34</sup> Traditional metrics of diagnostic performance, such as AUROC, sensitivity and specificity only measure the accuracy of one prediction model against another, but fail to consider whether patients will really benefit from a specific model with the high predictive accuracy.<sup>24</sup>

In addition, the PHLF score was validated externally and demonstrated satisfactory predictive accuracy and clinical utility. Furthermore, PHLF score can also stratify patients undergoing hepatectomy in terms of risk of PHLF in the external validation cohort.

The relatively low PPV indicates that patients who were actually at high risk of PHLF were not assigned to the high-risk group, and some factors that caused high risk of PHLF, such as repeated resection and tumor-related factors, were not included. Patients who underwent repeated resection were at higher risk of developing PHLF. In addition, this study enrolled patients either with benign or malignant lesions, so that tumor-related factors such as tumor number, size and biomarker were not included in the analysis.

This study has several limitations. First, we retrospectively investigated a group of patients with a relatively low proportion of grade B or C PHLF. Grade A PHLF represents a transient deterioration in liver function that does not require extra treatment. However, the hospital stay of grade A PHLF patients was longer than those without PHLF, indicating that this model is of clinical significance. Second, the predictive model cannot access the severity of PHLF and make a classification according to the ISGLS grade, where different grades of PHLF are subject to different treatments. Third, the extent of resection was defined as minor (<3 segments) or major (≥3 segments) in this study, which could not exactly reflect the FLR volume. Because the volume of segment II+III (left lateral section) is significantly smaller than that of segment VII+VIII (right lateral section), and the latter may exceed the volume of segment II+III+IV (left liver).<sup>35</sup> In addition, inadequate FLR volume can lead to PHLF.<sup>36</sup> The performance of the predictive model could be improved through measuring FLR volume and FLR function by three-dimensional CT reconstruction or other image fusion techniques preoperatively.<sup>12,37</sup>

In conclusion, this study showed that PHLF after hepatectomy can be accurately predicted by five simple and readily available perioperative variables, which may significantly contribute to the postoperative care of those patients and improving clinical outcomes.

## Funding

This work was supported by the Leading Investigator Program of the Shanghai municipal government (17XD1401100), the National Key Basic Research Program (973 Program; 2015CB554005) from the Ministry of Science and Technology of China, and the National Natural Science Foundation of China (81672326 and 81871928, and 81871929).

## Conflict of interest

The authors have no conflict of interests related to this publication.

## Author contributions

Study concept and design (BX, XLL, FY, YJC and HCS), acquisition of data (BX, XLL, FY, XDZ, CH and YHS), analysis of data (BX, XLL and FY), interpretation of data (BX, XLL, FY, XDZ, CH, YHS, YJC and HCS), drafting of the manuscript (BX, XLL and FY), critical revision of the manuscript for important intellectual content (YJC and HCS), administrative, technical, or material support, study supervision (JZ and JF).

## Data sharing statement

The data collected for this study will not be shared because the Institutional Ethics Committee of the two hospitals required that data involved in this study should be kept confidential. Other documents such as statistical analysis plan and informed consent form will be shared.

## References

- [1] Rahbari NN, Garden OJ, Padbury R, Brooke-Smith M, Crawford M, Adam R, *et al*. Posthepatectomy liver failure: a definition and grading by the International Study Group of Liver Surgery (ISGLS). *Surgery* 2011;149(5):713–724. doi:10.1016/j.surg.2010.10.001.
- [2] Citterio D, Facciorusso A, Sposito C, Rota R, Bhoori S, Mazzaferro V. Hierarchical interaction of factors associated with liver decompensation after resection for hepatocellular carcinoma. *JAMA Surg* 2016;151(9):846–853. doi:10.1001/jamasurg.2016.1121.
- [3] Schreckenbach T, Liese J, Bechstein WO, Moench C. Posthepatectomy liver failure. *Dig Surg* 2012;29(1):79–85. doi:10.1159/000335741.
- [4] Cescon M, Colecchia A, Cucchetti A, Peri E, Montrone L, Ercolani G, *et al*. Value of transient elastography measured with FibroScan in predicting the outcome of hepatic resection for hepatocellular carcinoma. *Ann Surg* 2012;256(5):706–712; discussion 712–713. doi:10.1097/SLA.0b013e3182724ce8.
- [5] Kamath PS, Kim WR, Advanced Liver Disease Study Group. The model for end-stage liver disease (MELD). *Hepatology* 2007;45(3):797–805. doi:10.1002/hep.21563.
- [6] Johnson PJ, Berhane S, Kagebayashi C, Satomura S, Teng M, Reeves HL, *et al*. Assessment of liver function in patients with hepatocellular carcinoma: a new evidence-based approach—the ALBI grade. *J Clin Oncol* 2015;33(6):550–558. doi:10.1200/JCO.2014.57.9151.
- [7] Roayaie S, Jibara G, Berhane S, Tabrizian P, Park J-W, Yang J, *et al*. PALBI: an objective score based on platelets, albumin & bilirubin stratifies HCC patients undergoing resection & ablation better than child's classification. *Hepatology* 2015;62(1, SI):631A–632A.
- [8] Kong FH, Miao XY, Zou H, Xiong L, Wen Y, Chen B, *et al*. End-stage liver disease score and future liver remnant volume predict post-hepatectomy liver failure in hepatocellular carcinoma. *World J Clin Cases* 2019;7(22):3734–3741. doi:10.12998/wjcc.v7.i22.3734.
- [9] Andreatos N, Amini N, Gani F, Margonis GA, Sasaki K, Thompson VM, *et al*. Albumin-bilirubin score: predicting short-term outcomes including bile leak and post-hepatectomy liver failure following hepatic resection. *J Gastrointest Surg* 2017;21(2):238–248. doi:10.1007/s11605-016-3246-4.
- [10] Zhang ZQ, Xiong L, Zhou JJ, Miao XY, Li QL, Wen Y, *et al*. Ability of the ALBI grade to predict posthepatectomy liver failure and long-term survival after liver resection for different BCLC stages of HCC. *World J Surg Oncol* 2018;16(1):208. doi:10.1186/s12957-018-1500-9.
- [11] Araki K, Harimoto N, Kubo N, Watanabe A, Igarashi T, Tsukagoshi M, *et al*. Functional remnant liver volumetry using Gd-EOB-DTPA-enhanced magnetic resonance imaging (MRI) predicts post-hepatectomy liver failure in resection of more than one segment. *HPB (Oxford)* 2020;22(2):318–327. doi:10.1016/j.hpb.2019.08.002.
- [12] Li C, Zhu A. Application of image fusion in diagnosis and treatment of liver cancer. *Applied Sciences* 2020;10(3):1171–1171. doi:10.3390/app10031171.
- [13] Kauffmann R, Fong Y. Post-hepatectomy liver failure. *Hepatobiliary Surg Nutr* 2014;3(5):238–246. doi:10.3978/j.issn.2304-3881.2014.09.01.
- [14] Shen Y, Shi G, Huang C, Zhu X, Chen S, Sun H, *et al*. Prediction of post-operative liver dysfunction by serum markers of liver fibrosis in hepatocellular carcinoma. *PLoS One* 2015;10(10):e0140932. doi:10.1371/journal.pone.0140932.
- [15] Shen Y, Zhou C, Zhu G, Shi G, Zhu X, Huang C, *et al*. Liver stiffness assessed by shear wave elastography predicts postoperative liver failure in patients with hepatocellular carcinoma. *J Gastrointest Surg* 2017;21(9):1471–1479. doi:10.1007/s11605-017-3443-9.
- [16] Perri RE, Chiorean MV, Fidler JL, Fletcher JG, Talwalkar JA, Stadheim L, *et al*. A prospective evaluation of computerized tomographic (CT) scanning as a screening modality for esophageal varices. *Hepatology* 2008;47(5):1587–1594. doi:10.1002/hep.22219.
- [17] Kim SH, Kim YJ, Lee JM, Choi KD, Chung YJ, Han JK, *et al*. Esophageal


- varices in patients with cirrhosis: multidetector CT esophagography-comparison with endoscopy. *Radiology* 2007;242(3):759–768. doi:10.1148/radiol.2423050784.
- [18] Lipp MJ, Broder A, Hudesman D, Suwandhi P, Okon SA, Horowitz M, *et al*. Detection of esophageal varices using CT and MRI. *Dig Dis Sci* 2011;56(9):2696–2700. doi:10.1007/s10620-011-1660-8.
- [19] Shin SU, Lee JM, Yu MH, Yoon JH, Han JK, Choi BI, *et al*. Prediction of esophageal varices in patients with cirrhosis: usefulness of three-dimensional MR elastography with echo-planar imaging technique. *Radiology* 2014;272(1):143–153. doi:10.1148/radiol.14130916.
- [20] Ronot M, Lambert S, Elkrief L, Doblas S, Rautou PE, Castera L, *et al*. Assessment of portal hypertension and high-risk oesophageal varices with liver and spleen three-dimensional multifrequency MR elastography in liver cirrhosis. *Eur Radiol* 2014;24(6):1394–1402. doi:10.1007/s00330-014-3124-y.
- [21] Bezerra AS, D'Ippolito G, Faintuch S, Szejnfeld J, Ahmed M. Determination of splenomegaly by CT: is there a place for a single measurement? *AJR Am J Roentgenol* 2005;184(5):1510–1513. doi:10.2214/ajr.184.5.01841510.
- [22] Gunes SO, Akturk Y. Determination of splenomegaly by coronal oblique length on CT. *Jpn J Radiol* 2018;36(2):142–150. doi:10.1007/s11604-017-0704-1.
- [23] Homrighausen D, McDonald DJ. Risk consistency of cross-validation with lasso-type procedures. *Statistica Sinica* 2018;27(3):1017–1036. doi:10.5705/ss.202015.0355.
- [24] Fitzgerald M, Saville BR, Lewis RJ. Decision curve analysis. *JAMA* 2015;313(4):409–410. doi:10.1001/jama.2015.37.
- [25] Makuuchi M, Kosuge T, Takayama T, Yamazaki S, Kakazu T, Miyagawa S, *et al*. Surgery for small liver cancers. *Semin Surg Oncol* 1993;9(4):298–304. doi:10.1002/ssu.2980090404.
- [26] Imamura H, Seyama Y, Kokudo N, Maema A, Sugawara Y, Sano K, *et al*. One thousand fifty-six hepatectomies without mortality in 8 years. *Arch Surg* 2003;138(11):1198–1206; discussion 1206. doi:10.1001/archsurg.138.11.1198.
- [27] Kobayashi Y, Kiya Y, Sugawara T, Nishioka Y, Hashimoto M, Shindoh J. Expanded Makuuchi's criteria using estimated indocyanine green clearance rate of future liver remnant as a safety limit for maximum extent of liver resection. *HPB (Oxford)* 2019;21(8):990–997. doi:10.1016/j.hpb.2018.12.001.
- [28] Fagenson AM, Gleeson EM, Pitt HA, Lau KN. Albumin-bilirubin score vs model for end-stage liver disease in predicting post-hepatectomy outcomes. *J Am Coll Surg* 2020;230(4):637–645. doi:10.1016/j.jamcollsurg.2019.12.007.
- [29] Lu LH, Zhang YF, Mu-Yan C, Kan A, Zhong XP, Mei J, *et al*. Platelet-albumin-bilirubin grade: risk stratification of liver failure, prognosis after resection for hepatocellular carcinoma. *Dig Liver Dis* 2019;51(10):1430–1437. doi:10.1016/j.dld.2019.04.006.
- [30] Khabbaz RC, Lokken RP, Chen YF, Lipnik AJ, Bui JT, Ray CE Jr, *et al*. Albumin-bilirubin and platelet-albumin-bilirubin grades do not predict survival after transjugular intrahepatic portosystemic shunt creation. *Cardiovasc Intervent Radiol* 2018;41(7):1029–1034. doi:10.1007/s00270-018-1923-2.
- [31] Hwang S, Ha TY, Song GW, Jung DH, Ahn CS, Moon DB, *et al*. Quantified risk assessment for major hepatectomy via the indocyanine green clearance rate and liver volumetry combined with standard liver volume. *J Gastrointest Surg* 2015;19(7):1305–1314. doi:10.1007/s11605-015-2846-8.
- [32] Pruvot FR, Truant S. Major hepatic resection: from volumetry to liver scintigraphy. *HPB (Oxford)* 2016;18(9):707–708. doi:10.1016/j.hpb.2016.08.001.
- [33] Guo P, Zeng F, Hu X, Zhang D, Zhu S, Deng Y, *et al*. Improved variable selection algorithm using a LASSO-type penalty, with an application to assessing hepatitis B infection relevant factors in community residents. *PLoS One* 2015;10(7):e0134151. doi:10.1371/journal.pone.0134151.
- [34] Vickers AJ, Van Calster B, Steyerberg EW. Net benefit approaches to the evaluation of prediction models, molecular markers, and diagnostic tests. *BMJ* 2016;352:i6. doi:10.1136/bmj.i6.
- [35] Abdalla EK, Denys A, Chevalier P, Nemr RA, Vauthey JN. Total and segmental liver volume variations: implications for liver surgery. *Surgery* 2004;135(4):404–410. doi:10.1016/j.surg.2003.08.024.
- [36] Kim HJ, Kim CY, Park EK, Hur YH, Koh YS, Kim HJ, *et al*. Volumetric analysis and indocyanine green retention rate at 15 min as predictors of post-hepatectomy liver failure. *HPB (Oxford)* 2015;17(2):159–167. doi:10.1111/hpb.12295.
- [37] Theilig D, Steffen I, Malinowski M, Stockmann M, Seehofer D, Pratschke J, *et al*. Predicting liver failure after extended right hepatectomy following right portal vein embolization with gadoxetic acid-enhanced MRI. *Eur Radiol* 2019;29(11):5861–5872. doi:10.1007/s00330-019-06101-2.





Original Article

# Integrative Characterization of Immune-relevant Genes in Hepatocellular Carcinoma

Wei-Feng Hong<sup>1#</sup>, Yu-Jun Gu<sup>2#</sup>, Na Wang<sup>3#</sup>, Jie Xia<sup>3</sup>, Heng-Yu Zhou<sup>3,4</sup>, Ke Zhan<sup>5</sup>, Ming-Xiang Cheng<sup>6</sup> and Ying Cai<sup>3,7\*</sup> 

<sup>1</sup>Department of Medical Imaging, The First Affiliated Hospital of Guangdong Pharmaceutical University, Guangzhou, Guangdong, China; <sup>2</sup>Department of Ultrasonic Medicine, The First Affiliated Hospital of Sun Yat-Sen University, Guangzhou, Guangdong, China; <sup>3</sup>Key Laboratory of Molecular Biology for Infectious Diseases (Ministry of Education), Institute for Viral Hepatitis, Department of Infectious Diseases, The Second Affiliated Hospital, Chongqing Medical University, Chongqing, China; <sup>4</sup>College of Nursing, Chongqing Medical University, Chongqing, China; <sup>5</sup>Department of Gastroenterology, The Second Affiliated Hospital, Chongqing Medical University, Chongqing, China; <sup>6</sup>Department of Hepatobiliary Surgery, The Second Affiliated Hospital, Chongqing Medical University, Chongqing, China; <sup>7</sup>Department of Intensive Care Medicine, The Second Affiliated Hospital, Chongqing Medical University, Chongqing, China

Received: 27 November 2020 | Revised: 18 February 2021 | Accepted: 21 February 2021 | Published: 8 March 2021

## Abstract

**Background and Aims:** Tumor microenvironment plays an essential role in cancer development and progression. Cancer immunotherapy has become a promising approach for the treatment of hepatocellular carcinoma (HCC). We aimed to analyze the HCC immune microenvironment characteristics to identify immune-related genetic changes. **Methods:** Key immune-relevant genes (KIRGs) were obtained through integrating the differentially expressed genes of The Cancer Genome Atlas, immune genes from the Immunology Database and Analysis Portal, and immune differentially expressed genes determined by single-sample gene set enrichment analysis scores. Cox regression analysis was performed to mine therapeutic target genes. A regulatory network based on KIRGs, transcription factors, and immune-related long non-coding RNAs (IRLncRNAs) was also generated. The outcomes of risk score model were validated in a testing cohort and in clinical samples using tissue immunohistochemistry staining. Correlation analysis

between risk score and immune checkpoint genes and immune cell infiltration were investigated. **Results:** In total, we identified 21 KIRGs, including programmed cell death-1 (PD-1) and cytotoxic T-lymphocyte associated protein 4 (CTLA4), and found IKBKE, IL2RG, EDNRA, and IGHA1 may be equally important to PD-1 or CTLA4. Meanwhile, KIRGs, various transcription factors, and IRLncRNAs were integrated to reveal that the NRF1-AC127024.5-IBKKE axis might be involved in tumor immunity regulation. Furthermore, the immune-related risk score model was established according to KIRGs and key IRLncRNAs, and verified more obvious discriminating power in the testing cohort. Correlation analysis indicated *TNFSF4*, *LGALS9*, *KIAA1429*, *IDO2*, and *CD276* were closely related to the risk score, and CD4 T cells, macrophages, and neutrophils were the primary immune infiltration cell types. **Conclusions:** Our results highlight the importance of immune genes in the HCC microenvironment and further unravel the underlying molecular mechanisms in the development of HCC.

**Citation of this article:** Hong WF, Gu YJ, Wang N, Xia J, Zhou HY, Zhan K, *et al.* Integrative characterization of immune-relevant genes in hepatocellular carcinoma. J Clin Transl Hepatol 2021;9(3):301–314. doi: 10.14218/JCTH.2020.00132.

**Keywords:** Hepatocellular carcinoma; Immune gene; Immunotherapy; Tumor microenvironment; Risk model.

**Abbreviations:** CTLA4, cytotoxic T-lymphocyte associated protein 4; DEGs, differentially expressed genes; DETFs, differentially expressed transcription factors; GSEA, gene set enrichment analysis; HCC, hepatocellular carcinoma; IDEGs, immune differentially expressed genes; IGs, immune genes; IKBKE, inhibitor of nuclear factor kappa-B kinase subunit epsilon; ImmPort, Immunology Database and Analysis Portal; IRG, immune-relevant gene; IRLncRNAs, immune-related long non-coding RNAs; KEGG, Kyoto Encyclopedia of Genes and Genomes; KIRGs, key immune-relevant genes; Lasso, least absolute shrinkage and selection operator; LIHC, liver hepatocellular carcinoma; PD-1, programmed cell death-1; ROC, receiver operating characteristic; ssGSEA, single sample gene set enrichment analysis; STRING, search tool for the retrieval of interacting genes/proteins database; TCGA, The Cancer Genome Atlas; TIMER, tumor immune estimation resource; WGCNA, weighted gene co-expression networks analysis.

\*These authors contributed equally to this study.

**Correspondence to:** Ying Cai, Key Laboratory of Molecular Biology for Infectious Diseases (Ministry of Education), Institute for Viral Hepatitis, Department of Infectious Diseases; Department of Intensive Care Medicine, The Second Affiliated Hospital, Chongqing Medical University, 1# Yixueyuan Road, Yuzhong District, Chongqing 400000, China. ORCID: <https://orcid.org/0000-0002-1782-719X>. Tel: +86-15923330181, E-mail: [caiying@cqmu.edu.cn](mailto:caiying@cqmu.edu.cn)

## Introduction

Liver cancer is the most common malignancy and the fourth leading cause of cancer-related mortality worldwide.<sup>1</sup> Hepatocellular carcinoma (HCC), a predominant type of primary liver cancer, has become a major public health problem. Although surgical resection is a potentially curative modality for a minority of early-stage HCC patients,<sup>2</sup> as many as 70% of these patients will experience disease recurrence within 5 years.<sup>3</sup> Due to the occult onset of HCC, most advanced patients are not eligible for the timely administration of effective treatment.<sup>4</sup> Sorafenib, as a multi-kinase

inhibitor, has been approved by the Food and Drug Administration and recommended as the first-line treatment in this population based on the “SHARP” trial, with median overall survival of 6.5 months.<sup>2,5,6</sup> Then, the “REFLECT” trial demonstrated that lenvatinib was non-inferior to sorafenib for overall survival in untreated advanced HCC patients.<sup>7</sup> It only showed some clinical benefits for secondary endpoints in progression-free survival, time to progression, and objective response rate. The current status of HCC recurrence and metastasis are not optimistic; therefore, novel and effective treatment options are desperately in need of further exploration to decrease recurrence rates.

Increasing evidence has shown that the tumor microenvironment plays an essential role in cancer development and progression. With improved understanding of biological interactions within the tumor microenvironment, immune system and tumor cells, cancer immunotherapy has appeared to provide tremendous promise as a cancer treatment modality in recent years. Typically, in the liver, large quantities of innate and adaptive immune cells play a critical role in immune surveillance to detect and eliminate pathogens and participate in immune response and regulation of host defenses.<sup>8</sup> However, the inflammatory state, due to risk factors that contribute to HCC, such as chronic infection with hepatitis B virus or hepatitis C virus, will change the tumor microenvironment and facilitate evasion of immune surveillance, leading to tumor tolerance and promoting the development of HCC.<sup>8</sup> Hence, targeted immunotherapy is actively researched with the goal of inhibiting aberrant oncogenic pathways and improving prognosis.

At present, immune checkpoint inhibitors are considered one of the immunotherapies for rapid development to promote immune reconstitution and restore immune cell function.<sup>9</sup> Programmed cell death-1 (PD-1) and cytotoxic T-lymphocyte associated protein 4 (CTLA4) blockage therapies have become promising approaches for the treatment of HCC.<sup>10–13</sup> Unfortunately, in some studies, overall survival and improved recurrence-free survival did not achieve the pre-defined statistical significance criteria.<sup>14</sup> It has been suggested that the HCC microenvironment can form a potent immune tolerance system, which greatly hinders the efficacy of immune checkpoint therapy. Therefore, remodeling the immune tolerant microenvironment of HCC could be of great significance for HCC immunotherapy.

Given the complexity of immunotherapy and tumor heterogeneity, extensive genomic analysis could provide clinical options, including personalized therapies for patients with cancer. We systematically integrated genomic profiling to illustrate the global portrait of the HCC immune microenvironment characteristics to further identify the immune-related genetic changes. In addition, immune-related models and networks were also established to shed light on the potential mechanism of immune therapeutic targets.

## Methods

### Datasets acquisition and pre-processing

Fragments per kilobase million upper quartile RNA-Seq gene expression profile of liver hepatocellular carcinoma (LIHC) were downloaded from The Cancer Genome Atlas (TCGA) (<https://portal.gdc.cancer.gov/>), including 50 normal tissue and 374 primary tumor samples.<sup>15</sup> A list of 1,811 immune genes (IGs), including 17 immune categories according to different molecular function, were obtained from the Immunology Database and Analysis Portal (ImmPort) (<https://www.immport.org/home>)<sup>16</sup> after eliminating reiterated genes. One of the major collections (C7: immunologic signatures) in the molecular signatures database

(MSigDB) of Gene Set Enrichment Analysis (GSEA) (<https://www.gsea-msigdb.org/gsea/index.jsp>)<sup>17</sup> is a collection of 4,872 annotated gene sets that represent cell types, states, and perturbations within the immune system.<sup>18</sup> The immunologic gene sets and 28 immune signaling pathways were also collected and processed for subsequent analyses. The data of tumor immune infiltration in TCGA-LIHC was downloaded from the tumor immune estimation resource (known as TIMER) (<https://cistrome.shinyapps.io/timer/>).<sup>19</sup>

### Screening immune-relevant genes (IRGs)

To evaluate the enrichment scores of every sample on each immune-related term in RNA-Seq data of TCGA-LIHC, single-sample gene set enrichment analysis (ssGSEA) was used to generate ssGSEA-score<sup>20</sup> implemented in the R package “GSVA” and “GSEABase”. Each score was corrected between 0 and 1. Patients were divided into a high-immune score (Immunity\_H) and a low-immune score (Immunity\_L) group using unsupervised hierarchical clustering of R package “sparcl”.

Differentially expressed gene (DEG) analysis was performed via the R package “Limma” based on the empirical Bayes method.<sup>21</sup> Immune differentially expressed genes (IDEGs) were determined by Immunity\_H to Immunity\_L ratio, with cutoff criteria of absolute log2 fold-change ( $|\log(2) FC|$ ) > 1.0 and false discovery rate < 0.05. Significant DEGs of RNA-Seq data from TCGA-LIHC project were also identified by the same approach. Then, overlapping DEGs, IDEGs, and IGs were assessed and provided 77 interacting genes as the IRGs in the present study.

### Construction of weighted gene co-expression networks and identification of key IRGs

Based on the expression of 77 IRGs with complete clinical data in tumor tissues from TCGA-LIHC project, weighted gene co-expression networks analysis (WGCNA) was carried out to create expression modules and analyze the correlation of each module with immune traits (ImmuneGroup, StromalScore, ImmuneScore, ESTIMATEScore, and TumorPurity) using the R package WGCNA by hierarchical clustering of adjacency-based dissimilarity.<sup>22</sup> Module eigengenes were defined as the first principle component of each gene module and regarded as representative of genes in each module. Gene significance was calculated to measure the Pearson correlation between gene expression and sample traits and to identify the significance of each module. We selected higher gene significance and defined survival-related modules according to  $p \leq 0.001$  for further analysis. A scale-free topology fit index (scale-free  $R^2$ ) > 0.95 was implemented to verify the soft threshold power and maintain optimal mean connectivity. A dynamic hybrid cut method, using a bottom-up algorithm, was applied to identify crucial modules, with cut height-off of 0.25. At last, key immune-relevant genes (KIRGs) in crucial modules were selected by those with module membership > 0.5. General characteristics of KIRGs were analyzed using GSCALite (<http://bioinfo.life.hust.edu.cn/web/GSCALite/>).<sup>23</sup>

### Construction of co-expression network based on KIRGs

To analyze the function of KIRGs, the relationship between transcription factors and KIRGs was explored. The transcription factors set was extracted from the Cistrome Project (<http://www.cistrome.org/>)<sup>24</sup> and subjected to expression

differential analysis by the R package “Limma”, with cut-off value of  $|\log FC| > 1.0$  and adjusted  $p$ -value of  $< 0.05$ . The significant correlations between the differentially expressed transcription factors (DETFs) and KIRGs (DETFs-KIRGs) were calculated by Pearson’s test, with  $p$ -value of  $< 0.0001$  and correlation coefficient of  $> 0.30$ , which was visualized by Cytoscape software (3.7.1) in the appropriate type of correlation network.

Meanwhile, considering immune-related long non-coding RNAs (lncRNAs) involved in the mRNA transcript process of KIRGs, the network of lncRNAs-KIRGs was established using the co-expression analysis approach as described above. The profile of long non-coding RNAs was taken from the annotation data of TCGA-LIHC. Subsequently, the network of DETFs and lncRNAs (DETFs-lncRNAs) was also generated (correlation coefficient  $> 0.30$  and  $p < 0.0001$ ). Finally, the DETFs-lncRNA-KIRGs regulatory network was integrated for the pairs of the above three networks’ data.

### Risk score model construction and verification

TCGA-LIHC patients were randomly divided at the ratio of 1:1 into two cohorts (training cohort and testing cohort). To avoid overfitting, least absolute shrinkage and selection operator (Lasso) Cox regression was applied to eliminate genes generated from univariate Cox analysis of all genes of lncRNAs-KIRGs. Then, we performed multivariate Cox regression to construct a risk score model, and the performance was evaluated in the testing cohort. Kaplan-Meier survival analysis and time-dependent receiver operating characteristic (commonly known as ROC) analysis were used to compare the survival states and evaluate the accuracy of the risk score model.

### Enrichment analysis and protein-protein interaction

To determine the function and potential regulatory pathways of identified genes, GSEA was explored for biological functions and pathways using the R package “clusterprofiler” and “GSVA”, with adjusted  $p$ -value of  $< 0.05$  and  $q$ -value of  $< 0.05$ , as each was regarded as statistically significant. Gene Ontology analysis and Kyoto Encyclopedia of Genes and Genomes (KEGG) pathway enrichment analysis were performed by the web tool “Metascape” (<http://metascape.org/>).<sup>25</sup> The search tool for the retrieval of interacting genes/proteins database (commonly known as STRING) was utilized to assess protein-protein interactions, with information minimum required interaction score: medium confidence (0.40) ([www.string-db.org/](http://www.string-db.org/)).<sup>26</sup>

### Experimental section

Paired tumor and peritumor tissues were obtained from patients diagnosed with HCC and who had undergone surgery at the Department of Hepatological Surgery of the Second Affiliated Hospital of Chongqing Medical University (Chongqing, China). All experiments were performed in accordance with the Declaration of Helsinki of the World Medical Association and were approved by the ethics committee of the Second Affiliated Hospital of Chongqing Medical University (No. 2020-004). All participants provided written informed consent.

Tissue proteins were lysed using radio immunoprecipitation assay lysis buffer (CWBIO, Beijing, China) with protease inhibitor cocktail (CWBIO). Protein concentration was measured with a bicinchoninic acid assay (CWBIO). The same amount of total proteins was subjected to SDS-PAGE, followed by a standard western blotting procedure with the

primary antibodies and secondary antibodies (Supplementary Table 1), and detection using an enhanced chemiluminescence system (Advansta, Menlo Park, CA, USA).

Tissue paraffin sections were prepared for immunohistochemistry staining, according to standard procedures. The slides were visualized using 3,3'-diaminobenzidine substrate kit (Abcam, Cambridge, UK) and counterstained with hematoxylin (Solarbio, Beijing, China). Stained slides were scanned by the Motic Easyscanner (Motic, Hong Kong, China) and the images were captured with Motic DS Assistant Lite (Motic VM V1 Viewer 2.0).

Tissue total RNA was extracted using TRIzol reagent (Invitrogen, Carlsbad, CA, USA), following the manufacturer’s instructions. The cDNA library was constructed by reverse transcription using a commercial reverse-transcription kit (Takara, Shiga, Japan) according to the manufacturer’s protocol. The cDNA was amplified using SYBR Green Master Mix (Bimake, Houston, TX, USA) and normalized by GAPDH. Quantitative polymerase chain reaction primers (Supplementary Table 2) were synthesized by Invitrogen.

### Statistical analysis

All statistical analyses were performed in R version 3.6.0 and GraphPad Prism software 8.0, and  $p$ -values  $< 0.05$  were considered significant. Continuous variables, such as difference analysis, were performed by  $t$ -test or Wilcoxon’s test, according to the normality of data distribution. Correlation analysis of categorical variables was carried out with the chi-squared test. Correlations between continuous variables were estimated using the Pearson correlation, while Spearman’s correlation was used to assess the association between non-normally distributed data.

## Results

### Initial screening IRGs

To screen significant immune biomarkers, we incorporated important databases in the initial workflow (Fig. 1A). A total of 7,667 DEGs were identified from TCGA-LIHC dataset (Supplementary Fig. 1A, B). To understand each tumor sample’s immune status, the corresponding enrichment scores on every immune-related term were calculated based on the ssGSEA method. By unsupervised hierarchical clustering, patients were clustered into the Immunity\_H group ( $n=170$ ) and the Immunity\_L group ( $n=204$ ) (Supplementary Fig. 1C). Stromal cells and immune cells were the non-tumor components of the immune microenvironment which reflected tumor immune infiltration and tumor purity. The stromal scores and immune scores were calculated and combined to estimate scores in order to display tumor purity by the ESTIMATE algorithm (Fig. 2A; Supplementary Table 3). Upon comparison with the Immunity\_L group, stromal scores, immune scores, and ESTIMATE scores were significantly higher in the Immunity\_H group, while the lower level of tumor purity represented the low activity of tumor cells ( $p < 0.001$ ) (Fig. 2B–E). Then, enrichment analysis of biological functions and pathways in the two groups was performed using GSEA. The Immunity\_H group was identified when the enrichment score was  $> 0$ , and found to be mainly enriched in complement activation (classical pathway), humoral immune response mediated by circulating immunoglobulin and MHC class II protein complex in the aspect of biological function (Fig. 2F). Allograft rejection, intestinal immune network for IgA production, and primary immunodeficiency embodied the pathway



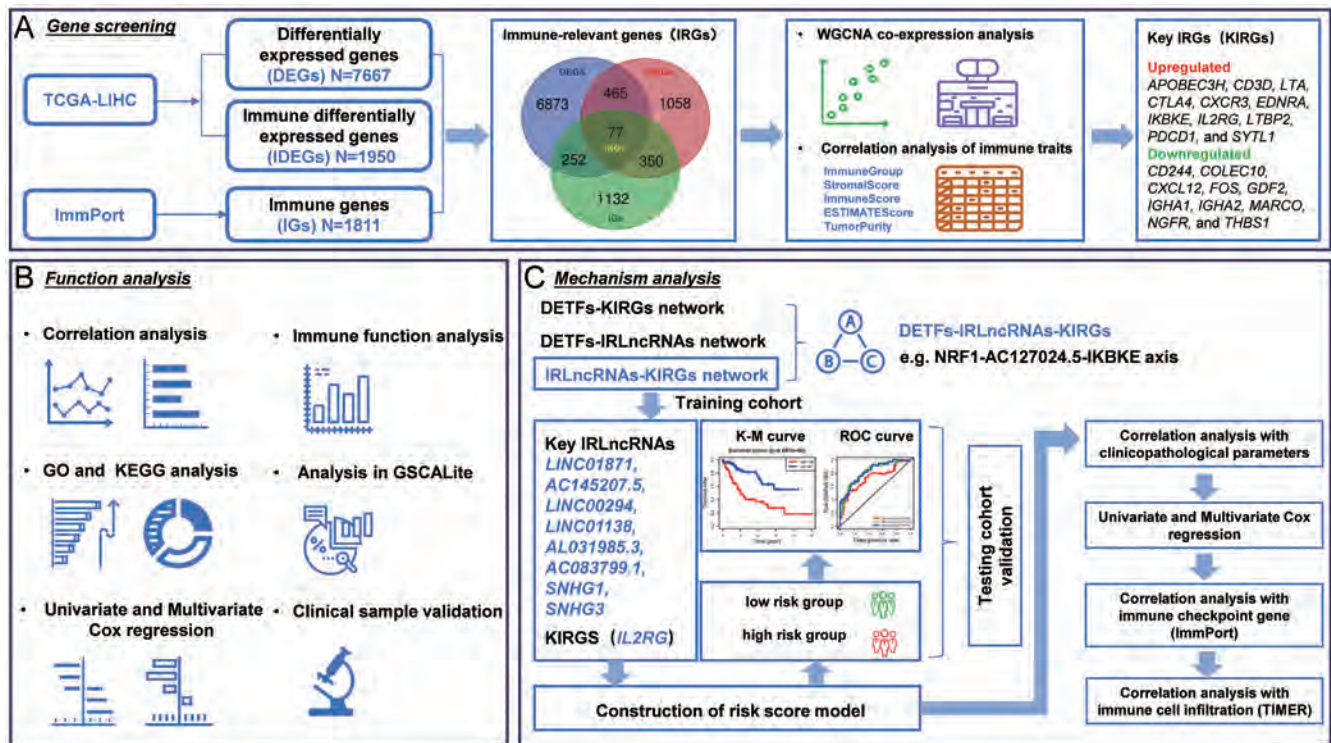


**Fig. 1.** Flow chart of immune-relevant gene screening, function analysis, and mechanism analysis. (A) Screening for KIRGs incorporated from TCGA and ImmPort. (B) Schematic diagram for function analysis of KIRGs. (C) Flow chart for underlying mechanism analysis of KIRGs combined with transcription factors and lncRNAs.

enrichment results (Fig. 2G). Next, the bubble chart showed the top 10 biological functions in the Immunity\_H group and the Immunity\_L group (Fig. 2H). Enrichment analysis of the pathway only focused on the Immunity\_H group (Supplementary Table 4). Meanwhile, 1,950 IDEGs were obtained by differential analysis for the Immunity\_H and Immunity\_L groups (Supplementary Fig. 1D, E). Finally, 77 IRGs were screened out by overlapping the DEGs, IDEGs, and IGs in this present study. Gene Ontology analysis and KEGG pathway enrichment analysis results were statistically confirmed via Metascape (Supplementary Fig. 1F, G).

#### Identification of the modules associated with immune traits by construction of WGCNA

WGCNA was applied to find important modules most associated with immune traits based on 77 IRGs. A total of seven modules were identified by setting soft threshold power and cut height-off value. IRGs in the gray module were identified as non-clustering genes (Fig. 3A, B). In the heatmap of module-trait relationships, the blue module (12 IRGs) and brown module (9 IRGs) manifested significant correlation of immune traits, especially by ImmuneScore (correlation coefficient of 0.73,  $p=4e-64$ ) and StromalScore (correlation coefficient of 0.65,  $p=7e-47$ ), respectively. Genes in these two modules with module membership of  $>0.5$  were defined as KIRGs (Fig. 3C).

#### Functional analysis of the KIRGs signature

We analyzed the fundamental functional of the KIRGs (Fig.

1B). Differential analysis of KIRGs' expressions was performed, with 11 genes (*APOBEC3H, CD3D, CTLA4, CXCR3, EDNRA, inhibitor of nuclear factor kappa-B kinase subunit epsilon (IKBKE), IL2RG, LTA, LTBP2, PDCD1, and SYTL1*) showing high expression and 9 genes (*CD244, COLEC10, CXCL12, FOS, GDF2, IGHA1, IGHA2, MARCO, NGFR, and THBS1*) showing low expression in tumor tissue ( $p<0.05$ ) (Fig. 4A). Correlation analysis of 21 KIRGs showed that *CXCR3* was highly associated with *CD3D* and *LTA* (correlation coefficient of  $>0.80$ ,  $p<0.05$ ) (Fig. 4B). To display interactive relationships among proteins of KIRGs, a protein-protein interaction network was constructed by the STRING database. *LTA, CTLA4, FOS, and CXCL12* had the most interactive lines ( $n>10$ ) in the bar graph, which totaled 60 lines (Fig. 4C, D). High node degrees could indicate an essential role in tumor immune processes.

Gene Ontology analysis and KEGG pathway enrichment analysis were performed using the R package "clusterprofiler". To demonstrate more information from the results, the top 20 Gene Ontology terms were enriched as a Gene Ontology heatmap, mainly in "leukocyte migration" and "humoral immune response" (Fig. 4E). We also found that the three terms of "response to oxygen levels", "response to hypoxia" and "response to decreased oxygen levels" enriched from the same genes (Fig. 4E). In the KEGG circle map, KIRGs were enriched in some common and critical pathways referring to tumorigenesis and progression, such as "T cell receptor signaling pathway", "Cytokine-cytokine receptor interaction" and "PI3K-Akt signaling pathway" and so on (Fig. 4F).

To further verify whether KIRGs were closely related to immune function, 29 terms from the ImmPort database served as the candidate profile and a gene set including 21 KIRGs was found to be enriched in eight immune



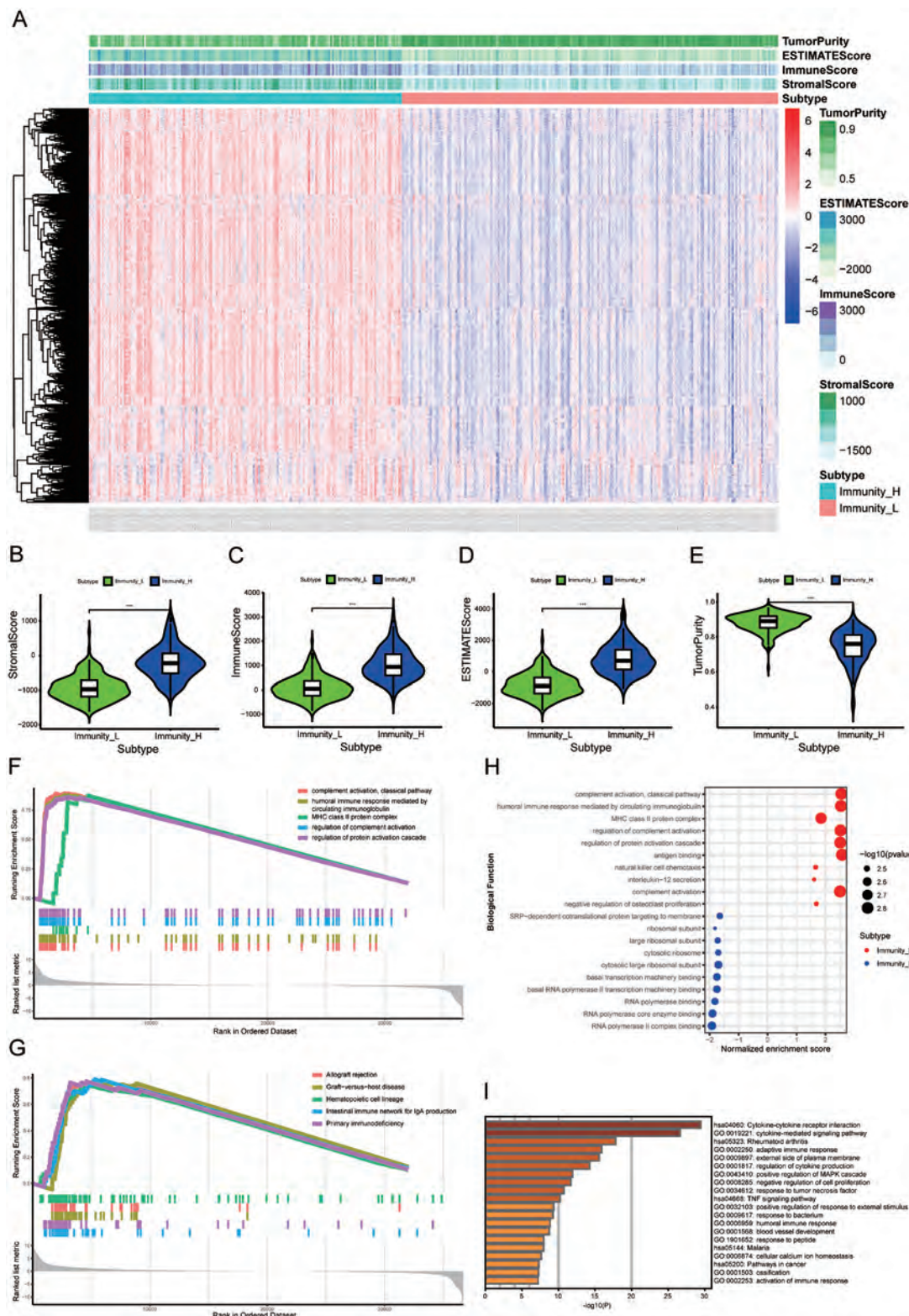


**Fig. 2. Microenvironment signatures of TCGA-LIHC cohort and enrichment analysis.** (A) Heatmaps showed expression profiles for microenvironment signatures of stromal scores, immune scores, ESTIMATE scores, and tumor purity with unsupervised hierarchical clustering analyses. (B–E) Stromal scores, immune scores, ESTIMATE scores and tumor purity in the Immunity\_H group and the Immunity\_L group. (\*\* $p < 0.001$ ) (F–G) Enrichment analysis of biological functions and pathways in the Immunity\_H group (top 5). (H) Bubble chart of top 10 biological functions in the Immunity\_H and Immunity\_L groups. (I) Heatmap of Gene Ontology and KEGG enrichment analysis for IRGs via Metascape.

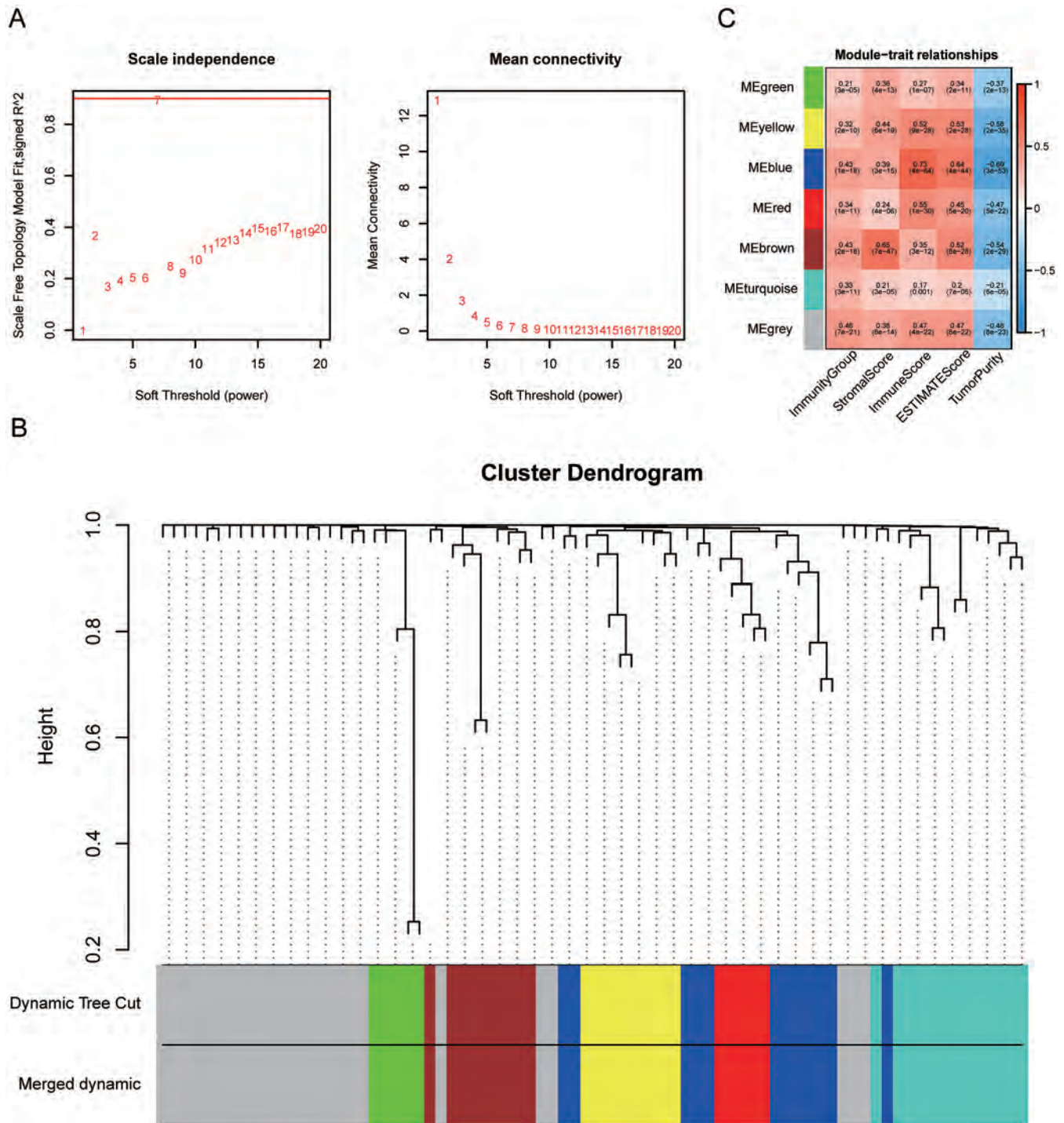


**Fig. 3. Construction of WGCNA co-expression modules and identification of modules associated with immune traits.** (A) Analyses of the scale-free topology fit index of the soft threshold power (left panel) and the mean connectivity of soft threshold power (right panel). (B) A cluster dendrogram of 77 IRGs with various modules constructed by hierarchical clustering of adjacency-based dissimilarity; different colors represent different modules. (C) Heatmap of relationships between module eigengenes and immune trait.

terms, namely Check-point, Th1 cells, Tfh, T cell coinhibition, plasmacytoid dendritic cells, CCR, TIL, and regulatory T cells, based on the ssGSEA-score of the R package “GSVA” (Supplementary Fig. 2A–C). Next, we extracted all the genes of some critical immune terms from TCGA-

LIHC project and differential analysis of expression was implemented between the Immunity\_H group and the Immunity\_L group (Supplementary Fig. 3A–E). Besides, due to multiple filters, *IKBKE*, *IL2RG*, *EDNRA*, and *IGHA1* were screened out more significantly with  $p < 0.2$  using



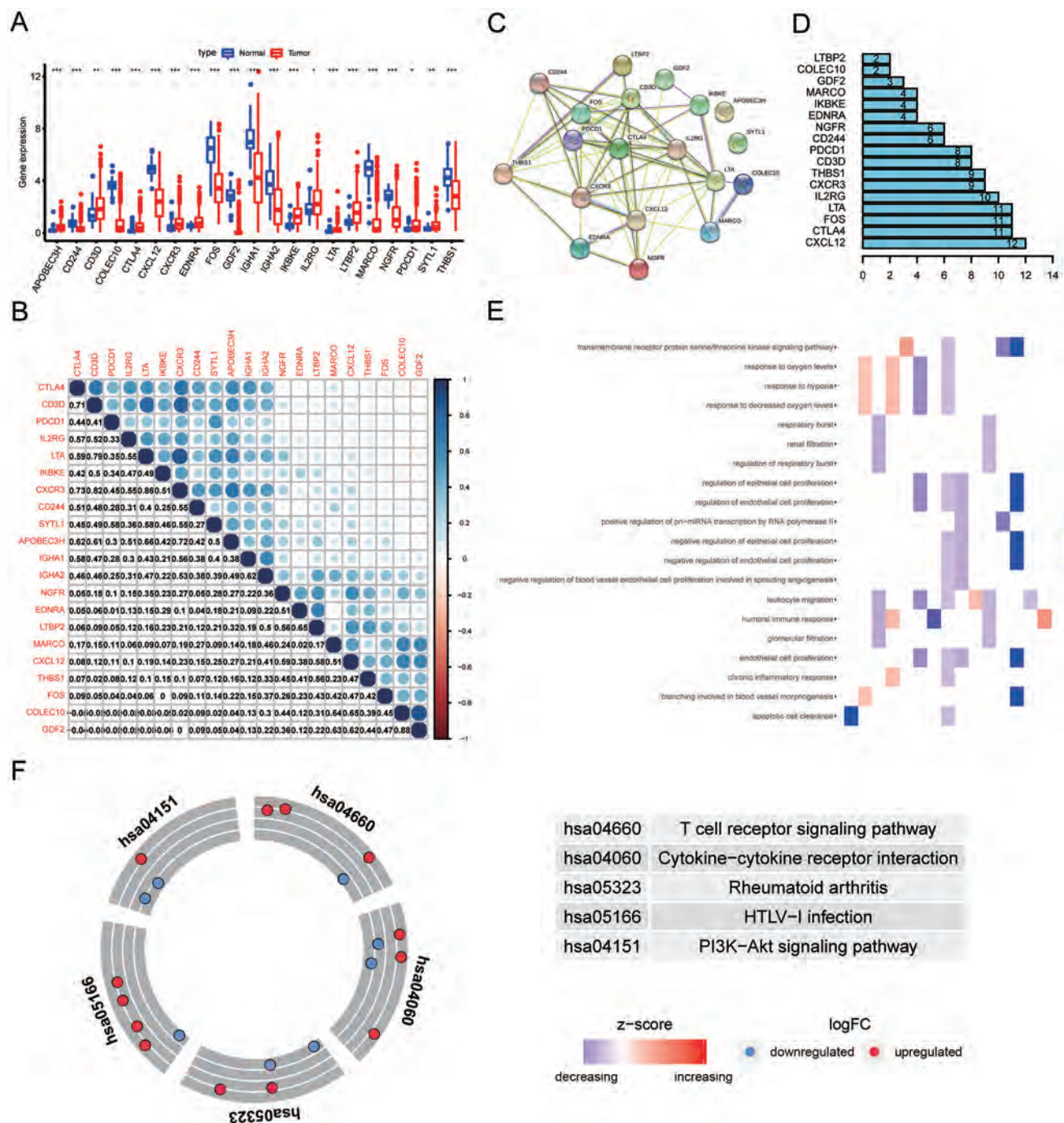


**Fig. 4. Functional analysis of the KIRGs signature.** (A) Differential analysis of KIRGs expression in normal and HCC tissues. (\*\* $p < 0.001$ , \*\* $p < 0.01$ , \* $p < 0.05$ ). (B) Correlation analysis of 21 KIRGs. (C) A protein-protein interaction network of 21 KIRGs was constructed via STRING. (D) The number of gene connections in the protein-protein interaction network. (E) Gene Ontology heatmap of KIRGs. (F) KEGG circle map of KIRGs.

univariate Cox regression and multivariate Cox regression of 21 KIRGs (Fig. 5A, B). We examined protein expression of these four markers in clinical HCC and corresponding peritumor tissues. Western blotting indicated that IKBKE, IL2RG, and EDNRA were highly expressed in most HCC tissue specimens, while IGHA1 had low expression in tumors (Fig. 5C). Immunohistochemical assay showed IKBKE and IL2RG were significantly higher in representative

HCC tissue (Fig. 5D).

#### Analysis of KIRGs in a web-based platform of GS-CALite

To understand gene set mutations, we observed single nucleotide variation frequency and analyzed the variant types.

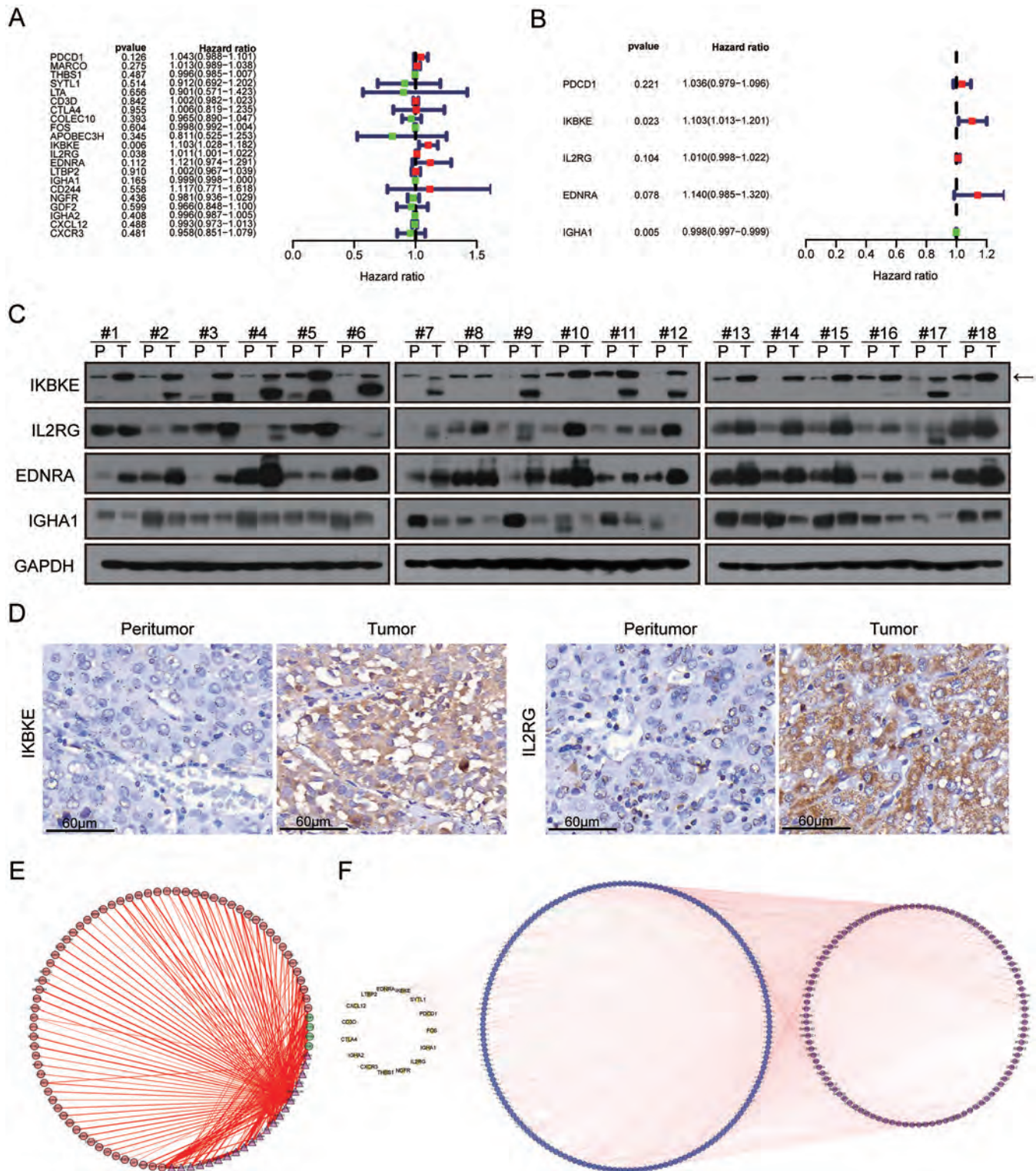


**Fig. 5. Cox regression of 21 KIRGs and construction of regulatory networks.** (A) Univariate Cox regression. (B) Multivariate Cox regression. (C) Western blot of protein expression in HCC and paired peritumor tissues from 18 patients. (D) Immunohistochemical staining of the representative KIRGs IKBKE and IL2RG in HCC and paired peritumor tissues. (E) Construction of DETFs-KIRGs networks. (F) Construction of DETFs-IRLncRNAs-KIRGs regulatory networks.

Of the 21 KIRGs, the vast majority of variants occurred as single nucleotide polymorphisms and missense muta-

tions in the included samples (Supplementary Fig. 4A, B). The top 10 frequently mutated genes were *GDF2*, *LTBP2*,



*THBS1*, *CXCR3*, *EDNRA*, *MARCO*, *NGFR*, *CD244*, *FOS* and *APOBEC3H*, with 91.18% alteration in at least one sample (Supplementary Fig. 4C, E). *GDF2*, *LTBP2*, and *THBS1* alterations were observed in 15% of tumors; *NGFR* had multiple alterations of missense mutation, splice site, and frame shift deletion (Supplementary Fig. 4E). C > T and C > A accounted for most of the single nucleotide mutation types (Supplementary Fig. 4D). Meanwhile, we noted that somatic copy number alterations occurred more often in heterozygous copy number variations than in homozygous ones (Supplementary Fig. 4F). *IKBKE*, *COLEG10*, and *CD244* manifested mainly in the statistical processing of heterozygous amplifications (Supplementary Fig. 4F).

Further, differential methylation between tumor and paired normal tissues were found, along with that of other tumor types (Supplementary Fig. 4G). *PDCD1*, *CTLA4*, and *MARCO* indicated high levels of methylation in HCC tissues, while *CXCL12* and *EDNRA* showed a high level in paired normal tissues. We also observed the relationships between methylation levels and corresponding gene expression, which displayed that *PDCD1* methylation had a positive correlation with expression, whereas *IKBKE* and *EDNRA* methylation showed negative relationships in most tumors (Supplementary Fig. 4H).

We also investigated the difference of gene expression between pathway activity groups (activation and inhibition). These KIRGs were also involved in apoptosis, cell cycle, DNA damage response, epithelial to mesenchymal transition, and the RAS/MAPK biological process (Supplementary Fig. 4I). *PDL1*, *CTLA4*, *IKBKE*, and *IL2RG* could promote apoptosis and activate DNA damage response and epithelial to mesenchymal transition (Supplementary Fig. 4J). Eventually, drug sensitivity analysis was performed for 21 KIRGs of HCC lines in the Genomics of Drug Sensitivity in Cancer<sup>27</sup> and Cancer Therapeutics Response Portal<sup>28</sup> databases by Spearman correlation analysis with small molecule/drug sensitivity (Supplementary Fig. 5 and 6).

### Construction of the DTFs-IRLncRNA-KIRGs network

Subsequently, in order to observe transcription factors involved in the regulation of KIRGs, the correlations of KIRGs to DTFs were generated according to co-expression analysis and visualized as a regulatory network (Fig. 1C). A total of 162 positive correlation pairs of DTFs-KIRGs were found; among these, the pairs of *FOS*-*ERG1* (correlation coefficient of 0.63,  $p=5.2E-43$ ), *CIITA*-*CTLA4* (correlation coefficient of 0.62,  $p=6.3E-43$ ) and *CXCR3*-*CIITA* (correlation coefficient of 0.62,  $p=9.1E-43$ ) showed very high correlation (Fig. 5E). Similarly, the IRLncRNAs-KIRGs network and DTFs-IRLncRNAs network were also constructed. Eventually, combining the three networks, the DTFs-IRLncRNAs-KIRGs regulatory network was built, comprised of 103 DTFs, 175 lncRNAs, and 15 KIRGs, to elucidate underlying regulatory mechanisms (Fig. 5F). Most of the pairs represented positive correlations within the network.

*IKBKE*, having a prominent role among the KIRGs, was related to numerous IRLncRNAs, most obviously *AC127024.5*. Interestingly, in the network, *NRF1* was regarded as the most relevant transcription factor to *AC127024.5* (correlation coefficient of 0.63,  $p=4.94E-43$ ), which indicated that the *NRF1*-*AC127024.5*-*IKBKE* axis might be involved in regulating many biological processes. We also explored the *NRF1*-*AC127024.5*-*IKBKE* axis for immune cell infiltration in TCGA-LIHC patients from the TIMER database, and found an involvement in the vast majority of immune cell infiltration processes, especially those related to B cells, CD4 T cells, neutrophils and macrophages ( $p<0.01$ ) (Supplementary Fig. 7).

Furthermore, univariate and Lasso Cox regressions were implemented to optimize the parameters for screening risk genes among the KIRGs and IRLncRNAs (Fig. 6A, B). In total, *IL2RG* and eight key IRLncRNAs (*LINC01871*, *AC145207.5*, *LINC00294*, *LINC01138*, *AL031985.3*, *AC083799.1*, *SNHG1*, and *SNHG3*) were obtained by multivariate Cox regression in the training cohort. The risk score model was constructed and verified the performance in the testing cohort. Patients in each cohort were divided into a low risk group and a high risk group, according to the median risk score of the training cohort. Survival status, risk scores, and expression patterns of each patient were reflected in Fig. 6C and 6D.

Kaplan-Meier curve analysis showed that the low risk group had a significantly better prognosis than that of the high risk group in the training cohort ( $p=4.70E-06$ ) and the testing cohort ( $p=4.70E-05$ ), respectively (Fig. 6E, G). Time-dependent ROC curve analysis of the risk score model in the training and testing cohorts all determined good predictive accuracy with area under the curve values of 0.826 and 0.724 for 1-year survival, and 0.822 and 0.736 for 3-year survival, respectively (Fig. 6F, H). Therefore, it appeared that the risk score model successfully stratified HCC from TCGA.

In addition, we found that the risk score model was associated with clinicopathological parameters, such as tumor-stage, clinical stage, and survival state by chi-squared test ( $p<0.01$ ) (Fig. 7A). Further analysis of univariate and multivariate Cox regression revealed that risk score could be an independent prognostic indicator for HCC patients ( $p<0.001$ ) (Fig. 7B, C). Representative markers (*IL2RG*, *SNHG1*, *SNHG3*, and *LINC01138*) showed obvious high expression in HCC samples at the mRNA level (Fig. 7D). Meanwhile, the forecast performance of the risk score model was superior to those models based on tumor-stage, node-stage, metastasis-stage, grade, American Joint Committee on Cancer stage, KIRGs and key IRLncRNAs (Supplementary Fig. 8A–G). The multiplex model seemed a dependable indicator for predicting the prognosis of HCC patients.

We analyzed the expression of each immune checkpoint gene of ImmPort for correlation with the integration of risk score resulting from the two cohorts. Pearson's correlation indicated *TNFSF4*, *LGALS9*, *KIAA1429*, *IDO2*, and *CD276* were closely related to risk score ( $p<0.05$ ), shown as a circle map (Fig. 8A). Ultimately, we investigated the measurement of the integrated risk score for immune cell infiltration in TCGA-LIHC patients from the TIMER database and observed that effects of risk score appeared to be concentrated among the CD4 T cells, macrophages, and neutrophils ( $p<0.05$ ), while the B cells, CD8 T cells and dendritic cells did not show significant correlation (Fig. 8B–G).

### Discussion

Rapidly emerged immunotherapy has demonstrated increasing promise in the application of treatment for human cancers. On account of tumor complexity and heterogeneity, only a minority of patients could have benefitted from immunotherapy. Interestingly, the tumor immune microenvironment is closely related to patients' responsiveness after receiving the therapy of immune-checkpoint blockade.<sup>29</sup> Thus, understanding the tumor immune microenvironment's diversity will likely uncover novel biomarkers and provide effective therapeutic targets.

According to the natural and fundamental immunological properties of the liver and the current dilemma of immunotherapy for HCC, in this study, we systematically identified 21 KIRGs that potentially participate in HCC pathogenesis and progression. To obtain more robust and reliable IGs, our results were analyzed by more comprehensive and

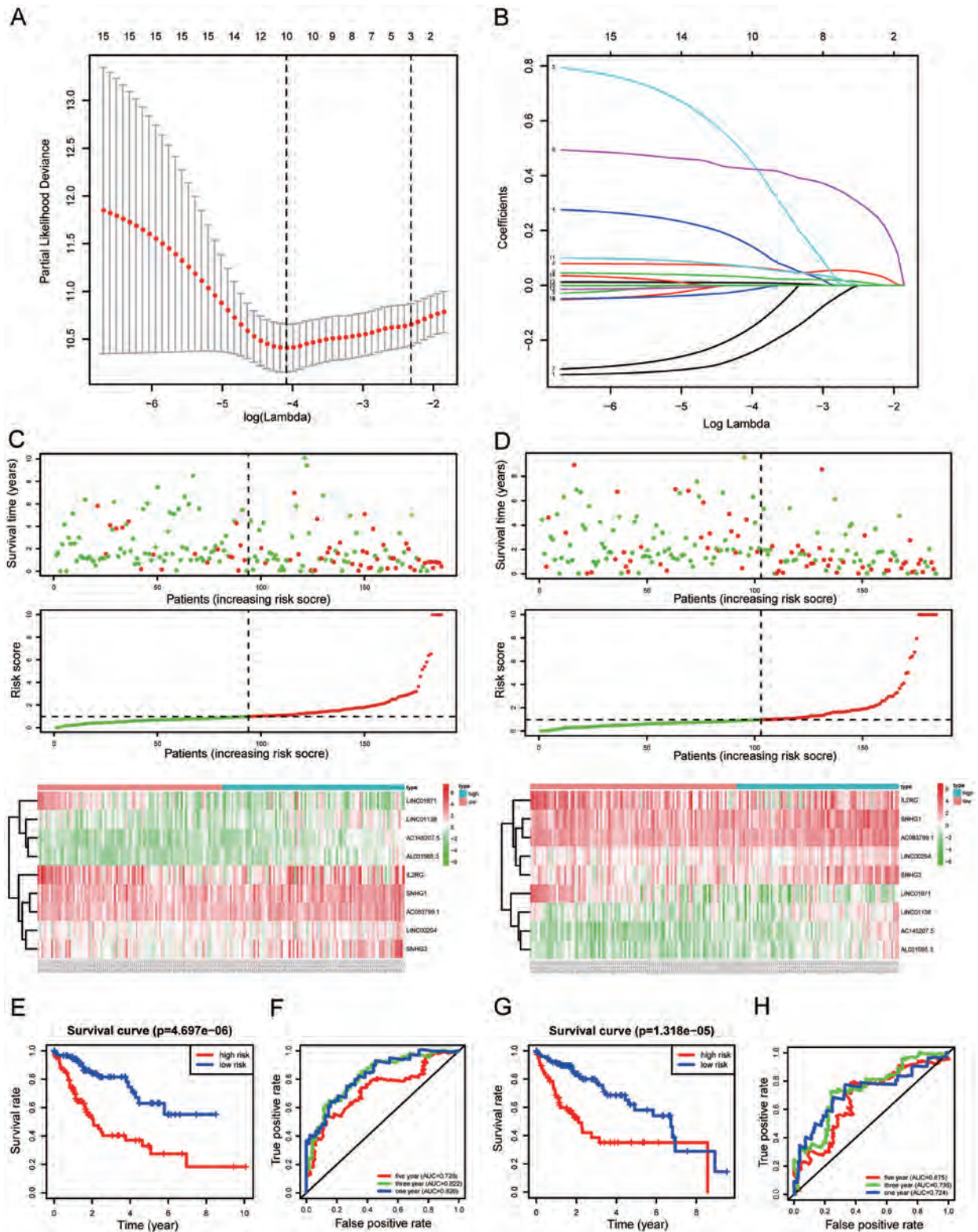


**Fig. 6. Construction of risk score model based on DETFs-IRLncRNAs-KIRGs network.** (A–B) KIRGs and IRLncRNAs were narrowed down by the Lasso algorithm. (C) Survival status scatter plots, risk score distribution, and expression patterns in the training cohort. (D) Survival status scatter plots, risk score distribution, and expression patterns in the testing cohort. (\*\*\*\* $p < 0.001$ ). (E) Kaplan-Meier curve analysis of the high risk and low risk groups in the training cohort. (F) Time-dependent ROC curve analysis of the risk score model in the training cohort. (G) Kaplan-Meier curve analysis of the high risk and low risk groups in the testing cohort. (H) Time-dependent ROC curve analysis of the risk score model in the testing cohort.



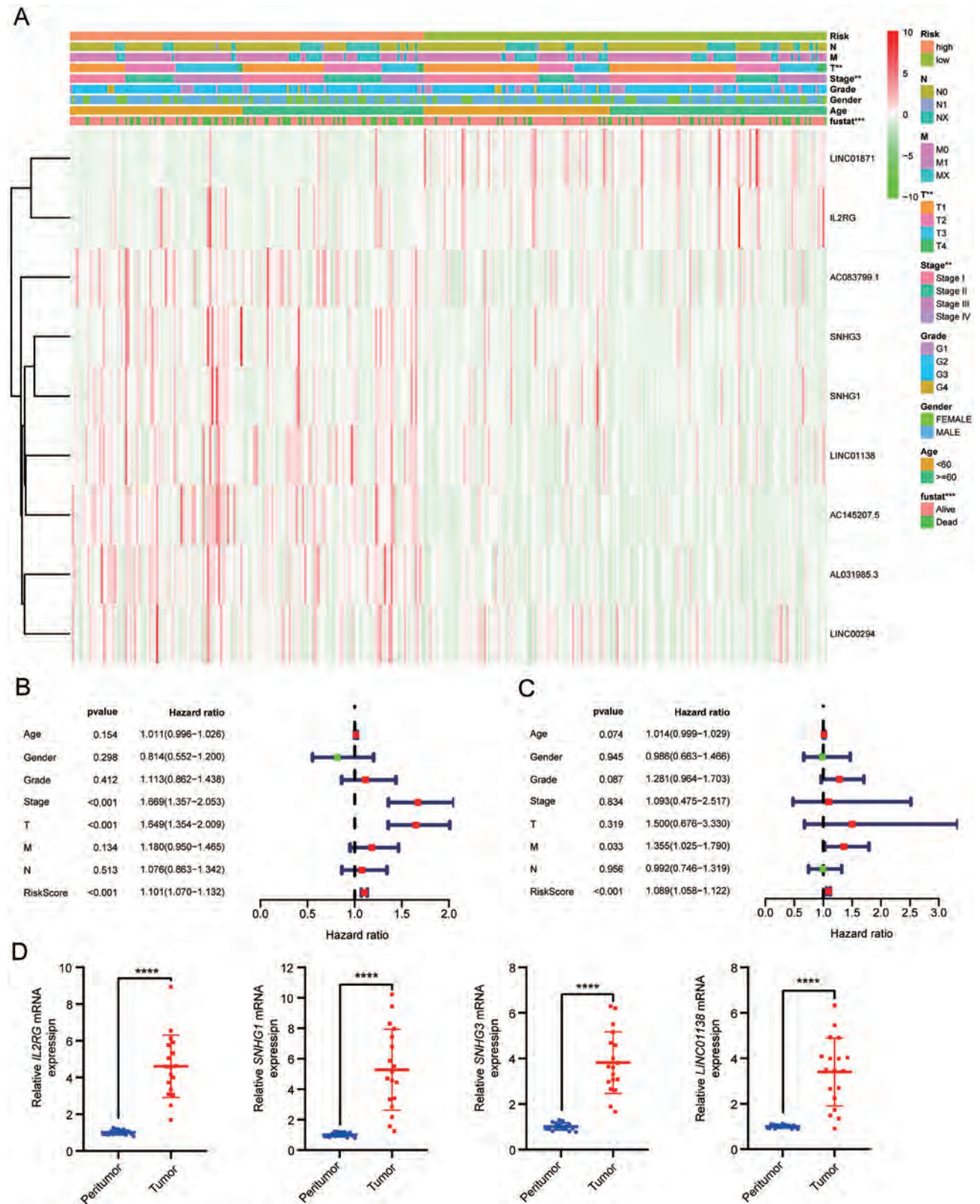


**Fig. 7. Relationship between risk score model and clinicopathological parameters.** (A) Expression profiles of risk genes and association with clinicopathological characteristics. (B–C) Univariate and multivariate Cox regression analyses of risk score and clinicopathological characteristics. (D) Representative key lncRNAs were detected by real-time polymerase chain reaction of HCC and paired peritumor tissues from 18 patients. Abbreviations: M, metastasis; N, node; T, tumor.

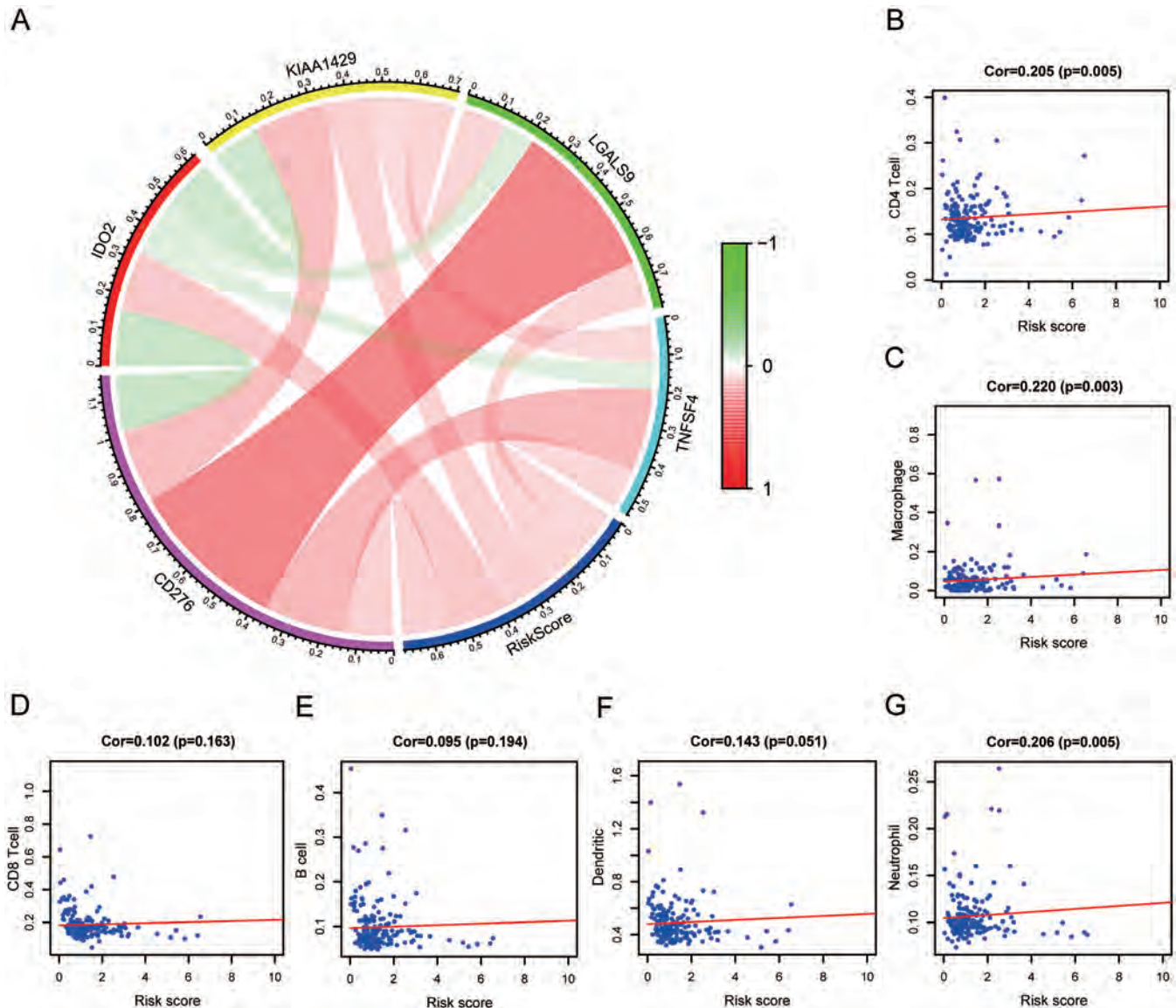


**Fig. 8. Correlation analysis between risk score and immune checkpoint gene and immune cell infiltration.** (A) Circle map of the relationships between immune checkpoint genes and integration of risk score. (B–G) Risk score for immune cell infiltration of CD4 T cells, macrophages, CD8 T cells, B cells, dendritic cells, and neutrophils.

strict screening methods on the basis of DEGs and IDEGs in TCGA database, and IGs retrieved from ImmPort. In its methodology, ssGSEA is a widely accepted algorithm to analyze statistical enrichment.<sup>30</sup> The ESTIMATE algorithm was used to calculate the stromal score, immune score and estimate score in the immune microenvironment for further immune assessment.<sup>31</sup> The Lasso algorithm, as one of the regression regularization methods, applies a Lasso Cox regression model and ensures optimal risk model, even when variables in the dataset have high dimensions and multicollinearity.<sup>32,33</sup>

As is known, binding of ligand and inhibitory receptors on immune cells will weaken the T cell mediated immune response. Antibodies against immune checkpoint proteins, such as CTLA4 or PD-1 (also called PDCD1), the first generation of antibody-based immunotherapy, has been implemented for the treatment of HCC patients. In consideration of partial immune response to these inhibitors, early

results of a recent study based on the CheckMate-040 trial (nivolumab plus ipilimumab) were obtained for patients of advanced HCC who previously received sorafenib, and demonstrated an objective response rate of 33% (95% confidence interval of 20–48) in these patients. The Food and Drug Administration has accelerated the approval of this combination therapy strategy.<sup>34</sup> Similar treatment regimens emerged for melanoma,<sup>35</sup> non-small-cell lung cancer,<sup>36</sup> and renal cell carcinoma.<sup>37</sup> Evidently, our results showed reliability and high practical utility from a clinical perspective.

Meanwhile, it is also imperative to develop novel immune therapeutic approaches. In the present study, we found *IKBKE*, *IL2RG*, *EDNRA*, and *IGHA1* to be statistically more significant with  $p < 0.2$  than *PDCD1* ( $p > 0.2$ ) among the 21 KIRGs by univariate Cox regression and multivariate Cox regression. Due to multi-step screening, we boldly defined the critical value as 0.2. *IKBKE*, a member of the nonclassical IKK family, is considered to be a potential target for



cancer therapy.<sup>38</sup> Typically, IKBKE was classified as an oncogenic effector during KRAS-induced pancreatic transformation and activated AKT signaling to promote tumorigenesis.<sup>39</sup> IKBKE-associated cytokine signaling was also shown to promote tumorigenicity of immune-driven triple-negative breast cancers.<sup>40</sup> IKBKE regulates androgen receptor levels via Hippo pathway inhibition in advanced prostate cancer.<sup>41</sup> However, the specific functions of these four factors in HCC still lack a deep understanding.

To investigate the regulatory mechanism of KIRGs, transcription factors and lncRNAs were analyzed according to their roles as crucial components of cancer regulatory networks. We identified lncRNAs associated with KIRGs and DETFs, and constructed a DETFs-lncRNAs-KIRGs regulatory network to reveal the possible functional relationship. To date, AC127024.5 has only been reported as a prognostic target for pancreatic cancer.<sup>42</sup> In HCC, we found that the NRF1-AC127024.5-IBKKE axis might be involved in the regulation of many biological processes, further underscoring its potential for clinical application. In addition, from the key lncRNAs-KIRGs network, we constructed a risk score model and verified the prognosis prediction efficiency, which could emphasize good compatibility and appropriate clinical applicability compared to several genes placed in a model based on only one data set. Our risk model showed more obvious discriminating power than that of tumor staging. Unfortunately, we could not find available data in the Gene Expression Omnibus and the International Cancer Genome Consortium, including KIRGs and lncRNAs simultaneously; thus, external validation was precluded. Ultimately, the correlation between any immune checkpoint gene and risk score indicated the current targets of immunotherapy, such as CD4 T cells and phagocytosis checkpoint immunotherapy.

Although we have identified relevant IGs, including related transcription factors and lncRNAs, there is still a long road ahead of us before these findings are able to be applied in clinical practice. This field of cancer immunotherapy also presents several obstacles and faces many challenges.<sup>43</sup> Implementation of combination therapy with immune checkpoint blockade or as an adjuvant treatment of HCC in patients will not be immediate and its potential still needs to be investigated systematically and thoroughly.

## Conclusions

In summary, our analysis results highlight the importance of IGs in the HCC microenvironment. Moreover, sufficient information on novel biomarkers, networks, and pathways further unravel the underlying molecular mechanisms in the development of HCC. Understanding the immune microenvironment signatures will be advantageous to provide persuasive justification to improve the clinical efficacy of the immunotherapy.

## Acknowledgments

We sincerely appreciate the guidance of Xinyuan Lao and Zhujun Tan of Helixlife, and the invaluable assistance of Huimei Wang, Yuanning Guo, and Liewang Qiu during the current study.

## Funding

This work was supported by the China Postdoctoral Science Foundation (grant number 2019M663445 to YC), National Natural Science Foundation of China (grant num-

ber 81602045 to JX, 81802454 to HYZ), Chongqing Basic and Frontier Research Project (grant number cstc2018jcyjAX0728 to NW), Science and Technology Planning Project of Yuzhong District of Chongqing city (grant number 20180118 to JX), and Open Research Fund Program of the Key Laboratory of Molecular Biology for Infectious Diseases, CQMU (grant number 202001 to YC).

## Conflict of interest

The authors have no conflict of interests related to this publication.

## Author contributions

Study concept and design (YC, WFH), analysis and interpretation of data (WFH, YJG), sample collection (HYZ, MXC), experimental processes and drafting of the manuscript (KZ, NW), critical revision of the manuscript for important intellectual content (YC and JX). All authors have read and approved the final manuscript.

## References

- Bray F, Ferlay J, Soerjomataram I, Siegel RL, Torre LA, Jemal A. Global cancer statistics 2018: GLOBOCAN estimates of incidence and mortality worldwide for 36 cancers in 185 countries. *CA Cancer J Clin* 2018;68:394–424. doi: 10.3322/caac.21492.
- Omata M, Cheng AL, Kokudo N, Kudo M, Lee JM, Jia J, *et al*. Asia-Pacific clinical practice guidelines on the management of hepatocellular carcinoma: a 2017 update. *Hepatol Int* 2017;11:317–370. doi: 10.1007/s12072-017-9799-9.
- Llovet JM, Zucman-Rossi J, Pikarsky E, Sangro B, Schwartz M, Sherman M, *et al*. Hepatocellular carcinoma. *Nat Rev Dis Primers* 2016;2:16018. doi: 10.1038/nrdp.2016.18.
- Hollebecque A, Malka D, Fertié C, Ducreux M, Boige V. Systemic treatment of advanced hepatocellular carcinoma: from disillusion to new horizons. *Eur J Cancer* 2015;51:327–339. doi: 10.1016/j.ejca.2014.12.005.
- Llovet JM, Ricci S, Mazzaferro V, Hilgard P, Gane E, Blanc JF, *et al*. Sorafenib in advanced hepatocellular carcinoma. *N Engl J Med* 2008;359:378–390. doi: 10.1056/NEJMoa0708857.
- Cheng AL, Kang YK, Chen Z, Tsao CJ, Qin S, Kim JS, *et al*. Efficacy and safety of sorafenib in patients in the Asia-Pacific region with advanced hepatocellular carcinoma: a phase III randomised, double-blind, placebo-controlled trial. *Lancet Oncol* 2009;10:25–34. doi: 10.1016/S1470-2045(08)70285-7.
- Kudo M, Finn RS, Qin S, Han KH, Ikeda K, Piscaglia F, *et al*. Lenvatinib versus sorafenib in first-line treatment of patients with unresectable hepatocellular carcinoma: a randomised phase 3 non-inferiority trial. *Lancet* 2018;391:1163–1173. doi: 10.1016/S0140-6736(18)30207-1.
- Jayant K, Habib N, Huang KW, Podda M, Warwick J, Arasaradnam R. Immunological basis of genesis of hepatocellular carcinoma: Unique challenges and potential opportunities through immunomodulation. *Vaccines (Basel)* 2020;8:247. doi: 10.3390/vaccines8020247.
- Zhou G, Sprengers D, Boor PPC, Doukas M, Schutz H, Mancham S, *et al*. Antibodies against immune checkpoint molecules restore functions of tumor-infiltrating T cells in hepatocellular carcinomas. *Gastroenterology* 2017;153:1107–1119.e10. doi: 10.1053/j.gastro.2017.06.017.
- El-Khoueiry AB, Sangro B, Yau T, Crocenzi TS, Kudo M, Hsu C, *et al*. Nivolumab in patients with advanced hepatocellular carcinoma (CheckMate 040): an open-label, non-comparative, phase 1/2 dose escalation and expansion trial. *Lancet* 2017;389:2492–2502. doi: 10.1016/S0140-6736(17)31046-2.
- Zhu AX, Finn RS, Edeline J, Cattani S, Ogasawara S, Palmer D, *et al*. Pembrolizumab in patients with advanced hepatocellular carcinoma previously treated with sorafenib (KEYNOTE-224): a non-randomised, open-label phase 2 trial. *Lancet Oncol* 2018;19:940–952. doi: 10.1016/S1470-2045(18)30351-6.
- Sangro B, Gomez-Martin C, de la Mata M, Inarrairaegui M, Garraza E, Barrera P, *et al*. A clinical trial of CTLA-4 blockade with tremelimumab in patients with hepatocellular carcinoma and chronic hepatitis C. *J Hepatol* 2013;59:81–88. doi: 10.1016/j.jhep.2013.02.022.
- Yau T, Kang YK, Kim TY, El-Khoueiry AB, Santoro A, Sangro B, *et al*. Nivolumab (NIVO) + ipilimumab (IPI) combination therapy in patients (pts) with advanced hepatocellular carcinoma (aHCC): Results from CheckMate 040. *J Clin Oncol* 2019;37:4012. doi: 10.1200/JCO.2019.37.15\_suppl.4012.
- Finn RS, Ryoo BY, Merle P, Kudo M, Bouattour M, Lim HY, *et al*. Pembrolizumab as second-line therapy in patients with advanced hepatocellular carcinoma in KEYNOTE-240: A randomized, double-blind, phase III trial. *J*

- Clin Oncol 2020;38:193–202. doi:10.1200/JCO.19.01307.
- [15] Hutter C, Zenklusen JC. The cancer genome atlas: Creating lasting value beyond its data. *Cell* 2018;173:283–285. doi:10.1016/j.cell.2018.03.042.
  - [16] Bhattacharya S, Andorf S, Gomes L, Dunn P, Schaefer H, Pontius J, *et al*. ImmPort: disseminating data to the public for the future of immunology. *Immunol Res* 2014;58:234–239. doi:10.1007/s12026-014-8516-1.
  - [17] Subramanian A, Tamayo P, Mootha VK, Mukherjee S, Ebert BL, Gillette MA, *et al*. Gene set enrichment analysis: a knowledge-based approach for interpreting genome-wide expression profiles. *Proc Natl Acad Sci U S A* 2005;102:15545–15550. doi:10.1073/pnas.0506580102.
  - [18] Godec J, Tan Y, Liberzon A, Tamayo P, Bhattacharya S, Butte AJ, *et al*. Compendium of immune signatures identifies conserved and species-specific biology in response to inflammation. *Immunity* 2016;44:194–206. doi:10.1016/j.immuni.2015.12.006.
  - [19] Li T, Fu J, Zeng Z, Cohen D, Li J, Chen Q, *et al*. TIMER2.0 for analysis of tumor-infiltrating immune cells. *Nucleic Acids Res* 2020;48:W509–W514. doi:10.1093/nar/gkaa407.
  - [20] Verhaak RG, Tamayo P, Yang JY, Hubbard D, Zhang H, Creighton CJ, *et al*. Prognostically relevant gene signatures of high-grade serous ovarian carcinoma. *J Clin Invest* 2013;123:517–525. doi:10.1172/JCI65833.
  - [21] Ritchie ME, Phipson B, Wu D, Hu Y, Law CW, Shi W, *et al*. limma powers differential expression analyses for RNA-sequencing and microarray studies. *Nucleic Acids Res* 2015;43:e47. doi:10.1093/nar/gkv007.
  - [22] Langfelder P, Horvath S. WGCNA: an R package for weighted correlation network analysis. *BMC Bioinformatics* 2008;9:559. doi:10.1186/1471-2105-9-559.
  - [23] Liu CJ, Hu FF, Xia MX, Han L, Zhang Q, Guo AY. GSCALite: a web server for gene set cancer analysis. *Bioinformatics* 2018;34:3771–3772. doi:10.1093/bioinformatics/bty411.
  - [24] Wang S, Sun H, Ma J, Zang C, Wang C, Wang J, *et al*. Target analysis by integration of transcriptome and ChIP-seq data with BETA. *Nat Protoc* 2013;8:2502–2515. doi:10.1038/nprot.2013.150.
  - [25] Zhou Y, Zhou B, Pache L, Chang M, Khodabakhshi AH, Tanaseichuk O, *et al*. Metascape provides a biologist-oriented resource for the analysis of systems-level datasets. *Nat Commun* 2019;10:1523. doi:10.1038/s41467-019-09234-6.
  - [26] Szklarczyk D, Gable AL, Lyon D, Junge A, Wyder S, Huerta-Cepas J, *et al*. STRING v11: protein-protein association networks with increased coverage, supporting functional discovery in genome-wide experimental datasets. *Nucleic Acids Res* 2019;47:D607–D613. doi:10.1093/nar/gky1131.
  - [27] Yang W, Soares J, Greninger P, Edelman EJ, Lightfoot H, Forbes S, *et al*. Genomics of Drug Sensitivity in Cancer (GDSC): a resource for therapeutic biomarker discovery in cancer cells. *Nucleic Acids Res* 2013;41:D955–D961. doi:10.1093/nar/gks1111.
  - [28] Seashore-Ludlow B, Rees MG, Cheah JH, Cokol M, Price EV, Coletti ME, *et al*. Harnessing connectivity in a large-scale small-molecule sensitivity dataset. *Cancer Discov* 2015;5:1210–1223. doi:10.1158/2159-8290.CD-15-0235.
  - [29] Binnewies M, Roberts EW, Kersten K, Chan V, Fearon DF, Merad M, *et al*. Understanding the tumor immune microenvironment (TIME) for effective therapy. *Nat Med* 2018;24:541–550. doi:10.1038/s41591-018-0014-x.
  - [30] Barbie DA, Tamayo P, Boehm JS, Kim SY, Moody SE, Dunn IF, *et al*. Systematic RNA interference reveals that oncogenic KRAS-driven cancers require TBK1. *Nature* 2009;462:108–112. doi:10.1038/nature08460.
  - [31] Yoshihara K, Shahmoradgol M, Martínez E, Vegesna R, Kim H, Torres-García W, *et al*. Inferring tumour purity and stromal and immune cell admixture from expression data. *Nat Commun* 2013;4:2612. doi:10.1038/ncomms3612.
  - [32] Atabaki-Pasdar N, Ohlsson M, Viñuela A, Frau F, Pomares-Millan H, Haid M, *et al*. Predicting and elucidating the etiology of fatty liver disease: A machine learning modeling and validation study in the IMI DIRECT cohorts. *PLoS Med* 2020;17:e1003149. doi:10.1371/journal.pmed.1003149.
  - [33] Lee BP, Vittinghoff E, Hsu C, Han H, Therapondos G, Fix OK, *et al*. Predicting low risk for sustained alcohol use after early liver transplant for acute alcoholic hepatitis: The sustained alcohol use post-liver transplant score. *Hepatology* 2019;69:1477–1487. doi:10.1002/hep.30478.
  - [34] Wright K. FDA approves nivolumab plus ipilimumab for the treatment of advanced HCC. *Oncology (Williston Park)* 2020;34:693606.
  - [35] Zimmer L, Livingstone E, Hassel JC, Fluck M, Eigentler T, Loquai C, *et al*. Adjuvant nivolumab plus ipilimumab or nivolumab monotherapy versus placebo in patients with resected stage IV melanoma with no evidence of disease (IMMUNED): a randomised, double-blind, placebo-controlled, phase 2 trial. *Lancet* 2020;395:1558–1568. doi:10.1016/S0140-6736(20)30417-7.
  - [36] Hellmann MD, Paz-Ares L, Bernabe Caro R, Zurawski B, Kim SW, Carcereny Costa E, *et al*. Nivolumab plus ipilimumab in advanced non-small-cell lung cancer. *N Engl J Med* 2019;381:2020–2031. doi:10.1056/NEJMoa1910231.
  - [37] Tomita Y, Kondo T, Kimura G, Inoue T, Wakumoto Y, Yao M, *et al*. Nivolumab plus ipilimumab versus sunitinib in previously untreated advanced renal-cell carcinoma: analysis of Japanese patients in CheckMate 214 with extended follow-up. *Jpn J Clin Oncol* 2020;50:12–19. doi:10.1093/jjco/hyz132.
  - [38] Yin M, Wang X, Lu J. Advances in IKBKE as a potential target for cancer therapy. *Cancer Med* 2020;9:247–258. doi:10.1002/cam4.2678.
  - [39] Rajurkar M, Dang K, Fernandez-Barrena MG, Liu X, Fernandez-Zapico ME, Lewis BC, *et al*. IKBKE is required during KRAS-induced pancreatic tumorigenesis. *Cancer Res* 2017;77:320–329. doi:10.1158/0008-5472.CAN-15-1684.
  - [40] Barbie TU, Alexe G, Aref AR, Li S, Zhu Z, Zhang X, *et al*. Targeting an IKBKE cytokine network impairs triple-negative breast cancer growth. *J Clin Invest* 2014;124:5411–5423. doi:10.1172/JCI75661.
  - [41] Bainbridge A, Walker S, Smith J, Patterson K, Dutt A, Ng YM, *et al*. IKBKE activity enhances AR levels in advanced prostate cancer via modulation of the Hippo pathway. *Nucleic Acids Res* 2020;48:5366–5382. doi:10.1093/nar/gkaa271.
  - [42] Wei C, Liang Q, Li X, Li H, Liu Y, Huang X, *et al*. Bioinformatics profiling utilized a nine immune-related long noncoding RNA signature as a prognostic target for pancreatic cancer. *J Cell Biochem* 2019;120:14916–14927. doi:10.1002/jcb.28754.
  - [43] Hegde PS, Chen DS. Top 10 challenges in cancer immunotherapy. *Immunity* 2020;52:17–35. doi:10.1016/j.immuni.2019.12.011.



Original Article

# Differentiation of Hepatocellular Carcinoma from Hepatic Hemangioma and Focal Nodular Hyperplasia using Computed Tomographic Spectral Imaging

Weixia Li<sup>1#</sup>, Ruokun Li<sup>1#</sup>, Xiangtian Zhao<sup>2#</sup>, Xiaozhu Lin<sup>3</sup>, Yixing Yu<sup>4</sup>, Jing Zhang<sup>1</sup>, Kemin Chen<sup>1</sup>, Weimin Chai<sup>1</sup> and Fuhua Yan<sup>1\*</sup>

<sup>1</sup>Department of Radiology, Ruijin Hospital Affiliated to Shanghai Jiao Tong University School of Medicine, Shanghai, China;

<sup>2</sup>Department of Radiology, Guangdong General Hospital, Guangdong Academy of Medical Sciences, Guangzhou, Guangdong, China;

<sup>3</sup>Department of Nuclear Medicine, Ruijin Hospital affiliated to Shanghai Jiao Tong University School of Medicine, Shanghai, China;

<sup>4</sup>Department of Radiology, The First Affiliated Hospital of Soochow University, Suzhou, Jiangsu, China

Received: 21 December 2020 | Revised: 26 February 2021 | Accepted: 7 March 2021 | Published: 31 March 2021

## Abstract

**Background and Aims:** Hepatocellular carcinoma (HCC) is the most common primary hepatic malignancy. This study was designed to investigate the value of computed tomography (CT) spectral imaging in differentiating HCC from hepatic hemangioma (HH) and focal nodular hyperplasia (FNH). **Methods:** This was a retrospective study of 51 patients who underwent spectral multiple-phase CT at 40–140 keV during the arterial phase (AP) and portal venous phase (PP). Slopes of the spectral curves, iodine density, water density derived from iodine- and water-based material decomposition images, iodine uptake ratio (IUR), normalized iodine concentration, and the ratio of iodine concentration in liver lesions between AP and PP were measured or calculated. **Results:** As energy level decreased, the CT values of HCC ( $n=31$ ), HH ( $n=17$ ), and FNH ( $n=7$ ) increased in both AP and PP. There were significant differences in IUR in the AP, IUR in the PP, normalized iodine concentration in the AP, slope in the AP, and slope in the PP among HCC, HH, and FNH. The CT values in AP, IUR in the AP and PP, normalized iodine concentration in the AP, slope in the AP and PP had high sensitivity and specificity in differentiating HH and HCC from FNH. Quantitative CT spectral data had higher sensitivity and specificity than conventional qualitative CT image analysis during the combined phases. **Conclusions:** Mean CT values at low energy (40–90 keV) and quantitative

analysis of CT spectral data (IUR in the AP) could be helpful in the differentiation of HCC, HH, and FNH.

**Citation of this article:** Li W, Li R, Zhao X, Lin X, Yu Y, Zhang J, *et al.* Differentiation of hepatocellular carcinoma from hepatic hemangioma and focal nodular hyperplasia using computed tomographic spectral imaging. J Clin Transl Hepatol 2021;9(3):315–323. doi: 10.14218/JCTH.2020.00173.

## Introduction

Hepatocellular carcinoma (HCC) is the most common primary hepatic malignant tumor and the third leading cause of cancer-related death worldwide, with annual mortality rates of 14.3 per 100,000 men and 5.1 per 100,000 women.<sup>1,2</sup> Hepatic hemangioma (HH) and focal nodular hyperplasia (FNH) are the most and the second most common benign hepatic lesions.<sup>3–5</sup> Since the three lesions may share some characteristics upon imaging examination, the differentiation of HCC from HH and FNH is very critical, as their clinical courses, prognosis, and treatment are markedly different.

About 80–90% of HCCs occur as a complication of chronic liver disease, secondary to viral hepatitis B- or C-induced cirrhosis or alcoholic cirrhosis; therefore, patient clinical history may be helpful for the differential diagnosis of HCC from HH and FNH.<sup>6–8</sup> Nevertheless, the remaining 10–20% of HCCs can be found in a low-risk population or in patients without alcohol abuse. Besides, typical HCC, HH, and FNH can be diagnosed with confidence using ultrasound, contrast-enhanced computed tomography (CT), or magnetic resonance imaging (commonly known as MRI),<sup>9–21</sup> but in some instances, HCC may display atypical imaging presentations if the tumor is well-differentiated,<sup>22,23</sup> small ( $\leq 2$  cm),<sup>24</sup> with fatty metamorphosis,<sup>25,26</sup> or with abundant interstitial fibrosis.<sup>10,27,28</sup> In addition, HH may show slow enhancement or homogeneous enhancement during the arterial phase (AP),<sup>29–32</sup> while atypical FNH may show non-enhancement of the central scar, less intense enhancement of the tumor, and pseudo-capsular enhancement in delayed images.<sup>33</sup> In the presence of atypical imaging appearances, it may not be easy to distinguish HCC from HH and FNH.

**Keywords:** Hepatocellular carcinoma; Hepatic hemangioma; Focal nodular hyperplasia; Computed tomography spectral imaging; Spectral curve.

**Abbreviations:** AP, arterial phase; AUC, the area under the ROC curve; CNR, contrast-to-noise ratio; CT, computed tomography; DECT, dual-energy computed tomography; FNH, focal nodular hyperplasia; GSI, gemstone spectral imaging; HCC, hepatocellular carcinoma; HH, hepatic hemangioma; ICR, iodine concentration ratio; ID, iodine density; IUR, iodine uptake ratio; LNR, lesion-to-normal parenchyma ratio; MD, material decomposition; MRI, magnetic resonance imaging; NIC, normalized iodine concentrations; PACS, picture archiving and communication system; PP, portal venous phase; ROC, receiver operating characteristic; ROI, Regions of interest; WD, water density.

\*These authors contributed equally to this work.

**\*Correspondence to:** Fuhua Yan, Department of Radiology, Ruijin Hospital Affiliated to Shanghai Jiao Tong University School of Medicine, 197 Ruijin Erlu, Huangpu District, Shanghai 200025, China. ORCID: <https://orcid.org/0000-0002-6385-499X>. Tel: +86-21-6437-0045-665724, Fax: +86-21-6384-2916, E-mail: [yfh11655@rjh.com.cn](mailto:yfh11655@rjh.com.cn)

Many studies have shown superior performance of MRI over conventional CT in the diagnosis of HCC;<sup>34,35</sup> however, it may be contraindicated in some patients or may result in insufficient image quality in some patients with ascites or patients incapable of holding their breath. With the introduction of dual-energy CT (commonly referred to as DECT) spectral imaging in the field of liver imaging, several studies have shown the benefit of DECT in the improved evaluation of microvascular invasion in HCC,<sup>36</sup> in the visualization and quantification of HCC,<sup>37</sup> and in the early detection of HCC and hypervascular liver tumors.<sup>38–40</sup> DECT improved soft tissue contrast by generating different monochromatic images,<sup>41,42</sup> which also showed that material decomposed images could provide increased contrast in the visualization of the AP hyperenhancement and washout in HCC compared to both monoenergetic 65 keV images and MRI.<sup>37</sup> Until now, only a few studies have reported spectral CT being used in differentiating small HH,<sup>43,44</sup> FNH<sup>45</sup> or angiomyolipoma<sup>46</sup> from HCC with only a few parameters, such as the contrast-to-noise ratio, normalized iodine concentrations (referred to as NIC), and lesion-to-normal parenchyma iodine concentration ratio. Nevertheless, there is almost no literature about systematic and comprehensive comparisons using CT attenuation values derived from a set of monochromatic images (40–140 keV) and other quantitative assessments, including iodine density (referred to as ID), water density (referred to as WD), and the slopes of the spectral curve between HCC, HH, and FNH.

Therefore, this study aimed to describe CT attenuation values derived from a set of monochromatic images and material density-related quantitative assessments for HCC, HH, and FNH, and to evaluate the value of CT spectral imaging in distinguishing HCC from HH and FNH.

## Methods

### Patients

This retrospective study included patients with known or suspected liver tumors, who underwent dynamic enhancement CT scanning in gemstone spectral imaging (GSI) mode on a Discovery CT750 HD scanner (GE Healthcare, Chicago, IL, USA) between February 2012 and January 2018. The exclusion criteria were: 1) no HCC, HH, or FNH; 2) no histological confirmation; 3) with prior trans-arterial chemoembolization or radiofrequency ablation; or 4) recurrent HCC after liver resection or transplantation. This study was approved by the ethics committee of Ruijin Hospital Affiliated to Shanghai Jiao Tong University School of Medicine. Individual consent was waived because of the retrospective nature of the study.

### Diagnostic procedures

All HCCs were confirmed pathologically after surgical resection. The HCCs were graded according to the Edmondson-Steiner classification.<sup>47</sup> The diagnosis of HH was established based on histological specimens obtained at partial hepatectomy or typical multiple-phase CT findings, including peripheral nodular enhancement similar to the enhancement of blood vessels at the AP and centripetal fill-in enhancement at the portal venous phase (PP). FNH was proven pathologically after surgical resection because of diagnostic uncertainty after MRI or initial misdiagnosis as HCC.

### CT examinations

All patients underwent triple-phase CT within a maximum

of 10 days of surgery, using the high-definition Discovery CT750 HD scanner. The detailed scan parameters are provided in the online supplementary materials. Three types of images were reconstructed from the single spectral CT acquisition for analysis, namely conventional polychromatic images obtained at 140 kVp, iodine- and water-based material decomposition (referred to as MD) images, and a set of monochromatic images obtained with energy levels ranging from 40 to 140 keV.

### Quantitative analyses

All measurements were performed on an advanced workstation (AW 4.4; GE Healthcare) using the GSI viewer software, by a single radiologist experienced in abdominal radiology and blind to the results of all patients. The 70 keV monochromatic images and iodine-based MD images were reviewed first. Regions of interest (referred to as ROIs) were placed in the lesions, normal liver parenchyma, and aorta on the default 70-keV monochromatic images (Fig. 1). The GSI viewer software automatically calculated the mean CT attenuation value and standard deviation at different energy levels (40–140 keV, at 10-keV intervals) from the set of monochromatic image and ID and WD values from the iodine- and water-based (IDM and WDM, respectively) images during AP and PP.<sup>48</sup> Four parameters were obtained from the measurements of CT values and iodine concentration. The NIC during AP was calculated as ratio of the iodine concentrations in AP in the lesions and aorta. Iodine concentrations in the lesions in AP were normalized to those of the aorta in order to minimize variations among patients. The iodine uptake ratio (IUR) was calculated as the ratio of the mean iodine concentrations in the lesions and in the non-tumor hepatic parenchyma surrounding the lesion. The iodine concentration ratio (ICR) in liver lesions between AP and PP was calculated as the difference of the iodine concentrations in the lesions during AP and PP. The slopes of the spectral curve in AP and PP were calculated as  $(CT_{40keV} - CT_{90keV})/50$ , where  $CT_{40keV}$  and  $CT_{90keV}$  were the mean CT attenuation values in the lesions at 40 keV and 90 keV of the spectral curves, respectively.

### Qualitative analysis

Two radiologists (WXL and XTZ, with 15 and 14 years of experience in abdominal CT imaging, respectively) qualitatively reviewed the 70 keV monochromatic images by consensus with the GSI viewer at the workstation. Neither observer was aware of clinical, surgical, and pathologic findings. The observers documented the following enhancement and morphologic features: number; maximal diameter on transverse images; necrosis or cyst; scar; and, enhancement pattern and degree. The enhancement patterns and degrees were evaluated for any enhancing portion of the lesion relative to the aorta and the adjacent liver parenchyma during AP and relative to the adjacent liver parenchyma during PP. The enhancement patterns were described as globular or nodular, diffuse homogeneous, or heterogeneous. The enhancement degree of the lesion was classified as hyper-, iso-, or hypo-enhancement compared with surrounding liver parenchyma. The changes in enhancement degree between AP and PP were characterized as expansion, washout, or none. The expansion was defined as a hyperenhancement area in the lesion during both AP and PP. Washout was defined as a change from hyper- or iso-enhancement area in the lesion during AP to a hypo-enhancement area in the lesion compared with surrounding liver parenchyma during PP, while none was defined as a hyper- or iso-enhancement



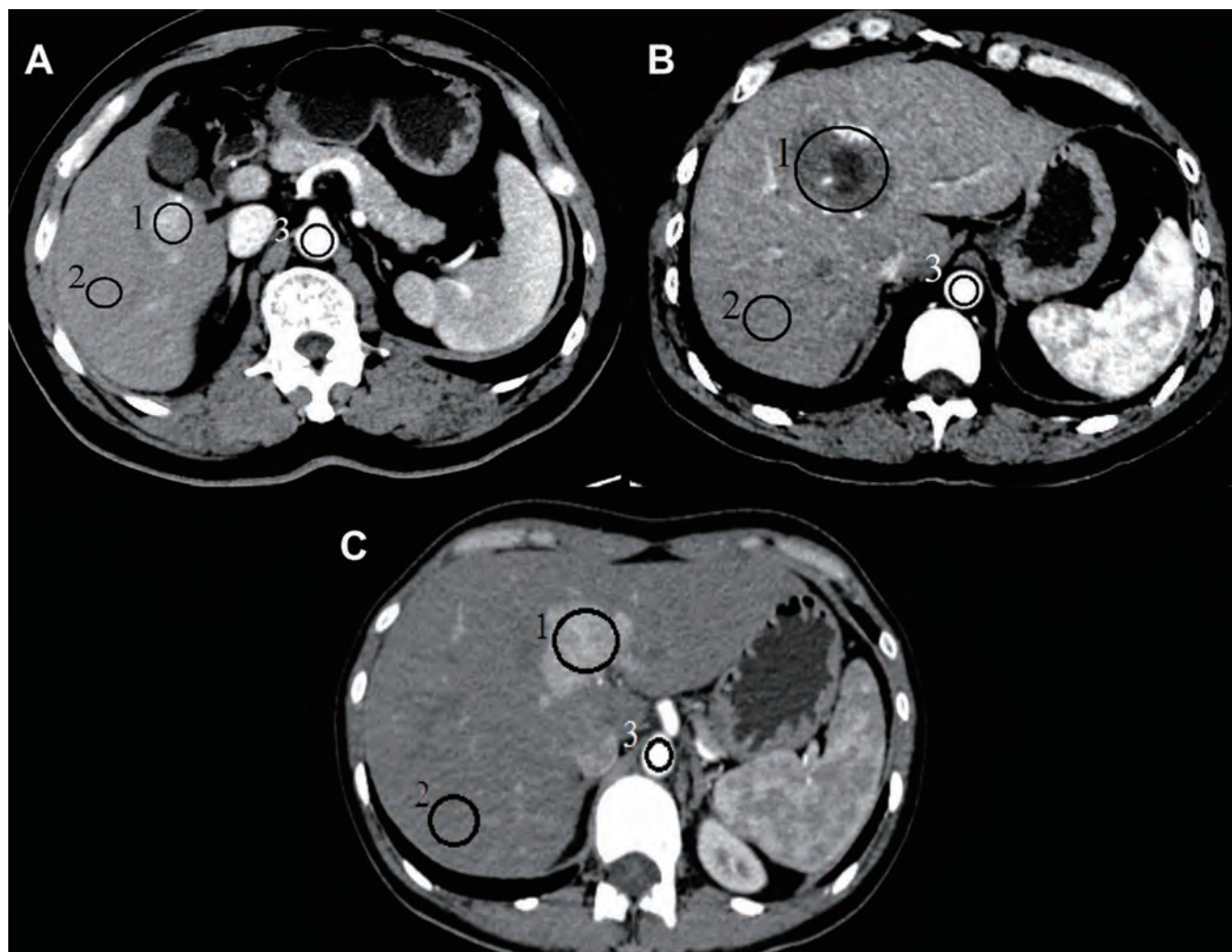


**Fig. 1. DECT imaging of liver lesions.** Circular or elliptical ROIs were placed in the lesion (#1), normal hepatic parenchyma (#2), and aorta (#3) on the default 70-keV monochromatic images. DECT, dual-energy computed tomography; ROI, region of interest.

area in the lesion during AP to an iso-enhancement area in the lesion compared with adjacent liver parenchyma during PP.

Finally, the observers, in consensus, characterized each lesion type as HCC, HH, and FNH based on imaging features (online supplementary materials). Differences among the observers were resolved by means of consensus discussion. The definition of the sensitivity and specificity for differential diagnosis of HCC, HH and FNH are demonstrated in the online supplementary materials.

### Statistical analysis

The data were analyzed using SPSS 13.0 (SPSS Inc., Chicago, IL, USA). Continuous variables were presented as median (interquartile range) after confirming their non-normal distribution using the Kolmogorov-Smirnov test. The estimated parameters were analyzed among HCC, HH, and FNH groups using the Kruskal-Wallis test, with the Wilcoxon rank-sum post hoc test. Receiver operating characteristic (ROC) curves were used to help establish the threshold values of the mean CT values at different energy levels (40–

140 keV), IDM, WDM, IUR and slope in AP, and PP, and ICR required for significant differentiation of HCC, HH, and FNH. The diagnostic capability was determined by calculating the area under the ROC curve (AUC). The best sensitivity and specificity were determined using the optimal thresholds based on the Youden's index. A two-sided *p* value of <0.05 was considered statistically significant. Qualitative CT imaging features were compared among HCC, HH, and FNH by Fisher's exact tests.

## Results

### Patients

From 476 potentially eligible patients, 425 were excluded based on the following exclusion criteria: 1) no HCC, HH, or FNH; 2) no histological confirmation; 3) with prior transarterial chemoembolization or radiofrequency ablation; or 4) recurrent HCC after liver resection or transplantation. Therefore, 51 patients (30 males and 21 females) were included, with 31 HCCs in 31 patients, 17 HHs in 13 patients, and 7

**Table 1. Characteristics of the patients**

Variable	HCC, <i>n</i> =31	HH, <i>n</i> =13	FNH, <i>n</i> =7
Number of lesions	31	17	7
Age in years, median (IQR)	57.0 (16.0)	48.0 (18.0)	24.0 (11.0)
Male, <i>n</i> (%)	26 (83.4)	2 (15.4)	2 (28.6)
Background liver status, <i>n</i> (%)			
Normal liver	2 (6.5)	13 (100)	7 (100)
Cirrhosis	29 (93.5)	0	0
Cause, <i>n</i> (%)			
HBV infection	28 (90.3)	0	0
HBV and alcoholic cirrhosis	1 (9.7)	0	0
Tumor size in cm, median (IQR)	3.00 (3.00)	5.30 (3.35)	5.00 (2.00)

FNH, focal nodular hyperplasia; HBV, hepatitis B virus; HCC, hepatocellular carcinoma; HH, hepatic hemangioma; IQR, interquartile range.

FNHs in 7 patients (Table 1). According to the Edmondson-Steiner classification, two HCCs were grade I, fourteen were grade II, thirteen were grade III, and two were grade IV. All patients who were diagnosed as HH with multiple-phase CT findings were followed for at least 3 years. No patient was lost to follow-up.

### Quantitative analysis

**CT values:** Regarding the CT values of HCC, HH, and FNH, there was a trend towards a decrease in mean CT values of HH, HCC, and FNH as energy level increased (40–140 keV) in both AP and PP (Table 2 and Fig. 2). HH had the lowest mean CT values, while FNH had the highest mean CT values at different energy levels (40–140 keV) in both AP and PP (Table 2 and Fig. 2). Moreover, there were significant differences in CT values at energy levels from 40 to 140 keV during AP and PP (Table 2) for HCC vs. FNH, and HH vs. FNH. There were significant differences between HCC and HH at energy levels from 40 to 140 keV in AP and only at energy levels from 40 to 100 keV in PP (Table 2).

ROC curve analysis revealed that the mean CT values from 40–140 keV in both AP and PP, especially at 40–120 keV in AP (all AUC=1) and 120 keV in PP (AUC=0.992) had the best performance in differentiating HH from FNH. The mean CT values at 80–90 keV in AP (both AUC=0.926) and 100 keV in PP (AUC=0.949) had better performance in differentiating HCC from FNH. Meanwhile, the mean CT values at 40–50 keV in AP (AUC=0.896) and 40–50 keV in PP (AUC=0.780) had high sensitivity and specificity in differentiating HCC from HH. See Supplementary Tables S1–S3.

**Standard deviation of the mean CT values:** For the standard deviation of the mean CT values of HCC, HH, and FNH in AP and PP (Table 3), there were significant differences at 40 to 100 keV during PP between HCC and HH, and from 40 to 140 keV during PP between HH and FNH. In addition, sensitivity (88.2%) and specificity (100%) showed that the standard deviation of mean CT values at 40 keV in PP (AUC=0.882) had the best performance in differentiating HH from FNH. The standard deviation of mean CT values from 40–140 keV in PP showed low sensitivity and specificity in differentiating between HCC and FNH. The standard deviation of mean CT values at 40–100 keV in PP, especially at 50 keV (AUC=0.846), had the best sensitivity and specificity in differentiating between HCC and HH. See Supplementary Tables S4–S6.

### Quantitative assessments

For the spectral CT imaging-specific quantitative assessments of HCC, HH, and FNH, there were significant differences in IUR, slope in AP and PP, NIC in AP (which tended to increase from HH, HCC to FNH) between every two groups of HCC, HH, and FNH (Table 4). IDM in both AP and PP, WDM in PP, and ICR revealed significant differences between HH and FNH, as well as IDM in AP and PP, and ICR between HH and HCC, WDM in PP between HCC and FNH also differed significantly (Table 4). ROC curve analysis demonstrated that ICR and slope in AP had the best diagnostic performance (AUC=0.992) in differentiating HH from FNH. While IUR in AP had better performance (AUC=0.903) in differentiating HCC from FNH. For distinguishing HCC from HH, IDM and slope in AP, ICR had good performance (AUC=0.890). See Supplementary Tables S7–S9.

### Qualitative analysis

The CT features of the HH, HCC, and FNH groups were analyzed and listed in Table 5. Feeding vessels were found in 15 (48.4%) of the 31 HCCs, 6 (85.7%) of the 7 FNHs, and none was found in HHs (both  $p<0.001$  for HCC vs. HH, FNH vs. HH, respectively). Thirteen (76.5%) of seventeen HHs showed globular or nodular enhancement during AP, whereas neither HCCs nor FNHs showed it (both  $p<0.001$  for HH vs. HCC and for HH vs. FNH). Fourteen (82.4%) of seventeen HHs demonstrated expansion change of enhancement between AP and PP ( $p<0.001$  for HH vs. HCC and  $p=0.001$  HCC vs. FNH, respectively), whereas twenty-two (71%) of the thirty-one lesions of HCC demonstrated washout change of enhancement between AP and PP ( $p<0.001$  for HH vs. HCC and  $p=0.001$  for HCC vs. FNH, respectively).

In the conventional qualitative analysis of imaging features with combined AP and PP, we achieved sensitivity of 83.9% (26 of 31 HCCs) and specificity of 82.4% (14 of 17 HHs), respectively, for differentiating between HCC and HH, which was lower than quantitative image analysis with CT spectral imaging, which had sensitivity of 87.1% and specificity of 88.2%. Meanwhile, for differentiating between FNH and HH, we achieved sensitivity of 76.5% (13 of 17 HHs) vs. 100%, specificity 71.4% (5 of 7 FNHs) vs. 100%. In addition, we achieved sensitivity of 80.6% (25 of 31 HCCs) vs. 100%, and specificity 71.4% (5 of 7 FNHs) vs. 90.3%, respectively.

Table 2. Mean CT attenuation values of HCC, HH, and FNH at energy levels ranging 40–140 keV (at 10-keV intervals) during AP and PP

Energy in keV	HH, <i>n</i> =17	HCC, <i>n</i> =31	FNH, <i>n</i> =7	<i>p</i>		
				HCC vs. HH	HCC vs. FNH	FNH vs. HH
AP						
40	102.77 (57.02)	210.02 (125.86)	318.74 (165.34)	<0.001*	0.004*	<0.001*
50	81.67 (36.37)	156.48 (83.43)	224.71 (113.64)	<0.001*	0.003*	<0.001*
60	66.45 (23.41)	115.87 (57.17)	166.84 (71.39)	<0.001*	0.006*	<0.001*
70	59.31 (17.24)	95.09 (41.81)	130.42 (42.74)	<0.001*	0.001*	<0.001*
80	54.65 (15.29)	81.35 (29.19)	113.65 (26.49)	<0.001*	<0.001*	<0.001*
90	48.65 (15.52)	71.15 (23.73)	103.64 (16.13)	<0.001*	<0.001*	<0.001*
100	47.45 (16.05)	65.59 (22.63)	90.07 (15.13)	<0.001*	0.001*	<0.001*
110	46.99 (15.41)	61.76 (20.84)	78.06 (17.20)	0.002*	0.001*	<0.001*
120	45.56 (15.06)	58.96 (20.06)	69.62 (18.75)	0.004*	0.001*	<0.001*
130	44.08 (14.76)	56.62 (17.53)	65.52 (21.27)	0.008*	0.002*	<0.001*
140	42.89 (14.21)	53.91 (16.29)	62.56 (23.54)	0.018*	0.004*	<0.001*
PP						
40	179.57 (89.33)	246.44 (78.64)	338.48 (63.72)	0.001*	0.004*	0.001*
50	131.95 (58.34)	176.12 (50.17)	238.85 (38.62)	0.001*	0.002*	0.001*
60	102.98 (40.96)	132.85 (36.90)	177.56 (32.60)	0.002*	0.001*	0.001*
70	84.44 (28.58)	105.22 (25.08)	142.38 (28.65)	0.003*	0.001*	0.001*
80	72.55 (22.82)	87.80 (19.26)	114.83 (26.14)	0.004*	<0.001*	<0.001*
90	64.49 (19.53)	74.59 (16.54)	98.60 (24.60)	0.010*	<0.001*	<0.001*
100	59.04 (18.46)	66.74 (16.56)	87.38 (23.48)	0.036*	<0.001*	<0.001*
110	54.73 (17.71)	60.70 (16.34)	79.44 (22.23)	0.065	<0.001*	<0.001*
120	50.80 (16.64)	56.48 (15.14)	73.88 (21.25)	0.113	0.001*	<0.001*
130	47.87 (15.76)	53.57 (13.83)	69.62 (21.17)	0.185	0.001*	<0.001*
140	47.05 (15.01)	50.92 (13.13)	66.25 (21.36)	0.200	0.002*	0.001*

Data are expressed as median (interquartile range). \**p*<0.05. AP: arterial phase; FNH, focal nodular hyperplasia; HCC, hepatocellular carcinoma; HH, hepatic hemangioma.

## Discussion

The present study suggests that spectral CT can be helpful for differentiating HCC from HH and FNH. HH had the lowest mean CT values, while FNH had the highest mean CT values at different energy levels. The different slopes clearly indicated that the CT spectral imaging could distinguish HCC, HH, and FNH.

Treatment options and the prognosis of HCC, HH, and FNH are markedly different. Previous studies discussed the role of CT in the diagnosis of HCC, HH, and FNH,<sup>9,11,19,20,30–33</sup> but they were primarily focusing on analyzing the imaging features of the lesions qualitatively. Some studies reported quantitative evaluations of spectral CT in differentiating small HH,<sup>43</sup> FNH,<sup>45</sup> or angiomyolipoma<sup>46</sup> from HCC with only a few parameters. This study systematically and comprehensively compared CT values derived from a set of monochromatic images (from 40 to 140 keV at 10-keV intervals), and quantitative assessments including ID, WD, and the slopes of the spectral curve for differentiating HCC, HH, and FNH. The study expands the results of previous studies<sup>43,45,46</sup> that only examined spectral CT features of HCC vs. one lesion type and with limited energy levels. This is supported by Wang *et al.*,<sup>48</sup> who showed that spectral CT

features could differ between malignant and benign liver lesions.

The present study shows that the mean CT values and the standard deviation of mean CT values measured on monochromatic images at low energy levels (40–90 keV), especially in AP, have better contrast resolution compared to monochromatic images at high energy levels (100–140 keV). This means that the CT values and their standard deviation (which represent the heterogeneity of lesions in CT values) measured on monochromatic images at certain energy levels could be helpful for the differential diagnosis of different hypervascular hepatic tumors. This is partly similar to the studies reported by Lv *et al.*<sup>40</sup> and Yu *et al.*,<sup>45</sup> who found that monochromatic images at energy levels of 40–70 keV could improve the differential diagnosis of small HCC compared to conventional polychromatic images. ROC curve analysis in the study also confirmed that quantitative analysis of CT spectral data had higher sensitivity and specificity with those of conventional qualitative CT image analysis during combined phases for differentiating HCC, FNH and HH.

According to the present study results, all values of IUR in the AP for HCC, FNH, and HH were >1, which means that all three groups showed hyperenhancement appearance during AP. The value of IUR in the PP of HCC was <1 during

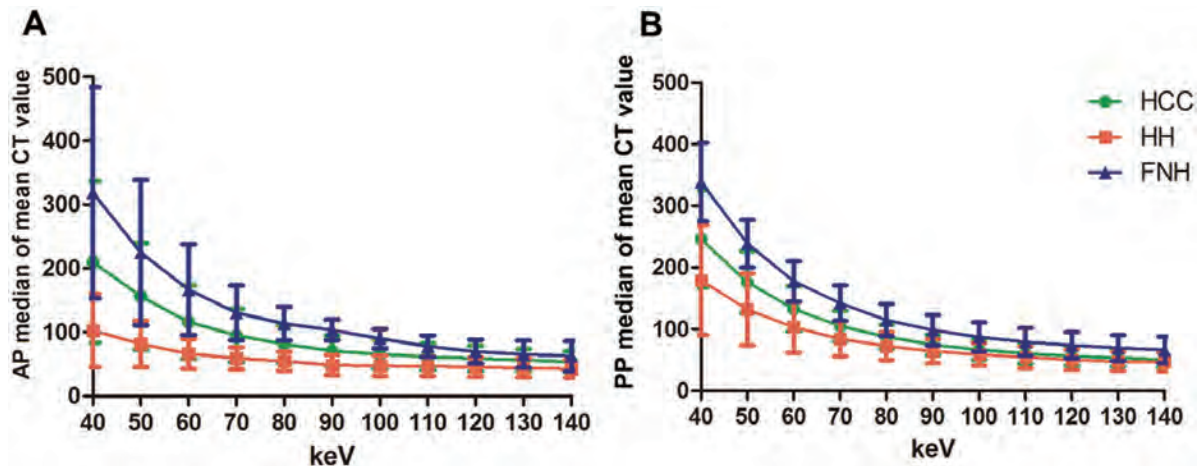


**Fig. 2. Spectral curves of HH, HCC, and FNH in AP and PP.** (A) The spectral curves of HH, HCC, FNH at different energy levels (40–140 keV). CT values peaked at 40 keV and decreased as photon energy increased in the AP for all three lesions. (B) The spectral curves of HH, HCC, and FNH at different energy levels (40–140 keV). CT values peaked at 40 keV and decreased as photon energy increased in the PP for all three lesions. AP, arterial phase; FNH, focal nodular hyperplasia; HCC, hepatocellular carcinoma; HH, hepatic hemangioma; PP, portal venous phase.

**Table 3. Standard deviations of mean CT attenuation values (the heterogeneity of lesions in mean CT values) of HCC, HH, and FNH at energy levels ranging 40–140 keV (at 10-keV intervals) during AP and PP**

Energy in keV	HH, <i>n</i> =17	HCC, <i>n</i> =31	FNH, <i>n</i> =7	<i>p</i>		
				HCC vs. HH	HCC vs. FNH	FNH vs. HH
AP						
40	74.15 (54.18)	62.04 (20.15)	58.32 (47.92)	0.407	0.985	0.589
50	48.04 (35.43)	42.05 (14.65)	41.27 (36.32)	0.438	0.778	0.727
60	33.63 (23.01)	31.79 (12.21)	34.00 (24.50)	0.659	0.665	0.924
70	23.63 (15.87)	21.77 (7.81)	23.16 (17.35)	0.643	0.624	0.775
80	21.84 (7.10)	20.42 (5.83)	19.89 (10.86)	0.316	0.585	0.727
90	23.60 (4.95)	19.87 (8.73)	22.82 (7.54)	0.152	0.721	0.727
100	24.24 (6.80)	19.71 (12.44)	22.88 (5.92)	0.337	0.836	0.193
110	23.00 (7.59)	20.26 (14.06)	21.16 (4.60)	0.407	0.985	0.216
120	23.23 (8.71)	19.52 (12.42)	19.82 (3.55)	0.525	0.778	0.172
130	23.45 (9.56)	19.64 (12.36)	18.73 (2.92)	0.553	0.679	0.266
140	23.67 (10.21)	19.44 (13.13)	17.92 (2.42)	0.511	0.638	0.357
PP						
40	125.30 (73.50)	52.41 (30.98)	54.04 (18.74)	<0.001*	0.778	0.001*
50	81.20 (46.81)	35.60 (16.82)	39.27 (11.48)	<0.001*	0.440	0.001*
60	54.92 (31.65)	25.12 (13.28)	31.96 (6.28)	<0.001*	0.463	0.001*
70	39.25 (21.45)	17.61 (8.43)	21.41 (4.70)	<0.001*	0.283	0.002*
80	32.81 (13.96)	18.22 (5.73)	18.30 (3.85)	<0.001*	0.865	0.001*
90	28.89 (8.62)	21.07 (10.46)	20.15 (5.14)	<0.001*	0.463	0.001*
100	27.20 (5.05)	21.02 (10.67)	19.20 (6.34)	0.011*	0.275	0.001*
110	24.88 (6.76)	20.76 (11.82)	17.73 (6.82)	0.054	0.251	0.003*
120	24.86 (8.45)	20.67 (13.16)	16.73 (7.17)	0.200	0.236	0.006*
130	24.72 (10.42)	20.86 (14.19)	15.98 (7.39)	0.258	0.236	0.010*
140	24.31 (11.75)	20.01 (15.08)	15.44 (7.55)	0.337	0.221	0.010*

Data are expressed as median (interquartile range). \**p*<0.05. AP: arterial phase; FNH, focal nodular hyperplasia; HCC, hepatocellular carcinoma; HH, hepatic hemangioma; PP, portal venous phase.



Table 4. Quantitative assessment of HCC, HH and FNH with CT spectral imaging

	HH, n=17	HCC, n=31	FNH, n=7	p		
				HCC vs. HH	HCC vs. FNH	FNH vs. HH
IDM in the AP (water mg/mL)	0.75 (0.70)	2.04 (1.51)	3.34 (2.56)	<0.001*	0.080	0.006*
IDM in the PP (water mg/mL)	1.73 (1.00)	2.56 (1.17)	3.53 (1.09)	0.002*	0.052	0.017*
WDM in the AP (iodine mg/mL)	1,037.77 (11.12)	1,038.99 (12.22)	1,046.02 (20.98)	0.872	0.087	0.105
WDM in the PP (iodine mg/mL)	1,038.22 (16.80)	1,035.67 (12.53)	1,047.36 (22.31)	0.643	0.010*	0.039*
ICR	0.45 (0.18)	0.81 (0.26)	0.95 (0.10)	<0.001*	0.118	<0.001*
IUR in the AP	1.22 (0.61)	2.70 (1.75)	6.94 (6.39)	<0.001*	0.001*	<0.001*
IUR in the PP	0.57 (0.30)	0.93 (0.32)	1.18 (0.29)	0.002*	0.009*	0.002*
NIC in the AP	0.06 (0.06)	0.17 (0.13)	0.29 (0.08)	<0.001*	0.002*	0.002*
Slope in the AP	1.01 (0.98)	2.78 (2.06)	4.54 (2.45)	<0.001*	0.008*	<0.001*
Slope in the PP	2.34 (1.36)	3.48 (1.58)	4.80 (1.32)	0.007*	0.004*	0.001*

Data are expressed as median (interquartile range). \*p<0.05. AP: arterial phase; FNH, focal nodular hyperplasia; HCC, hepatocellular carcinoma; HH, hepatic hemangioma; PP, portal venous phase.

Table 5. Qualitative CT assessment of lesions

Feature	HH, n=17	HCC, n=31	FNH, n=7	p		
				HCC vs. HH	HCC vs. FNH	FNH vs. HH
Necrosis or cyst	2 (11.8)	7 (22.6)	0 (0)	0.460	0.309	1
Central scars	2 (11.8)	0 (0)	4 (57.1)	0.121	0.001*	0.174
Presence of feeding vessels	0 (0)	15 (48.4)	6 (85.7)	<0.001*	0.104	<0.001*
Pseudocapsule	0 (0)	8 (25.8)	3 (42.9)	0.038	0.390	0.017*
Attenuation of enhancing area in AP						
Similar to aorta	7 (41.2)	0 (0)	0 (0)	<0.001*	–	0.065
Less than aorta, greater than adjacent liver parenchyma	10 (58.8)	31 (100)	7 (100)	<0.001*	–	0.065
Enhancement pattern in AP						
Globular or nodular	13 (76.5)	0 (0)	0 (0)	<0.001*	–	<0.001*
Diffuse homogeneous	4 (23.5)	10 (32.3)	5 (71.4)	0.741	0.089	0.061
Diffuse heterogeneous	0 (0)	21 (67.7)	2 (28.6)	<0.001*	0.089	0.076
Enhancement change between AP and PP						
Expansion	14 (82.4)	0 (0)	4 (57.1)	<0.001*	0.001*	0.307
Washout	0 (0)	22 (71)	0 (0)	<0.001*	0.001*	–
None	3 (17.6)	9 (29)	4 (42.9)	0.497	0.203	0.134

Data represent number of lesions. Numbers in parentheses are percentages. The p-values were calculated using Fisher's exact test. \*p<0.05; –, unable to calculate p-value using Fisher's exact test. FNH, focal nodular hyperplasia; HCC, hepatocellular carcinoma; HH, hepatic hemangioma.

PP, which was in line with the characteristics of “washout” feature of typical HCC during PP. While the value of IUR of FNH >1 during PP conformed to persistent enhancement characteristics of most FNH during PP. On the other hand, the value of IUR <1 in PP for HH, was contrary to the typically persistent enhancement feature. This could be due to the measurement of IDM in PP, including the part of HH without iodine filling during AP or PP. The ROI encompassed as much of the lesions as possible in order to measure the heterogeneity of lesion, and this caused the IUR in PP (IDM in PP of the lesion divided by the IDM in the PP of the liver) to be >1.

The present study did have some limitations. First, this was a retrospective study, with all the biases inherent to that study design. Second, this was a preliminary study with a small number of patients and needs to be verified by additional studies performed with a larger number of patients. Third, the HCCs in the present study were not classified by histopathological grade, because the numbers of patients in grades I and IV were too small. Fourth, because only one reader examined the images, intra- or inter-observer variability data were lacking. Fifth, and most importantly, there was a lack of correlation with conventional MDCT morphologic findings and typical features. Finally, quantitative analysis is time-consuming, and many of the described parameters could not be quantitated on picture archiving and communication system (PACS) and would need a dedicated AW workstation. Additional studies are necessary to address these issues.

## Conclusions

In conclusion, spectral CT provides a set of monochromatic images, iodine-based MD images, and the quantitative parameters based on iodine concentration analysis that may help to increase the accuracy of the differentiation of HCC, HH, and FNH.

## Acknowledgments

The authors are grateful to Dr. Jianying Li at GE Healthcare in revising the manuscript.

## Funding

This work was supported by the National Natural Science Foundation of China (Grant number 81401406) and the Innovative Research Team of High-Level Local Universities in Shanghai.

## Conflict of interest

The authors have no conflict of interests related to this publication.

## Author contributions

Carried out the studies, participated in collecting data and drafted the manuscript (WL), carried out the studies and participated in collecting data (RL, XZ), participated in collecting data (YY, JZ), performed the statistical analysis and participated in its design (XL, WC), participated in acquisition and analysis of data (KC), participated in interpretation of data (FY). Manuscript writing and final approval of manu-

script (all authors).

## Data sharing statement

No additional data are available.

## References

- [1] Ferlay J, Soerjomataram I, Dikshit R, Eser S, Mathers C, Rebelo M, *et al*. Cancer incidence and mortality worldwide: sources, methods and major patterns in GLOBOCAN 2012. *Int J Cancer* 2015;136(5):E359–386. doi:10.1002/ijc.29210.
- [2] Tapper EB, Parikh ND. Mortality due to cirrhosis and liver cancer in the United States, 1999–2016: observational study. *BMJ* 2018;362:k2817. doi:10.1136/bmj.k2817.
- [3] Toro A, Mahfouz AE, Ardori A, Malaguarnera M, Malaguarnera G, Loria F, *et al*. What is changing in indications and treatment of hepatic hemangiomas. A review. *Ann Hepatol* 2014;13(4):327–339.
- [4] Marrero JA, Ahn J, Rajender Reddy K, American College of Gastroenterology. ACG clinical guideline: the diagnosis and management of focal liver lesions. *Am J Gastroenterol* 2014;109(9):1328–1347; quiz 1348. doi:10.1038/ajg.2014.213.
- [5] Bioulac-Sage P, Laumonier H, Laurent C, Blanc JF, Balabaud C. Benign and malignant vascular tumors of the liver in adults. *Semin Liver Dis* 2008;28(3):302–314. doi:10.1055/s-0028-1085098.
- [6] Demirjian A, Peng P, Geschwind JF, Cosgrove D, Schutz J, Kamel IR, *et al*. Infiltrating hepatocellular carcinoma: seeing the tree through the forest. *J Gastrointest Surg* 2011;15(11):2089–2097. doi:10.1007/s11605-011-1614-7.
- [7] Llovet JM, Burroughs A, Bruix J. Hepatocellular carcinoma. *Lancet* 2003;362(9399):1907–1917. doi:10.1016/S0140-6736(03)14964-1.
- [8] Trevisani F, Frigerio M, Santi V, Grignaschi A, Bernardi M. Hepatocellular carcinoma in non-cirrhotic liver: a reappraisal. *Dig Liver Dis* 2010;42(5):341–347. doi:10.1016/j.dld.2009.09.002.
- [9] Leslie DF, Johnson CD, Johnson CM, Ilstrup DM, Harmsen WS. Distinction between cavernous hemangiomas of the liver and hepatic metastases on CT: value of contrast enhancement patterns. *AJR Am J Roentgenol* 1995;164(3):625–629. doi:10.2214/ajr.164.3.7863883.
- [10] Lee JH, Lee JM, Kim SJ, Baek JH, Yun SH, Kim KW, *et al*. Enhancement patterns of hepatocellular carcinomas on multiphasic multidetector row CT: comparison with pathological differentiation. *Br J Radiol* 2012;85(1017):e573–583. doi:10.1259/bjr/86767895.
- [11] Quinn SF, Benjamin GG. Hepatic cavernous hemangiomas: simple diagnostic sign with dynamic bolus CT. *Radiology* 1992;182(2):545–548. doi:10.1148/radiology.182.2.1732978.
- [12] Ito K, Mitchell DG, Outwater EK, Szklaruk J, Sadek AG. Hepatic lesions: discrimination of nonsolid, benign lesions from solid, malignant lesions with heavily T2-weighted fast spin-echo MR imaging. *Radiology* 1997;204(3):729–737. doi:10.1148/radiology.204.3.9280251.
- [13] Farrar SW, Jara H, Chang KJ, Ozonoff A, Soto JA. Differentiation of hepatocellular carcinoma and hepatic metastasis from cysts and hemangiomas with calculated T2 relaxation times and the T1/T2 relaxation times ratio. *J Magn Reson Imaging* 2006;24(6):1333–1341. doi:10.1002/jmri.20758.
- [14] Chan YL, Lee SF, Yu SC, Lai P, Ching AS. Hepatic malignant tumour versus cavernous haemangioma: differentiation on multiple breath-hold turbo spin-echo MRI sequences with different T2-weighting and T2-relaxation time measurements on a single slice multi-echo sequence. *Clin Radiol* 2002;57(4):250–257. doi:10.1053/crad.2001.0763.
- [15] Cieszanowski A, Szeszkowski W, Golebiowski M, Bielecki DK, Grodzicki M, Pruszyński B. Discrimination of benign from malignant hepatic lesions based on their T2-relaxation times calculated from moderately T2-weighted turbo SE sequence. *Eur Radiol* 2002;12(9):2273–2279. doi:10.1007/s00330-002-1366-6.
- [16] Santoro L, Grazioli L, Filippone A, Grassedonio E, Belli G, Colagrande S. Resonance enhanced MR imaging of the liver: does quantitative assessment help in focal lesion classification and characterization? *J Magn Reson Imaging* 2009;30(5):1012–1020. doi:10.1002/jmri.21937.
- [17] Soyer P, Corno L, Boudiaf M, Aout M, Sirol M, Placé V, *et al*. Differentiation between cavernous hemangiomas and untreated malignant neoplasms of the liver with free-breathing diffusion-weighted MR imaging: comparison with T2-weighted fast spin-echo MR imaging. *Eur J Radiol* 2011;80(2):316–324. doi:10.1016/j.ejrad.2010.08.011.
- [18] Turner MA, Fulcher AS. The cystic duct: normal anatomy and disease processes. *Radiographics* 2001;21(1):3–22; questionnaire 288–94. doi:10.1148/radiographics.21.1.g01ja093.
- [19] Ruppert-Kohlmaier AJ, Uggowitz MM, Kugler C, Zebedin D, Schaffler G, Ruppert GS. Focal nodular hyperplasia and hepatocellular adenoma of the liver: differentiation with multiphasic helical CT. *AJR Am J Roentgenol* 2001;176(6):1493–1498. doi:10.2214/ajr.176.6.1761493.
- [20] van den Esschert JW, van Gulik TM, Phoa SS. Imaging modalities for focal nodular hyperplasia and hepatocellular adenoma. *Dig Surg* 2010;27(1):46–55. doi:10.1159/000268407.
- [21] Sun M, Wang S, Song Q, Wang Z, Wang H, Ning D, *et al*. Utility of R2\* obtained from T2\*-weighted imaging in differentiating hepatocellular carcinomas from cavernous hemangiomas of the liver. *PLoS One* 2014;9(3):e91751. doi:10.1371/journal.pone.0091751.

- [22] Jang HJ, Kim TK, Burns PN, Wilson SR. Enhancement patterns of hepatocellular carcinoma at contrast-enhanced US: comparison with histologic differentiation. *Radiology* 2007;244(3):898–906. doi:10.1148/radiol.2443061520.
- [23] Okuda K. Hepatocellular carcinoma: recent progress. *Hepatology* 1992;15(5):948–963. doi:10.1002/hep.1840150532.
- [24] Forner A, Vilana R, Ayuso C, Bianchi L, Solé M, Ayuso JR, *et al.* Diagnosis of hepatic nodules 20 mm or smaller in cirrhosis: prospective validation of the noninvasive diagnostic criteria for hepatocellular carcinoma. *Hepatology* 2008;47(1):97–104. doi:10.1002/hep.21966.
- [25] Yoshikawa J, Matsui O, Takashima T, Ida M, Takanaka T, Kawamura I, *et al.* Fatty metamorphosis in hepatocellular carcinoma: radiologic features in 10 cases. *AJR Am J Roentgenol* 1988;151(4):717–720. doi:10.2214/ajr.151.4.717.
- [26] Martin J, Sents M, Zidan A, Donoso L, Puig J, Falcó J, *et al.* Fatty metamorphosis of hepatocellular carcinoma: detection with chemical shift gradient-echo MR imaging. *Radiology* 1995;195(1):125–130. doi:10.1148/radiology.195.1.7892452.
- [27] Luo M, Zhang L, Jiang XH, Zhang WD. Intravoxel incoherent motion: application in differentiation of hepatocellular carcinoma and focal nodular hyperplasia. *Diagn Interv Radiol* 2017;23(4):263–271. doi:10.5152/dir.2017.16595.
- [28] Leoni S, Piscaglia F, Golfieri R, Camaggi V, Vidili G, Pini P, *et al.* The impact of vascular and nonvascular findings on the noninvasive diagnosis of small hepatocellular carcinoma based on the EASL and AASLD criteria. *Am J Gastroenterol* 2010;105(3):599–609. doi:10.1038/ajg.2009.654.
- [29] Moody AR, Wilson SR. Atypical hepatic hemangioma: a suggestive sonographic morphology. *Radiology* 1993;188(2):413–417. doi:10.1148/radiology.188.2.8327687.
- [30] Vilgrain V, Boulos L, Vullierme MP, Denys A, Terris B, Menu Y. Imaging of atypical hemangiomas of the liver with pathologic correlation. *Radiographics* 2000;20(2):379–397. doi:10.1148/radiographics.20.2.g00mc01379.
- [31] Kim T, Federle MP, Baron RL, Peterson MS, Kawamori Y. Discrimination of small hepatic hemangiomas from hypervascular malignant tumors smaller than 3 cm with three-phase helical CT. *Radiology* 2001;219(3):699–706. doi:10.1148/radiology.219.3.r01jn45699.
- [32] Hanafusa K, Ohashi I, Himeno Y, Suzuki S, Shibuya H. Hepatic hemangioma: findings with two-phase CT. *Radiology* 1995;196(2):465–469. doi:10.1148/radiology.196.2.7617862.
- [33] Hussain SM, Terkivatan T, Zondervan PE, Lanjouw E, de Rave S, Ijzermans JN, *et al.* Focal nodular hyperplasia: findings at state-of-the-art MR imaging, US, CT, and pathologic analysis. *Radiographics* 2004;24(1):3–17. discussion 18-9. doi:10.1148/rg.241035050.
- [34] Li J, Wang J, Lei L, Yuan G, He S. The diagnostic performance of gadoteric acid disodium-enhanced magnetic resonance imaging and contrast-enhanced multi-detector computed tomography in detecting hepatocellular carcinoma: a meta-analysis of eight prospective studies. *Eur Radiol* 2019;29(12):6519–6528. doi:10.1007/s00330-019-06294-6.
- [35] Hanna RF, Miloushev VZ, Tang A, Finklestone LA, Brejt SZ, Sandhu RS, *et al.* Comparative 13-year meta-analysis of the sensitivity and positive predictive value of ultrasound, CT, and MRI for detecting hepatocellular carcinoma. *Abdom Radiol (NY)* 2016;41(1):71–90. doi:10.1007/s00261-015-0592-8.
- [36] Yang CB, Zhang S, Jia YJ, Yu Y, Duan HF, Zhang XR, *et al.* Dual energy spectral CT imaging for the evaluation of small hepatocellular carcinoma microvascular invasion. *Eur J Radiol* 2017;95:222–227. doi:10.1016/j.ejrad.2017.08.022.
- [37] Pfeiffer D, Parakh A, Patino M, Kambadakone A, Rummeny EJ, Sahani DV. Iodine material density images in dual-energy CT: quantification of contrast uptake and washout in HCC. *Abdom Radiol (NY)* 2018;43(12):3317–3323. doi:10.1007/s00261-018-1636-7.
- [38] Lv P, Lin XZ, Chen K, Gao J. Spectral CT in patients with small HCC: investigation of image quality and diagnostic accuracy. *Eur Radiol* 2012;22(10):2117–2124. doi:10.1007/s00330-012-2485-3.
- [39] Altenbernd J, Heusner TA, Ringelstein A, Ladd SC, Forsting M, Antoch G. Dual-energy-CT of hypervascular liver lesions in patients with HCC: investigation of image quality and sensitivity. *Eur Radiol* 2011;21(4):738–743. doi:10.1007/s00330-010-1964-7.
- [40] Marin D, Nelson RC, Samei E, Paulson EK, Ho LM, Boll DT, *et al.* Hypervascular liver tumors: low tube voltage, high tube current multidetector CT during late hepatic arterial phase for detection—initial clinical experience. *Radiology* 2009;251(3):771–779. doi:10.1148/radiol.2513081330.
- [41] Große Hokamp N, Hoink AJ, Doerner J, Jordan DW, Pahn G, Persigehl T, *et al.* Assessment of arterially hyper-enhancing liver lesions using virtual monoenergetic images from spectral detector CT: phantom and patient experience. *Abdom Radiol (NY)* 2018;43(8):2066–2074. doi:10.1007/s00261-017-1411-1.
- [42] Shuman WP, Green DE, Busey JM, Mitsumori LM, Choi E, Koprowicz KM, *et al.* Dual-energy liver CT: effect of monochromatic imaging on lesion detection, conspicuity, and contrast-to-noise ratio of hypervascular lesions on late arterial phase. *AJR Am J Roentgenol* 2014;203(3):601–606. doi:10.2214/AJR.13.11337.
- [43] Lv P, Lin XZ, Li J, Li W, Chen K. Differentiation of small hepatic hemangioma from small hepatocellular carcinoma: recently introduced spectral CT method. *Radiology* 2011;259(3):720–729. doi:10.1148/radiol.11101425.
- [44] Laroia ST, Bhadoria AS, Venigalla Y, Chibber GK, Bihari C, Rastogi A, *et al.* Role of dual energy spectral computed tomography in characterization of hepatocellular carcinoma: Initial experience from a tertiary liver care institute. *Eur J Radiol Open* 2016;3:162–171. doi:10.1016/j.ejro.2016.05.007.
- [45] Yu Y, Lin X, Chen K, Chai W, Hu S, Tang R, *et al.* Hepatocellular carcinoma and focal nodular hyperplasia of the liver: differentiation with CT spectral imaging. *Eur Radiol* 2013;23(6):1660–1668. doi:10.1007/s00330-012-2747-0.
- [46] Yu Y, He N, Sun K, Lin X, Yan F, Chen K. Differentiating hepatocellular carcinoma from angiolipoma of the liver with CT spectral imaging: a preliminary study. *Clin Radiol* 2013;68(9):e491–497. doi:10.1016/j.crad.2013.03.027.
- [47] Zhou L, Rui JA, Zhou WX, Wang SB, Chen SG, Qu Q. Edmondson-Steiner grade: a crucial predictor of recurrence and survival in hepatocellular carcinoma without microvascular invasion. *Pathol Res Pract* 2017;213(7):824–830. doi:10.1016/j.prp.2017.03.002.
- [48] Wang Q, Shi G, Qi X, Fan X, Wang L. Quantitative analysis of the dual-energy CT virtual spectral curve for focal liver lesions characterization. *Eur J Radiol* 2014;83(10):1759–1764. doi:10.1016/j.ejrad.2014.07.009.





Original Article

## 3-year Treatment of Tenofovir Alafenamide vs. Tenofovir Disoproxil Fumarate for Chronic HBV Infection in China

Jinlin Hou<sup>1\*</sup>, Qin Ning<sup>2\*</sup>, Zhongping Duan<sup>3</sup>, You Chen<sup>3</sup>, Qing Xie<sup>4</sup>, Fu-Sheng Wang<sup>5</sup>, Lunli Zhang<sup>6</sup>, Shanming Wu<sup>7</sup>, Hong Tang<sup>8</sup>, Jun Li<sup>9</sup>, Feng Lin<sup>10</sup>, Yongfeng Yang<sup>11</sup>, Guozhong Gong<sup>12</sup>, John F. Flaherty<sup>13</sup>, Anuj Gaggar<sup>13</sup>, Shuyuan Mo<sup>13</sup>, Cong Cheng<sup>13</sup>, Gregory Camus<sup>13</sup>, Chengwei Chen<sup>14</sup>, Yan Huang<sup>15</sup>, Jidong Jia<sup>16</sup>, Mingxiang Zhang<sup>17</sup> and GS-US-320-0110 and GS-US-320-0108 China Investigators

<sup>1</sup>Nanfang Hospital of Southern Medical University, Guangzhou, Guangdong, China; <sup>2</sup>Tongji Hospital, Tongji Medical College, Huazhong University of Science and Technology, Wuhan, Hubei, China; <sup>3</sup>Beijing YouAn Hospital, Capital Medical University, Beijing, China; <sup>4</sup>Shanghai Ruijin Hospital, Shanghai Jiao Tong University School of Medicine, Shanghai, China; <sup>5</sup>Beijing 302 Hospital, Beijing, China; <sup>6</sup>The First Affiliated Hospital of Nanchang University, Nanchang, Jiangxi, China; <sup>7</sup>Shanghai Public Health Clinical Center, Shanghai, China; <sup>8</sup>West China Hospital, Sichuan University, Chengdu, Sichuan, China; <sup>9</sup>The First Affiliated Hospital with Nanjing Medical University, Nanjing, Jiangsu, China; <sup>10</sup>Hainan General Hospital, Haikou, Hainan, China; <sup>11</sup>Nanjing No. 2 Hospital, Nanjing, Jiangsu, China; <sup>12</sup>The 2nd Xiangya Hospital, Central South University, Changsha, Hunan, China; <sup>13</sup>Gilead Sciences, Foster City, CA, USA; <sup>14</sup>Liver Disease Center of Naval 905 Hospital, Shanghai, China; <sup>15</sup>Xiangya Hospital, Central South University, Changsha, Hunan, China; <sup>16</sup>Beijing Friendship Hospital, Capital University, Beijing, China; <sup>17</sup>The Sixth People's Hospital of Shenyang, Shenyang, Liaoning, China

Received: 1 December 2020 | Revised: 18 February 2021 | Accepted: 8 March 2021 | Published: 28 April 2021

### Abstract

**Background and Aims:** Tenofovir alafenamide (TAF) has similar efficacy to tenofovir disoproxil fumarate (TDF) but with improved renal and bone safety in chronic hepatitis B patients studied outside of China. We report 3-year results from two phase 3 studies with TAF in China (ClinicalTrials.gov: NCT02836249 and NCT02836236). **Methods:** Chinese hepatitis B e antigen (HBeAg)-positive and -negative chronic hepatitis B patients with viremia and elevated alanine aminotransferase were randomized 2:1 to TAF or TDF treatment groups and treated in a double-blind fashion for 144 weeks (3 years). Efficacy responses were assessed by individual study while safety was assessed by a pooled analysis. **Results:** Of the 334 patients (180 HBeAg-positive and 154 HBeAg-negative) randomized and treated, baseline characteristics were similar between groups. The overall mean age was 38 years and 73% were male. The mean HBV DNA was

6.4 log<sub>10</sub> IU/mL. The median alanine aminotransferase was 88 U/L, and 37% had a history of antiviral use. At week 144, the proportion with HBV DNA <29 IU/mL was similar among the two groups, with TAF at 83% vs. TDF at 79%, and TAF at 93% vs. TDF at 92% for the HBeAg-positive and -negative patients, respectively. In each study, higher proportions of TAF than TDF patients showed normalized alanine aminotransferase (via the American Association for the Study of Liver Diseases and the China criteria) and showed loss of HBsAg; meanwhile, the HBeAg seroconversion rates were similar. Treatment was well-tolerated among the TAF patients, who showed a smaller median decline in creatinine clearance (−0.4 vs. −3.2 mL/min; *p*=0.014) and less percentage change in bone mineral density vs. TDF at hip (−0.95% vs. −1.93%) and spine (+0.35% vs. −1.40%). **Conclusions:** In chronic hepatitis B patients from China, TAF treatment provided efficacy similar to TDF but with better renal and bone safety at 3 years.

**Citation of this article:** Hou J, Ning Q, Duan Z, Chen Y, Xie Q, Wang FS, *et al.* 3-year treatment of tenofovir alafenamide vs. tenofovir disoproxil fumarate for chronic HBV infection in China. J Clin Transl Hepatol 2021;9(3):324–334. doi: 10.14218/JCTH.2020.00145.

**Keywords:** Chronic hepatitis B virus; Antiviral therapy; Bone safety; Renal safety.

**Abbreviations:** ADV, adefovir; AE, adverse event; ALT, alanine aminotransferase; AST, aspartate aminotransferase; BMD, bone mineral density; β<sub>2</sub>M:Cr, urine β<sub>2</sub>-microglobulin-to-creatinine ratio; CHB, chronic hepatitis B; CKD, chronic kidney disease; DXA, dual energy x-ray absorptiometry; EC<sub>50</sub>, half maximal effective concentration; eGFR<sub>CG</sub>, estimated creatinine clearance by the Cockcroft-Gault method; HBeAg, hepatitis B e antigen; HBsAg, hepatitis B surface antigen; HBV, hepatitis B virus; HCC, hepatocellular carcinoma; HDL, high-density lipoprotein; LDL, low-density lipoprotein; OAT, organic anion transporter; OAV, oral antiviral; pol/RT, polymerase/reverse transcriptase; RBP:Cr, urine retinol binding protein-to-creatinine ratio; TAF, tenofovir alafenamide; TDF, tenofovir disoproxil fumarate; TFV, tenofovir; UACR, urine albumin-to-creatinine ratio; ULN, upper limit of normal; UPCR, urine protein-to-creatinine ratio.

\*Correspondence to: Jinlin Hou, Nanfang Hospital of Southern Medical University, Guangzhou, Guangdong 510515, China. E-mail: jlhoumu@163.com; Ning Qin, Tongji Hospital, Tongji Medical College, Huazhong University of Science and Technology, Wuhan, Hubei 430030, China. E-mail: qning@vip.sina.com

### Introduction

The World Health Organization estimated that 257 million people worldwide are chronically infected with the hepatitis B virus (HBV) and recent modeling-based analyses suggested this figure could be as high as 292 million, which represents a global prevalence of 3.9%.<sup>1,2</sup> In China, the prevalence previously was higher; however, due to the in-

roduction of universal HBV immunization in 1992, combined with other public health measures, the prevalence reduced to 7.2% in 2006, and 6.15% recently.<sup>2,3</sup> Over 95 million people in China are chronic HBV carriers and ≥20 million have active disease.<sup>2,3</sup> If untreated, chronic HBV infection progresses to cirrhosis, hepatic decompensation, or hepatocellular carcinoma (HCC), or both.<sup>4,5</sup> Worldwide, liver cancer is the third leading cause of cancer deaths and is the second most common cancer in China where up to 80% of HCC cases are attributed to HBV.<sup>3</sup>

Treatment with potent antivirals that have a high resistance barrier allows for long-term suppression in the majority of patients; therefore, the risk of liver-related complications is reduced, and slowing or reversing the disease progression is possible.<sup>6</sup> However, a limited number achieve a functional cure for chronic hepatitis B (CHB) (long-lasting loss of hepatitis B surface antigen [HBsAg]); therefore, life-long treatment is normally required.<sup>7,8</sup> In an aging population with increased comorbidity risk, side effects, such as renal and bone complications that are seen with tenofovir disoproxil fumarate (TDF) use can become problematic.<sup>9–11</sup>

Tenofovir alafenamide (TAF) is a novel prodrug of tenofovir (TFV), which is a nucleotide analog that inhibits reverse transcription of HBV.<sup>12,13</sup> Compared with TDF, TAF has increased plasma stability that enables more efficient hepatic delivery of the active drug (TFV-diphosphate).<sup>12,14</sup> At the currently approved dose of 25 mg once daily, the levels of circulating TFV are approximately 90% lower than with the TDF 300 mg once daily dosing regimen which forms the basis for an improvement in renal and bone safety with TAF.<sup>15</sup>

Studies GS-US-320-0110 (Study 110, in HBeAg-positive patients) and GS-US-320-0108 (Study 108, in HBeAg-negative patients) are ongoing, randomized, double-blind, international (excluding China) Phase 3 studies that compare TAF versus TDF in a combined population of 1,298 treatment-naïve and treatment-experienced patients with CHB, which includes those with compensated cirrhosis. In each study, TAF demonstrated statistical non-inferiority to TDF in antiviral efficacy (HBV DNA <29 IU/mL at week 48), which was confirmed at week 96.<sup>16–18</sup> In addition, a smaller mean percentage decrease in bone mineral density (BMD) at the hip and spine, and a smaller median decline in the estimated creatinine clearance were seen with TAF versus TDF in each study at week 48 and by pooled safety analysis at week 96.<sup>16–18</sup> In addition, TAF-treated patients had significantly smaller changes in biomarkers for bone turnover and reductions in markers for proximal tubular function compared with TDF.<sup>18</sup> For the first time, the efficacy and safety results from 3 years of double-blind treatment in a separate cohort of patients that were enrolled in Studies 110 and 108 in China are presented.

## Methods

### Patients and study design

The randomized, double-blind, active-controlled phase 3 trials were identical in design and differed only by the patient population as previously described.<sup>16,17</sup> Briefly, patients were ≥18 years of age, HBsAg positive for ≥6 months with HBV DNA levels ≥20,000 IU/mL, and alanine transaminase (ALT) level of >60 U/L in men or >38 U/L in women. All patients had an estimated creatinine clearance ≥50 mL/min by using the Cockcroft-Gault (eGFR<sub>CG</sub>) equation. Patients were excluded with clinical or laboratory evidence of decompensated liver disease, aspartate transaminase or ALT >10 times the upper limit of normal (ULN), hepatocellular carcinoma, or co-infection with hepatitis C, hepatitis D, or the human immunodeficiency virus.

Patients were randomly assigned (2:1) to TAF 25 mg or TDF 300 mg given orally once a day for 144 weeks. All patients received placebo tablets that matched the alternative treatment; patients and investigators were blinded to the treatment assignment throughout the double-blind period. A limited number of individuals from the clinical research, biometrics, safety, and regulatory departments of the sponsor were unblinded at the 48-week time point to undertake measures that lead to the submission for TAF registration in China. Randomization was stratified by HBV DNA levels (≥8 log<sub>10</sub> IU/mL versus 7 to 8 log<sub>10</sub> IU/mL versus <7 log<sub>10</sub> IU/mL in Study 108, and ≥8 log<sub>10</sub> IU/mL versus <8 log<sub>10</sub> IU/mL in Study 110) and by previous oral antiviral (OAV) treatment (treatment-naïve status was defined as <12 weeks of previous OAVs for HBV, and treatment-experienced patients received ≥12 weeks of previous OAV therapy).

Written informed consent was obtained from all patients before enrollment and the study protocols were approved by the institutional review board or independent ethics committees at all participating sites and were conducted according to the principles of the Declaration of Helsinki and Good Clinical Practice. All authors had access to the study data and reviewed and approved the final manuscript.

### Procedures

During the first year, study visits occurred every 4 weeks that started at treatment week 4; however, during the second and third years study visits were conducted every 8 and 12 weeks, respectively. Laboratory assessments included a complete blood count with platelets, serum chemistries, fasting lipid panel, standard measures of renal function (serum creatinine, eGFR<sub>CG</sub>, proteinuria by dipstick), and quantitative markers of proteinuria (protein-to-creatinine ratio [UPCR], the albumin-to-creatinine ratio [UACR], retinol binding protein-to-creatinine ratio [RBP:Cr], and the β<sub>2</sub>-microglobulin-to-creatinine ratio [β<sub>2</sub>M:Cr]; Covance Laboratories, Shanghai, China). Changes in BMD were assessed in patients at sites that were able to perform dual-energy x-ray absorptiometry (DXA) scanning of the lumbar spine and hip. DXA scans were performed at screening, and then every 24 weeks. In addition, fasting serum biomarkers of bone turnover were measured, including C-type collagen sequences and procollagen type 1 N-terminal propeptide, which are sensitive markers of bone resorption and formation, respectively.

### Outcomes

Efficacy endpoints for the 144-week analysis were the proportions of patients with HBV DNA <29 IU/mL, proportions of patients with a serological response (loss of HBsAg with or without seroconversion to anti-HBs, quantitative change in HBsAg, and in HBeAg-positive patients, proportion with HBeAg loss with or without seroconversion to anti-HBe). Other efficacy endpoints included the proportions of patients with ALT normalization (defined as ALT >ULN at baseline becoming ≤ULN at week 144) by the criteria proposed by the AASLD; 35 U/L for males and 25 U/L for females).<sup>7</sup> In addition, a ULN of 40 U/L (for men and women) was assessed for ALT normalization, because this cutoff is often used as a reference in China, which is referred to as the China criteria in this study. Fibrosis was assessed noninvasively using serum FibroTest (BioPredictive S.A.S., Paris, France). In addition, categorical shifts from baseline were assessed using three categories of FibroTest ranges: 0.00–0.48 (approximately equivalent to Metavir F0/F1; no or minimal fibrosis), 0.49–0.74 (F2 or F3; moderate to severe fibrosis),

**Table 1. Patient characteristics in the pooled population of studies 110 (HBeAg-positive) and 108 (HBeAg-negative) in patients from China**

	TAF 25 mg (n = 227)	TDF 300 mg (n = 107)	Total (n = 334)
Mean age (years [range])	38 (18–69)	40 (20–73)	38 (18–73)
Age ≥ 50 years (n [%])	31 (14)	24 (22)*	55 (16)
Male (n [%])	162 (71)	82 (77)	244 (73)
Asian (n [%])	227 (100)	107 (100)	334 (100)
Mean BMI (kg/m <sup>2</sup> [SD])	24 (3.4)	24 (3.1)	24 (3.3)
Mean HBV DNA (log <sub>10</sub> IU/mL [SD])	6.4 (1.87)	6.4 (1.81)	6.4 (1.85)
HBV DNA ≥ 8 log <sub>10</sub> IU/mL (n [%])	55 (24)	22 (21)	77 (23)
Median ALT (Q1, Q3)	85 (53, 160)	90 (63, 185)	88 (56, 165)
HBeAg status			
Positive	121 (53)†	59 (55)†	180 (54)
Negative	106 (47)†	48 (45)†	154 (46)
HBV genotype			
B	90 (40)	33 (31)	123 (37)
C	131 (58)	74 (69)	205 (61)
B/C	2 (1)	0	2 (0.6)
D	2 (1)	0	2 (0.6)
Unknown	2 (1)	0	2 (0.6)
History of cirrhosis			
Yes	5/56 (9)	7/25 (28)‡	12/81 (15)
No	51/56 (91)	18/25 (72)	69/81 (85)
Indeterminate/unknown	171	82	253
Mean FibroTest score (range)	0.41 (0.04–0.98)	0.44 (0.06–0.96)	0.42 (0.04–0.98)
FibroTest score ≥ 0.75	24/224 (11)	13/103 (13)	37/327 (11)
Previous nucleos(t)ide use (n [%])	86 (38)	38 (36)	124 (37)
Previous adefovir dipivoxil (n [%])	47 (21)	23 (21)	70 (21)
Previous lamivudine (n [%])	35 (15)	18 (17)	53 (16)
Prior entecavir, n (%)	48 (21)	18 (17)	66 (20)
Median eGFR by Cockcroft-Gault (Q1, Q3)	113 (98, 129)	113 (97, 125)	113 (97, 128)
Diabetes mellitus	21 (9)	5 (5)	26 (8)
Cardiovascular disease	9 (4)	1 (1)	10 (3)
Hypertension	18 (8)	13 (12)	31 (9)
Hyperlipidemia	4 (2)	3 (3)	7 (2)
Total hip BMD clinical status			
Normal (T-score ≥ −1.0)	59/93 (63)	31/54 (57)	90/147 (61)
Osteopenia (−2.5 ≤ T-score < −1.0)	33/93 (35)	22/54 (41)	55/147 (37)
Osteoporosis (T-score < −2.5)	0/93	1/54 (2)	1/147 (0.7)
Status not determined	1/93 (1)	0/54	1/147 (0.7)
Lumbar spine BMD clinical status			
Normal (T-score ≥ −1.0)	38/94 (40)	25/54 (46)	63/148 (43)
Osteopenia (−2.5 ≤ T-score < −1.0)	51/94 (54)	25/54 (46)	76/148 (51)
Osteoporosis (T-score < −2.5)	4/94 (4)	4/54 (7)	8/148 (5)
Status not determined	1/94 (1)	0/54	1/148 (0.7)
Median 25-hydroxy vitamin D (ng/mL [Q1, Q3])	18.8 (13.2, 24.4)	18.4 (14, 23.6)	18.8 (13.6, 24.4)

\**p* = 0.044; †HBeAg status for 5 patients (TAF *n* = 3, TDF *n* = 2) in Study 108 changed from negative to positive between the screening and baseline visits, and in Study 110, HBeAg status for 5 patients (TAF *n* = 5) changed from positive to negative between the screening and baseline visits; ‡*p* = 0.0265.



Table 2. Efficacy outcomes at week 144 in patients from China

n/N or n/n (%) [95% CI]	HBeAg-positive patients (Study 110)			HBeAg-negative patients (Study 108)		
	TAF 25 mg (N = 123)	TDF 300 mg (N = 57)	Proportional Difference (95% CI)	TAF 25 mg (N = 104)	TDF 300 mg (N = 50)	Proportional Difference (95% CI)
HBV DNA <29 IU/mL	102 (83) [75–89]	45 (79) [66–89]	4.1% (–9.1%–17.3%)	97 (93) [87–97]	46 (92) [81–98]	1.5% (–8.9%–12.0%)
HBeAg loss*	27/118 (23)	16/57 (28)	ND	–	–	–
HBeAg seroconversion*	20/118 (17)	9/57 (16)	ND	–	–	–
HBsAg loss†	5 (4)	0	ND	3 (3)	0	ND
HBsAg seroconversion†	3 (2)	0	ND	1 (1)	0	ND
Mean change from baseline in HBsAg, log <sub>10</sub> IU/mL (SD)	–0.75 (1.190)	–0.68 (0.927)	–0.06 (–0.41–0.29)	–0.39 (0.764)	–0.23 (0.487)	–0.15 (–0.38–0.08)
ALT normalization by 2018 AASLD criteria§	87/114 (76)	37/55 (67)	10.4% (–3.9%–24.8%)	74/92 (80)	29/41 (71)	8.8% (–8.3%–25.8%)
ALT normalization by China criteria	83/107 (78)	36/54 (67)	12.2% (–2.3%–26.8%)	74/86 (86)	26/36 (72)	13.3% (–4.1%–30.8%)
Mean FibroTest score change from baseline (SD)	–0.09 (0.140)	–0.09 (0.184)	–0.01 (–0.06–0.05)	–0.06 (0.138)	–0.04 (0.185)	–0.02 (–0.07–0.04)

All efficacy results are missing equals failure except for log<sub>10</sub> IU/mL change from baseline in HBsAg; ALT, alanine aminotransferase; CI, confidence interval; ND, not done. \*Among patients who were seropositive for HBeAg and negative for anti-HBe at baseline. †Among patients who were seropositive for HBsAg and negative for anti-HBs at baseline. ‡Among patients with ALT at baseline above the central lab normal range. §Among patients with ALT at baseline above the AASLD-defined normal range (>35 U/L men and >25 U/L women). ||Among patients with ALT at baseline >40 U/L.

and 0.75–1.00 (F4; cirrhosis).<sup>19</sup> Safety endpoints included mean percent change in hip BMD, mean percent change in spine BMD, and changes in renal function, as measured by mean change in serum creatinine and median change in eGFR<sub>CC</sub>.

### Resistance analyses

Baseline samples for all patients were assessed for the presence of HBV resistance mutations in the polymerase/reverse transcriptase (pol/RT) region using the HBV INNO-LiPA Multi-DR v2/3 assay (WuXi AppTec [Shanghai] Co., Ltd., Shanghai, China). Resistance surveillance was performed annually and included population or deep sequencing of the HBV pol/RT at baseline and week 48 for patients only with virologic breakthrough (defined as HBV DNA ≥69 IU/mL at two consecutive visits if previously confirmed <69 IU/mL, or confirmed ≥1 log<sub>10</sub> increase in HBV DNA from nadir), and at weeks 96 and 144, pol/RT sequencing was performed for all patients with HBV DNA ≥69 IU/mL, either on treatment or at early discontinuation in those with viremia. Phenotyping was performed for patients that experienced virologic breakthrough and any pol/RT amino acid change or conserved site change, and in patients with a polymorphic site, substitution provided the change was observed in >1 patient. For phenotyping, >2-fold change in EC<sub>50</sub> for the patient's isolate relative to baseline was considered to indicate reduced sensitivity to TAF or TDF.

### Statistical analysis

A missing equals failure approach was employed for the efficacy endpoints. For HBV DNA <29 IU/mL results, 95% confidence intervals (CI) were generated by the treatment group at each time point. Because the non-inferiority of TAF compared with TDF for the proportion of patients with HBV DNA <29 IU/mL was previously established for both studies

in the global (non-China) population,<sup>16–18</sup> the sample sizes for each study in the China cohort were not determined based on statistical considerations, instead enough patients were included to show comparable efficacy and safety following local registration requirements in China. Instead, exploratory statistical analyses were performed for the treatment difference (using 95% CI or *p*-values) for key efficacy and safety endpoints.

## Results

### Patient disposition

Out of 180 HBeAg-positive patients that were randomized and treated in Study 110 (123 TAF and 57 TDF) and 154 HBeAg-negative patients in Study 108 (104 TAF and 50 TDF), 165 (92%; 113 TAF and 52 TDF) and 146 (95%; 99 TAF and 47 TDF), completed the double-blind treatment to week 144, respectively. Complete dispositions for each study are provided in Supplementary Tables 1A and B.

Baseline demographics for the 334 patients enrolled in both studies were similar between treatment groups (Table 1). Patients were mainly male, mean age 38 years (range 18–73 years) with a smaller proportion of TAF versus TDF patients ≥50 years of age (14% versus 22%; *p* = 0.044). Mean HBV DNA and median ALT at baseline were 6.4 log<sub>10</sub> IU/mL and 88 U/L, respectively. The percentages of HBeAg-positive and HBeAg-negative patients were comparable (54% and 46%, respectively), with HBV genotypes C (61%) and B (37%) most common. In a subset of patients, a history of cirrhosis was known: 5/56 (9%) in the TAF group and 7/25 (28%) in the TDF group (*p* = 0.0265); however, for most patients, the cirrhosis status was indeterminate or unknown (Table 1). Using a FibroTest score ≥0.75 (i.e., suggestive of cirrhosis or Metavir F4),<sup>19</sup> 11% of patients had cirrhosis with similar proportions for both groups. Previous oral nucleos(t)ide use was reported in 37%, with 21%,

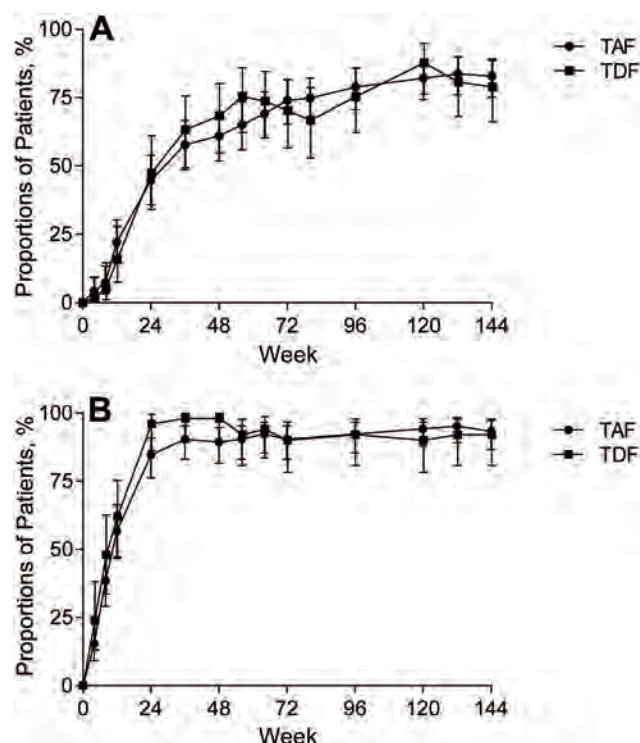


**Fig. 1. Viral suppression (HBV DNA <29 IU/mL) by visit week.** (A) Proportions of HBeAg-positive patients with HBV DNA <29 IU/mL. (B) Proportions of HBeAg-negative patients with HBV DNA <29 IU/mL. Analysis is missing equals failure.

20%, and 16% of patients previously treated with adefovir (ADV), entecavir, and lamivudine, respectively. Median (Q1, Q3) eGFR<sub>CG</sub> was 113 (97, 128) mL/min at baseline. Out of 147 patients that had available DXA data, 38% had evidence of bone loss (i.e., osteopenia or osteoporosis based on t-scores) at the hip and 57% showed bone loss at the spine. Comorbidities (hypertension, diabetes mellitus, cardiovascular disease, and hyperlipidemia) were present in <10% of study participants with a similar prevalence between treatment groups.

## Efficacy

**Antiviral efficacy:** In both studies, the rates of antiviral suppression were slightly higher for TDF versus TAF at week 48; however, from weeks 72 and 56 onward, similar suppression rates were achieved and maintained in Studies 110 and 108, respectively (Figs. 1A, B). The proportion of HBeAg-positive patients that received TAF with HBV DNA <29 IU/mL at week 144 was 83% compared with 79% in those that received TDF (proportional difference 4.1% [95% CI, -9.1%–17.3%]) (Table 2 and Fig. 1A). The proportion of patients with HBV DNA <29 IU/mL who had target not detected was 26% in both treatment groups, and the proportion with HBV DNA ≥29 IU/mL was 11% in both groups, and 7% and 11% of TAF and TDF patients, respectively, had missing data.

The proportion of HBeAg-negative patients that received TAF with HBV DNA <29 IU/mL at week 144 was 93% compared with 92% in those that received TDF (Table 2 and Fig. 1B). The proportions of HBeAg-negative patients with HBV DNA <29 IU/mL with target not detected were 61% and 48% in the TAF and TDF groups, respectively; there were a

few patients (2 TAF; 1 TDF) with HBV DNA ≥29 IU/mL, and similar proportions (TAF 5%; TDF 6%) had missing data at week 144.

**ALT normalization:** The proportion of HBeAg-positive patients that achieved ALT normalization at week 144 by the AASLD criteria was higher for TAF versus TDF-treated patients (76% versus 67%, respectively) (Table 2). In addition, patients that received TAF had consistently higher rates than those on TDF over the 3-year study (Fig. 2A). When assessed using the China cutoff of 40 U/L, a similar trend was seen with a higher rate of ALT normalization for TAF versus TDF at week 144 (78% versus 67%; Table 2).

In addition, HBeAg-negative patients that received TAF compared with those that received TDF showed a higher rate of ALT normalization at week 144 by the AASLD criteria (80% versus 71%; Table 2), with the difference in treatment response becoming more apparent from weeks 72 to 144 (Fig. 2B). When assessed by the China criteria, a similarly higher rate of ALT normalization was seen for TAF versus TDF at week 144 (86% versus 72%; Table 2).

**Serological efficacy:** The proportions of HBeAg-positive patients with HBeAg loss at week 144 were 23% and 28%, for the TAF and TDF groups, respectively, and rates of anti-HBe seroconversion were similar (17% versus 16%, respectively; Table 2). In the TAF group, for HBeAg-positive and HBeAg-negative patients, rates of HBsAg loss (4% and 3%, respectively) and HBsAg seroconversion (2% and 1%, respectively) were higher than in the TDF group, where no patients in either study achieved this endpoint (Table 2). Mean (SD) decreases in HBsAg levels were small and similar between treatment groups over 144 weeks of treatment in both studies.

## FibroTest changes

Mean (SD) FibroTest scores at baseline were similar between groups in each study (Study 110: TAF 0.37 [0.219] versus TDF 0.40 [0.219]; Study 108: TAF 0.46 [0.222] versus TDF 0.50 [0.265]). For HBeAg-positive patients, similar small mean (SD) decreases were seen with TAF and TDF at week 144 (Table 2); for HBeAg-negative patients, the mean declines were similar between treatments but were numerically smaller compared with HBeAg-positive patients. Fibrosis change was assessed by shifts from baseline in FibroTest categories (Supplementary Tables 2A, B). Although the numbers were small, the majority of HBeAg-positive patients in the highest fibrosis category (≥0.75; cirrhosis [F4]) at baseline improved by ≥1 category on study treatment, a finding that was present by week 48 with improvement remaining to week 144 (TAF 9/10 [90%] and TDF 2/3 [66%]). In contrast, nearly all patients in the lowest category at baseline (≤0.48; no or minimal fibrosis [F0/F1]) remained stable for the 144 weeks (TAF 79/80 [99%] and TDF 28/32 [88%]). For patients in the intermediate category (0.49 to 0.74; moderate to severe fibrosis [F2 or F3]), most showed a positive shift to the lowest category (TAF 12/24 [50%] and TDF 11/16 [69%]) with only a few having an increase in fibrosis category at week 144. Similar results were observed for HBeAg-negative patients for both study treatments (Supplementary Table 2B).

## Resistance surveillance

Results for resistance surveillance for the 144 weeks are provided in Supplementary Table 3. All patients with HBV DNA ≥ 69 IU/mL qualified for pol/RT sequencing at weeks 96 and 144; however, at week 48 only patients with virologic breakthrough were sequenced given the previous

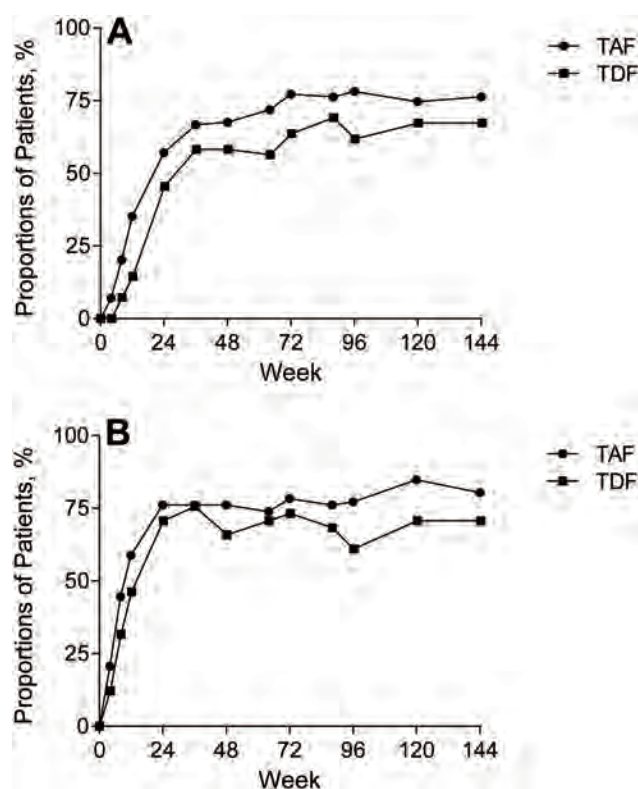


**Fig. 2. ALT normalization by visit week using 2018 AASLD criteria.** (A) Proportions of HBeAg-positive patients that achieved ALT normalization. (B) Proportions of HBeAg-negative patients that achieved ALT normalization. Analysis is missing equals failure and includes only patients with baseline ALT above the upper limit of normal for 2018 AASLD criteria (25 U/L and 35 U/L for males and females, respectively).

data that showed no resistance to TDF in patients with early viremia on treatment.<sup>20</sup> In both studies, there were 7 (6 TAF, 1 TDF), 23 (16 TAF, 7 TDF), and 14 (9 TAF, 5 TDF) patients who qualified for sequencing at weeks 48, 96, and 144, respectively, and of these, there were 1 out of 7, 8 out of 23, and 5 out of 14 patients, respectively, who had no sequence changes from baseline, and 3 out of 7, 6 out of 23, and 1 out of 14 patients with polymorphic site substitutions, and 0 out of 7, 4 out of 23, and 2 out of 14 patients who had conserved site substitutions. No specific conserved site substitution was found in >1 patient in either group. Overall, most patients that qualified for sequencing had viremia in the absence of virologic breakthrough (i.e., persistent viremia, or a viral blip, 24 out of 44 patients). Of the patients with available sequencing data, 1 out of 4, 8 out of 18, and 3 out of 8, qualified for phenotyping testing at weeks 48, 96, and 144, respectively. Overall, no pol/RT amino acid substitutions associated with resistance to TAF or tenofovir were detected during the 144 weeks in either group in each study.

### Safety

In the pooled safety analysis, which included 227 patients that were treated with TAF and 107 that were given TDF, each treatment was safe and well tolerated. Adverse events (AEs) were mostly mild or moderate in severity (88% and 92% experienced  $\geq 1$  AE in the TAF and TDF groups, respectively; proportional difference  $-3.9\%$  [95% CI:  $-10.7\%$ –

$2.9\%$ ]) (Table 3). One patient in each group experienced a Grade 3 or 4 AE related to the study drug, and 1 TDF-treated patient had treatment discontinued prematurely for renal impairment (moderate or Grade 2) which was a serious adverse event (SAE) and was determined to be related to study treatment. Common AEs ( $\geq 5\%$  of patients) were similar between treatment groups. No patient died during the study period and there were no cases of HCC or hepatic cancer.

Similar percentages of patients in each group experienced Grade 3 or 4 laboratory abnormalities (TAF 32%; TDF 34%), with a proportional difference of  $-1.9\%$  ( $-12.7\%$ – $8.9\%$ ) (Table 3). The most common laboratory abnormalities in  $\geq 3\%$  of patients were elevations in ALT and AST, and increased creatine kinase, each occurred at a similar frequency with TAF and TDF treatment. More patients had elevations in fasting LDL cholesterol or urine glucose abnormalities in the TAF group, both were transient and primarily seen in patients with pre-existing hyperlipidemia, diabetes mellitus, or both. Occult blood or urine erythrocytes were the most common urine abnormalities, which occurred mostly in menstruating women.

### Changes in fasting lipids

Baseline fasting lipid parameters were similar between treatment groups and median (Q1, Q3) values were within the normal ranges for each parameter (Supplementary Table 4). Following the initiation of study treatment, decreases in fasting total cholesterol were observed in both groups with a smaller decline for TAF versus TDF treatment (median [Q1, Q3] change at week 144: TAF  $-8$  [ $-21$ ,  $12$ ] mg/dL versus TDF  $-27$  [ $-40$ ,  $-10$ ] mg/dL;  $p < 0.001$ ). In addition, treatment with TAF resulted in smaller median declines in high-density lipoprotein (HDL) cholesterol at week 144 versus TDF ( $-8$  [ $-15$ ,  $-2$ ] mg/dL versus  $-12$  [ $-18$ ,  $-5$ ] mg/dL;  $p = 0.012$ ). Therefore, the median change in total cholesterol to HDL ratio at week 144, a commonly used measure to assess the relevance of lipid changes, was small and comparable between treatments (TAF 0.4 [0.0, 0.8] versus TDF 0.3 [ $-1.0$ , 0.6];  $p = 0.042$ ). A small increase in median fasting low-density lipoprotein (LDL) cholesterol was seen with TAF compared with a small decrease with TDF treatment at week 144 (11 [ $-4$ , 25] mg/dL versus  $-5$  [ $-15$ , 7];  $p < 0.001$ ); a similar trend was observed with fasting triglycerides (TAF 11 [ $-14$ , 41] mg/dL; TDF  $-6$  [ $-28$ , 15];  $p < 0.001$ ). In general, the observed differences in fasting lipid changes between the TAF and TDF groups were similar at week 48 compared with the results at week 144, which supported an early change that did not further progress over 3 years of treatment (Supplementary Table 4). Of note, 3 (1%) out of 227 TAF patients required initiation of lipid-lowering (i.e., statin) therapy compared with no patients in the TDF group ( $p = 0.554$ ).

### Changes in renal parameters

Table 4 provides a summary of renal laboratory results by treatment group at week 144. Median eGFR<sub>CG</sub> decreased slightly by week 144 in TAF-treated patients compared with a larger decrease in those that received TDF ( $-0.4$  mL/min versus  $-3.2$  mL/min;  $p = 0.014$ ). Of note, the larger decrease in eGFR<sub>CG</sub> with TDF occurred early (week 8) and remained significantly different versus TAF at each assessment for the 144 weeks, except for weeks 24 and 120 (Supplementary Table 5). When eGFR<sub>CG</sub> change was assessed as the percentage with  $\geq 25\%$  decrease at week 144, less TAF than TDF patients met this endpoint (10%



Table 3. Safety during 3 years of double-blind treatment

n (%) or n/N (%)	TAF 25 mg (N = 227)	TDF 300 mg (N = 107)
Any AE	199 (88)	98 (92)
Proportional difference (95% CI)	−3.9% (−10.7%–2.9%)	
Any AE related to study	50 (22)	37 (35)
AE that lead to study drug discontinuation	0	1 (<1)*
Any Grade 3 or 4 AE	16 (7)	4 (4)
Any Grade 3 or 4 AE related to study drug	1 (<1)	1 (<1)
Any SAE	17 (7)	10 (9)
Any SAE related to study drug	0	1 (<1)*
Deaths	0	0
AEs that occurred in ≥5% of patients in any treatment group		
Nasopharyngitis	72 (32)	24 (22)
Upper respiratory tract infection	52 (23)	27 (25)
Cough	21 (9)	5 (5)
Oropharyngeal pain	16 (7)	7 (7)
Pharyngitis	13 (6)	5 (5)
Influenza	8 (4)	7 (7)
Diarrhea	14 (6)	7 (7)
Nausea	4 (2)	7 (7)
Abdominal distension	8 (4)	6 (6)
Upper abdominal pain	13 (6)	7 (7)
Hepatic steatosis	12 (5)	6 (6)
Urinary tract infection	13 (6)	8 (7)
Increased amylase	2 (<1)	6 (6)
Osteopenia	1 (<1)	6 (6)
Increased blood parathyroid hormone	7 (3)	8 (7)
Weight decreased	4 (2)	7 (7)
Toothache	7 (3)	6 (6)
Grade 3 or 4 laboratory abnormalities that occurred in ≥3% of patients in any treatment group†		
Any Grade 3 or 4 laboratory abnormality	72/225 (32)	36/107 (34)
Proportional difference (95% CI)	−1.9% (−12.7%–8.9%)	
Alanine aminotransferase >5 × ULN	16 (7)	10 (9)
Aspartate aminotransferase >5 × ULN	5 (2)‡	4 (4)‡
Creatine kinase ≥10 × ULN	9 (4)	4 (4)
Fasting LDL cholesterol >190 mg/dL	9/224 (4)‡	0/106
Hemoglobin <9 g/dL	2 (<1)‡	5 (5)‡
Urine glucose (by dipstick) 4+	7 (3)¶	1 (1)¶
Occult blood	24 (11)¶	13 (12)¶
Urine erythrocytes	14/114 (12)¶	8/46 (17)‡

All AEs and Grade 3 or 4 laboratory abnormalities were treatment-emergent. ULN, upper limit of normal range; CI, confidence interval. \*64 yr-old woman had study treatment discontinued for an AE of Grade 2 renal impairment on Day 290 that was an SAE and related to study drug. †Laboratory results are based on 225 patients for TAF 25 mg, and 107 patients for TDF 300 mg, unless otherwise noted. ‡Only Grade 3 abnormalities were observed for these parameters. ¶Grade 3 was the highest grade for these parameters.

versus 22%;  $p = 0.003$ ). In addition, more patients that were given TAF versus TDF showed improvement in chronic kidney disease (CKD) stage at week 144 (e.g., Stage 2 →

Stage 1, Stage 3 → Stage 2), and a smaller proportion of TAF versus TDF-treated patients had CKD stage worsening (e.g., Stage 1 → Stage 2 [no patients negatively shifted to

**Table 4. Renal safety parameters at week 144**

	TAF (N = 227)	TDF (N = 107)
Mean serum creatinine (mg/dL [SD])		
Baseline	0.81 (0.144)	0.82 (0.151)
Change at week 144	−0.012 (0.090)	−0.002 (0.092)
Difference in least squares means (95% CI)	−0.011(−0.033–0.010)	
Median eGFR <sub>CG</sub> (mL/min [Q1, Q3])		
Baseline	113 (98, 129)	113 (97, 125)
Change at week 144	−0.4 (−8.2, 8.6)	−3.2 (−11.2, 5.2)
<i>p</i> -value	0.014	
≥25% decrease from baseline in eGFR <sub>CG</sub> (n/n)	22/225 (10)	24/107 (22)
<i>p</i> -value	0.003	
Shifts in CKD stage: baseline →week 144 <sup>*†</sup>		
<i>Improvement</i>		
Stage 2→1	7/32 (22)	1/12 (8)
Stage 3→2	1/1 (100)	0/2 (0)
<i>Worsening</i>		
Stage 1→2	12/180 (7)	10/85 (12)
Stage 2→3	0/32 (0)	0/12 (0)
<i>No change</i>		
Stage 1→1	168/180 (93)	75/85 (88)
Stage 2→2	25/32 (78)	11/12 (92)
Stage 3→3	0/1 (0)	2/2 (100)
<i>p</i> -value	0.064	
Median urinary proximal tubular markers (μg/g [Q1, Q3])		
RBP:Cr	n = 227	n = 107
Baseline	91 (65, 133)	93 (69, 138)
% change at week 144	−8 (−35, 41)	27 (−18, 71)
<i>p</i> -value	0.003	
β2M:Cr		
Baseline	94 (67, 152)	91 (58, 149)
% change at week 144	−29 (−56, 12.5)	18 (−35, 124)
<i>p</i> -value	<0.0001	

eGFR<sub>CG</sub>, estimated creatinine clearance by the Cockcroft-Gault method. RBP:Cr, urine retinol binding protein-to-creatinine ratio. β2M:Cr, urine beta-2 microglobulin to creatinine ratio. \*eGFR<sub>CG</sub>: Stage 1: ≥ 90 mL/min; Stage 2: ≥60 to < 90 mL/min; Stage 3: ≥ 30 to < 60 mL/min; Stage 4: ≥15 to <30 mL/min. <sup>†</sup>There were no Stage 4 CKD patients at baseline and no patients had moved to Stage 4 at week 144.

Stages 3 or 4]) (Table 4).

When median percentage changes from baseline were compared for the markers of proximal tubular function (RBP:Cr and β2M:Cr), significant differences were found that favored TAF treatment (Table 4 and Supplementary Figs. 1A, B). For both parameters, patients that received TAF had decreased results compared with increases for those on TDF. Significant differences in these highly sensitive markers by treatment were apparent by week 24 and were reconfirmed at week 144 (Supplementary Fig. 1A). Two TDF and no TAF patients had renal-related AEs: 1 patient in Study 110 had an AE of renal tubular disorder on day 85 that was nonserious, Grade 1 (mild), and resolved with continued study treatment on day 167, and another TDF patient in Study 108 had an AE of renal failure that was

associated with a decrease in creatinine clearance that led to discontinuation of the study drug during the first year of treatment.

### Changes in BMD

The mean (SD) percent change in hip BMD from baseline to week 144 was −0.95% (3.73%) for the subset of patients that underwent DXA scanning and received TAF, which was less than the −1.9% (3.83%) change in those that received TDF (Fig. 3A). Similarly, mean (SD) percent changes in spine BMD from baseline to week 144 were 0.35% (4.56%) and −1.4% (3.45%) for the subset of patients with DXA data

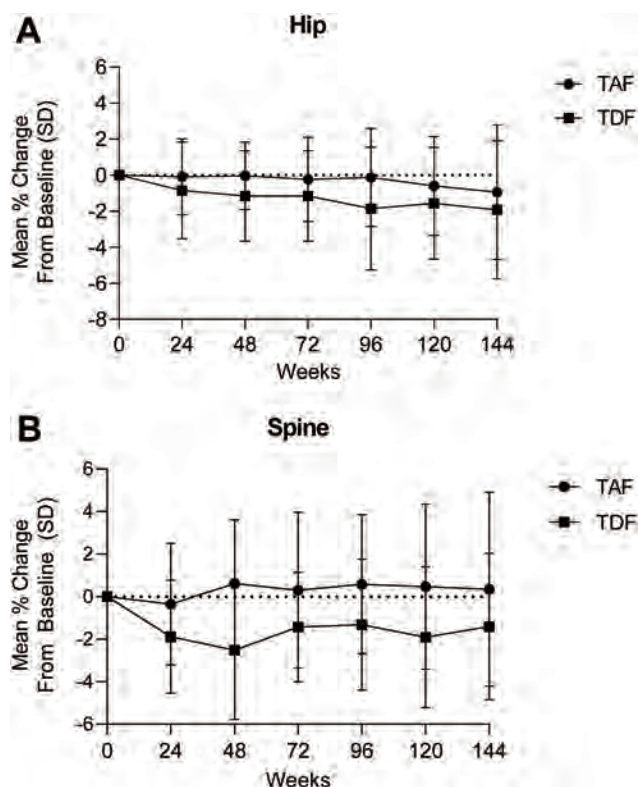


**Fig. 3. Mean percentage changes in BMD.** (A) Mean percentage change from baseline in hip BMD at weeks 24, 48, 72, 96, 120, and 144 of treatment in the subset of patients that underwent DXA scanning. (B) Mean percentage change from baseline in spine BMD at weeks 24, 48, 72, 96, 120, and 144 of treatment in the subset of patients that underwent DXA scanning. Analysis is missing equals excluded (observed data).

that received TAF and TDF, respectively (Fig. 3B). Using a cutoff of  $>5\%$  decrease at week 144, the proportions of patients were 25%–50% lower with TAF versus TDF treatment (hip BMD 8/67 [12%] versus 10/41 [24%] and spine BMD 6/71 [8%] versus 5/43 [12%], respectively) (Supplementary Tables 6A, B). Bone fracture was uncommon, usually trauma-related, and was observed at a similar frequency by treatment (TAF  $n = 4$  [clavicle, foot, pelvis, and spinal compression; 1 patient each] and TDF  $n = 2$  [forearm, 2 patients]).

## Discussion

In previous reports, the 48 and 96-week outcomes from the two double-blind, randomized, Phase 3 trials in the global (non-China) population confirmed that TAF has an antiviral efficacy that is noninferior to TDF with superior bone and renal safety in HBeAg-positive and negative patients.<sup>16–18</sup> The results in Chinese HBV patients presented in this study agree with the global data and, in November 2018, TAF was granted licensing approval by the National Medical Products Administration in China. In addition, the results represent the first randomized comparison of TAF versus TDF in CHB patients over a 3-year treatment period. Further, the population enrolled in study sites across multiple provinces in China (Supplemental Tables 1, 2) was representative of the population of Chinese patients that require HBV treatment.

In the China cohort, the proportions of patients that achieved and maintained HBV DNA  $<29$  IU/mL were simi-

lar between the TAF and TDF groups in each study over 3 years; the results are consistent with earlier data from the global program.<sup>16–18</sup> In HBeAg-positive and negative Chinese patients, high levels of viral suppression were observed at week 144 with TAF versus TDF (83% versus 79%, and 93% versus 92%, respectively). The numerically lower responses for TAF versus TDF (the 95% CI overlapped) at week 48 in each study was mainly due to some TAF patients with high baseline viral loads that took slightly longer to suppress and some that experienced a transient (one-time) viral blip. No difference in viral potency was noted as shown by similar proportions with an undetectable target for HBV DNA (i.e., full suppression), and similar small proportions with HBV DNA  $\geq 29$  IU/mL at week 144. Resistance surveillance that was conducted annually over 3 years showed no patients in either study had reduced susceptibility to TAF or TDF.

In the global studies, a significantly higher rate of ALT normalization was reported for TAF compared with TDF.<sup>16–18</sup> When the current ULN cutoffs for men and women recommended by AASLD were applied, results for the HBeAg-positive and negative patients showed higher ALT normalization with TAF treatment. In addition, this finding was observed when China ULN criteria were used. The mechanism(s) for improved ALT normalization with TAF versus TDF is unknown, this differential effect has been demonstrated in viremic, mostly treatment-naïve patients, and in virally suppressed, treatment-experienced patients that switched therapy from TDF to TAF.<sup>21</sup>

In HBeAg-positive Chinese patients, loss of HBeAg occurred at a slightly higher rate with TDF versus TAF at week 144 (28% versus 23%), although HBeAg seroconversion was similar (Table 2). The results for TAF were comparable with previously reported data from the global population; however, for TDF the rate of HBeAg loss was higher than previously reported (i.e., rates at week 96 were 22% and 18% for TAF and TDF, respectively).<sup>18</sup> Over 3 years of treatment, low rates of HBsAg loss ( $\leq 4\%$ ) and anti-HBs seroconversion ( $\leq 2\%$ ) were observed in patients that received TAF, and no TDF patients lost surface antigen. The low rate of HBsAg loss in Chinese patients was not unexpected, because of the previous data from TDF-treated patients that showed it to be genotype-related and occurred most often in patients with genotypes A and D.<sup>22</sup> After 3 years of treatment, mean declines in HBsAg were small ( $<1 \log_{10}$ ) in each study and similar between groups.

As in the Phase 3 registration program for TAF, histologic changes were not assessed in the Chinese cohort; instead, a serum FibroTest was utilized. The impact of treatment-induced changes in FibroTest with antivirals for CHB has not been well studied.<sup>19</sup> However, mean serum FibroTest scores decreased over 3 years to a similar magnitude with TAF and TDF treatment, and most patients in the highest FibroTest category (i.e.,  $\geq 0.75$  or Metavir F4) at baseline showed improvement on treatment with a few patients overall showing a categorical worsening. In Phase 3 studies with TDF, achievement and maintenance of long-term viral suppression in CHB patients over 5 years resulted in histologic regression of fibrosis and cirrhosis in most treated patients.<sup>8</sup> These two studies will continue for 8 years, and therefore, potentially the relationship between treatment response and fibrosis change could be better established.

Safety outcomes in Chinese patients were consistent with the results previously reported for the global population.<sup>16–18</sup> Overall, both treatments were safe and well tolerated with similar rates of SAEs and Grade 3 or 4 AEs and relatively few events were judged to be related to the study drug. No TAF patients required treatment discontinuation due to an AE and one TDF patient had treatment stopped within the first year after moderate renal impairment developed.



Differences were noted in fasting lipid profiles between TAF and TDF-treated patients, a finding that has been reported by other researchers.<sup>18,23,24</sup> In Chinese CHB patients, TDF treatment resulted in median decreases in HDL, LDL, and total cholesterol, as well as in triglycerides, which is consistent with its known lipid-lowering effect.<sup>23,24</sup> In comparison, TAF treatment produced decreases in total and HDL cholesterol (however, they were smaller in magnitude than TDF), and small increases in LDL and triglycerides were observed. The impact of TDF on fasting lipids has been reported to be correlated with increased plasma levels of TFV;<sup>23</sup> given that TFV exposures were approximately 90% lower when treated with TAF versus TDF,<sup>15</sup> this could explain these differences. The small difference observed between treatments in total cholesterol to HDL ratio change, as well as the small percent of TAF patients (1%) that started on statin therapy during the trial, the lipid differences were probably not clinically important for most patients. This point was recently made by the authors of a meta-analysis that involved >6,000 HIV-1-infected patients that participated in 7 randomized, controlled trials that compared TAF-based versus TDF-based antiretroviral therapy.<sup>24</sup> There were more TAF than TDF-treated patients with Grade 3 increases in LDL cholesterol in this pooled analysis; however, the elevations were nearly always transient (i.e., seen during a single study visit) and were in all cases preceded by an elevated baseline level of LDL, which suggested pre-existing hyperlipidemia.

In this analysis, differences that favored TAF versus TDF treatment were seen for several renal and bone safety parameters during the 144 weeks. The findings from this analysis were consistent with the global results where statistically prespecified key bone and renal safety endpoints demonstrated a safety benefit with TAF with the stipulation that noninferior efficacy to TDF must be established first.<sup>16–18</sup> Tenofovir, the main metabolite of both prodrugs, is taken up into renal proximal tubular cells via organic anion transporters 1 and 3 (OAT-1 and OAT-3), which is believed to play a central role in TDF-associated nephrotoxicity.<sup>25–27</sup> TAF has greater plasma stability than TDF and is not a substrate for uptake via OAT-1/OAT-3.<sup>14,27</sup> With TAF treatment the circulating levels of TFV are significantly reduced compared with TDF; therefore, there is less TFV available to the kidneys and improved renal safety is seen. This finding was reported in HBV and HIV-infected patients that were treated with TAF in clinical trials for ≤3 years.<sup>18,23,24,28</sup> In this analysis, significant differences in eGFR<sub>CG</sub> decrease and smaller changes in proximal tubular markers were observed. The results are particularly relevant because 21% of patients that entered these studies reported previous ADV use, a nucleotide antiviral that was previously shown to increase the potential risk of proximal tubulopathy when TDF was then used.<sup>29,30</sup>

The serial assessments of BMD by DXA were an important component of safety monitoring in TDF and TAF clinical programs for many years.<sup>16–18,23,24</sup> In this report, BMD was only assessed in a subset of patients at sites in China that could perform these scans. Apart from the subjects being a little older (mean age 40 versus 36 years;  $p = 0.002$ ), there were no notable differences between those enrolled at sites without ( $n = 186$ ) or with ( $n = 148$ ) DXA capability, which supports the BMD results generated were probably representative of the overall population. Over 3 years, TAF patients had only small changes in hip or spine BMD compared with the declines observed with TDF. Although the magnitude of BMD changes reported in this study was slightly different from the results in the global population (where all patients underwent DXA scanning),<sup>18</sup> these results confirm a differential difference in BMD in Chinese CHB patients that received TAF versus TDF.

This study has several limitations: the sample sizes for

the two studies could not confirm non-inferiority in efficacy; however, they were based on demonstrating comparability with global data to meet local registration requirements. Similar to the global studies, the inclusion of patients that were at a higher risk of TDF-associated bone and renal complications (e.g., older age, comorbidities including hyperlipidemia, history of bone, or renal disease, or both)<sup>7,8</sup> was limited; additional data from these more vulnerable populations are required. Finally, viremic patients with elevated levels of serum ALT were included, who meet the criteria to initiate treatment.<sup>7,8</sup> Additional studies on Chinese patients that are virally suppressed and changed to TAF from TDF or ETV would be beneficial, as would real world cohort studies that evaluate the use of TAF in clinical practice.

In conclusion, in CHB patients from China that were treated with TAF or TDF for 3 years, similar efficacy at suppressing HBV replication was found with no virologic resistance, and ALT normalization rates were higher with TAF. The safety results showed that TAF was well tolerated and was associated with less impact on bone and renal safety, as previously reported in the global HBV program.

## Acknowledgments

Editorial assistance was provided by Sandra Chen of Gilead Sciences.

## Funding

This study was sponsored by Gilead Sciences, Inc.

## Conflict of interest

Jinlin Hou has served as a consultant for AbbVie, Arbutus, Bristol Myers Squibb, Gilead Sciences, Johnson & Johnson, Roche and received grants from Bristol Myers Squibb, Gilead, and Johnson & Johnson. Qin Ning has served as a consultant for Gilead Sciences, Johnson & Johnson, AbbVie, Roche, Bristol-Myers Squibb, MSD, and has received research funding from Bristol-Myers Squibb, Roche, and Gilead Sciences. Qing Xie has served as a consultant for AbbVie, Bristol-Myers Squibb, Gilead Sciences, Johnson & Johnson, and Roche, and has received grants from Gilead Sciences. Shanming Wu has served as a consultant for Gilead Sciences, AbbVie, GSK, Bristol-Myers Squibb, and MSD, and has received research funding from Bristol-Myers Squibb, Roche, AbbVie, and Gilead Sciences. Hong Tang has served as a consultant for Gilead Sciences, MSD, AbbVie, GSK, Bristol-Myers Squibb, and has received research funding from Bristol-Myers Squibb, Roche, and Gilead Sciences. Jun Li has served as a consultant for Gilead, MSD, AbbVie, GSK, and Bristol-Myers Squibb. John F. Flaherty, Anuj Gaggar, Gregory Camus, Cong Cheng, and Shuyuan Mo are employees and stockholders of Gilead Sciences. Chengwei Chen has served as a consultant for Gilead, AbbVie, GSK, Bristol-Myers Squibb, MSD and received research funds from Bristol-Myers Squibb, Roche, AbbVie, and Gilead. Jidong Jia has served as a consultant for AbbVie, Bristol-Myers Squibb, Gilead and GSK, and received research funds from Bristol-Myers Squibb and Gilead. The other authors have no conflict of interests related to this publication.

## Author contributions

Contributed to the study concept and design (JH, JFF, AG),

the acquisition of data (JH, ZD, YC, QX, FSW, LZ, SW, HT, JL, FL, YY, GG, CC, YH, JJ, MZ, QN), and the statistical analysis (SM). All authors contributed to the analysis and interpretation of data, drafting of the manuscript, critical revision of the manuscript for important intellectual content.

## Data sharing statement

All data are available upon request.



## References

- [1] World Health Organization. Hepatitis B. Available from: <https://www.who.int/en/news-room/fact-sheets/detail/hepatitis-b>.
- [2] Global prevalence, treatment, and prevention of hepatitis B virus infection in 2016: a modelling study. *Lancet Gastroenterol Hepatol* 2018;3(6):383–403. doi:10.1016/S2468-1253(18)30056-6.
- [3] Wang FS, Fan JG, Zhang Z, Gao B, Wang HY. The global burden of liver disease: the major impact of China. *Hepatology* 2014;60(6):2099–2108. doi:10.1002/hep.27406.
- [4] Gish RG, Given BD, Lai CL, Locarnini SA, Lau JY, Lewis DL, *et al*. Chronic hepatitis B: Virology, natural history, current management and a glimpse at future opportunities. *Antiviral Res* 2015;121:47–58. doi:10.1016/j.antiviral.2015.06.008.
- [5] Peng CY, Chien RN, Liaw YF. Hepatitis B virus-related decompensated liver cirrhosis: benefits of antiviral therapy. *J Hepatol* 2012;57(2):442–450. doi:10.1016/j.jhep.2012.02.033.
- [6] Marcellin P, Gane E, Buti M, Afdhal N, Sievert W, Jacobson IM, *et al*. Regression of cirrhosis during treatment with tenofovir disoproxil fumarate for chronic hepatitis B: a 5-year open-label follow-up study. *Lancet* 2013;381(9865):468–475. doi:10.1016/S0140-6736(12)61425-1.
- [7] Terrault NA, Lok ASF, McMahon BJ, Chang KM, Hwang JP, Jonas MM, *et al*. Update on prevention, diagnosis, and treatment of chronic hepatitis B: AASLD 2018 hepatitis B guidance. *Hepatology* 2018;67(4):1560–1599. doi:10.1002/hep.29800.
- [8] Sarin SK, Kumar M, Lau GK, Abbas Z, Chan HL, Chen CJ, *et al*. Asian-Pacific clinical practice guidelines on the management of hepatitis B: a 2015 update. *Hepatol Int* 2016;10(1):1–98. doi:10.1007/s12072-015-9675-4.
- [9] Chen CH, Lin CL, Kao CH. Association between chronic hepatitis B virus infection and risk of osteoporosis: A nationwide population-based study. *Medicine (Baltimore)* 2015;94(50):e2276. doi:10.1097/MD.00000000000002276.
- [10] Chen YC, Su YC, Li CY, Hung SK. 13-year nationwide cohort study of chronic kidney disease risk among treatment-naïve patients with chronic hepatitis B in Taiwan. *BMC Nephrol* 2015;16:110. doi:10.1186/s12882-015-0106-5.
- [11] Maggi P, Montinaro V, Leone A, Fasano M, Volpe A, Bellacosa C, *et al*. Bone and kidney toxicity induced by nucleotide analogues in patients affected by HBV-related chronic hepatitis: a longitudinal study. *J Antimicrob Chemother* 2015;70(4):1150–1154. doi:10.1093/jac/dku502.
- [12] Lee WA, He GX, Eisenberg E, Cihlar T, Swaminathan S, Mulato A, *et al*. Selective intracellular activation of a novel prodrug of the human immunodeficiency virus reverse transcriptase inhibitor tenofovir leads to preferential distribution and accumulation in lymphatic tissue. *Antimicrob Agents Chemother* 2005;49(5):1898–1906. doi:10.1128/AAC.49.5.1898-1906.2005.
- [13] Delaney WE, Ray AS, Yang H, Qi X, Xiong S, *et al*. Intracellular metabolism and in vitro activity of tenofovir against hepatitis B virus. *Antimicrob Agents Chemother* 2006;50(7):2471–2477. doi:10.1128/AAC.00138-06.
- [14] Murakami E, Wang T, Park Y, Hao J, Lepist EI, Babusis D, *et al*. Implications of efficient hepatic delivery by tenofovir alafenamide (GS-7340) for hepatitis B virus therapy. *Antimicrob Agents Chemother* 2015;59(6):3563–3569. doi:10.1128/AAC.00128-15.
- [15] Agarwal K, Fung SK, Nguyen TT, Cheng W, Sicard E, Ryder SD, *et al*. Twenty-eight day safety, antiviral activity, and pharmacokinetics of tenofovir alafenamide for treatment of chronic hepatitis B infection. *J Hepatol* 2015;62(3):533–540. doi:10.1016/j.jhep.2014.10.035.
- [16] Buti M, Gane E, Seto WK, Chan HL, Chuang WL, Stepanova T, *et al*. Tenofovir alafenamide versus tenofovir disoproxil fumarate for the treatment of patients with HBeAg-negative chronic hepatitis B virus infection: a randomised, double-blind, phase 3, non-inferiority trial. *Lancet Gastroenterol Hepatol* 2016;1(3):196–206. doi:10.1016/S2468-1253(16)30107-8.
- [17] Chan HL, Fung S, Seto WK, Chuang WL, Chen CY, Kim HJ, *et al*. Tenofovir alafenamide versus tenofovir disoproxil fumarate for the treatment of HBeAg-positive chronic hepatitis B virus infection: a randomised, double-blind, phase 3, non-inferiority trial. *Lancet Gastroenterol Hepatol* 2016;1(3):185–195. doi:10.1016/S2468-1253(16)30024-3.
- [18] Agarwal K, Brunetto M, Seto WK, Lim YS, Fung S, Marcellin P, *et al*. 96 weeks treatment of tenofovir alafenamide vs. tenofovir disoproxil fumarate for hepatitis B virus infection. *J Hepatol* 2018;68(4):672–681. doi:10.1016/j.jhep.2017.11.039.
- [19] Salkic NN, Jovanovic P, Hauser G, Brcic M. FibroTest/FibroSure for significant liver fibrosis and cirrhosis in chronic hepatitis B: a meta-analysis. *Am J Gastroenterol* 2014;109(6):796–809. doi:10.1038/ajg.2014.21.
- [20] Liu Y, Corsi AC, Buti M, Cathcart AL, Flaherty JF, Miller MD, *et al*. No detectable resistance to tenofovir disoproxil fumarate in HBeAg+ and HBeAg- patients with chronic hepatitis B after 8 years of treatment. *J Viral Hepat* 2017;24(1):68–74. doi:10.1111/jvh.12613.
- [21] Lampertico P, Buti M, Fung S, Ahn SH, Chuang WL, Tak WY, *et al*. Switching from tenofovir disoproxil fumarate to tenofovir alafenamide in virologically suppressed patients with chronic hepatitis B: a randomised, double-blind, phase 3, multicentre non-inferiority study. *Lancet Gastroenterol Hepatol* 2020;5(5):441–453. doi:10.1016/S2468-1253(19)30421-2.
- [22] Marcellin P, Buti M, Krastev Z, de Man RA, Zeuzem S, Lou L, *et al*. Kinetics of hepatitis B surface antigen loss in patients with HBeAg-positive chronic hepatitis B treated with tenofovir disoproxil fumarate. *J Hepatol* 2014;61(6):1228–1237. doi:10.1016/j.jhep.2014.07.019.
- [23] Arribas JR, Thompson M, Sax PE, Haas B, McDonald C, Wohl DA, *et al*. Brief report: Randomized, double-blind comparison of tenofovir alafenamide (TAF) vs tenofovir disoproxil fumarate (TDF), each coformulated with elvitegravir, cobicistat, and emtricitabine (E/C/F) for initial HIV-1 treatment: week 144 results. *J Acquir Immune Defic Syndr* 2017;75(2):211–218. doi:10.1097/QAI.0000000000001350.
- [24] Tao X, Lu Y, Zhou Y, Zhang L, Chen Y. Efficacy and safety of the regimens containing tenofovir alafenamide versus tenofovir disoproxil fumarate in fixed-dose single-tablet regimens for initial treatment of HIV-1 infection: A meta-analysis of randomized controlled trials. *Int J Infect Dis* 2020;93:108–117. doi:10.1016/j.ijid.2020.01.035.
- [25] Cihlar T, Ho ES, Lin DC, Mulato AS. Human renal organic anion transporter 1 (hOAT1) and its role in the nephrotoxicity of antiviral nucleotide analogs. *Nucleosides Nucleotides Nucleic Acids* 2001;20(4-7):641–648. doi:10.1081/NCN-100002341.
- [26] Lampertico P, Chan HL, Janssen HL, Strasser SI, Schindler R, Berg T. Review article: long-term safety of nucleoside and nucleotide analogues in HBV-monoinfected patients. *Aliment Pharmacol Ther* 2016;44(1):16–34. doi:10.1111/apt.13659.
- [27] Bam RA, Yant SR, Cihlar T. Tenofovir alafenamide is not a substrate for renal organic anion transporters (OATs) and does not exhibit OAT-dependent cytotoxicity. *Antivir Ther* 2014;19(7):687–692. doi:10.3851/IMP2770.
- [28] Gupta SK, Post FA, Arribas JR, Eron JJ Jr, Wohl DA, Clarke AE, *et al*. Renal safety of tenofovir alafenamide vs. tenofovir disoproxil fumarate: a pooled analysis of 26 clinical trials. *AIDS* 2019;33(9):1455–1465. doi:10.1097/QAD.0000000000002223.
- [29] Gara N, Zhao X, Collins MT, Chong WH, Kleiner DE, Jake Liang T, *et al*. Renal tubular dysfunction during long-term adefovir or tenofovir therapy in chronic hepatitis B. *Aliment Pharmacol Ther* 2012;35(11):1317–1325. doi:10.1111/j.1365-2036.2012.05093.x.
- [30] Trinh S, Le AK, Chang ET, Hoang J, Jeong D, Chung M, *et al*. Changes in renal function in patients with chronic HBV infection treated with tenofovir disoproxil fumarate vs entecavir. *Clin Gastroenterol Hepatol* 2019;17(5):948–956.e1. doi:10.1016/j.cgh.2018.08.037.



Original Article

# Tenofovir Alafenamide Fumarate, Tenofovir Disoproxil Fumarate and Entecavir: Which is the Most Effective Drug for Chronic Hepatitis B? A Systematic Review and Meta-analysis

Xuefeng Ma<sup>1#</sup>, Shousheng Liu<sup>2,3#</sup>, Mengke Wang<sup>1</sup>, Yifen Wang<sup>1</sup>, Shuixian Du<sup>1</sup>, Yongning Xin<sup>1,3\*</sup>   
and Shiying Xuan<sup>1,3\*</sup> 

<sup>1</sup>Department of Infectious Disease, Qingdao Municipal Hospital, Qingdao University, Qingdao, Shandong, China; <sup>2</sup>Clinical Research Center, Qingdao Municipal Hospital, Qingdao University, Qingdao, Shandong, China; <sup>3</sup>Digestive Disease Key Laboratory of Qingdao, Qingdao, Shandong, China

Received: 14 December 2020 | Revised: 23 January 2021 | Accepted: 9 March 2021 | Published: 29 March 2021

## Abstract

**Background and Aims:** The therapeutic effect of tenofovir alafenamide fumarate (TAF), tenofovir disoproxil fumarate (TDF) and entecavir (ETV) on chronic hepatitis B (CHB) patients remains inconsistent. The aim of this study was to explore the differences in virological responses to TAF, TDF and ETV in patients with CHB. **Methods:** Literature searches were conducted of the PubMed, EMBASE, and the Cochrane Library databases to identify randomized controlled trials and observational studies published up to July 21, 2020. Statistical comparisons of virological response between TDF, ETV, and TAF were carried out with pooled odds ratio (OR) values. **Results:** The virological response in TDF-treated CHB patients was notably superior to that of the ETV-treated CHB patients after 12-weeks [OR=1.12, 95% confidence interval (CI): 0.89–1.41], 24-weeks (OR=1.33, 95% CI: 1.11–1.61), 48-weeks (OR=1.62, 95% CI: 1.16–2.25), 72-weeks (OR=1.43, 95% CI: 0.78–2.62), and 96-weeks (OR=1.56, 95% CI: 0.87–2.81) treatment. No significant difference was observed for the virological responses in CHB patients after 48-weeks treatment with TAF or TDF. The virological response in TDF+ETV-treated CHB patients was superior to that of TDF-treated CHB patients after 24-weeks, 48-weeks (OR=1.54, 95% CI: 1.17–2.02), 96-weeks, and 144-weeks. **Conclusions:** The virological response in TDF-treated CHB patients was superior to that in ETV-treated CHB patients, but there was no significant difference between TAF and TDF. In addition, the therapeutic

effect of TDF+ETV was superior to TDF alone.

**Citation of this article:** Ma X, Liu S, Wang M, Wang Y, Du S, Xin Y, *et al.* Tenofovir alafenamide fumarate, tenofovir disoproxil fumarate and entecavir: which is the most effective drug for chronic hepatitis B? a systematic review and meta-analysis. J Clin Transl Hepatol 2021;9(3):335–344. doi: 10.14218/JCTH.2020.00164.

## Introduction

Hepatitis B virus (HBV) infection is a serious global health problem and patients are considered to be at high risk of developing hepatic cirrhosis and hepatocellular carcinoma (referred to herein as HCC).<sup>1</sup> A report from the World Health Organization indicated that 292 million individuals are positive for the hepatitis B surface antigen across the globe, and the distribution of chronic hepatitis B (CHB) patients is region-dependent.<sup>2,3</sup> HBV infection has become one of the principal causes of liver-related mortality globally, and approximately 700,000 HBV-related deaths occurred in 2013 alone.<sup>3</sup>

Tenofovir alafenamide fumarate (TAF), tenofovir disoproxil fumarate (TDF) and entecavir (ETV) are recommended as the first-line oral drugs for patients with CHB.<sup>4,5</sup> Furthermore, these drugs exert good effect on the suppression of HBV replication, provide histologic improvement, and reduce the incidence of HCC after the long-term nucleos(t)ide analogue therapy.<sup>6,7</sup> TAF is a bioavailable prodrug of tenofovir (TFV), which is regarded as an effective therapeutic drug for both HBV and human immunodeficiency virus (*i.e.* HIV-1) infection.<sup>8,9</sup> A previous study found that TAF possesses greater plasma stability, safety and toleration than TDF.<sup>10</sup> According to the clinical trials, TAF was more likely to be safe compared to TDF, most notably for patients with bone and renal dysfunction.<sup>11,12</sup> Ridruejo *et al.*<sup>13</sup> reported that ETV had long-term effectiveness and safety for HBV patients, while some other studies have demonstrated that the rate of HBV DNA suppression achieved was less than that with TDF or TAF within 3 years.

In consideration of the inconsistency of the therapeutic effects of TAF, TDF, and ETV for patients with CHB, and whether the combination of TAF and ETV possesses a better

**Keywords:** Tenofovir alafenamide; Entecavir; Tenofovir disoproxil; Chronic hepatitis B; Virological response.

**Abbreviations:** CHB, chronic hepatitis B; CI, confidence interval; eGFR, estimated glomerular filtration rate; ETV, entecavir; HBV, hepatitis B virus; HCC, hepatocellular carcinoma; HIV, human immunodeficiency virus; NOS, Newcastle-Ottawa scale; OR, odds ratio; RCT, randomized controlled trial; PRISMA, Preferred Reporting Items for Systematic Reviews and Meta-Analyses; TAF, Tenofovir alafenamide fumarate; TDF, tenofovir disoproxil fumarate; TFV, tenofovir.

\*Both authors contributed equally to this work.

**Correspondence to:** Yongning Xin, Department of Infectious Disease, Qingdao Municipal Hospital, 1 Jiaozhou Road, Qingdao, Shandong 266011, China. ORCID: <https://orcid.org/0000-0002-3692-7655>. Tel: +86-532-8278-9463, Fax: +86-532-8596-8434, E-mail: [xinyongning@163.com](mailto:xinyongning@163.com); Shiying Xuan, Department of Infectious Disease, Qingdao Municipal Hospital, 1 Jiaozhou Road, Qingdao, Shandong 266011, China. ORCID: <https://orcid.org/0000-0002-9849-1877>. Tel: +86-532-8890-5508, Fax: +86-532-8890-5293, E-mail: [xuansydx@163.com](mailto:xuansydx@163.com)



effect than single-agent TAF treatment in CHB patients, this study was designed to explore the difference of virological response with TAF, TDF, and ETV, and the combination of TAF and ETV in the patients with CHB.

## Methods

### Study selection

A literature search was performed in the PubMed, Cochrane Library, and Embase databases according to the Preferred Reporting Items for Systematic Reviews and Meta-Analyses (commonly known as PRISMA) process. Studies published up to July 21, 2020 and in the English language were considered. Various combinations of the following keywords were applied in the search strategy: tenofovir alafenamide, TAF, emlidy, ETV, entecavir, ECV, Enti, En, Viread, tenofovir disoprox, TDF.

### Inclusion and exclusion criteria

The inclusive criteria were as follows: 1) research type: randomized controlled trial (RCT) and observational study; 2) research subjects: patients with chronic hepatitis B and only those patients diagnosed by HBV DNA test; 3) data on virological response, defined as undetectable HBV DNA level in serum and the lower limit for undetectable HBV DNA having been determined; and 4) receipt of treatment with TDF, TAF, or ENT or combination of these drugs. The exclusion criteria were as follows: 1) research type: review; 2) data unable to be extracted or utilized; 3) data based upon animal experiments; or 4) patients co-infected with HIV or other hepato-tropic viruses.

### Data extraction and quality assessment

Information including the first author, publication date, country, sample size, study type, intervention mode, and undetectable HBV DNA level were extracted from each study. The virological response rate of the intervention group and control group were pooled for the meta-analysis. The article list and extracted data were checked by a third researcher, to ensure no patient overlap was present among the different included studies. Quality of the included studies was assessed independently by two authors (Xuefeng Ma and Shousheng Liu). Any discrepancies were resolved through consensus decision upon discussion with a third author. The cohort studies were evaluated according to the Newcastle-Ottawa scale (commonly known as the NOS).<sup>14</sup> The NOS is comprised of the following three sections: selection (up to 4 points); comparability (up to 2 points); and, outcome (up to 3 points). The maximum score is 9 points. Study quality was classified as poor (score, 0–3), fair (score, 4–6), or good (score, 7–9). For RCTs, the updated Cochrane tool (<https://www.riskof-bias.info/>) was used to assess the risk of bias. The updated Cochrane tool was made up of the following domains: random sequence generation; allocation concealment; blinding of participants and personnel; blinding of outcome assessment; incomplete outcome data; selective reporting bias; and other sources of bias. The high, low, or unclear risks of bias of each study were determined in those domains.

### Statistical analysis

STATA 14 software (Stata Corporation, College Station, TX,

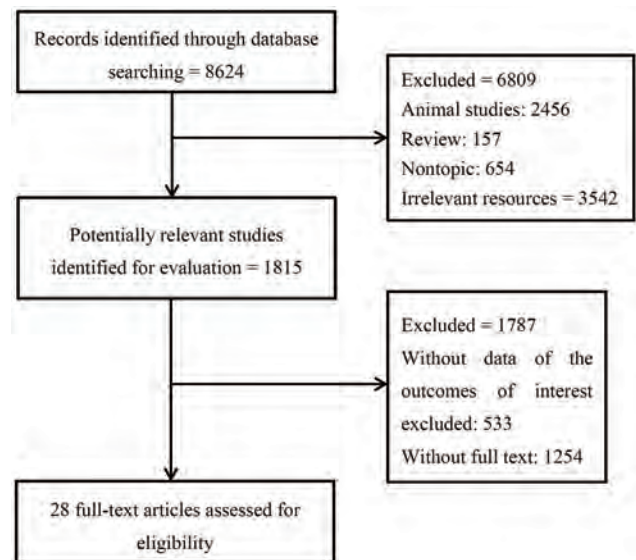


Fig. 1. Flow chart of the literature search process.

USA) was used for data analysis in this study. Dichotomous variables were expressed as odds ratio (OR; as an effective indicator) and the estimated value and 95% confidence interval (CI) were included as effect analysis statistics. For the Q statistic, heterogeneity was considered present when  $p$  was  $<0.1$  or  $I^2$  was  $>50\%$ . A fixed-effect model was used when literature heterogeneity did not exist; otherwise, a random-effect model was used. Publication bias was calculated visually with funnel plots. Publication bias was considered significant when  $p$  was  $<0.05$  in Begg's test. Subgroup analyses were performed according to undetectable HBV DNA level and design of the study.

## Results

### Literature search results and study characteristics

A total of 8,624 studies were identified as potentially relevant studies from the databases. After removing animal studies, reviews, non-topical studies and irrelevant resources, 1,815 studies were retrieved for further evaluation. After excluding studies which did not provide detailed information of virologic response and those without full-text, 28 studies were included for this meta-analysis (Fig. 1). Among these selected studies, 17 focused on the comparison of TDF vs. ETV, 5 focused on the comparison of TAF vs. TDF, and 6 focused on the comparison of TDF+ETV vs. TDF. Among these selected studies, 13 were RCTs,<sup>15–27</sup> 14 were cohort studies,<sup>28–41</sup> and only 1 was a cross-sectional study<sup>42</sup> (Table 1). Quality assessment suggested that all the cohort studies and RCTs possessed high quality (Table 1 and Fig. 2). Other characteristics of included studies are presented in Supplementary Table 1.

### Comparison of the virological response in TDF-treated vs. ETV-treated CHB patients

A total of 17 studies investigated the difference of virological response in patients with CHB after treatment with TDF and ETV<sup>19,22,26–34,36–39,41,42</sup> (Table 1). Among these studies,

Table 1. Characteristics of studies that met our inclusion criteria

Author	Year	Country	Sample size	Study type	Follow-up in weeks	Intervention	Undetectable HBV DNA level	Study quality
Batirel et al. <sup>28</sup>	2014	Turkey	195	Retrospective study	48	Received TDF (245 mg/day) or ETV (0.5 mg/day)	20 IU/mL	Good
Cai et al. <sup>19</sup>	2019	China	315	RCT	144	All the drugs, either TDF capsule or ETV capsule, were provided by Cosunter Pharmaceutical (Ningde, Fujian, China)	20 IU/mL	NA
Centeno et al. <sup>34</sup>	2016	Spain	64	Retrospective study	48	Initiated treatment with TDF or ETV between January 1998 and 2013	20 IU/mL	Good
Ceylan et al. <sup>29</sup>	2013	Turkey	117	Retrospective study	96	Treatment with TDF or ETV	20 IU/mL	Good
Ha et al. <sup>30</sup>	2016	USA	556	Retrospective study	96	Either ETV 0.5 mg daily or TDF 300 mg daily	40 IU/mL	Good
Jayakumar et al. <sup>31</sup>	2012	India	39	Prospective study	24	Treated with lamivudine (100 mg/day) plus adefovir (10 mg/day) combination ETV monotherapy (0.5 mg/day) and tenofovir monotherapy (300 mg/day)	400 copies/mL	Good
Kayaaslan et al. <sup>32</sup>	2017	Turkey	252	Retrospective study	96	Therapy with ETV 0.5–1 mg/day or TDF 245 mg/day	20 IU/mL	Good
Koike et al. <sup>22</sup>	2017	Japan	166	RCT	24	TDF 300 mg QD and ETV 0.5 mg QD	NA	NA
Kwon et al. <sup>33</sup>	2015	Korea	79	Retrospective study	48	Treatment with TDF or ETV	20 IU/mL	Good
Ozaras et al. <sup>36</sup>	2014	Turkey	251	Cohort study	72	Treatment with TDF or ETV	2*10 <sup>6</sup> IU/mL	Good
Park et al. <sup>37</sup>	2017	Korea	210	Cohort study	48	Treatment with TDF or ETV	20 IU/mL	Good
Riveiro-Barciela et al. <sup>38</sup>	2017	Spain	611	Cohort study	60	ETV at dose of 0.5 or 1 mg per day, and TDF at dose of 245 mg per day	69 IU/mL	Good
Pereira et al. <sup>42</sup>	2016	Brazil	294	Cross-sectional study	48	Treatment with TDF or ETV	NA	NA
Shi et al. <sup>39</sup>	2016	China	96	Retrospective study	96	Treated orally with ETV at 0.5 mg/day (ETV group) and tenofovir at 300 mg/day (TDF group)	100 IU/mL	Good
Sriprayoon et al. <sup>26</sup>	2016	Thailand	400	RCT	144	Receive either ETV 0.5 mg or TDF 300 mg daily	20 IU/mL	NA
Yim et al. <sup>27</sup>	2018	Korea	40	RCT	48	One group received 300 mg of TDF once daily and the other received 0.5 mg of ETV once daily	120 copies/mL	NA
Yu et al. <sup>41</sup>	2014	Korea	107	Retrospective study	48	Treated with TDF 300 mg daily, and the ETV group treated with ETV 0.5 mg daily	50 IU/mL	Good

(continued)

Table 1. (continued)

Author	Year	Country	Sample size	Study type	Follow-up in weeks	Intervention	Undetectable HBV DNA level	Study quality
Agarwal et al. <sup>15</sup>	2018	United Kingdom	1,298	RCT	48	Receive 25 mg TAF or 300 mg TDF	29 IU/mL	NA
Buti et al. <sup>16</sup>	2016	Spain	425	RCT	96	Receive once-daily oral doses of TAF 25 mg or TDF 300 mg, each with matching placebo	29 IU/mL	NA
Buti et al. <sup>17</sup>	2017	Spain	1,298	RCT	48	Receive oral tablets containing 150 mg elvitegravir, 150 mg cobicistat, 200 mg emtricitabine, and 10 mg TAF (elvitegravir/cobicistat/emtricitabine/TAF) or 300 mg TDF (elvitegravir/cobicistat/emtricitabine /TDF)	29 IU/mL	NA
TAF vs. TDF	Byrne et al. <sup>18</sup>	Spain	1,298	RCT	96	Different doses of TAF (8, 25, 40 or 120 mg) or to TDF 300 mg	29 IU/mL	NA
	Chan et al. <sup>20</sup>	China	873	RCT	96	Received TAF 25 mg orally once daily or TDF 300 mg orally once daily.	29 IU/mL	NA
	Jeon et al. <sup>21</sup>	Korea	54	RCT	96	Related with TDF monotherapy (n=12), TDF+LAM (n=19), or TDF+ETV (n=42)	12 IU/mL	NA
TDF+ETV vs. TDF	Lim et al. <sup>23</sup>	Korea	90	RCT	48	Receive TDF (300 mg/day) monotherapy or TDF and ETV (1 mg/day) combination therapy	15 IU/mL and 60 IU/mL	NA
	Lim et al. <sup>24</sup>	Korea	192	RCT	144	After completing 48 weeks of randomized, parallel comparisons of TDF monotherapy (300 mg once daily) vs. TDF/ETV combination therapy, patients were eligible to continue TDF monotherapy (TDF-TDF group) or switch to TDF monotherapy (TDF/ETV-TDF group)	15 IU/mL and 60 IU/mL	NA
	Lok et al. <sup>25</sup>	Turkey	379	RCT	96	Receive ETV 0.5 mg plus TDF 300mg once daily or ETV 0.5 mg once daily for 100 weeks	50 IU/mL	NA
	Lu et al. <sup>35</sup>	USA	68	Retrospective cohort study	68	At least 12 months of ETV, and were switched to TDF monotherapy (n=25) or ETV+TDF (n=43)	60 IU/mL	Good
	Wang et al. <sup>40</sup>	China	143	Retrospective study	143	CHB patients with PVR to ETV were switched to TDF monotherapy or TDF+ETV combination therapy	100IU/mL	Good



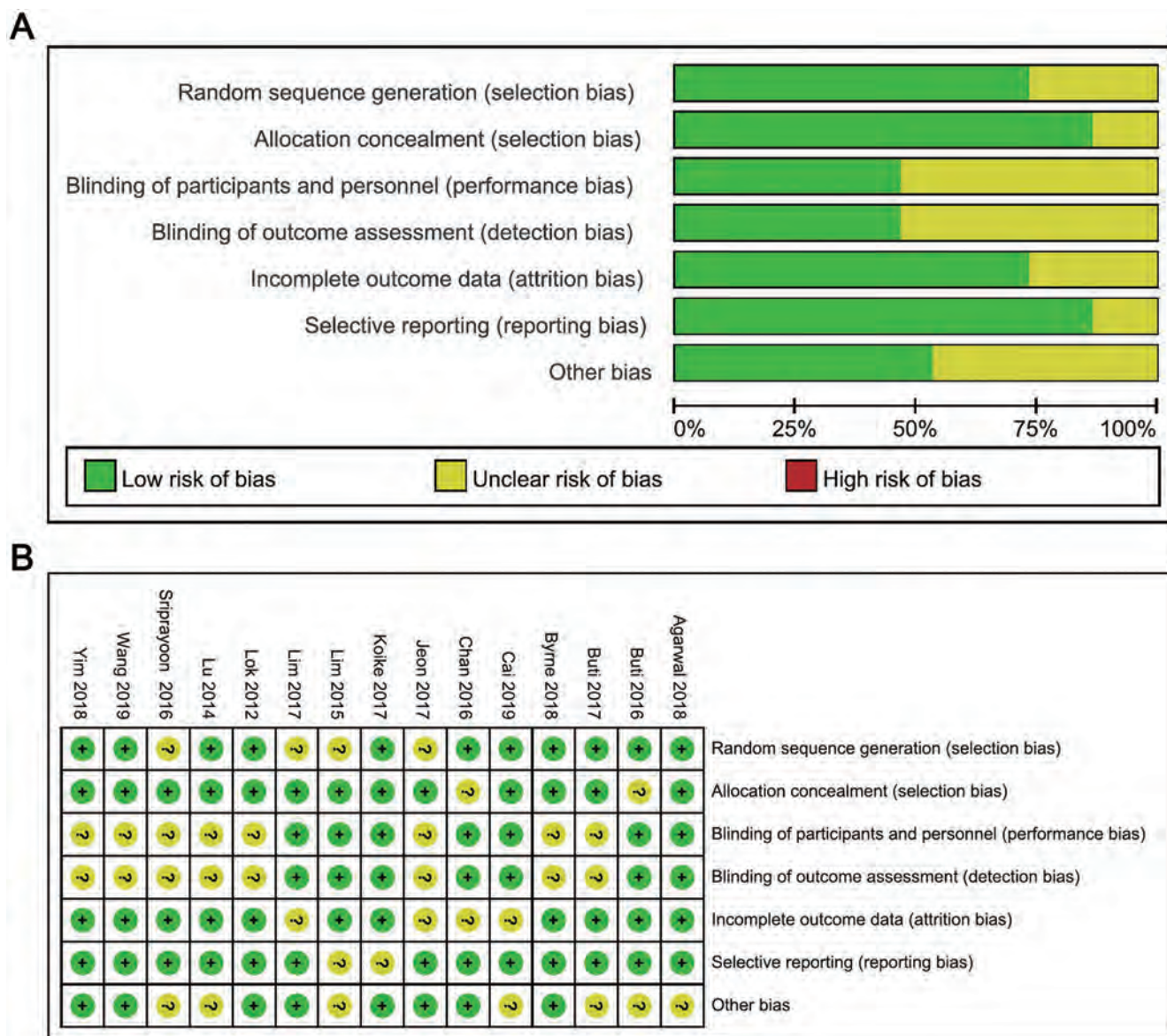


**Fig. 2. Risk-of-bias summary for the included randomized controlled trials (RCTs).** (A) Overall risk of bias of the included RCTs. (B) Performance of bias in each study. RCT, randomized controlled trial.

four were conducted in South Korea, four in Turkey, two in China, one in Japan, one in India, one in Brazil, one in Thailand, and one in the USA. Furthermore, 13 were observational studies, which included 12 cohort studies and 1 cross-sectional study, and 4 were RCTs. A total of 3,792 patients were involved in the 17 total studies.

Nine studies reported the virological response of patients with CHB after 12 weeks of treatment with TDF and ETV. The pooled effects of TDF and ETV on virological response were analyzed by using the fixed-effects model ( $p=0.547$ ,  $I^2=0.0\%$ ). The results showed that the virological response of TDF was superior to that of ETV (OR=1.12, 95% CI: 0.89–1.41), but the difference was not statistically significant ( $p>0.05$ ) (Fig. 3A). Thirteen studies reported the virological response of patients with CHB after 24 weeks of treatment with TDF and ETV. The outcome was demonstrated by a fixed fixed-effects model ( $p=0.053$ ,  $I^2=42.3\%$ ),

and the pooled OR was 1.33 (95% CI: 1.11–1.61,  $p<0.05$ ) (Fig. 3B). Three studies reported the virological response of patients with CHB after 36 weeks of treatment with TDF and ETV. The outcome was demonstrated by the random-effects model ( $p=0.128$ ,  $I^2=51.4\%$ ), and the pooled OR was 0.93 (95% CI: 0.46–1.87,  $p>0.05$ ) (Fig. 3C). Twelve studies reported the virological response of patients with CHB after 48 weeks of treatment with TDF and ETV. The outcome was demonstrated by the random-effects model ( $p=0.007$ ,  $I^2=51.8\%$ ), and the pooled OR was 1.62 (95% CI: 1.16–2.25,  $p<0.05$ ) (Fig. 3D). Six studies reported the virological response of patients with CHB after 72 weeks of treatment with TDF and ETV. The outcome was demonstrated by the random-effects model ( $p=0.001$ ,  $I^2=75.1\%$ ), and the pooled OR was 1.43 (95% CI: 0.78–2.62,  $p>0.05$ ) (Fig. 3E). Six studies reported the virological response of patients with CHB after 96 weeks of treatment with TDF and

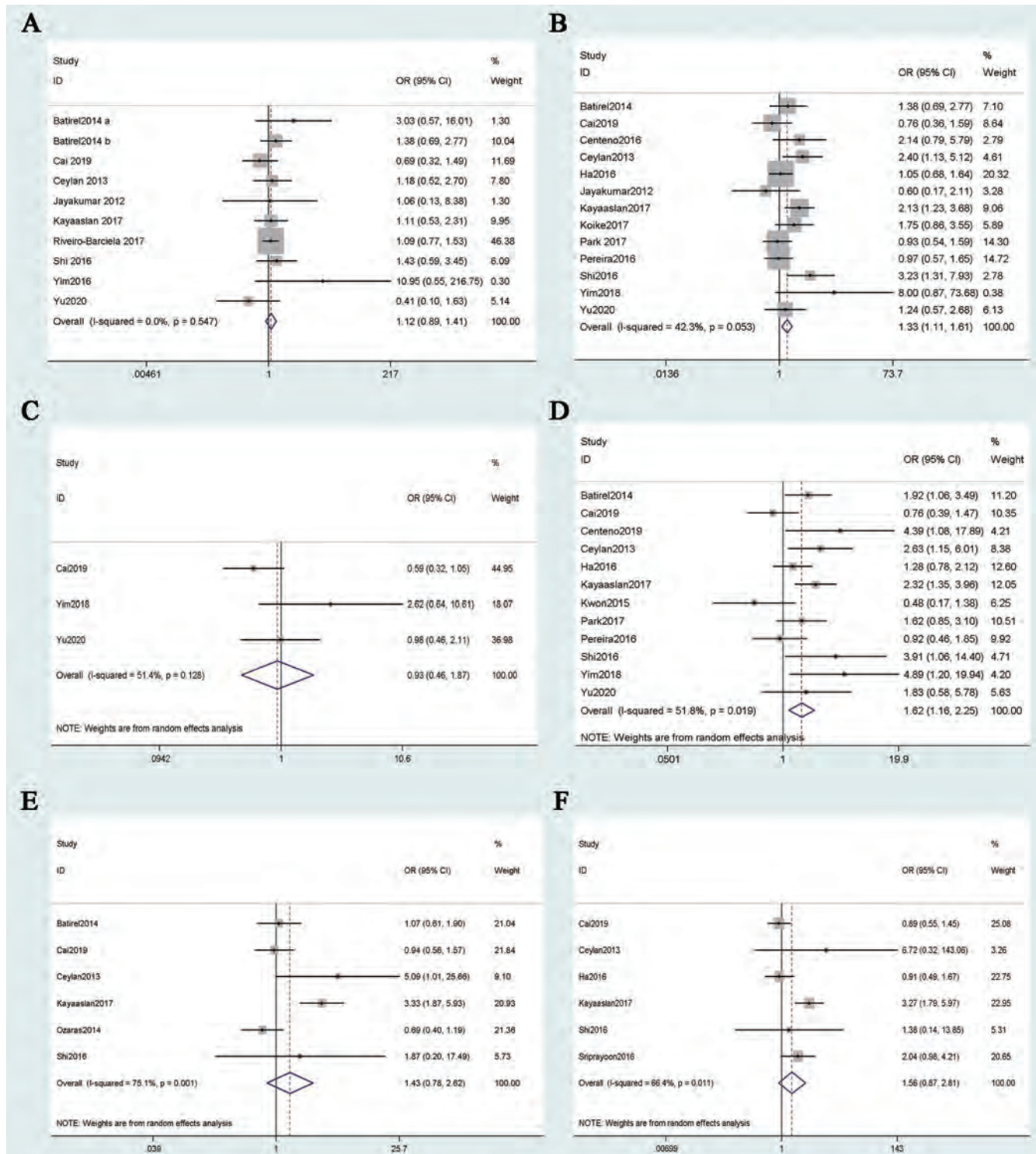


**Fig. 3. Pooled odds ratios (ORs) of virological response in tenofovir disoproxil fumarate (TDF)-treated vs. entecavir (ETV)-treated chronic hepatitis B (CHB) patients.** After (A) 12 weeks, (B) 24 weeks, (C) 36 weeks, (D) 48 weeks, (E) 72 weeks and (F) 96 weeks of treatment. CHB, chronic hepatitis B; ETV, entecavir; OR, odds ratio; TDF, tenofovir disoproxil fumarate.

ETV. The outcome was demonstrated by the random-effects model ( $p < 0.001$ ,  $I^2 = 88.0\%$ ), and the pooled OR was 1.56 (95% CI: 0.87–2.81,  $p > 0.05$ ) (Fig. 3F). The virological response of patients with CHB after 120 weeks of treatment

with TDF and ETV was reported in one study and after 144 weeks treatment was reported in two studies; the results suggested that there was no strong difference in the virological response after treatment with TDF or ETV.



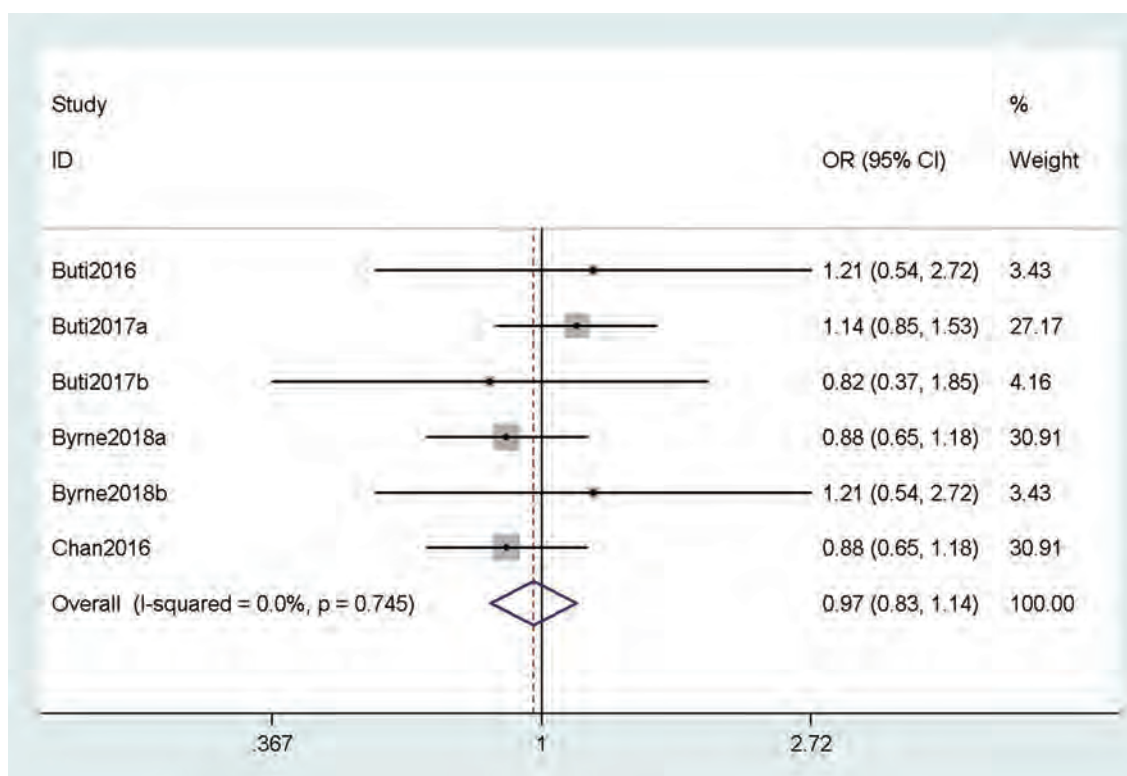


**Fig. 4. Pooled OR of virological response in tenofovir alafenamide fumarate (TAF)-treated vs. TDF-treated CHB patients after 48 weeks of treatment.** CHB, chronic hepatitis B; OR, odds ratio; TAF, Tenofovir alafenamide fumarate; TDF, tenofovir disoproxil fumarate.

#### Comparison of the virological response in TAF-treated vs. TDF-treated CHB patients

Five of the studies investigated the difference of virological response in patients with CHB after treatment with TAF and TDF<sup>15–18,20</sup> (Table 1). Among those studies, three were conducted in Spain, one was conducted in the UK and 1 was conducted in China. All were RCTs, and a total of 5,192 patients were included in these studies.

Four studies reported the virological response of patients with CHB after 48 weeks of treatment with TAF and TDF. The pooled effects of TAF and TDF on the virological response were analyzed by using the fixed-effects model ( $p=0.783$ ,  $I^2=0.0\%$ ). The results showed that the virological response of TAF was equivalent to that of TDF (OR=0.97, 95% CI: 0.83–1.14,  $p>0.05$ ) (Fig. 4). The virological response of patients with CHB after 96 weeks of treatment with TAF and TDF was reported in two studies, the results suggested that there was no obvious differences in the virological response after treatment with TAF and TDF.

#### Comparison of the virological response in TDF+ETV-treated vs. TDF-treated CHB patients

Six studies investigated the difference of virological response in patients with CHB after treatment with TDF+ETV and TDF<sup>21,23–25,35,40</sup> (Table 1). Among these, four were conducted in South Korea, one was conducted in China and one was conducted in the USA. Furthermore, two studies were cohort studies and one was an RCT; a total of 926 patients were included in these studies.

The virological response of patients with CHB after 24

weeks of treatment with TDF+ETV or TDF alone was reported in two studies. The results suggested that the therapeutic effect of TDF+ETV was significantly superior to that of TDF alone. Six studies reported the virological response of patients with CHB after 48 weeks of treatment with TDF+ETV or TDF alone. The outcome was demonstrated by the random-effects model ( $p=0.529$ ,  $I^2=0.0\%$ ), and the pooled OR was 1.54 (95% CI: 1.17–2.02,  $p<0.05$ ) (Fig. 5). The virological response of patients with CHB after 96 weeks and 144 weeks of treatment with TDF+ETV or TDF alone was reported in two studies and one study, respectively. The results suggested that the therapeutic effect of TDF+ETV was significantly superior to that of TDF alone.

#### Discussion

In this study, we systematically compared the therapeutic effect of TDF, TAF, ETV, and TDF+ETV on CHB patients. Our results suggest that in the TDF-treated CHB patients, the virological response was markedly superior to that of ETV-treated CHB patients after 12-, 24-, 48-, 72-, and 96-weeks treatment, which supports that TDF can be superior to ETV for the treatment of CHB patients. When compared to the therapeutic effect of TAF and TDF, no obvious difference was observed, which suggests that TAF is comparable to TDF for the treatment of CHB patients. In addition, we found that the virological response in TDF+ETV-treated CHB patients was superior to that of TDF-treated CHB patients after 24-, 48-, 96-, and 144-weeks treatment, which suggests that TDF combined with ETV exerts a better therapeutic effect for CHB patients than TDF alone.

TDF and ETV are two types of nucleos(t)ide analogues that can efficiently inhibit the replication of HBV via the

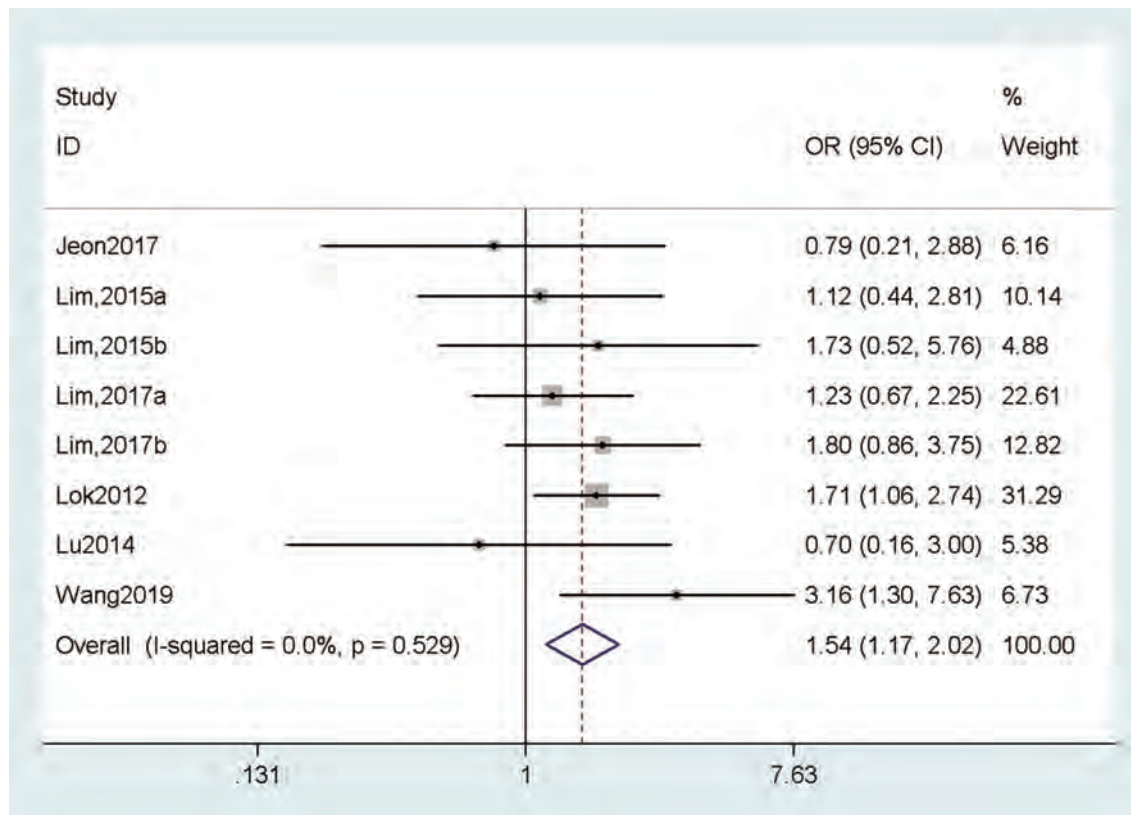


**Fig. 5. Pooled OR of virological response in TDF+ETV-treated vs. TDF-treated CHB patients after 48 weeks of treatment.** CHB, chronic hepatitis B; ETV, entecavir; OR, odds ratio; TDF, tenofovir disoproxil fumarate.

blockade of DNA polymerase and reverse transcriptase, respectively.<sup>43</sup> Nowadays, TDF and ETV are widely used for patients with CHB, due to their potent antiviral activities. The therapeutic effect of TDF and ETV in CHB patients has been investigated in some studies, but the conclusions have not been consistent. Yim *et al.*<sup>27</sup> conducted a RCT to investigate the virological response in CHB patients upon treatment with TDF or ETV. They found that when patients were switched to TDF from ETV, the HBV DNA level was significantly lower than that detected in the ETV treatment group.

In this meta-analysis, we summarized all the relative studies to compare the value of TDF and ETV on the treatment of CHB. We found that TDF was superior to ETV for the treatment of CHB patients. However, there were some inconsistencies observed regarding safety. Cai *et al.*<sup>19</sup> reported that both TDF and ETV were generally well tolerated, and the common adverse events were similar with no obvious fluctuation of the estimated glomerular filtration rate (commonly known as eGFR) found during the observational period between the TDF group and ETV group. Meanwhile, Centeno *et al.*<sup>34</sup> reported that after 48 weeks of treatment, 19.4% of patients in the TDF group showed eGFR <60 mL/min/1.73m<sup>2</sup> vs. 15.6% in the ETV group, which demonstrated the better effect achieved with TDF than ETV.

TAF is a newly developed prodrug of TFV, which can facilitate better entry of TFV into hepatocytes than TDF. Agarwal *et al.*<sup>15</sup> reported that after treatment with TAF, patients possessed higher intracellular concentrations of TFV and lower plasma concentrations of TFV compared to those who were on treatment with TDF. Our meta-analysis indicated that there was no significant difference in the virological responses of patients treated with TAF vs. TDF. Regarding

safety, Chan *et al.*<sup>7,20</sup> found that the unique pharmacokinetic profile of TAF had caused the declined rates of TFV-related major adverse events, kidney dysfunction, and bone mineralization, when compared with TDF. Furthermore, many studies have displayed that the levels of low-density lipoprotein, fasting total cholesterol, and high-density lipoprotein were all reduced in patients with HIV co-infection;<sup>44,45</sup> although, the precise mechanism for these changes remains unclear. Besides the TAF vs. TDF comparison results, we also found the TDF+ETV combination can bring about an effective virological response compared to TDF alone in CHB patients. Whereas, Wang *et al.*<sup>40</sup> found slightly increased serum creatinine level and decreased serum phosphorus level in TDF+ETV-treated CHB patients, but with both of which being within the normal range.

The therapeutic effect of TDF or ETV in CHB patients may be influenced by the genotype of HBV. Lok *et al.*<sup>25</sup> demonstrated that loss of hepatitis B surface antigen and hepatitis B e antigen seroconversion signifies that patients with HBV genotype C infection enjoyed better performance of TDF+ETV combination than ETV alone; however, the performance of TDF+ETV combination was poorer than ETV alone for HBV genotypes A, B and D. In addition, the main indication and characteristics of patients treated by TDF+ETV combination was drug resistance. Except for patients in the study by Lok *et al.*,<sup>26</sup> most of the patients in the studies using TDF+ETV combination have been reported to have resistance to ETV, lamivudine or adefovir dipivoxil.<sup>25</sup>

There are several inherent limitations to this study, which must be considered. First, only two studies were included to compare the therapeutic effect of TDF+ENT vs. TDF alone; therefore, more RCTs are needed to supported our conclu-



sions. Second, almost all of the included studies were RCTs or interventional cohort studies, and a potential source of bias might have been introduced. Third, age, sex, hepatitis B e antigen status, cirrhosis stage, and HBV DNA level before therapy, duration of previous therapy, and baseline HBV DNA level may be factors associated with virologic response but which were not taken into account in our meta-analysis.

## Conclusions

In summary, the therapeutic effect of TDF, ETV, TAF, and TDF+ETV in patients with CHB was investigated in this study. The virological response in TDF-treated CHB patients was superior to that achieved in the ETV-treated CHB patients, but no significant difference of virological response was found between TAF-treated and TDF-treated CHB patients. In addition, the therapeutic effect of TDF+ETV was superior to that of TDF. These conclusions were made from the available studies published to recent time, and more clinical RCTs or observational studies should be conducted to verify them. Also, the drug safety of TAF, TDF, and TDF+ETV should be investigated more systematically.

NA, not available or not applicable. CHB, chronic hepatitis B; ETV, entecavir; TAF, Tenofovir alafenamide fumarate; TDF, tenofovir disoproxil fumarate.

## Acknowledgments

We thanks Jie Zhang for the assistance in this study.

## Funding

This study was supported by a grant from the National Natural Science Foundation of China (No. 31770837). The funding agency did not have any role in the design of the study, the collection, analysis and interpretation of data, nor writing of the manuscript.

## Conflict of interest

The authors have no conflict of interests related to this publication.

## Author contributions

Acquisition of data, analysis and interpretation of data, drafting and final approval of the article (XM, SL); acquisition, analysis and interpretation of data (MW, YW, SD); study design and revision of the article (YX, SX). All authors have read and approved the manuscript.

## Data sharing statement

No additional data are available.

## References

- [1] Trépo C, Chan HL, Lok A. Hepatitis B virus infection. *Lancet* 2014; 384(9959): 2053–2063. doi:10.1016/S0140-6736(14)60220-8.
- [2] Fattovich G, Bortolotti F, Donato F. Natural history of chronic hepatitis B: special emphasis on disease progression and prognostic factors. *J Hepatol*

- 2008; 48(2): 335–352. doi:10.1016/j.jhep.2007.11.011.
- [3] GBD 2013 Mortality and Causes of Death Collaborators. Global, regional, and national age-sex specific all-cause and cause-specific mortality for 240 causes of death, 1990–2013: a systematic analysis for the global burden of disease study 2013. *Lancet* 2015; 385(9963): 117–171. doi:10.1016/S0140-6736(14)61682-2.
- [4] Terrault NA, Lok ASF, McMahon BJ, Chang KM, Hwang JP, Jonas MM, *et al.* Update on prevention, diagnosis, and treatment of chronic hepatitis B: AASLD 2018 hepatitis B guidance. *Clin Liver Dis (Hoboken)* 2018; 12(1): 33–34. doi:10.1002/cld.728.
- [5] European Association for the Study of the Liver. EASL 2017 clinical practice guidelines on the management of hepatitis B virus infection. *J Hepatol* 2017; 67(2): 370–398. doi:10.1016/j.jhep.2017.03.021.
- [6] Gordon SC, Lamerato LE, Rupp LB, Li J, Holmberg SD, Moorman AC, *et al.* Antiviral therapy for chronic hepatitis B virus infection and development of hepatocellular carcinoma in a US population. *Clin Gastroenterol Hepatol* 2014; 12(5): 885–893. doi:10.1016/j.cgh.2013.09.062.
- [7] Chen Y, Li JJ, Chen R, Li G, Ji J. Dynamics of HBV surface antigen related end points in chronic hepatitis B infection: a systematic review and meta-analysis. *Antivir Ther* 2020; 25: 203–215. doi:10.3851/IMP3366.
- [8] Molina JM, Ward D, Brar I, Mills A, Stellbrink HJ, López-Cortés L, *et al.* Switching to fixed-dose bicitragravir, emtricitabine, and tenofovir alafenamide from dolutegravir plus abacavir and lamivudine in virologically suppressed adults with HIV-1: 48 week results of a randomised, double-blind, multicentre, active-controlled, phase 3, non-inferiority trial. *Lancet HIV* 2018; 5(7): e357–e365. doi:10.1016/S2352-3018(18)30092-4.
- [9] Sax PE, Wohl D, Yin MT, Post F, DeJesus E, Saag M, *et al.* Tenofovir alafenamide versus tenofovir disoproxil fumarate, coformulated with elvitegravir, cobicistat, and emtricitabine, for initial treatment of HIV-1 infection: two randomised, double-blind, phase 3, non-inferiority trials. *Lancet* 2015; 385(9987): 2606–2615. doi:10.1016/S0140-6736(15)60616-X.
- [10] Agarwal K, Fung SK, Nguyen TT, Cheng W, Sicard E, Ryder SD, *et al.* Twenty-eight day safety, antiviral activity, and pharmacokinetics of tenofovir alafenamide for treatment of chronic hepatitis B infection. *J Hepatol* 2015; 62(3): 533–540. doi:10.1016/j.jhep.2014.10.035.
- [11] Fong TL, Lee BT, Tien A, Chang M, Lim C, Ahn A, *et al.* Improvement of bone mineral density and markers of proximal renal tubular function in chronic hepatitis B patients switched from tenofovir disoproxil fumarate to tenofovir alafenamide. *J Viral Hepat* 2019; 26(5): 561–567. doi:10.1111/jvh.13053.
- [12] Lampertico P, Buti M, Fung S, Ahn SH, Chuang WL, Tak WY, *et al.* Switching from tenofovir disoproxil fumarate to tenofovir alafenamide in virologically suppressed patients with chronic hepatitis B: a randomised, double-blind, phase 3, multicentre non-inferiority study. *Lancet Gastroenterol Hepatol* 2020; 5(5): 441–453. doi:10.1016/S2468-1253(19)30421-2.
- [13] Ridruejo E. Treatment of chronic hepatitis B in clinical practice with entecavir or tenofovir. *World J Gastroenterol* 2014; 20(23): 7169–7180. doi:10.3748/wjg.v20.i23.7169.
- [14] Wells G, Shea JB, O'Connell J. The Newcastle-Ottawa scale (NOS) for assessing the quality of nonrandomised studies in meta-analyses. Ottawa Health Research Institute Web site 2014; 7.
- [15] Agarwal K, Brunetto M, Seto WK, Lim YS, Fung S, Marcellin P, *et al.* 96 weeks treatment of tenofovir alafenamide vs. tenofovir disoproxil fumarate for hepatitis B virus infection. *J Hepatol* 2018; 68(4): 672–681. doi:10.1016/j.jhep.2017.11.039.
- [16] Buti M, Gane E, Seto WK, Chan HL, Chuang WL, Stepanova T, *et al.* Tenofovir alafenamide versus tenofovir disoproxil fumarate for the treatment of patients with HBeAg-negative chronic hepatitis B virus infection: a randomised, double-blind, phase 3, non-inferiority trial. *Lancet Gastroenterol Hepatol* 2016; 1(3): 196–206. doi:10.1016/S2468-1253(16)30107-8.
- [17] Buti M, Riveiro-Barciela M, Esteban R. Tenofovir alafenamide fumarate: a new tenofovir prodrug for the treatment of chronic hepatitis B infection. *J Infect Dis* 2017; 216(suppl\_8): S792–S796. doi:10.1093/infdis/jix135.
- [18] Byrne R, Carey I, Agarwal K. Tenofovir alafenamide in the treatment of chronic hepatitis B virus infection: rationale and clinical trial evidence. *Therap Adv Gastroenterol* 2018; 11: 1756284818786108. doi:10.1177/1756284818786108.
- [19] Cai D, Pan C, Yu W, Dang S, Li J, Wu S, *et al.* Comparison of the long-term efficacy of tenofovir and entecavir in nucleos(t)ide analogue-naïve HBeAg-positive patients with chronic hepatitis B: a large, multicentre, randomized controlled trials. *Medicine (Baltimore)* 2019; 98(1): e13983. doi:10.1097/MD.00000000000013983.
- [20] Chan HL, Fung S, Seto WK, Chuang WL, Chen CY, Kim HJ, *et al.* Tenofovir alafenamide versus tenofovir disoproxil fumarate for the treatment of HBeAg-positive chronic hepatitis B virus infection: a randomised, double-blind, phase 3, non-inferiority trial. *Lancet Gastroenterol Hepatol* 2016; 1(3): 185–195. doi:10.1016/S2468-1253(16)30024-3.
- [21] Jeon HJ, Jung SW, Park NH, Yang Y, Noh JH, Ahn JS, *et al.* Efficacy of tenofovir-based rescue therapy for chronic hepatitis B patients with resistance to lamivudine and entecavir. *Clin Mol Hepatol* 2017; 23(3): 230–238. doi:10.3350/cmh.2017.0003.
- [22] Koike K, Suyama K, Ito H, Itoh H, Sugiura W. Randomized prospective study showing the non-inferiority of tenofovir to entecavir in treatment-naïve chronic hepatitis B patients. *Hepatol Res* 2018; 48(1): 59–68. doi:10.1111/hepr.12902.
- [23] Lim YS, Byun KS, Yoo BC, Kwon SY, Kim YJ, An J, *et al.* Tenofovir monotherapy versus tenofovir and entecavir combination therapy in patients with entecavir-resistant chronic hepatitis B with multiple drug failure: results of a randomised trial. *Gut* 2016; 65(5): 852–860. doi:10.1136/gutjnl-2014-308353.
- [24] Lim YS, Lee YS, Gwak GY, Byun KS, Kim YJ, Choi J, *et al.* Monotherapy with

- tenofovir disoproxil fumarate for multiple drug-resistant chronic hepatitis B: 3-year trial. *Hepatology* 2017;66(3):772–783. doi:10.1002/hep.29187.
- [25] Lok AS, Trinh H, Carosi G, Akarca US, Gadano A, Habersetzer F, *et al*. Efficacy of entecavir with or without tenofovir disoproxil fumarate for nucleos(t)ide-naïve patients with chronic hepatitis B. *Gastroenterology*. 2012;143(3):619–628.e1. doi:10.1053/j.gastro.2012.05.037.
- [26] Sriprayoon T, Mahidol C, Ungtrakul T, Chun-On P, Soonklang K, Pongpun W, *et al*. Efficacy and safety of entecavir versus tenofovir treatment in chronic hepatitis B patients: a randomized controlled trial. *Hepatol Res* 2017;47(3):E161–E168. doi:10.1111/hepr.12743.
- [27] Yim HJ, Kim IH, Suh SJ, Jung YK, Kim JH, Seo YS, *et al*. Switching to tenofovir vs continuing entecavir for hepatitis B virus with partial virologic response to entecavir: a randomized controlled trial. *J Viral Hepat* 2018;25(11):1321–1330. doi:10.1111/jvh.12934.
- [28] Batirel A, Guclu E, Arslan F, Kocak F, Karabay O, Ozer S, *et al*. Comparable efficacy of tenofovir versus entecavir and predictors of response in treatment-naïve patients with chronic hepatitis B: a multicenter real-life study. *Int J Infect Dis* 2014;28:153–159. doi:10.1016/j.ijid.2014.09.004.
- [29] Ceylan B, Yardimci C, Fincanci M, Eren G, Tozalgan U, Muderrisoglu C, *et al*. Comparison of tenofovir and entecavir in patients with chronic HBV infection. *Eur Rev Med Pharmacol Sci* 2013;17(18):2467–2473.
- [30] Ha NB, Trinh HN, Rosenblatt L, Nghiem D, Nguyen MH. Treatment outcomes with first-line therapies with entecavir and tenofovir in treatment-naïve chronic hepatitis B patients in a routine clinical practice. *J Clin Gastroenterol* 2016;50(2):169–174. doi:10.1097/MCG.0000000000000345.
- [31] Jayakumar R, Joshi YK, Singh S. Laboratory evaluation of three regimens of treatment of chronic hepatitis B: tenofovir, entecavir and combination of lamivudine and adefovir. *J Lab Physicians* 2012;4(1):10–16. doi:10.4103/0974-2727.98664.
- [32] Kayaaslan B, Akinci E, Ari A, Tufan ZK, Alpat SN, Gunal O, *et al*. A long-term multicenter study: entecavir versus tenofovir in treatment of nucleos(t)ide analogue-naïve chronic hepatitis B patients. *Clin Res Hepatol Gastroenterol* 2018;42(1):40–47. doi:10.1016/j.clinre.2017.06.008.
- [33] Kwon YJ, Lee HS, Park MJ, Shim SG. Comparison of the efficacy of tenofovir and entecavir for the treatment of nucleos(t)ide-naïve patients with chronic hepatitis B. *Niger J Clin Pract*. 2015;18(6):796–801. doi:10.4103/1119-3077.163296.
- [34] López Centeno B, Collado Borrell R, Pérez Encinas M, Gutiérrez García ML, Sanmartín Fenollera P. Comparison of the effectiveness and renal safety of tenofovir versus entecavir in patients with chronic hepatitis B. *Farm Hosp* 2016;40(4):279–286; English. doi:10.7399/fh.2016.40.4.10492.
- [35] Lu L, Yip B, Trinh H, Pan CQ, Han SH, Wong CC, *et al*. Tenofovir-based alternate therapies for chronic hepatitis B patients with partial virological response to entecavir. *J Viral Hepat* 2015;22(8):675–681. doi:10.1111/jvh.12368.
- [36] Ozaras R, Mete B, Ceylan B, Ozgunes N, Gunduz A, Karaosmanoglu H, *et al*. First-line monotherapies of tenofovir and entecavir have comparable efficacies in hepatitis B treatment. *Eur J Gastroenterol Hepatol* 2014;26(7):774–780. doi:10.1097/MEG.000000000000099.
- [37] Park JW, Kwak KM, Kim SE, Jang MK, Suk KT, Kim DJ, *et al*. Comparison of the long-term efficacy between entecavir and tenofovir in treatment-naïve chronic hepatitis B patients. *BMC Gastroenterol* 2017;17(1):39. doi:10.1186/s12876-017-0596-7.
- [38] Riveiro-Barciela M, Tabernero D, Calleja JL, Lens S, Manzano ML, Rodríguez FG, *et al*. Effectiveness and safety of entecavir or tenofovir in a spanish cohort of chronic hepatitis B patients: validation of the page-B score to predict hepatocellular carcinoma. *Dig Dis Sci* 2017;62(3):784–793. doi:10.1007/s10620-017-4448-7.
- [39] Shi H, Huang M, Lin G, Li X, Wu Y, Jie Y, *et al*. Efficacy comparison of tenofovir and entecavir in HBsAg-positive chronic hepatitis B patients with high HBV DNA. *Biomed Res Int* 2016;2016:6725073. doi:10.1155/2016/6725073.
- [40] Wang YH, Liao J, Zhang DM, Wu DB, Tao YC, Wang ML, *et al*. Tenofovir monotherapy versus tenofovir plus entecavir combination therapy in HBsAg-positive chronic hepatitis patients with partial virological response to entecavir. *J Med Virol* 2020;92(3):302–308. doi:10.1002/jmv.25608.
- [41] Yu HM, Kwon SY, Kim J, Chung HA, Kwon SW, Jeong TG, *et al*. Virologic response and safety of tenofovir versus entecavir in treatment-naïve chronic hepatitis B patients. *Saudi J Gastroenterol* 2015;21(3):146–151. doi:10.4103/1319-3767.157558.
- [42] Pereira CV, Tovo CV, Grossmann TK, Miranda H, Dal-Pupo BB, Almeida PR, *et al*. Efficacy of entecavir and tenofovir in chronic hepatitis B under treatment in the public health system in southern Brazil. *Mem Inst Oswaldo Cruz* 2016;111(4):252–257. doi:10.1590/0074-02760150390.
- [43] Scaglione SJ, Lok AS. Effectiveness of hepatitis B treatment in clinical practice. *Gastroenterology* 2012;142(6):1360–1368.e1. doi:10.1053/j.gastro.2012.01.044.
- [44] Santos JR, Saumoy M, Curran A, Bravo I, Llibre JM, Navarro J, *et al*. The lipid-lowering effect of tenofovir/emtricitabine: a randomized, crossover, double-blind, placebo-controlled trial. *Clin Infect Dis* 2015;61(3):403–408. doi:10.1093/cid/civ296.
- [45] Tungsiripat M, Kitch D, Glesby MJ, Gupta SK, Mellors JW, Moran L, *et al*. A pilot study to determine the impact on dyslipidemia of adding tenofovir to stable background antiretroviral therapy: ACTG 5206. *AIDS* 2010;24(11):1781–1784. doi:10.1097/QAD.0b013e32833ad8b4.



Original Article

# Validation of the Nanjing Criteria for Diagnosing Pyrrolizidine Alkaloids-induced Hepatic Sinusoidal Obstruction Syndrome

Wei Zhang<sup>1#</sup>, Lu Liu<sup>1,2#</sup>, Ming Zhang<sup>1</sup>, Feng Zhang<sup>1</sup>, Chunyan Peng<sup>1</sup>, Bin Zhang<sup>1</sup>, Jun Chen<sup>3</sup>, Lin Li<sup>3</sup>, Jian He<sup>4</sup>, Jiangqiang Xiao<sup>1</sup>, Yanhong Feng<sup>5</sup>, Xunjiang Wang<sup>6</sup>, Aizhen Xiong<sup>6</sup>, Li Yang<sup>6</sup>, Xiaoping Zou<sup>1</sup>, Yuecheng Yu<sup>7\*</sup> and Yuzheng Zhuge<sup>1\*</sup>

<sup>1</sup>Department of Gastroenterology, The Affiliated Drum Tower Hospital of Nanjing University Medical School, Nanjing, Jiangsu, China; <sup>2</sup>Department of Gastroenterology, The Affiliated Jiangning Hospital of Nanjing Medical University, Nanjing, Jiangsu, China; <sup>3</sup>Department of Pathology, The Affiliated Drum Tower Hospital of Nanjing University Medical School, Nanjing, Jiangsu, China; <sup>4</sup>Department of Imaging, The Affiliated Drum Tower Hospital of Nanjing University Medical School, Nanjing, Jiangsu, China; <sup>5</sup>Department of Hepatology, Nanjing Second Hospital, Nanjing University of Chinese Medicine, Nanjing, Jiangsu, China; <sup>6</sup>The Ministry of Education Key Laboratory for Standardization of Chinese Medicines, Institute of Chinese Materia Medica, Shanghai University of Traditional Chinese Medicine, Shanghai, China; <sup>7</sup>Liver Diseases Center of PLA and Department of Infectious Diseases, General Hospital of Eastern Theater Command, and Bayi Hospital Affiliated to Nanjing University of Chinese Medicine, Nanjing, Jiangsu, China

Received: 19 November 2020 | Revised: 31 January 2021 | Accepted: 8 March 2021 | Published: 31 March 2021

## Abstract

**Background and Aims:** Hepatic sinusoidal obstruction syndrome (HSOS) is caused by toxic injury to sinusoidal endothelial cells in the liver. The intake of pyrrolizidine alkaloids (PAs) in some Chinese herbal remedies/plants remains the major etiology for HSOS in China. Recently, new diagnostic criteria for PA-induced HSOS (i.e. PA-HSOS) have been developed; however, the efficacy has not been clinically validated. This study aimed to assess the performance of the Nanjing criteria for PA-HSOS. **Methods:** Data obtained from consecutive patients in multiple hospitals, which included 86 PA-HSOS patients and 327 patients with other liver diseases, were retrospectively analyzed. Then, the diagnostic performance of the Nanjing criteria and simplified Nanjing criteria were evaluated and validated. The study is registered in www.chictr.org.cn (ID: ChiCTR1900020784). **Results:** The

Nanjing criteria have a sensitivity and specificity of 95.35% and 100%, respectively, while the simplified Nanjing criteria have a sensitivity and specificity of 96.51% and 96.33%, respectively, for the diagnosis of PA-HSOS. Notably, a proportion of patients with Budd-Chiari syndrome (11/49) was misdiagnosed as PA-HSOS on the basis of the simplified Nanjing criteria, and this was mainly due to the overlapping features in the enhanced computed tomography/magnetic resonance imaging examinations. Furthermore, most of these patients (10/11) had occlusion or thrombosis of the hepatic vein, and communicating vessels in the liver were found in 8/11 patients, which were absent in PA-HSOS patients. **Conclusions:** The Nanjing criteria and simplified Nanjing criteria exhibit excellent performance in diagnosing PA-HSOS. Thus, both could be valuable diagnostic tools in clinical practice.

**Citation of this article:** Zhang W, Liu L, Zhang M, Zhang F, Peng C, Zhang B, et al. Validation of the Nanjing criteria for diagnosing pyrrolizidine alkaloids-induced hepatic sinusoidal obstruction syndrome. J Clin Transl Hepatol 2021; 00(00):345–352. doi: 10.14218/JCTH.2020.00124.

**Keywords:** Drug-induced liver injury; Hepatic sinusoidal obstruction syndrome; Pyrrolizidine alkaloids; Sensitivity; Specificity.

**Abbreviations:** ALF, acute liver failure; ALT, alanine transaminase; AST, aspartate aminotransferase; AUC, area under the receiver operating characteristic curve; BCS, Budd-Chiari syndrome; CECT, contrast-enhanced computed tomography; CI, confidence interval; CT, computed tomography; DILI, drug-induced liver injury; EASL, European Association for the Study of the Liver; FN, false negative; FP, false positive; HSCT, hematopoietic stem cell transplantation; HSOS, hepatic sinusoidal obstruction syndrome; HVOD, hepatic veno-occlusive disease; MELD, model for end-stage liver disease; MRI, magnetic resonance imaging; NPV, negative predictive value; PA, pyrrolizidine alkaloid; PPA, pyrrole-protein adduct; PPV, positive predictive value; PT, prothrombin time; SALT, subacute liver failure; SD, standard deviation; TBIL, total bilirubin; TBLB, transjugular liver biopsy; TN, true negative; TP, true positive.

\*These authors contributed equally to this work.

**\*Correspondence to:** Yuzheng Zhuge, Department of Gastroenterology, The Affiliated Drum Tower Hospital of Nanjing University Medical School, Nanjing, Jiangsu 210008, China. Tel: +86-15996289206, Fax: +86-25-83106666, E-mail: yuzheng9111963@aliyun.com; Yuecheng Yu, Liver Diseases Center of PLA and Department of Infectious Diseases, General Hospital of Eastern Theater Command, and Bayi Hospital Affiliated to Nanjing University of Chinese Medicine, Nanjing, Jiangsu 210008, China. ORCID: <http://orcid.org/0000-0003-3480-1829>. Tel: +86-13805168619, Fax: +86-25-84546576, E-mail: gslsycy@163.com

## Introduction

Hepatic sinusoidal obstruction syndrome (HSOS), which is also referred to as hepatic veno-occlusive disease (or simply HVOD), is a hepatic vascular disease featured by edema, detachment of endothelial cells in the small sinusoidal hepatic and interlobular veins, necrosis, portal hypertension, intrahepatic congestion, and liver dysfunction.<sup>1–6</sup> It has been demonstrated that HSOS is caused by toxic injury to sinusoidal endothelial cells in the liver, and that this injury can be induced by different etiological factors. In Western countries, HSOS usually occurs as a consequence of bone marrow hematopoietic stem cell transplantation (HSCT) treatment for hematological malignancies.<sup>7</sup> In China, the in-

**Table 1. Nanjing criteria for the diagnosis of PA-HSOS**

No.	Diagnostic criteria
i	A definite history of PA-containing plants
ii	Abdominal distention and/or pain in the hepatic region, hepatomegaly and ascites
iii	Elevation of serum TBil or abnormal liver function
iv	Typical features in the enhanced CT or MRI

Patients with i, ii, iii, iv or i, and pathological evidence, and the ruling out the other known causes of liver injury can be diagnosed as PA-HSOS.

take of pyrrolizidine alkaloids (PAs) in certain Chinese herbal remedies/plants (e.g., *Senecio*, *Crotalaria*, *heliotropes*, and *Tusanqi*) remains the major etiology for HSOS.<sup>8</sup> The manifestations in HSOS patients include jaundice, abdominal distention, hepatomegaly and ascites, which overlap with other liver diseases, such as Budd-Chiari syndrome (BCS), acute liver failure, or decompensated cirrhosis of various causes.<sup>9,10</sup> This has posed challenges in the diagnosis of HSOS. In recent years, the incidence of PA-induced HSOS (i.e. PA-HSOS) in China has been increasing. However, PA-HSOS has been frequently misdiagnosed as the following diseases: acute/subacute severe hepatitis, decompensated cirrhosis, BCS, etc. This misdiagnosis delays the proper treatment of patients with PA-HSOS, in which a proportion of severe cases can progress into severe dysfunction, and even multiple organ failure. Therefore, there is an urgent need to develop diagnostic criteria specific to PA-HSOS.<sup>4</sup>

For HSOS caused by bone marrow HSCT (HSCT-HSOS), the diagnosis is made according to the improved Seattle and Baltimore criteria.<sup>11</sup> However, it has been noted that there are significant differences, in terms of epidemiology, ethnicity, etiology and underlying diseases, between PA-HSOS and HSCT-HSOS, and that patients with PA-HSOS have specific clinical characteristics. For instance, previous study<sup>2</sup> revealed that PA-HSOS patients have a relatively longer incubation period from the initial exposure to PA, which ranges from 3 days to 3 months, and that serum total bilirubin (TBil) <34.2  $\mu\text{mol/L}$  can be found in approximately 40% of PA-HSOS patients. In addition, as high as 90% of PA-HSOS patients presented with distinctive imaging findings, such as hepatomegaly, uneven liver perfusion in the balance phase, compressive stenosis of the hepatic segmental inferior vena cava in the imaging findings of the enhanced computed tomography (CT) scan or magnetic resonance imaging (MRI), and decreased peak velocity of portal vein blood flow in the Doppler ultrasonography. On the other hand, a history of chemotherapeutic exposure for 20 or 21 days before onset and 2%–5% weight gain at onset are required in the improved Seattle and Baltimore criteria. However, PA-HSOS patients do not often have the experience of using chemotherapy. Doctors do not usually have accurate weight-change data due to the sporadic nature of the disease. Based on these reasons, the improved Seattle and Baltimore criteria are not suitable for the diagnosis of PA-HSOS. Therefore, in 2017, the Chinese Society of Gastroenterology Committee of Hepatobiliary Disease reached a consensus, and proposed the Nanjing criteria for the diagnosis of PA-HSOS (Table 1).<sup>6</sup> Nevertheless, to date, the clinical efficacy of the Nanjing criteria has not been validated.

The present multi-center retrospective study intends to validate the diagnostic performance of the Nanjing criteria for Chinese patients with PA-HSOS.

## Methods

### Study population

During the period between November 2011 and Decem-

ber 2018, a total of 994 consecutive patients in multiple centers were retrospectively evaluated for eligibility in the present study. The participating hospitals were, as follows: (1) Department of Gastroenterology, The Affiliated Drum Tower Hospital of Nanjing University Medical School; (2) Department of Hepatology, Nanjing Second Hospital, Nanjing University of Chinese Medicine; and (3) Liver Diseases Center of PLA and Department of Infectious Diseases, General Hospital of Eastern Theater Command, and Bayi Hospital Affiliated to Nanjing University of Chinese Medicine. The inclusion criteria used for the enrollment of patients were, as follows: (1) presentation of clinical symptoms at  $\leq 6$  months; (2) abnormal liver function [elevated alanine transaminase (ALT), aspartate aminotransferase (AST), or total bilirubin (Tbil)]; (3) ascites and/or abdominal distension; or (4) anorexia. Patients with the following criteria were excluded from the present study: (1) suspected, but not pathologically diagnosed, with PA-HSOS; (2) two or more liver diseases, or PA-HSOS in combination with biliary diseases; (3) unknown cause of liver disease; (4) missing clinical data; and (5) duplicate data from the previous study of the Nanjing Criteria.

Finally, 86 patients with PA-HSOS and 327 patients with other liver diseases of various etiologies were retrospectively investigated (Fig. 1). All patients with PA-HSOS underwent transjugular liver biopsy (TJLB).

The present study was reviewed and approved by the Ethics Committee of each participating hospital. The requirement for written informed consent was waived due to the retrospective nature of the study.

### Diagnostic criteria

The reference standards of the diagnostic criteria for PA-HSOS were, as follows: (1) pathologically proven edema, necrosis, detachment of hepatic sinusoidal endothelial cells in the hepatic acinus zone III, and significant dilation and congestion of hepatic sinusoids; and (2) confirmed history of intake of PA-containing herbs/plants, or the detection of blood pyrrole-protein adducts (PPAs). All liver tissue specimens were independently examined by two experienced hepatopathologists.

The clinical components of the Nanjing criteria for PA-HSOS were, as follows: (1) definite history of intake of PA-containing plants; (2) abdominal distention and/or pain in the hepatic region, hepatomegaly and ascites; (3) elevated serum TBil or abnormal serum markers for liver function; and (4) typical features in the enhanced CT or MRI examinations (e.g., diffuse hepatomegaly, ascites, and plain scans revealing a heterogeneous decreased density of the hepatic parenchyma; enhancement characterized by a map-like or mottle-like nonhomogeneous appearance in the venous phase and equilibrium phase; hepatic vein lumen being stenotic or obscured; hepatic segment of the inferior vena cava being compressed and thinner; and MRI findings being similar to CT findings).

The diagnostic criteria for other liver diseases were de-



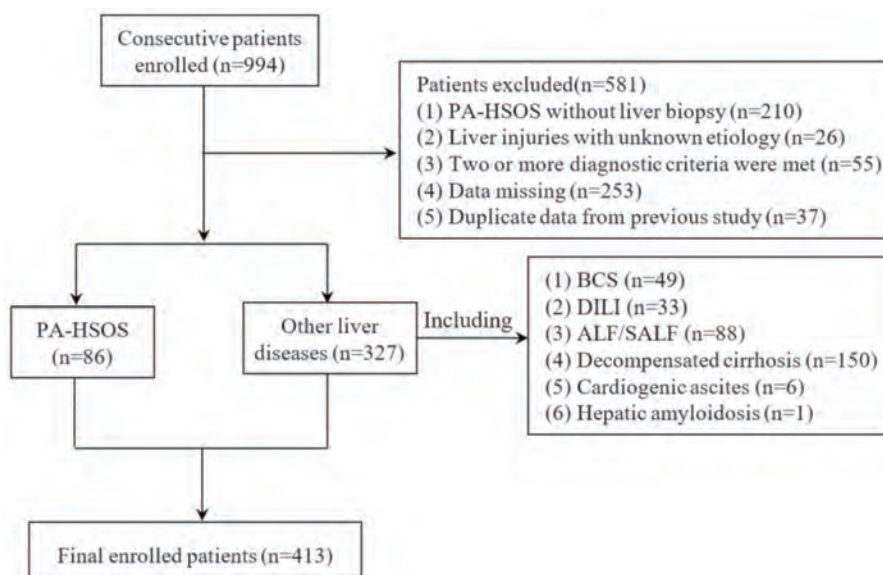


Fig. 1. Flow diagram for the patient enrollment.

terminated upon referring to established guidelines or text books. The diagnosis was independently performed by two experienced hepatologists (Wei Zhang and Yuzheng Zhuge), according to the diagnostic criteria. Simply, patients with a consistent diagnosis were included in the study, and those with inconsistent diagnosis were excluded. The diagnosis of BCS was made in accordance with the 2016 European Association for the Study of the Liver (EASL) Clinical Practice Guidelines.<sup>12</sup>

The diagnosis of decompensated cirrhosis was made according to the 2018 EASL Clinical Practice Guidelines for the management of patients with decompensated cirrhosis, which was based on the characteristic clinical manifestation, laboratory tests, imaging performance, and histological data.<sup>13</sup> In addition, the cause of chronic liver damage was determined by medical history and laboratory examination.<sup>14–18</sup>

The diagnostic criteria for acute liver failure (ALF) or sub-acute liver failure (SALF) were determined by reference to the 2017 EASL Clinical Practical Guidelines on the management of acute (fulminant) liver failure.<sup>19</sup>

The diagnosis for drug-induced liver injury (DILI) was made according to the American College of Gastroenterology Clinical Guidelines on the diagnosis and management of idiosyncratic DILI.<sup>20</sup> PA-HSOS is a unique sub-group of DILI, and has its own diagnostic criteria. Thus, DILI cases in the present study were defined as DILI except when HSOS was induced by PA or other drugs.

### Quantification of PPAs

Serum PPAs were examined using the pre-column derivatization liquid chromatography-tandem mass spectrometry method, as previously reported, with minor modifications.<sup>3</sup>

### Statistical analysis

The statistical analyses were carried out using the SPSS version 22.0 software (IBM Corp., Armonk, NY, USA). Continuous data were expressed as mean  $\pm$  standard deviation (SD), or median and interquartile range (25 and 75 percentiles), according to the data distribution.

Baseline data were compared between PA-HSOS and other liver diseases (BCS, decompensated cirrhosis, DILI, ALF/SALF, and cardiogenic ascites), respectively. Continuous variables were compared using Student's *t*-test or Mann-Whitney *U*-test, when an abnormal distribution was detected. In addition, Pearson's chi-square test or Fisher's exact test was used to compare the categorical variables among different groups. The sensitivity, specificity, overall accuracy, positive predictive value (PPV), negative predictive value (NPV), 95% confidence interval (CI), likelihood ratio, Kappa value, and area under the receiver operating characteristics curve (commonly referred to as AUC) were calculated to evaluate the diagnostic accuracy of the Nanjing criteria. A two-tailed *p*-value of  $<0.05$  was considered statistically significant.

## Results

### Characteristics of the study subjects

A total of 413 patients, treated between November 2011 and December 2018, who fulfilled the eligibility criteria, were retrospectively enrolled in the present study (Fig. 1). Among these patients, 86 underwent TJLB and had ascites, and the PA of these patients met the criteria for the diagnosis of HSOS. The pathological findings confirmed edema, necrosis, detachment of hepatic sinusoidal endothelial cells in hepatic acinus zone III, and significant dilation and congestion of hepatic sinusoids (Fig. 2). Among the 86 PA-HSOS patients, 85 were found to have a clear history of intake of PA-containing herbal medicine/plants, and 1 was diagnosed with PA-HSOS through a blood test of PPAs that confirmed the history of PA intake. The remaining 327 patients were diagnosed with other various liver diseases, according to the diagnostic criteria described in the Materials and Methods section (BCS: *n*=49, DILI: *n*=33, ALF/SALF: *n*=88, decompensated cirrhosis: *n*=150, cardiogenic ascites: *n*=6, and liver amyloidosis: *n*=1).

The demographic, laboratory and clinical characteristics of these patients are summarized in Table 2. Patients with PA-HSOS were older than patients with other liver diseases.

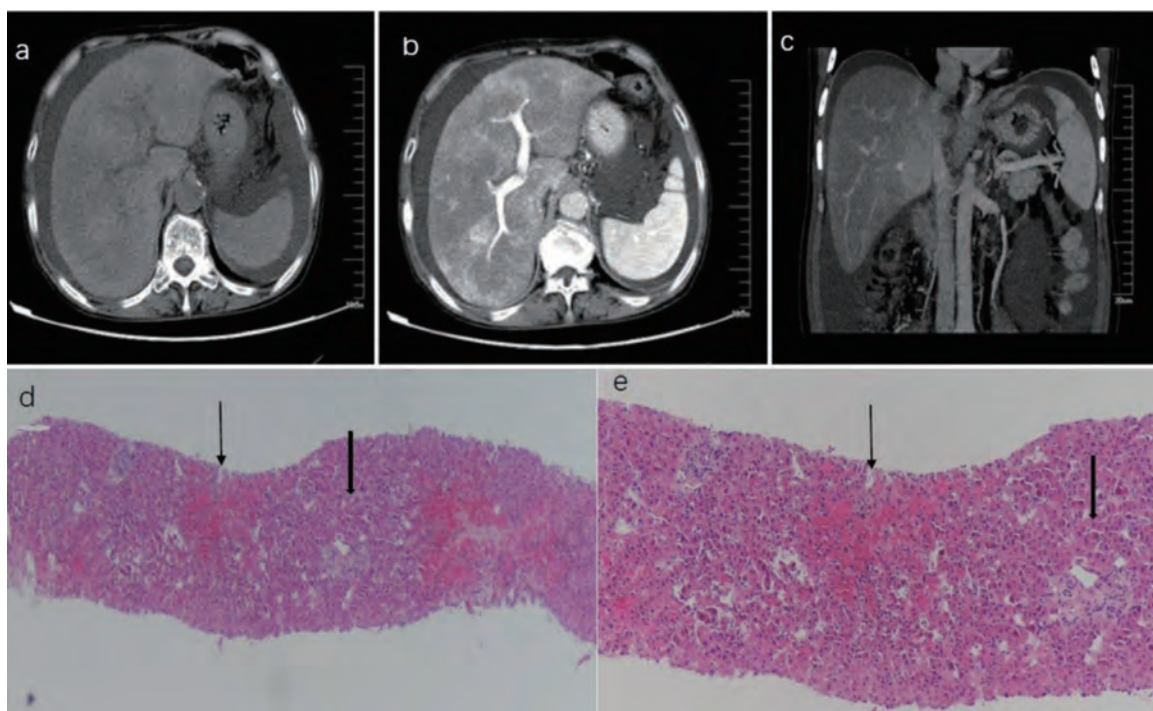


**Fig. 2. Representative CT images and pathological findings for PA-HSOS patients.** (A) The CT imaging revealed diffuse hepatomegaly, ascites, and plain scans showing the heterogeneous decreased density of the hepatic parenchyma. (B) The CT enhancement characterized a map-like or mottle-like nonhomogeneous appearance in the equilibrium phase. (C) The CT images showed that the hepatic vein lumen was obscured, and the hepatic segment of the inferior vena cava was compressed and thinner. (D) hematoxylin-eosin (HE)  $\times 40$ , Zone III, Zone I; (E) HE  $\times 100$ , Zone III, Zone I. The pathological findings confirmed edema, necrosis, detachment of hepatic sinusoidal endothelial cells in hepatic acinus zone III, significant dilation and congestion of hepatic sinusoids, but showed no significant changes in zone I.

es, and ascites was present in all PA-HSOS patients. The findings of the enhanced CT/MRI were significantly different between PA-HSOS and other liver injuries ( $p < 0.001$ ). Patchy enhancement and heterogeneous hypoattenuation were the typical features (Fig. 2). The majority of these PA-HSOS patients had mildly elevated TBil, and nearly normal transaminase and platelet levels. The laboratory characteristics were similar to those in BCS patients but were different from patients with decompensated cirrhosis, who had decreased platelet levels. For the Child-Turcotte-Pugh and Model for End-Stage Liver Disease (commonly known as MELD) scores, patients with ALF/SALF had the highest scores, followed by patients with DILI, PA-HSOS, decompensated cirrhosis, BCS, and cardiogenic ascites.

#### **Performance of the Nanjing criteria in the diagnosis of PA-HSOS**

The diagnostic performance of the Nanjing criteria and simplified Nanjing criteria (ii, iii and iv in the Nanjing criteria) in diagnosing PA-HSOS was assessed. The results are presented in Table 3. The Nanjing criteria demonstrated a good ability in diagnosing PA-HSOS, with a sensitivity of 95.35% (95% CI: 90.81–99.89), a specificity of 100%, a PPV of 100%, a NPV of 98.79% (95% CI: 97.61–99.97), and an overall accuracy of as high as 99.03%. In contrast, the simplified Nanjing criteria had a sensitivity of 96.51% (95% CI: 92.55–100) and a specificity of 96.33% (95% CI: 94.28–98.38) for the diagnosis of PA-HSOS. It was noteworthy that the PPV and NPV of the simplified Nanjing criteria was 87.37% (95% CI: 80.57–94.17) and 99.06% (95% CI: 97.99–100), respectively, for the diagnosis of HSOS. The positive likelihood ratio for the simplified Nanjing criteria was 25.98. The negative

likelihood ratios for the Nanjing criteria and simplified criteria were 0.046 and 0.036, respectively. The AUC for the Nanjing criteria in the diagnosis of PA-HSOS was 0.977 (95% CI: 0.951–1.000,  $p < 0.01$ ), while the AUC for the simplified Nanjing criteria was 0.964 (95% CI: 0.939–0.990,  $p < 0.01$ ) (Fig. 3). As shown in Table 4, the Kappa value between the Nanjing criteria and the liver pathology for the diagnosis of PA-HSOS was 0.970. In addition, the Kappa value for the simplified Nanjing criteria was 0.894, indicating a strong consistency with the gold standard.

#### **Performance of the Nanjing criteria in differentiating PA-HSOS from BCS**

Performance of the Nanjing criteria in distinguishing PA-HSOS from BCS was further evaluated. Both conditions share similar clinical characteristics and imaging features, which has posed difficulties to differential diagnosis. It was found that 11 of 49 (22.45%) BCS patients had typical features of patchy enhancement on the CT/MRI, and these patients were misdiagnosed as PA-HSOS according to simplified Nanjing Criteria. In order to differentiate BCS from PA-HSOS in patients with similar typical features of enhanced CT or MRI, the characteristics of the hepatic vein were further compared in the Doppler ultrasound and venography for the 44 PA-HSOS patients who underwent Doppler ultrasound examinations and the above mentioned 11 BCS patients. As shown in Table 5, among the 11 BCS patients with typical features of patchy enhancement on the CT/MRI, 5 had the hepatic vein type, 5 had the mixed type, and 1 had the inferior vena cava type. The Doppler ultrasound detected thrombosis or occlusion of the hepatic vein in 10 of 11 (90.9%) BCS patients and this was confirmed in

Table 2. Demographic, laboratory and clinical characteristics of the study patients

	PA-HSOS, n=86	BCS, n=49	Decompensated cirrhosis, n=150	DILI, n=33	ALF/SALF, n=88	Cardiogenic ascites, n=6
Age in years, median (range)	65 (60.75, 70)	40 (30, 52)***	57.5 (50, 68)***	59 (46.5, 68)*	54 (42, 62.8)***	59 (31.25, 73.25)
Male, n (%)	49 (56.98)	20 (40.82)	90(60)	15 (45.45)	67 (76.14)**	3 (50)
Disease course in days, median (range)	30 (20, 60)	60 (30, 90)***	30 (20, 90)	20 (9.5, 30)**	20 (12.5, 30)**	45 (13.75, 135)
History of ingesting PA- containing plants, n (%)	85 (98.84)	0	0	0	0	1 (16.67)
Ascites						
No, n (%)	0 (0)	13 (26.53)***	10 (6.67)*	3 (9.09)	12 (13.64)**	0 (0)
MI, n (%)	5 (5.81)	7 (14.29)	49 (32.67)***	12 (36.36)	22 (25)**	1 (16.67)
MO, n (%)	72 (83.72)	23 (46.94)***	84 (56)***	17 (51.52)***	53 (60.23)**	4 (66.66)
SE, n (%)	9 (10.47)	6 (12.24)	7 (4.66)	1 (3.03)**	1 (1.13)*	1 (16.67)
ALT in U/L, median (range)	40.9 (25.98, 70.88)	23.6 (15.4, 34.45)***	34.3 (24.53, 64)	201.5 (120.85, 505)***	238.7 (80.68, 894.35)***	18.45 (12.78, 25.85)**
Elevated ALT, n (%)	43 (50)	16 (32.65)	73 (48.67)	33 (100)**	84 (95.45)***	2 (33.33)
AST in U/L, median (range)	56.7 (38.25, 91)	29.1 (20.35, 43.8)***	50.55 (32.13, 95)	186.5 (85.05, 444.15)***	242.95 (111.23, 635.13)***	27.75 (21.88, 38.7)**
Elevated AST, n (%)	63 (73.26)	44 (89.80)*	97 (64.67)	33 (100)**	88 (100)***	4 (66.67)
TBI in $\mu\text{mol/L}$ , median (range)	33.7 (22.38, 46.2)	26.6 (19.45, 47.33)	29.25 (18.33, 56)	164.2 (73.8, 308.6)***	273.05 (174.7, 419.83)***	20.9 (8.28, 36.7)
Elevated bilirubin, n (%)	76 (88.37)	8 (16.33)***	121 (80.67)	32 (96.97)	81 (92.05)	2 (33.33)**
PT in s, median (range)	14.55 (13, 16.93)	13.8 (12.5, 15.6)*	14.6 (13.13, 16.38)	13.7	20.9	13.15
PLT as $\times 10^9/\text{L}$ , median (range)	99.5 (72.5, 133.25)	106 (77.5, 190.5)	71 (49, 112.25)***	158 (113, 238)***	109.5 (72.5, 144)	144 (115.75, 215.75)*
Typical imaging features, n (%)	83 (96.51)	11 (22.45)***	0 (0)***	0 (0)***	0 (0)***	3 (50)***
Child-Pugh stage, n	86	49	150	29	87	6
A, n (%)	1 (1.16)	14 (28.57)***	16 (10.67)*	0 (0)	0 (0)	1 (16.67)
B, n (%)	65 (75.58)	28 (57.14)	102 (68)	20 (68.97)	23 (26.44)***	5 (83.33)
C, n (%)	20 (23.26)	7 (14.29)	32 (21.33)	9 (31.03)	64 (73.56)***	0 (0)
MELD, median (range)	12 (10, 16.25)	10 (8, 14.75)	10 (6, 13)**	17 (14, 20)***	24 (21, 28)***	8.5 (4.5, 12)*

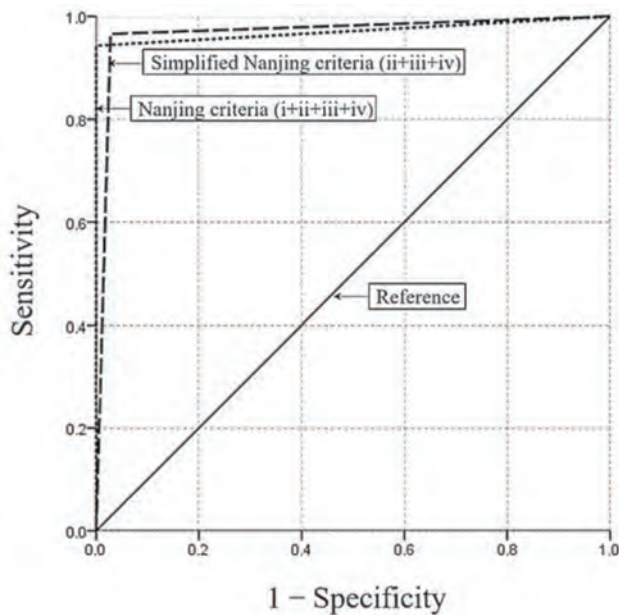
\*p<0.05, \*\*p<0.01, \*\*\*p<0.001, PA-HSOS vs. other liver diseases (BCS, decompensated cirrhosis, DILI, ALF/SALF, cardiogenic ascites). MI, mild; MO, moderate; SE, severe. Elevated bilirubin: serum total bilirubin >17.1  $\mu\text{mol/L}$ ; Elevated ALT: ALT >40 U/L; Elevated AST: AST >40 U/L.

Table 3. Performance of the Nanjing criteria and simplified Nanjing criteria for the diagnosis of PA-HSOS

Diagnostic criteria	Reference standard				Sensitivity, % (95% CI)	Specificity, % (95% CI)	PPV, % (95% CI)	NPV, % (95% CI)	Positive likelihood ratio	Negative likelihood ratio	Overall accu- racy
	TP	FP	TN	FN							
Nanjing criteria (i+ii+iii+iv)	82	0	327	4	95.35 (90.81–99.89)	100	100	98.79 (97.61–99.97)	—	0.046	99.03
Simplified Nanjing criteria (ii+iii+iv)	83	12	315	3	96.51 (92.55–100)	96.33 (94.28–98.38)	87.37 (80.57–94.17)	99.06 (97.99–100)	25.98	0.036	96.37

i. History of ingesting PA-containing plants; ii. Clinical manifestation; iii. Abnormal liver function (abnormal liver function: ALT >40 U/L, AST >40 U/L or serum TBI >17.1  $\mu\text{mol/L}$ ); iv. Imaging performance. TP, true positive; FP, false positive; TN, true negative; FN, false negative.





**Fig. 3. Receiver operating characteristic curves for the Nanjing criteria and simplified Nanjing criteria in the study patients.** The AUC for the Nanjing criteria in the diagnosis of PA-HSOS was 0.977 (95% CI: 0.951–1.000,  $p < 0.01$ ), while the AUC for the simplified Nanjing criteria was 0.964 (95% CI: 0.939–0.990,  $p < 0.01$ ).

the venography, while no thrombosis or occlusion was found in PA-HSOS patients. In addition, 8 of 11 (72.7%) BCS patients had a communicating branched vein within the liver detected by Doppler ultrasound, while none of the PA-HSOS patients had such feature. Furthermore, 35 of 44 (79.5%) PA-HSOS patients and 1 of 11 (9.1%) BCS patients had reductions in the diameter or velocity of the hepatic vein. However, none of the 11 BCS patients had a history of intake of PA. All differences between these two groups were statistically significant ( $p < 0.001$ ).

## Discussion

The Nanjing criteria has been recently proposed for the diagnosis of PA-HSOS. However, its efficacy and reliability has not been clinically validated. The present study demonstrated that the Nanjing criteria exhibits excellent performance in the diagnosis of PA-HSOS. This was demonstrated by multiple lines of evidence, including high sensitivity and specificity.

A variety of diagnostic criteria, such as the Baltimore criteria and Modified Seattle criteria, are available for the diagnosis of HSCT-HSOS.<sup>21–23</sup> However, these criteria were specifically developed for the diagnosis of HSCT-HSOS and the clinical efficacy remains argumentative when applied for the diagnosis of PA-HSOS. For example, the first item in both the Baltimore criteria and Modified Seattle criteria is absent in PA-HSOS patients. Since PA-HSOS is a form of sporadic disease, it is difficult to obtain accurate data on the patient's weight gain following the onset of the disease. In addition, more than 40% of PA-HSOS patients have mildly abnormal hepatic function at the time of the disease onset, with TBil  $< 34.2 \mu\text{mol/L}$ , and this largely differs from that in HSCT-HSOS patients. Previously, the diagnosis of PA-HSOS has largely relied on the pathological examination of the liver biopsy specimen. Nevertheless, ascites has been detected in nearly all PA-HSOS patients, and percutaneous liver biopsy might be the cause of severe complications (e.g., intraperitoneal bleeding and liver rupture). TJLB has been considered to be better than percutaneous liver biopsy for PA-HSOS patients. However, TJLB has not become a routine procedure in most hospitals, mainly because it is relatively difficult to perform and costly. Recently, the Nanjing criteria was proposed and issued in the Expert consensus on the clinical management of PA-HSOS.<sup>6</sup> To date, no clinical validation has been made by assessing the diagnostic performance of the criteria. In this context, the present study focused on the clinical items in the criteria to verify the diagnostic value of the Nanjing criteria for PA-HSOS.

Among the 86 PA-HSOS patients examined in this study, 82 were diagnosed with PA-HSOS on the basis of the Nanjing criteria, while 4 were determined to have been misdiagnosed, giving a false negative rate of 4.70% (4/86). Among these four patients, one had no history of PA-containing plant intake but showed positivity for PPA detection in the blood, while the remaining three patients had no typical imaging features in their enhanced CT/MRI scans. These results suggest that the intake of PA is subjective. Therefore, an objective proof of PA intake through the examination of serum PPAs might be necessary for the confirmation of the etiology. Previous studies have indicated that serum PPAs have a diagnostic sensitivity of 100%, a specificity of 94.1%, and a NPV of 100%.<sup>24</sup> Thus, PPAs can be regarded as a specific biomarker of PA intake. In addition, not every PA-HSOS patient has typical features in the enhanced CT/MRI. Therefore, TJLB might be useful in the diagnosis of PA-HSOS.

In clinic, many PA-HSOS patients were not clear in their history of intake of PA-containing plants. Therefore, the diagnostic performance of the simplified Nanjing criteria (ii, iii and iv in the Nanjing criteria) was evaluated. Notably, 83 PA-HSOS patients were accurately diagnosed, while the remaining 3 patients were misdiagnosed due to the absence

**Table 4. Kappa analysis of the Nanjing criteria or simplified Nanjing criteria with the gold standard**

	Nanjing criteria (i+ii+iii+iv)	Simplified Nanjing criteria (ii+iii+iv)
Gold standard	0.970	0.894

**Table 5. Comparison of the characteristics of PA-HSOS and BCS**

	PA-HSOS, <i>n</i> =44	BCS, <i>n</i> =11	<i>p</i> -value
Thrombosis or occlusion of hepatic vein by Doppler ultrasound, <i>n</i> (%)	0 (0)	10 (90.9)	$< 0.001$
Reduction of diameters or velocities of hepatic vein by Doppler ultrasound, <i>n</i> (%)	35 (79.5)	1 (9.1)	$< 0.001$
Communicating branched vessels found by Doppler ultrasound, <i>n</i> (%)	0 (0)	8 (72.7)	$< 0.001$
Thrombosis or occlusion of hepatic vein confirmed by venography, <i>n</i> (%)	0 (0)	10 (90.9)	$< 0.001$
History of PA intake, <i>n</i>	44	0	$< 0.001$



of typical features in the enhanced CT/MRI. Previous studies have demonstrated that the typical imaging features of PA-HSOS are critical for the diagnosis of PA-HSOS. In a single-center retrospective study, 293 patients, who were diagnosed with PA-HSOS ( $n=71$ ), BCS ( $n=57$ ) and liver cirrhosis ( $n=165$ ), were enrolled, and the findings revealed that the radiologic finding of patchy liver enhancement yielded a sensitivity of 92.96%, a specificity of 92.79%, a PPV of 80.49%, a NPV of 97.63%, and an accuracy of 91.83%. The values for the heterogeneous hypoattenuation were 100%, 95.05%, 86.59%, 100% and 96.25%, respectively. A study indicated that contrast-enhanced CT (commonly referred to as CECT) is effective for diagnosing PA-HSOS.<sup>25</sup> However, it was observed that 11 patients with BCS and 1 patient with liver amyloids were misdiagnosed as PA-HSOS in accordance with the simplified Nanjing criteria, and this was mainly due to the overlapping imaging findings with those in PA-HSOS. Thus, special caution should be taken in the differential diagnosis of PA-HSOS from BCS. Furthermore, it may merit attention in the present study that the communicating veins in the liver, thrombosis and occlusion of the hepatic vein were largely different between BCS and PA-HSOS cases. Furthermore, the history of ingesting PA-containing herbal medicine/plants and the detection of blood PPAs were critical for distinguishing between PA-HSOS and BCS cases, especially when the history of ingesting PA-containing plants was not clear and the simplified Nanjing criteria (ii, iii and iv in the Nanjing criteria) was used.<sup>24,26</sup>

The present study may have some limitations. First, the present study was retrospectively performed and not all patients had liver biopsy results. Hence, selection bias may exist in the retrospective design of the study. Second, a significant number of patients exposed to PA but who did not present with significant clinical symptoms might have been missed. In fact, people can be exposed to toxic PAs mainly through the consumption of PA-producing plants used as herbal medicines, teas, and dietary supplements and/or PA-contaminated staple foods, such as wheat and millets. In addition, the carry-over of PA through livestock into dietary foodstuffs (e.g., milk, eggs, honey and their downstream contamination in the food chain) significantly increases PA exposure in humans.<sup>27–29</sup> Thus, these patients were not even aware that they had been exposed to PA. Blood PPAs might represent the specific biomarkers for determining exposure to PAs. Hence, a prospective study is needed to evaluate the diagnostic value of blood PPAs and the modified Nanjing criteria.

## Conclusions

The present study suggests that the Nanjing criteria and simplified Nanjing criteria have excellent performance in diagnosing PA-HSOS, thereby representing a valuable diagnostic tool. It also merits attention that the differential diagnosis of PA-HSOS from BCS is highly recommended due to the shared imaging features.

## Funding

This study was funded in full by the National Natural Science Foundation of China, with grant numbers 8157040652 and 81900552, and the Key Project of Nanjing Health and Technology Development, with grant number ZKX19015.

## Conflict of interest

The authors have no conflict of interests related to this publication.

## Author contributions

Conception and design of the study (WZ, YZ), generation, collection, and assembly of data (QZ, LL, MZ, FZ, BZ, JC, LL, JH, HX, YF), analysis and/or interpretation of data (WZ, LL), drafting or revision of the manuscript (WZ, LL, YZ, FZ, CP).

## Data sharing statement

All data are available upon request.

## References

- [1] Fan CQ, Crawford JM. Sinusoidal obstruction syndrome (hepatic veno-occlusive disease). *J Clin Exp Hepatol* 2014;4(4):332–346. doi:10.1016/j.jceh.2014.10.002.
- [2] Zhuge YZ, Wang Y, Zhang F, Zhu CK, Zhang W, Zhang M, *et al*. Clinical characteristics and treatment of pyrrolizidine alkaloid-related hepatic vein occlusive disease. *Liver Int* 2018;38(10):1867–1874. doi:10.1111/liv.13684.
- [3] Lin G, Wang JY, Li N, Li M, Gao H, Ji Y, *et al*. Hepatic sinusoidal obstruction syndrome associated with consumption of *Gynura segetum*. *J Hepatol* 2011;54(4):666–673. doi:10.1016/j.jhep.2010.07.031.
- [4] Wang JY, Gao H. Tusangqi and hepatic sinusoidal obstruction syndrome. *J Dig Dis* 2014;15(3):105–107. doi:10.1111/1751-2980.12112.
- [5] Xu Z, Zhuge Y, Xu T. Raise the recognition of hepatic veno-occlusive disease induced by chrysanthemum-like groundsel. *Chin J Gastroenterol* 2009;14(10):577–579.
- [6] Zhuge Y, Liu Y, Xie W, Zou X, Xu J, Wang J. Expert consensus on the clinical management of pyrrolizidine alkaloid-induced hepatic sinusoidal obstruction syndrome. *J Gastroenterol Hepatol* 2019;34(4):634–642. doi:10.1111/jgh.14612.
- [7] Dalle JH, Giral SA. Hepatic veno-occlusive disease after hematopoietic stem cell transplantation: risk factors and stratification, prophylaxis, and treatment. *Biol Blood Marrow Transplant* 2016;22(3):400–409. doi:10.1016/j.bbmt.2015.09.024.
- [8] Chen Z, Huo JR. Hepatic veno-occlusive disease associated with toxicity of pyrrolizidine alkaloids in herbal preparations. *Neth J Med* 2010;68(6):252–260.
- [9] Zhu W, Chen S, Chen W, Li Y. Clinical analysis of 50 cases of hepatic veno-occlusive disease. *Chin J Dig* 2012;32(9):620–624.
- [10] Gu C, Zou XP, Xu ZM, Zhuge Y. Clinical features of hepatic veno-occlusive disease caused by *Gynura segetum* (Lour.) Merr. *Chin J Dig* 2010;30(10):771–772.
- [11] Dignan FL, Wynn RF, Hadzic N, Karani J, Quaglia A, Pagliuca A, *et al*. BCSH/BSBMT guideline: diagnosis and management of veno-occlusive disease (sinusoidal obstruction syndrome) following haematopoietic stem cell transplantation. *Br J Haematol* 2013;163(4):444–457. doi:10.1111/bjh.12558.
- [12] EASL Clinical Practice Guidelines: Vascular diseases of the liver. *J Hepatol* 2016;64(1):179–202. doi:10.1016/j.jhep.2015.07.040.
- [13] EASL Clinical Practice Guidelines for the management of patients with decompensated cirrhosis. *J Hepatol* 2018;69(2):406–460. doi:10.1016/j.jhep.2018.03.024.
- [14] EASL Clinical Practice Guidelines: Management of alcohol-related liver disease. *J Hepatol* 2018;69(1):154–181. doi:10.1016/j.jhep.2018.03.018.
- [15] EASL Clinical Practice Guidelines: The diagnosis and management of patients with primary biliary cholangitis. *J Hepatol* 2017;67(1):145–172. doi:10.1016/j.jhep.2017.03.022.
- [16] EASL 2017 Clinical Practice Guidelines on the management of hepatitis B virus infection. *J Hepatol* 2017;67(2):370–398. doi:10.1016/j.jhep.2017.03.021.
- [17] EASL Recommendations on Treatment of Hepatitis C 2016. *J Hepatol* 2017;66(1):153–194. doi:10.1016/j.jhep.2016.09.001.
- [18] EASL Clinical Practice Guidelines: Autoimmune hepatitis. *J Hepatol* 2015;63(4):971–1004. doi:10.1016/j.jhep.2015.06.030.
- [19] EASL Clinical Practice Guidelines on the management of acute (fulminant) liver failure. *J Hepatol* 2017;66(5):1047–1081. doi:10.1016/j.jhep.2016.12.003.
- [20] Chalasani NP, Hayashi PH, Bonkovsky HL, Navarro VJ, Lee WM, Fontana RJ. ACG Clinical Guideline: the diagnosis and management of idiosyncratic drug-induced liver injury. *Am J Gastroenterol* 2014;109(7):950–966. quiz 967. doi:10.1038/ajg.2014.131.
- [21] McDonald GB, Sharma P, Matthews DE, Shulman HM, Thomas ED. Venocclusive disease of the liver after bone marrow transplantation: diagnosis, incidence, and predisposing factors. *Hepatology* 1984;4(1):116–122. doi:10.1002/hep.1840040121.
- [22] McDonald GB, Hinds MS, Fisher LD, Schoch HG, Wolford JL, Banaji M, *et al*. Veno-occlusive disease of the liver and multiorgan failure after bone marrow transplantation: a cohort study of 355 patients. *Ann Intern Med* 1993;118(4):255–267. doi:10.7326/0003-4819-118-4-199302150-00003.
- [23] Jones RJ, Lee KS, Beschornor WE, Vogel VG, Grochow LB, Braine HG, *et al*. Venocclusive disease of the liver following bone marrow transplantation. *Transplantation* 1987;44(6):778–783. doi:10.1097/00007890-

- 198712000-00011.
- [24] Gao H, Ruan JQ, Chen J, Li N, Ke CQ, Ye Y, *et al*. Blood pyrrole-protein adducts as a diagnostic and prognostic index in pyrrolizidine alkaloid-hepatic sinusoidal obstruction syndrome. *Drug Des Devel Ther* 2015;9:4861–4868. doi: 10.2147/DDDT.S87858.
  - [25] Kan X, Ye J, Rong X, Lu Z, Li X, Wang Y, *et al*. Diagnostic performance of Contrast-enhanced CT in Pyrrolizidine Alkaloids-induced Hepatic Sinusoidal Obstructive Syndrome. *Sci Rep* 2016;6:37998. doi:10.1038/srep37998.
  - [26] Gao H, Li N, Wang JY, Zhang SC, Lin G. Definitive diagnosis of hepatic sinusoidal obstruction syndrome induced by pyrrolizidine alkaloids. *J Dig Dis* 2012;13(1):33–39. doi: 10.1111/j.1751-2980.2011.00552.x.
  - [27] Ma C, Liu Y, Zhu L, Ji H, Song X, Guo H, *et al*. Determination and regulation of hepatotoxic pyrrolizidine alkaloids in food: A critical review of recent research. *Food Chem Toxicol* 2018;119:50–60. doi: 10.1016/j.fct.2018.05.037.
  - [28] Xia Q, Zhao Y, Lin G, Beland FA, Cai L, Fu PP. Pyrrolizidine alkaloid-protein adducts: Potential non-invasive biomarkers of pyrrolizidine alkaloid-induced liver toxicity and exposure. *Chem Res Toxicol* 2016;29(8):1282–1292. doi:10.1021/acs.chemrestox.6b00120.
  - [29] Fu PP, Yang YC, Xia Q, Chou MW, Cui YY, Lin G. Pyrrolizidine Alkaloids-Tumorigenic Components in Chinese Herbal Medicines and Dietary Supplements. *J Food Drug Anal* 2002;10(4):198–211.



Original Article

# Efficacy of Intra-gastric Balloons in the Markers of Metabolic Dysfunction-associated Fatty Liver Disease: Results from Meta-analyses

Zi-Yuan Zou<sup>#</sup> , Jing Zeng<sup>#</sup>, Tian-Yi Ren, Yi-Wen Shi, Rui-Xu Yang and Jian-Gao Fan<sup>\*</sup>

Center for Fatty Liver, Department of Gastroenterology, Xinhua Hospital Affiliated to Shanghai Jiao Tong University School of Medicine, Shanghai Key Lab of Pediatric Gastroenterology and Nutrition, Shanghai, China

Received: 27 December 2020 | Revised: 25 February 2021 | Accepted: 1 March 2021 | Published: 16 March 2021

## Abstract

**Background and Aims:** Nonalcoholic fatty liver disease, now renamed metabolic dysfunction-associated fatty liver disease (MAFLD), is common in obese patients. Intra-gastric balloon (IGB), an obesity management tool with low complication risk, might be used in MAFLD treatment but there is still unexplained heterogeneity in results across studies. **Methods:** We conducted a systematic search of 152 citations published up to September 2020. Meta-analyses, stratified analyses, and meta-regression were performed to evaluate the efficacy of IGB on homeostasis model assessment of insulin resistance (HOMA-IR), alanine aminotransferase (ALT), aspartate aminotransferase (AST), and gamma-glutamyl transpeptidase (GGT), and to identify patients most appropriate for IGB therapy. **Results:** Thirteen observational studies and one randomized controlled trial met the inclusion criteria (624 participants in total). In the overall estimate, IGB therapy significantly improved the serum markers change from baseline to follow-up [HOMA-IR: 1.56, 95% confidence interval (CI)=1.16–1.95; ALT: 11.53 U/L, 95% CI=7.10–15.96; AST: 6.79 U/L, 95% CI=1.69–11.90; GGT: 10.54 U/L, 95% CI=6.32–14.75]. In the stratified analysis, there were trends among participants with advanced age having less change in HOMA-IR (1.07 vs. 1.82). The improvement of insulin resistance and liver biochemistries with swallowable IGB therapy was no worse than that with endoscopic IGB. Multivariate meta-regression analyses showed that greater HOMA-IR loss was predicted by younger age ( $p=0.0107$ ). Furthermore, effectiveness on ALT and GGT was predicted by basal ALT ( $p=0.0004$ ) and

GGT ( $p=0.0026$ ), respectively. **Conclusions:** IGB is effective among the serum markers of MAFLD. Younger patients had a greater decrease of HOMA-IR after IGB therapy.

**Citation of this article:** Zou ZY, Zeng J, Ren TY, Shi YW, Yang RX, Fan JG. Efficacy of intra-gastric balloons in the markers of metabolic dysfunction-associated fatty liver disease: results from meta-analyses. J Clin Transl Hepatol 2021; 00(00):353–363. doi: 10.14218/JCTH.2020.00183.

## Introduction

As the prevalence of obesity and insulin resistance continues to rise, nonalcoholic fatty liver disease (NAFLD), now rebranded as metabolic dysfunction-associated fatty liver disease (MAFLD), has emerged as the most prevalent parenchymal liver disease worldwide and explains 9% of deaths from liver cirrhosis.<sup>1–3</sup> Currently, there are no approved pharmacotherapies for fatty liver disease.<sup>4</sup> Bariatric surgery for fatty liver disease has enjoyed a high profile due to its remarkable capacity for improving liver enzyme, NAFLD activity score, and fibrosis.<sup>5,6</sup> However, unexpected rates of liver fibrosis progression in patients who undergo bariatric surgery and excessive risks of postoperative complications limit the acceptance of bariatric surgery.<sup>7,8</sup> Additionally, lifestyle modification strategies are difficult to address the disadvantage regarding treatment compliance.<sup>9,10</sup> As a result, novel therapeutic applications, which take all efficacy, safety, and treatment compliance into account, are urgently needed for all MAFLD patients.

Recently, the potential role of endoscopic bariatric and metabolic therapies (EBMT) in the management of fatty liver disease has been highlighted.<sup>11,12</sup> EBMT are developed to avoid the invasive nature of laparoscopic or open bariatric surgery, in contrast, reproducing similar gastrointestinal physiological alterations and therapeutic effects.<sup>13</sup> Among these interventions, intra-gastric balloon (IGB), as a space-occupying EBMT device with proven efficacy in inducing weight loss, has been used in diminishing liver volume to reduce the risks of subsequent bariatric surgery and has met with success.<sup>14,15</sup> Prior study has demonstrated that the change in liver volume was positively correlated with the change in intrahepatic fat,<sup>16</sup> which suggested the potential therapeutic effect of using IGB in fatty liver disease. In terms of current evidence, a randomized controlled

**Keywords:** Intra-gastric balloon; Nonalcoholic fatty liver disease; Insulin resistance; Age groups; Treatment outcome.

**Abbreviations:** ALT, alanine aminotransferase; AST, aspartate aminotransferase; BMI, body mass index; CI, confidence interval; EBMT, endoscopic bariatric and metabolic therapies; GGT, gamma-glutamyl transpeptidase; HOMA-IR, homeostasis model assessment of insulin resistance; IGB, intra-gastric balloon; I<sup>2</sup>, inconsistency index; MD, mean difference; NAFLD, nonalcoholic fatty liver disease; NOS, Newcastle-Ottawa scale; MAFLD, metabolic dysfunction-associated fatty liver disease; RCT, randomized controlled trial.

<sup>#</sup>Both authors contributed equally to this work.

**\*Correspondence to:** Jian-Gao Fan, Center for Fatty Liver, Department of Gastroenterology, Xinhua Hospital Affiliated to Shanghai Jiao Tong University School of Medicine, Shanghai Key Lab of Pediatric Gastroenterology and Nutrition, Shanghai 200092, China. ORCID: <https://orcid.org/0000-0001-7443-5056>. Tel: +86-21-2507-7340, Fax: +86-21-2507-7340, E-mail: fanjiangao@xinhamed.com.cn



trial (RCT) evaluated changes in histological scores after 6-month IGB therapy and showed a beneficial effect on the severity of fatty liver disease.<sup>17</sup> However, due to the limited sample size of this trial, we still need to combine the existing RCT findings with observational longitudinal studies to present the effectiveness of IGB in larger sample size, before it is widely recommended for the treatment of MAFLD. Therefore, we performed a systematic review with meta-analyses to evaluate the therapeutic effect of IGB on the markers of MAFLD, such as homeostasis model assessment of insulin resistance (HOMA-IR) index, alanine aminotransferase (ALT), aspartate aminotransferase (AST), and gamma-glutamyl transpeptidase (GGT). Furthermore, to identify patients most appropriate for IGB therapy, stratified analyses and meta-regression were both implemented.

## Methods

### Data sources and search strategy

This systematic review was performed according to the preferred reporting items for systematic reviews and meta-analysis statement (see Table S1).<sup>18</sup> The protocol for this review is registered in PROSPERO (no. CRD42020214315).

To collect all full-text articles describing the effect of IGB on the markers of MAFLD, we performed a search of the Medline, Cochrane Library, and Web Of Science with English-language restriction and up to September 2020 using the following strategy: ("Intragastric balloon" OR "Gastric balloon") AND ("Alanine aminotransferase" OR "Alanine transaminase" OR "ALT" OR "Liver" OR "Nonalcoholic fatty liver disease" OR "Non-alcoholic fatty liver disease" OR "NASH" OR "NAFLD" OR "HOMA-IR" OR "Homeostasis model assessment" OR "Insulin resistance"). The detailed search strategy is summarized in Table S2. Furthermore, the reference lists of each article were manually searched to prevent the omission of any pertinent study.

### Study eligibility and selection criteria

Only observational longitudinal studies and RCTs were included. Inclusion criteria of the articles were as follows: (a) population: all patients who are obese or in need of obesity treatment; (b) intervention: liquid-filled IGB procedure; (c) comparator: the participants at baseline before IGB placement; and (d) outcome: the decrease of ALT, AST, GGT, or HOMA-IR index in all the participants treated with IGB. Moreover, the studies which recruited only pediatric patients or utilized the gas-filled IGB as an intervention were excluded to prevent bias.

### Data extraction and quality assessment

Data extraction was performed independently by two investigators (ZYZ, JZ). The information and characteristics extracted from the included study were first author, year of publication, study design, country, study size of participants with IGB therapy, IGB type, dwelling time of IGB, filling of IGB, method of IGB implantation, additional nutrition and exercise prescription, description of liver disease in exclusion criteria, percentage of male individuals, prevalence of diabetes, participants' age and body mass index (BMI) at baseline, and participants' ALT, AST, GGT and HOMA-IR before and after IGB therapy. When standard deviation was unavailable, it was replaced with a quarter of the range.<sup>19</sup> The risk of bias of the selected studies was evaluated using

the modified Newcastle-Ottawa scale (NOS) for observational longitudinal studies<sup>20</sup> and Cochrane Collaboration's tool for RCT.<sup>21</sup>

## Data analysis

Using R software version 3.6.3 (R Foundation for Statistical Computing, Vienna, Austria) and Review Manager version 5.3 (Nordic Cochrane Centre, The Cochrane Collaboration, Copenhagen, Denmark), meta-analyses (quantitative synthesis) were performed to evaluate the pooled mean difference (MD) in HOMA-IR, ALT, AST and GGT from baseline to end of IGB therapy using the inverse variance method and random-effect model, with 95% confidence interval (CI) and *p*-value. A *p*-value <0.05 was considered statistically significant. Publication bias was evaluated by Egger's test and funnel plot.<sup>22,23</sup> Heterogeneity was evaluated with inconsistency index (*I*<sup>2</sup>), classified as a low (*I*<sup>2</sup>≥25%), substantial (*I*<sup>2</sup>≥50%), or considerable (*I*<sup>2</sup>≥75%).<sup>24</sup> Stratified analyses were conducted to investigate sources of heterogeneity based on the following characteristics: method of IGB implantation; mean basal level of serum markers (HOMA-IR, ALT, AST, or GGT); age and BMI of the participants; study region; and NOS score. When meta-regression analysis was performed, univariate and multivariate linear regression models were utilized to evaluate the slope coefficient between the reduced value of serum marker (HOMA-IR, ALT, AST, or GGT) after IGB therapy and the following covariates: mean basal level of serum marker; percentage of male individuals; and age and BMI of the participants. To summarize the results, the scatter plots were mapped to materialize the linear relationship between the changed value after IGB therapy and covariates which had statistical significance with both univariate and multivariate meta-regression analysis (*p*<0.05). Each study was represented by a circle of size proportional to the inverse of the variance of MD.

## Results

### Literature search results

Figure 1 summarizes the flow diagram of the selection process performed to identify eligible studies in this systematic review. Out of 152 references, a total of 14 studies<sup>25–38</sup> comprising 624 participants met the predefined inclusion criteria. All studies were published prior to September 13, 2020.

### Improvement of insulin resistance after IGB on therapy

**Summary of study characteristics:** Eight studies<sup>25–27,29,33,35,36,38</sup> with a total of 352 individuals were included in this meta-analysis of HOMA-IR level, and their characteristics are summarized in Table 1. All included studies were published after 2007. Of these, one<sup>38</sup> was a two-arm RCT, and the rest<sup>25–27,29,33,35,36</sup> were observational longitudinal studies, meaning that a total of nine intervention arms were included in this analysis. The participants came from three countries (Brazil, Italy, Japan). Seven intervention arms<sup>25–27,29,33,35</sup> applied the Orbera IGB system, one arm<sup>36</sup> used the Orbera/Spatz IGB system, and the single remaining arm<sup>38</sup> reported results with the Elipse IGB system. Furthermore, the range of average baseline HOMA-IR was from 2.36 to 12.30. The results of the quality assessment using

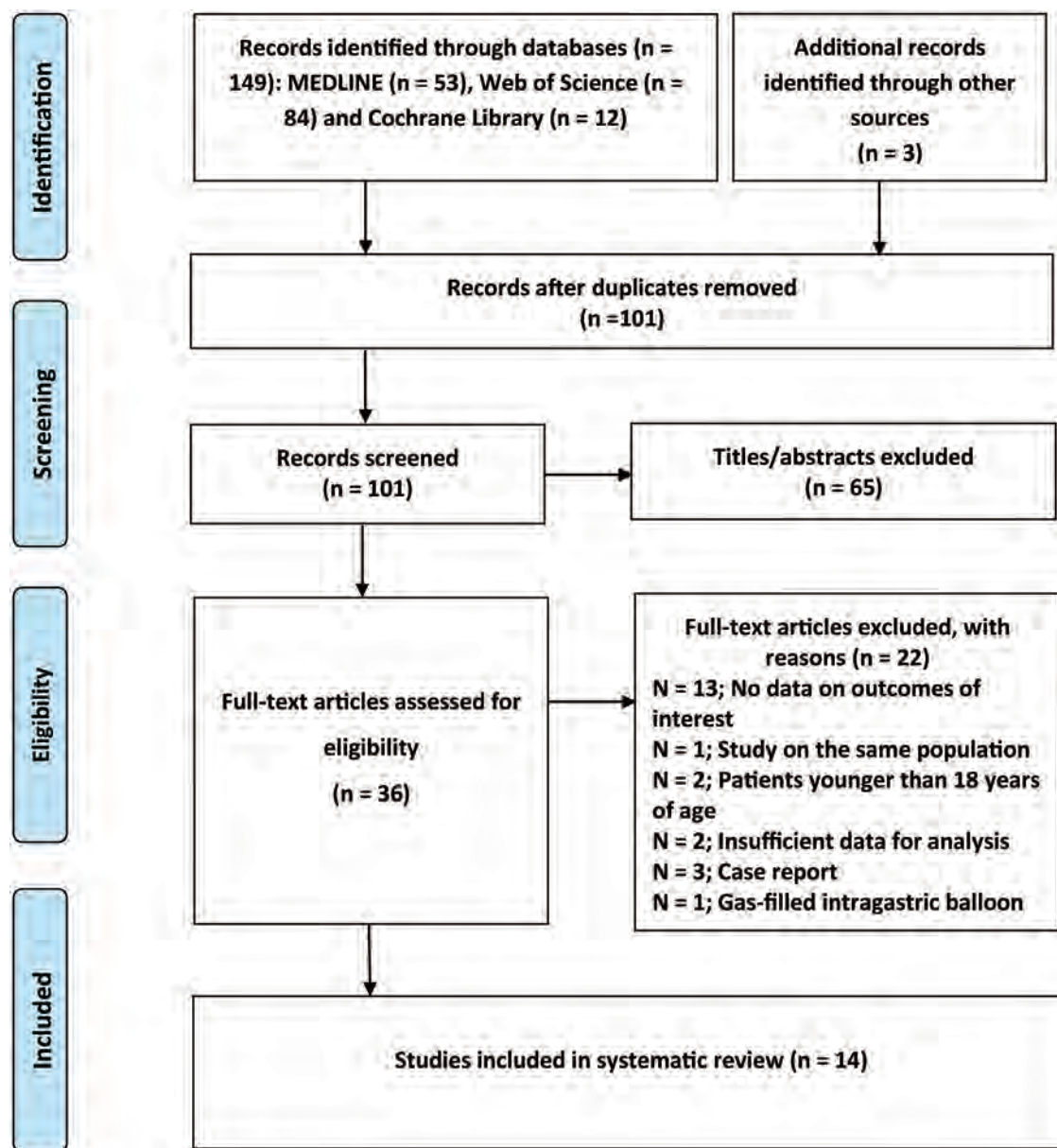


Fig. 1. Flow diagram of the study selection process.

the modified NOS and Cochrane Collaboration's tool can be found in Table S3 and Figure S1.

**Quantitative synthesis and stratified analyses:** Nine intervention arms<sup>25–27,29,33,35,36,38</sup> of 352 participants evaluated the effect of IGB on HOMA-IR. The pooled mean decrease in HOMA-IR levels with IGB therapy was 1.56 (95% CI=1.16–1.95,  $I^2=61.1$ ; Fig. 2A). According to the Egger's test and funnel plot, no significant publication bias was present ( $p=0.2665$ ; Fig. S2A). Table 2 presents the results of the stratified analyses. Both endoscopic IGB (MD=1.68, 95% CI=1.24–2.11) and swallowable IGB (MD=0.90, 95% CI=0.26–1.54) were effective in inducing HOMA-IR loss. There were trends showing the advanced age group had less change in HOMA-IR (MD=1.07, 95% CI=0.57–1.56) compared to those  $\leq 40$  years (MD=1.82, 95% CI=1.25–2.40), but the findings were not statistically significant ( $p=0.0502$ ). Higher baseline HOMA-IR ( $>5$ ) was associat-

ed with more significant reductions in HOMA-IR [MD=3.48 (95% CI=2.46–4.50) vs. MD=1.40 (95% CI=1.25–1.54),  $p<0.0001$ ]. Consequently, intra-subgroup heterogeneity was significantly diminished and almost absent with different basal HOMA-IR (basal HOMA-IR  $\leq 5$ :  $I^2=0.0$ ; basal HOMA-IR  $>5$ :  $I^2=0.0$ ).

**Meta-regression:** Table 3 presents the meta-regression findings of HOMA-IR. In univariate meta-regression, basal HOMA-IR of the participants (slope coefficient=0.3966, 95% CI=0.1119–0.6814,  $p=0.0063$ ) and percentage of male individuals (slope coefficient=0.0433, 95% CI=0.0183 to 0.0684,  $p=0.0007$ ) seemed to be factors significantly associated with reductions in HOMA-IR. Subsequently, using a multivariate meta-regression approach, our final model consisted of four covariates: basal HOMA-IR, percentage of male individuals, age and BMI of the participants. Greater HOMA-IR loss was predicted by younger age (slope coeffi-

Table 1. Characteristics of the included studies

Author	IGB group, n	Type of study; Country; Prevalence of diabetes	Nutrition and exercise prescription	IGB type; IGB duration; Filling; Implantation of IGB	Liver disease excluded
Bazerbachi et al. <sup>37</sup>	21	Observational study; USA; 52%	Low-calorie diet + lifestyle therapy	Orbera; 6 months; Liquid-filled; Endoscopically	Other primary causes of liver disease
Maekawa et al. <sup>38</sup>	18	RCT; Japan; Not described	Low-carbohydrate diet	Orbera; 6 months; Liquid-filled; Endoscopically	Not described
Maekawa et al. <sup>38</sup>	13	RCT; Japan; Not described	Low-calorie diet	Orbera; 6 months; Liquid-filled; Endoscopically	Not described
Guedes et al. <sup>36</sup>	42	Observational study; Brazil; Not described	Low-calorie diet	Orbera/Spatz; 6 months; Liquid-filled; Endoscopically	Not described
Genco et al. <sup>35</sup>	38	Observational study; Italy; Not described	Low-calorie diet + exercise counseling	Elipse; 4 months; Liquid-filled; Swallowable	Not described
Raftopoulos et al. <sup>34</sup>	12	Observational study; Greece; Not described	Diet and exercise counseling	Elipse; 4 months; Liquid-filled; Swallowable	No history of alcohol
Folini et al. <sup>32</sup>	13	Observational study; Italy; Not described	Low-calorie diet + exercise counseling	Orbera; 6 months; Liquid-filled; Endoscopically	Alcohol consumption, presence of any predisposing disorders for liver diseases, pregnancy, and lactation
Takahata et al. <sup>33</sup>	8	Observational study; Japan; Not described	Low-calorie diet	Orbera; 6 months; Liquid-filled; Endoscopically	Not described
Tai et al. <sup>31</sup>	28	Observational study; China (Taiwan); Not described	Low-calorie diet	Orbera; Median 200 days; Liquid-filled; Endoscopically	Alcoholism or drug addiction
Nikolic et al. <sup>28</sup>	33	Observational study; Croatia; Not described	Low-calorie diet	Orbera; 6 months; Liquid-filled; Endoscopically	Not described
Sekino et al. <sup>29</sup>	8	Observational study; Japan; Not described	Not described	Orbera; 6 months; Liquid-filled; Endoscopically	Not described
Stimac et al. <sup>30</sup>	165	Observational study; Croatia; Not described	Not described	Orbera; 6 months; Liquid-filled; Endoscopically	Present alcohol or drug abuse
Forlano et al. <sup>27</sup>	120	Observational study; Italy; 13.3%	Low-calorie diet	Orbera; 6 months; Liquid-filled; Endoscopically	Use of drugs reported to cause liver damage, alcohol intake of 30 g/day or more, and viral hepatitis
Donadio et al. <sup>26</sup>	40	Observational study; Italy; Not described	Not described	Orbera; 6 months; Liquid-filled; Endoscopically	Alcoholism
Ricci et al. <sup>25</sup>	65	Observational study; Italy; Not described	Low-calorie diet	Orbera; 6 months; Liquid-filled; Endoscopically	Positivity for hepatitis B virus or hepatitis C virus, previous or current alcohol consumption >30 g/day, use of medications with reported hepatosteatogenic effect (amiodarone, tamoxifen, estrogens), and type 1 diabetes

IGB, intragastric balloon; RCT, randomized controlled trial.



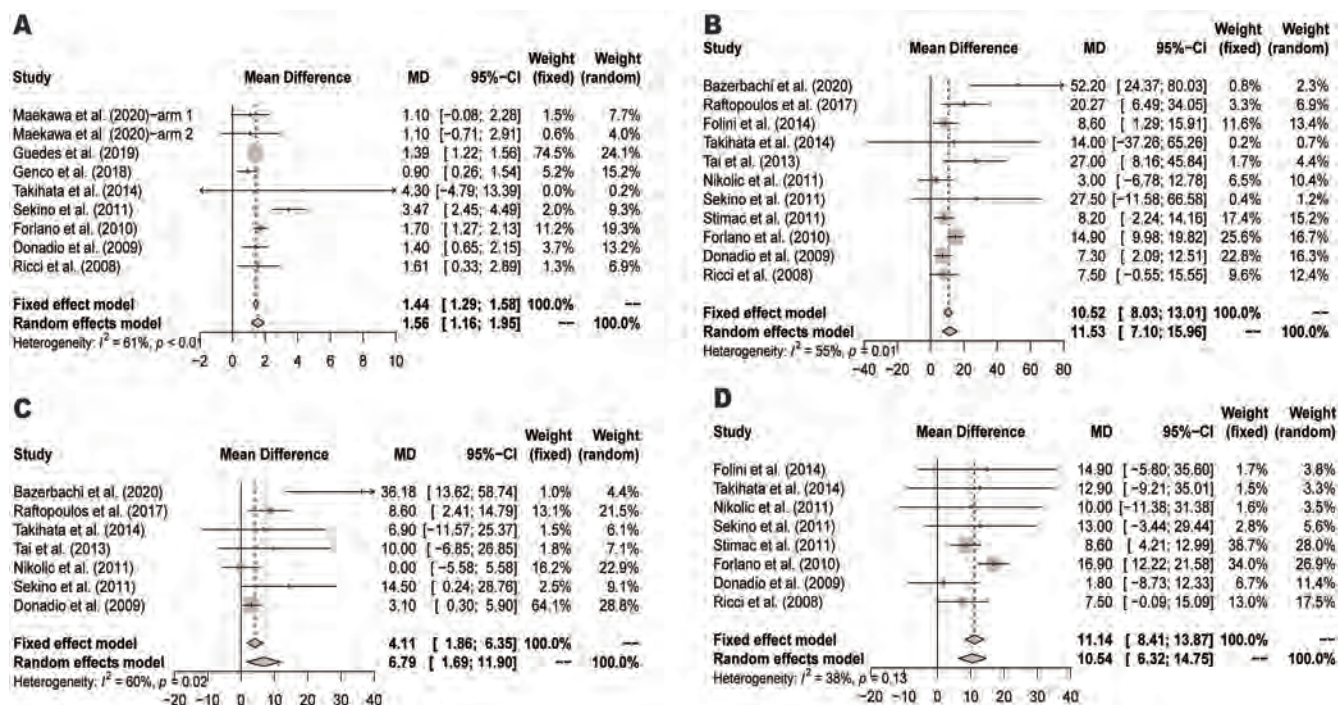


Fig. 2. Forest plots. HOMA-IR (A), ALT (B), AST (C), and GGT (D) decreased after IGB treatment and removal. ALT, alanine aminotransferase; AST, aspartate aminotransferase; GGT, gamma-glutamyl transpeptidase; HOMA-IR, homeostasis model assessment of insulin resistance; IGB, intragastric balloon.

cient = -0.0932, 95% CI = -0.1647 to -0.0216,  $p = 0.0107$ ).

### Decrease in ALT after IGB therapy

**Summary of study characteristics:** Eleven observational longitudinal studies<sup>25–34,37</sup> with a total of 513 individuals were included in this meta-analysis of ALT level, and their characteristics are summarized in Table 1. All included studies were published after 2007. The participants included in the meta-analysis of ALT level came from six countries (China, Croatia, Greece, Italy, Japan, USA). Ten studies<sup>25–33,37</sup> applied the Orbera IGB system, and one study<sup>34</sup> reported results with the Elipse IGB system. Furthermore, the range of average baseline ALT was from 26.0 to 91.6 U/L. The results of the quality assessment using the modified NOS can be found in Table S3.

**Quantitative synthesis and stratified analyses:** Eleven studies<sup>25–34,37</sup> of 513 participants evaluated the effect of IGB on ALT. The pooled mean decrease of ALT with IGB therapy was 11.53 U/L (95% CI = 7.10–15.96,  $I^2 = 55.4$ ; Fig. 2B). According to the Egger's test and funnel plot, no significant publication bias was present ( $p = 0.2422$ ; Fig. S2B). Table 2 presents the results of the stratified analyses. Both endoscopic IGB (MD = 10.85 U/L, 95% CI = 6.31–15.39) and swallowable IGB (MD = 20.27 U/L, 95% CI = 6.49–34.05) were effective in inducing ALT loss. The advanced age group had similar change in ALT (MD = 15.57 U/L, 95% CI = 5.20–25.93) compared to those  $\leq 40$  years (MD = 10.40 U/L, 95% CI = 5.38–15.41). Higher baseline ALT ( $> 40$  U/L) was associated with more significant reductions in ALT [MD = 32.43 U/L (95% CI = 18.49–46.37) vs. MD = 9.58 U/L (95% CI = 6.18–12.98),  $p = 0.0018$ ]. Overall, intra-subgroup heterogeneity in different basal ALT diminished significantly and was classified as a low (basal ALT  $\leq 40$  U/L:  $I^2 = 38.7$ ; basal ALT  $> 40$  U/L:  $I^2 = 0.0$ ).

**Meta-regression:** Table 3 presented the meta-regression

findings of ALT. In univariate meta-regression, basal ALT of the participants (slope coefficient = 0.7314, 95% CI = 0.3862–1.0767,  $p < 0.0001$ ) seemed to be a factor significantly associated with reductions in ALT. Subsequently, using a multivariate meta-regression approach, our final model consisted of four covariates: basal ALT; percentage of male individuals; age; and BMI. Effectiveness on ALT was predicted by basal ALT (slope coefficient = 0.7135, 95% CI = 0.3213–1.1057,  $p = 0.0004$ ). The scatter plot showed a linear trend towards increasing effectiveness of IGB therapy with increasing basal ALT of the participants (Fig. 3A).

### Decrease in AST after IGB therapy

**Summary of study characteristics:** Seven observational longitudinal studies<sup>26,28,29,31,33,34,37</sup> with a total of 150 individuals were included in this meta-analysis of AST level, and their characteristics are summarized in Table 1. The participants included in the meta-analysis of AST level came from six countries (China, Croatia, Greece, Italy, Japan, USA). Six studies<sup>26,28,29,31,33,37</sup> applied the Orbera IGB system, and one study<sup>34</sup> reported results with the Elipse IGB system. Furthermore, the range of average baseline AST was from 21.7 to 67.5 U/L. The results of the quality assessment using the modified NOS can be found in Table S3.

**Quantitative synthesis and stratified analyses:** Seven studies of 150 participants evaluated the effect of IGB on AST. The pooled mean decrease of AST with IGB therapy was 6.79 U/L (95% CI = 1.69–11.90,  $I^2 = 59.9$ ; Fig. 2C). According to the Egger's test and funnel plot, no significant publication bias was present ( $p = 0.3768$ ; Fig. S2C). Table 2 presents the results of the stratified analyses. Both endoscopic IGB (MD = 6.74 U/L, 95% CI = 0.53–12.96) and swallowable IGB (MD = 8.60 U/L, 95% CI = 2.41–14.79) were effective in inducing AST loss. The advanced age group had a similar change in AST (MD = 14.54 U/L, 95% CI = -0.04 to 29.12) compared



**Table 2. Pooled change in HOMA-IR, ALT, AST, and GGT after IGB treatment and removal: Stratified analyses**

	Intervention arm, n	MD (95% CI)	I <sup>2</sup>
Pooled change in HOMA-IR after IGB treatment and removal			
Insertion of IGB (IGB type)			
Endoscopic (Orbera/Spatz)	8	1.68 (1.24–2.11)	60.3
Swallowable (Elipse)	1	0.90 (0.26–1.54)	–
Basal HOMA-IR			
≤5	7	1.40 (1.25–1.54)	0.0
>5	2	3.48 (2.46–4.50)	0.0
Mean age, years			
≤40	4	1.82 (1.25–2.40)	82.0
>40	5	1.07 (0.57–1.56)	0.0
Mean BMI, kg/m <sup>2</sup>			
≤40	4	1.35 (1.19–1.51)	0.0
>40	5	2.01 (1.25–2.77)	66.4
Region			
Asia	4	1.35 (1.19–1.51)	72.4
Europe	4	1.41 (1.01–1.81)	29.1
South America	1	1.39 (1.22–1.56)	–
NOS scale			
High	3	1.37 (0.88–1.87)	52.0
Fair	4	2.16 (0.87–3.44)	81.2
Pooled change in ALT after IGB treatment and removal			
Insertion of IGB (IGB type)			
Endoscopic (Orbera)	10	10.85 (6.31–15.39)	55.9
Swallowable (Elipse)	1	20.27 (6.49–34.05)	–
Basal ALT, U/L			
≤40	7	9.58 (6.18–12.98)	38.7
>40	4	32.43 (18.49–46.37)	0.0
Mean age, years			
≤40	6	10.40 (5.38–15.41)	54.6
>40	5	15.57 (5.20–25.93)	64.6
Mean BMI, kg/m <sup>2</sup>			
≤40	2	22.61 (11.49–33.74)	0.0
>40	9	9.98 (5.59–14.38)	53.7
Region			
Asia	3	25.80 (9.69–41.91)	0.0
Europe	7	9.58 (6.18–12.98)	38.7
North America	1	9.88 (7.33–12.44)	–
NOS scale			
High	4	12.71 (5.27–20.16)	78.0
Fair	7	10.59 (4.84–16.35)	29.4
Pooled change in AST after IGB treatment and removal			
Insertion of IGB (IGB type)			
Endoscopic (Orbera)	6	6.74 (0.53–12.96)	60.4

(continued)

Table 2. (continued)

	Intervention arm, n	MD (95% CI)	I <sup>2</sup>
Swallowable (Elipse)	1	8.60 (2.41–14.79)	–
Basal AST, U/L			
≤40	6	4.52 (1.05–7.99)	29.8
>40	1	36.18 (13.62–58.74)	0
Mean age, years			
≤40	4	3.30 (–0.66 to 7.26)	29.9
>40	3	14.54 (–0.04 to 29.12)	63.5
Mean BMI, kg/m <sup>2</sup>			
≤40	2	8.77 (2.95–14.58)	0.0
>40	5	6.64 (–0.20 to 13.49)	66.8
Region			
Asia	3	11.15 (1.77–20.53)	0
Europe	3	3.59 (–0.34 to 7.52)	52.1
North America	1	36.18 (13.62–58.74)	–
NOS scale			
High	2	17.67 (–14.52 to 49.86)	87.7
Fair	5	6.17 (0.53–11.81)	38.2
Pooled change in GGT after IGB treatment and removal			
Insertion of IGB (IGB type)			
Endoscopic (Orbera)	8	9.45 (4.46–14.45)	53.0
Swallowable (Elipse)	0	–	–
Basal GGT, U/L			
≤40	6	8.74 (2.89–14.59)	66.2
>40	2	12.96 (–0.23 to 26.15)	0.0
Mean age, years			
≤40	5	8.75 (1.71–15.79)	71.3
>40	3	8.80 (2.02–15.58)	0.0
Mean BMI, kg/m <sup>2</sup>			
≤40	8	9.45 (4.46–14.45)	53.0
>40	0	–	–
Region			
Asia	2	12.96 (–0.23 to 26.15)	0.0
Europe	6	8.74 (2.89–14.59)	66.2
NOS scale			
High	3	10.10 (2.49–17.72)	80.1
Fair	5	7.88 (1.86–13.89)	0.0

ALT, alanine aminotransferase; AST, aspartate aminotransferase; GGT, gamma-glutamyl transpeptidase; HOMA-IR, homeostasis model assessment of insulin resistance; IGB, intragastric balloon.

to those ≤40 years (MD=3.30 U/L, 95% CI=–0.66 to 7.26). Higher baseline AST (>40 U/L) was associated with more significant reductions in AST [MD=36.18 U/L (95% CI=13.62–58.74) vs. MD=4.52 U/L (95% CI=1.05–7.99,  $p=0.0065$ )]. Overall, intra-subgroup heterogeneity in different basal AST diminished significantly and was classified as a low (basal AST ≤40 U/L:  $I^2=29.8$ ; basal AST >40 U/L:  $I^2=0.0$ ).

**Meta-regression:** Table 3 presents the meta-regres-

sion findings of AST. In univariate meta-regression, basal AST of the participants (slope coefficient=0.7650, 95% CI=0.3319–1.1982,  $p=0.0005$ ) and age of the participants (slope coefficient=1.4430, 95% CI=0.5644–2.3216,  $p=0.0013$ ) seemed to be factors significantly associated with reductions in AST. Subsequently, using a multivariate meta-regression approach, our final model consisted of four covariates: basal AST; percentage of male individuals; age;

and BMI. Effectiveness on AST could not be predicted by all of the above covariates.

### Decrease in GGT after IGB therapy

**Summary of study characteristics:** Eight observational longitudinal studies<sup>25–30,32,33</sup> with a total of 452 individuals were included in this meta-analysis of GGT level, and their characteristics are summarized in Table 1. The participants included in the meta-analysis of GGT level came from three countries (Croatia, Italy, Japan). All eight studies<sup>25–30,32,33</sup> applied the Orbera IGB system. Furthermore, the range of average baseline GGT was from 29.8 to 53.0 U/L. The results of the quality assessment using the modified NOS can be found in Table S3.

**Quantitative synthesis and stratified analyses:** Eight studies<sup>25–30,32,33</sup> of 452 participants evaluated the effect of IGB on GGT. The pooled mean decrease of GGT with IGB therapy was 10.54 U/L (95% CI=6.32–14.75,  $I^2=37.6$ ; Fig. 2D). According to the Egger's test and funnel plot, no significant publication bias was present ( $p=0.8620$ ; Fig. S2D). Table 2 presented the results of the stratified analyses. The advanced age group had a similar change in GGT (MD=8.80 U/L, 95% CI=2.02–15.58) compared to those  $\leq 40$  years (MD=8.75 U/L, 95% CI=1.71–15.79). There were trends showing that the higher basal GGT group had more change in GGT (MD=12.96, 95% CI=–0.23 to 26.15) compared to those  $\leq 40$  U/L (MD=8.74, 95% CI=2.89–14.59) but the findings were not statistically significant ( $p=0.6919$ ). Overall, intra-subgroup heterogeneity diminished significantly in the higher basal GGT group ( $I^2=0.0$ ).

**Meta-regression:** Table 3 presents the meta-regression findings of GGT. In univariate meta-regression, basal GGT of the participants (slope coefficient=0.7968, 95% CI=0.2032–1.3904,  $p=0.0085$ ) seemed to be a factor significantly associated with reductions in GGT. Subsequently, using a multivariate meta-regression approach, our final model consisted of four covariates: basal GGT; percentage of male individuals; age; and BMI. Effectiveness on GGT was predicted by basal GGT (slope coefficient=1.3773, 95% CI=0.4793–2.2754,  $p=0.0026$ ). The scatter plot showed a linear trend towards increasing effectiveness of IGB therapy with increasing basal GGT of the participants (Fig. 3B).

## Discussion

### Principal findings and relevant mechanisms

IGB is the most widely available EBMT with proven efficacy in inducing weight loss. According to the IGB type, an empty balloon is introduced into the stomach by an upper gastrointestinal endoscopy or by swallowing the balloon capsule directly. The liquid-filled IGB is inflated with saline and methylene blue to occupy the space in the stomach. After that, the IGB dwells in the stomach for 4 to 6 months until it ruptures or is removed.<sup>14,39</sup> Due to its moderate efficacy of weight loss and excellent safety profiles, the potential utility of IGB was mentioned by the Asian-Pacific clinical practice guideline on MAFLD.<sup>40</sup> IGB has also been employed for clinical research of fatty liver disease. However, there is still substantial heterogeneity in results across studies. One explanation is that patients with fatty liver disease can be subdivided into IGB responder and non-responder groups. In this systematic review with meta-analysis, we demonstrated that IGB could reverse the serum markers of MAFLD, including HOMA-IR, ALT, AST, and GGT levels. Furthermore, the change of ALT and GGT with IGB therapy

had a positive linear relationship with the basal value. This means that even at higher levels of disease severity, abnormal liver enzymes can be controlled within the reported range of included studies (ALT: 26.0–91.6 U/L; GGT: 29.8–53.0 U/L).

Due to the dearth of eligible studies, the histological and radiological findings cannot be quantitatively pooled through meta-analyses and can only be described in the discussion. In terms of histological variables, a small RCT,<sup>17</sup> with 18 patients who completed the study, reported that NAFLD activity score at post-therapy was significantly lower among the IGB-treated compared with the sham-treated arm. On the other hand, there seemed to be no difference between the IGB-treated arm and the sham-treated arm in improving fibrosis. Consistent with this finding, according to another observational study,<sup>37</sup> significant improvement of NAFLD activity score was reached in most NAFLD patients treated with IGB ( $p<0.001$ ). Apart from these, some of the studies assessed non-invasive radiological parameters of NAFLD. A prospective single-arm study<sup>27</sup> showed that after 6 months of IGB therapy, the number of patients with severe hepatic steatosis confirmed by abdominal ultrasound decreased from 52% to 4%. Two other clinical studies,<sup>32,37</sup> respectively, demonstrated that hepatic fat fraction and fibrosis by magnetic resonance imaging could be significantly alleviated by IGB therapy. Taken together, these histological and radiological findings were consistent with the results of serum markers (HOMA-IR, ALT, AST, and GGT) in our meta-analyses.

To date, no study has looked at the impact of age on insulin resistance amelioration in patients receiving IGB therapy. In our meta-analysis, multivariate linear meta-regression and stratified analyses indicated that participants with advanced age had less change in HOMA-IR after IGB therapy. Several weight-dependent and non-weight-dependent hypotheses may explain this phenomenon. A previously published study reported that advanced age was significantly correlated with less excess weight loss in females after IGB intervention.<sup>41</sup> Given that clinically significant weight loss can alleviate insulin resistance,<sup>42</sup> age-related differences in insulin resistance outcomes might be partly attributed to the different weight loss during treatment. Additionally, both obesity and aging are linked to and engender insulin resistance.<sup>43</sup> Among elderly patients, the effect of aging is strongly amplified and cannot be eliminated by the obesity management tools. Taken together, age might be considered as a predictor of insulin resistance amelioration in patients undergoing IGB therapy.

### Comparison with other studies or reviews

In terms of the impact of IGB on liver enzymes, a commendable meta-analysis published in 2016 showed that the use of IGB could decrease ALT (MD=10.02, 95% CI=6.8–13.2),<sup>19</sup> which was in line with our findings. When their meta-analysis was published, swallowable IGB had not been widely used and investigated.<sup>14</sup> To help clinicians and researchers keep up to date with current evidence, we performed this systematic review including more updated studies. Our stratified analysis revealed that the improvement of ALT, AST, and HOMA-IR with swallowable IGB therapy was no worse than that with endoscopic IGB. Future RCTs are needed to comprehensively compare the efficacy and safety between these two IGBs.

### Limitations and strengths

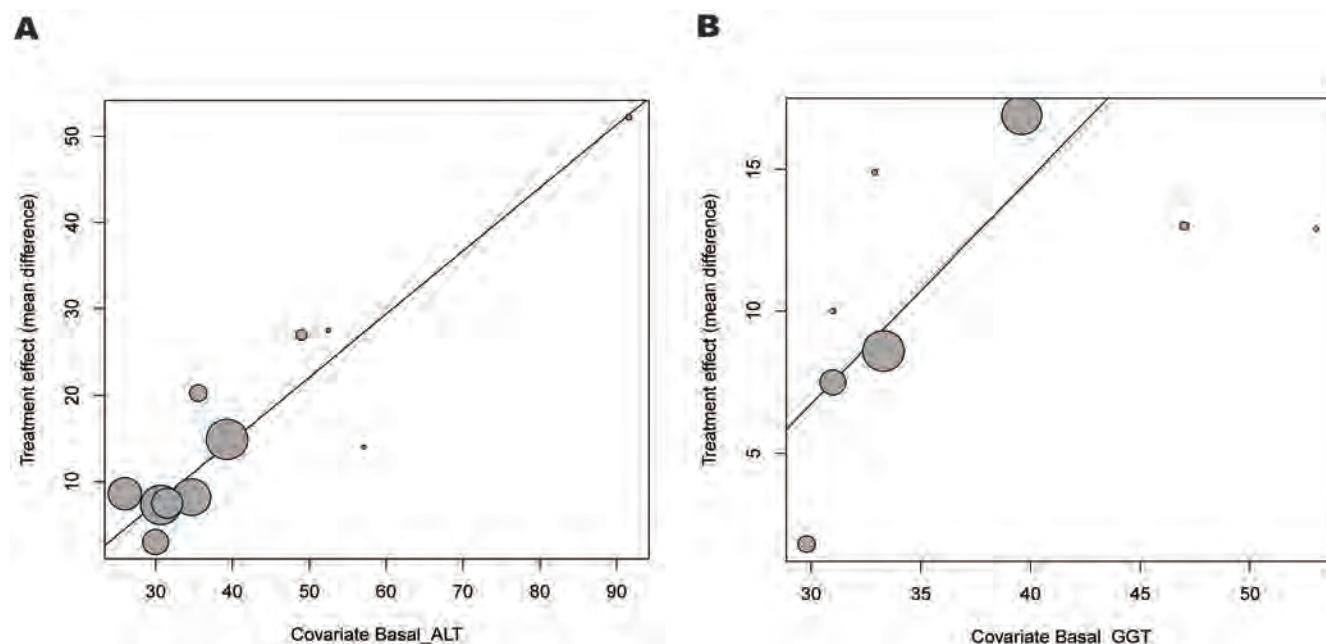
Our systematic review does have some shortcomings. First,

Table 3. Univariate and multivariate meta-regression analyses on the mean difference of HOMA-IR, ALT, AST, and GGT after IGB treatment and removal

Moderators	Intervention arm, n	Univariable analysis			Multivariable analysis		
		Slope coefficient (95% CI)	p		Slope coefficient (95% CI)	p	
Mean difference of HOMA-IR after IGB treatment and removal							
Basal HOMA-IR	9	<b>0.3966 (0.1119–0.6814)</b>	<b>0.0063</b>		0.2361 (–0.2764 to 0.7487)	0.3665	
Mean age	9	–0.0753 (–0.1891 to 0.0386)	0.1950		<b>–0.0932 (–0.1647 to –0.0216)</b>	<b>0.0107</b>	
Mean BMI	9	0.0975 (–0.0288 to 0.2238)	0.1302		–0.0473 (–0.1298 to 0.0351)	0.2607	
Male	9	<b>0.0433 (0.0183–0.0684)</b>	<b>0.0007</b>		0.0381 (–0.0094 to 0.0856)	0.1159	
Mean difference of ALT after IGB treatment and removal							
Basal ALT	11	<b>0.7314 (0.3862–1.0767)</b>	<b>&lt;0.0001</b>		<b>0.7135 (0.3213–1.1057)</b>	<b>0.0004</b>	
Mean age	11	0.8603 (–0.3376 to 2.0582)	0.1593		0.3408 (–0.5602 to 1.2417)	0.4585	
Mean BMI	11	–1.1489 (–2.6746 to 0.3767)	0.1399		–0.5035 (–1.6750 to 0.6681)	0.3996	
Male	11	0.0851 (–0.3480 to 0.5181)	0.7002		–0.0652 (–0.3742 to 0.2437)	0.6791	
Mean difference of AST after IGB treatment and removal							
Basal AST	7	<b>0.7650 (0.3319–1.1982)</b>	<b>0.0005</b>		0.5438 (–0.0501 to 1.1378)	0.0727	
Mean age	7	<b>1.4430 (0.5644–2.3216)</b>	<b>0.0013</b>		0.5348 (–0.8576 to 1.9272)	0.4516	
Mean BMI	7	–0.1374 (–1.5495 to 1.2747)	0.8488		–0.1086 (–0.8199 to 0.6028)	0.7648	
Male	7	0.1362 (–0.2020 to 0.4744)	0.4299		0.0699 (–0.2378 to 0.3777)	0.6562	
Mean difference of GGT after IGB treatment and removal							
Basal GGT	8	<b>0.7968 (0.2032–1.3904)</b>	<b>0.0085</b>		<b>1.3773 (0.4793–2.2754)</b>	<b>0.0026</b>	
Mean age	8	0.5022 (–2.0156 to 3.0201)	0.6958		0.3219 (–1.9139 to 2.5577)	0.7778	
Mean BMI	8	–0.2371 (–4.2184 to 3.7441)	0.9071		–1.3277 (–4.6165 to 1.9612)	0.4288	
Male	8	0.0996 (–0.3201 to 0.5193)	0.6418		–0.4310 (–0.9670 to 0.1051)	0.1151	

Boldface font denotes statistical significance. ALT, alanine aminotransferase; AST, aspartate aminotransferase; GGT, gamma-glutamyl transpeptidase; HOMA-IR, homeostasis model assessment of insulin resistance; IGB, intragastric balloon.





**Fig. 3. Scatter plots.** (A) Change in ALT is positively correlated with basal ALT. (B) Change in GGT is positively correlated with basal GGT. ALT, alanine aminotransferase; GGT, gamma-glutamyl transpeptidase.

although our review included studies of both endoscopic and swallowable IGB, there were still a number of IGB types (such as ReShape Duo Balloon and Obalon Gastric Balloon) not mentioned in the current review due to the lack of relevant clinical research.<sup>14</sup> Second, at the time of the preliminary search, we found that most of the clinical studies in this field were of longitudinal observational design. Thus, when formal screening of the search was performed, we defined the patient at baseline, but not the sham-treated group, as comparators. However, this approach ignored the potential for spontaneous remission of the disease.<sup>44</sup> Despite these limitations, our systematic review provides the most comprehensive evaluation of the effect of IGB on the serum markers of MAFLD, with low intra-subgroup heterogeneity in stratified analysis, suggesting that the evidence is highly credible. More impressively, our observations demonstrate for the first time that age has an adverse effect on IGB treatment of insulin resistance.

### Conclusions and perspectives

IGB therapy has led to improvements in the serum markers of MAFLD, including HOMA-IR, ALT, AST, and GGT. Significant reductions in HOMA-IR and liver biochemical parameters were seen across different methods of balloon implantation and different age/BMI classes. The improvement of insulin resistance and liver biochemistries with swallowable IGB therapy was no worse than that with endoscopic IGB. Furthermore, greater insulin resistance amelioration with IGB therapy was predicted by younger age and the relevant mechanism needs further investigation. Although IGB has the potential to become a multidisciplinary management tool of MAFLD, it cannot be ignored that IGB is a temporary measure. If the patient cannot maintain an active lifestyle after the first balloon is removed, relapse of MAFLD is an expected result. In this regard, IGB combined with other pharmacotherapy or sequential IGB therapy could be a po-

tential solution, and further RCT is warranted.

### Funding

This study was supported by the National Key R&D Program of China (2017YFC0908903), National Natural Science Foundation of China (81873565, 81900507), Shanghai Leading Talent Plan 2017, Innovative Research Team of High-Level Local Universities in Shanghai, and Hospital Funded Clinical Research, Clinical Research Unit, Xinhua Hospital Affiliated to Shanghai Jiao Tong University School of Medicine (17CSK04).

### Conflict of interest

The authors have no conflict of interests related to this publication.

### Author contributions

Conception and design (JGF), funding acquisition and supervision (JGF, TYR), collection and assembly of data (ZYZ, JZ), data analysis and interpretation (ZYZ), manuscript writing (ZYZ, JZ, TYR, YWS, RXY, JGF), final approval of manuscript (ZYZ, JZ, TYR, YWS, RXY, JGF).

### Data sharing statement

No additional data are available.

### References

- [1] Sanyal AJ. Past, present and future perspectives in nonalcoholic fat-

- ty liver disease. *Nat Rev Gastroenterol Hepatol* 2019;16(6):377–386. doi:10.1038/s41575-019-0144-8.
- [2] Paik JM, Golabi P, Younossi Y, Mishra A, Younossi ZM. Changes in the global burden of chronic liver diseases from 2012 to 2017: the growing impact of NAFLD. *Hepatology* 2020; 72(5):1605–1616. doi:10.1002/hep.31173.
  - [3] Eslam M, Newsome PN, Sarin SK, Anstee QM, Targher G, Romero-Gomez M, *et al*. A new definition for metabolic dysfunction-associated fatty liver disease: an international expert consensus statement. *J Hepatol* 2020; 73(1):202–209. doi:10.1016/j.jhep.2020.03.039.
  - [4] Friedman SL, Neuschwander-Tetri BA, Rinella M, Sanyal AJ. Mechanisms of NAFLD development and therapeutic strategies. *Nat Med* 2018; 24(7):908–922. doi:10.1038/s41591-018-0104-9.
  - [5] Baldwin D, Chennakesavalu M, Gangemi A. Systematic review and meta-analysis of Roux-en-Y gastric bypass against laparoscopic sleeve gastrectomy for amelioration of NAFLD using four criteria. *Surg Obes Relat Dis* 2019; 15(12):2123–2130. doi:10.1016/j.soard.2019.09.060.
  - [6] Fakhry TK, Mhaskar R, Schmittalla T, Muradova E, Gonzalvo JP, Murr MM. Bariatric surgery improves nonalcoholic fatty liver disease: a contemporary systematic review and meta-analysis. *Surg Obes Relat Dis* 2019; 15(3):502–511. doi:10.1016/j.soard.2018.12.002.
  - [7] Lee Y, Doumouras AG, Yu J, Brar K, Banfield L, Gmora S, *et al*. Complete resolution of nonalcoholic fatty liver disease after bariatric surgery: a systematic review and meta-analysis. *Clin Gastroenterol Hepatol* 2019; 17(6):1040–1060.e11. doi:10.1016/j.cgh.2018.10.017.
  - [8] Martin M, Beekley A, Kjørstad R, Sebesta J. Socioeconomic disparities in eligibility and access to bariatric surgery: a national population-based analysis. *Surg Obes Relat Dis* 2010; 6(1):8–15. doi:10.1016/j.soard.2009.07.003.
  - [9] Penn L, Moffatt SM, White M. Participants' perspective on maintaining behaviour change: a qualitative study within the European Diabetes Prevention Study. *BMC Public Health* 2008; 8:235. doi:10.1186/1471-2458-8-235.
  - [10] Chalasani N, Younossi Z, Lavine JE, Charlton M, Cusi K, Rinella M, *et al*. The diagnosis and management of nonalcoholic fatty liver disease: practice guidance from the American Association for the Study of Liver Diseases. *Hepatology* 2018; 67(1):328–357. doi:10.1002/hep.29367.
  - [11] Abu Dayyeh BK, Bazerbachi F, Graupera I, Cardenas A. Endoscopic bariatric and metabolic therapies for non-alcoholic fatty liver disease. *J Hepatol* 2019; 71(6):1246–1248. doi:10.1016/j.jhep.2019.07.026.
  - [12] Salomone F, Sharaiha RZ, Boskoski I. Endoscopic bariatric and metabolic therapies for non-alcoholic fatty liver disease: evidence and perspectives. *Liver Int* 2020; 40(6):1262–1268. doi:10.1111/liv.14441.
  - [13] Abu Dayyeh BK, Edmundowicz S, Thompson CC. Clinical practice update: expert review on endoscopic bariatric therapies. *Gastroenterology* 2017; 152(4):716–729. doi:10.1053/j.gastro.2017.01.035.
  - [14] Bazerbachi F, Vargas EJ, Abu Dayyeh BK. Endoscopic bariatric therapy: a guide to the intragastric balloon. *Am J Gastroenterol* 2019; 114(9):1421–1431. doi:10.14309/ajg.0000000000000239.
  - [15] Frutos MD, Morales MD, Luján J, Hernández Q, Valero G, Parrilla P. Intra-gastric balloon reduces liver volume in super-obese patients, facilitating subsequent laparoscopic gastric bypass. *Obes Surg* 2007; 17(2):150–154. doi:10.1007/s11695-007-9040-3.
  - [16] Lewis MC, Phillips ML, Slavotinek JP, Kow L, Thompson CH, Tooouli J. Change in liver size and fat content after treatment with optifast very low calorie diet. *Obes Surg* 2006; 16(6):697–701. doi:10.1381/096089206777346682.
  - [17] Lee YM, Low HC, Lim LG, Dan YY, Aung MO, Cheng CL, *et al*. Intra-gastric balloon significantly improves nonalcoholic fatty liver disease activity score in obese patients with nonalcoholic steatohepatitis: a pilot study. *Gastrointest Endosc* 2012; 76(4):756–760. doi:10.1016/j.gie.2012.05.023.
  - [18] Page MJ, Moher D. Evaluations of the uptake and impact of the Preferred Reporting Items for Systematic reviews and Meta-Analyses (PRISMA) statement and extensions: a scoping review. *Syst Rev* 2017; 6(1):263. doi:10.1186/s13643-017-0663-8.
  - [19] Popov VB, Thompson CC, Kumar N, Ciarleglio MM, Deng Y, Laine L. Effect of intragastric balloons on liver enzymes: a systematic review and meta-analysis. *Dig Dis Sci* 2016; 61(9):2477–2487. doi:10.1007/s10620-016-4178-2.
  - [20] Stang A. Critical evaluation of the Newcastle-Ottawa scale for the assessment of the quality of nonrandomized studies in meta-analyses. *Eur J Epidemiol* 2010; 25(9):603–605. doi:10.1007/s10654-010-9491-z.
  - [21] Higgins JP, Altman DG, Gotzsche PC, Juni P, Moher D, Oxman AD, *et al*. The cochrane collaboration's tool for assessing risk of bias in randomised trials. *BMJ* 2011; 343:d5928. doi:10.1136/bmj.d5928.
  - [22] Egger M, Davey Smith G, Schneider M, Minder C. Bias in meta-analysis detected by a simple, graphical test. *BMJ* 1997; 315(7109):629–634. doi:10.1136/bmj.315.7109.629.
  - [23] Egger M, Smith GD, Phillips AN. Meta-analysis: principles and procedures. *BMJ* 1997; 315(7121):1533–1537. doi:10.1136/bmj.315.7121.1533.
  - [24] Higgins JP, Thompson SG, Deeks JJ, Altman DG. Measuring inconsistency in meta-analyses. *BMJ* 2003; 327(7414):557–560. doi:10.1136/bmj.327.7414.557.
  - [25] Ricci G, Bersani G, Rossi A, Pigò F, De Fabritiis G, Alvisi V. Bariatric therapy with intragastric balloon improves liver dysfunction and insulin resistance in obese patients. *Obes Surg* 2008; 18(11):1438–1442. doi:10.1007/s11695-008-9487-x.
  - [26] Donadio F, Sburlati LF, Masserini B, Lunati EM, Lattuada E, Zappa MA, *et al*. Metabolic parameters after BioEnterics intragastric balloon placement in obese patients. *J Endocrinol Invest* 2009; 32(2):165–168. doi:10.1007/BF03345708.
  - [27] Forlano R, Ippolito AM, Iacobellis A, Merla A, Valvano MR, Niro G, *et al*. Effect of the BioEnterics intragastric balloon on weight, insulin resistance, and liver steatosis in obese patients. *Gastrointest Endosc* 2010; 71(6):927–933. doi:10.1016/j.gie.2009.06.036.
  - [28] Nikolic M, Mirosevic G, Ljubcic N, Boban M, Supanc V, Nikolic BP, *et al*. Obesity treatment using a Bioenterics intragastric balloon (BiB)—preliminary Croatian results. *Obes Surg* 2011; 21(8):1305–1310. doi:10.1007/s11695-010-0101-7.
  - [29] Sekino Y, Imajo K, Sakai E, Uchiyama T, Iida H, Endo H, *et al*. Time-course of changes of visceral fat area, liver volume and liver fat area during intragastric balloon therapy in Japanese super-obese patients. *Intern Med* 2011; 50(21):2449–2455. doi:10.2169/internalmedicine.50.5672.
  - [30] Stimac D, Majanović SK, Turk T, Kezele B, Licul V, Orlić ZC. Intra-gastric balloon treatment for obesity: results of a large single center prospective study. *Obes Surg* 2011; 21(5):551–555. doi:10.1007/s11695-010-0310-0.
  - [31] Tai CM, Lin HY, Yen YC, Huang CK, Hsu WL, Huang YW, *et al*. Effectiveness of intragastric balloon treatment for obese patients: one-year follow-up after balloon removal. *Obes Surg* 2013; 23(12):2068–2074. doi:10.1007/s11695-013-1027-7.
  - [32] Folini L, Veronelli A, Benetti A, Pozzato C, Cappelletti M, Masci E, *et al*. Liver steatosis (LS) evaluated through chemical-shift magnetic resonance imaging liver enzymes in morbid obesity: effect of weight loss obtained with intragastric balloon gastric banding. *Acta Diabetol* 2014; 51(3):361–368. doi:10.1007/s00592-013-0516-4.
  - [33] Takihata M, Nakamura A, Aoki K, Kimura M, Sekino Y, Inamori M, *et al*. Comparison of intragastric balloon therapy and intensive lifestyle modification therapy with respect to weight reduction and abdominal fat distribution in super-obese Japanese patients. *Obes Res Clin Pract* 2014; 8(4):e331–338. doi:10.1016/j.orcp.2013.07.002.
  - [34] Raftopoulos I, Giannakou A. The Elipse Balloon, a swallowable gastric balloon for weight loss not requiring sedation, anesthesia or endoscopy: a pilot study with 12-month outcomes. *Surg Obes Relat Dis* 2017; 13(7):1174–1182. doi:10.1016/j.soard.2017.02.016.
  - [35] Genco A, Ernesti I, Ienca R, Casella G, Mariani S, Francomano D, *et al*. Safety and efficacy of a new swallowable intragastric balloon not needing endoscopy: early Italian experience. *Obes Surg* 2018; 28(2):405–409. doi:10.1007/s11695-017-2877-1.
  - [36] Guedes MR, Fittipaldi-Fernandez RJ, Diestel CF, Klein MRST. Impact of intragastric balloon treatment on adipokines, cytokines, and metabolic profile in obese individuals. *Obes Surg* 2019; 29(8):2600–2608. doi:10.1007/s11695-019-03891-8.
  - [37] Bazerbachi F, Vargas EJ, Rizk M, Maselli DB, Mounajjed T, Venkatesh SK, *et al*. Intra-gastric balloon placement induces significant metabolic and histologic improvement in patients with nonalcoholic steatohepatitis. *Clin Gastroenterol Hepatol* 2021; 19(1):146–154.e4. doi:10.1016/j.cgh.2020.04.068.
  - [38] Maekawa S, Niizawa M, Harada M. A comparison of the weight loss effect between a low-carbohydrate diet and a calorie-restricted diet in combination with intragastric balloon therapy. *Intern Med* 2020; 59(9):1133–1139. doi:10.2169/internalmedicine.4153-19.
  - [39] Laing P, Pham T, Taylor LJ, Fang J. Filling the void: a review of intragastric balloons for obesity. *Dig Dis Sci* 2017; 62(6):1399–1408. doi:10.1007/s10620-017-4566-2.
  - [40] Eslam M, Sarin SK, Wong VW, Fan JG, Kawaguchi T, Ahn SH, *et al*. The Asian Pacific Association for the Study of the Liver clinical practice guidelines for the diagnosis and management of metabolic associated fatty liver disease. *Hepatol Int* 2020; 14(6):889–919. doi:10.1007/s12072-020-10094-2.
  - [41] Diab AF, Abdurassul EM, Diab FH. The effect of age, gender, and baseline BMI on weight loss outcomes in obese patients undergoing intragastric balloon therapy. *Obes Surg* 2019; 29(11):3542–3546. doi:10.1007/s11695-019-04023-y.
  - [42] Swift DL, Johannsen NM, Lavie CJ, Earnest CP, Blair SN, Church TS. Effects of clinically significant weight loss with exercise training on insulin resistance and cardiometabolic adaptations. *Obesity (Silver Spring)* 2016; 24(4):812–819. doi:10.1002/oby.21404.
  - [43] Gong Z, Tas E, Yakar S, Muzumdar R. Hepatic lipid metabolism and non-alcoholic fatty liver disease in aging. *Mol Cell Endocrinol* 2017; 455:115–130. doi:10.1016/j.mce.2016.12.022.
  - [44] Han MAT, Altayar O, Hamdeh S, Takyar V, Rotman Y, Etzion O, *et al*. Rates of and factors associated with placebo response in trials of pharmacotherapies for nonalcoholic steatohepatitis: systematic review and meta-analysis. *Clin Gastroenterol Hepatol* 2019; 17(4):616–629.e26. doi:10.1016/j.cgh.2018.06.011.



Original Article

# Roles of SET7/9 and LSD1 in the Pathogenesis of Arsenic-induced Hepatocyte Apoptosis

Bing Han<sup>1,2#</sup>, Yi Yang<sup>1,2#</sup>, Lei Tang<sup>3#</sup>, Qin Yang<sup>1,2</sup> and Rujia Xie<sup>1,2\*</sup>

<sup>1</sup>Department of Pathophysiology, College of Basic Medical Sciences, Guizhou Medical University, Guiyang, Guizhou, China;

<sup>2</sup>Guizhou Provincial Key Laboratory of Pathogenesis and Drug Research on Common Chronic Diseases, Guizhou Medical University, Guiyang, Guizhou, China; <sup>3</sup>Medical College of Guizhou University, Guiyang, Guizhou, China

Received: 28 December 2020 | Revised: 22 February 2021 | Accepted: 11 March 2021 | Published: 16 April 2021

## Abstract

**Background and Aims:** Multiple regulatory mechanisms play an important role in arsenic-induced liver injury. To investigate whether histone H3 lysine 4 (H3K4) methyltransferase (SET7/9) and histone H3K4 demethyltransferase (LSD1/KDM1A) can regulate endoplasmic reticulum stress (ERS)-related apoptosis by modulating the changes of H3K4 methylations in liver cells treated with arsenic. **Methods:** Apoptosis, proliferation and cell cycles were quantified by flow cytometry and real-time cell analyzer. The expression of ERS- and epigenetic-related proteins was detected by Western blot analysis. The antisense SET7/9 expression vector and the overexpressed LSD1 plasmid were used for transient transfection of LO2 cells. The effects of NaAsO<sub>2</sub> on the methylation of H3 in the promoter regions of 78 kDa glucose-regulated protein, activating transcription factor 4 and C/EBP-homologous protein were evaluated by chromatin immunoprecipitation assay. **Results:** The protein expression of LSD1 (1.25±0.08 vs. 1.77±0.08, *p*=0.02) was markedly decreased by treatment with 100 μM NaAsO<sub>2</sub>, whereas the SET7/9 (0.68±0.05 vs. 1.10±0.13, *p*=0.002) expression level was notably increased, which resulted in increased H3K4me1/2 (0.93±0.64, 1.19±0.22 vs. 0.71±0.13, 0.84±0.13, *p*=0.03 and *p*=0.003). After silencing SET7/9 and overexpressing LSD1 by transfection, apoptosis rate (in percentage: 3.26±0.34 vs. 7.04±0.42, 4.80±0.32 vs. 7.52±0.38, *p*=0.004 and *p*=0.02) was significantly decreased and proliferation rate was notably increased, which is reversed after inhibiting LSD1 (in percentage: 9.31±0.40 vs. 7.52±0.38, *p*=0.03). Furthermore, the methylation levels of H3 in the promoter regions of GRP78 (20.80±2.40 vs. 11.75±2.47, 20.46±2.23 vs. 14.37±0.91, *p*=0.03 and *p*=0.01) and CHOP (48.67±4.04

vs. 16.67±7.02, 59.33±4.51 vs. 20.67±3.06, *p*=0.004 and *p*=0.001) were significantly increased in LO<sub>2</sub> cells exposed to 100 μM NaAsO<sub>2</sub> for 24 h. **Conclusions:** Histone methyltransferase SET7/9 and histone demethyltransferase LSD1 jointly regulate the changes of H3K4me1/me2 levels in arsenic-induced apoptosis. NaAsO<sub>2</sub> induces apoptosis in LO2 cells by activating the ERS-mediated apoptotic signaling pathway, at least partially by enhancing the methylation of H3 on the promoter regions of ERS-associated genes, including GRP78 and CHOP.

**Citation of this article:** Han B, Yang Y, Tang L, Xie R, Yang Q. Roles of SET7/9 and LSD1 in the pathogenesis of arsenic-induced hepatocyte apoptosis. J Clin Transl Hepatol 2021;9(3):364–372. doi: 10.14218/JCTH.2020.00185.

## Introduction

Arsenic is a non-metal element, widely distributed in soil, water, minerals and plants in nature; and long-term exposure to a high-arsenic environment can cause arsenic poisoning in the organism.<sup>1–3</sup> A large number of epidemiological investigations and animal experiments have shown that arsenic poisoning can cause liver damage, and even lead to cirrhosis and liver cancer, which has become the main cause of death in patients with arsenic poisoning.<sup>4,5</sup> Therefore, there is an urgent need to identify novel therapeutic targets and to develop effective strategies for liver damage therapy. At present, studies on the mechanism of liver injury caused by arsenic poisoning mainly focus on oxidative stress,<sup>6</sup> influence on enzyme activity,<sup>7</sup> DNA damage, DNA methylation,<sup>8</sup> and apoptosis.<sup>9,10</sup> Observations of involvement of many various mechanisms indicate that arsenic-induced hepatocyte apoptosis is one of the core events.<sup>11,12</sup>

Arsenic can upregulate the expression levels of Fas and Fas ligand (i.e. FasL) in liver cells, and increase the apoptosis of cells through the death receptor pathway, causing liver damage.<sup>13,14</sup> Some scholars have found that arsenic can increase the expression levels of Bax and p53 proteins and induce hepatocyte apoptosis through a mitochondrial pathway.<sup>15,16</sup> While the endoplasmic reticulum (ER) is physiologically responsible for the control of proper protein folding and function, many factors such as the unfolded protein response, ER overload response and others, can disturb ER function, leading to ER stress (ERS). Apoptosis induced by ERS is a newly-discovered apoptosis pathway

**Keywords:** Arsenic; SET7/9; LSD1; H3K4me1/2; ER stress.

**Abbreviations:** AI, artificial intelligence; ATF4, activating transcription factor 4; ChIP, chromatin immunoprecipitation assay; CHOP, C/EBP-homologous protein; EDTA, ethylene diamine tetraacetic acid; ER, endoplasmic reticulum; ERS, endoplasmic reticulum stress; GRP78, 78 kDa glucose-regulated protein; H3K4, histone 3 lysine 4; LSD1/KDM1A, histone 3 lysine 4 demethyltransferase; me, methylation; PBS, phosphate-buffered saline; PERK, PRKR-like endoplasmic reticulum kinase; RTCA, real-time cell analyzer; RUCAM, Roussel Uclaf causality assessment method; SET7/9, histone 3 lysine 4 methyltransferase; shRNA, small hairpin; siRNA, small interfering RNA.

#These authors contributed equally to this study.

\*Correspondence to: Rujia Xie, Department of Pathophysiology, College of Basic Medical Sciences, Guizhou Medical University, Guiyang, Guizhou 550000, China. ORCID: <https://orcid.org/0000-0001-5991-2678>. Tel: +86-13985441220, E-mail: 592153968@qq.com

following the death receptor pathway and the mitochondrial pathway.<sup>17,18</sup> Previous studies have also demonstrated ERS-mediated hepatocyte apoptosis in rats.<sup>19</sup> Further study found the PRKR-like endoplasmic reticulum kinase (PERK) signaling pathway were activated in arsenic-mediated liver cells.<sup>20</sup>

However, how the PERK signaling pathway is activated has not been deeply researched. In recent years, epigenetics has gradually become a research hotspot. Epigenetics is a branch of genetics that studies the heritable changes in gene expression without changes in nucleotide sequence. Some scholars have found that the expression levels of 78 kDa glucose-regulated protein (GRP78), histone 3 lysine 4 methyltransferase (SET7/9) and histone 3 lysine 4 (H3K4) me2 are significantly increased in the renal tissues of diabetic nephrotic mice,<sup>21</sup> suggesting that epigenetic histone modification may be associated with ERS. SET/9 specifically monomethylates the fourth lysine of histone 3 (i.e. H3K4) in multiple modifiable sites of histones.<sup>22,23</sup> Studies have shown that sodium arsenite can upregulate the level of dimethyl and methyl modification of H3K4 by downregulating the expression level of LSD1, which can open or increase the transcription of some genes.<sup>24</sup> Lysine-specific histone demethylase 1 (LSD1, also known as KDM1A), is a member of the amine oxidase family and a member of the demethylase family. LSD1 serves as a demethylase that specifically removes dimethyl and methyl modifications of H3K4 *in vitro*.

Based on the above research background, this experiment was designed to investigate whether SET7/9 and LSD1/KDM1A can regulate ERS-related apoptosis by modulating the changes of H3K4 methylations in liver cells treated with arsenic.

## Methods

### Cells and reagents

Human normal hepatocyte LO2 cells were obtained from the Shanghai Cell Bank of Chinese Academy of Sciences (China) and sodium arsenite was obtained from Shandong Xiya Reagent Chemical Industry (China). Fetal bovine serum, Dulbecco's modified Eagle's medium (GIBCO, New York, NY, USA), antibodies against GRP78, C/EBP-homologous protein (CHOP), LSD1, H3 and H3K4me1 (Abcam, Cambridge, UK), antibodies against H3K4me2 (Active Motif, Carlsbad, CA, USA), GAPDH (Bioprimacy Biotechnology, Wuhan, China), secondary antibodies (Boster Biological Engineering, Wuhan, China), SET7/9-specific small interfering RNAs (siRNAs) were purchased from Shanghai Jima Gene (China), negative small hairpin (sh)RNA and LSD1 overexpressed plasmids were obtained from Shanghai Jima Gene. OG-LO02, an effective and selective LSD1 inhibitor, was obtained from Selleck Chemicals Company (Houston, USA). The chromatin immunoprecipitation assay (ChIP) kit and Lipofectamine 2000 were procured from Thermo Fisher Scientific (Waltham, MA, USA). The cell cycle and apoptosis detection kit were purchased from Bormai Biotechnology (Beijing, China)

### Real-time cellular analysis

Cell proliferation was monitored using an xCELLigence Real-Time Cell Analysis instrument (xCELLigence DP System; ACEA Biosciences, Inc., San Diego, CA, USA), which can continuously monitor live cell proliferation, morphology and viability with a label-free assay. A 100  $\mu$ L aliquot of LO2 sus-

pended droplets were added to an E-Plate, including 10,000 cells, which was placed at 37°C in a humidified incubator containing 5% CO<sub>2</sub> for 6–8 h. After LO2 cells adhered to the plate, arsenic was added at 100  $\mu$ M,<sup>20</sup> and we performed continuous monitoring of the cell growth and proliferation process for 36 to 48 h.

### Western blot

Taking out each cell culture, and adding "protein lysis solution" and protease inhibitors at a ratio of 99:1, each cell suspension was collected into a 1.5 mL centrifuge tube after lysing on the ice for 10 m; then, the 1.5 mL centrifuge tubes were centrifuged at 4°C and 12,000 r/m for 20 m. After precipitating, collecting the supernatant, and transferring the proteins to PVDF membranes, non-specific binding was blocked with 5% non-fat dry milk in Tris-buffered saline with Tween-20, and the membranes were probed overnight at 4°C with primary antibodies against GRP78 (1:1,500), CHOP (1:1,500), GAPDH (1:1,000), H3 (1:1,000), H3K4me1 (1:1,000), and H3K4me2 (1:1,000). The bound antibodies were detected with horseradish peroxidase-conjugated secondary antibodies and visualized using enhanced chemiluminescence reagents. The signal intensity was measured using Bio-Rad imaging system (Hercules, CA, USA) and analyzed by Quantity One software (Bio-Rad).

### Apoptosis assay

Cells were digested with 0.25% trypsin without ethylene diamine tetraacetic acid (commonly referred to as EDTA) and washed with phosphate-buffered saline (PBS) 2–3 times; then, suspension liquids were collected into 10 mL centrifuge tubes. After centrifugation at 1,500 r/m for 5 m, 500  $\mu$ L of binding buffer was added into tubes and resuspended. Annexin V-FITC (5  $\mu$ L) and propidium iodide staining solution (5  $\mu$ L) were added for a 5–15 m incubation.

### Cell cycle assay

After the supernatant of each group was discarded and washed with PBS for 2–3 times, the cells of each group were digested with trypsin, free of EDTA, and the cell suspension was collected. The supernatant was discarded after centrifugation at 2,000 r/m for 5 m, and then washed with PBS to repeat the above steps. After the supernatant of the centrifuged tube was discarded, 250  $\mu$ L PBS was added for resuspending, and 750  $\mu$ L precooled anhydrous ethanol was added to each group to make the final concentration of ethanol 75%; after resuspension, the cells were incubated overnight at 4°C. On the second day, the cell suspensions of each group were centrifuged at 2,000 r/m for 5 m, and the supernatant was discarded. Then, the supernatant was processed with PBS in the same way. After the supernatant was discarded, the mixture of 500  $\mu$ L was configured for each group in the proportion of RNase: Propidium Iodide=1:9.

### ChIP-qPCR

LO2 cells (1  $\times$  10<sup>6</sup>) were seeded onto 10-cm diameter dishes and were mock-treated with PBS (0  $\mu$ M/L NaAsO<sub>2</sub>) or 100  $\mu$ M/L NaAsO<sub>2</sub> for 24 h. After treatment, ChIP kit (purchased from Thermo Fisher Scientific) was used to perform



**Table 1.** DNA sequences of primers used for reverse transcription- and ChIP-quantitative PCR

Gene	Forward, 5'–3'	Reverse, 5'–3'
GRP78	GGGATGGAGGAAGGGAGAAC	GAGGCATTCCGCTGTAAC
ATF4	GGTGGGTTCCATGGTCAAAT	AACACATCCACCACTGC
CHOP	CACGACCTCAGCCTGTCAAG	ACTGGAGTGGTGTGGCAATG

a ChIP assay. According to the manufacturer's instructions, LO2 cells were cross-linked with 16% formaldehyde, and 1× glycine was added to terminate the cross-linking. The cells were lysed with 2 µL cell nuclease (ChIP grade) lysis buffer and the lysates were ultrasound-crushed to a length of 150–1,000 bp. Immunoprecipitation was performed at 4°C for overnight using magnetic beads A/G and the following antibodies: rabbit IgG (1:10), anti-RNA polymerase II (1:10), anti-H3K4me1 (1:10), and anti-H3K4me2 (1:10). The immunoprecipitates were washed and eluted using magnetic scaffolding (purchased from Thermo Fisher Scientific). Immunoprecipitated DNA was recovered by reverse cross-linking, then purified and dissolved in distilled water. The corresponding sample without any antibody added served as input control. Objective DNA and input DNA were analyzed by reverse transcription-qPCR. The abundance of immunoprecipitated target DNA was expressed as the percentage of input chromatin DNA. The primer sequences of the target genes GRP78, activating transcription factor 4 (ATF4), and CHOP are listed in Table 1.

### Statistical analysis

SPSS 20.0 statistical software was used for analysis. Data were expressed as the mean±standard deviation. The one-way analysis of variance method was used for the multivariate comparison, and the least significant difference method was used as a post hoc test. A *p*-value of <0.05 was considered to indicate a statistically significant difference.

### Results

#### Arsenic significantly upregulates ERS-related proteins and H3K4me1/me2 in L02 cells

Compared with control group, the levels of SET7/9,<sup>20</sup> CHOP and H3K4me1 were significantly increased (Fig. 1B and Fig. 2B), whereas the level of LSD1 was obviously decreased

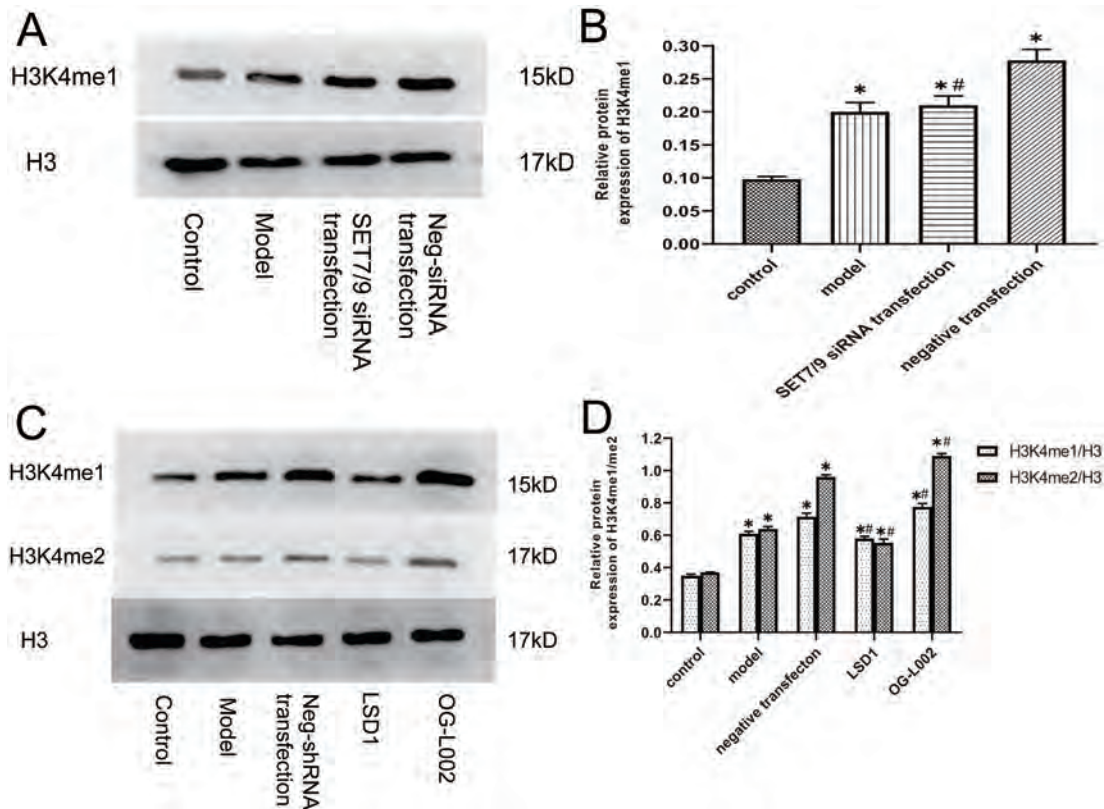


**Fig. 1.** Effect of arsenic on H3K4 methylation in L02 hepatocytes. Cells were exposed to arsenic at 100 µmol/L for 24 h. Proteins, prepared from whole cell extracts, were analyzed by western blotting. The activities of H3K4me1/me2 were determined with respective specific antibodies. (A) SET7/9 protein knock-down efficiency. H3K4me1 expression was measured in control, model and SET7/9 knock-down L02 cells. (B) Data shown are mean±standard deviation of three independent experiments, \**p*<0.05 vs. control group; #*p*<0.05 vs. negative transfection group. (C) LSD1 protein knock-down and overexpression efficiency. H3K4me1/me2 expression was measured in control, model and LSD1 knock-down and OG-L002 group of L02 cells. (D) Data shown are mean±standard deviation of three independent experiments, \**p*<0.05 vs. control group; #*p*<0.05 vs. negative transfection group.

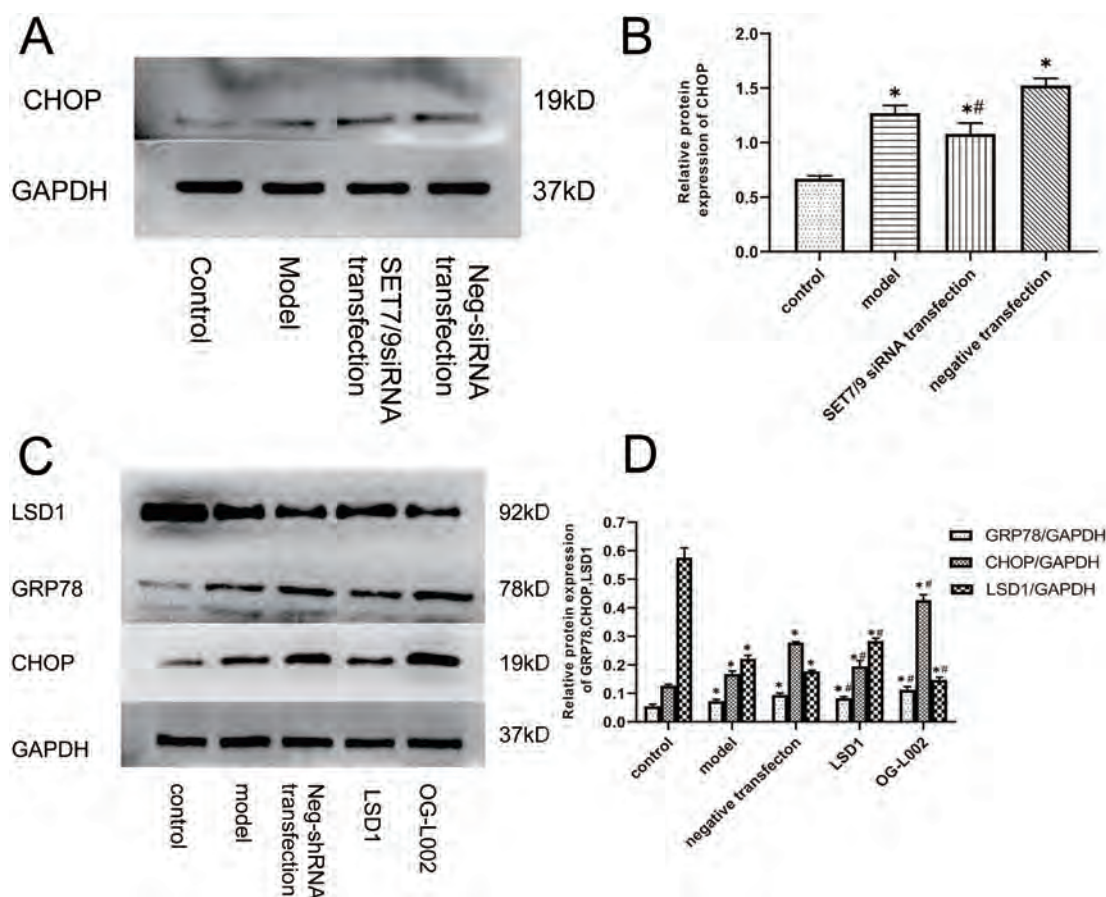


**Fig. 2. Effect of arsenic on ERS-related proteins in L02 hepatocytes.** Cells were exposed to arsenic at 100  $\mu\text{mol/L}$  for 24 h. Proteins, prepared from whole cell extracts, were analyzed by western blotting. The activities of GRP78, CHOP, and LSD1 were determined with respective specific antibodies. (A) SET7/9 protein knock-down efficiency. CHOP expression was measured in control, model and SET7/9 knock-down in L02 cells. (B) Data shown are mean  $\pm$  standard deviation of three independent experiments, \* $p < 0.05$  vs. control group; # $p < 0.05$  vs. negative transfection group. (C) LSD1 protein knock-down and overexpression efficiency. GRP78, CHOP, and LSD1 expression was measured in control, model and LSD1 knock-down and OG-L002 group of L02 cells. (D) Data shown are mean  $\pm$  standard deviation of three independent experiments, \* $p < 0.05$  vs. control group; # $p < 0.05$  vs. negative transfection group.

in the model group (Fig. 2D). Compared with the negative siRNA transfection group, the expression levels of GRP78, CHOP, and H3K4me1 in the SET7/9 siRNA transfection group (Fig. 1B and Fig. 2B) were significantly decreased.

Compared with the negative shRNA transfection group, the expression levels of GRP78, CHOP, H3K4me1, and H3K4me2 were significantly decreased in the LSD1 group (Fig. 1D and Fig. 2D); the expression levels of GRP78, CHOP, H3K4me1 and H3K4me2 were notably increased in the OG-L002 group (Fig. 1D and Fig. 2D).

#### **SET7/9 and LSD1 induce changes in apoptosis and cell cycle in L02 hepatocytes treated with arsenic**

Flow cytometry showed that the apoptosis rate and the proportion of G1 phase cells were significantly increased in the model group compared with the control group. Compared with the negative transfection group, the apoptosis rate and the proportion of G1 phase cells were notably decreased in the SET7/9 siRNA transfection group and the LSD1 overexpression group, while the apoptosis rate and the proportion of G1 phase cells were obviously increased in the OG-L002 group [Fig. 3A(f)]. These results indicate that arsenic could promote apoptosis and increase the proportion of G1 phase

cells, and histone modifying enzyme of SET7/9 and LSD1 could regulate apoptosis and cycle in arsenic-induced L02 cells [Fig. 3B(b) and 3C(b)]. The apoptotic data on SET7/9 has been published.<sup>20</sup>

#### **SET7/9 and LSD1 mediate proliferation changes in arsenic-induced L02 hepatocytes**

Real-time cellular analysis showed that the proliferation was significantly decreased in the model group compared with the control group. The proliferation rate was notably increased in the SET7/9 siRNA transfection group and in the LSD1 overexpression group compared with the negative transfection group, while the proliferation was obviously decreased in the OG-L002 group (Fig. 4B and 4D). These results illustrate that the histone modifying enzymes of SET7/9 and LSD1 could regulate proliferation in L02 cells.

#### **Arsenic treatment enhances the methylation level of histone H3 in the promoter regions of the GRP78 and CHOP genes in L02 hepatocytes**

In order to confirm whether the regulation of transcription



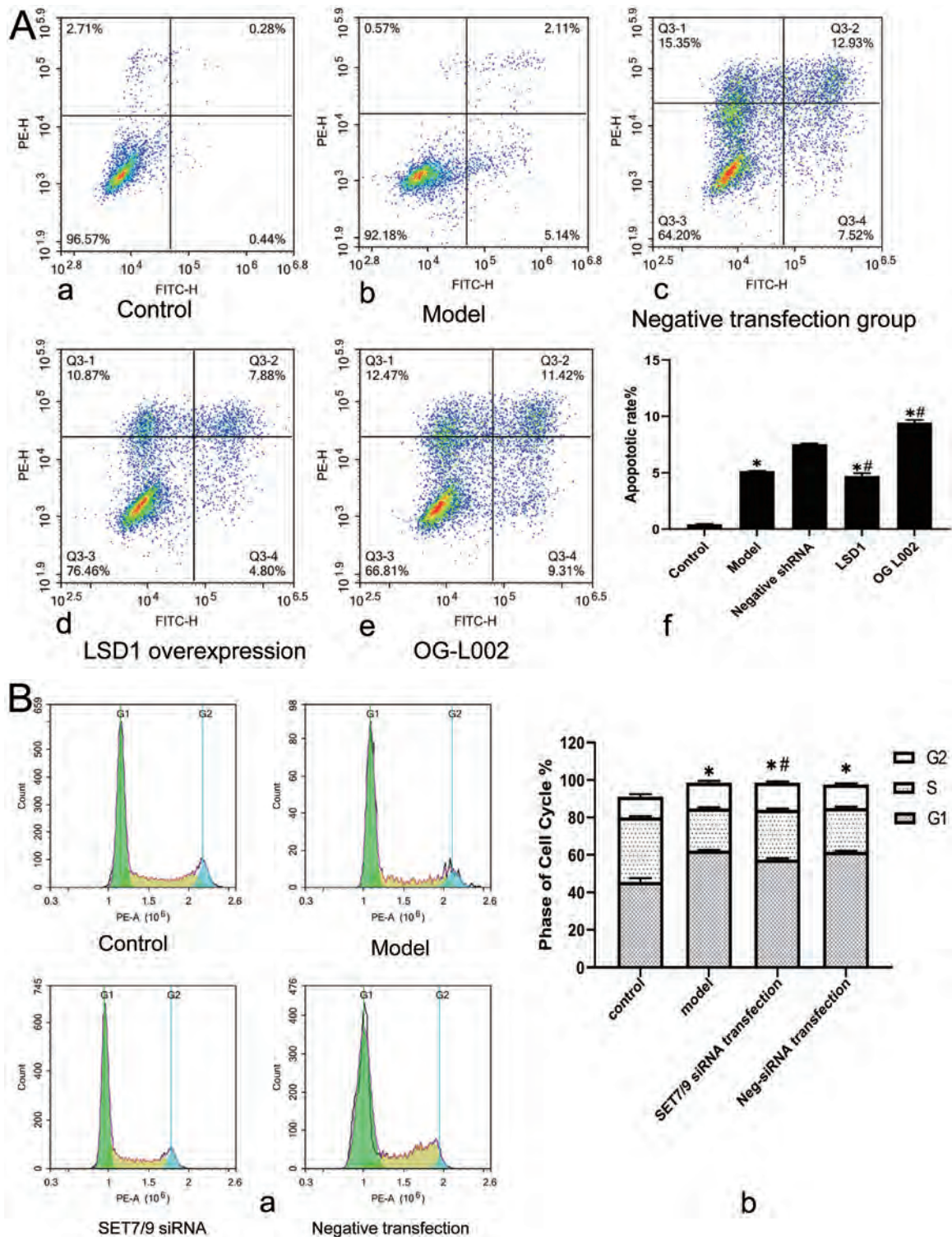
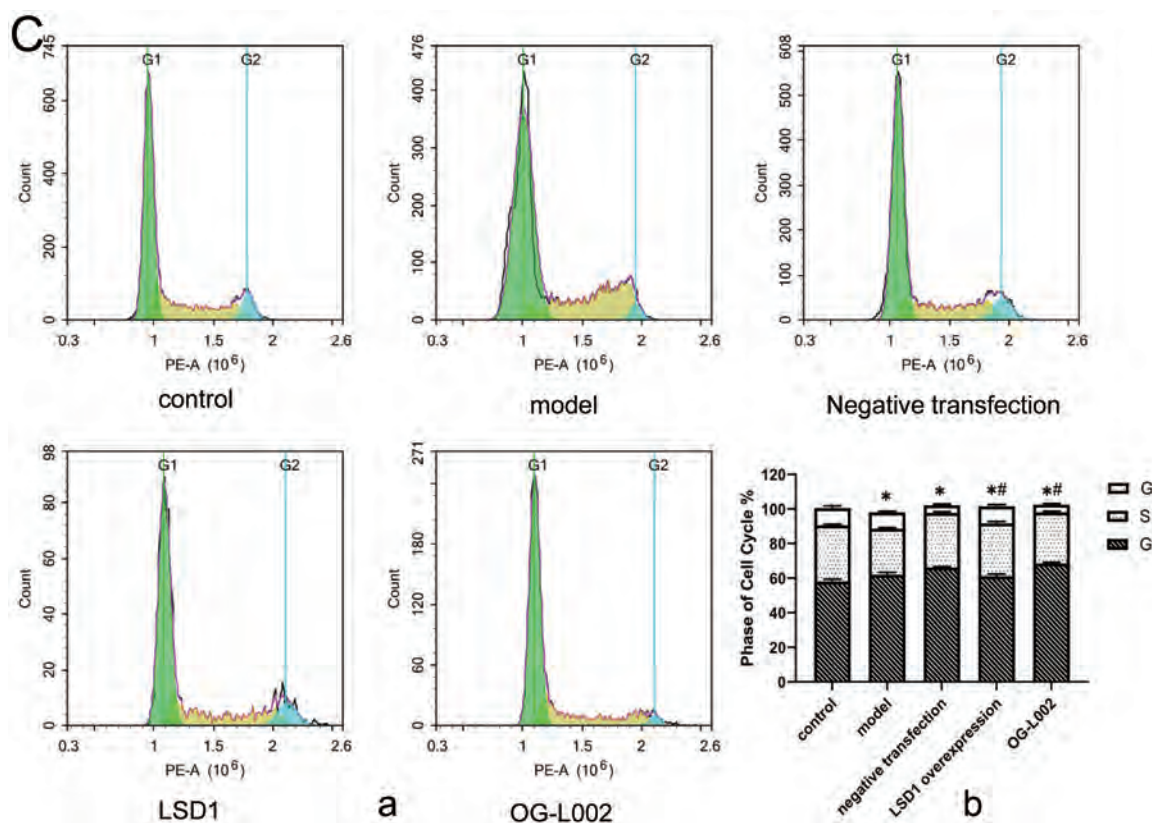


**Fig. 3. Effect of arsenic on apoptosis and cycles in L02 hepatocytes.** (A) The changes of apoptosis in the L02 cells of different groups were analyzed by flow cytometry. LSD1 protein knock-down and overexpression efficiency. Apoptosis was measured in control, model and LSD1 knock-down and OG-L002 group of L02 cells. (a: control; b: model; c: negative transfection; d: LSD1 overexpression group; e: OG L002; f: the apoptosis rate of different groups) Data shown are mean±standard deviation of three independent experiments, \* $p < 0.05$  vs. control group; # $p < 0.05$  vs. negative transfection group. (B) The cell cycle distribution of each group. SET7/9 protein knock-down efficiency. Cell cycles were assessed in control, model and SET7/9 knock-down of L02 cells. (a: cycles diagram for each group; f: the cycles of different groups) Data shown are mean±standard deviation of three independent experiments, \* $p < 0.05$  vs. control group; # $p < 0.05$  vs. negative transfection group. (C) The cell cycle distribution of each group. Cycles were assessed in control, model and LSD1 knock-down and OG-L002 group of L02 cells. (a: cycles diagram for each group; f: the cycles of different groups) Data shown are mean±standard deviation of three independent experiments, \* $p < 0.05$  vs. control group; # $p < 0.05$  vs. negative transfection group.

Fig. 3. (continued)



of GRP78, ATF4 and CHOP genes by arsenic is mediated by the upregulation of H3K4me1/me2, ChIP was performed. Following treatment with arsenic, the L02 cells were lysed and immunoprecipitated with specific anti-H3K4me1/me2 antibody. qPCR results demonstrated a significant increase in the H3K4me1/me2-associated promoter regions of the GRP78 and CHOP genes in L02 cells treated with 100  $\mu$ M NaAsO<sub>2</sub> (Fig. 5A and 5C), while the promoter region of ATF4 did not show a significant increase in H3K4me1/me2 (Fig. 5B). These results confirmed that arsenic induces the expression of ERS-associated molecules by increasing their transcription, at least partially through enhancing the methylation of histone H3 in the promoter regions of these genes.

## Discussion

Arsenic can cause injury to many organs of the body,<sup>25</sup> among which liver injury has always been the focus.<sup>26,27</sup> In addition to endemic arsenic poisoning, medicine-induced arsenic poisoning also occurs.<sup>28</sup> Since ancient times, raw plants as well as refined plant products have been in common use, including as traditional Chinese medicine, Ayurveda in India, Kampo in Japan, traditional Korean medicine, and Unani in old Greece, all of which have well known associations with increased risk of liver damage.<sup>29</sup> In many countries, rice grains and complementary medicines are important sources of arsenic consumption.<sup>30</sup> Ayurvedic is an arsenic-containing compound, which is currently in use in India to control blood counts of patients with hematological malignancies.<sup>31</sup> Long-term use of the Ayurvedic drug can also cause liver damage.<sup>32</sup>

The Roussel Uclaf Causality Assessment Method (com-

monly known as RUCAM) is the best way to assess cause and effect in liver damage caused by arsenic poisoning from herbs and drugs. RUCAM, in its original version (published in 1993)<sup>33</sup> and its updated version (from 2016),<sup>34</sup> represents sophisticated diagnostic algorithms based on principles of artificial intelligence (commonly referred to as AI), as outlined in a recent editorial.<sup>35</sup>

At present, a clinical study of arsenic detoxification *in vivo* is under way. The arsenic detoxification treatment with dimercaptopropanol and sodium dimercaptopropanesulfonate has not achieved the expected efficacy in patients. The antagonistic effect of selenium on arsenic, the antioxidant effect of superoxide dismutase on patients with arsenic poisoning and the protective effect on liver, lung, kidney, heart and other organs have been widely reported in treatment studies. Guizhou province reports of Chinese herbal medicine preparation for the treatment of chronic arsenic poisoning causing liver damage, such as Lu *et al.*<sup>36</sup> showing that whether by clinical manifestations or through the preparation before and after the organizational structure of the liver samples of vivisection, compound preparation of the Chinese herbal medicine HanDan diisopropylamine dichloroacetate liver damage caused by arsenic poisoning still produces obvious curative effect. Yun *et al.*<sup>37</sup> used ginkgo biloba leaves to treat 84 cases of chronic arsenic poisoning caused by coal burning, with anti-liver fibrosis intent. Serology and pathological histology observations indicated that the serum platelet activation factor (an important factor involved in liver injury and fibrosis) and four liver fibrosis indexes in the treatment group were significantly decreased ( $p < 0.01$ ), and the liver pathology was also improved to a certain extent in the treatment group, which was statistically significant when compared with the non-ginkgo biloba control group ( $p > 0.01$ ).



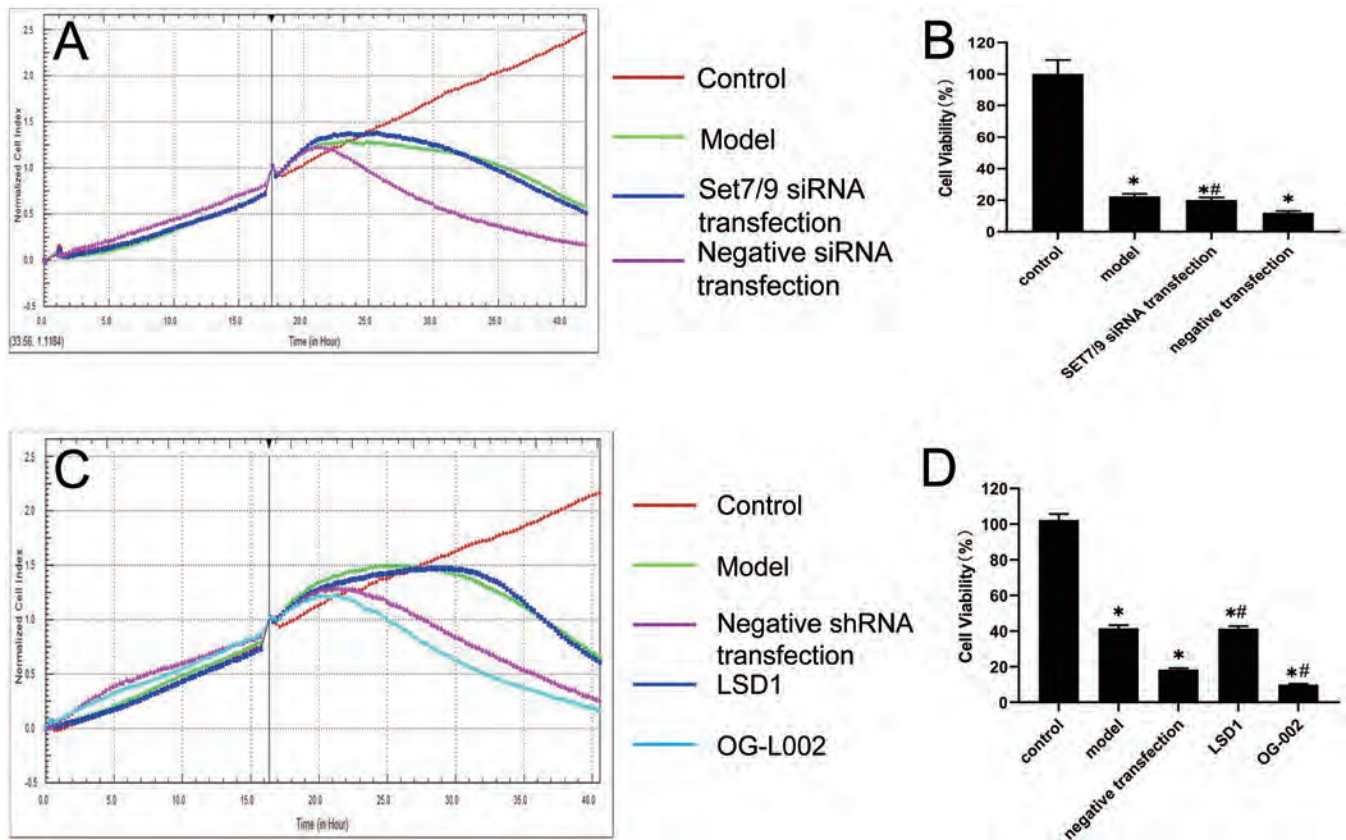


**Fig. 4. Effect of arsenic on growth in L02 hepatocytes.** (A) Real-time cellular analysis was employed to detect the SET7/9 protein knock-down efficiency. Proliferation was measured in control, model and SET7/9 knock-down of L02 cells. (B) The proliferation rate in control, model and SET7/9 knock-down. Data shown are mean±standard deviation of three independent experiments, \* $p<0.05$  vs. control group; # $p<0.05$  vs. negative transfection group. (C) Real-time cellular analysis was employed to detect the LSD1 protein knock-down and overexpression efficiency. D: The proliferation rate was measured in control, model and LSD1 knock-down and overexpression LSD1 group. Data shown are mean±standard deviation of three independent experiments, \* $p<0.05$  vs. control group; # $p<0.05$  vs. negative transfection group.

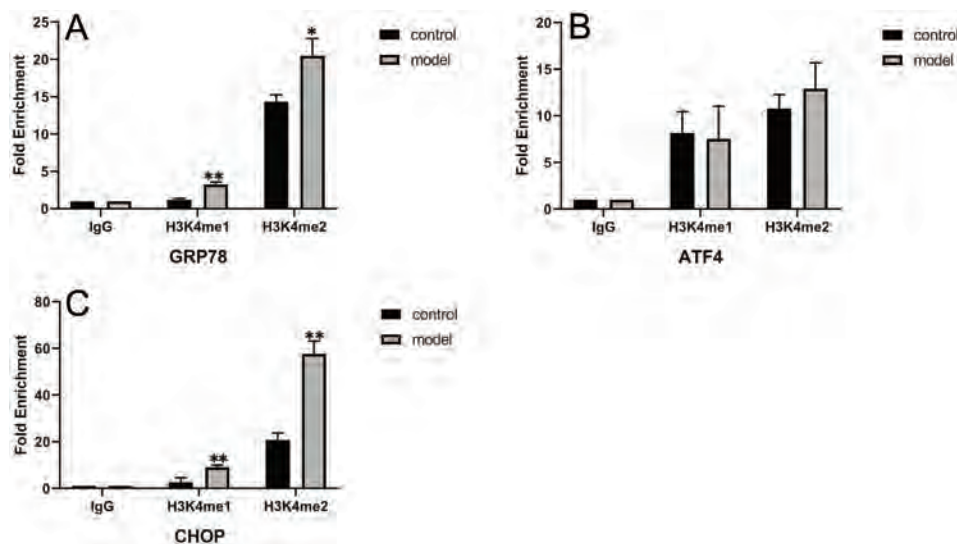


**Fig. 5. Effect of H3K4me1 and H3K4me2 on GRP78, ATF4, and CHOP promoter activity in L02 hepatocytes.** (A) Changes in enrichment of H3K4me1 and H3K4me2 in the GRP78 promoter region. Data shown are mean±standard deviation of three independent experiments; \* $p<0.05$  vs. control group, \*\* $p<0.01$  vs. control group. (B) Changes of the enrichment of H3K4me1 and H3K4me2 in the ATF4 promoter region. Data shown are mean±standard deviation of three independent experiments; \* $p<0.05$  vs. control group, \*\* $p<0.01$  vs. control group. (C) Changes of the enrichment of H3K4me1 and H3K4me2 in the CHOP promoter region. Data shown are mean±standard deviation of three independent experiments; \* $p<0.05$  vs. control group, \*\* $p<0.01$  vs. control group.

Our studies have shown that arsenic can regulate the changes of H3K4me1/me2 level by regulating histone methyltransferase SET7/9 and histone demethyltransferase LSD1 in the process of arsenic-induced hepatocyte apoptosis. Histone H3K4me1/me2 is involved in the activation of ERS-related proteins of GRP78 and CHOP during the process of arsenic-induced hepatocyte apoptosis. This provides a theoretical basis for further elucidating the pathogenesis of arsenic-induced liver injury.

## Acknowledgments

We thank Leng Liang for technical advice in using flow cytometry and microscopy (Basic Medical Science Research Center of Guizhou Medical University). We would like to thank Liu Li for her comments on this manuscript.

## Funding

The present study was supported by the National Natural Science Foundation of China (Grant No. 81100284), Guizhou Science and Technology Cooperation Platform Personnel [2018] (Grant No. 5779-10,5779-19), and Science and Technology Foundation of Guizhou Province (Grant No. ZK [2021]-364).

## Conflict of interest

The authors have no conflict of interests related to this publication.

## Author contributions

Study concept and design (BH), acquisition of data (YY, LT), analysis and interpretation of data (YY, LT), drafting of the manuscript (YY), critical revision of the manuscript for important intellectual content (BH), administrative, technical, or material support, study supervision (BH, QY, RX).

## Data sharing statement

All data are available upon request.

## References

- [1] Kumar R, Mukherji MD, Chakraborty S, Mukherji R. A review on a heavy metal (arsenic) contamination in ground water, soil and translocation in plants. *Indian Journal of Environmental Protection* 2018; 38(7):591–600.
- [2] Adeyemi OS, Meyakno E, Akanji MA. Inhibition of Kupffer cell functions modulates arsenic intoxication in Wistar rats. *Gen Physiol Biophys* 2017; 36(2):219–227. doi:10.4149/gpb\_2016041.
- [3] Abu El-Saad AM, Al-Kahtani MA, Abdel-Moneim AM. N-acetylcysteine and meso-2,3-dimercaptosuccinic acid alleviate oxidative stress and hepatic dysfunction induced by sodium arsenite in male rats. *Drug Des Devel Ther* 2016; 10:3425–3434. doi:10.2147/DDDT.S115339.
- [4] Pompili M, Vichi M, Dinelli E, Erbutto D, Pycha R, Serafini G, *et al*. Arsenic: Association of regional concentrations in drinking water with suicide and natural causes of death in Italy. *Psychiatry Res* 2017; 249:311–317. doi:10.1016/j.psychres.2017.01.041.
- [5] El-Bahnasawy MM, Mohammad Ael-H, Morsy TA. Arsenic pesticides and environmental pollution: exposure, poisoning, hazards and recommendations. *J Egypt Soc Parasitol* 2013; 43(2):493–508. doi:10.12816/0006406.
- [6] Li C, Li J, Zhang A, Yu C, Xu Y, Xiong X, *et al*. Intervention effects of curcumin on hepatic oxidative stress injury in water arsenic-exposed rats. *Chinese Journal of Endemiology* 2015; 34(6):406–410. doi:10.3760/cma.j.issn.2095-4255.2015.06.005.
- [7] Bronkowska M, Łożna K, Figurska-Ciura D, Styczyńska M, Orzeł D, Biernat J, *et al*. Influence of arsenic on selected biochemical blood parameters in

- rats fed diet with different fat and protein content. *Rocz Panstw Zakl Hig* 2015; 66(3):233–237.
- [8] Chen L, Zhang A, Yu C, Dong X, Huang X. Arsenic exposure causes human 8-hydroxyguanine DNA glycosylase 1 gene methylation and DNA oxidative damage. *Chinese Journal of Pharmacology and Toxicology* 2014; 28(2):216–220. doi:10.3867/j.issn.1000-3002.2014.02.012.
- [9] Santra A, Chowdhury A, Ghatak S, Biswas A, Dhali GK. Arsenic induces apoptosis in mouse liver is mitochondria dependent and is abrogated by N-acetylcysteine. *Toxicol Appl Pharmacol* 2007; 220(2):146–155. doi:10.1016/j.taap.2006.12.029.
- [10] Liu S, Li X, Tan C, Liu H, Wu B. Effects of ER stress and PUMA on 5-FU-induced liver cell injury and apoptosis. *Journal of Sun Yat-sen University* 2019; 3:364–371. doi:10.13471/j.cnki.j.sun.yat-sen.univ(med.sci).2019.0052.
- [11] Yang DP, Li J, Huang XX, Zhang AH, Yun H, Xie ZJ. Apoptosis in arsenic poisoning hepatic injury caused by coal burning. *Journal of Military Surgeon in Southwest China* 2005; 7(4):1–3. doi:10.3969/j.issn.1672-7193.2005.04.001.
- [12] Xie TT, Zhang AH. Role of p53-mediated mitochondrial apoptotic pathway in arsenic liver injury caused by coal-burning. *Chin J Pharmacol Toxicol* 2014; 28(2):210–215. doi:10.3867/j.issn.1000-3002.2014.02.011.
- [13] Liu J, Zhao H, Wang Y, Shao Y, Li J, Xing M. Alterations of antioxidant indexes and inflammatory cytokine expression aggravated hepatocellular apoptosis through mitochondrial and death receptor-dependent pathways in Gallus gallus exposed to arsenic and copper. *Environ Sci Pollut Res Int* 2018; 25(16):15462–15473. doi:10.1007/s11356-018-1757-0.
- [14] Zhao H, He Y, Li S, Sun X, Wang Y, Shao Y, *et al*. Subchronic arsenism-induced oxidative stress and inflammation contribute to apoptosis through mitochondrial and death receptor dependent pathways in chicken immune organs. *Oncotarget* 2017; 8(25):40327–40344. doi:10.18632/oncotarget.16960.
- [15] Choudhury S, Ghosh S, Mukherjee S, Gupta P, Bhattacharya S, Adhikary A, *et al*. Pomegranate protects against arsenic-induced p53-dependent ROS-mediated inflammation and apoptosis in liver cells. *J Nutr Biochem* 2016; 38:25–40. doi:10.1016/j.jnutbio.2016.09.001.
- [16] Wang C, Ning Z, Wan F, Huang R, Chao L, Kang Z, *et al*. Characterization of the cellular effects and mechanism of arsenic trioxide-induced hepatotoxicity in broiler chickens. *Toxicol In Vitro* 2019; 61:104629. doi:10.1016/j.tiv.2019.104629.
- [17] Zhang XQ, Xu CF, Yu CH, Chen WX, Li YM. Role of endoplasmic reticulum stress in the pathogenesis of nonalcoholic fatty liver disease. *World J Gastroenterol* 2014; 20(7):1768–1776. doi:10.3748/wjg.v20.i7.1768.
- [18] Rasheva VI, Domingos PM. Cellular responses to endoplasmic reticulum stress and apoptosis. *Apoptosis* 2009; 14(8):996–1007. doi:10.1007/s10495-009-0341-y.
- [19] Xue QX, Shen X, Tian T, Han B, Xie RJ, He Y, *et al*. Metallothionein decreases the expression of GRP78 and CHOP proteins followed by apoptosis of liver cells in arsenic poisoning rats. *Basic & Clinical Medicine* 2015; 35(6):739–743. doi:10.16352/j.issn.1001-6325.2015.06.005.
- [20] Tang L, Xie RJ, Zheng L, Tian T, Yu L, Hu XX, *et al*. Effect of SET7/9-mediated endoplasmic reticulum stress on arsenic-induced hepatocyte apoptosis. *Chinese Journal of Pathophysiology* 2019; 35(02):186–189. doi:10.3969/j.issn.1000-4718.2019.02.029.
- [21] Chen J, Guo Y, Zeng W, Huang L, Pang Q, Nie L, *et al*. ER stress triggers MCP-1 expression through SET7/9-induced histone methylation in the kidneys of db/db mice. *Am J Physiol Renal Physiol* 2014; 306(8):F916–F925. doi:10.1152/ajprenal.00697.2012.
- [22] Nishioka K, Chuiikov S, Sarma K, Erdjument-Bromage H, Allis CD, Tempst P, *et al*. Set9, a novel histone H3 methyltransferase that facilitates transcription by precluding histone tail modifications required for heterochromatin formation. *Genes Dev* 2002; 16(4):479–489. doi:10.1101/gad.967202.
- [23] Tamura R, Doi S, Nakashima A, Sasaki K, Maeda K, Ueno T, *et al*. Inhibition of the H3K4 methyltransferase SET7/9 ameliorates peritoneal fibrosis. *PLoS One* 2018; 13(5):e0196844. doi:10.1371/journal.pone.0196844.
- [24] Li ZR, Wang S, Yang L, Yuan XH, Suo FZ, Yu B, *et al*. Experience-based discovery (EBD) of aryl hydrazines as new scaffolds for the development of LSD1/KDM1A inhibitors. *Eur J Med Chem* 2019; 166:432–444. doi:10.1016/j.ejmech.2019.01.075.
- [25] Pagrut N, Ganguly S, Tekam S, Pendharkar R, Kumar V. Histological alterations in arsenic induced various organs in rats. *Journal of Entomology and Zoology Studies* 2018; 6(3):1428–1429.
- [26] Bali İ, Bilir B, Emir S, Turan F, Yılmaz A, Gökkuş T, Aydın M. The effects of melatonin on liver functions in arsenic-induced liver damage. *Ulus Cerrahi Derg* 2016; 32(4):233–237. doi:10.5152/UCD.2015.3224.
- [27] Bambino K, Zhang C, Austin C, Amarasiriwardena C, Arora M, Chu J, *et al*. Inorganic arsenic causes fatty liver and interacts with ethanol to cause alcoholic liver disease in zebrafish. *Dis Model Mech* 2018; 11(2):dmm031575. doi:10.1242/dmm.031575.
- [28] Wang LM. Chronic arsenic poisoning caused by long-term taken Niu Huang Ninggong tablet: a report of 2 cases. *Zhongguo Zhong Xi Yi Jie He Za Zhi* 2005; 25(3):213.
- [29] Quan NV, Dang Xuan T, Teschke R. Potential hepatotoxins found in herbal medicinal products: A systematic review. *Int J Mol Sci* 2020; 21(14):5011. doi:10.3390/ijms21145011.
- [30] Sharma S, Kaur I, Nagpal AK. Assessment of arsenic content in soil, rice grains and groundwater and associated health risks in human population from Ropar wetland, India, and its vicinity. *Environ Sci Pollut Res Int* 2017; 24(23):18836–18848. doi:10.1007/s11356-017-9401-y.
- [31] Treleaven J, Meller S, Farmer P, Birchall D, Goldman J, Pillar G. Arsenic and ayurveda. *Leuk Lymphoma* 1993; 10(4-5):343–345. doi:10.3109/10428199309148558.

- [32] Khandpur S, Malhotra AK, Bhatia V, Gupta S, Sharma VK, Mishra R, *et al*. Chronic arsenic toxicity from Ayurvedic medicines. *Int J Dermatol* 2008;47(6):618–621. doi:10.1111/j.1365-4632.2008.03475.x.
- [33] Danan G, Benichou C. Causality assessment of adverse reactions to drugs—I. A novel method based on the conclusions of international consensus meetings: application to drug-induced liver injuries. *J Clin Epidemiol* 1993;46(11):1323–1330. doi:10.1016/0895-4356(93)90101-6.
- [34] Danan G, Teschke R. RUCAM in drug and herb induced liver injury: The update. *Int J Mol Sci* 2015;17(1):14. doi:10.3390/ijms17010014.
- [35] Teschke R. DILI, HILI, RUCAM algorithm, and AI, the artificial intelligence: Provocative issues, progress, and proposals. *Arch Gastroenterol Res* 2020;1(1):4–11.
- [36] Wu J, Lu T, Cheng ML. Therapeutic effects of the Chinese Medicine Han-Dan-Gan-Le, on arsenic-induced liver injury in Guizhou, China. *Chinese Journal of Endemiology* 2006;25(1):86–89. doi:10.3760/cma.j.issn.1000-4955.2006.01.028.
- [37] He Y, Zhang A, Yang D, Wang J, Wei X, Huang X. Clinical study on treatment to hepatic fibrosis of coal-brunt arsenic with ginkgo leaf. *Journal of Military Surgeon in Southwest China* 2005;7(1):1–3. doi:10.3969/j.issn.1672-7193.2005.01.001.



Original Article

# Icaritin Attenuates Lipid Accumulation by Increasing Energy Expenditure and Autophagy Regulated by Phosphorylating AMPK

Yue Wu<sup>1#</sup>, Ying Yang<sup>1#</sup>, Fang Li<sup>2#</sup>, Jie Zou<sup>1</sup>, Yu-Hao Wang<sup>1</sup>, Meng-Xia Xu<sup>1</sup>, Yong-Lun Wang<sup>1</sup>, Rui-Xi Li<sup>1</sup>, Yu-Ting Sun<sup>1</sup>, Shun Lu<sup>3,4</sup>, Yuan-Yuan Zhang<sup>1,5\*</sup>  and Xiao-Dong Sun<sup>1,6\*</sup> 

<sup>1</sup>West China School of Basic Medical Sciences & Forensic Medicine, Sichuan University, Chengdu, Sichuan, China; <sup>2</sup>Department of Medical Oncology, Sichuan Cancer Hospital & Institute, School of Medicine, University of Electronic Science and Technology of China, Chengdu, Sichuan, China; <sup>3</sup>Department of Radiation Oncology, Sichuan Cancer Hospital & Institute, Sichuan Cancer Center, School of Medicine, University of Electronic Science and Technology of China, Chengdu, Sichuan, China; <sup>4</sup>Department of Radiological Protection, Radiation Oncology Key Laboratory of Sichuan Province, Chengdu, Sichuan, China; <sup>5</sup>Department of Gastroenterology, The Second Affiliated Hospital of Chengdu Medical College, China National Nuclear Corporation 416 Hospital, Chengdu, Sichuan, China; <sup>6</sup>State Key Laboratory of Medicinal Chemical Biology, Nankai University, Tianjin, China

Received: 3 February 2021 | Revised: 3 March 2021 | Accepted: 4 March 2021 | Published: 8 March 2021

## Abstract

**Background and Aims:** Lipid accumulation is the major characteristic of non-alcoholic fatty liver disease, the prevalence of which continues to rise. We aimed to investigate the effects and mechanisms of icaritin on lipid accumulation. **Methods:** Cells were treated with icaritin at 0.7, 2.2, 6.7, or 20  $\mu$ M for 24 h. The effects on lipid accumulation in L02 and Huh-7 cells were detected by Bodipy and oil red O staining, respectively. Mitochondria biogenesis of L02 cells was detected by MitoTracker Orange staining. Glucose uptake and adenosine triphosphate content of 3T3-L1 adipocytes and C2C12 myotubes were detected. The expression levels of proteins in the adenosine 5'-monophosphate-activated protein kinase (AMPK) signaling pathway, biomarkers of autophagy, and mitochondria biogenesis were measured by western blotting. LC3 puncta were detected by immunofluorescence. **Results:** Icaritin significantly attenuated lipid accumulation in L02 and Huh-7 cells and boosted the mitochondria biogenesis of L02 cells. Icaritin enhanced glu-

cose uptake, decreased adenosine triphosphate content, and activated the AMPK signaling pathway in 3T3-L1 adipocytes and C2C12 myotubes. Icaritin boosted autophagy and also enhanced the initiation of autophagic flux in 3T3-L1 preadipocytes and C2C12 myoblasts. However, icaritin decreased autophagy and promoted mitochondria biogenesis in 3T3-L1 adipocytes and C2C12 myotubes. **Conclusions:** Icaritin attenuates lipid accumulation by increasing energy expenditure and regulating autophagy by activating the AMPK pathway.

**Citation of this article:** Wu Y, Yang Y, Li F, Zou J, Wang YH, Xu MX, *et al.* Icaritin attenuates lipid accumulation by increasing energy expenditure and autophagy regulated by phosphorylating AMPK. J Clin Transl Hepatol 2021;00(00): 373–383. doi: 10.14218/JCTH.2021.00050.

## Introduction

The global prevalence of non-alcoholic fatty liver disease (NAFLD) is estimated to be about 24% to 25% of the population, which has steadily rose over recent decades.<sup>1</sup> NAFLD represents a range of diseases, from simple hepatic steatosis to steatohepatitis that eventually leads to cirrhosis and hepatocellular carcinoma.<sup>2</sup> Lipid accumulation in the liver is the major characteristic of NAFLD. Lipid accumulation in skeletal muscles is associated with the development of insulin resistance, which is an early marker and significantly contributes to NAFLD.<sup>3</sup> Adipose acts as a fuel reservoir, which controls the mobilization of lipids.<sup>4</sup> As such, we employed hepatic cells (L02 and Huh-7 cells), C2C12 myoblasts, C2C12 myotubes, 3T3-L1 preadipocytes, and 3T3-L1 adipocytes in this study.

No effective medical interventions can completely reverse NAFLD, other than lifestyle and dietary changes, to date. Although some drugs show benefits, such as vitamin E and pioglitazone, no drugs have been approved by the US Food and Drug Administration.<sup>5</sup> NAFLD results from the

**Keywords:** Icaritin; Lipid accumulation; NAFLD; AMPK; Autophagy.

**Abbreviations:** ACC, acetyl-CoA carboxylase; AMPK, adenosine 5'-monophosphate-activated protein kinase; ATCC, American type culture collection; ATP, adenosine triphosphate; CaMKK $\beta$ , Calcium/calmodulin-dependent protein kinase kinase  $\beta$ ; CQ, chloroquine; DMEM, Dulbecco's modified Eagle's medium; FBS, fetal bovine serum; GAPDH, glyceraldehyde 3-phosphate dehydrogenase; LKB1, liver kinase B1; NAFLD, non-alcoholic fatty liver disease; NBSC, newborn calf serum; NRF1, nuclear respiratory factor 1; p-ACC, phospho-ACC; p-AMPK, phospho-AMPK; PBS, phosphate buffer saline; PFA, paraformaldehyde; PGC-1 $\alpha$ , peroxisome proliferator-activated receptor gamma coactivator 1-alpha; p-LKB1, phospho-LKB1; PVDF, polyvinylidene fluoride; RT, room temperature; SDS-PAGE, sodium dodecyl sulfate-polyacrylamide gel electrophoresis; SIRT1, silent mating type information regulation 2 homolog 1; TFAM, transcription factor A; 2-NBDG, 2-[N-(7-nitrobenz-2-oxa-1,3-diazol-4-yl) amino]-2-deoxy-D-glucose.

\*Contributed equally to this work.

**\*Correspondence to:** Yuan-Yuan Zhang, West China School of Basic Medical Sciences & Forensic Medicine, Sichuan University, Chengdu, Sichuan 610041, China. ORCID: <http://orcid.org/0000-0002-9263-6262>. Tel: +86-28-8550-1278, Fax: +86-28-8550-1278, E-mail: zhangyy@scu.edu.cn, sarahyyzhang@hotmail.com; Xiao-Dong Sun, West China School of Basic Medical Sciences & Forensic Medicine, Sichuan University, Chengdu, Sichuan 610041, China. ORCID: <http://orcid.org/0000-0002-7062-8931>. Tel: +86-28-8550-1278, Fax: +86-28-8550-1278, E-mail: sunxdelta@hotmail.com



chronic energy imbalance. Increasing energy expenditure is an effective strategy to attenuate lipid accumulation and combat NAFLD. There is an urgent need to develop candidate agents to combat NAFLD through enhancing energy expenditure and attenuating lipid accumulation.

Icaritin is a naturally bioactive flavonoid of the traditional Chinese herbal medicine *Herba Epimedii*. Flavonoids of *Herba Epimedii* have been widely used for their metabolic regulation, anti-oxidation, and hepatoprotective effects.<sup>6</sup> Icaritin is also the metabolite of the major flavonoid of *Herba Epimedii*, icariin (Fig. 1A).<sup>6</sup> Icaritin's lipid-lowering effects have attracted widespread attention recently.<sup>7</sup> Icaritin inhibited intravascular thrombosis and extravascular lipids deposition.<sup>8</sup> However, icaritin's effects on lipid accumulation have not been explored. In this study, we investigated the effects and mechanisms of icaritin on lipid accumulation.

## Methods

### Cell culture and treatments

Human hepatic L02 cells were obtained from the American Type Culture Collection (commonly known as the ATCC). L02 cells were cultured in RPMI-1640 medium (HyClone, Logan, UT, USA) supplemented with 10% fetal bovine serum (FBS) (Biological Industries, Cromwell, CT, USA) and 1% penicillin-streptomycin (HyClone). Huh-7 cells were a kind gift from Prof. Lang Bai of West China Hospital, Sichuan University. Huh-7 cells were cultured in Dulbecco's Modified Eagle's Medium (DMEM) (HyClone) supplemented with 10% FBS and 1% penicillin-streptomycin.

3T3-L1 preadipocytes were obtained from the ATCC, cultured in DMEM supplemented with 10% newborn calf serum (referred to herein as "NBCS") (Biological Industries) and 1% penicillin-streptomycin. When the cells reached 50% confluence, they were induced to differentiate into adipocytes by changing the medium to a differentiation medium which was composed of DMEM supplemented with 10% NBCS, 0.5 mM 3-isobutyl-1-methylxanthine, 1  $\mu$ M dexamethasone, and 10  $\mu$ g/mL insulin, for 48 h. Then, the cells were cultured with DMEM supplemented with 10% FBS and 1% penicillin-streptomycin for another 48 h. After being induced for 8 to 10 days, more than 90% of the 3T3-L1 preadipocytes differentiated into adipocytes, which showed features of insulin resistance and a fat cellular phenotype filled with lipid droplets.

C2C12 myoblasts were cultured in the DMEM supplemented with 10% FBS and 1% penicillin-streptomycin. When the cells reached 80% confluence, they were induced to differentiate into myotubes by changing the medium to a differentiation medium which was composed of DMEM containing 2% horse serum (HyClone). C2C12 myoblasts were cultured in the differentiation medium for 4 to 6 days, with medium change every 48 h, until they differentiated into insulin-resistant mature myotubes. Numerous mature myotubes formed and aligned regularly as observed by optical microscope (Zeiss, Oberkochen, Germany). All cells were cultured at 37 °C in an atmosphere of 5% CO<sub>2</sub>.

Icaritin (3,7-dihydroxy-8-prenyl-4'-methoxychrysin, PubChem CID: 5318980, CAS: 118525-40-9) with purity above 99% was commercially obtained from Shanghai Yuanye Biotechnology (Cat# B21277; Shanghai, China).

### Determination of lipid accumulation

Huh-7 and L02 cells were seeded in 24-well plates and treated with sodium oleate at 100  $\mu$ M for 24 h when 40–

50% confluence was reached. Then, the cells were treated with icaritin for 24 h. For Bodipy staining, L02 cells were stained with 4  $\mu$ M Bodipy staining solution (Thermo Fisher Scientific, Waltham, MA, USA) in dark at 37 °C for 15 m after treatments.<sup>9</sup> Then, the cells were washed twice with phosphate buffer saline (PBS) and fixed with 4% paraformaldehyde (PFA) (Sangon, Shanghai, China) for 20 m. Finally, the nucleus was stained with Hoechst 33258 (Sigma, St. Louis, MO, USA) for 3 m. For oil red O staining, L02 and Huh-7 cells were washed with PBS and fixed with 4% PFA for 20 m at room temperature (RT). Then, the 4% PFA was discarded and the cells were washed with PBS. Following, 60% oil red O solution was added for staining for 45 m at RT. The cells were then washed with 60% isopropanol in PBS, and the nucleus was stained with hematoxylin for 5 m. Finally, the cells were washed with PBS and double-distilled water, and sealed with glycerin. Lipid droplets in the cells were observed and photographed by an optical microscope (Zeiss).

### Determination of mitochondria biogenesis

L02 cells, C2C12 myotubes, and 3T3-L1 adipocytes were seeded on coverslips in 24-well plates for 24 h. Then, the cells were incubated with icaritin at 0.7, 2.2, 6.7, or 20  $\mu$ M for 24 h. The number of mitochondria in the cells was evaluated by MitoTracker Orange staining.<sup>10</sup> The cells were first stained with a staining solution containing MitoTracker probe (Thermo Fisher Scientific) for 30 m. Then, the cells were fixed with 4% PFA for 20 m and permeabilized with 0.5% Triton X-100 (BBI, Shanghai, China) for 15 m. The nucleus was stained with Hoechst 33258 for 3 m. Finally, cells were sealed with an anti-fluorescence quenching agent and stored at –20 °C. The biogenesis and morphology of mitochondria were observed and photographed by confocal microscopy (Zeiss).

### Glucose uptake analysis

Both C2C12 myotubes and 3T3-L1 adipocytes were seeded on coverslips in 24-well plates. After reaching 80% confluence, the cells were treated with icaritin (2.2, 6.7, or 20  $\mu$ M), metformin (2.5 mM), or phloretin (100  $\mu$ M) for 4 h. Phloretin, a glucose uptake inhibitor, was employed as the negative control and metformin as the positive control. The 2-NBDG glucose uptake assay kit (BioVision, San Francisco, CA, USA) was employed to measure the amount of glucose uptake.<sup>11</sup> The cells were incubated with the glucose uptake mix for 30 m after washing. Then, the cells were washed, fixed, and observed. Amounts of 2-NBDG taken-up were determined by fluorescence microscopy (Olympus, Tokyo, Japan).

### Adenosine triphosphate (ATP) content analysis

C2C12 myotubes and 3T3-L1 adipocytes were treated with icaritin at 0.7, 2.2, 6.7, or 20  $\mu$ M, or metformin at 2.5 mM, for 24 h, and harvested with trypsin. Total ATP content was measured using an ATP colorimetric/fluorometric assay kit (BioVision).<sup>12</sup> A 100  $\mu$ L aliquot of ATP assay buffer was added. Interfering proteins were removed by perchloric acid. Then, samples were centrifuged at 13,000 rpm for 15 m at 4 °C. A 50  $\mu$ L aliquot of supernatant was added to each well of the 96-well plate and mixed with 50  $\mu$ L reaction mix in dark for 30 m. The absorbance was measured at 570 nm using a microplate reader (Thermo Fisher Scientific).

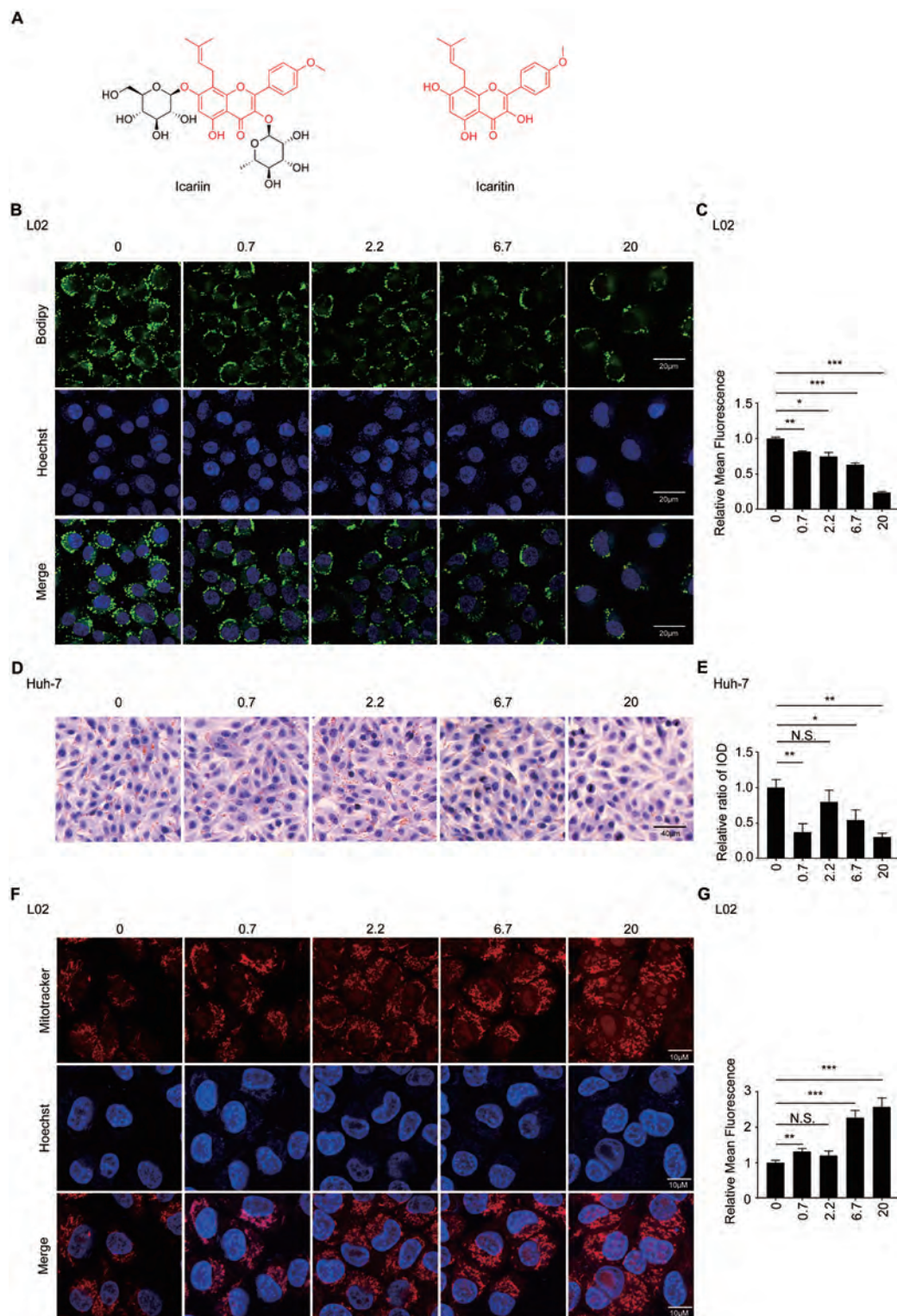


**Fig. 1. Icaritin attenuated lipid accumulation in sodium oleate-induced L02 and Huh-7 cells, and enhanced the mitochondria biogenesis of L02 cells.** (A) The chemical structure of icaritin and icaritin. (B, C) L02 cells were induced by sodium oleate at 100  $\mu$ M for 24 h to establish a NAFLD cell model. Then, L02 cells were treated with icaritin at 0.7, 2.2, 6.7, or 20  $\mu$ M for 24 h. Lipid accumulation in L02 cells was attenuated by icaritin, as visualized by Bodipy staining and observed by a confocal microscope. (D, E) Huh-7 cells were induced by sodium oleate at 100  $\mu$ M for 24 h to establish a NAFLD cell model. Then, Huh-7 cells were treated with icaritin at 0.7, 2.2, 6.7, or 20  $\mu$ M for 24 h. Lipid accumulation in Huh-7 cells was attenuated by icaritin, as visualized by oil red O staining. (F, G) L02 cells were induced by sodium oleate at 100  $\mu$ M for 24 h and treated with icaritin for 24 h. The mass of mitochondria in L02 cells was enhanced by icaritin, as detected by MitoTracker Orange staining (red). Abbreviation: NAFLD, non-alcoholic fatty liver disease.

### Western blot analysis

C2C12 myoblasts, C2C12 myotubes, 3T3-L1 preadipocytes, and 3T3-L1 adipocytes were incubated with icaritin at 0.7, 2.2, 6.7, or 20  $\mu$ M, or metformin at 2.5 mM, for 24 h. Cells were harvested by trypsin and lysed by 1 $\times$  sodium dodecyl sulfate-polyacrylamide gel electrophoresis (commonly known as SDS-PAGE) loading buffer. Then, samples were boiled at 98  $^{\circ}$ C for 10 m. Proteins were separated by SDS-PAGE and transferred to a polyvinylidene fluoride (commonly known as PVDF) membrane. Non-specific binding was blocked with 5% skim milk (BBI) for 1 h. Then, the PVDF membranes were incubated with primary antibodies, including CaMKK $\beta$  (D262840; Sango), LKB1 (D163053; Sango), p-LKB1 (D151527; Sango), AMPK (2532s; Cell Signaling Technology, Danvers, MA, USA), p-AMPK (2535; Cell Signaling Technology), ACC (3662; Cell Signaling Technology), p-ACC (11818; Cell Signaling Technology), p-62 (PM045; MBL, Tokyo, Japan), LC3 (M186-3; MBL), SIRT1 (sc-135791; Santa Cruz Biotechnology, Dallas, TX, USA), PGC-1 $\alpha$  (66369-1; Proteintech, Rosemont, IL, USA), NRF1 (66832-1; Proteintech), TFAM (22586-1; Proteintech), and GAPDH (sc-32233; Santa Cruz Biotechnology), for 2 h at RT. Then, the PVDF membranes were incubated with a secondary antibody to rabbit or mouse IgG conjugated to horseradish peroxidase at RT for 1 h after washing. Blots were developed using enhanced chemiluminescence detection reagents (Mei5bio, Beijing, China) and images were taken by chemiluminescence imager (Clinx, Shanghai, China).

### Immunofluorescence analysis

C2C12 myotubes, C2C12 myoblasts, 3T3-L1 preadipocytes, and 3T3-L1 adipocytes were seeded on round coverslips in 24-well plates for 24 h. Then, the cells were treated with icaritin (6.7  $\mu$ M) alone, or in combination with chloroquine (CQ) at 10  $\mu$ M for 24 h. After, the cells were fixed with 4% PFA for 20 m, permeabilized with 0.5% Triton X-100 for 15 m, and blocked with 4% bovine serum albumin (BioFroxx, Einhausen, Germany) for 1 h. Then, the cells were incubated with anti-LC3 antibody (MBL) at RT for 2 h, and with the secondary antibody conjugated to fluorescein isothiocyanate in dark at RT for 1 h. Finally, nuclei were stained with Hoechst 33258 for 3 m after washing. The intensity of fluorescence was observed and pictured by confocal microscopy (Zeiss).

### Statistical analysis

All experiments were performed in triplicate. Results were expressed as the mean  $\pm$  standard deviation. All data were analyzed with *t*-test using GraphPad Prism 7.0 (GraphPad Software Inc., La Jolla, CA, USA). A *p*-value of  $<0.05$  was defined as statistically significant.

## Results

### Icaritin attenuated lipid accumulation in L02 and Huh-7 cells, and enhanced the mass of mitochondria of L02 cells

L02 and Huh-7 cells were treated with sodium oleate at 100  $\mu$ M for 24 h to establish the NAFLD cell model. Icaritin attenuated lipid accumulation in L02 cells at 0.7, 2.2, 6.7, and 20  $\mu$ M, as detected by Bodipy staining (Fig. 1B, C). As

shown in Fig. 1D and E, icaritin significantly attenuated lipid accumulation in Huh-7 cells, as detected by oil red O staining. Besides, the mass and fluorescence intensity of mitochondria in L02 cells was enhanced by icaritin (Fig. 1F, G).

### Icaritin enhanced the glucose uptake, decreased the ATP content, and activated the LKB1/AMPK/ACC pathway in 3T3-L1 adipocytes and C2C12 myotubes

Icaritin significantly enhanced glucose uptake of both 3T3-L1 adipocytes (Fig. 2A, B) and C2C12 myotubes (Fig. 2C, D) in a dose-dependent manner, compared with the untreated cells. Meanwhile, icaritin decreased the ATP content in 3T3-L1 adipocytes (Fig. 2E) and C2C12 myotubes (Fig. 2F). Icaritin significantly enhanced the expression of CaMKK $\beta$ , p-LKB1, p-AMPK, and p-ACC in both 3T3-L1 adipocytes (Fig. 3A–F) and C2C12 myotubes (Fig. 3G–L). The changes of p-LKB1 and p-AMPK in 3T3-L1 adipocytes occurred in a dose-dependent manner (Fig. 3C, E). As for C2C12 myotubes, the changes of expression of CaMKK $\beta$ , p-LKB1, and p-ACC also occurred in a dose-dependent manner (Fig. 3G–L). Interestingly, the constitutive expression of AMPK was decreased in both 3T3-L1 adipocytes and C2C12 myotubes (Fig. 3D, J).

### Icaritin enhanced autophagy and promoted the initiation of autophagy in autophagic flux in both 3T3-L1 preadipocytes and C2C12 myoblasts

Icaritin enhanced the number of endogenous LC3 puncta in both 3T3-L1 preadipocytes (Fig. 4A, B) and C2C12 myoblasts (Fig. 4C, D) at 0.7, 2.2, 6.7, and 20  $\mu$ M, as detected by immunofluorescence. For 3T3-L1 preadipocytes, the enhanced trend of LC3 puncta slightly decreased at 20  $\mu$ M, while it was still higher than that observed in the untreated cells. Meanwhile, the expression of p62 was decreased by icaritin in both 3T3-L1 preadipocytes (Fig. 4E, F) and C2C12 myoblasts (Fig. 4H, I), compared to the untreated cells. The ratio of LC3II/LC3I in both cells was increased by icaritin (Fig. 4E, G, H, J). To investigate the role of icaritin on autophagic flux, we employed CQ. As shown in Fig. 5A and B, the combination of CQ and icaritin further increased LC3 puncta than icaritin alone (Fig. 5A, B, F, G). Consistent with the above observations, the ratio of LC3-II/I in 3T3-L1 preadipocytes (Fig. 5C, E) and C2C12 myoblasts (Fig. 5H, J) was also increased by icaritin alone or in combination with CQ. Meanwhile, the expression of p62 was also increased by icaritin in combination with CQ (Fig. 5D, I).

### Icaritin inhibited autophagy and enhanced the mitochondrial biogenesis in 3T3-L1 adipocytes and C2C12 myotubes

Given that icaritin induced autophagy in undifferentiated 3T3-L1 preadipocytes and C2C12 myoblasts, we wondered whether icaritin was able to work uniformly in insulin-resistant cells, 3T3-L1 adipocytes, and C2C12 myotubes. The western blotting analysis showed that the expression of p62 was increased by icaritin in both 3T3-L1 adipocytes (Fig. 6A, B) and C2C12 myotubes (Fig. 6D, E). Accordingly, the ratio of LC3-II/LC3-I in 3T3-L1 adipocytes and C2C12 myotubes was decreased by icaritin to some extent (Fig. 6A, C, D, F). Icaritin significantly boosted the mass and density of mitochondria of 3T3-L1 adipocytes (Fig. 7A, B) and C2C12 myotubes (Fig. 7H, I). The expression of several proteins (SIRT1, PGC-1 $\alpha$ , NRF1, and TFAM) which play



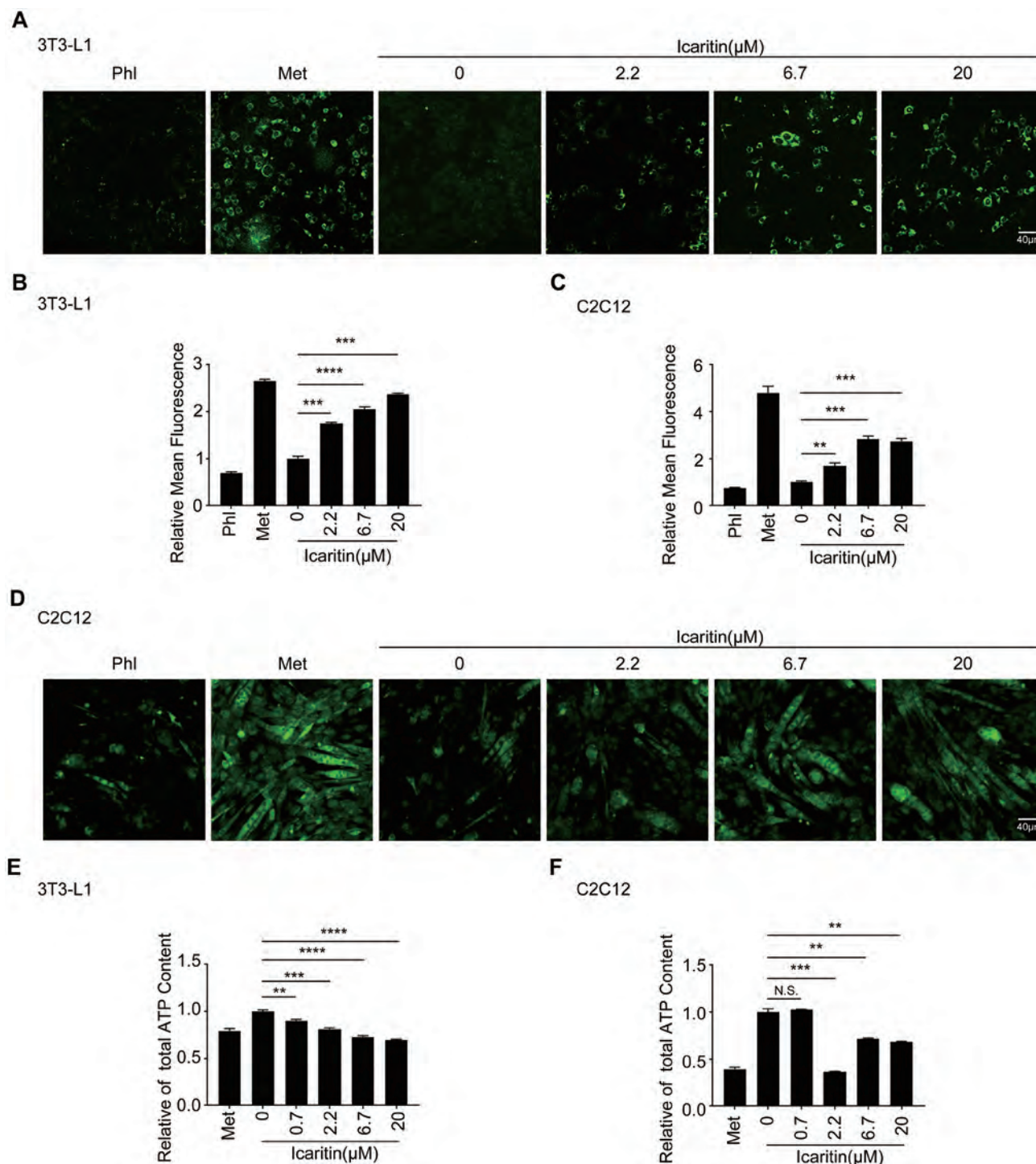


**Fig. 2. Icaritin increased the glucose uptake and decreased the ATP content in 3T3-L1 adipocytes and C2C12 myotubes.** (A, B) 3T3-L1 adipocytes were treated with icaritin (0, 2.2, 6.7, or 20 μM), metformin (2.5 mM), or phloretin (100 μM) for 4 h. Glucose uptake in 3T3-L1 adipocytes was dose-dependently increased by icaritin, as observed by fluorescence microscopy after being stained with 2-NBDG. (C, D) C2C12 myotubes were treated as in (A). Icaritin increased the glucose uptake of C2C12 myotubes. (E, F) 3T3-L1 adipocytes and C2C12 myotubes were treated with icaritin (0, 2.2, 6.7, or 20 μM), or metformin (2.5 mM) for 24 h. The ATP content was decreased by icaritin, as determined using an ATP calorimetric assay kit. All values are presented as mean±standard deviation ( $n=3$ ). \* $p<0.05$ ; \*\* $p<0.01$ ; \*\*\* $p<0.001$  vs. untreated cells. Abbreviations: ATP, adenosine triphosphate; Met, metformin; Phl, phloretin; 2-NBDG, 2-[N-(7-nitrobenz-2-oxa-1,3-diazol-4-yl) amino]-2-deoxy-D-glucose.

prominent roles in mitochondria biogenesis, were all significantly increased by icaritin in both cells (Fig. 7C–G, J–N).

However, icaritin significantly enhanced the expression of TFAM in 3T3-L1 adipocytes only at 6.7 μM (Fig. 7C, G).



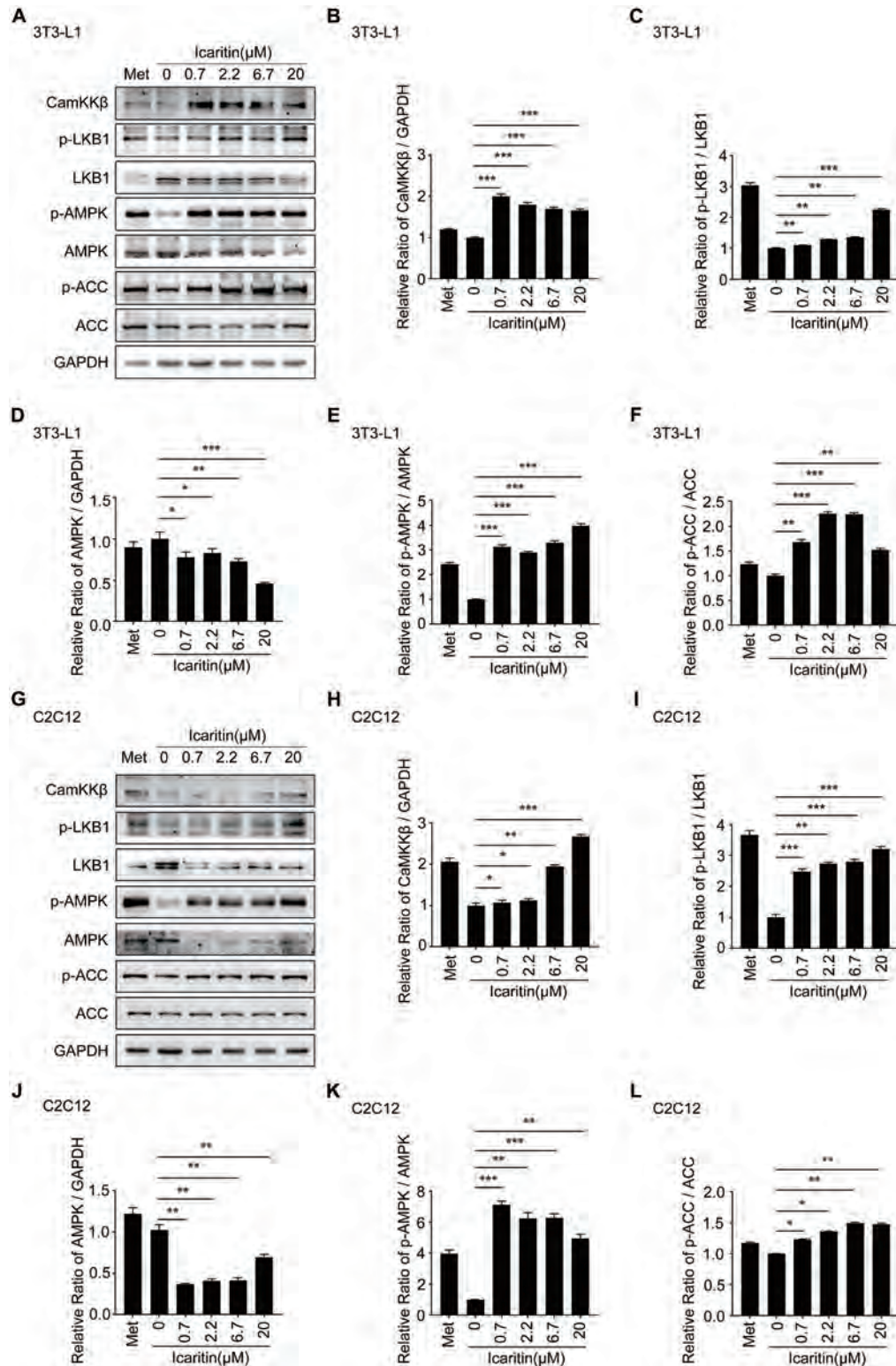


**Fig. 3. Icaritin activated the AMPK pathway in 3T3-L1 adipocytes and C2C12 myotubes.** 3T3-L1 adipocytes and C2C12 myotubes were treated with icaritin (0, 0.7, 2.2, 6.7, or 20  $\mu$ M), or metformin (2.5 mM) for 24 h. (A–F) Icaritin increased the expression of CaMKK $\beta$ , the ratio of p-LKB1/LKB1, p-AMPK/AMPK, and p-ACC/ACC in 3T3-L1 adipocytes, as detected by western blotting. (G–L) Icaritin increased the expression of CaMKK $\beta$ , the ratio of p-LKB1/LKB1, p-AMPK/AMPK, and p-ACC/ACC in C2C12 myotubes, as detected by western blotting. Values are presented as mean  $\pm$  standard deviation ( $n=3$ ). \* $p<0.05$ ; \*\* $p<0.01$ ; \*\*\* $p<0.001$  vs. untreated cells. Abbreviations: ACC, Acetyl-CoA carboxylase; AMPK, adenosine 5'-monophosphate-activated protein kinase; CaMKK $\beta$ , Calcium/calmodulin-dependent protein kinase kinase  $\beta$ ; GAPDH, glyceraldehyde 3-phosphate dehydrogenase; LKB1, liver kinase B1; p-ACC, phospho-ACC; p-AMPK, phospho-AMPK; p-LKB1, phosphor-LKB1.

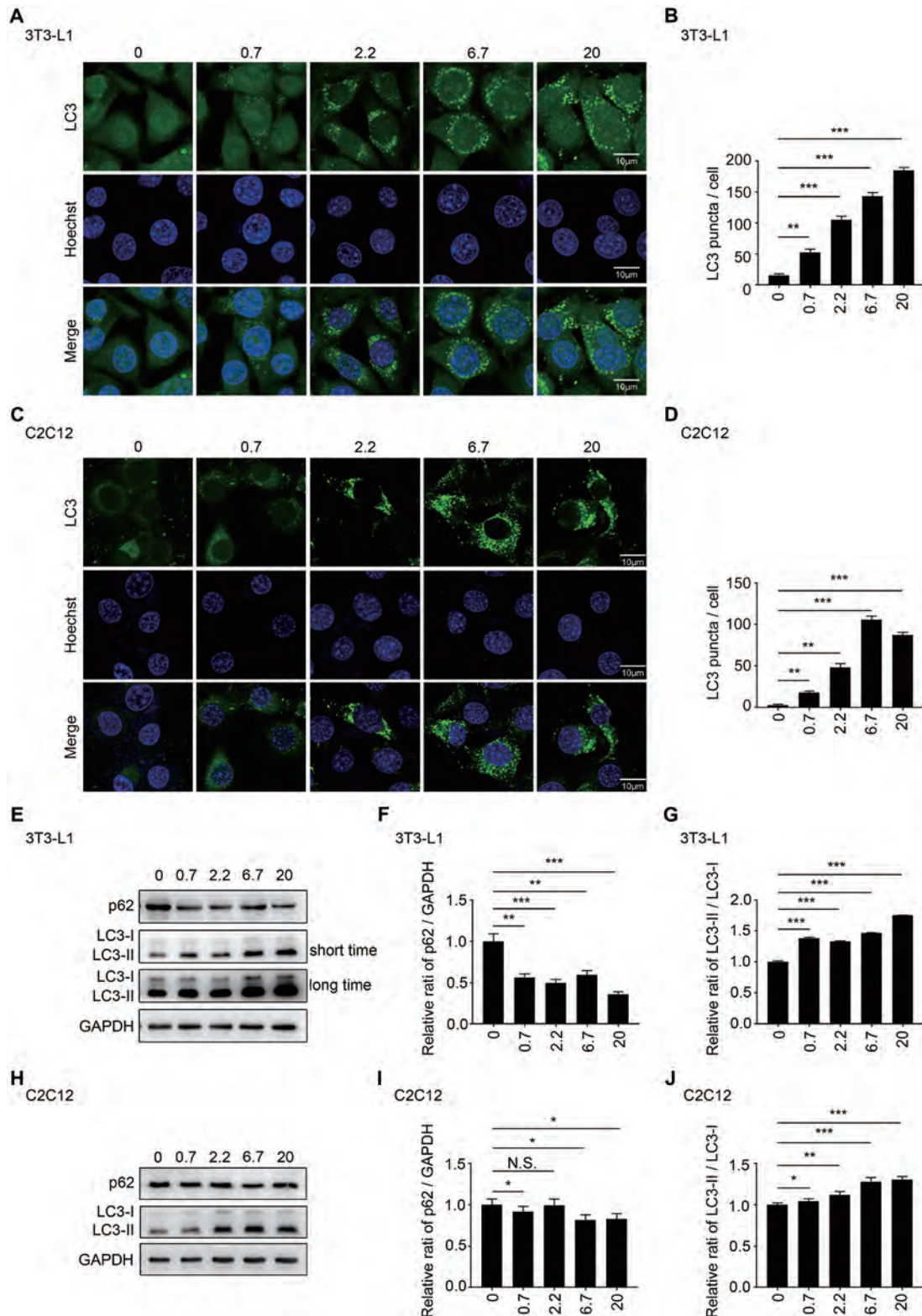


**Fig. 4.** Icaritin promoted autophagy in 3T3-L1 preadipocytes and C2C12 myoblasts. 3T3-L1 preadipocytes and C2C12 myoblasts were treated with icaritin (0, 0.7, 2.2, 6.7, or 20  $\mu$ M) for 24 h. (A–D) 3T3-L1 preadipocytes and C2C12 myoblasts were incubated with an anti-LC3 antibody and the secondary antibody conjugated to fluorescein isothiocyanate. Icaritin increased endogenous LC3 puncta in 3T3-L1 preadipocytes and C2C12 myoblasts, as observed by confocal microscopy. (E–J) Icaritin decreased the expression of p62 and increased LC3II/LC3I in 3T3-L1 preadipocytes and C2C12 myoblasts, as detected by western blotting. All values were presented as mean  $\pm$  standard deviation ( $n=3$ ). \* $p<0.05$ ; \*\* $p<0.01$ ; \*\*\* $p<0.001$  vs. untreated cells. Abbreviation: GAPDH, glyceraldehyde 3-phosphate dehydrogenase.



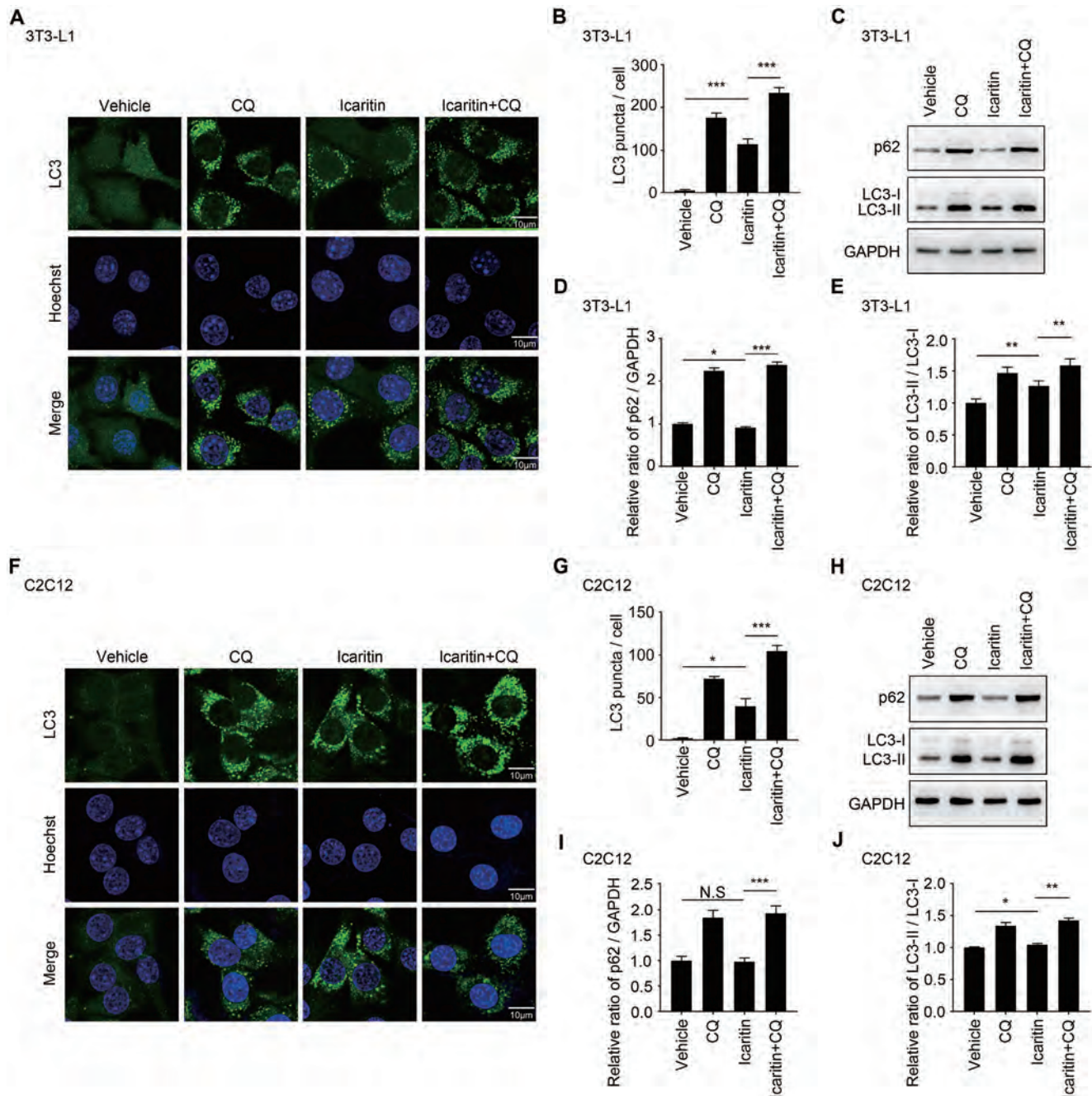


**Fig. 5. Icaritin promoted initiation of autophagy in autophagic flux of 3T3-L1 preadipocytes and C2C12 myoblasts.** 3T3-L1 preadipocytes and C2C12 myoblasts were treated with icaritin (6.7  $\mu$ M) alone or in combination with CQ (10  $\mu$ M) for 24 h. (A, B) 3T3-L1 preadipocytes were incubated with an anti-LC3 antibody and the secondary antibody conjugated to FITC. Icaritin increased the endogenous LC3 puncta in 3T3-L1 preadipocytes, which was further increased by the combination of CQ, as observed by confocal microscopy. (C-E) Icaritin increased the expression of p62 and enhanced LC3II/LC3I of 3T3-L1 preadipocytes, which was further increased by the combination of CQ, as detected by western blotting. (F, G) C2C12 myoblasts were treated as in (A). Icaritin increased the endogenous LC3 puncta in C2C12 myoblasts, which was further increased by the combination of CQ. (H-J) Icaritin increased the expression of p62 and enhanced LC3II/LC3I of C2C12 myoblasts, which was further increased by the combination of CQ, as detected by western blotting. Values are presented as mean  $\pm$  standard deviation ( $n=3$ ). \* $p<0.05$ ; \*\* $p<0.01$ ; \*\*\* $p<0.001$  vs. vehicle or as indicated. Abbreviations: CQ, chloroquine; GAPDH, glyceraldehyde 3-phosphate dehydrogenase.

## Discussion

Accumulating evidence has demonstrated the anti-cancer effects of icaritin. However, there have been no reports on its roles in NAFLD, so far. Enhancing energy expenditure

and inhibiting lipid accumulation is an effective strategy to combat NAFLD. Our results showed that icaritin significantly attenuated sodium oleate-induced lipid accumulation in L02 and Huh-7 cells. Icaritin increased the number and fluorescence intensity of mitochondria in L02 cells. Accordingly, icaritin decreased the ATP content of 3T3-L1 adipocytes.



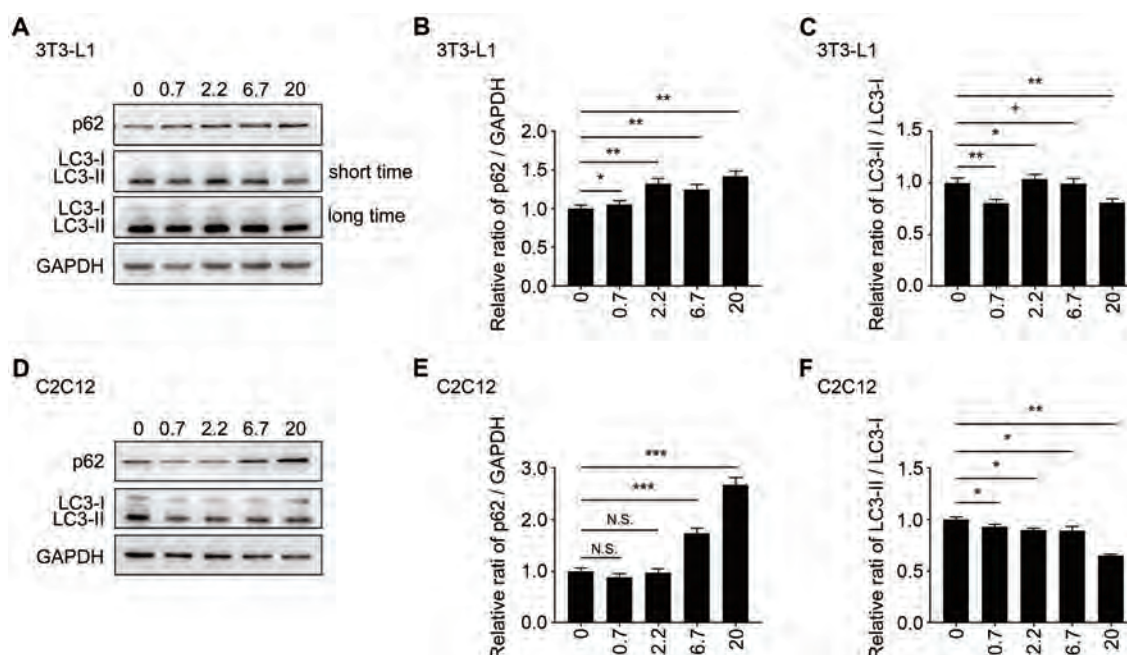


**Fig. 6. Icaritin inhibited autophagy in 3T3-L1 adipocytes and C2C12 myotubes.** 3T3-L1 adipocytes and C2C12 myotubes were treated with icaritin (0, 0.7, 2.2, 6.7, or 20  $\mu$ M) for 24 h. (A–C) Icaritin increased the expression of p62 and decreased LC3II/LC3I to some extent in 3T3-L1 adipocytes, as detected by western blotting. (D–F) Icaritin increased the expression of p62 and decreased LC3II/LC3I to some extent in C2C12 myotubes, as detected by western blotting. Values are presented as mean  $\pm$  standard deviation ( $n=3$ ). \* $p<0.05$ ; \*\* $p<0.01$ ; \*\*\* $p<0.001$  vs. untreated cells. Abbreviation: GAPDH, glyceraldehyde 3-phosphate dehydrogenase.

cytes and C2C12 myotubes. Our results demonstrated that icaritin does attenuate lipid accumulation through increasing energy expenditure, making it a promising candidate for NAFLD.

As a well-recognized energy sensor, AMPK is in the central position of energy status in the eukaryotic cytoplasm, which activates multiple signaling pathways to regulate mitochondrial function.<sup>13</sup> It is worth noting that enhancing AMPK activity has been considered a feasible strategy for increasing energy expenditure and improving NAFLD.<sup>14</sup> Our study demonstrated that icaritin activates the LKB1/AMPK/ACC pathway. Interestingly, it also decreased the constitutive expression of AMPK $\alpha$ . Decreased expression of AMPK $\alpha$  may be compensation or adaptation to the changed energy metabolism due to changed cellular status.<sup>15</sup> Chronic energy imbalance is the common ground for many metabolic diseases, such as obesity, type 2 diabetes mellitus, and NAFLD. Since icaritin can increase energy expenditure by activating AMPK, we hypothesized that it may be a promising candidate for these metabolic diseases, including NAFLD.

Autophagy acts as a dynamic recycling system to generate new components and energy for cell repair and energy homeostasis.<sup>16</sup> Autophagy stimulates cholesterol efflux, which in turn inhibits lipid accumulation.<sup>17</sup> Our results showed that icaritin regulates autophagy according to the cellular status. Icaritin increased autophagy in 3T3-L1 preadipocytes and C2C12 myoblasts. Similar to our results, icaritin induced autophagy in human GBM cell line U87 cells at 10 and 20  $\mu$ M.<sup>18</sup> The process between fusing with the lysosome and then degrading is termed as “the initiation of autophagy”.<sup>19</sup> CQ has been widely used to inhibit the last stage of autophagy, functioning through blocking lysosomal degradation.<sup>19</sup> Our results showed that the LC3 puncta were significantly increased in both 3T3-L1 preadipocytes and C2C12 myoblasts when treated with icaritin and CQ. Our results, thus, indicate that icaritin promotes the initiation of autophagy. However, activating autophagy also poses some risks since excess autophagy

induces cell death.<sup>20</sup> Icaritin rescued 3T3-L1 adipocytes and C2C12 myotubes out of this danger, which reduced the autophagy to a normal level. Fig. 8 summarizes our findings.

Our study has a couple of limitations. The effects of icaritin on lipid accumulation were explored by *in vitro* experiments, which should be further confirmed in animal models. Besides energy expenditure, whether or not icaritin decreases energy intake should also be explored in animal models. Dysregulated autophagy leads to both impaired mitochondrial biogenesis and mitochondrial dysfunction. The effects of icaritin on mitochondrial dysfunction should be measured in further studies.

In conclusion, our study demonstrated that icaritin attenuates lipid accumulation by enhancing energy expenditure and regulating autophagy. These effects were induced by activating the LKB1/AMPK/ACC pathway.

## Acknowledgments

Huh-7 cells were a kind gift from Prof. Lang Bai of West China Hospital, Sichuan University.

## Funding

This work was financially supported by the National Natural Science Foundation of China (Grant No. 81770580) and open funding from the Sichuan Provincial Key Laboratory of Radiation Oncology (Grant No. 2020FSZX-02).

## Conflict of interest

The authors declare that they have no conflicts of interest

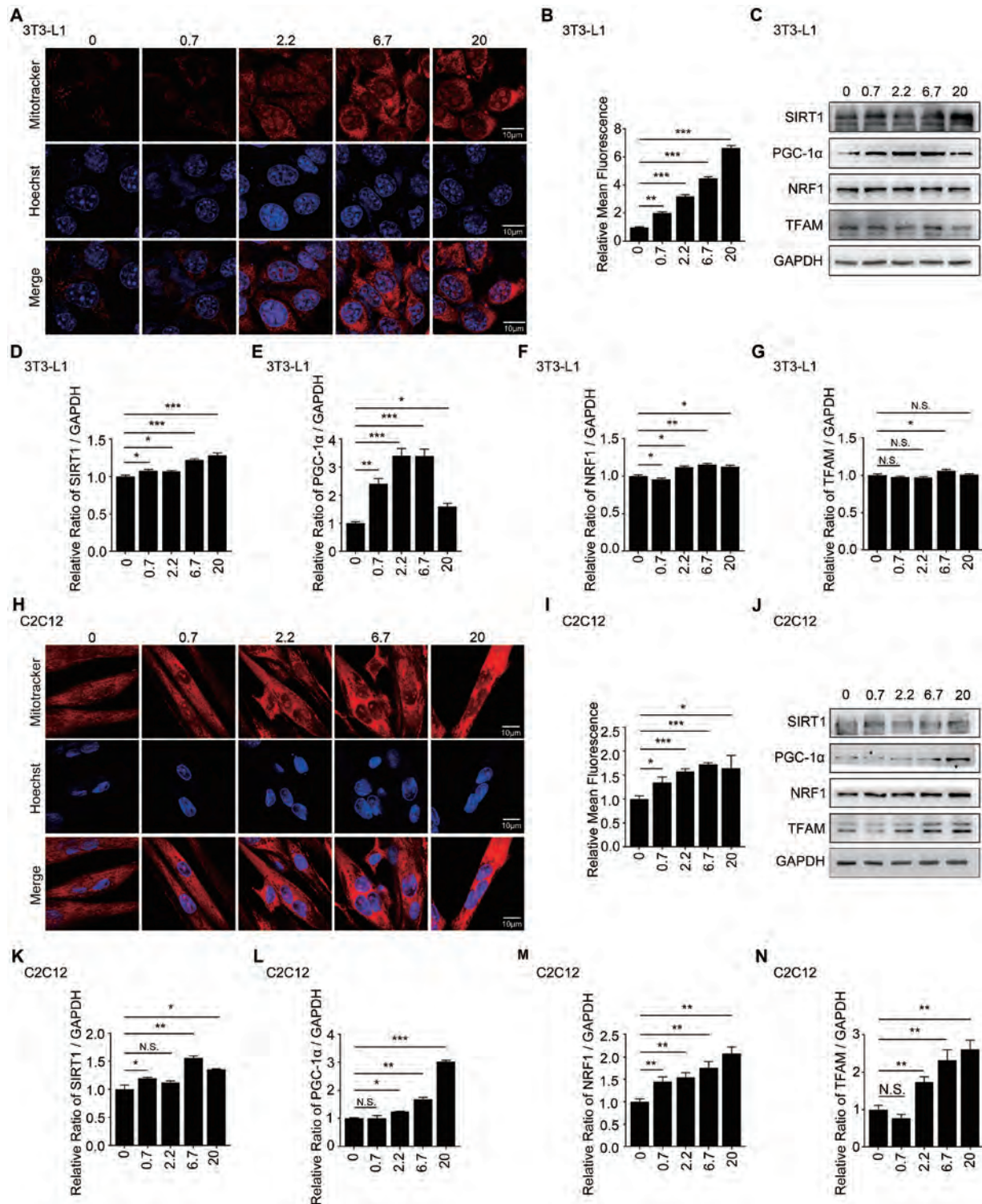


**Fig. 7. Icaritin promoted mitochondria biogenesis of 3T3-L1 adipocytes and C2C12 myotubes.** 3T3-L1 adipocytes and C2C12 myotubes were treated with icaritin (0, 0.7, 2.2, 6.7, or 20 μM) for 24 h. (A, B) Icaritin enhanced the mitochondria biogenesis of 3T3-L1 adipocytes, as detected by MitoTracker Orange staining (red). (C–G) Expression of SIRT1, PGC-1α, NRF1, and TFAM was increased by icaritin in 3T3-L1 adipocytes, as detected by western blotting. Icaritin enhanced the ratio of SIRT1/GAPDH, PGC-1α/GAPDH, NRF1/GAPDH, and TFAM/GAPDH in 3T3-L1 adipocytes. (H, I) Icaritin enhanced mitochondria biogenesis of C2C12 myotubes, as detected by MitoTracker Orange staining (red). (J–N) Icaritin enhanced the ratio of SIRT1/GAPDH, PGC-1α/GAPDH, NRF1/GAPDH, and TFAM/GAPDH in C2C12 myotubes. Values are presented as mean±standard deviation ( $n=3$ ). \* $p<0.05$ ; \*\* $p<0.01$ ; \*\*\* $p<0.001$  vs. untreated cells. Abbreviations: GAPDH, glyceraldehyde 3-phosphate dehydrogenase; NRF1, nuclear respiratory factor 1; PGC-1α, peroxisome proliferator-activated receptor gamma coactivator 1-alpha; SIRT1, silent mating type information regulation 2 homolog 1; TFAM, transcription factor A.

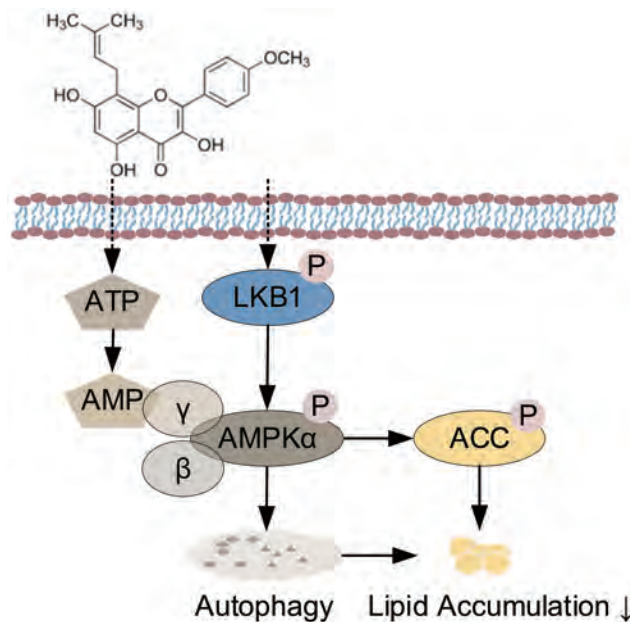


**Fig. 8. Proposed mechanisms of icaritin on lipid accumulation.** Icaritin attenuates lipid accumulation by enhancing energy expenditure and regulating autophagy. These effects were induced by activating the LKB1/AMPK/ACC pathway. Abbreviations: ACC, Acetyl-CoA carboxylase; AMPK, adenosine 5'-monophosphate-activated protein kinase; LKB1, liver kinase B1.

related to this publication.

## Author contributions

Optimized and performed the experiments (YW, YY, FL), drafted the manuscript (YW) performed the immunofluorescence experiment (JZ, YHW, MXX), helped with part of the experimentation (YLW, RXL, YTS) optimized the experiments (SL), designed the study and edited the manuscript (YYZ, XDS). All authors analyzed the data and contributed to the study.

## Data sharing statement

All data are available upon request.

## References

- [1] Younossi ZM. Non-alcoholic fatty liver disease - a global public health perspective. *J Hepatol* 2019; 70(3):531–544. doi:10.1016/j.jhep.2018.10.033.
- [2] Duvnjak M, Stojaković S, Jukić LV, Duvnjak LS. Risk factors for colorectal adenoma - acknowledging the burden of NAFLD. *J Clin Transl Hepatol* 2019; 7(2):97–98. doi:10.14218/JCTH.2019.00022.
- [3] van Herpen NA, Schrauwen-Hinderling VB. Lipid accumulation in non-adipose tissue and lipotoxicity. *Physiol Behav* 2008; 94(2):231–241. doi:10.1016/j.physbeh.2007.11.049.
- [4] Luo L, Liu M. Adipose tissue in control of metabolism. *J Endocrinol* 2016; 231(3):R77–R99. doi:10.1530/JOE-16-0211.
- [5] Adams LA, Angulo P. Treatment of non-alcoholic fatty liver disease. *Postgrad Med J* 2006; 82(967):315–322. doi:10.1136/pgmj.2005.042200.
- [6] Wu T, Shu T, Kang L, Wu J, Xing J, Lu Z, *et al*. Icaritin, a novel plant-derived osteoinductive agent, enhances the osteogenic differentiation of human bone marrow- and human adipose tissue-derived mesenchymal stem cells. *Int J Mol Med* 2017; 39(4):984–992. doi:10.3892/ijmm.2017.2906.
- [7] Wang M, Gao H, Li W, Wu B. Icaritin and its metabolites regulate lipid metabolism: from effects to molecular mechanisms. *Biomed Pharmacother* 2020; 131:110675. doi:10.1016/j.biopha.2020.110675.
- [8] Zhang G, Qin L, Sheng H, Wang XL, Wang YX, Yeung DK, *et al*. A novel semisynthesized small molecule icaritin reduces incidence of steroid-associated osteonecrosis with inhibition of both thrombosis and lipid-deposition in a dose-dependent manner. *Bone* 2009; 44(2):345–356. doi:10.1016/j.bone.2008.10.035.
- [9] Govender T, Ramanna L, Rawat I, Bux F. BODIPY staining, an alternative to the Nile Red fluorescence method for the evaluation of intracellular lipids in microalgae. *Bioresour Technol* 2012; 114:507–511. doi:10.1016/j.biortech.2012.03.024.
- [10] Agnello M, Morici G, Rinaldi AM. A method for measuring mitochondrial mass and activity. *Cytotechnology* 2008; 56(3):145–149. doi:10.1007/s10616-008-9143-2.
- [11] Kuroda S, Yamazaki M, Abe M, Sakimura K, Takayanagi H, Iwai Y. Basic leucine zipper transcription factor, ATF-like (BATF) regulates epigenetically and energetically effector CD8 T-cell differentiation via Sirt1 expression. *Proc Natl Acad Sci USA* 2011; 108(36):14885–14889. doi:10.1073/pnas.1105133108.
- [12] Su YC, Hong JR. Betanodavirus B2 causes ATP depletion-induced cell death via mitochondrial targeting and complex II inhibition in vitro and in vivo. *J Biol Chem* 2010; 285(51):39801–39810. doi:10.1074/jbc.M110.164988.
- [13] Hardie DG, Ross FA, Hawley SA. AMPK: a nutrient and energy sensor that maintains cellular homeostasis. *Nat Rev Mol Cell Biol* 2012; 13(4):251–262. doi:10.1038/nrm3311.
- [14] Smith BK, Marcinko K, Desjardins EM, Lally JS, Ford RJ, Steinberg GR. Treatment of nonalcoholic fatty liver disease: role of AMPK. *Am J Physiol Endocrinol Metab* 2016; 311(4):E730–E740. doi:10.1152/ajpendo.00225.2016.
- [15] Viana AY, Sakoda H, Anai M, Fujishiro M, Ono H, Kushiya A, *et al*. Role of hepatic AMPK activation in glucose metabolism and dexamethasone-induced regulation of AMPK expression. *Diabetes Res Clin Pract* 2006; 73(2):135–142. doi:10.1016/j.diabres.2005.12.011.
- [16] Mizushima N, Komatsu M. Autophagy: renovation of cells and tissues. *Cell* 2011; 147(4):728–741. doi:10.1016/j.cell.2011.10.026.
- [17] Filfan M, Sandu RE, Zăvăleanu AD, Greșit A, Glăvan DG, Olaru DG, *et al*. Autophagy in aging and disease. *Rom J Morphol Embryol* 2017; 58(1):27–31.
- [18] Li Z, Meng X, Jin L. Icaritin induces apoptotic and autophagic cell death in human glioblastoma cells. *Am J Transl Res* 2016; 8(11):4628–4643.
- [19] Mauthe M, Orhon I, Rocchi C, Zhou X, Luhr M, Hijlkema KJ, *et al*. Chloroquine inhibits autophagic flux by decreasing autophagosome-lysosome fusion. *Autophagy* 2018; 14(8):1435–1455. doi:10.1080/15548627.2018.1474314.
- [20] Levine B, Kroemer G. Autophagy in the pathogenesis of disease. *Cell* 2008; 132(1):27–42. doi:10.1016/j.cell.2007.12.018.





Original Article

# Predictive Value of Inflammation Biomarkers in Patients with Portal Vein Thrombosis

Jian-Bo Han<sup>#</sup>, Qing-Hua Shu<sup>#</sup>, Yu-Feng Zhang<sup>\*</sup> and Yong-Xiang Yi<sup>\*</sup>

Department of Hepatopancreatobiliary Surgery, The Second Hospital of Nanjing, Nanjing University of Chinese Medicine, Nanjing, Jiangsu, China

Received: 11 December 2020 | Revised: 9 February 2021 | Accepted: 26 February 2021 | Published: 30 March 2021

## Abstract

**Background and Aims:** To investigate the usefulness of inflammation biomarkers to serve as predictors of portal vein thrombosis (PVT) postoperatively (post) in patients with portal hypertension after splenectomy and periesophagogastric devascularization. **Methods:** A total of 177 liver cirrhosis patients were recruited from January 2013 to December 2017. They were divided into a PVT group ( $n=71$ ) and a non-PVT group ( $n=106$ ), according to ultrasound examination findings at 7-day post. Inflammation biomarkers involving platelet-to-lymphocyte ratio (PLR), neutrophil-to-lymphocyte ratio (NLR), monocyte-to-lymphocyte ratio (MLR), red blood cell distribution width-to-platelet ratio (RPR), mean platelet volume-to-platelet ratio (MPR) preoperatively (pre) and at 1, 3, 7-days post were recorded. **Results:** The univariate logistic regression analysis indicated that PLR (pre) (odds ratio (OR)=3.963, 95% confidence interval (CI)=2.070–7.587,  $p<0.000$ ), MLR (pre) (OR=2.760, 95% CI=1.386–5.497,  $p=0.004$ ), PLR (post-day 7) (OR=3.345, 95% CI=1.767–6.332,  $p=0.000$ ) were significantly associated with the presence of PVT. The multivariate logistic regression analysis results indicated that PLR (pre) (OR=3.037, 95% CI=1.463–6.305,  $p=0.003$ ), MLR (pre) (OR=2.188, 95% CI=1.003–4.772,  $p=0.049$ ), PLR (post-day 7) (OR=2.166, 95% CI=1.053–4.454,  $p=0.036$ ) were independent factors for predicting PVT. **Conclusions:** The PLR (pre), MLR (pre), and PLR (post-day 7) are predictors of portal vein thrombosis post in patients with portal hypertension after splenectomy and periesophagogastric devascularization.

**Citation of this article:** Han JB, Shu QH, Zhang YF, Yi YX. Predictive value of inflammation biomarkers in patients with portal vein thrombosis. J Clin Transl Hepatol 2021;9(3):384–391. doi: 10.14218/JCTH.2020.00159.

**Keywords:** Inflammation biomarker; Thrombosis; Splenectomy; Portal vein.

**Abbreviations:** AUC, area under the curve; CI, confidence interval; CTP, Child-Turcotte-Pugh; MELD, model for end-stage liver disease; MLR, monocyte-to-lymphocyte ratio; MPR, mean platelet volume-to-platelet ratio; NLR, neutrophil-to-lymphocyte ratio; OR, odds ratio; PLR, platelet-to-lymphocyte ratio; PLT, platelet; PNI, prognostic nutritional index; post, postoperatively; pre, preoperatively; PVT, portal vein thrombosis; RPR, red blood cell distribution width-to-platelet ratio; WBC, white blood cell.

<sup>#</sup>These two authors contributed equally to this study.

**\*Correspondence to:** Yu-Feng Zhang and Yong-Xiang Yi, Department of Hepatopancreatobiliary Surgery, The Second Hospital of Nanjing, Nanjing University of Chinese Medicine, No. 1 Zhongfu Road, Nanjing, Jiangsu 210003, China. Tel/Fax: +86-25-83626570, E-mail: znn9053@sina.com (YFZ) and sygyssqh@sina.com (YXY)

## Introduction

Splenectomy and periesophagogastric devascularization is one of the main procedures for the management of portal hypertension and hypersplenism, especially for patients with variceal bleeding. The incidence of portal vein thrombosis (PVT) after such surgery can be as high as 6.3%–39.0%.<sup>1</sup> PVT is characterized by partial or total occlusion of the portal vein, with the presence of solid intraluminal material. It can elevate the resistance to portal inflow as the portal venous pressure is increased. Consequently, liver function becomes deteriorated due to the decreased blood flow to the liver. It also shows increased rate of re-bleeding and aggravated progression of bleeding.<sup>2,3</sup> The rate of bleeding in liver cirrhosis patients with PVT is higher than in those without PVT.<sup>4</sup> Besides these harmful effects, PVT even influences the eligibility for liver transplantation, since it makes the operative technique more complicated and decreases the 1-year survival rate of the recipient.<sup>5,6</sup>

Vascular endothelial injury, blood flow alteration, and prothrombotic condition are the three major determinants of venous thrombosis, described as Virchow's triad.<sup>7</sup> Previous research has indicated that a higher model for end-stage liver disease (MELD) score, wider splenic vein diameter, increased antithrombin III concentration and prolonged prothrombin time are risk factors of PVT after splenectomy in patients with liver cirrhosis.<sup>8–11</sup>

However, an accumulation of evidence suggests that systemic inflammatory response is associated with the development of venous thrombosis.<sup>12–17</sup> Some inflammation biomarkers involving platelet-to-lymphocyte ratio (PLR), lymphocyte-to-monocyte ratio (LMR), and neutrophil-to-lymphocyte ratio (NLR) have been demonstrated to be useful in predicting venous thromboembolism (deep vein thrombosis of the lower limbs and/or pulmonary embolism or cerebral vein thrombosis).<sup>18–21</sup> Another series of an index involving the monocyte-to-lymphocyte ratio (MLR), NLR, prognostic nutritional index (PNI), red blood cell distribution width-to-platelet ratio (RPR), and mean platelet volume-to-platelet ratio (MPR) consists of inflammation response biomarkers associated with the prognostic of inflammatory disease, viral infection disease, coronary artery disease, and malignant tumor.<sup>18–24</sup> However, whether these inflammation biomarkers are able to detect the probability of PVT formation is still unclear.

In previous studies, inflammation biomarkers were not dynamically observed, and the surgery itself may cause the ongoing inflammatory response resulting in change of these markers. In this study, inflammatory biomarkers were de-

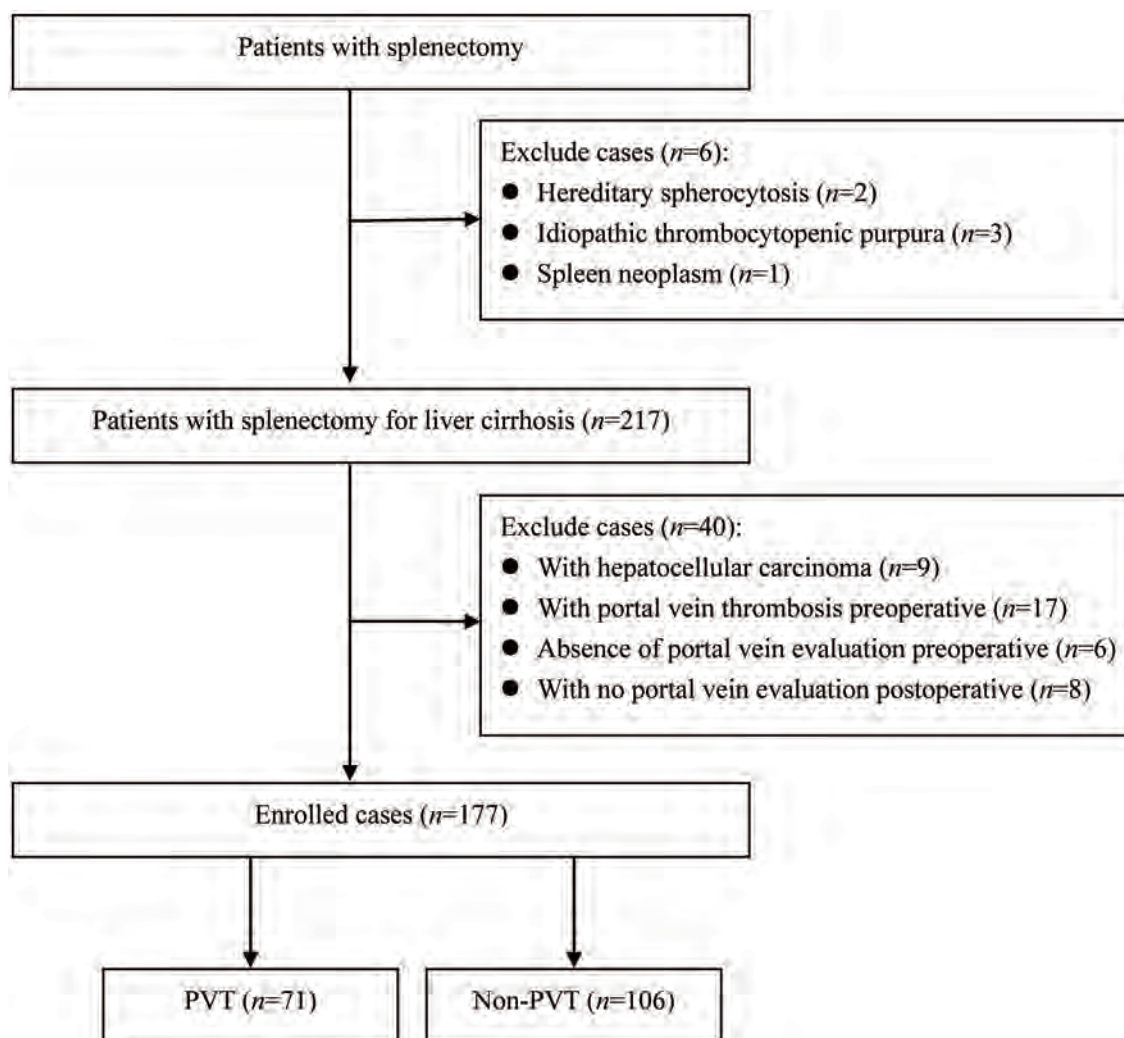


Fig. 1. Flow diagram of the study population. PVT, portal vein thrombosis.

tested at certain times before and after surgery. We aimed to determine whether these inflammation biomarkers could serve as predictors of PVT in liver cirrhosis patients with portal hypertension after splenectomy and periesophagegastic devascularization.

## Methods

### Patients

We conducted a retrospective analysis of the patients consecutively admitted to the Hospital for portal hypertension, who had been diagnosed according to the following criteria: hypersplenism (platelet count  $<100 \times 10^9/L$ ) or gastroesophageal varices between the dates of January 2013 to December 2017 (Fig. 1). All selected patients had undergone splenectomy combined with periesophagegastic devascularization. Exclusion criteria were as follows: 1) liver tumor; 2) liver cirrhosis patients associated with preoperative PVT; 3) liver cirrhosis patients associated with congenital thrombotic disease or hematopoietic disease; 4) use of anticoagulation or anti-inflammation drugs; 5) severe organ

dysfunction; or 6) incomplete clinical information. Before surgical procedures, all patients or their relatives provided informed consent and the investigation was carried out in line with the principles of the Declaration of Helsinki (as revised in Fortaleza, Brazil, October 2013). The Ethics Committee of the Second Hospital of Nanjing approved the study protocol.

### Laboratory tests

Blood specimens were collected from the peripheral vein. Data collected from blood tests included assessment of liver function, renal function, coagulation parameters, etiology of liver disease, and blood morphology. Electrocardiography, chest radiography, ultrasound examination, endoscopy of the upper gastrointestinal tract, and contrast-enhanced spiral computed tomography were performed on each patient before the operation. Cirrhosis was confirmed by pathological investigation postoperatively (post). The severity of cirrhosis was evaluated by the MELD and Child-Turcotte-Pugh (CTP) scores. Blood tests, including assessment of liver function, renal function, blood coagulation, and blood morphology, were conducted again on days 1, 3, and 7 after

the operation. Two independent radiologists evaluated the presence and extent of PVT, velocity of portal blood flow of PVT preoperatively (pre) and at day 7 post by color Doppler ultrasound examination. Besides, the basic demographic and clinical characteristics (age, gender, body mass index), etiology of liver cirrhosis, and emergency surgery were also recorded.

## Definitions

PLR was defined as the absolute platelet count divided by lymphocyte count ( $10^9/L$ ). NLR was the ratio of absolute neutrophils count to lymphocyte count ( $10^9/L$ ). MLR was calculated as absolute monocyte count divided by lymphocyte ratio count ( $10^9/L$ ), and the MPR as mean platelet volume divided by platelet count ( $10^9/L$ ). While RPR referred to the ratio of red cell distribution width to platelet count ( $10^9/L$ ). PNI was calculated as albumin (g/L) + 5 × total lymphocyte count ( $10^9/L$ ).<sup>20</sup>

## Operation

Although the standard surgical procedure of splenectomy with periesophagogastric devascularization has been commonly described, we still need to make a brief statement. The open operation was performed by using an extended left subcostal incision. The routine splenectomy was firstly performed, and then periesophagogastric devascularization was performed. Firstly, the gastric branch of the right gastric vein near the gastric angular incisura and small branches of the gastric coronary veins were disconnected. Secondly, the esophageal branch (i.e. esophageal branch of the gastric coronary vein; high esophageal branch of the gastric coronary vein; aberrant high esophageal branch of the gastric coronary vein) was disconnected and suture-ligated, involving up to 10 cm of the esophageal inferior segment. The gastric posterior veins and short gastric veins were disconnected, and then the left subphrenic vein was also disconnected. In addition, the corresponding arteries, including the left gastric artery, left gastroepiploic artery, gastric posterior artery, and left subphrenic artery, were also ligated.

## Statistical analysis

The measurement data were presented as mean ± standard deviation (normal distribution). Statistically significant differences were evaluated with Student's *t*-test (normal distribution). Qualitative data were summarized as *n* (%), and statistically significant differences were evaluated using the chi-square test. Receiver operating characteristic curves were constructed to assess the indicative values of the inflammation biomarkers. The areas under the curves (AUCs) were calculated with 95% confidence intervals (CIs). The Youden index was applied to determine the optimal cutoff value for every indicator. Significant variables of PVT from univariate analysis were included in multivariate analysis when performing forward stepwise logistic regression modeling. Data were analyzed by SPSS version 16 (SPSS Inc., Chicago, IL, USA). A *p*-value of less than 0.05 was considered statistically significant.

## Results

We collected data for 223 patients with splenectomy. In total, 46 patients were excluded for the following reasons:

hematopoietic disease (*n*=6); liver tumor (*n*=9); PVT pre (*n*=17); no portal vein evaluation pre and post (*n*=14). Finally, 177 patients who meet the criteria were enrolled in this study. The patients were divided into the PVT group (*n*=71) and the non-PVT group (*n*=106) according to the finding of PVT post. Baseline characteristics and clinical and laboratory parameters of the two groups are presented in Table 1. There were no significant differences between the two groups, with respect to gender, body mass index, etiology of liver cirrhosis, emergency surgery, portal blood flow velocity, CTP score, and MELD score.

Significant differences in basic characteristics of the patients, including age (*p*=0.027), PLR (*p*=0.007), NLR (*p*=0.035), MLR (*p*=0.037), and lymphocyte count (*p*=0.002), were observed between the two groups. On day 3 post, the PLR of the PVT group was higher than that of the non-PVT group (*p*=0.027). In day 7 post, PLR (*p*=0.001), MLR (*p*=0.023), PLT (*p*=0.030), and lymphocyte count (*p*=0.009) were significantly different among the groups. The data are illustrated in Table 2.

Youden index analysis showed the optimal cutoff points for NLR (pre), PLR (post-day 3), MLR (post-day 7), and PLT (post-day 7) were 3.7, 139, 1.055, and 263.5, respectively. The cutoff value for PLR (pre) was 70.5, with a sensitivity of 0.714 and a specificity of 0.614. The cutoff value for MLR (pre) was 0.295, with a sensitivity of 0.783 and a specificity of 0.434. The cutoff value for PLR (post-day 7) was 230.5, with a sensitivity of 0.657 and a specificity of 0.647 (Table 3). Receiver operating characteristic curve analysis identified the AUC for PLR (pre), MLR (pre), PLR (post-day 7), and PLR (pre) combined with MLR (pre) as 0.665, 0.618, 0.655, and 0.697, respectively (Fig. 2). Obviously, they were all better than the AUC values for NLR (pre) (0.600), PLR (post-day 3) (0.595), MLR (post-day 7) (0.607), and PLT (post-day 7) (0.604).

The univariate logistic regression analysis indicated that age [odds ratio (OR)=1.958, 95% CI=1.051–3.647, *p*=0.034], NLR (pre) (OR=2.969, 95% CI=1.417–6.220, *p*=0.004), PLR (pre) (OR=3.963, 95% CI=2.070–7.587, *p*<0.000), MLR (pre) (OR=2.760, 95% CI=1.386–5.497, *p*=0.004), PLR (post-day 3) (OR=2.615, 95% CI=1.342–5.098, *p*=0.005), PLR (post-day 7) (OR=3.345, 95% CI=1.767–6.332, *p*=0.000), MLR (post-day 7) (OR=2.567, 95% CI=1.312–5.022, *p*=0.006), and PLT (post-day 7) (OR=2.437, 95% CI=1.313–4.527, *p*=0.005) were significantly associated with the presence of PVT.

Multivariate logistic regression analysis was conducted to verify the predictive value of the factors including age, NLR (pre), PLR (pre), MLR (pre), PLR (post-day 3), PLR (post-day 7), MLR (post-day 7), and PLT (post-day 7). The results indicated that PLR (pre) (OR=3.037, 95% CI=1.463–6.305, *p*=0.003), MLR (pre) (OR=2.188, 95% CI=1.003–4.772, *p*=0.049), and PLR (post-day 7) (OR=2.166, 95% CI=1.053–4.454, *p*=0.036) were independent factors for predicting PVT (Table 4).

According to the cutoff values for PLR (pre) and MLR (pre), the patients were divided into the following three groups: PLR (pre) ≤70.5 with MLR (pre) ≤0.295; PLR (pre) ≤70.5 with MLR (pre) > 0.295 or PLR (pre) >70.5 with MLR (pre) ≤0.295; and, PLR (pre) >70.5 with MLR (pre) > 0.295. PLR (pre) ≤70.5 with MLR (pre) ≤0.295 was selected as reference. Multivariate logistic regression analysis was performed and showed that PLR (pre) >70.5 and MLR (pre) >0.295 were associated with the greatest predictive value between the three groups (Table 5).

## Discussion

PVT after splenectomy and periesophagogastric devascu-



**Table 1. Demographic and clinical characteristics of the study population at baseline**

Variable	PVT, <i>n</i> =71	Non-PVT, <i>n</i> =106	<i>p</i> -value
Age in years	45.90±9.50	49.36±10.48	0.027
Gender, male/female	51/20	68/38	0.286
BMI	23.29±2.88	22.94±3.22	0.478
Etiology, hepatitis B/others	62/9	87/19	0.348
Emergency surgery, yes/no	23/48	26/80	0.252
Velocity of portal blood flow in cm/s	18.33±4.87	17.85±5.34	0.598
Thickness of spleen in mm	61.56±12.59	58.31±15.28	0.184
Longitudinal diameter of spleen in mm	184.84±31.55	169.81±22.87	0.053
CTP score, A/B/C	53/18/0	75/31/0	0.570
MELD score	10.94±2.37	10.77±2.36	0.639
PT in s	15.83±2.04	15.56±2.25	0.423
TBIL in µmol/L	22.88±13.20	23.52±11.64	0.732
DBIL in µmol/L	9.24±5.49	10.95±6.76	0.079
ALB in g/L	37.21±5.07	36.43±5.51	0.345
GLB in g/L	25.77±4.79	27.13±6.92	0.152
AKP in U/L	145.61±53.14	85.42±40.41	0.348
GGT in U/L	143.38±47.89	134.29±73.39	0.299
ACE	3,876.00±1,320.28	3,866.90±1,398.56	0.966
BUN in mmol/L	5.65±2.36	6.73±7.48	0.244
Cr in µmol/L	65.54±15.42	62.97±18.62	0.341
INR	1.37±0.17	1.34±0.20	0.278

ACE, acetylcholinesterase; AKP, alkaline phosphatase; ALB, albumin; BMI, body mass index; BUN, blood urea nitrogen; Cr, creatine; DBIL, direct bilirubin; GGT, glutamyl transpeptidase; GLB, globulin; INR, international normalized ratio; PT, prothrombin time; TBIL, total bilirubin.

larization is a life-threatening complication for its serious consequences involving the increased rate of re-bleeding, complicated liver transplantation technique, and deterioration of liver function.<sup>25</sup> The relationship between venous thromboembolism and inflammation response has been controversial, with it being unknown whether inflammation is casual in the development of venous thrombosis or instead a consequence of venous thrombosis. A growing body of data suggests that inflammation plays a vital role in the pathogenesis of venous thromboembolism.<sup>13–17</sup> The inflammatory process can influence coagulation from the following three aspects: down-regulation of physiological anticoagulant pathways, inhibition of fibrin removal, and initiation of coagulation activation.<sup>26</sup> This would result in the shift of hemostatic balance toward a prothrombotic state. Besides, inflammation may increase the damage of endothelial cells. Some inflammatory biomarkers, such as PLR, NLR, and LMR, have been confirmed as useful predictive measures of deep vein thrombus.<sup>27–30</sup>

There is no significant difference with respect to pre platelet count and monocyte count between the PVT group and the non-PVT group. Elevated levels of pre PLR and MLR in the PVT group primarily result from a decreased number of lymphocytes compared with that in the control group. The lymphocyte is the major cell component of the immune system that represents the immunomodulatory pathway and plays a crucial role in regulating systemic inflammation.<sup>31</sup> As systemic inflammation worsens, peripheral lymphocyte count becomes reduced as a result of cell apoptosis, necrosis, and redistribution. In hepatitis B virus-related acute-on-chronic liver failure, systemic inflammation is the

result of depletion in circulating lymphocytes.<sup>32</sup> The lymphocyte count in the PVT group of our study was lower than that of the control group, indicating suppressed immunity. We hypothesized that the intestinal lumen bacterial products penetrated into the circulation in patients with advanced cirrhosis and portal hypertension due to depressed immunity. The combination of bacterial distribution and suppressed immunity ultimately may result in more critical portal vein and systemic inflammation in the PVT group. The inflammation of the vessel wall will initiate thrombus formation.

The elevated level of PLR (post-day 7) may primarily result from an increased platelet count and a decreased lymphocyte count compared to counts in the control group. We found the platelet count to be increasing gradually after splenectomy, and the platelet count of the PVT group in the 7-day post group to be significantly higher than that of the non-PVT group; there were no significant differences for that between the groups at pre and post-day 1 or post-day 3. Evidence suggest that platelets play a less important role in venous thrombosis than in arterial thrombosis. This was supported by the findings from pathological analysis, which showed the arterial thrombi to mainly consist of platelets and the venous thrombi to mainly consist of red blood cells and fibrin, at least initially. The involvement of platelets in the formation of venous thrombosis is slight at an early stage; at a later stage, platelets appear to play a slightly more major role because the subsequent layers of venous thrombi contain some platelets.<sup>14</sup> To concretely determine the roles of platelets in the formation of venous thrombosis more research is needed. This may be helpful for clinical

Table 2. Characteristics of inflammation biomarkers at pre and post-days 1, 3, and 7

Variables	PVT (pre)	Non-PVT (pre)	P-value	PVT (post-D1)	Non-PVT (post-D1)	p-value
WBC as 10 <sup>9</sup> /L	2.60±2.40	2.66±1.75	0.867	17.61±6.92	16.96±6.80	0.537
Neutrophils as 10 <sup>9</sup> /L	1.82±2.14	1.69±1.41	0.609	15.55±6.53	15.06±6.47	0.623
Lymphocytes as 10 <sup>9</sup> /L	0.51±0.25	0.67±0.37	0.002	0.69±0.45	0.65±0.37	0.526
Monocytes as 10 <sup>9</sup> /L	0.22±0.14	0.23±0.14	0.720	1.29±0.76	1.20±0.63	0.403
PLT as 10 <sup>9</sup> /L	44.39±25.68	43.74±24.90	0.869	83.01±29.72	82.69±30.02	0.944
PNI	39.86±5.06	39.62±6.02	0.780	39.48±4.50	38.59±4.55	0.205
PLR	92.61±43.68	73.72±46.13	0.007	175.92±176.30	168.51±112.74	0.735
NLR	3.63±3.21	2.70±2.18	0.035	37.78±59.96	32.26±29.37	0.421
MLR	0.46±0.25	0.38±0.24	0.037	2.69±2.62	2.36±1.87	0.322
RPR	0.49±0.23	0.47±0.21	0.411	0.25±0.14	0.23±0.12	0.307
MPR	0.30±0.14	0.32±0.17	0.334	0.180±0.181	0.16±0.08	0.376

Variables	PVT (post-D3)	Non-PVT (post-D3)	p-value	PVT (post-D7)	Non-PVT (post-D7)	p-value
WBC as 10 <sup>9</sup> /L	13.64±4.75	14.03±5.04	0.608	11.30±4.20	11.65±4.96	0.628
Neutrophils as 10 <sup>9</sup> /L	11.21±4.40	11.49±4.70	0.688	8.45±3.67	8.64±4.45	0.770
Lymphocytes as 10 <sup>9</sup> /L	0.84±0.43	0.93±0.51	0.266	1.00±0.41	1.19±0.52	0.009
Monocytes as 10 <sup>9</sup> /L	1.37±0.65	1.36±0.63	0.927	1.45±0.69	1.39±0.67	0.552
PLT as 10 <sup>9</sup> /L	143.35±54.45	130.39±64.60	0.162	275.17±122.08	233.98±123.30	0.030
PNI	39.59±3.69	40.09±4.55	0.458	40.56±4.19	40.75±5.50	0.811
PLR	230.60±160.50	182.03±121.49	0.027	319.23±192.50	223.99±137.22	0.001
NLR	17.19±11.53	15.44±10.42	0.311	9.16±4.74	8.34±5.38	0.301
MLR	2.04±1.23	1.77±1.25	0.166	1.60±0.87	1.31±0.77	0.023
RPR	0.147±0.083	0.153±0.089	0.651	0.08±0.05	0.10±0.08	0.155
MPR	0.096±0.062	0.108±0.057	0.214	0.05±0.04	0.07±0.05	0.071

WBC, white blood cell count.

cians to determine when and which anticoagulation therapy should be recommended. The result indicates that taking an anti-platelet drug from the post-day 7 time point should be an alternative.

The use of anticoagulation for PVT is strongly recommended because of the fact that spontaneous recanalization of PVT rarely happens; however, this therapy is associated with anticoagulation-related bleeding. Which subgroup of patients who undergo surgery and will benefit most from anticoagulant therapy remains an unresolved issue. Early selection of appropriate patients is critical. The two inflammation biomarkers, pre PLR and MLR, are significantly asso-

ciated with a diagnosis of PVT. Further analysis demonstrated that with a combination index of pre PLR >70.5 and MLR >0.295, the risk of PVT increased 8.148-fold compared with that of PLR ≤70.5 and MLR ≤0.295. Patients with PLR >70.5 and MLR >0.295 are at high risk for development of post PVT. The increased PLR and MLR preoperatively may reflect a serious thrombus burden. As the thrombus burden becomes aggravated, the risk of PVT becomes increased. This contributes to enhancing our ability to identify the high-risk population and provide a bias for clinic intervention at an early stage. Resveratrol has been demonstrated to reduce the incidence of PVT after splenectomy in an animal model,

Table 3. Receiver operating characteristics curve of predictive variables for patients with PVT

Variable	Cutoff value	AUC (95%CI)	Sensitivity, %	Specificity, %	p-value
NLR (pre)	3.7	0.600 (0.515–0.685)	32.9	85.8	0.025
PLR (pre)	70.5	0.665 (0.585–0.746)	71.4	61.4	0.000
MLR (pre)	0.295	0.618 (0.534–0.703)	78.3	43.4	0.008
PLR (post-day 3)	139	0.595 (0.508–0.682)	73.1	48	0.037
PLR (post-day 7)	230.5	0.655 (0.571–0.739)	65.7	64.7	0.001
MLR (post-day 7)	1.055	0.607 (0.523–0.692)	75.4	45.6	0.017

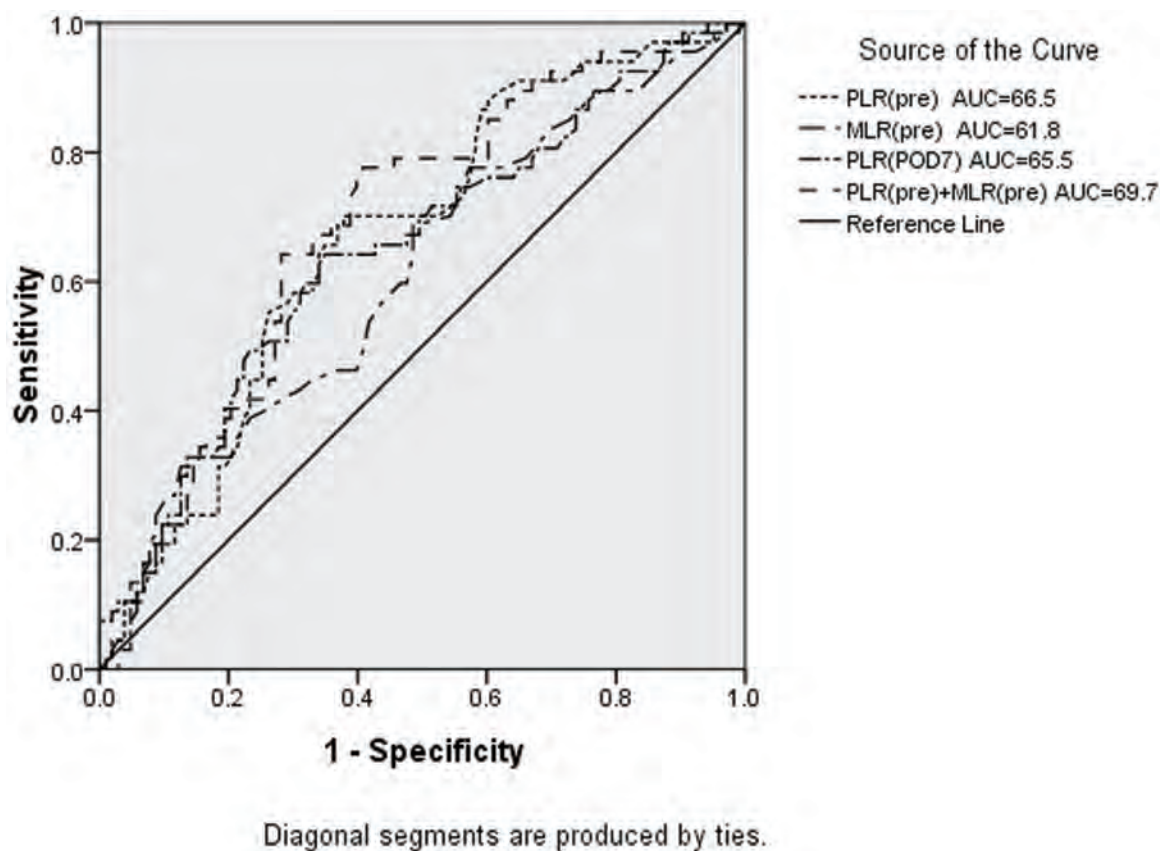


Fig. 2. ROC curve analysis for predicting PVT by PLR (pre), MLR (pre), PLR (post-D7) and combined markers in the estimation cohort. ROC, receiver operating characteristic.

via a regulation of platelet function and induction of platelet apoptosis.<sup>33</sup> Besides that, statins have been used as anti-thrombotic therapy for their anti-inflammatory effect.<sup>34</sup> This type of therapy could decrease the rate of venous throm-

bosis via the reduction of proinflammatory cytokines and chemokines. However, the current guideline of anticoagulation management did not recommend the treatment of inhibiting inflammation. This study may help to suggest the

Table 4. Predictive variables of portal vein thrombosis by univariate and multivariate analyses

Variable	Univariate analysis		Multivariate analysis	
	OR (95% CI)	p-value	OR (95% CI)	p-value
Age ( $\leq 50$ vs. $> 50$ years)	1.958 (1.051–3.647)	0.034		
NLR (pre) ( $> 3.7$ vs. $\leq 3.7$ )	2.969 (1.417–6.220)	0.004		
PLR (pre) ( $> 70.5$ vs. $\leq 70.5$ )	3.963 (2.070–7.587)	0.000	3.037 (1.463–6.305)	0.003
MLR (pre) ( $> 0.295$ vs. $\leq 0.295$ )	2.760 (1.386–5.497)	0.004	2.188 (1.003–4.772)	0.049
PLR (post-day 3) ( $> 139$ vs. $\leq 139$ )	2.615 (1.342–5.098)	0.005		
PLR (post-day 7) ( $> 230.5$ vs. $\leq 230.5$ )	3.345 (1.767–6.332)	0.000	2.166 (1.053–4.454)	0.036
MLR (post-day 7) ( $> 1.055$ vs. $\leq 1.055$ )	2.567 (1.312–5.022)	0.006		

Table 5. Multivariate logistic regression analysis of predictive variables

Variable	OR	95%CI	P-value
PLR (pre) $\leq 70.5$ and MLR (pre) $\leq 0.295$			
PLR (pre) $> 70.5$ and MLR (pre) $\leq 0.295$	2.750	1.008–7.502	0.048
PLR (pre) $\leq 70.5$ and MLR (pre) $> 0.295$			
PLR (pre) $> 70.5$ and MLR (pre) $> 0.295$	8.148	3.005–22.093	$< 0.000$



role of anti-inflammation therapy as an optimal prophylactic strategy. The identification of inflammation markers relevant to the formation of PVT could provide definite targets for future therapy.

In this study, we found that PLR (pre), MLR (pre), and PLR (post-day7) are predictors of PVT post in patients undergoing splenectomy and periesophagogastric devascularization. Some potential limitations of this study should be noted. Firstly, this is a retrospective study performed in a single-center, and additional prospective and multicenter studies are needed. Secondly, the portal vein was assessed only on the seventh day after surgery. Dynamic observation of portal vein is proposed, as changes of inflammation biomarkers may represent an after-effect. Thirdly, former research confirmed that the anatomic extent of deep vein thrombosis was associated with changes of inflammation marker levels;<sup>12</sup> the PVT group was not divided into any subgroups according to the extent of PVT.

### Acknowledgments

The authors would like to thank all the individuals who participated in this study.

### Funding

This work was supported by the Nanjing Medical Science and Technology Development Fund (Grant numbers YKK17169).

### Conflict of interest

The authors have no conflict of interests related to this publication.

### Author contributions

Study concept and design (YXY, YFZ), acquisition of data (JBH, QHS), analysis and interpretation of data (JBH, QHS, YFZ, YXY), drafting of the manuscript (JBH, QHS), critical revision of the manuscript for important intellectual content (JBH, QHS), administrative, technical, or material support, study supervision (YXY, YFZ).

### Data sharing statement

All data are available upon request.

### References

- [1] Webster GJ, Burroughs AK, Riordan SM. Review article: portal vein thrombosis — new insights into aetiology and management. *Aliment Pharmacol Ther* 2005;21(1):1–9. doi:10.1111/j.1365-2036.2004.02301.x.
- [2] Stine JG, Shah PM, Cornella SL, Rudnick SR, Ghazil MS, Stukenborg GJ, *et al*. Portal vein thrombosis, mortality and hepatic decompensation in patients with cirrhosis: A meta-analysis. *World J Hepatol* 2015;7(27):2774–2780. doi:10.4254/wjh.v7.i27.2774.
- [3] Qi X, Su C, Ren W, Yang M, Jia J, Dai J, *et al*. Association between portal vein thrombosis and risk of bleeding in liver cirrhosis: A systematic review of the literature. *Clin Res Hepatol Gastroenterol* 2015;39(6):683–691. doi:10.1016/j.clinre.2015.02.012.
- [4] Dell'Era A, Iannuzzi F, Fabris FM, Fontana P, Reati R, Grillo P, *et al*. Impact of portal vein thrombosis on the efficacy of endoscopic variceal band ligation. *Dig Liver Dis* 2014;46(2):152–156. doi:10.1016/j.dld.2013.08.138.
- [5] Lendoire J, Raffin G, Cejas N, Duek F, Barros Schelotto P, *et al*. Liver transplantation in adult patients with portal vein thrombosis: risk factors, management and outcome. *HPB (Oxford)* 2007;9(5):352–356. doi:10.1080/13651820701599033.
- [6] Qi X, Dai J, Jia J, Ren W, Yang M, Li H, *et al*. Association between portal vein thrombosis and survival of liver transplant recipients: a systematic review and meta-analysis of observational studies. *J Gastrointest Liver Dis* 2015;24(1):51–59. doi:10.15403/jgld.2014.1121.qix.
- [7] Kyrle PA, Eichinger S. Deep vein thrombosis. *Lancet* 2005;365(9465):1163–1174. doi:10.1016/S0140-6736(05)71880-8.
- [8] Zocco MA, Di Stasio E, De Cristofaro R, Novi M, Aiora ME, Ponzi F, *et al*. Thrombotic risk factors in patients with liver cirrhosis: correlation with MELD scoring system and portal vein thrombosis development. *J Hepatol* 2009;51(4):682–689. doi:10.1016/j.jhep.2009.03.013.
- [9] Danno K, Ikeda M, Sekimoto M, Sugimoto T, Takemasa I, Yamamoto H, *et al*. Diameter of splenic vein is a risk factor for portal or splenic vein thrombosis after laparoscopic splenectomy. *Surgery* 2009;145(5):457–464; discussion 465–466. doi:10.1016/j.surg.2008.06.030.
- [10] Kawanaka H, Akahoshi T, Kinjo N, Konishi K, Yoshida D, Aneawa G, *et al*. Impact of antithrombin III concentrates on portal vein thrombosis after splenectomy in patients with liver cirrhosis and hypersplenism. *Ann Surg* 2010;251(1):76–83. doi:10.1097/SLA.0b013e3181bdf8ad.
- [11] Li MX, Zhang XF, Liu ZW, Lv Y. Risk factors and clinical characteristics of portal vein thrombosis after splenectomy in patients with liver cirrhosis. *Hepatobiliary Pancreat Dis Int* 2013;12(5):512–519. doi:10.1016/s1499-3872(13)60081-8.
- [12] Rabinovich A, Cohen JM, Cushman M, Kahn SR. Association between inflammation biomarkers, anatomic extent of deep venous thrombosis, and venous symptoms after deep venous thrombosis. *J Vasc Surg Venous Lymphat Disord* 2015;3(4):347–353.e1. doi:10.1016/j.jvsv.2015.04.005.
- [13] Riva N, Donadini MP, Ageno W. Epidemiology and pathophysiology of venous thromboembolism: similarities with atherothrombosis and the role of inflammation. *Thromb Haemostasis* 2015;113(6):1176–1183. doi:10.1160/TH14-06-0563.
- [14] Saghaizadeh A, Hafizi S, Rezaei N. Inflammation in venous thromboembolism: Cause or consequence? *Int Immunopharmacol* 2015;28(1):655–665. doi:10.1016/j.intimp.2015.07.044.
- [15] Vazquez-Garza E, Jerjes-Sanchez C, Navarrete A, Joya-Harrison J, Rodriguez D. Venous thromboembolism: thrombosis, inflammation, and immunothrombosis for clinicians. *J Thromb Thrombolysis* 2017;44(3):377–385. doi:10.1007/s11239-017-1528-7.
- [16] Branchford BR, Carpenter SL. The role of inflammation in venous thromboembolism. *Front Pediatr* 2018;6:142. doi:10.3389/fped.2018.00142.
- [17] Saghaizadeh A, Rezaei N. Inflammation as a cause of venous thromboembolism. *Crit Rev Oncol Hematol* 2016;99:272–285. doi:10.1016/j.critrevonc.2016.01.007.
- [18] Budzianowski J, Piesko K, Burchardt P, Rzeźniczak J, Hiczkiewicz J. The role of hematological indices in patients with acute coronary syndrome. *Dis Markers* 2017;2017:3041565. doi:10.1155/2017/3041565.
- [19] Cai J, Wang K, Han T, Jiang H. Evaluation of prognostic values of inflammation-based markers in patients with HBV-related acute-on-chronic liver failure. *Medicine (Baltimore)* 2018;97(46):e13324. doi:10.1097/MD.00000000000013324.
- [20] Kinoshita A, Onoda H, Imai N, Iwaku A, Oishi M, Fushiya N, *et al*. Comparison of the prognostic value of inflammation-based prognostic scores in patients with hepatocellular carcinoma. *Br J Cancer* 2012;107(6):988–993. doi:10.1038/bjc.2012.354.
- [21] Sun Y, Zhang L. The clinical use of pretreatment NLR, PLR, and LMR in patients with esophageal squamous cell carcinoma: evidence from a meta-analysis. *Cancer Manag Res* 2018;10:6167–6179. doi:10.2147/CMAR.S171035.
- [22] Cetinkaya E, Senol K, Saylam B, Tez M. Red cell distribution width to platelet ratio: new and promising prognostic marker in acute pancreatitis. *World J Gastroenterol* 2014;20(39):14450–14454. doi:10.3748/wjg.v20.i39.14450.
- [23] Cai YJ, Dong JJ, Dong JZ, Chen Y, Lin Z, Song M, *et al*. A nomogram for predicting prognostic value of inflammatory response biomarkers in decompensated cirrhotic patients without acute-on-chronic liver failure. *Aliment Pharmacol Ther* 2017;45(11):1413–1426. doi:10.1111/apt.14046.
- [24] Li Y, Zhao Y, Feng L, Guo R. Comparison of the prognostic values of inflammation markers in patients with acute pancreatitis: a retrospective cohort study. *BMJ Open* 2017;7(3):e013206. doi:10.1136/bmjopen-2016-013206.
- [25] Violi F, Ferro D. Clotting activation and hyperfibrinolysis in cirrhosis: implication for bleeding and thrombosis. *Semin Thromb Hemost* 2013;39(4):426–433. doi:10.1055/s-0033-1334144.
- [26] Levi M, van der Poll T, Büller HR. Bidirectional relation between inflammation and coagulation. *Circulation* 2004;109(22):2698–2704. doi:10.1161/01.CIR.0000131660.51520.9A.
- [27] Artoni A, Abbattista M, Bucciarelli P, Giannelli F, Scalabrino E, Pappalardo E, *et al*. Platelet to lymphocyte ratio and neutrophil to lymphocyte ratio as risk factors for venous thrombosis. *Clin Appl Thromb Hemost* 2018;24(5):808–814. doi:10.1177/1076029617733039.
- [28] Ming L, Jiang Z, Ma J, Wang Q, Wu F, Ping J. Platelet-to-lymphocyte ratio, neutrophil-to-lymphocyte ratio, and platelet indices in patients with acute deep vein thrombosis. *Vasa* 2018;47(2):143–147. doi:10.1024/0301-1526/a000683.
- [29] Zhu X, Yao Y, Yao C, Jiang Q. Predictive value of lymphocyte to monocyte ratio and monocyte to high-density lipoprotein ratio for acute deep vein thrombosis after total joint arthroplasty: a retrospective study. *J Orthop Surg Res* 2018;13(1):211. doi:10.1186/s13018-018-0910-2.
- [30] Akboga YE, Bektas H, Anlar O. Usefulness of platelet to lymphocyte and neutrophil to lymphocyte ratios in predicting the presence of cerebral venous sinus thrombosis and in-hospital major adverse cerebral events. *J Neurol Sci* 2017;380:226–229. doi:10.1016/j.jns.2017.07.036.

- [31] Mo C, Zeng Z, Deng Q, Ding Y, Xiao R. Imbalance between T helper 17 and regulatory T cell subsets plays a significant role in the pathogenesis of systemic sclerosis. *Biomed Pharmacother* 2018; 108: 177–183. doi: 10.1016/j.biopha.2018.09.037.
- [32] Wu W, Yan H, Zhao H, Sun W, Yang Q, Sheng J, *et al*. Characteristics of systemic inflammation in hepatitis B-precipitated ACLF: Differentiate it from No-ACLF. *Liver Int* 2018; 38(2): 248–257. doi: 10.1111/liv.13504.
- [33] Xu M, Xue W, Ma Z, Bai J, Wu S. Resveratrol reduces the incidence of portal vein system thrombosis after splenectomy in a rat fibrosis model. *Oxid Med Cell Longev* 2016; 2016: 7453849. doi: 10.1155/2016/7453849.
- [34] Sexton T, Wallace EL, Smyth SS. Anti-thrombotic effects of statins in acute coronary syndromes: At the intersection of thrombosis, inflammation, and platelet-leukocyte interactions. *Curr Cardiol Rev* 2016; 12(4): 324–329. doi: 10.2174/1573403x12666160504100312.



Original Article

# Characteristics and Inpatient Outcomes of Primary Biliary Cholangitis and Autoimmune Hepatitis Overlap Syndrome

Yi Jiang<sup>1\*</sup>, Bing-Hong Xu<sup>2</sup>, Brandon Rodgers<sup>1</sup> and Nikolaos Pyrsopoulos<sup>3\*</sup>

<sup>1</sup>Department of Medicine, Rutgers New Jersey Medical School, Newark, New Jersey, USA; <sup>2</sup>Liver Center & Center for Asian Health, RWJBH-Saint Barnabas Medical Center, Florham Park, New Jersey, USA; <sup>3</sup>Division of Gastroenterology and Hepatology, Rutgers New Jersey Medical School, Newark, New Jersey, USA

Received: 2 January 2021 | Revised: 23 February 2021 | Accepted: 26 February 2021 | Published: 11 March 2021

## Abstract

**Background and Aims:** Primary biliary cholangitis (PBC) and autoimmune hepatitis (AIH) are hepatobiliary diseases of presumed immune-mediated origin that have been shown to overlap. The aim of this retrospective trial was to use national data to examine the characteristics and outcomes of patients hospitalized with overlapping PBC and AIH (PBC/AIH). **Methods:** The National Inpatient Sample was used to identify hospitalized adult patients with PBC, AIH, and PBC/AIH from 2010 to 2014 by International Classification of Diseases-Ninth Edition Revision codes; patients with hepatitis B virus and hepatitis C virus infection were excluded. Primary outcomes measures were in-hospital outcomes that included mortality, respiratory failure, septic shock, length of stay, and total hospital charges. Secondary outcomes were the clinical characteristics of PBC/AIH, including the comorbid extrahepatic autoimmune disease pattern and complications of cirrhosis. **Results:** A total of 3,478 patients with PBC/AIH were included in the study. PBC/AIH was associated with higher rates of Sjögren's syndrome ( $p<0.001$ ;  $p<0.001$ ), lower rates of Crohn's disease ( $p<0.05$ ;  $p<0.05$ ), and higher rates of cirrhosis-related complications when compared to PBC or AIH alone. There were similar rates of mortality between the PBC/AIH, PBC, and AIH groups. The PBC/AIH group had higher rates of septic shock when compared to the PBC group ( $p<0.05$ ) and AIH group ( $p<0.05$ ) after adjusting for possible confounders. **Conclusions:** PBC/AIH is associated with a lower rate of Crohn's disease, a higher rate of Sjögren's syndrome, higher rates of cirrhosis-related complications, and significantly increased risk of septic shock compared to PBC

and AIH individually.

**Citation of this article:** Jiang Y, Xu BH, Rodgers B, Pyrsopoulos N. Characteristics and inpatient outcomes of primary biliary cholangitis and autoimmune hepatitis overlap syndrome. J Clin Transl Hepatol 2021;9(3):392–398. doi: 10.14218/JCTH.2021.00008.

## Introduction

Primary biliary cholangitis (PBC) and autoimmune hepatitis (AIH) are diseases of presumed immune-mediated origin that affect the hepatobiliary system. They are distinct entities, though they share some similarities clinicopathologically.<sup>1</sup> Previous studies have suggested that variant forms of AIH develop in patients with PBC at diagnosis or during follow-up, and vice versa.<sup>2–4</sup> It has also been reported that patients with typical features of PBC or AIH can switch from one disease to another over time.<sup>3</sup> Moreover, some patients present with overlapping features of these two disorders within the spectrum of autoimmune liver diseases.<sup>5</sup> As a result of these observed clinical correlations, there has been an increased focus on the overlap of PBC and AIH.

Whether the coexistence of PBC and AIH are sequential, a concurrent occurrence of two independent autoimmune liver diseases (AILDs), or a primary AILD with one or more features of another AILD, is still under debate.<sup>6</sup> Nevertheless, it is important to recognize the coexisting disease pattern because it demonstrates unique clinical characteristics and outcomes that are different from either PBC or AIH. Previous studies have found that patients with both features of PBC and AIH developed cirrhosis more rapidly and had decreased responses to ursodeoxycholic acid and steroid therapy compared to AIH alone.<sup>7</sup> Compared to the PBC group, patients with PBC and AIH overlap have shown higher rates of mortality and orthotopic liver transplantation, with more cirrhosis-related complications, such as symptomatic portal hypertension, esophageal varices, gastrointestinal bleeding, and ascites.<sup>8,9</sup> Additionally, a large number of extrahepatic autoimmune diseases were found to be associated with AIH and PBC.<sup>10</sup>

Due to the relatively low prevalence of both PBC and AIH, systemic studies with sufficient numbers have been challenging. Indeed, the previous studies have been limited by small population sizes; thus, variable results have been ob-

**Keywords:** Primary biliary cholangitis; Autoimmune hepatitis; Extrahepatic autoimmune diseases; Cirrhosis-related complications; Septic shock; Hospital burden.

**Abbreviations:** AIH, autoimmune hepatitis; AILD, autoimmune liver disease; AITD, autoimmune thyroid disease; aOR, adjusted odds ratio; CI, confidence interval; ERCP, endoscopic retrograde cholangiopancreatography; ICD-9 CM, International Classification of Diseases-Ninth Edition Revision, Clinical Modification; LOS, length of stay; NIS, Nationwide Inpatient Sample; PBC, primary biliary cholangitis; SJS, Sjögren's syndrome; Treg, regulatory T cell.

**\*Correspondence to:** Nikolaos Pyrsopoulos, Division of Gastroenterology and Hepatology, Rutgers-New Jersey Medical School, University Hospital, 185 S. Orange Avenue, Medical Science Building H level Room – 536, Newark, NJ 07101-1709, USA. ORCID: <https://orcid.org/0000-0002-6950-8174>. Tel: +1-973-972-5252, E-mail: [pyrsopni@njms.rutgers.edu](mailto:pyrsopni@njms.rutgers.edu); Yi Jiang, Department of Medicine, Rutgers-New Jersey Medical School, Newark, NJ 07101, USA. ORCID: <https://orcid.org/0000-0001-5114-0183>. Tel: +1-973-972-6056, E-mail: [yi.jiang@rutgers.edu](mailto:yi.jiang@rutgers.edu)



tained, without firm conclusions. To date, there have not been large nationally representative studies to elucidate the characteristics and outcomes of PBC and AIH overlap syndrome.

In this nationwide study, we aimed to examine the characteristics (including demographics, comorbidities, related interventions) and inpatient outcomes [including length of stay (LOS), total hospital charges, in-hospital mortality, respiratory failure, and septic shock] for patients admitted with concomitant PBC and AIH (i.e. PBC/AIH). Specifically, we investigated the comorbid extrahepatic autoimmune disease pattern and complications of cirrhosis in this patient population.

## Methods

### Data source

Data were obtained from the Nationwide Inpatient Sample (NIS) database, which is the largest all-payer inpatient care database in the USA. It is designed to approximate a 20% sample of the USA community hospitals. Yearly sampling weights are applied to generate national estimates.<sup>11</sup> This database has been used previously to provide estimate burdens of AIH<sup>12</sup> and PBC<sup>13</sup> hospitalizations in the USA. The data includes demographics (age, sex, race/ethnicity), hospital information (bed size, type), insurance, discharge disposition, total hospital charges, and LOS. Diagnoses and procedures were identified by International Classification of Diseases-Ninth Edition Revision, Clinical Modification (ICD-9 CM) codes.

### Study design and inclusion criteria

This study was a retrospective cohort study of adult (18–90 years-old) patients hospitalized with discharge diagnoses of both PBC (ICD-9 CM code: 571.6) and AIH (ICD-9 CM code: 571.42) across the USA, from 2010 to 2014. Two control groups from the same time period were selected. One control group was all PBC patients without diagnosis of AIH (the PBC group), while the other control group was all AIH patients without diagnosis of PBC (the AIH group). All three groups excluded patients with the diagnoses of hepatitis B virus infection or hepatitis C virus infection. Demographic and clinical characteristics were collected (Table 1).

The Elixhauser Comorbidity Index,<sup>14</sup> which measures 29 common medical conditions and assigns different weights to compile a score, was used to analyze the severity of comorbidities. Other comorbid conditions included were hypercholesterolemia, vitamin D deficiency, osteoporosis, obesity, cirrhosis-related complications, hepatocellular carcinoma, inflammatory bowel disease (ulcerative colitis and Crohn's disease), lymphoma, non-dialysis dependent chronic kidney disease, end-stage renal disease and autoimmune diseases, including Sjögren's syndrome (SJS), systemic sclerosis (SS), rheumatoid arthritis, systemic lupus erythematosus, autoimmune thyroid disease (AITD), psoriasis and celiac disease. Hepatobiliary procedures or interventions such as liver transplantation and endoscopic retrograde cholangiopancreatography (commonly referred to as ERCP) were also included. ICD-9-CM codes are provided in the Supplementary Table 1.

Primary outcomes measures were in-hospital outcomes that included mortality, respiratory failure, septic shock, LOS, and total hospital charges. Secondary outcomes were the clinical characteristics of PBC/AIH, including the comorbid extrahepatic autoimmune disease pattern and complica-

tions of cirrhosis.

### Statistical analysis

SAS survey procedures (SAS 9.4; SAS Institute Inc, Cary, NC, USA) were used for all statistical analyses. The national estimates were calculated after accounting for the sample design elements (clusters, strata, and trend weights) provided by the NIS. Continuous variables were reported as weighted means±standard errors, and categorical variables were reported as weighted numbers (*n*) and percentages (%). The standard errors of weighted means were estimated by using the Taylor linearization method that incorporates the sample design. Rao-Scott modified chi-square test was used to test the difference of distribution for categorical variables, while weighted Student's *t*-test was used to analyze the normally distributed continuous variables. Variables that are not normally-distributed were tested by Wilcoxon rank-sum tests. A multivariate logistic regression was used to estimate the odds ratio of in-hospital mortality, respiratory failure, and septic shock after adjusting for patient demographics, hospital bed size, hospital location/teaching status, insurance type, median household income, Elixhauser Comorbidity Index score, and other comorbidities that showed statistically significant difference in comparisons between groups. In addition, a multivariate linear regression was used to estimate the average change in LOS and hospital charges after adjusting for the same covariates mentioned above.

### Ethical information

Only de-identified patient demographics from the NIS database were used and there were no patients actively involved in this study. Therefore, Institutional Review Board approval was deemed unnecessary.

## Results

### Patient characteristics (Table 1)

In this study, a total of 56,369 patients were admitted with PBC, 82,747 with AIH, and 3,478 with PBC/AIH. Those with PBC/AIH, PBC, and AIH were predominantly women (89.3%, 84.3%, and 80.2%, respectively) with a Caucasian prevalence (58.2%, 71.2%, and 60%), as shown in Table 1. Compared to the PBC group, patients with PBC/AIH were younger in age (57.3 vs. 64.4 years, *p*<0.001) and more likely to be admitted to large (69.1% vs. 63.3%) and urban teaching (65.8% vs. 58.6%) hospitals. The PBC/AIH cohort was also associated with less hypercholesterolemia (2.3% vs. 3.8%, *p*<0.05), a lower rate of non-dialysis dependent chronic kidney disease (10.5% vs. 13.9%, *p*<0.05) and fewer comorbid Crohn's disease cases (0.4% vs. 0.9%, *p*<0.05). However, the PBC/AIH cohort was associated with significantly more SJS (7.2% vs. 3.1%, *p*<0.001) and systemic lupus erythematosus (5.7% vs. 2.2%, *p*<0.05). Compared with the AIH group, patients with PBC/AIH were demographically similar but were associated with higher rates of vitamin D deficiency (4.1% vs. 2%, *p*<0.05) and osteoporosis (11.4% vs. 7.4%, *p*=0.002), and a lower rate of obesity (10.2% vs. 13%, *p*<0.05). Fewer comorbid Crohn's disease (0.4% vs. 0.9%, *p*<0.05) cases and more SJS (7.2% vs. 2.4%, *p*<0.001) and systemic sclerosis (4.7% vs. 0.8%, *p*=0.001) cases were seen in the PBC/AIH group. Interestingly, the PBC/AIH group did not show significantly

Table 1. Comparison of selected variables in patients hospitalized with PBC, AIH, and concomitant PBC and AIH (PBC/AIH)

Variable	PBC/AIH (n=3,478)	PBC (n=56,369)	p-value <sup>a</sup>	AIH (n=82,747)	p-value <sup>b</sup>
Age	57.3±0.6	64.4±0.2	<0.001	57.0±0.2	0.657
ECI score	11.2±0.5	11.6±0.1	0.333	10.7±0.1	0.206
Female	3,105 (89.3)	47,515 (84.3)	<0.001	66,318 (80.2)	<0.001
Caucasian	2,024 (58.2)	40,127 (71.2)	<0.001	49,616 (60.0)	<0.001
Large hospital bed	2,393 (69.1)	35,459 (63.3)	<0.05	53,479 (64.9)	0.076
Urban teaching hospital	2,280 (65.8)	32,854 (58.6)	<0.05	50,931 (61.8)	0.202
Hypercholesterolemia	79 (2.3)	2,116 (3.8)	<0.05	2,381 (2.9)	0.313
Vitamin D deficiency	144 (4.1)	1,688 (3.0)	0.157	1,677 (2.0)	<0.05
Osteoporosis	398 (11.4)	6,209 (11.0)	0.741	6,096 (7.4)	<0.05
Obesity	355 (10.2)	4,998 (8.9)	0.264	10,786 (13.0)	<0.05
Crohn's disease	13 (0.4)	499 (0.9)	<0.05	718 (0.9)	<0.05
Lymphoma	44 (1.3)	683 (1.2)	0.945	836 (1.0)	0.763
Non-dialysis dependent chronic kidney disease	366 (10.5)	7,836 (13.9)	<0.05	8,907 (10.8)	0.854
End-stage renal disease	46 (1.3)	813 (1.4)	0.781	819 (1.0)	0.466
Sjögren's syndrome	251 (7.2)	1,756 (3.1)	<0.001	1,957 (2.4)	<0.001
Systemic sclerosis	162 (4.7)	1,541 (2.7)	0.112	623 (0.8)	<0.05
Systemic lupus erythematosus	199 (5.7)	1,250 (2.2)	<0.05	4,775 (5.8)	0.961
Rheumatoid arthritis	119 (3.4)	2,153 (3.8)	0.590	3,522 (4.3)	0.244
Autoimmune thyroid disease	15 (0.4)	193 (0.3)	0.716	478 (0.6)	0.591
Psoriasis	44 (1.3)	742 (1.3)	0.918	886 (1.1)	0.714
Celiac disease	45 (1.3)	392 (0.7)	0.160	618 (0.7)	0.198
Ascites	720 (20.7)	8,327 (14.8)	<0.001	11,260 (13.6)	<0.001
Hepatic encephalopathy	185 (5.3)	2,072 (3.7)	0.073	2,920 (3.5)	<0.05
Variceal bleeding	56 (1.6)	648 (1.2)	0.379	577 (0.7)	0.080
Portal hypertension	682 (19.6)	8,696 (15.4)	<0.05	10,362 (12.5)	<0.001
Hepatorenal syndrome	80 (2.3)	803 (1.4)	0.124	912 (1.1)	<0.05
Spontaneous bacterial peritonitis	45 (1.3)	380 (0.7)	0.194	539 (0.7)	0.175
Respiratory failure	105 (3.0)	1,942 (3.4)	0.529	2,425 (2.9)	0.881
Septic shock	126 (3.6)	1,019 (1.8)	<0.05	1,406 (1.7)	<0.05
Mortality	110 (3.2)	2,301 (4.1)	0.190	3,122 (3.8)	0.380
LOS in days	5.9±0.2	5.8±0.1	0.628	5.8±0.1	0.628
Total hospital charges in dollars	61,539.8±3,977.3	54,295.5±1,565.4	0.075	51,638.1±1,215.1	<0.05

Values are reported as weighted means±standard errors and weighted numbers (%).

<sup>a</sup>p-value, comparison between PBC/AIH and PBC.<sup>b</sup>p-value, comparison between PBC/AIH and AIH.

Abbreviation: ECI, elixhauser comorbidity index.

**Table 2. Multivariate analysis for cirrhosis-related complications in patients hospitalized with primary biliary cholangitis (PBC), autoimmune hepatitis (AIH) and concomitant PBC and AIH (PBC/AIH)**

Cirrhosis-related complications	Unadjusted OR or coefficient (95% CI)	p-value	aOR or coefficient* (95% CI)	p-value
Ascites <sup>a</sup>	0.6 (0.55, 0.66)	<0.001	0.58 (0.48, 0.71)	<0.001
Hepatic encephalopathy <sup>a</sup>	0.65 (0.56, 0.76)	<0.001	0.71 (0.5, 1.02)	0.063
Variceal bleeding <sup>a</sup>	0.43 (0.32, 0.56)	<0.001	0.47 (0.25, 0.88)	<0.05
Portal hypertension <sup>a</sup>	0.59 (0.54, 0.64)	<0.001	0.57 (0.47, 0.7)	<0.001
Hepatorenal syndrome <sup>a</sup>	0.47 (0.38, 0.6)	<0.001	0.49 (0.29, 0.84)	0.009
Spontaneous bacterial peritonitis <sup>a</sup>	0.5 (0.37, 0.67)	<0.001	0.55 (0.27, 1.11)	0.093
Ascites <sup>b</sup>	0.66 (0.61, 0.72)	<0.001	0.69 (0.56, 0.84)	<0.001
Hepatic encephalopathy <sup>b</sup>	0.68 (0.58, 0.8)	<0.001	0.79 (0.55, 1.13)	0.195
Variceal bleeding <sup>b</sup>	0.71 (0.54, 0.93)	<0.05	0.84 (0.45, 1.57)	0.582
Portal hypertension <sup>b</sup>	0.75 (0.69, 0.82)	<0.001	0.85 (0.69, 1.04)	0.105
Hepatorenal syndrome <sup>b</sup>	0.62 (0.49, 0.78)	<0.001	0.69 (0.41, 1.19)	0.184
Spontaneous bacterial peritonitis <sup>b</sup>	0.51 (0.38, 0.7)	<0.001	0.63 (0.31, 1.3)	0.215

<sup>a</sup>PBC/AIH as reference, results for the AIH group.<sup>b</sup>PBC/AIH as reference, results for the PBC group.

\*Adjusted for age, sex, race, primary insurance payer, hospital type, hospital bed size, income quartile, Elixhauser Comorbidity Index score, hypercholesterolemia, vitamin D deficiency, osteoporosis, obesity, Crohn's disease, Sjögren's syndrome, systemic sclerosis, systemic lupus erythematosus, autoimmune thyroid disease, and non-dialysis dependent chronic kidney disease.

different Elixhauser Comorbidity Index scores when compared to the PBC or AIH groups.

### Liver-related comorbid conditions

This study's analysis revealed that PBC/AIH was associated with higher rates of ascites (20.7% vs. 14.8%,  $p<0.001$ ) and portal hypertension (19.6% vs. 15.4%,  $p<0.05$ ) compared to PBC. Similarly, compared to AIH, PBC/AIH cases were associated with higher rates of ascites (20.7% vs. 13.6%,  $p<0.001$ ) and portal hypertension (19.6% vs. 12.5%,  $p<0.001$ ), and associated with higher rates of hepatic encephalopathy (5.3% vs. 3.5%,  $p<0.05$ ) and hepatorenal syndrome (2.3% vs. 1.1%,  $p<0.05$ ). Furthermore, multivariate analysis (Table 2) demonstrated that PBC/AIH was associated with higher rates of ascites compared to PBC [adjusted odds ratio (aOR): 0.69, 95% confidence interval (CI): 0.56–0.84,  $p<0.001$ ] or AIH (aOR: 0.58, 95% CI: 0.48–0.71,  $p<0.001$ ). In addition, PBC/AIH was associated with higher rates of variceal bleeding (aOR: 0.47, 95% CI: 0.25–0.88,  $p<0.05$ ), portal hypertension (aOR: 0.57, 95% CI: 0.47–0.7,  $p<0.001$ ) and hepatorenal syndrome (aOR: 0.49, 95% CI: 0.29–0.84,  $p<0.05$ ). Interestingly, when comparing the rates of hepatocellular carcinoma, liver transplantation, and interventions including diagnostic and therapeutic ERCP, there was no difference between PBC/AIH vs. PBC, or PBC vs. AIH.

### In-hospital outcomes

For the measures of hospital stay outcomes, there was a similar rate of mortality (3.2% vs. 4.1%,  $p=0.190$ ) and respiratory failure (3% vs. 3.4%,  $p=0.529$ ) between the PBC/AIH and PBC groups. Moreover, there was no statistically significant difference in hospitalization burden found in terms of LOS ( $5.9\pm0.2$  days vs.  $5.8\pm0.1$  days,  $p=0.628$ ) or total hospital charges ( $\$61539.8\pm3977.3$  vs.  $\$54295.5\pm1565.4$ ,  $p=0.075$ ). However, the PBC/AIH group had a significantly

higher rate of septic shock (3.6% vs. 1.8%,  $p<0.05$ ) than the PBC group. Additionally, compared to the AIH group, the PBC/AIH group was associated with a higher rate of septic shock (3.6% vs. 1.7%,  $p<0.05$ ) and higher total hospital charges ( $\$61539.8\pm3977.3$  vs.  $\$51638.1\pm1215.1$ ,  $p<0.05$ ). The rates of mortality (3.2% vs. 3.8%,  $p=0.380$ ), respiratory failure (3% vs. 2.9%,  $p=0.881$ ), and LOS ( $5.9\pm0.2$  days vs.  $5.8\pm0.1$  days,  $p=0.628$ ) were not markedly different between the PBC/AIH and AIH groups (Table 1). Patients with PBC (aOR: 0.54, 95% CI: 0.35–0.83,  $p<0.05$ ) and AIH (aOR: 0.49, 95% CI: 0.32–0.75,  $p=0.001$ ) retained the lower rates of septic shock compared to patients with PBC/AIH (Table 3) after adjusting for possible confounders.

### Discussion

This nationwide study examined the characteristics and inpatient outcomes of PBC/AIH compared to PBC or AIH alone. The major finding included that PBC/AIH was associated with a specific extrahepatic autoimmune disease pattern, with SJS being the most common extrahepatic autoimmune disease. PBC/AIH patients had significantly higher rates of cirrhosis-related complications. Furthermore, this study found that PBC/AIH was associated with a higher rate of septic shock compared to PBC and AIH, individually. This finding remained significant after adjusting for possible confounders, which suggests that PBC/AIH patients may present with an increased level of immunosuppression that increases the risk of dysregulated response leading to disseminated infection.

In regards to the higher rate of septic shock observed in the PBC/AIH cohort in this study, one possible explanation is the compromised immune system in PBC/AIH patients. It has been reported that PBC and AIH have a shared altered immune regulatory mechanism. Lohse *et al.*<sup>15</sup> described the concept of "spontaneous immunosuppression" in AIH, based upon observations in a murine model of experimental AIH as well as in patients. T cells obtained during remission markedly suppressed the liver-specific T cell responses by



Table 3. Multivariate analysis for outcomes in patients hospitalized with PBC, AIH, and concomitant PBC and AIH (PBC/AIH)

Outcomes	Unadjusted OR or coefficient (95% CI)	p-value	aOR or coefficient* (95% CI)	p-value
Mortality <sup>a</sup>	1.2 (0.99, 1.45)	0.07	1.19 (0.76, 1.86)	0.44
Respiratory failure <sup>a</sup>	0.97 (0.79, 1.18)	0.74	0.95 (0.61, 1.49)	0.83
Septic shock <sup>a</sup>	0.46 (0.38, 0.55)	<0.001	0.49 (0.32, 0.75)	<0.05
LOS in days <sup>a</sup>	-0.13 (-0.68, 0.41)	0.63	-0.1 (-0.63, 0.43)	0.71
Total hospital charges <sup>a</sup> in dollars	-9,901.76 (-17,517.55, -2,285.96)	<0.05	-8,557.16 (-16,148.88, -965.43)	<0.05
Mortality <sup>b</sup>	1.3 (1.07, 1.58)	<0.05	1.21 (0.78, 1.9)	0.40
Respiratory failure <sup>b</sup>	1.14 (0.94, 1.39)	0.19	1.1 (0.7, 1.74)	0.67
Septic shock <sup>b</sup>	0.49 (0.4, 0.59)	<0.001	0.54 (0.35, 0.83)	<0.05
LOS in days <sup>b</sup>	-0.13 (-0.68, 0.42)	0.64	-0.01 (-0.55, 0.53)	0.97
Total hospital charges <sup>b</sup> in dollars	-7,244.33 (-14,931.49, 442.84)	0.07	-3,376.62 (-11,056.4, 4,303.17)	0.39

<sup>a</sup>PBC/AIH as reference, results for the AIH group.<sup>b</sup>PBC/AIH as reference, results for the PBC group.

\*Adjusted for age, sex, race, primary insurance payer, hospital type, hospital bed size, income quartile, Elixhauser Comorbidity Index score, hypercholesterolemia, vitamin D deficiency, osteoporosis, obesity, Crohn's disease, Sjögren's syndrome, systemic sclerosis, systemic lupus erythematosus, autoimmune thyroid disease, and non-dialysis dependent chronic kidney disease, cirrhosis.

T cells obtained during the active phase of the AIH. Thus, it is postulated that spontaneous remission and long-lasting remission after discontinuance of immunosuppressive therapy may result from spontaneous immunosuppression. In addition, more data have suggested that regulatory T cells (Tregs) are numerically impaired in AILDs, especially during its active phase.<sup>16</sup> Similarly, it was reported that the pathogenesis of PBC likely involves an imbalance in immune tolerance rather than an over-reactive immune system directed against a self-antigen,<sup>17,18</sup> which explains the extensive failure of immunosuppressants in treating PBC.<sup>19</sup> Hence, immunoregulatory failure and dysfunction of Tregs play a vital role in the initiation and pathogenesis of both PBC and AIH, leading to further altered immune regulation in PBC/AIH, which may contribute to the increased rate of septic shock. An alternative explanation for the higher rate of septic shock in patients with PBC/AIH could be attributed to the treatment method. We hypothesize that more aggressive immunosuppressive induction and maintenance therapy offered to patients with PBC/AIH based on the rapid progression of disease course and higher rates of complications may further compromise the ability to protect against infection. Taken together, underlying dysregulation of the immune system from concomitant AILDs and related immunosuppressive treatment may increase the risk of septic shock.

Despite having the highest rate of septic shock, PBC/AIH had similar in-hospital mortality rates and LOS compared to PBC and AIH individually after adjusting for confounding factors. Previous studies have shown worse long-term mortality rates and more liver-related deaths in the PBC/AIH overlap group.<sup>8,20</sup> A plausible explanation for the contrary finding in this study is that PBC/AIH concomitant disease is a chronic progressive disease, either by its pathophysiology or as a result of effective treatment, and is associated with less acute decompensation that would contribute to in-hospital mortality.

This analysis revealed that PBC/AIH patients were relatively young and more likely to be admitted to a large teaching hospital when compared to PBC patients. This finding reflects the complexity and severity of PBC/AIH. Not surprisingly, PBC/AIH was associated with more vitamin D deficiency and osteoporosis. These patients were also less likely to be obese when compared to AIH patients. These findings can be explained by steatorrhea and weight loss from malabsorption due to decreased biliary secretion of bile acids, which are commonly seen in advanced PBC.<sup>21,22</sup> Interestingly, this study found significantly less Crohn's disease in the PBC/AIH group compared to either PBC or AIH. However, there was no difference in the incidence of ulcerative colitis found between all three groups. Ulcerative colitis has been reported to share similar human leukocyte antigen haplotypes with PBC,<sup>23</sup> and the same atypical antineutrophil cytoplasmic antibodies with AIH.<sup>24</sup> However, the data available regarding the association between Crohn's disease and PBC or AIH are very limited. The authors of one Japanese study commented on genetic polymorphisms, suggesting that they may be related to PBC and Crohn's disease susceptibility. Three alleles involved in the interleukin-12 signaling pathway perform in opposite directions in these two diseases, indicating an opposite pathogenic pathway that leads to a different balance of immune responses.<sup>25</sup> Further investigation on how PBC and AIH interaction can affect the pathogenesis of Crohn's disease is needed.

The observation of concurrent extrahepatic autoimmune diseases has been reported frequently in patients with AILDs.<sup>26,27</sup> The "mosaic of autoimmunity" has been proposed to describe this condition.<sup>28</sup> In our study's hospitalized patient cohort, SJS was the most common extrahepatic autoimmune comorbidity of PBC/AIH. Consistently, two other studies documented SJS as the most common

systemic autoimmune disease in AILDs.<sup>10,26</sup> It is reported that both PBC and SJS are characterized by inflammation of target epithelial elements sharing a similar target antigen.<sup>10,29</sup> Similarly, an inflammatory process with CD3+ T cell predominant lymphocytic infiltration on histological examination has been found in both liver and labial salivary glands in AIH patients.<sup>30</sup> These findings support a close relationship between PBC/AIH and SJS. AITD was reported to have a high prevalence rate in AILDs. In one study that focused on the gastroenterology clinic population, AITD was found in 18.3% of patients.<sup>10</sup> Conversely, this study's inpatient population cohort did not show a significantly high number of patients with AITD. This result may be attributed to underestimation by lacking specific ICD-9 codes or missing documentation in hospitalized patients, given the relative chronic course of AITD.

This study revealed higher rates of cirrhosis-related complications, most notably in ascites in the PBC/AIH group compared with PBC or AIH alone. Moreover, the PBC/AIH group demonstrated higher rates of variceal bleeding, portal hypertension and hepatorenal syndrome when compared to the AIH group. These results are consistent with previous findings<sup>7–9</sup> in which clinically significant progression to cirrhosis-related complications were more likely to be seen in the PBC/AIH population. In AILDs such as PBC or AIH, liver fibrogenesis is a complex process, influenced by immune and inflammatory mechanisms. The activation of hepatic stellate cells is considered the most important event in the fibrogenesis of both PBC<sup>31</sup> and AIH.<sup>32</sup> Portal fibroblasts, located around portal tracts, have been reported to be of particular importance in PBC and differentiate from hepatic stellate cells in regards to their profibrogenic function.<sup>33</sup> The targets of the autoimmune response in AIH are hepatocytes, whereas the target in PBC is the biliary epithelial cells. In addition to the classic wound healing reaction from unresolved inflammation and persistent liver injury, the proliferation of bile ducts and the direct or indirect contribution of bile acid to the fibrogenic process has been reported in PBC.<sup>34,35</sup> Furthermore, other mediators (such as CD4+ and CD8+ T cell response<sup>36,37</sup> and nitric oxide<sup>38,39</sup>) and other mechanisms (such as oxidant stress liver injury<sup>40,41</sup>) for the process of liver fibrogenesis have been shown to be shared by PBC and AIH. Considering the shared and disease-specific features between PBC and AIH fibrogenesis pathways, it can be hypothesized that an overlapping immune-mediated process accelerates the liver fibrogenesis in PBC/AIH overlap syndrome by targeting both hepatocytes and biliary epithelial cells, which may subsequently cause a higher prevalence of cirrhosis-related complications. Although the exact pathways of the overlapping immune-mediated process are unclear, this hypothesis is supported by several retrospective studies on the treatment of PBC/AIH, in which stable and decreased liver fibrosis states were observed in the patients with PBC/AIH who received combined immunosuppressive therapy.<sup>5,42,43</sup>

This study has several strengths and limitations. With nationwide samples, the NIS database provided the largest sample size to study two concomitant uncommon conditions, PBC and AIH. Therefore, our results are based on a high-power study and provide a national review of the disease. However, all diagnoses are dependent on the accuracy of ICD-9 codes, for which validation is routinely performed by the Agency for Healthcare Research and Quality, although coding errors may compromise the quality of the data. A recent study using the main diagnostic ICD-9-CM code (571.6) for PBC showed a good accuracy with most clinical and demographic parameters, comparable to the previously reported data.<sup>13</sup> There are other inherent limitations of this NIS study. For example, NIS provides inpatient data but none of the laboratory values, images, or pharmacological interventions are recorded. Therefore, in-

formation about outpatient follow-up, long-term outcomes or prognosis are not available, and additional information that may help better classify PBC/AIH overlap syndrome, such as liver function test results and histologic findings are not available. Also, a small proportion of patients who had readmissions were counted more than once, and this group of patients was non-identifiable. Therefore, the prevalence of disease might be overreported.

In conclusion, this national study used a large data set from the USA to examine the characteristics and in-hospital outcomes of PBC/AIH. Our results strengthened previous data showing high rates of cirrhosis-related complications, and also SJS as the most common extrahepatic autoimmune disease associated with AILDs in patients with PBC/AIH. The study identified that PBC/AIH is independently associated with a higher rate of septic shock compared to PBC and AIH individually. This result provokes clinicians to consider sepsis screening early in patients' presentations to the hospital and optimize the treatment of infections. Although previous studies reported worse liver-related mortality and long-term survival, this study did not observe worse in-patient mortality in PBC/AIH patients. These findings will inspire more work to be done in the future. Prospective studies at genetic and clinicopathological levels will assist in gaining a better understanding of the mechanism of the overlap between PBC and AIH, including the role of Treg cells and their interactions with immunosuppressive therapy. Ultimately, more progress in the field of immunomodulated therapy is expected.

## Acknowledgments

We thank Reza Hashemipour, MD, Krish Gandhi, MD from the gastroenterology department of Rutgers-New Jersey Medical School, and Chunyi Wu, PhD from the Institute of Gerontology, University of Michigan Medical School for their suggestions and proofreading of our project.

## Funding

None to declare.

## Conflict of interest

The authors have no conflict of interests related to this publication.

## Author contributions

Study concept and design (YJ, NP), acquisition of data (YJ, BX), analysis and interpretation of data (YJ, BX, BR), drafting of the manuscript (YJ, BX, BR, NP), critical revision of the manuscript for important intellectual content (YJ, BX, BR, NP), administrative, technical, or material support, study supervision (NP).

## References

- [1] Gonzalez RS, Washington K. Primary biliary cholangitis and autoimmune hepatitis. *Surg Pathol Clin* 2018;11:329–349. doi:10.1016/j.path.2018.02.010.
- [2] Czaja AJ. Frequency and nature of the variant syndromes of autoimmune liver disease. *Hepatology* 1998;28:360–365. doi:10.1002/hep.510280210.
- [3] Poupon R, Chazouilleres O, Corpechot C, Chrétien Y. Development of autoimmune hepatitis in patients with typical primary biliary cirrhosis. *Hepatology* 2006;44:85–90. doi:10.1002/hep.21229.

- [4] Bonder A, Retana A, Winston DM, Leung J, Kaplan MM. Prevalence of primary biliary cirrhosis-autoimmune hepatitis overlap syndrome. *Clin Gastroenterol Hepatol* 2011;9:609–612. doi:10.1016/j.cgh.2011.03.019.
- [5] Boberg KM, Chapman RW, Hirschfield GM, Lohse AW, Manns MP, Schrupf E. Overlap syndromes: the International Autoimmune Hepatitis Group (IAIHG) position statement on a controversial issue. *J Hepatol* 2011;54:374–385. doi:10.1016/j.jhep.2010.09.002.
- [6] Vierling JM. Autoimmune hepatitis and overlap syndromes: Diagnosis and management. *Clin Gastroenterol Hepatol* 2015;13:2088–2108. doi:10.1016/j.cgh.2015.08.012.
- [7] Park Y, Cho Y, Cho EJ, Kim YJ. Retrospective analysis of autoimmune hepatitis-primary biliary cirrhosis overlap syndrome in Korea: characteristics, treatments, and outcomes. *Clin Mol Hepatol* 2015;21:150–157. doi:10.3350/cmh.2015.21.2.150.
- [8] Silveira MG, Talwalkar JA, Angulo P, Lindor KD. Overlap of autoimmune hepatitis and primary biliary cirrhosis: long-term outcomes. *Am J Gastroenterol* 2007;102:1244–1250. doi:10.1111/j.1572-0241.2007.01136.x.
- [9] Yang F, Wang Q, Wang Z, Miao Q, Xiao X, Tang R, *et al*. The natural history and prognosis of primary biliary cirrhosis with clinical features of autoimmune hepatitis. *Clin Rev Allergy Immunol* 2016;50:114–123. doi:10.1007/s12016-015-8516-5.
- [10] Efe C, Wahlin S, Ozaslan E, Berlot AH, Purnak T, Muratori L, *et al*. Autoimmune hepatitis/primary biliary cirrhosis overlap syndrome and associated extrahepatic autoimmune diseases. *Eur J Gastroenterol Hepatol* 2012;24:531–534. doi:10.1097/MEG.0b013e328350f95b.
- [11] Agency for Healthcare Research and Quality. HCUP NIS database documentation. Available from: <https://www.hcup-us.ahrq.gov/db/nation/nis/nisdbdocumentation.jsp>.
- [12] Wen JW, Kohn MA, Wong R, Somsouk M, Khalili M, Maher J, *et al*. Hospitalizations for autoimmune hepatitis disproportionately affect black and Latino Americans. *Am J Gastroenterol* 2018;113:243–253. doi:10.1038/ajg.2017.456.
- [13] Shahab O, Sayiner M, Paik J, Felix S, Golabi P, Younossi ZM. Burden of primary biliary cholangitis among inpatient population in the United States. *Hepatol Commun* 2019;3:356–364. doi:10.1002/hep4.1314.
- [14] Moore BJ, White S, Washington R, Coenen N, Elixhauser A. Identifying increased risk of readmission and in-hospital mortality using hospital administrative data: The AHRQ elixhauser comorbidity index. *Med Care* 2017;55:698–705. doi:10.1097/MLR.0000000000000735.
- [15] Lohse AW, Kögel M, Meyer zum Büschenfelde KH. Evidence for spontaneous immunosuppression in autoimmune hepatitis. *Hepatology* 1995;22:381–388.
- [16] Liberal R, Grant CR, Holder BS, Cardone J, Martinez-Llordella M, Ma Y, *et al*. In autoimmune hepatitis type 1 or the autoimmune hepatitis-sclerosing cholangitis variant defective regulatory T-cell responsiveness to IL-2 results in low IL-10 production and impaired suppression. *Hepatology* 2015;62:863–875. doi:10.1002/hep.27884.
- [17] Wang L, Wang FS, Chang C, Gershwin ME. Breach of tolerance: primary biliary cirrhosis. *Semin Liver Dis* 2014;34:297–317. doi:10.1055/s-0034-1383729.
- [18] Mousa HS, Carbone M, Malinverno F, Ronca V, Gershwin ME, Invernizzi P. Novel therapeutics for primary biliary cholangitis: Toward a disease-stage-based approach. *Autoimmun Rev* 2016;15:870–876. doi:10.1016/j.autrev.2016.07.003.
- [19] Molinaro A, Marschall HU. Why doesn't primary biliary cholangitis respond to immunosuppressive medications? *Curr Hepatol Rep* 2017;16:119–123. doi:10.1007/s11901-017-0345-y.
- [20] Neuhauser M, Björnsson E, Treeprasertsuk S, Enders F, Silveira M, Talwalkar J, *et al*. Autoimmune hepatitis-PBC overlap syndrome: a simplified scoring system may assist in the diagnosis. *Am J Gastroenterol* 2010;105:345–353. doi:10.1038/ajg.2009.616.
- [21] Levy C, Lindor KD. Management of osteoporosis, fat-soluble vitamin deficiencies, and hyperlipidemia in primary biliary cirrhosis. *Clin Liver Dis* 2003;7:901–910. doi:10.1016/s1089-3261(03)00097-7.
- [22] Lanspa SJ, Chan AT, Bell JS 3rd, Go VL, Dickson ER, DiMaggio EP. Pathogenesis of steatorrhea in primary biliary cirrhosis. *Hepatology* 1985;5:837–842. doi:10.1002/hep.1840050522.
- [23] Xiao WB, Liu YL. Primary biliary cirrhosis and ulcerative colitis: a case report and review of literature. *World J Gastroenterol* 2003;9:878–880. doi:10.3748/wjg.v9.i4.878.
- [24] Terjung B, Spengler U, Sauerbruch T, Worman HJ. "Atypical p-ANCA" in IBD and hepatobiliary disorders react with a 50-kilodalton nuclear envelope protein of neutrophils and myeloid cell lines. *Gastroenterology* 2000;119:310–322. doi:10.1053/gast.2000.9366.
- [25] Aiba Y, Yamazaki K, Nishida N, Kawashima M, Hitomi Y, Nakamura H, *et al*. Disease susceptibility genes shared by primary biliary cirrhosis and Crohn's disease in the Japanese population. *J Hum Genet* 2015;60:525–531. doi:10.1038/jhg.2015.59.
- [26] Guo L, Zhou L, Zhang N, Deng B, Wang B. Extrahepatic autoimmune diseases in patients with autoimmune liver diseases: A phenomenon neglected by gastroenterologists. *Gastroenterol Res Pract* 2017;2017:2376231. doi:10.1155/2017/2376231.
- [27] Floreani A, De Martin S, Secchi MF, Cazzagon N. Extrahepatic autoimmunity in autoimmune liver disease. *Eur J Intern Med* 2019;59:1–7. doi:10.1016/j.ejim.2018.10.014.
- [28] Amital H, Gershwin ME, Shoenfeld Y. Reshaping the mosaic of autoimmunity. *Semin Arthritis Rheum* 2006;35:341–343. doi:10.1016/j.semarthrit.2005.09.002.
- [29] Selmi C, Meroni PL, Gershwin ME. Primary biliary cirrhosis and Sjögren's syndrome: autoimmune epithelitis. *J Autoimmun* 2012;39:34–42. doi:10.1016/j.jaut.2011.11.005.
- [30] Matsumoto T, Morizane T, Aoki Y, Yamasaki S, Nakajima M, Enomoto N, *et al*. Autoimmune hepatitis in primary Sjögren's syndrome: pathological study of the livers and labial salivary glands in 17 patients with primary Sjögren's syndrome. *Pathol Int* 2005;55:70–76. doi:10.1111/j.1440-1827.2005.01790.x.
- [31] Li YK, Li YM, Li Y, Wei YR, Zhang J, Li B, *et al*. CTHRC1 expression in primary biliary cholangitis. *J Dig Dis* 2019;20:371–376. doi:10.1111/1751-2980.12791.
- [32] Maia JM, Maranhão Hde S, Sena LV, Rocha LR, Medeiros IA, Ramos AM. Hepatic stellate cell activation and hepatic fibrosis in children with type 1 autoimmune hepatitis: an immunohistochemical study of paired liver biopsies before treatment and after clinical remission. *Eur J Gastroenterol Hepatol* 2010;22:264–269. doi:10.1097/MEG.0b013e328326cab6.
- [33] Dranoff JA, Wells RG. Portal fibroblasts: Underappreciated mediators of biliary fibrosis. *Hepatology* 2010;51:1438–1444. doi:10.1002/hep.23405.
- [34] Sveglia-Baroni G, Ridolfi F, Hannivoort R, Saccomanno S, Homan M, De Minicis S, *et al*. Bile acids induce hepatic stellate cell proliferation via activation of the epidermal growth factor receptor. *Gastroenterology* 2005;128:1042–1055. doi:10.1053/j.gastro.2005.01.007.
- [35] Fiorucci S, Baldelli F. Farnesoid X receptor agonists in biliary tract disease. *Curr Opin Gastroenterol* 2009;25:252–259. doi:10.1097/MOG.0b013e328324f87e.
- [36] Tsuda M, Ambrosini YM, Zhang W, Yang GX, Ando Y, Rong G, *et al*. Fine phenotypic and functional characterization of effector cluster of differentiation 8 positive T cells in human patients with primary biliary cirrhosis. *Hepatology* 2011;54:1293–1302. doi:10.1002/hep.24526.
- [37] Ichiki Y, Aoki CA, Bowlus CL, Shimoda S, Ishibashi H, Gershwin ME. T cell immunity in autoimmune hepatitis. *Autoimmun Rev* 2005;4:315–321. doi:10.1016/j.autrev.2005.01.005.
- [38] Beyazit Y, Efe C, Tanoglu A, Purnak T, Sayilir A, Taskiran I, *et al*. Nitric oxide is a potential mediator of hepatic inflammation and fibrogenesis in autoimmune hepatitis. *Scand J Gastroenterol* 2015;50:204–210. doi:10.3109/00365521.2014.974203.
- [39] Battista S, Bar F, Mengozzi G, Pollet C, Torchio M, Cavalli G, *et al*. Evidence of an increased nitric oxide production in primary biliary cirrhosis. *Am J Gastroenterol* 2001;96:869–875. doi:10.1111/j.1572-0241.2001.03470.x.
- [40] Pinzani M, Luong TV. Pathogenesis of biliary fibrosis. *Biochim Biophys Acta Mol Basis Dis* 2018;1864:1279–1283. doi:10.1016/j.bbdis.2017.07.026.
- [41] Pemberton PW, Aboutwerat A, Smith A, Burrows PC, McMahon RF, Warnes TW. Oxidant stress in type I autoimmune hepatitis: the link between necroinflammation and fibrogenesis? *Biochim Biophys Acta* 2004;1689:182–189. doi:10.1016/j.bbdis.2004.01.005.
- [42] Wu CH, Wang QH, Tian GS, Xu XY, Yu YY, Wang GQ. Clinical features of the overlap syndrome of autoimmune hepatitis and primary biliary cirrhosis: retrospective study. *Chin Med J (Engl)* 2006;119:238–241.
- [43] Chazouillères O, Wendum D, Serfaty L, Rosmorduc O, Poupon R. Long term outcome and response to therapy of primary biliary cirrhosis-autoimmune hepatitis overlap syndrome. *J Hepatol* 2006;44:400–406. doi:10.1016/j.jhep.2005.10.017.





Review Article

# HBV Integration Induces Complex Interactions between Host and Viral Genomic Functions at the Insertion Site

Dake Zhang<sup>1\*</sup> , Ke Zhang<sup>2,3</sup>, Urlike Protzer<sup>3,4</sup> and Changqing Zeng<sup>5,6</sup>

<sup>1</sup>Beijing Advanced Innovation Centre for Biomedical Engineering, Key Laboratory for Biomechanics and Mechanobiology of Ministry of Education, School of Biological Science and Medical Engineering, Beihang University, Beijing, China; <sup>2</sup>SCG Cell Therapy Pte. Ltd, Singapore; <sup>3</sup>Institute of Virology, Technical University of Munich/Helmholtz Zentrum München, Munich, Germany; <sup>4</sup>German Center for Infection Research (DZIF), Munich, Germany; <sup>5</sup>Key Laboratory of Genomic and Precision Medicine, Beijing Institute of Genomics, Chinese Academy of Sciences, Beijing, China; <sup>6</sup>University of Chinese Academy of Sciences, Beijing, China

Received: 7 February 2021 | Revised: 29 March 2021 | Accepted: 31 March 2021 | Published: 25 April 2021

## Abstract

Hepatitis B virus (HBV), one of the well-known DNA oncogenic viruses, is the leading cause of hepatocellular carcinoma (HCC). In infected hepatocytes, HBV DNA can be integrated into the host genome through an insertional mutagenesis process inducing tumorigenesis. Dissection of the genomic features surrounding integration sites will deepen our understanding of mechanisms underlying integration. Moreover, the quantity and biological activity of integration sites may reflect the DNA damage within affected cells or the potential survival benefits they may confer. The well-known human genomic features include repeat elements, particular regions (such as telomeres), and frequently interrupted genes (e.g., telomerase reverse transcriptase [i.e. *TERT*], lysine methyltransferase 2B [i.e. *KMT2B*], cyclin E1 [*CCNE1*], and cyclin A2 [*CCNA2*]). Consequently, distinct genomic features within diverse integrations differentiate their biological functions. Meanwhile, accumulating evidence has shown that viral proteins produced by integrants may cause cell damage even after the suppression of HBV replication. The integration-derived gene products can also serve as tumor markers, promoting the development of novel therapeutic strategies for HCC. Viral integrants can be single copy or multiple copies of different fragments with complicated rearrangement, which warrants elucidation of the whole viral integrant arrangement in future studies. All of these considerations underlie an urgent need to develop novel methodology and technology for sequence char-

acterization and function evaluation of integration events in chronic hepatitis B-associated disease progression by monitoring both host genomic features and viral integrants. This endeavor may also serve as a promising solution for evaluating the risk of tumorigenesis and as a companion diagnostic for designing therapeutic strategies targeting integration-related disease complications.

**Citation of this article:** Zhang D, Zhang K, Protzer U, Zeng C. HBV integration induces complex interactions between host and viral genomic functions at the insertion site. *J Clin Transl Hepatol* 2021;9(3):399–408. doi: 10.14218/JCTH.2021.00062.

## Introduction

There are still more than 250 million people infected with chronic hepatitis B virus (HBV) worldwide. Hepatocellular carcinoma (HCC) imposes a heavy socioeconomic public health burden. Among patients with cirrhosis, HBV infection has a reported annual incidence of 3%.<sup>1</sup> In 1980, shortly after the discovery of HBV, its integration was reported into HCC tissue cells and hepatoma cell lines.<sup>2,3</sup> There has been a long debate on the oncogenic roles of HBV integrations.<sup>4–6</sup> It is considered to be involved in the oncogenic process due to its intrinsic insertional mutagenesis (Fig. 1). Although current treatment using nucleoside or nucleotide analogs can efficiently suppress HBV replication, it is still not able to eliminate the virus from infected hepatocytes, mainly due to the persistent existence of covalently closed circular DNA (commonly referred to as cccDNA).<sup>7</sup>

Meanwhile, double-stranded linear DNA (dsDNA) is the alleged dominant substrate that gets incorporated into the host genome via repair of DNA double-stranded breaks (DSBs).<sup>8</sup> Indeed, HBV integrations tend to locate at either sites of host genomic instability,<sup>9,10</sup> or sites of cellular DNA damage.<sup>11</sup> Meanwhile, the HBV genome does not encode either integrase or other proteins recognizing specific genomic regions for integration,<sup>9,12,13</sup> and it is unlikely that HBV could deliberately “target” certain genes or regions. By far, only repeat elements or short homologous sequences, mediating the DNA repairing via non-homologous end joining,

**Keywords:** Double-strand break; Chimeric reads; Junction reads; Fusion transcript; Virus cellular junction; Virus cell junction; Virus host junction.

**Abbreviations:** cccDNA, covalently closed circular DNA; *CCN*, cyclin; cfDNA, cell-free DNA dsDNA, double-stranded linear DNA; DSB, DNA double-stranded breaks; *FN1*, fibronectin 1; HBV, hepatitis B virus; HBx, hepatitis B X; HCC, hepatocellular carcinoma; *hTERT*, human telomerase reverse transcriptase; *KMT2B*, lysine methyltransferase 2B; LINE1, long interspersed nuclear elements 1; mtDNA, mitochondrial DNA; NGS, next-generation of sequencing; *NTCP*, Na<sup>+</sup>/taurocholate polypeptide cotransporter; NUMT, nuclear copies of mtDNA; pgRNA, pregenomic RNA; SINE, short interspersed nuclear elements; *TP53*, tumor protein p53; TSS, transcriptional start site.

**\*Correspondence to:** Dake Zhang, Beijing Advanced Innovation Centre for Biomedical Engineering, Key Laboratory for Biomechanics and Mechanobiology of Ministry of Education, School of Biological Science and Medical Engineering, Beihang University, Beijing 100083, China. ORCID: <https://orcid.org/0000-0001-9508-8209>. E-mail: [dakezhang@buaa.edu.cn](mailto:dakezhang@buaa.edu.cn)

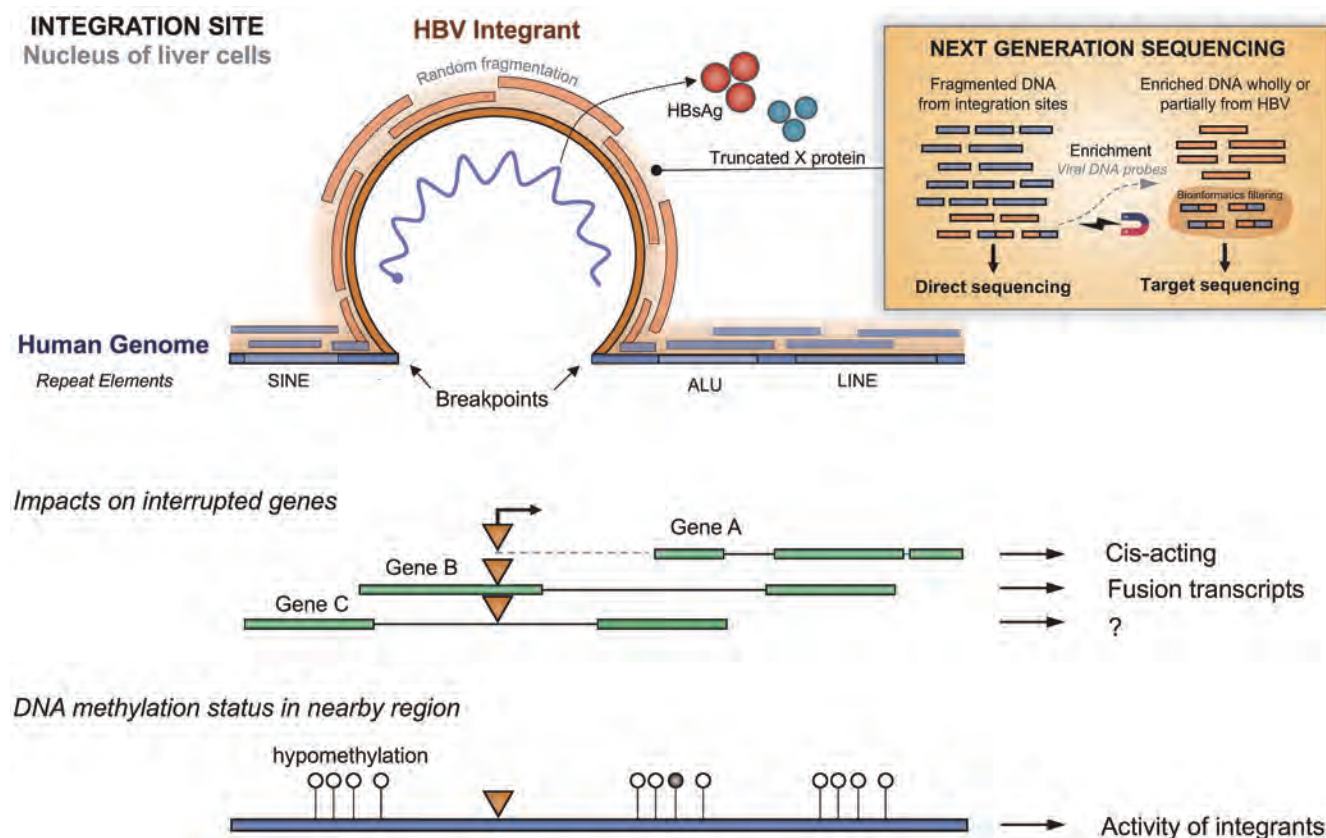


**Fig. 1. HBV integrations in the host nuclear genome.** HBV DNA fragments are incorporated into sites in the host nuclear genome, which may include double-stranded breaks due to diverse factors. Viral integrants can also be transcribed and translated to express viral proteins such as hepatitis B surface antigen and truncated X protein, which are involved in liver disease progression. It is well known that repeat elements are characteristic of the integration region, such as ALUs, SINE and LINES. Recently, solutions based on the NGS platform directly determine all of the DNA fragments from the integration sites. Viral-host chimeric fragments are evidence of the integration events. Particularly, these chimeric fragments can be enriched by using viral probes to capture those containing viral DNA, which increases the sensitivity of integration detection and extensively reduce the sequencing volume. The “breakpoints” of integrations refer to the position on the chimeric fragments where viral and human DNA fragments ligate with each other. They are also the boundaries of the integrations. Integrations may generate either a new promoter region to *cis*-activate the transcription of downstream genes, or directly interrupt the genes and potentially produce fusion transcripts. DNA methylation status in a nearby region may regulate the transcriptional activity of integrants.

are the main genomic feature of integration sites.<sup>14</sup> It has been known for a long time that the ends of an integrant most likely terminate at a 11 bp repeat region (5'-TTCAC-CTCTGC-3'), namely the cohesive-end regions termed DR1 and DR2.<sup>15</sup> About 37–40% of the reported viral breakpoints are mapped within the DR2-DR1 region,<sup>16–18</sup> where transcription and replication of the genome are initiated. During HBV replication, the reverse transcription from pregenomic RNA (commonly referred to as pgRNA) to cccDNA or dsDNA uses an 18 nucleotide RNA primer, which is the hydrolysate of pgRNA, to initiate the synthesis of the positive-sense DNA strand.<sup>12</sup> In about 90% of nucleocapsids, the RNA primer translocates to the DR2, leading to the synthesis of relaxed circular DNA; while in the remaining 10%, it binds to the DR1, priming the synthesis of dsDNA as the main source of viral DNA incorporated into the host genome.<sup>12</sup>

The HCC risk due to viral integrations remains as long as viral replication continues in liver cells. However, the detailed processes underlying viral integration still need clarification by investigators attempting to identify novel options to cure HBV infection. Recently, much attention has been dedicated to reviewing biological processes and consequences related to viral integrations in the background of the HBV life cycle.<sup>9,12</sup> The development of high-throughput sequencing solutions significantly facilitates resolving thousands of viral

integration breakpoints.<sup>16,18–22</sup> Our objective here is to summarize the features of host genomic sequences surrounding integration sites and viral fragments as integrants. These features of distinct integrations may be crucial to unraveling their contribution to liver disease progression. Pinpointing their involvement may aid efforts to identify novel diagnostic markers of disease progression and targets for improved therapeutic management of HBV infection.

#### HBV integration detection: Hybridization, cloning, amplification and next-generation sequencing (NGS) solutions

The short HBV DNA fragments are difficult to identify after being inserted into a large human genome (3Gb) in each affected cell. Meanwhile, these cells may also harbor limited integrations. In relative homogeneous populations of cell lines carrying HBV integrations, there are no more than 10 dominant integrations. For instance, the HepG2.2.15 cell line may contain at most five integrations,<sup>21</sup> and the PLC/PRF/5 cell line had nine integration regions reported.<sup>23</sup> Among the cell populations of the infected liver, it is estimated that there is about 1 integration per  $10^3$ – $10^4$  cells according to observations in an *in vitro* infection model.<sup>8</sup> Therefore, it

requires detection methods that have adequate sensitivity to identify such limited events in bulk tissue samples.

Early in the 1980s, the hybridization method was first applied to prove the existence of HBV integrations in cell lines and tumor tissues.<sup>2,24</sup> In Southern blot hybridization, digested DNA after a restriction enzyme treatment hybridized with <sup>32</sup>P-labeled HBV DNA probes, and researchers took the autoradiograph of the bands of digested DNA in the separation gel to identify the fragment harboring HBV DNA. Target fragments could be ligated into plasmid as integrant clones, which can be further fragmented and radiolabeled as probes for *in situ* hybridization. Prior to Sanger sequencing of integrant clones,<sup>25</sup> *in situ* hybridization was applied to see the cytogenetic locus of these probes binding to metaphase chromosomes and thereby determine the chromosome position of viral integrants.<sup>26</sup> The hybridization strategy and clone sequencing without an NGS platform are inefficient and insensitive to profile integrations.

To improve the methodology of HBV integration profiling, Minami *et al.*<sup>27</sup> (1995) developed the Alu PCR strategy, which is more practical for integration screening. Briefly, Alu elements, which have over one million copies dispersed throughout the human genome,<sup>28</sup> separate the entire genome into relatively small regions, the length of which is suitable for performing PCR amplification; the primer pair, one of which is Alu-specific and the other binds HBV sequences (X gene), may successfully amplify the virus-host chimeric regions. With this approach, Devrim *et al.*<sup>29</sup> identified 21 viral integrations from 18 patients in one study. Likewise, Mason *et al.*<sup>30–33</sup> first cleaved total liver cell DNA into fragments by NcoI, which cuts HBV DNA at nucleotide 1374, and then ligated these fragments into circles for nested PCR of virus-cellular junctions. This sensitive inverse-PCR assay is a quantitative method for integration detection. Nevertheless, since not all integrations are next to an Alu element or the cleavage site of NcoI, some may be omitted in subsequent analysis.

NGS solutions, either by direct sequencing or target sequencing after viral DNA enrichment (Fig. 1), can presumably achieve unbiased parallel analysis of tens to hundreds of samples. Extracted tissue DNA is randomly fragmented for sequencing library construction, the bioinformatic analysis aims to identify the so-called “junction read” or “chimeric read” in sequencing data, which is composed of both HBV and human DNA together and originates from the boundaries of integration events. Considering the relatively low frequencies of integrations, directly sequencing the whole nuclear genome for bulk tissues requires adequate sequencing coverage/depth to capture these chimeric fragments. Jiang *et al.*<sup>19</sup> adopted deep whole-genome sequencing (80X, 240G per sample; and 240X, 720G per sample) and identified 255 integrations in paired tumor and adjacent liver tissues from three HBV-positive HCC patients. The high cost and data analysis requirement will limit its application at the population scale. Target DNA enrichment has proven to be highly effective in exome sequencing of the human genome. It inspires the usage of viral DNA probes for HBV DNA enrichment prior to NGS analysis, which significantly reduces the sequencing volume to less than 2G per sample.<sup>16,21</sup> With the increased throughput, Zhao *et al.*<sup>16</sup> obtained 4,225 integration breakpoints (host-virus boundaries at the integration site) from 426 patients to characterize a viral integration pattern in one study, followed by other teams.<sup>17,34–37</sup>

Most NGS studies only took the single breakpoint as the indicator for one integration event. But one integration has two breakpoints (Fig. 1), and they may overestimate the number of integrations in each sample.<sup>21</sup> Fortunately, different integration events are likely to be far apart from each other in the cellular genome of hepatocytes. Therefore, we developed a strategy to pair adjacent breakpoints in the

human genome for the same integration event.<sup>21</sup> After the breakpoints in the human genome have been successfully paired, the corresponding viral breakpoints can then be paired. The boundaries of integration events are indicated by the sharp and consistent positions of the mapped reads, the particular distribution patterns of which have shown diverse modes of integrations (Fig. 2A). This pairing strategy can be used to predict the integrants and show their protein-coding ability or harbored regulatory elements. It can also illustrate insertion orientation and HBV fragments within the integration site. Besides, this strategy successfully uncovered the possibility of multiple fragments with different orientations in the same site (Fig. 2B), which have been validated in long-read sequencing studies.<sup>38</sup> The orientation of inserted fragments will determine their upstream and downstream directions and hence influence their regulatory roles for involved genes in the aforementioned biological effects of integrations. Therefore, further complicating the regulatory activity of the integration.

Viral integrations have been reported to locate at the boundaries of chromosome arrangements, such as large deletions, translocations, and inversions (Fig. 2C), which make the start and end of the same integrant distant from each other even in different chromosomes respectively.<sup>39,40</sup> Only when the structure variations of the host genome are dissected, can they have both breakpoints identified. Therefore, short-read sequencing will fail to predict the entire integrant for integration sites with complicated local sequence rearrangement. To meet the requirement for the characterization of entire integrants, long-read sequencing, with the longest single read over 2 Mb, is able to directly read through the entire integration region.<sup>23</sup> It can not only reveal integrations affected by large structure variations within the host genome but also characterize the organization of multiple copies of HBV fragments within the same integration site.<sup>23</sup>

## Recurrent genes interrupted by integration events

From the 1980s to the early 1990s, a few studies began to report HBV integration that affected the expression levels of a series of genes related to tumor development. They include *HST-1*,<sup>41</sup> tumor protein p53 (i.e. *TP53*),<sup>25,42</sup> cyclin A2 (*CCNA2*),<sup>43</sup> *myc* family oncogenes,<sup>44,45</sup> retinoic acid receptor beta or erb-B-like genes,<sup>46,47</sup> and mevalonate kinase gene.<sup>48</sup> With the accumulation of identified integration events, the frequencies of common recurrent genes affected by viral integrations become well characterized. The human telomerase reverse transcriptase (i.e. *hTERT*), which prevents telomere shortening after cell division, is not only the first reported recurrent gene affected by HBV integrations but it is also the most common one in HCC samples, ranging from nearly 20% (i.e. 17%, 14/82, Fujimoto *et al.*;<sup>49</sup> 24%, 101/426, Sun *et al.*;<sup>18</sup> 24%, 101/426, Zhao *et al.*;<sup>16</sup> 27%, 48/177, Péneau *et al.*<sup>50</sup>) to over 35% (36%, 34/95, Sze *et al.*<sup>37</sup>). The second most common recurrent gene was lysine methyltransferase 2B (*KMT2B*, also known as *MLL4* or *MLL2*), encoding histone methyltransferases, with a frequency of about 10% (2%, Péneau *et al.*;<sup>50</sup> 7%, Zhao *et al.*;<sup>16</sup> 7%, Fujimoto *et al.*;<sup>49</sup> 12%, Sun *et al.*;<sup>18</sup> 12%, Sze *et al.*<sup>37</sup>). They were followed by *CCNE1* (1%, Fujimoto *et al.*;<sup>49</sup> 1.6%, Zhao *et al.*;<sup>16</sup> 2%, Péneau *et al.*;<sup>50</sup> 3%, Sze *et al.*;<sup>37</sup> 5% Sun *et al.*<sup>18</sup>) and *CCNA2* (1%, Fujimoto *et al.*;<sup>49</sup> 1.8%, Zhao *et al.*;<sup>16</sup> 2%, Sze *et al.*<sup>37</sup>).

Whereas, integrations seem to account for a relatively small proportion of crucial genomic changes of total HCC.<sup>51</sup> For instance, about 70% of all HCC carry *TERT* mutations, and HBV integrations contribute to about 7% of them.<sup>52</sup> In other words, 5% of HCC are due to *TERT* integration;



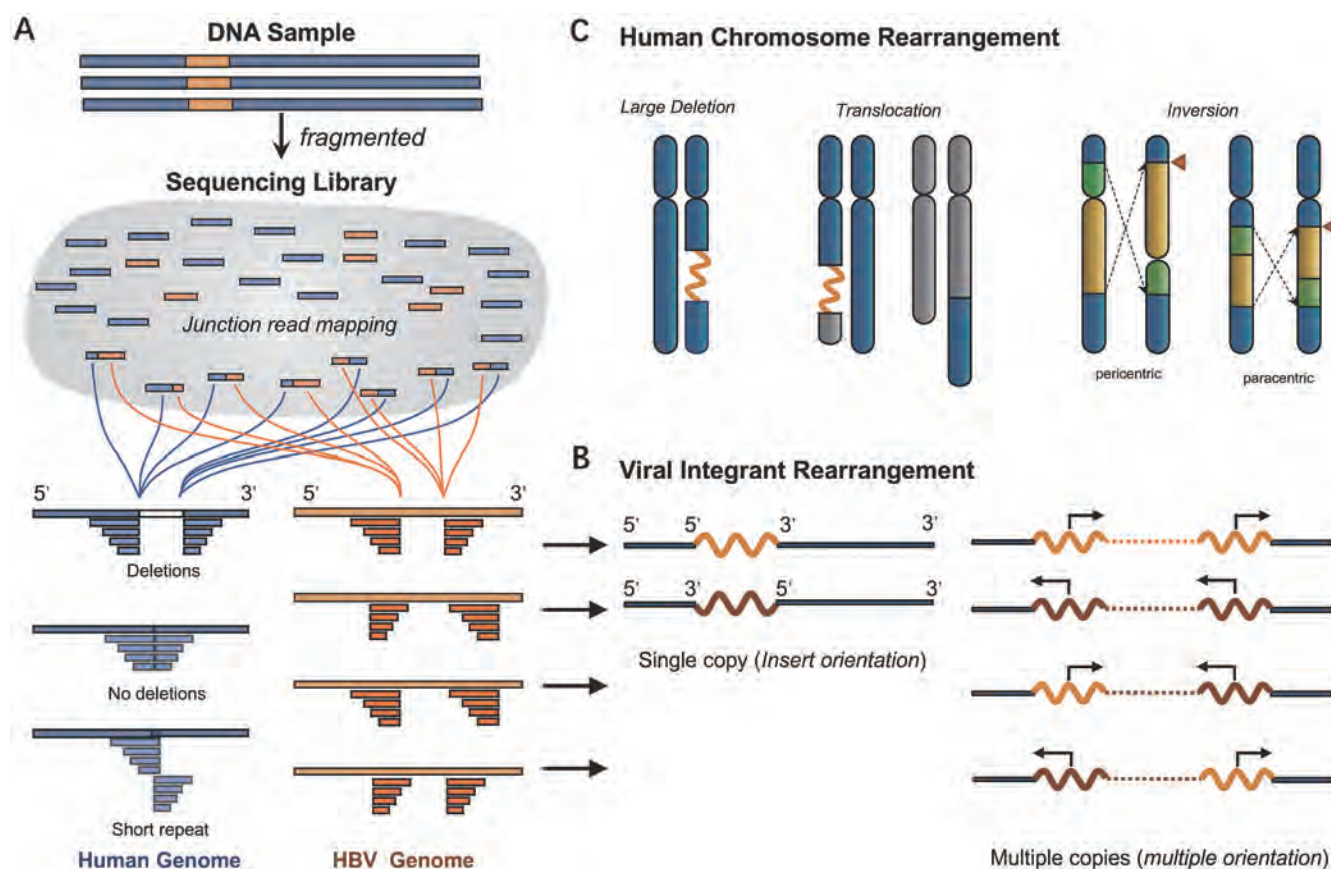


**Fig. 2. Integration identification based on short-read sequencing and confounding factors.** (A) In current solutions based on short-read sequencing, DNA samples will be fragmented into ideal size for subsequent library construction. Sequencing experiments will generate millions of reads, generally 150 bp in length, which need further bioinformatic analysis to map the reference host and viral genomes. Junction or chimeric reads, originating from an integration boundary, will be split into two pieces that are mapped to the host or viral reference genomes, respectively. Each integration event has two breakpoints, which can be paired according to their positions in the human genome. After successful pairing, read mapping patterns of paired breakpoints indicate the complicated rearrangement of viral integrants within the integration sites. (B) A single copy of an integrant may have either forward or reverse 5'-3' orientations with the host genome. The multiple copies of viral fragments are joined at distinct orientations before being incorporated into the integration site. Their orientation will determine which of them are downstream and affected by the integrant due to the *cis*-activation effect. (C) Large deletions, translocations and inversions are capable of joining two distant regions together and integration events tend to occur at the boundary of these structural variations. Such interaction will prevent pairing two breakpoints far apart from one another in the same integration event without any information about structural variations.

moreover, 58% of HCC have genomic changes affecting cell cycle control, and HBV integrations account for about 8% of those interrupting the *CCNE1*.<sup>52</sup> Considering HBV infection contributing to 50% of HCC cases, the contribution of integrations should be doubled in HBV-related HCC.<sup>53</sup>

#### HBV integration in gene promoter region: *cis*-activation effect

Integrations can influence the transcription of nearby genes by changing the promoter activity (Fig. 1; Gene Annotation), contributing to phenotype changes of affected cells. The integration site can be either only hundreds of base pairs (e.g., 257 bp upstream of *hTERT*<sup>54</sup>) or over 100 kb (e.g., 2,582 kb upstream of *CCNE1*<sup>55</sup>) from the genes in the vicinity along the human genome. In the first large-scale screening for HBV integrations in HCC, Sun *et al.*<sup>18</sup> explored integrations in the promoter region which were from 0 to -5 kb relative to the transcriptional start site (commonly referred to as TSS), while Fujimoto *et al.*<sup>49</sup> enlarged this region up to 10 kb upstream, which has become widely adopted. Nevertheless, the frequency and influence of inte-

gration in the promoter may be underestimated since some are located beyond the 10 kb region,<sup>56</sup> and Ding *et al.*<sup>35</sup> further extended the annotation region to 150 kb. However, analysis of the effects of long-range integration on gene expression regulation may be challenging and need further extensive validation.

Meanwhile, both the insertion orientation and the integration-TSS distance may influence their effect on the promoter activity of viral integrations. Telomerase expression was absent in mature hepatocytes, but 90% of the HCC<sup>57</sup> had *TERT*-related integrations, of which 80% are located in the promoter region.<sup>18</sup> In 2001, Horikawa *et al.*<sup>58</sup> first described the HBV integrations in the *cis*-activated *TERT* promoter in an orientation-independent manner. Recently, Sze *et al.*<sup>37</sup> found that when the orientation of an inserted HBV fragment (harboring enhancer I) was opposite to the *TERT* transcription direction, the promoter activity was reduced by 40% in comparison to the same-orientation integration. In 2012, Toh *et al.*<sup>34</sup> found that for *TERT* promoter integrations within 3 kb upstream in HCC tumor samples, the nearer it occurred to the TSS, the higher was the level of downstream *TERT* transcription. In tumors, the transcriptional levels of *TERT* could be over 10-fold higher, and this



increase has been associated with poorer survival of affected patients.<sup>16,35,37,49</sup>

### **Intragenic and intergenic integrations: fusion transcripts and trans-activation**

Fusion transcript detection from RNA-Seq has revealed that integration sites harboring a DR1 fragment, neighbored by regulatory elements such as the enhancer II, the preC promoter and the hormone response element, may produce virus-host chimeric transcripts.<sup>19</sup> This type of fusion transcript, commonly originating from interrupted genes, may have *trans*-acting effects on the regulation of gene expression (Fig. 1; Gene Annotation). In 1990, Takada *et al.*<sup>59</sup> reported the 3' truncated hepatitis B X gene (HBx)-cell fusion product; in 1995, Graef *et al.*<sup>60</sup> showed that HBV-mevalonate kinase fusion protein may lead to abnormal phosphorylation of cellular proteins by the affecting metabolism of mevalonate. Saigo *et al.*<sup>61</sup> described several HBV integrations located within a 300bp region within intron 3 flanked by the Alu element of *MLL4*, resulting in HBx/*MLL4* chimeric transcripts and fusion proteins that suppressed expression of certain genes. Then, Dong *et al.*<sup>62</sup> found integrations within *MLL4* could also occur in exon 3 and intron 5. In their study, the exonic integration resulted in an over 5-fold up-regulation of *MLL4* transcription, while the intronic one did not lead to significant changes in gene expression.<sup>62</sup> Meanwhile, Jiang *et al.*<sup>19</sup> observed the one integration, inserting two copies of HBV fragments in the 3' end of the exon 3 of *MLL4* gene, causing an over 20-fold up-regulation of its overall expression level; five HBV-*MLL4* integrations interrupting exon 3, 5 and 6 respectively in Furuta *et al.*'s<sup>63</sup> study all led to increased *MLL4* transcription in tumor samples. Viral integrations within fibronectin 1 (i.e. *FN1*) are most frequently observed in adjacent, non-tumor samples, and those at intronic ones are in the majority.<sup>18</sup> However, the frequency of HBV-*FN1* integration differs greatly among studies (4%, 17/426, Zhao *et al.*;<sup>16</sup> 8%, 14/170, Péneau *et al.*;<sup>50</sup> 12.5%, 5/40, Ding *et al.*;<sup>35</sup> 19%, 8/42, Furuta *et al.*;<sup>63</sup> 40%, 15/41, Furuta *et al.*<sup>63</sup>). HBV-*FN1* integrations were unlikely to significantly influence the expression level of *FN1* revealed in all these studies, which indicates different transcriptional activity and subsequent biological effects of integrations. Furuta *et al.*<sup>63</sup> speculated that HBV-*FN1* fusion transcripts might produce fusion protein, which can be involved in the pathogenesis of liver fibrosis, considering the regulatory roles of *FN1* in fibrosis. Nevertheless, Péneau *et al.*<sup>50</sup> argued that HBV-*FN1* may not have a functional effect since the *FN1* was not overexpressed due to integration. Future efforts should be made to answer why non-neoplastic hepatocytes carrying this common integration are not more likely to transform into tumor cells.

Intergenic integrations possibly account for functional chimeric noncoding transcripts. The HBx-long interspersed nuclear elements 1 (i.e. LINE1) is another type of fusion transcript, acting as a non-coding RNA.<sup>10,64</sup> Lau *et al.*<sup>64</sup> showed functions of HBx-*LINE1* did not rely on the fusion protein and it may affect  $\beta$ -catenin trans-activity, which is suggestive of a role played by Wnt signaling activation. Subsequently, Liang *et al.*<sup>65</sup> used the cell-line model to confirm that HBx-*LINE1* can serve as a miR-122 sponge, which is a liver-specific miRNA and a key regulator in liver diseases.<sup>66</sup> Lau *et al.*<sup>64</sup> reported the incidence of HBx-*LINE1* in HCC samples from the Chinese population reached 23.3% (21/90), but Trung *et al.*<sup>67</sup> did not detect this transcript in their 119 Vietnamese patients with HBV-associated HCC. Further efforts may need to clarify the underlying confounding factors, such as heterogeneity of

tumor samples and diversity of inserted HBx fragments with different RNA production ability. LINE1-related genes have attracted more and more interest in their roles in tumorigenesis and have been proposed as novel targets in HCC treatment.<sup>10,68,69</sup>

### **Chimeric fragments of HBV DNA and mitochondrial DNA (mtDNA)**

HBV-mtDNA integrations were observed, and the most frequently inserted site reported by Furuta *et al.*<sup>63</sup> is hypervariable region I (also known as HV I or HV1) in the control region of mtDNA, which contains the mitochondrial origin of replication and transcription. Although there is no evidence that HBV DNA can directly integrate into mtDNA, mtDNA can enter the cell nucleus via an uncharacterized process and is widely believed to integrate into the nuclear genome via non-homologous end joining at DSBs, forming nuclear copies of mtDNA (NUMTs).<sup>70</sup> Therefore, either HBV DNA was incorporated into the NUMTs or mtDNA and HBV dsDNA could also be ligated together via the same mechanism, but this possibility requires further validation by long-read sequencing to read through the entire integration site to determine if HBV-mtDNA chimeric fragments were definitely incorporated into the nuclear genome. Similar to HBV integrations in hepatocytes, the NUMTs also have diverse orientations and multiple fragments within the same site.<sup>71</sup> Multiple mtDNA fragment insertional mutagenesis at a single genomic site is unlikely. This is apparent since integration into a specific site is a random rather than a directed process. This consideration accounts for why DSB insertion is not likely to occur at a specific site (e.g., previous integration site) in a particular clone. They may originate from multiple copies of mtDNA fragments ligated or concatenated before being incorporated into the nuclear genome.<sup>71</sup> Delineating the similarities and differences between NUMTs and HBV integrations may provide more clues for clarifying the complicated underlying biological process.

**Repeat elements:** Alu PCR was first applied in HBV integration detection due to its ability to narrow the breadth of regions for analysis,<sup>27</sup> while accumulated evidence has shown that viral integrations (>50%) tend to locate at repeat regions within the human genome.<sup>35,72</sup> They include short interspersed nuclear elements (SINE) (including Alu repeats), LINES and simple repeats (also termed microsatellites). The top repeat element is LINE, followed by LTR, SINE and SINE-VNTR-Alu according to Budzinska *et al.*'s<sup>73</sup> observation in chronic hepatitis patients and an *in vitro* cell model. Nevertheless, we found the most common repeat region, was directly interrupted rather than abutting the cancer-enriched human alpha satellite (ALR/Alpha) identified in over 40% of the HCC cases.<sup>21</sup>

(TTAGGG)<sub>n</sub> is the featured sequence of nucleotides in telomeres, which are commonly affected by integrations. It indicates that the insertion of viral fragments may change the telomere length. The telomeres are 8–10 kb long in young individuals, decreasing at a rate of 24.8–27.7 bp per year;<sup>74</sup> viral integrations may range from hundreds of base pairs to over 3 kb, that increase the length significantly. The elongation of telomeres can prevent affected cells from replicative senescence and sustain cell division activity, leading to genomic instability.<sup>74</sup> This potential effect may need further experimental validation.

Besides, we found the L1ME1 of family LINE-1 (L1) (~20% cases) is the most frequently affected LINE element.<sup>21</sup> Interestingly, more evidence has been provided revealing that the activation of L1 contributes to hepatitis virus-related HCC.<sup>69,75</sup> Particularly, HBV infection suppresses interferon signal transduction by disrupting either STAT1 nuclear im-

port or phosphorylation.<sup>76</sup> The inhibition of interferon is believed to activate the L1 retrotransposon,<sup>77</sup> which subsequently creates DSBs in host cells.<sup>78</sup> LINEs and SINEs are subtypes of transposable elements, which are attracting increasing amounts of attention in recent studies. This interest is due to the realization that they play roles in shaping genome structure by their insertional activity and alteration of transcriptional networks.<sup>79</sup>

### DNA methylation of HBV integration sites

DNA methylation is one of the main epigenetic modifications regulating gene expression through chromosomal structural alteration, changes in both DNA conformation, and DNA stability.<sup>80</sup> Aberrant methylations of a CpG island in the promoter and gene body are known to lead to transcriptional changes of genes.<sup>81</sup> HBV infection is known to cause changes in the DNA methylation status of hepatocytes, which may not only regulate the viral replication but also contribute to host immune responses.<sup>82,83</sup> Transcription activity at integration sites is likely to be also under epigenetic regulation of host cells, and most of “functional” viral integrations may have to remain “unsilenced” to continue their involvement in inducing phenotype changes in the infected cells. In 2015, Watanabe *et al.*<sup>84</sup> described that the methylation status was consistent in the integrant and flanking regions in the host genome in PLC/PRF/5 cell lines and HBV-HCC tumor and adjacent tissues. In 2016, Wang *et al.*<sup>16</sup> pointed out that HBV integrations in tumor tissues were significantly enriched in the CpG islands, which are crucial sites wherein changes in the DNA methylation status can alter gene expression regulation. In 2020, Zhang *et al.*<sup>85</sup> found that, within 6,073 different previously identified integration regions, methylation levels of neighboring nucleotides reflected the global hypomethylation in the tumor genome well, regardless of whether integration occurred. This agreement is supportive of the notion that the integration regions tend to be hypomethylated during HCC development independent of integration occurrence. All of these findings point to the idea that the ability of integrations to induce altered biological functions may depend on the corresponding epigenetic status of inserted sites.

### HBV integrants: Latent danger after HBV clearance?

Even after cccDNA clearance, viral integrants can still exist stably in the host nuclear genome and replicate along with the host genome, as well as most likely not being lost during cell divisions.<sup>86</sup> To the best of our knowledge, there is so far no evidence for the spontaneous removal of viral integrants in affected cells. Genome editing technology is a feasible solution to eliminate the target fragment in the genome.<sup>87</sup> In 2017, Li *et al.*<sup>88</sup> excised a full-length 3,175-bp integrant in a stable HBV cell line HepG2.A64 using the CRISPR-Cas9 system and also disrupted HBV cccDNA. Assuming viral proteins produced by integrants act as neoantigens in tumor cells, this possibility forms the basis of novel immune therapeutic strategies for HBV-related HCC.<sup>89,90</sup> In 2019, Tan *et al.*<sup>91</sup> proposed using expression profiling of HBV integrants in HCC to select T cells for immunotherapy of HCC, and showed that even integrants, which encode not whole HBsAg but fragmented S genes, may produce hepatitis B surface antigen-derived epitopes for T cell receptor-engineered T cell therapy. In 2020, de Beijer *et al.*<sup>92</sup> attempted to identify the HBx and polymerase-derived T cell epitopes for effective HBV antigen-specific immunotherapies.

Most of the identified integrants only cover partial fragments and no more than one copy of the entire HBV ge-

nome. At least a 1.1-fold over-length HBV genome is required to achieve viral replication when being cloned into plasmids.<sup>93</sup> Therefore, natural HBV integrants are “defective”, which means they are not able to produce viruses.<sup>94</sup> Nevertheless, diverse integrants still have differential activities. In the aforementioned *cis*-activation effect of integrations within gene promoter regions, regulatory elements in the viral genome, particularly enhancer I, are believed to play important roles. Meanwhile, HBV integrations always harbor the complete open reading frames pre-S/S, and a 3' truncated X gene.<sup>12</sup> Without viral replication, they still can produce peptides of surface and X proteins, which play crucial roles in tumorigenesis during a long history of HBV infection. Oncogenic roles of HBx include its pleiotropic activities on DNA repair, cell cycle regulation, and diverse signaling pathways.<sup>95</sup> Particularly, most of the integrated X genes are 3' truncated and able to produce chimeric proteins.<sup>34</sup> Meanwhile, COOH-terminally truncated HBx is known to regulate cell cycle and apoptosis,<sup>96,97</sup> activate C-Jun/matrix metalloproteinase protein 10 to increase cell proliferation,<sup>98</sup> and enhance tumor cell invasion and metastasis.<sup>99</sup> Early in 1987, Nagaya *et al.*<sup>94</sup> summarized integrants in 31 reported cases, among which 4 were preS partially deleted. These mutants produce truncated surface proteins that accumulate in liver cells and may cause endoplasmic reticulum stress, with the consequent induction of oxidative DNA damage and genomic instability.<sup>100</sup> In 2017, Wooddell *et al.*<sup>101</sup> revealed that viral integrations may be a non-negligible source of hepatitis B surface antigen, which may interfere with the endpoint expectations of antiviral therapies, depending on the levels of viral proteins.

Indeed, not all integrations are active and some may be silenced with epigenetic modifications, consistent with surrounding host genomic regions.<sup>84</sup> Nevertheless, genome instability and aberrant methylation of infected hepatocytes may lead to variant accumulation or DNA hypomethylation during liver disease progression. There would be newly-established regulatory relations between integrations and affected genes due to structure variations, or production and accumulation of viral proteins coding by an integrant after abnormal activation, which may act as a latent risk factor in HBV infection that may cause diverse damage to infected liver cells.

### Reflection of integration events on clone expansion of affected hepatocytes

HBV integration may occur frequently in the chronic hepatitis stage. As early as 1981, Br  chot *et al.*<sup>102</sup> pointed out that HBV integrations may occur early during infection,<sup>103</sup> and other studies showed viral integrations are already present in acute or chronic hepatitis patients. By development and application of the inversed PCR, Summers and Mason<sup>31–33</sup> were first able to comprehensively investigate the clonal expansion by quantitative analysis of hepadnaviral DNA integrations in the woodchuck, chimpanzee, and human hepatocytes. Integration can occur immediately after infection, and large hepatocyte clones with viral integrations can be detected in all the stages of chronic hepatitis.<sup>8,21,104</sup> For spontaneous DSBs required for viral integrations, the majority appear in the context of DNA replication,<sup>105</sup> and about 10 to 50 DSBs occur per cell per day in any given cell, depending on cell cycle and tissue.<sup>106</sup> Considering the sparse and random feature of DSBs, it may require adequate dsIDNA as substrates or generate more DSBs in the host genome.<sup>107</sup> In the chronic hepatitis stage, both hepatocyte clone expansion and high HBV replication levels are common, and studies have observed more integration events in relatively normal liver tissues.<sup>35,63</sup> Mason *et al.*<sup>108</sup> believe

After tumor formation, HCC may not be able to accumulate integrations with the same frequency as in normal hepatocytes. First, HCC has undergone down-regulation of HBV receptor expression, the Na<sup>+</sup>/taurocholate polypeptide cotransporter (i.e. *NTCP*),<sup>109</sup> is not susceptible to infection, during which 10% of the viral particles introduce dsDNA into infected cells. Second, efficient HBV replication requires infected cells to maintain a state of cell differentiation,<sup>110</sup> which is missing in HCC. Therefore, the HBV replication level in HCC tissues is likely to be incompatible with that in normal tissues. Halgand *et al.*<sup>111</sup> observed that HBV pgRNA was detectable in most (90%) HCC non-tumor tissues but in only 67% of the HCC in tumor tissues. Fewer new infections and reduced HBV replication reduce the integration possibility. Regardless of more clone expansion with increased accumulation of DSBs, fewer integration events were detected in HCC tissues.<sup>35,63</sup>

9 1 9 9 9

## Conclusions



Medical University for language editing and proofreading of the manuscript.

Funding

This work was supported by the 111Project (Project No.: B13003), Innovation Promotion Association CAS (2016098), and National Natural Science Foundation of China (81201700) to D.Z.

Conflict of interest

Dake Zhang has an authorized patent for the probe-based HBV DNA capture in plasma as a liquid biopsy to monitor HCC development. The other authors have no conflict of interests related to this publication.

Author contributions

Substantial contributions to conception (DZ, KZ), manuscript writing and organizing, collection of data and data interpretation (DZ, KZ, CZ, UP).

References

[1] Zamor PJ, deLemos AS, Russo MW. Viral hepatitis and hepatocellular carcinoma: etiology and management. *J Gastrointest Oncol* 2017;8(2):229–242. doi:10.21037/jgo.2017.03.14.

[2] Brechot C, Pourcel C, Louise A, Rain B, Tiollais P. Presence of integrated hepatitis B virus DNA sequences in cellular DNA of human hepatocellular carcinoma. *Nature* 1980;286(5772):533–535. doi:10.1038/286533a0.

[3] Edman JC, Gray P, Valenzuela P, Rall LB, Rutter WJ. Integration of hepatitis B virus sequences and their expression in a human hepatoma cell. *Nature* 1980;286(5772):535–538. doi:10.1038/286535a0.

[4] Jiang S, Yang Z, Li W, Li X, Wang Y, Zhang J, et al. Re-evaluation of the carcinogenic significance of hepatitis B virus integration in hepatocarcinogenesis. *PLoS One* 2012;7(9):e40363. doi:10.1371/journal.pone.0040363.

[5] Davison FD, Fagan EA, Portmann B, Williams R. HBV-DNA sequences in tumor and nontumor tissue in a patient with the fibrolamellar variant of hepatocellular carcinoma. *Hepatology* 1990;12(4 Pt 1):676–679. doi:10.1002/hep.1840120410.

[6] Shafritz DA. Integration of HBV-DNA into liver and hepatocellular carcinoma cells during persistent HBV infection. *J Cell Biochem* 1982;20(3):303–316. doi:10.1002/jcb.240200310.

[7] Xia Y, Liang TJ. Development of direct-acting antiviral and host-targeting agents for treatment of hepatitis B virus infection. *Gastroenterology* 2019;156(2):311–324. doi:10.1053/j.gastro.2018.07.057.

[8] Tu T, Budzinska MA, Vondran FWR, Shackel NA, Urban S. Hepatitis B virus DNA integration occurs early in the viral life cycle in an *in vitro* infection model via sodium taurocholate cotransporting polypeptide-dependent uptake of enveloped virus particles. *J Virol* 2018;92(11):e02007–17. doi:10.1128/JVI.02007-17.

[9] Tu T, Budzinska MA, Shackel NA, Urban S. HBV DNA integration: Molecular mechanisms and clinical implications. *Viruses* 2017;9(4):75. doi:10.3390/v9040075.

[10] Heikenwalder M, Protzer U. LINE(1)s of evidence in HBV-driven liver cancer. *Cell Host Microbe* 2014;15(3):249–250. doi:10.1016/j.chom.2014.02.015.

[11] Bill CA, Summers J. Genomic DNA double-strand breaks are targets for hepadnaviral DNA integration. *Proc Natl Acad Sci U S A* 2004;101(30):11135–11140. doi:10.1073/pnas.0403925101.

[12] Zhao K, Liu A, Xia Y. Insights into hepatitis B virus DNA integration-55 years after virus discovery. *The Innovation* 2020;1(2):100034. doi:10.1016/j.xinn.2020.100034.

[13] Tsukuda S, Watashi K. Hepatitis B virus biology and life cycle. *Antiviral Res* 2020;182:104925. doi:10.1016/j.antiviral.2020.104925.

[14] Budzinska MA, Shackel NA, Urban S, Tu T. Cellular genomic sites of hepatitis B virus DNA integration. *Genes (Basel)* 2018;9(7):365. doi:10.3390/genes9070365.

[15] Dejean A, Sonigo P, Wain-Hobson S, Tiollais P. Specific hepatitis B virus integration in hepatocellular carcinoma DNA through a viral 11-base-pair direct repeat. *Proc Natl Acad Sci U S A* 1984;81(17):5350–5354. doi:10.1073/pnas.81.17.5350.

[16] Zhao LH, Liu X, Yan HX, Li WY, Zeng X, Yang Y, et al. Genomic and oncogenic preference of HBV integration in hepatocellular carcinoma. *Nat Commun* 2016;7:12992. doi:10.1038/ncomms12992.

[17] Li X, Zhang J, Yang Z, Kang J, Jiang S, Zhang T, et al. The function of targeted host genes determines the oncogenicity of HBV integration in hepa-

Zhang D. et al: Genomic functions at HBV integration sites

tocellular carcinoma. *J Hepatol* 2014;60(5):975–984. doi:10.1016/j.jhep.2013.12.014.

[18] Sung WK, Zheng H, Li S, Chen R, Liu X, Li Y, et al. Genome-wide survey of recurrent HBV integration in hepatocellular carcinoma. *Nat Genet* 2012;44(7):765–769. doi:10.1038/ng.2295.

[19] Jiang Z, Jhunhunjwala S, Liu J, Haverty PM, Kennemer MI, Guan Y, et al. The effects of hepatitis B virus integration into the genomes of hepatocellular carcinoma patients. *Genome Res* 2012;22(4):593–601. doi:10.1101/gr.133926.111.

[20] Fujimoto A, Totoki Y, Abe T, Boroevich KA, Hosoda F, Nguyen HH, et al. Whole-genome sequencing of liver cancers identifies etiological influences on mutation patterns and recurrent mutations in chromatin regulators. *Nat Genet* 2012;44(7):760–764. doi:10.1038/ng.2291.

[21] Chen W, Zhang K, Dong P, Fanning G, Tao C, Zhang H, et al. Noninvasive chimeric DNA profiling identifies tumor-originated HBV integrants contributing to viral antigen expression in liver cancer. *Hepatol Int* 2020;14(3):326–337. doi:10.1007/s12072-020-10016-2.

[22] Li CL, Ho MC, Lin YY, Tzeng ST, Chen YJ, Pai HY, et al. Cell-free virus-host chimera DNA from hepatitis B virus integration sites as a circulating biomarker of hepatocellular cancer. *Hepatology* 2020;72(6):2063–2076. doi:10.1002/hep.31230.

[23] Meng G, Tan Y, Fan Y, Wang Y, Yang G, Fanning G, et al. TSD: A computational tool to study the complex structural variants using PacBio targeted sequencing data. *G3 (Bethesda)* 2019;9(5):1371–1376. doi:10.1534/g3.118.200900.

[24] Chakraborty PR, Ruiz-Opazo N, Shouval D, Shafritz DA. Identification of integrated hepatitis B virus DNA and expression of viral RNA in an HBsAg-producing human hepatocellular carcinoma cell line. *Nature* 1980;286(5772):531–533. doi:10.1038/286531a0.

[25] Zhou YZ, Slagle BL, Donehower LA, vanTuijn P, Ledbetter DH, Butel JS. Structural analysis of a hepatitis B virus genome integrated into chromosome 17p of a human hepatocellular carcinoma. *J Virol* 1988;62(11):4224–4231. doi:10.1128/JVI.62.11.4224-4231.1988.

[26] Tokino T, Matsubara K. Chromosomal sites for hepatitis B virus integration in human hepatocellular carcinoma. *J Virol* 1991;65(12):6761–6764. doi:10.1128/JVI.65.12.6761-6764.1991.

[27] Minami M, Poussin K, Bréchet C, Paterlini P. A novel PCR technique using Alu-specific primers to identify unknown flanking sequences from the human genome. *Genomics* 1995;29(2):403–408. doi:10.1006/geno.1995.9004.

[28] Deininger P. Alu elements: know the SINEs. *Genome Biol* 2011;12(12):236. doi:10.1186/gb-2011-12-12-236.

[29] Gozuacik D, Murakami Y, Salgo K, Chami M, Mugnier C, Lagorce D, et al. Identification of human cancer-related genes by naturally occurring Hepatitis B Virus DNA tagging. *Oncogene* 2001;20(43):6233–6240. doi:10.1038/sj.onc.1204835.

[30] Mason WS, Liu C, Aldrich CE, Litwin S, Yeh MM. Clonal expansion of normal-appearing human hepatocytes during chronic hepatitis B virus infection. *J Virol* 2010;84(16):8308–8315. doi:10.1128/JVI.00833-10.

[31] Mason WS, Jilbert AR, Summers J. Clonal expansion of hepatocytes during chronic woodchuck hepatitis virus infection. *Proc Natl Acad Sci U S A* 2005;102(4):1139–1144. doi:10.1073/pnas.0409332102.

[32] Summers J, Jilbert AR, Yang W, Aldrich CE, Saputelli J, Litwin S, et al. Hepatocyte turnover during resolution of a transient hepadnaviral infection. *Proc Natl Acad Sci U S A* 2003;100(20):11652–11659. doi:10.1073/pnas.1635109100.

[33] Mason WS, Low HC, Xu C, Aldrich CE, Scougall CA, Grosse A, et al. Detection of clonally expanded hepatocytes in chimpanzees with chronic hepatitis B virus infection. *J Virol* 2009;83(17):8396–8408. doi:10.1128/JVI.00700-09.

[34] Toh ST, Jin Y, Liu L, Wang J, Babrzadeh F, Ghazizadeh B, et al. Deep sequencing of the hepatitis B virus in hepatocellular carcinoma patients reveals enriched integration events, structural alterations and sequence variations. *Carcinogenesis* 2013;34(4):787–798. doi:10.1093/carcin/bgs406.

[35] Ding D, Lou X, Hua D, Yu W, Li L, Wang J, et al. Recurrent targeted genes of hepatitis B virus in the liver cancer genomes identified by a next-generation sequencing-based approach. *PLoS Genet* 2012;8(12):e1003065. doi:10.1371/journal.pgen.1003065.

[36] Zapotka M, Borozan I, Brewer DS, Iskar M, Grundhoff A, Alawi M, et al. The landscape of viral associations in human cancers. *Nat Genet* 2020;52(3):320–330. doi:10.1038/s41588-019-0558-9.

[37] Sze KM, Ho DW, Chiu YT, Tsui YM, Chan LK, Lee JM, et al. Hepatitis B virus-telomerase reverse transcriptase promoter integration harnesses host ELF4, resulting in telomerase reverse transcriptase gene transcription in hepatocellular carcinoma. *Hepatology* 2021;73(1):23–40. doi:10.1002/hep.31231.

[38] Amarasinghe SL, Su S, Dong X, Zappia L, Ritchie ME, Gouil Q. Opportunities and challenges in long-read sequencing data analysis. *Genome Biol* 2020;21(1):30. doi:10.1186/s13059-020-1935-5.

[39] Chen XP, Long X, Jia WL, Wu HJ, Zhao J, Liang HF, et al. Viral integration drives multifocal HCC during the occult HBV infection. *J Exp Clin Cancer Res* 2019;38(1):261. doi:10.1186/s13046-019-1273-1.

[40] Takada S, Gotoh Y, Hayashi S, Yoshida M, Koike K. Structural rearrangement of integrated hepatitis B virus DNA as well as cellular flanking DNA is present in chronically infected hepatic tissues. *J Virol* 1990;64(2):822–828. doi:10.1128/JVI.64.2.822-828.1990.

[41] Hatada I, Tokino T, Ochiya T, Matsubara K. Co-amplification of integrated hepatitis B virus DNA and transforming gene hst-1 in a hepatocellular carcinoma. *Oncogene* 1988;3(5):537–540.

[42] Slagle BL, Zhou YZ, Butel JS. Hepatitis B virus integration event in human chromosome 17p near the p53 gene identifies the region of the chromo-

- some commonly deleted in virus-positive hepatocellular carcinomas. *Cancer Res* 1991;51(1):49–54.
- [43] Wang J, Zindy F, Chenivresse X, Lamas E, Henglein B, Br  chot C. Modification of cyclin A expression by hepatitis B virus DNA integration in a hepatocellular carcinoma. *Oncogene* 1992;7(8):1653–1656.
- [44] Wei Y, Ponzetto A, Tiollais P, Buendia MA. Multiple rearrangements and activated expression of c-myc induced by woodchuck hepatitis virus integration in a primary liver tumour. *Res Virol* 1992;143(2):89–96. doi:10.1016/s0923-2516(06)80086-5.
- [45] Baba M, Hasegawa H, Nakayabu M, Tamaki S, Watanabe S, Shima T, *et al*. Characteristics of human hepatocellular carcinoma cell lines (Hep-KANO) derived from a non-hepatic, non-cirrhotic hepatitis B virus carrier. *Jpn J Cancer Res* 1994;85(11):1105–1111. doi:10.1111/j.1349-7006.1994.tb02914.x.
- [46] Zhang XK, Egan JO, Huang D, Sun ZL, Chien VK, Chiu JF. Hepatitis B virus DNA integration and expression of an erb B-like gene in human hepatocellular carcinoma. *Biochem Biophys Res Commun* 1992;188(1):344–351. doi:10.1016/0006-291x(92)92391-a.
- [47] Dejean A, Bougu  leret L, Grzeschik KH, Tiollais P. Hepatitis B virus DNA integration in a sequence homologous to v-erb-A and steroid receptor genes in a hepatocellular carcinoma. *Nature* 1986;322(6074):70–72. doi:10.1038/322070a0.
- [48] Graef E, Caselmann WH, Wells J, Koshy R. Insertional activation of mevalonate kinase by hepatitis B virus DNA in a human hepatoma cell line. *Oncogene* 1994;9(1):81–87.
- [49] Fujimoto A, Furuta M, Totoki Y, Tsunoda T, Kato M, Shiraishi Y, *et al*. Whole-genome mutational landscape and characterization of noncoding and structural mutations in liver cancer. *Nat Genet* 2016;48(5):500–509. doi:10.1038/ng.3547.
- [50] P  neau C, Imbeaud S, La Bella T, Hirsch TZ, Caruso S, Calderaro J, *et al*. Hepatitis B virus integrations promote local and distant oncogenic driver alterations in hepatocellular carcinoma. *Gut* 2021. doi:10.1136/gutjnl-2020-323153.
- [51] Villanueva A. Hepatocellular carcinoma. *N Engl J Med* 2019;380(15):1450–1462. doi:10.1056/NEJMra1713263.
- [52] Schulze K, Nault JC, Villanueva A. Genetic profiling of hepatocellular carcinoma using next-generation sequencing. *J Hepatol* 2016;65(5):1031–1042. doi:10.1016/j.jhep.2016.05.035.
- [53] Llovet JM, Kelley RK, Villanueva A, Singal AG, Pikarsky E, Roayaie S, *et al*. Hepatocellular carcinoma. *Nat Rev Dis Primers* 2021;7(1):6. doi:10.1038/s41572-020-00240-3.
- [54] Kekul   AS, Lauer U, Meyer M, Caselmann WH, Hofschneider PH, Koshy R. The preS2/S region of integrated hepatitis B virus DNA encodes a transcriptional transactivator. *Nature* 1990;343(6257):457–461. doi:10.1038/343457a0.
- [55] Tsuei DJ, Hsu TY, Chen JY, Chang MH, Hsu HC, Yang CS. Analysis of integrated hepatitis B virus DNA and flanking cellular sequences in a childhood hepatocellular carcinoma. *J Med Virol* 1994;42(3):287–293. doi:10.1002/jmv.1890420316.
- [56] Murakami Y, Saigo K, Takashima H, Minami M, Okanoue T, Br  chot C, *et al*. Large scaled analysis of hepatitis B virus (HBV) DNA integration in HBV related hepatocellular carcinomas. *Gut* 2005;54(8):1162–1168. doi:10.1136/gut.2004.054452.
- [57] Nault JC, Ningharhari M, Rebouissou S, Zucman-Rossi J. The role of telomeres and telomerase in cirrhosis and liver cancer. *Nat Rev Gastroenterol Hepatol* 2019;16(9):544–558. doi:10.1038/s41575-019-0165-3.
- [58] Horikawa I, Barrett JC. cis-Activation of the human telomerase gene (hTERT) by the hepatitis B virus genome. *J Natl Cancer Inst* 2001;93(15):1171–1173. doi:10.1093/jnci/93.15.1171.
- [59] Takada S, Koike K. Trans-activation function of a 3' truncated X gene-cell fusion product from integrated hepatitis B virus DNA in chronic hepatitis tissues. *Proc Natl Acad Sci U S A* 1990;87(15):5628–5632. doi:10.1073/pnas.87.15.5628.
- [60] Graef E, Caselmann WH, Hofschneider PH, Koshy R. Enzymatic properties of overexpressed HBV-mevalonate kinase fusion proteins and mevalonate kinase proteins in the human hepatoma cell line PLC/PRF/5. *Virology* 1995;208(2):696–703. doi:10.1006/viro.1995.1201.
- [61] Saigo K, Yoshida K, Ikeda R, Sakamoto Y, Murakami Y, Urashima T, *et al*. Integration of hepatitis B virus DNA into the myeloid/lymphoid or mixed-lineage leukemia (MLL4) gene and rearrangements of MLL4 in human hepatocellular carcinoma. *Hum Mutat* 2008;29(5):703–708. doi:10.1002/humu.20701.
- [62] Dong H, Zhang L, Qian Z, Zhu X, Zhu G, Chen Y, *et al*. Identification of HBV-MLL4 integration and its molecular basis in Chinese hepatocellular carcinoma. *PLoS One* 2015;10(4):e0123175. doi:10.1371/journal.pone.0123175.
- [63] Furuta M, Tanaka H, Shiraishi Y, Unida T, Imamura M, Fujimoto A, *et al*. Characterization of HBV integration patterns and timing in liver cancer and HBV-infected livers. *Oncotarget* 2018;9(38):25075–25088. doi:10.18632/oncotarget.25308.
- [64] Lau CC, Sun T, Ching AK, He M, Li JW, Wong AM, *et al*. Viral-human chimeric transcript predisposes risk to liver cancer development and progression. *Cancer Cell* 2014;25(3):335–349. doi:10.1016/j.ccr.2014.01.030.
- [65] Liang HW, Wang N, Wang Y, Wang F, Fu Z, Yan X, *et al*. Hepatitis B virus-human chimeric transcript HBx-LINE1 promotes hepatic injury via sequestering cellular microRNA-122. *J Hepatol* 2016;64(2):278–291. doi:10.1016/j.jhep.2015.09.013.
- [66] Fu X, Calin GA. miR-122 and hepatocellular carcinoma: from molecular biology to therapeutics. *EBioMedicine* 2018;37:17–18. doi:10.1016/j.ebiom.2018.10.032.
- [67] Trung NT, Hai LT, Giang DP, Hoan PQ, Binh MT, Hoan NX, *et al*. No expression of HBV-human chimeric fusion transcript (HBx-LINE1) among Vietnamese patients with HBV-associated hepatocellular carcinoma. *Ann Hepatol* 2019;18(2):404–405. doi:10.1016/j.aohp.2019.02.002.
- [68] Ardeljan D, Wang X, Oghbaie M, Taylor MS, Husband D, Deshpande V, *et al*. LINE-1 ORF2p expression is nearly imperceptible in human cancers. *Mob DNA* 2019;11:1. doi:10.1186/s13100-019-0191-2.
- [69] Honda T. Links between human LINE-1 retrotransposons and hepatitis virus-related hepatocellular carcinoma. *Front Chem* 2016;4:21. doi:10.3389/fchem.2016.00021.
- [70] Hazkani-Covo E, Zeller RM, Martin W. Molecular poltergeists: mitochondrial DNA copies (numts) in sequenced nuclear genomes. *PLoS Genet* 2010;6(2):e1000834. doi:10.1371/journal.pgen.1000834.
- [71] Wei W, Pagnamenta AT, Gleadall N, Sanchis-Juan A, Stephens J, Broxholme J, *et al*. Nuclear-mitochondrial DNA segments resemble paternally inherited mitochondrial DNA in humans. *Nat Commun* 2020;11(1):1740. doi:10.1038/s41467-020-15336-3.
- [72] Yan H, Yang Y, Zhang L, Tang G, Wang Y, Xue G, *et al*. Characterization of the genotype and integration patterns of hepatitis B virus in early- and late-onset hepatocellular carcinoma. *Hepatology* 2015;61(6):1821–1831. doi:10.1002/hep.27722.
- [73] Budzinska MA, Shackel NA, Urban S, Tu T. Sequence analysis of integrated hepatitis B virus DNA during HBeAg-seroconversion. *Emerg Microbes Infect* 2018;7(1):142. doi:10.1038/s41426-018-0145-7.
- [74] Shammass MA. Telomeres, lifestyle, cancer, and aging. *Curr Opin Clin Nutr Metab Care* 2011;14(1):28–34. doi:10.1097/MCO.0b013e32834121b1.
- [75] Schauer SN, Carreira PE, Shukla R, Gerhardt DJ, Gerdes P, Sanchez-Luque FJ, *et al*. L1 retrotransposition is a common feature of mammalian hepatocarcinogenesis. *Genome Res* 2018;28(5):639–653. doi:10.1101/gr.226693.117.
- [76] L  tgehetmann M, Bornscheuer T, Volz T, Allweiss L, Bockmann JH, Pollok JM, *et al*. Hepatitis B virus limits response of human hepatocytes to interferon-  in chimeric mice. *Gastroenterology* 2011;140(7):2074–2083. doi:10.1053/j.gastro.2011.02.057.
- [77] Yu C, Carbone CJ, Katlinskaya YV, Zheng H, Zheng K, Luo M, *et al*. Type I interferon controls propagation of long interspersed element-1. *J Biol Chem* 2015;290(16):10191–10199. doi:10.1074/jbc.M114.612374.
- [78] Gasior SL, Wakeman TP, Xu B, Deininger PL. The human LINE-1 retrotransposon creates DNA double-strand breaks. *J Mol Biol* 2006;357(5):1383–1393. doi:10.1016/j.jmb.2006.01.089.
- [79] Payer LM, Burns KH. Transposable elements in human genetic disease. *Nat Rev Genet* 2019;20(12):760–772. doi:10.1038/s41576-019-0165-8.
- [80] Greenberg MVC, Bourc'his D. The diverse roles of DNA methylation in mammalian development and disease. *Nat Rev Mol Cell Biol* 2019;20(10):590–607. doi:10.1038/s41580-019-0159-6.
- [81] Baylin SB. DNA methylation and gene silencing in cancer. *Nat Clin Pract Oncol* 2005;2(Suppl 1):S4–S11. doi:10.1038/npcnc0354.
- [82] Hong X, Kim ES, Guo H. Epigenetic regulation of hepatitis B virus covalently closed circular DNA: Implications for epigenetic therapy against chronic hepatitis B. *Hepatology* 2017;66(6):2066–2077. doi:10.1002/hep.29479.
- [83] Dandri M. Epigenetic modulation in chronic hepatitis B virus infection. *Semin Immunopathol* 2020;42(2):173–185. doi:10.1007/s00281-020-00780-6.
- [84] Watanabe Y, Yamamoto H, Oikawa R, Toyota M, Yamamoto M, Kokudo N, *et al*. DNA methylation at hepatitis B viral integrants is associated with methylation at flanking human genomic sequences. *Genome Res* 2015;25(3):328–337. doi:10.1101/gr.175240.114.
- [85] Zhang H, Dong P, Guo S, Tao C, Chen W, Zhao W, *et al*. Hypomethylation in HBV integration regions aids non-invasive surveillance to hepatocellular carcinoma by low-pass genome-wide bisulfite sequencing. *BMC Med* 2020;18(1):200. doi:10.1186/s12916-020-01667-x.
- [86] Summers J, Mason WS. Residual integrated viral DNA after hepadnavirus clearance by nucleoside analog therapy. *Proc Natl Acad Sci U S A* 2004;101(2):638–640. doi:10.1073/pnas.0307422100.
- [87] Ran FA, Hsu PD, Wright J, Agarwala V, Scott DA, Zhang F. Genome engineering using the CRISPR-Cas9 system. *Nat Protoc* 2013;8(11):2281–2308. doi:10.1038/nprot.2013.143.
- [88] Li H, Sheng C, Wang S, Yang L, Liang Y, Huang Y, *et al*. Removal of integrated hepatitis B virus DNA using CRISPR-Cas9. *Front Cell Infect Microbiol* 2017;7:91. doi:10.3389/fcimb.2017.00091.
- [89] Ni L, Feng Y, Dong C. The advancement of immunotherapy in hepatocellular carcinoma. *Hepatoma Res* 2020;6:25. doi:10.20517/2394-5079.2020.14.
- [90] Lim CJ, Chew V. Impact of viral etiologies on the development of novel immunotherapy for hepatocellular carcinoma. *Semin Liver Dis* 2020;40(2):131–142. doi:10.1055/s-0039-3399534.
- [91] Tan AT, Yang N, Lee Krishnamoorthy T, Oei V, Chua A, Zhao X, *et al*. Use of expression profiles of HBV-DNA integrated into genomes of hepatocellular carcinoma cells to select T cells for immunotherapy. *Gastroenterology* 2019;156(6):1862–1876.e9. doi:10.1053/j.gastro.2019.01.251.
- [92] de Beijer MTA, Jansen DTS, Dou Y, van Esch WJE, Mok JY, Maas MJP, *et al*. Discovery and selection of hepatitis B virus-derived T cell epitopes for global immunotherapy based on viral indispensability, conservation, and HLA-binding strength. *J Virol* 2020;94(7):e01663–19. doi:10.1128/JVI.01663-19.
- [93] Guidotti LG, Matzke B, Schaller H, Chisari FV. High-level hepatitis B virus replication in transgenic mice. *J Virol* 1995;69(10):6158–6169. doi:10.1128/JVI.69.10.6158-6169.1995.
- [94] Nagaya T, Nakamura T, Tokino T, Tsurimoto T, Imai M, Mayumi T, *et al*. The mode of hepatitis B virus DNA integration in chromosomes of human hepatocellular carcinoma. *Genes Dev* 1987;1(8):773–782. doi:10.1101/gad.1.8.773.
- [95] Geng M, Xin X, Bi LQ, Zhou LT, Liu XH. Molecular mechanism of hepatitis B virus X protein function in hepatocarcinogenesis. *World J Gastroenterol* 2015;21(38):10732–10738. doi:10.3748/wjg.v21.i38.10732.
- [96] Tu H, Bonura C, Giannini C, Mouly H, Soussan P, Kew M, *et al*. Biological

- impact of natural COOH-terminal deletions of hepatitis B virus X protein in hepatocellular carcinoma tissues. *Cancer Res* 2001;61(21):7803–7810.
- [97] Ma NF, Lau SH, Hu L, Xie D, Wu J, Yang J, *et al*. COOH-terminal truncated HBV X protein plays key role in hepatocarcinogenesis. *Clin Cancer Res* 2008;14(16):5061–5068. doi:10.1158/1078-0432.CCR-07-5082.
- [98] Sze KM, Chu GK, Lee JM, Ng IO. C-terminal truncated hepatitis B virus x protein is associated with metastasis and enhances invasiveness by C-Jun/matrix metalloproteinase protein 10 activation in hepatocellular carcinoma. *Hepatology* 2013;57(1):131–139. doi:10.1002/hep.25979.
- [99] Li W, Li M, Liao D, Lu X, Gu X, Zhang Q, *et al*. Carboxyl-terminal truncated HBx contributes to invasion and metastasis via deregulating metastasis suppressors in hepatocellular carcinoma. *Oncotarget* 2016;7(34):55110–55127. doi:10.18632/oncotarget.10399.
- [100] Pollicino T, Cacciola I, Saffioti F, Raimondo G. Hepatitis B virus PreS/S gene variants: pathobiology and clinical implications. *J Hepatol* 2014;61(2):408–417. doi:10.1016/j.jhep.2014.04.041.
- [101] Wooddell CI, Yuen MF, Chan HL, Gish RG, Locarnini SA, Chavez D, *et al*. RNAi-based treatment of chronically infected patients and chimpanzees reveals that integrated hepatitis B virus DNA is a source of HBsAg. *Sci Transl Med* 2017;9(409):eaan0241. doi:10.1126/scitranslmed.aan0241.
- [102] Bréchot C, Hadchouel M, Scotto J, Fonck M, Potet F, Vyas GN, *et al*. State of hepatitis B virus DNA in hepatocytes of patients with hepatitis B surface antigen-positive and -negative liver diseases. *Proc Natl Acad Sci U S A* 1981;78(6):3906–3910. doi:10.1073/pnas.78.6.3906.
- [103] Kimbi GC, Kramvis A, Kew MC. Integration of hepatitis B virus DNA into chromosomal DNA during acute hepatitis B. *World J Gastroenterol* 2005;11(41):6416–6421. doi:10.3748/wjg.v11.i41.6416.
- [104] Tu T, Mason WS, Clouston AD, Shackel NA, McCaughan GW, Yeh MM, *et al*. Clonal expansion of hepatocytes with a selective advantage occurs during all stages of chronic hepatitis B virus infection. *J Viral Hepat* 2015;22(9):737–753. doi:10.1111/jvh.12380.
- [105] Syeda AH, Hawkins M, McGlynn P. Recombination and replication. *Cold Spring Harb Perspect Biol* 2014;6(11):a016550. doi:10.1101/cshperspect.a016550.
- [106] Vilenchik MM, Knudson AG. Endogenous DNA double-strand breaks: production, fidelity of repair, and induction of cancer. *Proc Natl Acad Sci U S A* 2003;100(22):12871–12876. doi:10.1073/pnas.2135498100.
- [107] Weitzman MD, Fradet-Turcotte A. Virus DNA replication and the host DNA damage response. *Annu Rev Virol* 2018;5(1):141–164. doi:10.1146/annurev-virology-092917-043534.
- [108] Mason WS, Gill US, Litwin S, Zhou Y, Peri S, Pop O, *et al*. HBV DNA integration and clonal hepatocyte expansion in chronic hepatitis B patients considered immune tolerant. *Gastroenterology* 2016;151(5):986–998.e4. doi:10.1053/j.gastro.2016.07.012.
- [109] Yan H, Zhong G, Xu G, He W, Jing Z, Gao Z, *et al*. Sodium taurocholate cotransporting polypeptide is a functional receptor for human hepatitis B and D virus. *Elife* 2012;1:e00049. doi:10.7554/eLife.00049.
- [110] Ozer A, Khaoustov VI, Mearns M, Lewis DE, Genta RM, Darlington GJ, *et al*. Effect of hepatocyte proliferation and cellular DNA synthesis on hepatitis B virus replication. *Gastroenterology* 1996;110(5):1519–1528. doi:10.1053/gast.1996.v110.pm8613059.
- [111] Halgand B, Desterke C, Rivière L, Fallot G, Sebah M, Calderaro J, *et al*. Hepatitis B virus pregenomic RNA in hepatocellular carcinoma: A nosological and prognostic determinant. *Hepatology* 2018;67(1):86–96. doi:10.1002/hep.29463.
- [112] Wang A, Wu L, Lin J, Han L, Bian J, Wu Y, *et al*. Whole-exome sequencing reveals the origin and evolution of hepato-cholangiocarcinoma. *Nat Commun* 2018;9(1):894. doi:10.1038/s41467-018-03276-y.
- [113] Qu C, Wang Y, Wang P, Chen K, Wang M, Zeng H, *et al*. Detection of early-stage hepatocellular carcinoma in asymptomatic HBsAg-seropositive individuals by liquid biopsy. *Proc Natl Acad Sci U S A* 2019;116(13):6308–6312. doi:10.1073/pnas.1819799116.
- [114] Wang YC, Li CL, Ho MC, Lin YY, Tzeng ST, Chen YJ, *et al*. Cell-free junctional DNA fragment from hepatitis B virus integration in HCC for monitoring postresection recurrence and clonality. *J Clin Oncol* 2019;37(15\_suppl):4090. doi:10.1200/JCO.2019.37.15\_suppl.4090.





## Review Article

# A Review of Hepatitis B Virus and Hepatitis C Virus Immunopathogenesis

Corey Saraceni\* and John Birk

University of Connecticut School of Medicine, Department of Medicine, Division of Gastroenterology and Hepatology, Farmington, CT, USA

Received: 20 October 2020 | Revised: 21 February 2021 | Accepted: 22 April 2021 | Published: 31 May 2021

## Abstract

Despite the advances in therapy, hepatitis B virus (HBV) and hepatitis C virus (HCV) still represent a significant global health burden, both as major causes of cirrhosis, hepatocellular carcinoma, and death worldwide. HBV is capable of incorporating its covalently closed circular DNA into the host cell's hepatocyte genome, making it rather difficult to eradicate its chronic stage. Successful viral clearance depends on the complex interactions between the virus and host's innate and adaptive immune response. One encouraging fact on hepatitis B is the development and effective distribution of the HBV vaccine. This has significantly reduced the spread of this virus. HCV is a RNA virus with high mutagenic capacity, thus enabling it to evade the immune system and have a high rate of chronic progression. High levels of HCV heterogeneity and its mutagenic capacity have made it difficult to create an effective vaccine. The recent advent of direct acting antivirals has ushered in a new era in hepatitis C therapy. Sustained virologic response is achieved with DAAs in 85–99% of cases. However, this still leads to a large population of treatment failures, so further advances in therapy are still needed. This article reviews the immunopathogenesis of HBV and HCV, their properties contributing to host immune system avoidance, chronic disease progression, vaccine efficacy and limitations, as well as treatment options and common pitfalls of said therapy.

**Citation of this article:** Saraceni C, Birk J. A review of hepatitis B virus and hepatitis C virus immunopathogenesis.

**Keywords:** Hepatitis B immunopathogenesis; Hepatitis C immunopathogenesis.

**Abbreviations:** +ssRNA, positive sense single-stranded RNA; -ssRNA, negative sense single stranded RNA; AHB, acute hepatitis B; ALT, alanine aminotransferase; anti-HBc or HBcAb, hepatitis B core antibody; anti-HBs or HBsAb, hepatitis B surface antibody; cccDNA, covalently closed circular DNA; CHB, chronic hepatitis B; cLD, cytosolic lipid droplet; CLDN1, claudin 1; DAA, direct-acting antiviral; ESCRT, endosomal sorting complex required for transport; HBcAg, hepatitis B virus core antigen; HBsAg, hepatitis B virus e-antigen antibody; HBeAg, hepatitis B virus e-antigen; HBsAg, hepatitis B surface antigen; HBV, hepatitis B virus; HCC, hepatocellular carcinoma; HCV, hepatitis C virus; HLA, human leukocyte antigen; IFN, interferon; IFN- $\alpha$ , interferon 1; IFN- $\alpha$ , interferon-alpha; IFN- $\gamma$ , interferon-gamma; IL, interleukin; LCMV, lymphocytic choriomeningitis virus; LDL, low density lipid; NAS, nucleos(t)ide analogues; NK, natural killer; NKT, natural killer T; NPC1L1, Niemann-Pick C1-like 1 cholesterol absorption receptor; NTCP, sodium taurocholate cotransport polypeptide; OCLN, occludin; PCR, polymerase chain reaction; pDC, plasmacytoid dendritic cell; rcDNA, relaxed circular DNA; SR-BI, scavenger receptor class B type I; ssRNA, single-stranded RNA; SVR, sustained virological response; TGF- $\beta$ , transforming growth factor-beta; TLR3, Toll-like receptor 3; TNF- $\alpha$ , tumor necrosis factor alpha; Treg, regulatory T cell; VLDL, very low density lipid.

\*Correspondence to: Corey Saraceni, University of Connecticut School of Medicine, Department of Medicine, Division of Gastroenterology and Hepatology, 263 Farmington Avenue, Farmington, CT 06030-8074, USA. Tel: +1-203-733-7408, Fax: +1-860-679-3159, E-mail: saraceni@uchc.edu

J Clin Transl Hepatol 2021;9(3):409–418. doi: 10.14218/JCTH.2020.00095.

## Introduction

Hepatitis B virus (HBV) and hepatitis C virus (HCV) infections remain major global health issues. Although the two viruses directly infect the liver, they have very different courses. Worldwide, there are an estimated more than 250 million HBV carriers, of whom roughly 600,000 die annually from HBV-related liver disease.<sup>1,2</sup> Acute HBV infection in adults is normally self-limited and subclinical, resulting in chronic infection in about 5%, as compared to neonatal HBV infection, where the acute infection results in chronic infection in 90% of cases. As a DNA virus, it is capable of incorporating its covalently closed circular DNA (cccDNA) into the host cell's genome, making it rather difficult to eradicate once the infection progresses to the chronic stage.

HCV was first identified in 1989 as a major cause of non A or B viral hepatitis.<sup>3,4</sup> Approximately 100 million people around the world have serologic evidence of HCV exposure and 71 million have chronic hepatitis C infection, according to a 2015 World Health Organization study.<sup>5</sup> It is estimated that 60–80% of patients with acute HCV infection will develop chronic infection, with about 20% of these chronically-infected HCV patients developing cirrhosis over a 25 year period. Those with cirrhosis have a yearly incidence of HCC of about 4–5%.<sup>6,7</sup> HCV is an inconstant RNA virus with high mutagenic capacity, and this leads to frequent genome mutations that enable it to evade the immune system and thereby have a high rate of chronic progression.<sup>8</sup> Furthermore, due to this high level of HCV heterogeneity, it has been difficult to create an effective vaccine.

Understanding the immunopathogenesis of HBV and HCV is essential in determining disease progression, chronicity, and treatment. The purpose of this article was to review the factors associated with HBV and HCV immunopathogenesis, disease progression, and pitfalls of current treatment options (Table 1).

## Hepatitis B

### Background

HBV is an enveloped DNA virus from the Hepadnaviridae

Table 1. HBV and HCV immunopathogenesis

	Hepatitis B	Hepatitis C
Virus structure	rcDNA	ssRNA
Receptor entry	Hepatocyte-specific NTCP receptor: Bile acid uptake from portal blood	Multi-step entry mechanism: LDL-R, SR-BI, CD-81, CLDN1, OCLN, NPC1L
Chronic progression	Adult infection: Clearance: 95%, Chronic progression: 5% Neonatal vertical transmission: Clearance: 10%, Chronic progression: 90%	All patients: Clearance: 60–80%, Chronic progression: 20–40%
Mechanisms of immune evasion	CD4+ cell inhibiting factors: IL-10, TNF-B CD8+ cell inhibiting factors: PD-1, CD244, CTLA-4	CD4+ cell inhibiting factors (including Tregs): IL-10, TNF-B, Overall Reduced CD4+ response CD8+ cell escape mutations: PD-1, CTLA-4
Approved therapies	Interferon therapy: Standard INF- $\alpha$ , Pegylated-INF- $\alpha$ NAs Treatment initiation decision: Presence of cirrhosis, ALT level, HBV DNA level	Interferon therapy: Pegylated-INF- $\alpha$ + ribavirin DAAs Treatment selection varies by: Genotype, presence of cirrhosis, treatment history, human immunodeficiency virus co-infection, renal impairment
Goals of therapy	Attain disease suppression: Suppression of HBV DNA, Loss of HBeAg, Normalization of ALT, Decrease necroinflammatory activity, Decrease in fibrosis	Eradicate HCV RNA – attain SVR: Undetectable RNA level 12 wk after completion of therapy
Vaccines	Approved and effective vaccines: Plasma-derived vaccination, HBV three-series vaccine	No available effective vaccines

family. The virus particle consists of an exterior envelope surrounding a viral capsid containing relaxed circular DNA (rcDNA). When the virus infects hepatocytes, it leaves a stable cccDNA template within the cell's nucleus. This provides a stable, long-lasting template for viral replication and accounts for HBV's viral persistence. HBV hepatocyte

infection can be divided into the following steps: cell entry, capsid uncoating, DNA repair and transcription, RNA packaging, reverse transcription, enveloping, and virus secretion (Fig. 1).

Viral entry into the hepatocyte is mediated by hepatocyte-binding specific envelope proteins. The HBV viral sur-

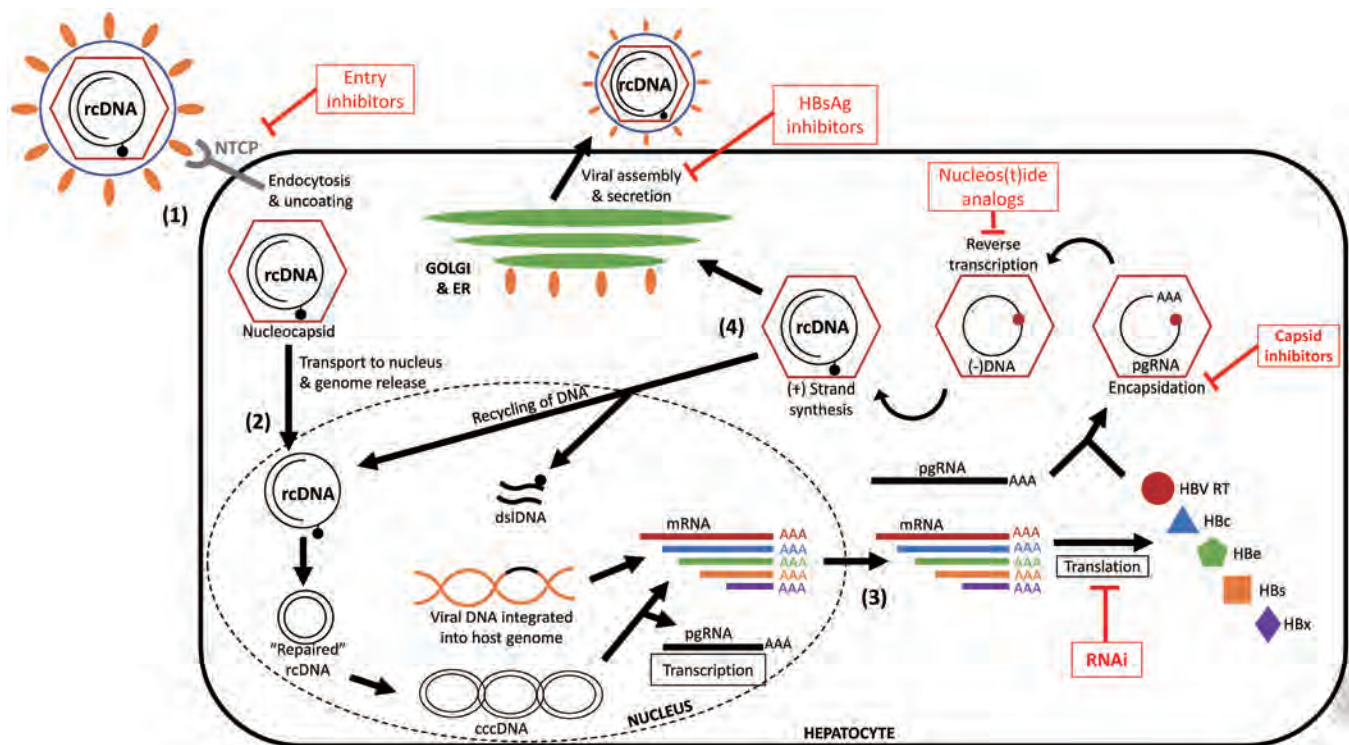
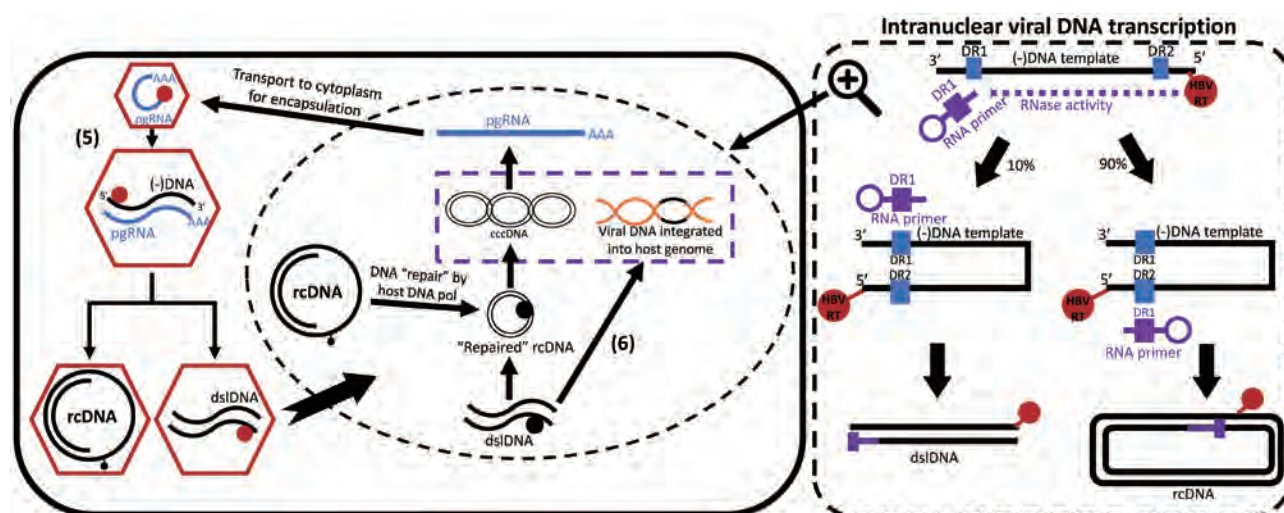


Fig. 1. Hepatitis B viral life cycle.



**Fig. 2. Hepatitis B DNA integration.** 1) HBV pre-S1 domain of envelope L protein binds to the hepatocyte-specific NTCP receptor (involved in bile acid uptake from portal blood flow), leading to cell entry.<sup>9,10</sup> The antigenic loop of HBV surface protein S between regions I and II interact with hepatocyte heparin sulfate proteoglycans and aid in HBV-NTCP receptor interaction.<sup>11</sup> 2) The viral nucleocapsid containing rcDNA is transported to the nucleus where it is "repaired" by the host cell's DNA repair mechanisms closing or "derelaxing" the rcDNA to form cccDNA. The cccDNA remains permanently in the hepatocyte's nucleus and acts as a template for viral mRNA and pgRNA.<sup>12,13</sup> 3) Viral mRNA and pgRNA are transported to the cytoplasm. Here, mRNA undergoes translation by host ribosomes to form viral proteins. The viral proteins and pgRNA are then assembled and encapsulated. pgRNA undergoes reverse transcription by newly transcribed HBV reverse transcriptase, producing a (-)DNA intermediate. pgRNA is then degraded and HBV reverse transcriptase completes transcription, producing an rcDNA containing nucleocapsid. 4) rcDNA containing nucleocapsids can either a) be enveloped and secreted as virions or b) cycle back to the nucleus to replenish the cccDNA pool.<sup>11,17</sup> 5) Transcription of pgRNA by HBV reverse transcriptase in a 3' to 5' direction resulting in a (-)DNA. pgRNA is then partially hydrolyzed by HBV reverse transcriptase, leaving an 18 nucleotide RNA primer for synthesis of (+) DNA strand. In ~90% of nucleocapsids, the RNA primer translocates to DR2 resulting in rcDNA as HBV reverse transcriptase synthesizes the (+)DNA resulting in an rcDNA containing nucleocapsid. In ~10% of pgRNA containing nucleocapsids, priming for reverse transcription occurs at the DR1 region (instead of DR2 region) of the (-)DNA template with resulting in dsIDNA. 6) Viral dsIDNA can then be transported to the nucleus and can incorporate into host DNA at double-strand DNA breaks.<sup>27</sup>

face contains three proteins: L, M, and S. The virus binds and uses the hepatocyte-specific sodium taurocholate cotransport polypeptide (NTCP) receptor, which is involved in bile acid uptake from portal blood flow for hepatocyte cell entry. In a seminal article by Yan *et al.*,<sup>9,10</sup> (2012), the pre-S1 domain of the HBV envelope L protein was described to bind to the hepatocyte-specific NTCP receptor, leading to cell binding and entry. The antigenic loop of HBV surface protein S between regions I and II interact with hepatocyte heparin sulfate proteoglycans and aid in HBV-NTCP receptor interaction and HBV infectivity (Fig. 2).<sup>11</sup>

Following binding and entry into the hepatocyte, the viral nucleocapsid containing rcDNA is released into the cytoplasm and transported to the cell's nucleus, where the rcDNA is delivered. In the nucleus, the rcDNA is "repaired" by the host cell's DNA repair mechanisms, closing or derelaxing the rcDNA to form cccDNA. This cccDNA remains permanently in the hepatocyte's nucleus and acts as a template for viral RNA transcription. The RNA transcripts are transported into the hepatocytes cytoplasm, where HBV reverse transcriptase uses the RNA as templates to produce viral rcDNA. The rcDNA is then either repackaged and enveloped for cellular export or recycled back to the nucleus, amplifying cccDNA concentration.<sup>12,13</sup>

### Acute hepatitis b infection

Acute hepatitis B (AHB) infection occurs by the exchange of bodily fluids such as blood, semen, or vaginal fluid. About 70% of adults who are acutely infected have a subclinical and anicteric phase, while the other 30% develop clinically significant symptoms and icteric hepatitis. Studies in chimpanzees by Wieland *et al.*,<sup>14</sup> (2004) and transgenic mice studies by Baron *et al.*,<sup>15</sup> (2002) have demonstrated the immune response during HBV infection. In an acute infection,

HBV has a prolonged incubation period of 45–180 days. The initial immune response is mediated by the innate immune system. Typically, the innate immune response results in about a 90% reduction in serum HBV DNA. In the chimpanzee and other model systems, it has been shown that natural killer (NK) cells and natural killer T (NKT) cells play an important role in the early viral control of acute HBV infection through interferon-gamma (IFN- $\gamma$ ) and tumor necrosis factor-alpha (TNF- $\alpha$ ) secretion. A surge of IFN- $\gamma$  mediated by NK cells, NKT cells, and T cells has been found to coincide with a reduction in serum HBV DNA.<sup>14</sup> Subsequent *ex vivo* studies have shown that IFN- $\gamma$  and TNF- $\alpha$  stimulation could destabilize cccDNA via activation of APOBEC3A and APOBEC3B.<sup>16</sup> These studies also suggested that the innate immune response is important for rapid viral clearance during AHB infection, although they cannot clear the virus alone.

The adaptive immune response during an acute infection function is crucial in three ways: 1) inhibition of HBV attachment and entry, 2) eradication of infected hepatocytes, and 3) conferral of viral immunity. B cell response and antibody production is focused on the various HBV proteins, including core protein, surface protein, e-antigen, and polymerase. The antibodies specific for the envelope (hepatitis B surface antibody, known as anti-HBs or HBsAb) and nucleocapsid antigen (hepatitis B core antibody, known as anti-HBc or HBcAb) are both clinically important and useful to distinguish between different acute phases of HBV infection.<sup>17</sup> The discovery of the NTCP and pre-S1 on protein L and the antigenic loop on protein S contributing to hepatocyte infection has led to the understanding of how anti-HBs leads to disease resolution and virus control. Antibodies against these entry antigens effectively block HBV infection, contributing to disease resolution and long-term immunity.<sup>18,19</sup>

HBV-specific T lymphocytes are responsible for viral



clearance as well as halting liver inflammation. HBV specific CD8<sup>+</sup> T cells are found in the liver during acute HBV infection and cause lysis of HBV-infected hepatocytes. This is thought to be the mechanism of clearing cccDNA-containing hepatocytes and effectively eliminating HBV infection.<sup>20</sup> CD8<sup>+</sup> T cells have also been shown to release INF- $\gamma$  and TNF- $\alpha$  during acute HBV infection, stimulating the innate immune response, a key mechanism in serum HBV DNA clearance.<sup>21</sup> T cell response is modulated during an acute infection by both inhibitory and activating regulatory mechanisms, including expression of PD-1, IL-10, and CD4 T regulatory cells (Tregs).<sup>22</sup> Higher expression of T cell inhibitory mechanisms (i.e. PD-1, CD244, and CTLA-4) are seen in patients who develop chronic hepatitis B (CHB), indicating that inhibition of the T cell response may contribute to development of CHB.<sup>23–25</sup>

## CHB

CHB is characterized by both persistent liver inflammation and HBV infection. Liver inflammation leading to fibrosis and cirrhosis occurs due to chronic inflammation as the immune system destroys the cccDNA-containing hepatocytes but is unable to clear the HBV infection. Clinically, this is identified by the presence of hepatitis B surface antigen (HBsAg), elevated HBV DNA, with elevated alanine aminotransferase (ALT). CHB can be further subdivided into two types: HBV e-antigen (HBeAg)-positive and HBeAg-negative. HBeAg is an immunologically distinct soluble antigen, located between the viral nucleocapsid and envelope processed from the pre-core protein. Loss of HBeAg is typically associated with remission of liver disease; however, in a subset of HBeAg-negative patients, viral reactivation can occur. The phases of HBV infection are detailed below.

The course of HBV infection can be divided into four phases that are determined by the host-virus immune response. The first phase is the immune tolerance phase, characterized by active replication of HBV without substantial hepatic inflammation but with HBeAg positivity and normal ALT level. HBeAg accumulates in the serum as an immunologically distinct soluble antigen and is used as a marker of active viral replication. The function of HBeAg is not clearly understood and is dispensable for replication, as mutant viruses without HBeAg exist and are both infectious and pathogenic. The second phase is the immune clearance phase, characterized by elevated ALT levels and decreased HBV DNA load. The third phase is the inactive carrier state, known as the immune control phase, defined by low HBV replication in which HBeAg positive patients lose HBeAg and gain antibodies to HBeAg (HBeAb). This phase is characterized by disease remission. The fourth phase is viral relapse, known as the immune escape phase, and is associated with a relatively high rate of liver inflammation, fibrosis, hepatocellular carcinoma (HCC) development, and mortality. In this phase, patients who were inactive carriers develop increased viral replication of HBeAg-negative HBV and hepatic inflammation with elevated ALT. This phase transition may occur in 20–30% of patients in the inactive carrier phase. HBeAg-negative CHB is the main form of CHB worldwide and is associated with defective T cell function.<sup>26</sup> It remains unclear what triggers the progression through the various phases of infection or the mechanism of defective T cell function during the immune escape.

Dysregulation of T cell immune response has been associated with progression to CHB. CD4<sup>+</sup> helper T cells perform antiviral functions and produce a variety of cytokines crucial for viral clearance and progression to fibrosis, specifically the ratio between Tregs and Th17 T-helper cell subtypes. These two subtypes remain antagonistic to each other,

where Th17 cells mediate inflammatory response leading to liver damage and fibrosis while Tregs mediate immune tolerance and contribute to the chronicity of infection. Nan *et al.*,<sup>27</sup> (2012) found elevated levels of both Tregs and Th17 cells in peripheral blood in patients with HBV infection; however, Th17 cells were significantly higher in patients with AHB compared to patients with CHB, who showed a higher Treg/Th17 ratio. These findings suggest Treg/Th17 imbalance is closely associated with progression of CHB. Further studies have shown higher interleukin (IL)-35, which stimulates Treg production, in CHB patients, contributing to the dysregulation of the Treg/Th17 ratio and that higher Treg/Th17 ratios are closely associated with cirrhosis.<sup>28,29</sup> CD4<sup>+</sup> helper T cells play an important role in stimulating and maintaining CD8<sup>+</sup> T cell response, and insufficient CD4<sup>+</sup> helper T cell response is strongly associated with impairment of CD8<sup>+</sup> T cell function and viral persistence.

Sterilizing cure is defined as the eradication of intrahepatic HBV DNA (intranuclear cccDNA or integrated HBV DNA), loss of HBsAg, and undetectable serum HBV DNA. This was the goal of interferon (IFN)-based therapies. Once viral DNA is incorporated into the host genome or cccDNA in the host nucleus, it is a challenge to remove it and may require immune modulation to destroy the infected hepatocyte due to the dysregulation of T cell immune response. Luneman *et al.*,<sup>30</sup> (2014) discovered that CHB patients paradoxically produce CD56<sup>bright</sup> NK cells that inhibit cytokine production and blunt the cytolytic activity of CD8<sup>+</sup> T-cells. Studies have shown that interferon-alpha (IFN- $\alpha$ ) treatment induces normal CD56<sup>bright</sup> NK cell activity, thereby increasing IFN- $\gamma$  expression and cytotoxic function of CD8<sup>+</sup> T cells with an associated decline viral load.<sup>31,32</sup> In a study by Wursthorn *et al.*,<sup>33</sup> (2006) IFN therapy can decrease intrahepatic HBV DNA in most patients and achieve undetectable levels on about 50% of patients based on real-time polymerase chain reaction (PCR) of post-treatment liver biopsies. Although IFN- $\alpha$  therapy may lead to seroconversion and viral clearance, there is a poor response rate, with about a 30% HBeAg seroconversion and 3% HBsAg seroconversion.<sup>26</sup> Due to the side effect profile, and the mediocre sterilizing cure rate, IFN-based therapies have fallen out of use. Functional cure, defined by seroclearance of HBsAg with persistence of HBV DNA only in the liver, is associated with improved clinical outcomes and is the current therapeutic target. Functional cure is the goal of nucleus(t)ide analogues (NAs) and is achieved by inhibiting viral replication. Due to the persistence of cccDNA in hepatocytes, NAs must be administered long term, if not indefinitely. However, some studies have shown that NA treatment improves CD8<sup>+</sup> T cell cytotoxic function and occasionally clearance of HBV DNA-containing hepatocytes is achieved.<sup>34,35</sup> In a subset of patients, cure can occur after prolonged NA treatment.

## HBV vaccines and limitations

HBV vaccination has been an effective measure to prevent HBV infection. Plasma-derived vaccinations were first developed then replaced by recombinant HBV vaccines in the 1980's, both with similar efficacy.<sup>36</sup> These vaccines stimulate anti-HBs antibodies in noninfected individuals, with a 95% effective rate of seroconversion. The reason for 5% non-response remains unclear; however, there are certain populations affected, including those with chronic disease, certain genetic mutations, and those on immunomodulatory medications at higher risk for non-response to vaccination.<sup>37</sup> Chronic diseases include old age (>60 years-old), human immunodeficiency virus-coinfection, and chronic kidney disease. Genetic mutations associated with non-response include homozygous mutations for human leukocyte

antigen (HLA) DRB1\*0301, HLA-B8, SC01, DR-3, HLAB44, FC-31, and DR-7.<sup>38,39</sup> Methods that induce seroconversion include administering a 4th dose of vaccine or a repeat administration of the three-series vaccine at a higher dose. Other vaccine methods currently under investigation include intradermal administration of the vaccine, the use of adjuvants (including 3-deacylatedmonophosphoryl lipid A), use of triple S antigen recombinants, and a vaccine with the combination HBsAg and HBcAg.<sup>37</sup>

The implementation of a rigorous vaccination program worldwide has led to a decrease in incidence of hepatitis B infection. However, the widespread use of vaccines has led to the emergence of certain point escape mutations leading to vaccination failure. This phenomenon has been shown to cause hepatitis B infection in previously vaccinated patients. A prospective Chinese study showed 6/176 adults to be HBV DNA-positive by PCR at 1 year after receiving the HBV vaccine. Four out of these six cases had known HBV escape mutations.<sup>40</sup> Despite awareness of this emerging issue, there is no consensus currently on the need for vaccine redevelopment or need for therapy in individuals infected with these mutants.<sup>41</sup>

### Experimental treatments in the pipeline

Currently, there are many classes of medications with various targets under investigation for hepatitis B therapy. One class under investigation are entry inhibitors targeting NTCP and therefore protecting against *de novo* infection of hepatocytes.<sup>42</sup> Myrcludex-B has been shown safe and effective in HBV/hepatitis D virus coinfection and is in phase II trials for the treatment of chronic HBV.<sup>43</sup> Another class undergoing active investigation includes small interfering RNAs, which target viral RNA and lead to their degradation preventing translation of viral proteins crucial for viral capsid formation and cccDNA formation.<sup>44</sup> Multiple small interfering RNA candidates are currently in phase I/II trials.<sup>45</sup> Capsid inhibitors are another class of drugs currently under investigation. The integrity of viral capsids, the protein surrounding the viral genome, are physically altered, causing both disruption of capsid integrity and preventing hepatocyte entry, thereby preventing cccDNA formation. This mechanism is distinct from entry inhibitors, as capsid inhibitors also exhibit antiviral properties.<sup>46</sup> Another class of agents, HBsAg inhibitors, which are currently in phase II trials, work by inhibiting the processing of HBsAg and release from the infected cell. Interestingly, they also seem to trigger an antiviral immune response, as serum HBsAg titer falls and occasionally HBsAb seroconversion occurs after monotherapy use.<sup>47</sup> This antiviral effect suggests that viral surface proteins in circulation may contribute to impairment of the immune system's antiviral response.<sup>47</sup> The role of HBsAg on antiviral suppression remains unclear and is an intriguing area of study in understanding the progression to chronic HBV and potential future immunomodulating therapies.

Investigational therapies using vaccines to stimulate cytotoxic T cell response have yielded unsatisfactory results. Fontaine *et al.*,<sup>48</sup> (2015) performed a phase I/II trial using NAs alongside an HBV envelope expressing DNA vaccine. The trial showed no benefit in regard to risk of relapse of HBV treated patients, rate of virologic breakthrough, or restoration of anti-HBV immune response. Lok *et al.*,<sup>49</sup> (2016) performed a phase II trial using T cell-based vaccine after 1 year of therapy with NAs. The vaccine did not provide significant reductions in HBsAg in virally suppressed patients with CHB. Currently, PD-1 inhibitors are being studied to explore if durable control of CHB can be achieved. Phase 1 trials have shown that in virally suppressed HBeAg-negative patients, that nivolumab (PD-1 inhibitor) led to HBsAg

decline in most patients and sustained HBsAg loss in one patient.<sup>50</sup> Clinical trials are currently ongoing, studying various vaccines and immunomodulatory to achieve sustained CHB control.<sup>51</sup>

## Hepatitis C

### Background

HCV was isolated in 1989 and is a member of the Flaviviridae family (which includes Dengue and Zika virus). HCV has infected nearly 3% of the world's population. It is a major cause of liver disease and cancer, where about 30% of chronically infected individuals develop cirrhosis, and infected individuals are at a 17-fold increased risk of developing HCC. In the USA, HCV accounts for 50% of the cases of HCC.<sup>52</sup> The virus consists of a single lipid bilayer envelope surrounding a viral nucleocapsid, containing multiple viral core proteins and single-stranded RNA (ssRNA) that encodes for a single large polyprotein transcript. The single transcript is further processed into three structural proteins (core, envelope-1, envelope-2) and seven proteins involved in viral replication. In chronic HCV infection, the actions of the virus along with host immune factors cause dysregulation of the immune system, leading to failure of the immune response to clear the HCV infection. The inability of the immune system to clear the infection leads to persistent hepatic inflammation, itself leading to cirrhosis, liver failure, or the development of HCC. The virus's high mutation rate due to the lack of proofreading capability by its RNA-dependent RNA polymerase leads to escape mutations, allowing the virus to evade the immune system and contributes to treatment and vaccine failure.

This high mutation rate leads to a broad range of genetic variants categorized into seven main genotypes, each with multiple different subtypes. Each genotype has more than a 25–35% difference in their nucleotide sequence.<sup>53</sup> Genotype subtypes differ in nucleotide sequence from each other by 15–25%.<sup>54</sup> Further genetic variability can be found in each individual patient, where multiple viral quasiespecies containing different mutations can co-exist. Prevalence of distribution of HCV genotypes varies geographically. Among all the genotypes, genotype 1 (i.e. HCV-1) is the most prevalent worldwide. In the USA, HCV-1a and HCV-1b subtypes account for 60–70% of all patients. HCV-2 is the most prevalent in middle and west Africa, HCV-3 in east Asia and India, HCV-4 in Egypt and sub-Saharan Africa, HCV-5 in South Africa, HCV-6 in China and southwest Asia, and HCV-7 in central Africa.<sup>53,55</sup>

### HCV infection

HCV circulates in the blood, accessing basolateral hepatocyte surface receptors. The HCV particle has a very low density that closely resembles very low density lipoprotein (VLDL) and low density lipoprotein (LDL) and uses apolipoprotein and serum lipid uptake mechanisms to enter the hepatocyte. HCV entry is complex and uses multiple cell entry factors that are spatially arranged and bind in a temporally ordered manner. Five cell surface proteins are essential for HCV particle binding and entry, namely CD81, scavenger receptor class B type I (SR-BI), claudin 1 (CLDN1), occludin (OCLN) and Niemann-Pick C1-like 1 cholesterol absorption receptor (NPC1L1). First, HCV attaches to the hepatocyte LDL-R via viral apolipoprotein E-like protein.<sup>56</sup> Next, SR-BI surface protein binds to viral lipoproteins expressed by HCV surface E2 gene. SR-BI is involved in high density lipopro-

tein (HDL) and VLDL binding and is highly expressed by hepatocytes, which may explain HCV hepatotropism. SR-BI then serves to unmask virus particles and exposes the CD81 cell membrane protein which binds to HCV E2 surface protein.<sup>57</sup> The CD81-HCV complex moves laterally across the cell membrane to tight junctions, where CLDN1 is located, and activates CLDN1 mediated viral entry via clathrin-dependent endocytosis.<sup>58</sup> OCLN and NPC1L1 are tight junction proteins that are involved with HCV entry, however their exact roles are unknown. Targeting NPC1L1 with antibodies or its antagonist ezetimibe (already Food and Drug Administration-approved as a cholesterol lowering medication) has been shown to halt or delay cell entry of all seven HCV genotypes, providing an intriguing potential therapeutic target.<sup>59</sup>

The HCV assembly and release processes is not yet fully understood; however, it seems to be closely related to lipid packaging and release.<sup>60</sup> Once inside the cell, the virus particles are uncoated, the capsid is destroyed, and the viral positive sense single-stranded RNA (+ssRNA) is released into the cytoplasm.<sup>61</sup> The viral RNA then takes over the hepatocytes ribosome on the rough endoplasmic reticulum to synthesize a single long polyprotein that is later proteolytically processed by viral and cellular proteases into its 10 proteins, which include 3 structural proteins (core, E1, E2) and 7 nonstructural proteins (p7, NS2, NS3, NS4A, NS4B, NS5A, NS5B).<sup>61</sup> Here in the cytoplasm, newly formed HCV RNA-dependent RNA polymerase transcribes the viral +ssRNA into an intermediate negative sense single stranded RNA (-ssRNA), which is then later transcribed into +ssRNA. The newly transcribed +ssRNA is then either packaged into new HCV virions or used for further HCV polyprotein translation by endoplasmic reticulum ribosomes. It is during this process, due to the high error rate and lack of proofreading ability of the HCV RNA polymerase, that many mutations are introduced and the many HCV quasispecies are formed.<sup>61</sup> The error rate of HCV RNA-dependent RNA polymerase is estimated to be between one mutation per every  $10^3$ – $10^6$  nucleotides copied compared to one mutation per every  $10^8$ – $10^{11}$  nucleotides copied for DNA polymerases.<sup>62–64</sup> The virus proteins then arrange on the endoplasmic reticulum intracellular lipid membrane, where core proteins are shaped and bind to cytosolic lipid droplets (cLDs).<sup>65</sup> The cLD-bound core proteins assemble into the core nucleocapsid via microtubules and dyneins, and +ssRNA are encapsulated. The HCV nucleocapsids, containing RNA and core proteins, then bud into the endoplasmic reticulum, where surface proteins are attached.

The detailed mechanism of HCV viral release is yet unknown; however, hepatocyte exit seems to depend on the pathway for producing VLDLs and on the presence of apolipoprotein B and E. It is thought that the HCV particle complexes with apolipoprotein B and apolipoprotein E containing VLDLs in order to exit the hepatocyte. A study by Huang *et al.*,<sup>66</sup> (2007) showed that blocking VLDL secretion reduced HCV viral release from the hepatocytes in a growth media by 80%. Recently, another cellular pathway has been implicated in HCV release. The endosomal sorting complex required for transport (ESCRT) pathway has been implicated in HCV secretion out of the endoplasmic reticulum and cell. This pathway is normally used to bud vesicles out of the cell, and HCV may use the ESCRT system too, but little is known about this process.<sup>67</sup>

### **Innate immune response to hepatitis C infection**

The innate immune response is important in HCV infection by both limiting viral dissemination through inducing infected hepatocyte apoptosis and stimulating the antigen specific

ic adaptive immune response.<sup>68</sup> During an acute HCV infection, viral RNA is detected within the hepatocyte cytoplasm. The presence of intracellular HCV RNA after the uncoating of HCV virion activates TLR3, RIG-I, and MDA5 of infected hepatocytes, which in turn release interferon 1 (IFN-I,  $\alpha$  and  $\beta$ ) and IFN- $\gamma$ . Circulating HCV RNA is also detected by plasmacytoid dendritic cells (pDCs). The activated pDCs produce IFN- $\alpha$ . Both IFN-I ( $\alpha$  and  $\beta$ ) and IFN- $\gamma$  released by infected hepatocytes and circulating pDCs act to directly inhibit HCV replication and activate NK cells.<sup>69</sup> NK cells play a crucial role in the innate immune response to acute HCV infection by cytolytic destruction of infected hepatocytes and cytokine release, which both directly inhibit HCV replication and stimulate the adaptive immune response. Activated NK cells directly induce infected hepatocyte perforin- and granzyme B-mediated apoptosis. The cytolytic action of NK cells through the perforin/granzyme mechanism causes collateral damage to uninfected surrounding hepatocytes. NK cells also produce IFN- $\gamma$  and TNF- $\alpha$ , which cause dendritic cell maturation, leading to IL-12 release which induces the adaptive immune response with the differentiation of CD4 and CD8 T cells.<sup>70,71</sup> Lastly, *in vitro* studies have shown that IFN produced by NK cells directly inhibits HCV replication.<sup>72</sup>

### **Adaptive immune response, its shortcomings, and progression to chronic hepatitis C**

Generally, T cell response is the adaptive immune system's main mechanism of viremia control. In HCV, specific CD8+ T cells destroy infected hepatocytes via HLA class I antigen presenting cells as well as by inducing cytokine secretion (TNF- $\alpha$ , IFN- $\gamma$ ).<sup>73</sup> Helper CD4+ T cells support this function via IL-2 to stimulate CD8+ T cell and NK cell activation.<sup>74,75</sup>

Chronic HCV infection is defined as persistent viremia for more than 6 months.<sup>76</sup> In chronic HCV, a continuous yet impaired activation of the adaptive immune system occurs. HCV has multiple mechanisms to defend against immune clearance, resulting in immune system evasion and chronic infection.

The first major mechanism of chronic infection is the loss of T cell function due to chronic T cell activation. Essentially, T cell function is inhibited and their cytotoxic capacity is lost. First described in persistently-infected mice with lymphocytic choriomeningitis virus (LCMV), high levels of persistent viral antigen production results in chronic T cell activation, leading to sequential loss of T cell function.<sup>77</sup> During chronic infection, HCV specific CD4+ helper T cells show a reduced production of IL-2, resulting in impaired CD8+ T cells activation.<sup>78</sup> Additionally, HCV core antibody has been implicated in T cell suppression, as it binds to complement C1q inhibiting Lck/Akt activation of CD4+ and CD8+ T cells.<sup>79</sup> PD-1-mediated CD8+ T cell suppression has also been implicated in inhibiting T cells. Studies have shown that isolating CD8+ T cells from chronically infected patients and exposing the cells to PD-1 blocking drugs *in vitro* can restore T cell function.<sup>80,81</sup> Further studies have shown that CTLA4 (an inhibitory signal produced by Tregs) along with PD-1 may synergistically inhibit CD8+ T cell function.<sup>82</sup>

CD4+ T cell activity plays an important role in chronic HCV infection. It is widely known that a vigorous CD4+ T cell response during an acute HCV infection is correlated with viral clearance.<sup>83–85</sup> Conversely, progression of acute HCV infection to chronic infection is strongly associated with the downfall of HCV specific CD4+ T cell response.<sup>74,83</sup> Both the lack of robust CD4+ T cell response during acute infection and the decrease CD4+ T cell response after the acute phase of infection have both been observed and associated with the development of chronic progression.<sup>86</sup> The mechanism by which CD4+ T cell response dwindles during the



acute infection remains unclear. One mechanism proposed is HCV escape mutations occurring in patients with various HLA epitopes (including HLA-DRB1\*15 epitope).<sup>86,87</sup>

Other Tregs, such as CD25+ T cells, play a role in suppressing immune system activation.<sup>88–90</sup> These cells work through various mechanisms to suppress the immune response during chronic HCV infection, including CD8+ T cell inhibition and inhibition of cytokine release such as IL-10 and transforming growth factor-beta (TGF- $\beta$ ) immunomodulating cytokines.<sup>89,91,92</sup> Tregs upregulated during chronic infection, decrease to the level of control individuals after spontaneous viral clearance and after treatment induced sustained virologic response (SVR).<sup>89,93</sup> The mechanism of Treg upregulation occurring during HCV infection remains unclear; however, it has been proposed that HCV itself can induce Treg upregulation specifically by HCV core protein.<sup>93,94</sup> Viral escape mutations are a major factor in the development of chronic HCV. HCV viral RNA is highly prone to mutations due to its RNA-dependent RNA polymerase and its lack of proofreading function. Multiple virus mutants can co-exist, eventually leading to the selection of CD8+ T cell escape variants. Up to 50–70% of patients with chronic HCV infections exhibit mutations at viral epitopes targeted by CD8+ T cells.<sup>95,96</sup> Viral escape mutations emerge during the early acute infection and remain fixed in the quasispecies for years, implicating themselves as a mechanism for immune system evasion and chronic progression.<sup>97</sup> However, many viral mutations have been shown to reduce fitness and viral replicative capacity.<sup>98,99</sup> Thus, as a consequence of the viral mutant-impaired fitness, most viral escape mutations will revert to wild-type long term and be the primary transmission agent to a new host.<sup>100</sup> Some HLA alleles have been shown to be protective of the viral escape mutants and are associated with a decrease in chronicity. HLA-B27 positivity is protective against chronic HCV progression; however, escape mutations can still occur. HLA-B27-binding anchor encodes a highly conserved region on viral RNA polymerase, where mutations at this epitope often lead to a non-functional RNA polymerase.<sup>101</sup>

### IFN and DAA HCV therapy

IFN remains an important immunomodulator involved in host defense and treatment of chronic HCV. Upon viral entry into the host cell, HCV RNA is detected by TLR3 in the endosome and by RIG-I in the cytoplasm. Activation of these receptor pathways lead to interferon transcription. There are 3 major types of interferon, Type I and III IFN are produced by the infected hepatocyte and Type II IFN are produced by NK-cells and natural killer T cells (NKT cells). IFN bind to specific transmembrane JAK–STAT receptor signaling pathways to regulate gene transcription in the nucleus inducing an “antiviral state” in the cell activating both the innate and adaptive immune systems through various stimulatory pathways.<sup>102–104</sup>

Historically, pegylated-IFN and ribavirin have been the mainstay of treatment of chronic HCV. Today, DAAs remain the preferred treatment choice; however, IFN-based therapies remain a treatment option. With IFN use, HCV genotypes play an important role in treatment strategy and outcome. HCV genotypes 1 and 4 require longer treatment (48 weeks) and achieve a SVR of 50%. Meanwhile, HCV genotypes 2 and 3 require a shorter treatment time, with a higher SVR around 80%.<sup>105–107</sup> The divergent response to IFN treatment has stimulated intense research, examining the mechanisms of non-response in an attempt to identify predictors of non-response that may guide therapy. The exact mechanism of IFN therapy failure remains unclear; however, it is thought that various viral mutations and host

immune factors contribute to divergent responses to IFN. Various mechanisms of IFN treatment failure via inhibition of IFN signaling pathways have been shown.<sup>108–110</sup> Besides HCV genotypes, multiple host factors have also been shown to affect IFN treatment response, including host sex, age, and race. Male sex, older age and African-American race are associated with inferior response to IFN therapy.<sup>111</sup>

The development of non-IFN-based therapy with DAAs have resulted in a much better safety profile and shorter duration of therapy, with a dramatic increase in virus cure rates, especially in difficult to treat HCV genotypes. The use of HCV screening in high risk populations (i.e. intravenous drug users) and highly effective DAA treatments have also proven cost-effective in avoiding liver-related mortality and liver transplantations.<sup>112</sup> There are three targets of DAA therapy, including NS3/4A protease inhibitors, NS5A polymerase inhibitors, NS5B polymerase inhibitors. DAA therapy is highly effective, with SVR rates >95% in genotype 1-infected patients without cirrhosis including those co-infected with human immunodeficiency virus, and about 78–87% effective in decompensated cirrhotics with Child–Turcotte–Pugh class C disease.<sup>113</sup> Despite the high rate of DAA effectiveness in achieving SVR, the sheer magnitude of individuals infected with HCV leaves a significant cohort of patients who fail their initial therapy. Clinical trials of re-treatment after failure of initial DAA therapy have shown high rates of SVR with DAA salvage therapy. Re-treatment regimens utilize strategies such as adding additional active agents (other DAA classes and/or ribavirin), using longer treatment courses, or both. Clinical trials such as POLARIS-1, POLARIS-4, MAGELLAN-3 have shown a 90–98% effective re-treatment cure rate after initial DAA failure.<sup>114,115</sup> The mechanism of DAA resistance is thought to be due to various mutations seen in the different HCV genotypes and the DAA interaction sites that render the drugs ineffective. After DAA initiation, wild-type DAA-susceptible HCV species are eliminated, selecting for resistant variants. Some studies have shown that some of the acquired mutations in resistant quasispecies may increase viral fitness, which may explain the rapid viral replication seen on treatment (known as breakthrough) or after treatment (known as relapse).<sup>116</sup> Genotype-specific DAA treatment regimens and the emergence of drug-resistant variants remain a significant concern. Genotype-specific DAA resistance is associated with polymorphisms present in the various HCV genotypes, such as the NS5A resistance-associated substitutions present in genotype 1, that lead to the decreased efficacy of ledipasvir/sofosbuvir regimens, or genotype 3 variations within the NS5A region, leading to reduced sensitivity to NAs. The emergence of genotype-specific DAA resistance has led to an increase in demand for pangenotypic therapies that have a higher barrier to drug resistance (such as sofosbuvir/velpatasvir or glecaprevir/pibrentasvir) for treatment of all HCV genotypes, especially in resource-limited areas when genotype testing is unavailable.

### Conclusions

Understanding the immune response to acute HBV infection and the immune system's dysregulation that results in chronic HBV infection are important in developing preventive and therapeutic strategies. Both adaptive and innate immune responses play major roles in the eradication of HBV infection with the dysregulation of T cell immune response associated with progression to chronic HBV infection. Persistence of viral DNA in the form of cccDNA or incorporated into the host's genome, along with the failure of the immune system to clear these infected cells, contributes to the persistence of HBV infection. The implementation of

a vaccination program worldwide has led to an overall decrease in incidence of HBV infection. IFN, with its poor rate of viral clearance and significant side effects, has fallen out of favor for therapy in hepatitis B. NAs are currently the treatment of choice and are aimed at suppressing viral replication by suppressing reverse transcriptase but are rarely curative. New strategies for targeting HBV production (RNA interference, HBsAg inhibitors, capsid inhibitors) and immune response (PD-1 inhibitors, therapeutic vaccines) are currently under investigation as possible curative treatments.

Unlike HBV infection, effective curative regimens using DAAs have been developed and successfully implemented for HCV; however, no effective vaccinations exist yet. It is the sheer magnitude of infected individuals and the cost of treatment that have proven to be significant barriers to disease elimination and persistence of HCV-related morbidity and mortality. It is the combination of HCV viral escape mutations along with host immune factors that are major contributors in the development of chronic HCV. Although the exact mechanism remains unclear, persistent viral infection results in chronic suppressor T cell activation, which leads to a loss of T cell response. Ongoing research to develop a safe and effective vaccine will help decrease incidence and spread of HCV.

## Funding

None to declare.

## Conflict of interest

The authors have no conflict of interests related to this publication.

## Author contributions

Study concept and design (CS), acquisition of data (CS), analysis and interpretation of data (CS), drafting of the manuscript (CS), critical revision of the manuscript for important intellectual content (JWB), administrative, technical, or material support, study supervision (JWB).

## References

- Ott JJ, Stevens GA, Groeger J, Wiersma ST. Global epidemiology of hepatitis B virus infection: new estimates of age-specific HBsAg seroprevalence and endemicity. *Vaccine* 2012;30(12):2212–2219. doi:10.1016/j.vaccine.2011.12.116.
- Goldstein ST, Zhou F, Hadler SC, Bell BP, Mast EE, Margolis HS. A mathematical model to estimate global hepatitis B disease burden and vaccination impact. *Int J Epidemiol* 2005;34(6):1329–1339. doi:10.1093/ije/dyi206.
- Choo QL, Kuo G, Weiner AJ, Overby LR, Bradley DW, Houghton M. Isolation of a cDNA clone derived from a blood-borne non-A, non-B viral hepatitis genome. *Science* 1989;244(4902):359–362. doi:10.1126/science.2523562.
- Kuo G, Choo QL, Alter HJ, Gitnick GL, Redeker AG, Purcell RH, *et al*. An assay for circulating antibodies to a major etiologic virus of human non-A, non-B hepatitis. *Science* 1989;244(4902):362–364. doi:10.1126/science.2496467.
- World Health Organization. Web Annex B. WHO estimates of the prevalence and incidence of hepatitis C virus infection by WHO region, 2015. Available from: <https://apps.who.int/iris/bitstream/handle/10665/277005/WHO-CDS-HIV-18.46-eng.pdf>.
- Kamal SM. Acute hepatitis C: a systematic review. *Am J Gastroenterol* 2008;103(5):1283–1297, quiz 1298. doi:10.1111/j.1572-0241.2008.01825.x.
- Rustgi VK. The epidemiology of hepatitis C infection in the United States. *J Gastroenterol* 2007;42(7):513–521. doi:10.1007/s00535-007-2064-6.
- Yamane D, McGivern DR, Masaki T, Lemon SM. Liver injury and disease pathogenesis in chronic hepatitis C. *Curr Top Microbiol Immunol* 2013;369:263–288. doi:10.1007/978-3-642-27340-7\_11.
- Yan H, Zhong G, Xu G, He W, Jing Z, Gao Z, Huang Y, Qi Y, Peng B, *et al*. Sodium taurocholate cotransporting polypeptide is a functional receptor for human hepatitis B and D virus. *Elife* 2012;1:e00049. doi:10.7554/eLife.00049.
- Li H, Zhuang Q, Wang Y, Zhang T, Zhao J, Zhang Y, *et al*. HBV life cycle is restricted in mouse hepatocytes expressing human NTCP. *Cell Mol Immunol* 2014;11(2):175–183. doi:10.1038/cmi.2013.66.
- Jaoué GA, Sureau C. Role of the antigenic loop of the hepatitis B virus envelope proteins in infectivity of hepatitis delta virus. *J Virol* 2005;79(16):10460–10466. doi:10.1128/JVI.79.16.10460-10466.2005.
- Tuttleman JS, Pourcel C, Summers J. Formation of the pool of covalently closed circular viral DNA in hepadnavirus-infected cells. *Cell* 1986;47(3):451–460. doi:10.1016/0092-8674(86)90602-1.
- Wu TT, Coates L, Aldrich CE, Summers J, Mason WS. In hepatocytes infected with duck hepatitis B virus, the template for viral RNA synthesis is amplified by an intracellular pathway. *Virology* 1990;175(1):255–261. doi:10.1016/0042-6822(90)90206-7.
- Wieland S, Thimme R, Purcell RH, Chisari FV. Genomic analysis of the host response to hepatitis B virus infection. *Proc Natl Acad Sci U S A* 2004;101(17):6669–6674. doi:10.1073/pnas.0401771101.
- Baron JL, Gardiner L, Nishimura S, Shinkai K, Locksley R, Ganem D. Activation of a nonclassical NKT cell subset in a transgenic mouse model of hepatitis B virus infection. *Immunity* 2002;16(4):583–594. doi:10.1016/S1074-7613(02)00305-9.
- Xia Y, Stadler D, Lucifora J, Reisinger F, Webb D, Hösel M, *et al*. Interferon- $\gamma$  and tumor necrosis factor- $\alpha$  produced by T cells reduce the HBV persistence form, cccDNA, without cytotoxicity. *Gastroenterology* 2016;150(1):194–205. doi:10.1053/j.gastro.2015.09.026.
- Gerlich WH. Medical virology of hepatitis B: how it began and where we are now. *Viral J* 2013;10:239. doi:10.1186/1743-422X-10-239.
- Glebe D, Aliakbari M, Krass P, Knoop EV, Valerius KP, Gerlich WH. Pre-s1 antigen-dependent infection of Tupaia hepatocyte cultures with hepatitis B virus. *J Virol* 2003;77(17):9511–9521. doi:10.1128/jvi.77.17.9511-9521.2003.
- Neurath AR, Seto B, Strick N. Antibodies to synthetic peptides from the preS1 region of the hepatitis B virus (HBV) envelope (env) protein are virus-neutralizing and protective. *Vaccine* 1989;7(3):234–236. doi:10.1016/0264-410x(89)90235-1.
- Thimme R, Wieland S, Steiger C, Ghayeb J, Reimann KA, Purcell RH, *et al*. CD8(+) T cells mediate viral clearance and disease pathogenesis during acute hepatitis B virus infection. *J Virol* 2003;77(1):68–76. doi:10.1128/jvi.77.1.68-76.2003.
- Guidotti LG, Ishikawa T, Hobbs MV, Matzke B, Schreiber R, Chisari FV. Intracellular inactivation of the hepatitis B virus by cytotoxic T lymphocytes. *Immunity* 1996;4(1):25–36. doi:10.1016/S1074-7613(00)80295-2.
- Zhang Z, Zhang JY, Wherry EJ, Jin B, Xu B, Zou ZS, *et al*. Dynamic programmed death 1 expression by virus-specific CD8 T cells correlates with the outcome of acute hepatitis B. *Gastroenterology* 2008;134(7):1938–1949. doi:10.1053/j.gastro.2008.03.037.
- Schurich A, Khanna P, Lopes AR, Han KJ, Peppas D, Micco L, *et al*. Role of the coinhibitory receptor cytotoxic T lymphocyte antigen-4 on apoptosis-Prone CD8 T cells in persistent hepatitis B virus infection. *Hepatology* 2011;53(5):1494–1503. doi:10.1002/hep.24249.
- Fisicaro P, Valdatta C, Massari M, Loggi E, Biasini E, Sacchelli L, *et al*. Anti-viral intrahepatic T-cell responses can be restored by blocking programmed death-1 pathway in chronic hepatitis B. *Gastroenterology* 2010;138(2):682–693. doi:10.1053/j.gastro.2009.09.052.
- Raziorrouh B, Schraut W, Gerlach T, Nowack D, Grüner NH, Ulsenheimer A, *et al*. The immunoregulatory role of CD244 in chronic hepatitis B infection and its inhibitory potential on virus-specific CD8+ T-cell function. *Hepatology* 2010;52(6):1934–1947. doi:10.1002/hep.23936.
- Lau GK, Piratvisuth T, Luo KX, Marcellin P, Thongsawat S, Cooksley G, *et al*. Peginterferon Alfa-2a, lamivudine, and the combination for HBeAg-positive chronic hepatitis B. *N Engl J Med* 2005;352(26):2682–2695. doi:10.1056/NEJMoa043470.
- Nan XP, Zhang Y, Yu HT, Sun RL, Peng MJ, Li Y, *et al*. Inhibition of viral replication downregulates CD4(+)CD25(high) regulatory T cells and programmed death-ligand 1 in chronic hepatitis B. *Viral Immunol* 2012;25(1):21–28. doi:10.1089/vim.2011.0049.
- Ferri C, Ramos-Casals M, Zignego AL, Arcaini L, Roccatello D, Antonelli A, *et al*. International diagnostic guidelines for patients with HCV-related extrahepatic manifestations. A multidisciplinary expert statement. *Autoimmun Rev* 2016;15(12):1145–1160. doi:10.1016/j.autrev.2016.09.006.
- Rasul I, Shepherd FA, Kamel-Reid S, Krajden M, Pantalony D, Heathcote EJ. Detection of occult low-grade B-cell non-Hodgkin's lymphoma in patients with chronic hepatitis C infection and mixed cryoglobulinemia. *Hepatology* 1999;29(2):543–547. doi:10.1002/hep.510290224.
- Lunemann S, Malone DF, Hengst J, Port K, Grabowski J, Deterding K, *et al*. Compromised function of natural killer cells in acute and chronic viral hepatitis. *J Infect Dis* 2014;209(9):1362–1373. doi:10.1093/infdis/jit561.
- Tan AT, Hoang LT, Chin D, Rasmussen E, Lopatin U, Hart S, *et al*. Reduction of HBV replication prolongs the early immunological response to IFN $\alpha$  therapy. *J Hepatol* 2014;60(1):54–61. doi:10.1016/j.jhep.2013.08.020.
- Gill US, Peppas D, Micco L, Singh HD, Carey I, Foster GR, *et al*. Interferon alpha induces sustained changes in NK cell responsiveness to hepatitis B viral load suppression in vivo. *PLoS Pathog* 2016;12(8):e1005788. doi:10.1371/journal.ppat.1005788.
- Wurstthorn K, Lutgehetmann M, Dandri M, Volz T, Buggisch P, Zollner B, *et al*. Peginterferon alpha-2b plus adefovir induce strong cccDNA decline and HBsAg reduction in patients with chronic hepatitis B. *Hepatology* 2006;44(3):675–684. doi:10.1002/hep.21282.
- Boni C, Laccabue D, Lampertico P, Giuberti T, Viganò M, Schivazappa S, *et al*. Restored function of HBV-specific T cells after long-term effective therapy with nucleos(t)ide analogues. *Gastroenterology* 2012;143(4):963–973. doi:10.1053/j.gastro.2012.07.014.

- [35] Boni C, Penna A, Ogg GS, Bertoletti A, Pilli M, Cavallo C, *et al*. Lamivudine treatment can overcome cytotoxic T-cell hyporesponsiveness in chronic hepatitis B: new perspectives for immune therapy. *Hepatology* 2001;33(4):963–971. doi:10.1053/jhep.2001.23045.
- [36] Gerety RJ, Ellis RW. Plasma-derived vs recombinant hepatitis B vaccine. *JAMA* 1987;258(11):1474. doi:10.1001/jama.1987.03400110056011.
- [37] Walayat S, Ahmed Z, Martin D, Puli S, Cashman M, Dhillon S. Recent advances in vaccination of non-responders to standard dose hepatitis B virus vaccine. *World J Hepatol* 2015;7(24):2503–2509. doi:10.4254/wjh.v7.i24.2503.
- [38] Godkin A, Davenport M, Hill AV. Molecular analysis of HLA class II associations with hepatitis B virus clearance and vaccine nonresponsiveness. *Hepatology* 2005;41(6):1383–1390. doi:10.1002/hep.20716.
- [39] Egea E, Iglesias A, Salazar M, Morimoto C, Kruskall MS, Awdeh Z, *et al*. The cellular basis for lack of antibody response to hepatitis B vaccine in humans. *J Exp Med* 1991;173(3):531–538. doi:10.1084/jem.173.3.531.
- [40] He C, Nomura F, Ito S, Isobe K, Nakai T. Prevalence of vaccine-induced escape mutants of hepatitis B virus in the adult population in China: a prospective study in 176 restaurant employees. *J Gastroenterol Hepatol* 2001;16(12):1373–1377. doi:10.1046/j.1440-1746.2001.02654.x.
- [41] Purdy MA. Hepatitis B virus S gene escape mutants. *Asian J Transfus Sci* 2007;1(2):62–70. doi:10.4103/0973-6247.33445.
- [42] Kohara M, Tanaka T, Tsukiyama-Kohara K, Tanaka S, Mizokami M, Lau JY, *et al*. Hepatitis C virus genotypes 1 and 2 respond to interferon-alpha with different virologic kinetics. *J Infect Dis* 1995;172(4):934–938. doi:10.1093/infdis/172.4.934.
- [43] Hadziyannis SJ, Sette H Jr, Morgan TR, Balan V, Diago M, Marcellin P, *et al*. Peginterferon-alpha2a and ribavirin combination therapy in chronic hepatitis C: a randomized study of treatment duration and ribavirin dose. *Ann Intern Med* 2004;140(5):346–355. doi:10.7326/0003-4819-140-5-200403020-00010.
- [44] Zeisel MB, Felmlee DJ, Baumert TF. Hepatitis C virus entry. *Curr Top Microbiol Immunol* 2013;369:87–112. doi:10.1007/978-3-642-27340-7\_4.
- [45] Hepatitis C guidance: AASLD-IDA recommendations for testing, managing, and treating adults infected with hepatitis C virus. *Hepatology* 2015;62(3):932–954. doi:10.1002/hep.27950.
- [46] Kamal SM, Rasenack JW, Bianchi L, Al Tawil A, El Sayed Khalifa K, Peter T, *et al*. Acute hepatitis C without and with schistosomiasis: correlation with hepatitis C-specific CD4(+) T-cell and cytokine response. *Gastroenterology* 2001;121(3):646–656. doi:10.1053/gast.2001.27024.
- [47] Maier I, Wu GY. Hepatitis C and HIV co-infection: a review. *World J Gastroenterol* 2002;8(4):577–579. doi:10.3748/wjg.v8.i4.577.
- [48] Fontaine H, Kahl S, Chazallon C, Bourguin M, Varaut A, Buffet C, *et al*. Anti-HBV DNA vaccination does not prevent relapse after discontinuation of analogues in the treatment of chronic hepatitis B: a randomised trial—ANRS HB02 VAC-ADN. *Gut* 2015;64(11):139–147. doi:10.1136/gutjnl-2013-305707.
- [49] Lok AS, Pan CQ, Han SH, Trinh HN, Fessel WJ, Rodell T, *et al*. Randomized phase II study of GS-4774 as a therapeutic vaccine in virally suppressed patients with chronic hepatitis B. *J Hepatol* 2016;65(3):509–516. doi:10.1016/j.jhep.2016.05.016.
- [50] Gane E, Verdon DJ, Brooks AE, Gaggar A, Nguyen AH, Subramanian GM, *et al*. Anti-PD-1 blockade with nivolumab with and without therapeutic vaccination for virally suppressed chronic hepatitis B: A pilot study. *J Hepatol* 2019;71(5):900–907. doi:10.1016/j.jhep.2019.06.028.
- [51] Féray C, López-Labrador FX. Is PD-1 blockade a potential therapy for HBV? *JHEP Rep* 2019;1(3):142–144. doi:10.1016/j.jhep.2019.07.007.
- [52] Altekruse SF, Henley SJ, Cucinelli JE, McGlynn KA. Changing hepatocellular carcinoma incidence and liver cancer mortality rates in the United States. *Am J Gastroenterol* 2014;109(4):542–553. doi:10.1038/ajg.2014.11.
- [53] Gower E, Estes C, Blach S, Razavi-Shearer K, Razavi H. Global epidemiology and genotype distribution of the hepatitis C virus infection. *J Hepatol* 2014;61(1 Suppl):S45–S57. doi:10.1016/j.jhep.2014.07.027.
- [54] Simmonds P, Becher P, Bukh J, Gould EA, Meyers G, Monath T, *et al*. ICTV virus taxonomy profile: Flaviviridae. *J Gen Virol* 2017;98(1):2–3. doi:10.1099/jgv.0.000672.
- [55] Murphy DG, Sablon E, Chamberland J, Fournier E, Dandavino R, Tremblay CL. Hepatitis C virus genotype 7, a new genotype originating from central Africa. *J Clin Microbiol* 2015;53(3):967–972. doi:10.1128/JCM.02831-14.
- [56] Agnello V, Abel G, Elfahal M, Knight GB, Zhang QX. Hepatitis C virus and other flaviviridae viruses enter cells via low density lipoprotein receptor. *Proc Natl Acad Sci U S A* 1999;96(22):12766–12771. doi:10.1073/pnas.96.22.12766.
- [57] Zahid MN, Turek M, Xiao F, Th VL, Guérin M, Fofana I, *et al*. The postbinding activity of scavenger receptor class B type I mediates initiation of hepatitis C virus infection and viral dissemination. *Hepatology* 2013;57(2):492–504. doi:10.1002/hep.26097.
- [58] Harris HJ, Davis C, Mullins JG, Hu K, Goodall M, Farquhar MJ, *et al*. Claudin association with CD81 defines hepatitis C virus entry. *J Biol Chem* 2010;285(27):21092–21102. doi:10.1074/jbc.M110.104836.
- [59] Sainz B Jr, Barretto N, Martin DN, Hiraga N, Imamura M, Hussain S, *et al*. Identification of the Niemann-Pick C1-like 1 cholesterol absorption receptor as a new hepatitis C virus entry factor. *Nat Med* 2012;18(2):281–285. doi:10.1038/nm.2581.
- [60] Targett-Adams P, Boulant S, Douglas MW, McLauchlan J. Lipid metabolism and HCV infection. *Viruses* 2010;2(5):1195–1217. doi:10.3390/v2051195.
- [61] Morozov VA, Lagaye S. Hepatitis C virus: Morphogenesis, infection and therapy. *World J Hepatol* 2018;10(2):186–212. doi:10.4254/wjh.v10.i2.186.
- [62] Powdrill MH, Tchesnokov EP, Kozak RA, Russell RS, Martin R, Svarovskaia ES, *et al*. Contribution of a mutational bias in hepatitis C virus replication to the genetic barrier in the development of drug resistance. *Proc Natl Acad Sci U S A* 2011;108(51):20509–20513. doi:10.1073/pnas.1105797108.
- [63] Ribeiro RM, Li H, Wang S, Stoddard MB, Learn GH, Korber BT, *et al*. Quantifying the diversification of hepatitis C virus (HCV) during primary infection: estimates of the in vivo mutation rate. *PLoS Pathog* 2012;8(8):e1002881. doi:10.1371/journal.ppat.1002881.
- [64] Choi KH. *Viral molecular machines*. New York, NY, USA: Springer Science. 2012.
- [65] Barba G, Harper F, Harada T, Kohara M, Goulinet S, Matsuura Y, *et al*. Hepatitis C virus core protein shows a cytoplasmic localization and associates to cellular lipid storage droplets. *Proc Natl Acad Sci U S A* 1997;94(4):1200–1205. doi:10.1073/pnas.94.4.1200.
- [66] Huang H, Sun F, Owen DM, Li W, Chen Y, Gale M Jr, *et al*. Hepatitis C virus production by human hepatocytes dependent on assembly and secretion of very low-density lipoproteins. *Proc Natl Acad Sci U S A* 2007;104(14):5848–5853. doi:10.1073/pnas.0700760104.
- [67] Corless L, Crump CM, Griffin SD, Harris M. Vps4 and the ESCRT-III complex are required for the release of infectious hepatitis C virus particles. *J Gen Virol* 2010;91(Pt 2):362–372. doi:10.1099/vir.0.017285-0.
- [68] Chang KM. Immunopathogenesis of hepatitis C virus infection. *Clin Liver Dis* 2003;7(1):89–105. doi:10.1016/s1089-3261(02)00068-5.
- [69] Nellore A, Fishman JA. NK cells, innate immunity and hepatitis C infection after liver transplantation. *Clin Infect Dis* 2011;52(3):369–377. doi:10.1093/cid/ciq156.
- [70] Chigbu DI, Loonawar R, Sehgal M, Patel D, Jain P. Hepatitis C virus infection: Host-virus interaction and mechanisms of viral persistence. *Cells* 2019;8(4):376. doi:10.3390/cells8040376.
- [71] Xu Y, Zhong J. Innate immunity against hepatitis C virus. *Curr Opin Immunol* 2016;42:98–104. doi:10.1016/j.coi.2016.06.009.
- [72] Wang SH, Huang CX, Ye L, Wang X, Song L, Wang YJ, *et al*. Natural killer cells suppress full cycle HCV infection of human hepatocytes. *J Viral Hepat* 2008;15(12):855–864. doi:10.1111/j.1365-2893.2008.01014.x.
- [73] Jo J, Aichele U, Kersting N, Klein R, Aichele P, Bisse E, *et al*. Analysis of CD8+ T-cell-mediated inhibition of hepatitis C virus replication using a novel immunological model. *Gastroenterology* 2009;136(4):1391–1401. doi:10.1053/j.gastro.2008.12.034.
- [74] Gerlach JT, Diepolder HM, Jung MC, Gruener NH, Schraut WW, Zachoval R, *et al*. Recurrence of hepatitis C virus after loss of virus-specific CD4(+) T-cell response in acute hepatitis C. *Gastroenterology* 1999;117(4):933–941. doi:10.1016/s0016-5085(99)70353-7.
- [75] Nascimbeni M, Mizukoshi E, Bosmann M, Major ME, Mihalik K, Rice CM, *et al*. Kinetics of CD4+ and CD8+ memory T-cell responses during hepatitis C virus rechallenge of previously recovered chimpanzees. *J Virol* 2003;77(8):4781–4793. doi:10.1128/jvi.77.8.4781-4793.2003.
- [76] Thimme R, Binder M, Bartenschlager R. Failure of innate and adaptive immune responses in controlling hepatitis C virus infection. *FEMS Microbiol Rev* 2012;36(3):663–683. doi:10.1111/j.1574-6976.2011.00319.x.
- [77] Wherry EJ, Blattman JN, Murali-Krishna K, van der Most R, Ahmed R. Viral persistence alters CD8 T-cell immunodominance and tissue distribution and results in distinct stages of functional impairment. *J Virol* 2003;77(8):4911–4927. doi:10.1128/jvi.77.8.4911-4927.2003.
- [78] Francavilla V, Accapezzato D, De Salvo M, Rawson P, Cosimi O, Lipp M, *et al*. Subversion of effector CD8+ T cell differentiation in acute hepatitis C virus infection: exploring the immunological mechanisms. *Eur J Immunol* 2004;34(2):427–437. doi:10.1002/eji.200324539.
- [79] Yao ZQ, Eisen-Vandervelde A, Waggoner SN, Cale EM, Hahn YS. Direct binding of hepatitis C virus core to gC1qR on CD4+ and CD8+ T cells leads to impaired activation of Lck and Akt. *J Virol* 2004;78(12):6409–6419. doi:10.1128/JVI.78.12.6409-6419.2004.
- [80] Urbani S, Amadei B, Tola D, Massari M, Schivazappa S, Missale G, *et al*. PD-1 expression in acute hepatitis C virus (HCV) infection is associated with HCV-specific CD8 exhaustion. *J Virol* 2006;80(22):11398–11403. doi:10.1128/JVI.011177-06.
- [81] Nakamoto N, Kaplan DE, Coleclough J, Li Y, Valiga ME, Kaminski M, *et al*. Functional restoration of HCV-specific CD8 T cells by PD-1 blockade is defined by PD-1 expression and compartmentalization. *Gastroenterology* 2008;134(7):1927–1937. doi:10.1053/j.gastro.2008.02.033.
- [82] Nakamoto N, Cho H, Shaked A, Olthoff K, Valiga ME, Kaminski M, *et al*. Synergistic reversal of intrahepatic HCV-specific CD8 T cell exhaustion by combined PD-1/CTLA-4 blockade. *PLoS Pathog* 2009;5(2):e1000313. doi:10.1371/journal.ppat.1000313.
- [83] Schulze zur Wiesch J, Lauer GM, Day CL, Kim AY, Ouchi K, Duncan JE, *et al*. Broad repertoire of the CD4+ Th cell response in spontaneously controlled hepatitis C virus infection includes dominant and highly promiscuous epitopes. *J Immunol* 2005;175(6):3603–3613. doi:10.4049/jimmunol.175.6.3603.
- [84] Diepolder HM, Zachoval R, Hoffmann RM, Wierenga EA, Santantonio T, Jung MC, *et al*. Possible mechanism involving T-lymphocyte response to non-structural protein 3 in viral clearance in acute hepatitis C virus infection. *Lancet* 1995;346(8981):1006–1007. doi:10.1016/s0140-6736(95)91691-1.
- [85] Eckels DD, Wang H, Bian TH, Tabatabai N, Gill JC. Immunobiology of hepatitis C virus (HCV) infection: the role of CD4 T cells in HCV infection. *Immunol Rev* 2000;174:90–97. doi:10.1034/j.1600-0528.2002.017403.x.
- [86] Wang JH, Layden TJ, Eckels DD. Modulation of the peripheral T-cell response by CD4 mutants of hepatitis C virus: transition from a Th1 to a Th2 response. *Hum Immunol* 2003;64(7):662–673. doi:10.1016/s0198-8859(03)00070-3.
- [87] Eckels DD, Zhou H, Bian TH, Wang H. Identification of antigenic escape variants in an immunodominant epitope of hepatitis C virus. *Int Immunol* 1999;11(4):577–583. doi:10.1093/intimm/11.4.577.
- [88] Cabrera R, Tu Z, Xu Y, Firpi RJ, Rosen HR, Liu C, *et al*. An immunomodulatory



- tory role for CD4(+)CD25(+) regulatory T lymphocytes in hepatitis C virus infection. *Hepatology* 2004;40(5):1062–1071. doi:10.1002/hep.20454.
- [89] Boettler T, Spangenberg HC, Neumann-Haefelin C, Panther E, Urbani S, Ferrari C, *et al*. T cells with a CD4+CD25+ regulatory phenotype suppress in vitro proliferation of virus-specific CD8+ T cells during chronic hepatitis C virus infection. *J Virol* 2005;79(12):7860–7867. doi:10.1128/JVI.79.12.7860-7867.2005.
- [90] Ward SM, Fox BC, Brown PJ, Worthington J, Fox SB, Chapman RW, *et al*. Quantification and localisation of FOXP3+ T lymphocytes and relation to hepatic inflammation during chronic HCV infection. *J Hepatol* 2007;47(3):316–324. doi:10.1016/j.jhep.2007.03.023.
- [91] Barrat FJ, Cua DJ, Boonstra A, Richards DF, Crain C, Savelkoul HF, *et al*. In vitro generation of interleukin 10-producing regulatory CD4(+) T cells is induced by immunosuppressive drugs and inhibited by T helper type 1 (Th1)- and Th2-inducing cytokines. *J Exp Med* 2002;195(5):603–616. doi:10.1084/jem.20011629.
- [92] Cerwenka A, Swain SL. TGF-beta1: immunosuppressant and viability factor for T lymphocytes. *Microbes Infect* 1999;1(15):1291–1296. doi:10.1016/s1286-4579(99)00255-5.
- [93] Sugimoto K, Ikeda F, Stadanlick J, Nunes FA, Alter HJ, Chang KM. Suppression of HCV-specific T cells without differential hierarchy demonstrated ex vivo in persistent HCV infection. *Hepatology* 2003;38(6):1437–1448. doi:10.1016/j.jhep.2003.09.026.
- [94] Zhai N, Chi X, Li T, Song H, Li H, Jin X, *et al*. Hepatitis C virus core protein triggers expansion and activation of CD4(+)CD25(+) regulatory T cells in chronic hepatitis C patients. *Cell Mol Immunol* 2015;12(6):743–749. doi:10.1038/cmi.2014.119.
- [95] Cox AL, Mosbruger T, Mao Q, Liu Z, Wang XH, Yang HC, *et al*. Cellular immune selection with hepatitis C virus persistence in humans. *J Exp Med* 2005;201(11):1741–1752. doi:10.1084/jem.20050121.
- [96] Neumann-Haefelin C, Timm J, Spangenberg HC, Wischniowski N, Nazarova N, Kersting N, *et al*. Virological and immunological determinants of intrahepatic virus-specific CD8+ T-cell failure in chronic hepatitis C virus infection. *Hepatology* 2008;47(6):1824–1836. doi:10.1002/hep.22242.
- [97] Erickson AL, Kimura Y, Igarashi S, Eichelberger J, Houghton M, Sidney J, *et al*. The outcome of hepatitis C virus infection is predicted by escape mutations in epitopes targeted by cytotoxic T lymphocytes. *Immunity* 2001;15(6):883–895. doi:10.1016/s1074-7613(01)00245-x.
- [98] Dazert E, Neumann-Haefelin C, Bressanelli S, Fitzmaurice K, Kort J, Timm J, *et al*. Loss of viral fitness and cross-recognition by CD8+ T cells limit HCV escape from a protective HLA-B27-restricted human immune response. *J Clin Invest* 2009;119(2):376–386. doi:10.1172/JCI36587.
- [99] Salloum S, Oniangue-Ndza C, Neumann-Haefelin C, Hudson L, Giugliano S, aus dem Siepen M, *et al*. Escape from HLA-B\*08-restricted CD8 T cells by hepatitis C virus is associated with fitness costs. *J Virol* 2008;82(23):11803–11812. doi:10.1128/JVI.00997-08.
- [100] Timm J, Lauer GM, Kavanagh DG, Sheridan I, Kim AY, Lucas M, *et al*. CD8 epitope escape and reversion in acute HCV infection. *J Exp Med* 2004;200(12):1593–1604. doi:10.1084/jem.20041006.
- [101] Neumann-Haefelin C, Oniangue-Ndza C, Kuntzen T, Schmidt J, Nitschke K, Sidney J, *et al*. Human leukocyte antigen B27 selects for rare escape mutations that significantly impair hepatitis C virus replication and require compensatory mutations. *Hepatology* 2011;54(4):1157–1166. doi:10.1002/hep.24541.
- [102] Timme R, Oldach D, Chang KM, Steiger C, Ray SC, Chisari FV. Determinants of viral clearance and persistence during acute hepatitis C virus infection. *J Exp Med* 2001;194(10):1395–1406. doi:10.1084/jem.194.10.1395.
- [103] Marcello T, Grakoui A, Barba-Spaeth G, Machlin ES, Kitenko SV, MacDonald MR, *et al*. Interferons alpha and lambda inhibit hepatitis C virus replication with distinct signal transduction and gene regulation kinetics. *Gastroenterology* 2006;131(6):1887–1898. doi:10.1053/j.gastro.2006.09.052.
- [104] Darnell JE Jr, Kerr IM, Stark GR. Jak-STAT pathways and transcriptional activation in response to IFNs and other extracellular signaling proteins. *Science* 1994;264(5164):1415–1421. doi:10.1126/science.8197455.
- [105] Fried MW, Shiffman ML, Reddy KR, Smith C, Marinos G, Goncalves FL Jr, *et al*. Peginterferon alfa-2a plus ribavirin for chronic hepatitis C virus infection. *N Engl J Med* 2002;347(13):975–982. doi:10.1056/NEJMoa020047.
- [106] Manns MP, McHutchison JG, Gordon SC, Rustgi VK, Shiffman M, Reindollar R, *et al*. Peginterferon alfa-2b plus ribavirin compared with interferon alfa-2b plus ribavirin for initial treatment of chronic hepatitis C: a randomised trial. *Lancet* 2001;358(9286):958–965. doi:10.1016/s0140-6736(01)06102-5.
- [107] Kamal SM, El Tawil AA, Nakano T, He Q, Rasenack J, Hakam SA, *et al*. Peginterferon {alpha}-2b and ribavirin therapy in chronic hepatitis C genotype 4: impact of treatment duration and viral kinetics on sustained virological response. *Gut* 2005;54(6):858–866. doi:10.1136/gut.2004.057182.
- [108] Meylan E, Curran J, Hofmann K, Moradpour D, Binder M, Bartenschlager R, *et al*. Cardif is an adaptor protein in the RIG-I antiviral pathway and is targeted by hepatitis C virus. *Nature* 2005;437(7062):1167–1172. doi:10.1038/nature04193.
- [109] Garaigorta U, Chisari FV. Hepatitis C virus blocks interferon effector function by inducing protein kinase R phosphorylation. *Cell Host Microbe* 2009;6(6):513–522. doi:10.1016/j.chom.2009.11.004.
- [110] Heim MH, Moradpour D, Blum HE. Expression of hepatitis C virus proteins inhibits signal transduction through the Jak-STAT pathway. *J Virol* 1999;73(10):8469–8475. doi:10.1128/JVI.73.10.8469-8475.
- [111] Conjeevaram HS, Fried MW, Jeffers LJ, Terrault NA, Wiley-Lucas TE, Afdhal N, *et al*. Peginterferon and ribavirin treatment in African American and Caucasian American patients with hepatitis C genotype 1. *Gastroenterology* 2006;131(2):470–477. doi:10.1053/j.gastro.2006.06.008.
- [112] Tatar M, Keeshin SW, Mailliard M, Wilson FA. Cost-effectiveness of universal and targeted hepatitis C virus screening in the United States. *JAMA Netw Open* 2020;3(9):e2015756. doi:10.1001/jamanetworkopen.2020.15756.
- [113] Pawlotsky JM. New hepatitis C therapies: the toolbox, strategies, and challenges. *Gastroenterology* 2014;146(5):1176–1192. doi:10.1053/j.gastro.2014.03.003.
- [114] Bourlière M, Gordon SC, Flamm SL, Cooper CL, Ramji A, Tong M, *et al*. Sofosbuvir, velpatasvir, and voxilaprevir for previously treated HCV infection. *N Engl J Med* 2017;376(22):2134–2146. doi:10.1056/NEJMoa1613512.
- [115] Wyles D, Weiland O, Yao B, Weillert F, Dufour JF, Gordon SC, *et al*. Retreatment of patients who failed glecaprevir/pibrentasvir treatment for hepatitis C virus infection. *J Hepatol* 2019;70(5):1019–1023. doi:10.1016/j.jhep.2019.01.031.
- [116] Seeff LB. Natural history of chronic hepatitis C. *Hepatology* 2002;36(5 Suppl 1):S35–S46. doi:10.1053/jhep.2002.36806.
- [117] Shi ST, Polyak SJ, Tu H, Taylor DR, Gretch DR, Lai MM. Hepatitis C virus NS5A colocalizes with the core protein on lipid droplets and interacts with apolipoproteins. *Virology* 2002;292(2):198–210. doi:10.1006/viro.2001.1225.



## Review Article

# Direct-acting Antiviral Regimens for Patients with Chronic Infection of Hepatitis C Virus Genotype 3 in China

Xiaozhong Wang<sup>1</sup> and Lai Wei<sup>2\*</sup>

<sup>1</sup>Department of Hepatology, Affiliated Hospital of Traditional Chinese Medicine of Xinjiang Medical University, Urumqi, Xinjiang, China; <sup>2</sup>Hepatopancreatobiliary Center, Beijing Tsinghua Changgung Hospital, School of Clinical Medicine, Tsinghua University, Beijing, China

Received: 26 October 2020 | Revised: 20 March 2021 | Accepted: 24 March 2021 | Published: 12 May 2021

## Abstract

Hepatitis C virus (HCV) genotype (GT)3 infection is associated with a more rapid hepatic disease progression than the other genotypes. Hence, early HCV clearance slows down the disease progression and is important for improving prognosis in GT3-infected patients. Nevertheless, compared with other genotypes, GT3 is difficult-to-treat with direct-acting antivirals, especially in the presence of cirrhosis. Current guidelines recommend several regimens which have been proven to be effective in GT3-infected patients from the Western world (North America, Europe, and Oceania). In China, GT3 infection comprises 8.7–11.7% of the 10 million patients infected with HCV and has strikingly different characteristics from that in Western countries. Unlike the Western countries, where GT3a is the predominant subtype, GT3a and 3b each affect roughly half of Chinese GT3-infected patients, with 94–96% of the GT3b-infected patients carrying A30K+L31M double NS5A resistance-associated substitutions. Phase 3 clinical trials including GT3b-infected patients have suggested that GT3b infection is difficult to cure, making the regimen choice for GT3b-infected patients an urgent clinical gap to be filled. This review includes discussions on the epidemiology of HCV GT3 in China, recommendations from guidelines, and clinical data from both Western countries and China. The aim is to provide knowledge that will elucidate the challenges in treating Chinese GT3-infected patients and propose potential solutions and future research directions.

**Citation of this article:** Wang X, Wei L. Direct-acting antiviral regimens for patients with chronic infection of hepatitis C virus genotype 3 in China. *J Clin Transl Hepatol* 2021;9(3):419–427. doi: 10.14218/JCTH.2020.00097.

**Keywords:** Cirrhosis; Direct-acting antivirals; Hepatitis C; Genotype 3; Resistance-associated substitutions.

**Abbreviations:** AASLD, American Association for the Study of Liver Diseases; CLV, coblopassvir; CMA, Chinese Medical Association; DAA, direct-acting antiviral agent; DCV, daclatasvir; EASL, European Association for the Study of the Liver; EBR, elbasvir; FDA, Food and Drug Administration; GLE, glecaprevir; GT, genotype; GZR, grazoprevir; HCV, hepatitis C virus; HD, hemodialysis; IFN, interferon; LDV, ledipasvir; mITT, modified intention-to-treat; NHSA, National Health Security Administration; PegIFN, pegylated interferon; PI, protease inhibitor; PIB, pibrentasvir; PWID, people who inject drugs; RAS, resistance-associated substitution; RBV, ribavirin; SOF, sofosbuvir; SVR, sustained virological response; VEL, velpatasvir; VOX, voxilaprevir; WHO, World Health Organization.

\*Correspondence to: Lai Wei, Hepatopancreatobiliary Center, Beijing Tsinghua Changgung Hospital, School of Clinical Medicine, Tsinghua University, 168 Litang Rd, Changping District, Beijing 102218, China. Tel: +86-10-56118881, Fax: +86-10-56118566, E-mail: weelai@163.com

## Introduction

Direct-acting antivirals (DAAs), with their proven efficacy and safety, have replaced pegylated interferon (PegIFN) plus ribavirin (RBV) as the first-line treatment for chronic hepatitis C virus (HCV) infection in international guidelines.<sup>1–4</sup> However, compared with patients infected with other genotypes (GTs) of HCV, GT3-infected patients, especially those with cirrhosis, tend to achieve lower rates of sustained virological response (SVR) from DAA regimens.<sup>5</sup> Given that China has drastically different distributions of HCV GT3 subtypes and resistance-associated substitutions (RASs) from those of Western countries,<sup>6</sup> it remains unclear whether findings from clinical studies on DAAs in GT3-infected patients from those countries would be generalizable to Chinese patients. This article will discuss the epidemiology of HCV GT3 in China and review guidelines recommendations as well as clinical data from GT3-infected patients on DAAs, to provide direction for treatment and research among the Chinese and the broader Asian GT3-infected population.

## HCV GT3 epidemiology in China

There are currently over 71 million HCV-infected patients worldwide,<sup>7</sup> of which 44–46% are of GT1 and 25–30% are of GT3.<sup>7,8</sup> South and Southeast Asian countries like Pakistan, India, and Malaysia see a higher proportion of GT3 infection, with 79% of the Pakistani HCV-infected patients being of GT3.<sup>7</sup> China has around 10 million HCV-infected patients,<sup>7</sup> with the most common genotypes being GT1b (52.2–62.8%) and GT2a (16.7–28.7%).<sup>7,9–11</sup> GT3 comprises 8.7% to 11.7% of all the local infections,<sup>7,9,11</sup> with both incidence and prevalence showing an increasing trend in recent years.<sup>10,11</sup> For instance, one retrospective study conducted at a hospital in Shanghai, China found that the percentage of GT3-infected patients increased from 13.4% in 2011 to 22.6% in 2014.<sup>12</sup> Geographically, GT3 has spread from the south and southwest regions to the entire country over the last two decades,<sup>11,13</sup> albeit with an uneven distribution across different regions; up to 38% of HCV-infected patients in the southwest region are of GT3, while that percentage is only 3% in the northeast region.<sup>9</sup> GT3a and GT3b subtypes each constitute about 50% of the Chinese GT3-infected population,<sup>6,9,11</sup> with the southwest region reporting up to 70% of GT3-infected patients carrying the GT3b subtype.<sup>9</sup> The GT3b subtype comprised 90%

Table 1. Approved DAA agents in China

DAA agent	Therapeutic class	Indicated GTs
Asunaprevir <sup>a</sup>	NS3/4A protease inhibitor	1b
CLV <sup>a</sup>	NS5A inhibitor	1, 2, 3, 6
Danoprevir/ritonavir <sup>a</sup>	NS3/4A protease inhibitor+CYP3A inhibitor	1b
Dasabuvir <sup>a</sup>	None-nucleotide analogue NS5B polymerase inhibitor	1
DCV <sup>a</sup>	NS5A inhibitor	1–6
SOF <sup>a</sup>	Nucleotide analogue NS5B polymerase inhibitor	1–6
EBR/GZR	NS3/4A protease inhibitor+NS5A inhibitor	1, 4
GLE/PIB	NS3/4A protease inhibitor+NS5A inhibitor	1–6
LDV/SOF	NS5A inhibitor+Nucleotide analogue NS5B polymerase inhibitor	1–6
Ombitasvir/paritaprevir/ritonavir <sup>a</sup>	NS5A inhibitor+NS3/4A protease inhibitor+CYP3A inhibitor	1, 4
SOF/VEL	Nucleotide analogue NS5B polymerase inhibitor+NS5A inhibitor	1–6
SOF/VEL/VOX	Nucleotide analogue NS5B polymerase inhibitor+NS5A inhibitor+NS3/4A protease inhibitor	1–6

<sup>a</sup>The drug needs to be used in combination with other medications to treat chronic HCV infection; more details can be found in the relevant prescribing information.

of the GT3-infected patients in a hospital-based study conducted in Myanmar bordering southwest China.<sup>14</sup> These are markedly different from the patient composition pattern in the Western world (North America, Europe, and Oceania), where close to 99% of the GT3-infected patients carry the GT3a subtype.<sup>15</sup>

Prior research in South Korea and the USA has shown that compared with GT1- or GT2-infected patients, GT3-infected patients tend to have a more rapid hepatic disease progression, with a higher risk of liver complications, such as hepatocellular carcinoma.<sup>16–18</sup> Similarly, the Chinese prospective, observational cohort study “CCgenos” reported that the median time from infection to disease progression was shorter in GT3b-infected patients than in GT1-infected patients (27.1 vs. 35.6 years).<sup>19</sup> The aforementioned study at the Shanghai hospital also reported a younger age and a shorter duration of infection in cirrhotic patients with GT3 infection,<sup>12</sup> lending further evidence to the rapid disease progression associated with GT3.

NS5A RASs such as Y93H, A30K, L31M as well as A30K and L31M double substitutions can affect the efficacy of NS5A inhibitor-based DAA regimens,<sup>20</sup> and are thus a potential key consideration when choosing DAAs for HCV treatment. The global prevalence of the Y93H RAS in GT3a-infected patients is 6%.<sup>15</sup> The phase 3 clinical trials of ALLY-3 in the USA and ASTRAL-3 in Europe, Northern America, and Oceania both reported a Y93H prevalence of 9% among GT3-infected patients.<sup>21,22</sup> However, only 1.6% of GT3-infected and 3.3% of GT3a-infected patients in China have the Y93H RAS.<sup>6,23</sup> As for GT3b, both Chinese and global patient populations have reported a very low prevalence of Y93H.<sup>15,23</sup> In China, 94–96% of GT3b-infected patients carry both A30K and L31M RASs,<sup>6,23</sup> which confer high resistance to currently-approved NS5A inhibitors, as shown by the elevated half maximal effective concentrations for HCV with the RASs.<sup>20</sup>

Injection drug use is a strong risk factor for HCV infection worldwide.<sup>24</sup> A 2017 global meta-analysis reported an HCV antibody prevalence of 43.1% among Chinese people who inject drugs (PWID),<sup>25</sup> while a 2019 study focusing on HCV high-risk populations in China found the prevalence to be 72.4% among PWID.<sup>26</sup> Most of the early GT3-infected patients in China contracted the virus via this route.<sup>11</sup> GT3 is still highly prevalent among the HCV-infected PWID in China, with a 2015 study reporting that GT3 accounted for

55% of HCV-infected PWID.<sup>27</sup> A recent study in heroin users undergoing methadone maintenance therapy in Jiangsu Province reported that up to 74.0% of these patients were HCV antibody-positive,<sup>28</sup> with GT3a and GT3b comprising 24.6% and 41.7% of the cohort with viremia, respectively.<sup>28</sup>

### Treatment recommendations for GT3-infected patients

All the DAAs currently approved in China can be found in Table 1. All of them except sofosbuvir (SOF) are available only as brand-name drugs in China. Seven DAA regimens have been approved in China for GT3-infected patients, namely SOF+RBV, SOF plus daclatasvir (DCV), SOF plus coblopasvir (CLV), ledipasvir (LDV)/SOF+RBV, SOF/velpatasvir (VEL), glecaprevir/pibrentasvir (GLE/PIB), and SOF/VEL/voxilaprevir (VOX); however, not all of them are recommended in the guidelines. The Chinese Medical Association (CMA), American Association for the Study of Liver Diseases (AASLD), European Association for the Study of the Liver (EASL), and World Health Organization (WHO) recently updated their HCV treatment guidelines.<sup>1–4,29</sup> The recommendations for GT3-infected patients without or with compensated cirrhosis are summarized in Table 2. It is worth noting that the international guidelines were formulated primarily based on clinical studies conducted in Western countries, where the GT3a subtype predominates among GT3-infected patients.<sup>15</sup> Therefore, the recommendations for “GT3-infected patients” in these guidelines would likely be more applicable to those with GT3a infection.

### Non-cirrhotic patients

According to the CMA, AASLD, EASL, and WHO guidelines, 12-week SOF/VEL is recommended for non-cirrhotic, GT3-infected patients, regardless of prior PegIFN+RBV treatment (Table 2).<sup>1–4</sup> Co-administration of RBV with SOF/VEL can be considered in GT3b-infected patients, according to the CMA guidelines.<sup>1</sup> GLE/PIB is recommended for non-cirrhotic, GT3-infected patients in the CMA, EASL and WHO guidelines, and the treatment duration is dependent on patient



**Table 2. Treatment recommendations for GT3-infected patients without and with compensated cirrhosis**

Cirrhosis status	Regimen	Treatment history	CMA <sup>1</sup> 2019	AASLD <sup>2</sup> 2019	EASL <sup>3,29</sup> 2018	WHO <sup>4</sup> 2018
No cirrhosis	SOF/VEL	Naïve	12 weeks <sup>b</sup>	12 weeks	12 weeks	12 weeks
		Experienced <sup>a</sup>	12 weeks <sup>b</sup>	12 weeks <sup>c</sup>	12 weeks	12 weeks
	GLE/PIB	Naïve	8 weeks	8 weeks	8 weeks	8 weeks
		Experienced <sup>a</sup>	16 weeks	–	12 weeks <sup>e</sup>	16 weeks
	SOF+DCV	Naïve	–	–	–	12 weeks
		Experienced <sup>a</sup>	–	–	–	12 weeks
Compensated cirrhosis	SOF/VEL	Naïve	12 weeks ± RBV	12 weeks <sup>d</sup>	12 weeks <sup>f</sup>	12 weeks
		Experienced <sup>a</sup>	12 weeks ± RBV	–	12 weeks <sup>f</sup>	12 weeks
	GLE/PIB	Naïve	12 weeks	8 weeks	12 weeks	12 weeks
		Experienced <sup>a</sup>	16 weeks	16 weeks	16 weeks	16 weeks
	SOF/VEL/VOX	Naïve	12 weeks	–	12 weeks	–
		Experienced <sup>a</sup>	12 weeks	12 weeks	12 weeks	–
	SOF+DCV	Naïve	–	–	–	24 weeks
		Experienced <sup>a</sup>	–	–	–	24 weeks

<sup>a</sup>Treatment “experienced” refers to prior treatment with PegIFN+RBV in the guidelines by AASLD, EASL and WHO, but with PegIFN+RBV±SOF or SOF+RBV in the CMA guidelines. <sup>b</sup>Consider the co-administration of RBV in GT3b-infected patients. <sup>c</sup>Baseline RAS testing for Y93H is recommended. When Y93H is present, RBV should be co-administered, or an alternative regimen (12 weeks of SOF/VEL/VOX or 16 weeks of GLE/PIB for those treatment-experienced) should be used. <sup>d</sup>Only applicable for patients without Y93H. When Y93H is present, another regimen should be used (12 weeks of SOF/VEL+RBV or SOF/VEL/VOX as alternatives for such patients). <sup>e</sup>The European prescribing information for GLE/PIB suggests a 16-week course for PegIFN+RBV-experienced, non-cirrhotic patients with GT3 infection. <sup>f</sup>Only applicable for patients without Y93H. If Y93H is present, an alternative regimen such as SOF/VEL/VOX should be used, or RBV should be co-administered with SOF/VEL when SOF/VEL/VOX is not available.

treatment history.<sup>1,3,4</sup> The regimen is also recommended by AASLD as a first-line treatment for treatment-naïve patients and as an alternative for PegIFN+RBV-experienced patients.<sup>2</sup> Recent clinical data showed that with 8 weeks of GLE/PIB in non-cirrhotic patients, a lower SVR12 rate was observed in GT3b-infected patients than in GT3a-infected patients,<sup>30</sup> indicating that 8 weeks is not an optimal course in the former group. Additionally, SOF+DCV is recognized only by the WHO as a first-line regimen in non-cirrhotic, GT3-infected patients.<sup>4</sup>

### Patients with compensated cirrhosis

Both SOF/VEL and GLE/PIB are recommended regimens for GT3-infected patients with compensated cirrhosis in the CMA, AASLD, EASL and WHO guidelines.<sup>1–4,29</sup> All the guidelines recommend an extended course (16 weeks) of GLE/PIB for treatment-experienced patients.<sup>1–4</sup> Co-administration of RBV with SOF/VEL can be considered irrespective of treatment experience according to the CMA guidelines,<sup>1</sup> while SOF/VEL+RBV is included only as an alternative for PegIFN+RBV-experienced patients in the AASLD guidelines.<sup>2</sup> According to EASL and AASLD, GT3-infected patients with compensated cirrhosis should receive RAS testing for Y93H before initiating treatment with SOF/VEL.<sup>2,29</sup> In the presence of Y93H, RBV should be co-administered or an alternative regimen should be used.<sup>2,29</sup> In contrast, the CMA does not recommend RAS testing at baseline in general and suggests considering RBV co-administration with SOF/VEL in cirrhotic, GT3-infected patients.<sup>1</sup> SOF/VEL/VOX is recommended for both treatment-naïve and treatment-experienced GT3-infected patients with compensated cirrhosis by the CMA and EASL guidelines, but only for those who are treatment-experienced in the AASLD guidelines.<sup>1–3</sup> Besides this, SOF+DCV is recommended only by the WHO

guidelines, for GT3-infected patients with compensated cirrhosis.<sup>4</sup>

### Patients with decompensated cirrhosis

Liver transplantation is the primary option for decompensated cirrhosis, whereas antiviral treatment may help prevent reinfection among liver recipients. Due to the safety concerns attributable to markedly increased drug exposure in patients with decompensated cirrhosis, protease inhibitor (PI)-containing regimens, such as GLE/PIB, SOF/VEL/VOX, and elbasvir/grazoprevir (EBR/GZR), are contraindicated in them.<sup>3</sup> The CMA, AASLD, and EASL guidelines recommend 12 weeks of SOF/VEL+RBV for GT3-infected patients with decompensated cirrhosis, and 24 weeks of SOF/VEL if RBV is contraindicated or not tolerated.<sup>1–3</sup> Additionally, 12 weeks of SOF+DCV+RBV or 24 weeks of SOF+DCV (when RBV is contraindicated or not tolerated) is also recommended for such patients in the CMA guidelines.<sup>1</sup> No treatment recommendations were provided by the WHO guidelines for patients with decompensated cirrhosis; although, the guidelines have noted the efficacy and safety of SOF/VEL and SOF+DCV in this patient population.<sup>4</sup>

Inappropriate use of PI-containing regimens in patients with decompensated cirrhosis could result in serious complications. In August 2019, the USA's Food and Drug Administration (known as the FDA) issued a warning on the risk of serious liver injury in patients with advanced liver disease receiving PI-containing regimens, following publication of several case reports.<sup>31</sup> Many of these cases should avoid PI-containing regimens, given the presence of signs and symptoms of decompensated cirrhosis or other serious liver problems.<sup>31</sup> The FDA thus recommends assessing liver disease severity at baseline, and close monitoring for worsening liver function when patients with compensated

cirrhosis receive PI-containing regimens.<sup>31</sup> The FDA also advises discontinuation upon the emergence of signs and symptoms of decompensation.<sup>31</sup> Therefore, a PI-free regimen like SOF/VEL would be more convenient for patients with compensated cirrhosis.

## Clinical data for DAAs in GT3-infected patients

### GT3a-infected patients

A large body of evidence has been generated in patients with GT3 infection from Western countries. Given the predominance of the GT3a subtype in GT3 infections, findings from Western GT3-infected patients in clinical trials could be largely regarded as those from GT3a-infected patients, although the distributions of GT3 subtypes were not always reported in studies. A smaller amount of data among GT3a-infected patients are also available from phase 3 clinical trials conducted in China. This section will review these two sets of efficacy data and discuss their implications and relevance for guiding the treatment of Chinese patients with GT3a infection.

**Western GT3a-infected patients treated with SOF/VEL:** In ASTRAL-3, an international multicenter phase 3 clinical trial, the overall SVR12 rate in GT3-infected patients (with 96% [265/277] infected with GT3a) receiving 12-week SOF/VEL was 95% (264/277); of patients with GT3a infection, 95% (253/265) achieved SVR12.<sup>22</sup> Efficacy was independent of cirrhosis status, with the SVR12 rates in patients without and with compensated cirrhosis reported as 97% (191/197) and 91% (73/80), respectively (Supplementary Fig. 1).<sup>22</sup> An integrated analysis of five phase 3 clinical trials with 12 weeks of SOF/VEL, performed by Hezode *et al.*,<sup>32</sup> reported an SVR12 rate of 93% (53/57) in GT3-infected patients with baseline NS5A RASs from ASTRAL-3 and POLARIS-3. The analysis also found that 86% (19/22) of Y93H carriers, 96% (27/28) of A30K carriers, and all five of the A30K+L31M carriers achieved SVR12,<sup>32</sup> suggesting that the efficacy of SOF/VEL in GT3a-infected patients is largely unaffected by the A30K RAS. In another integrated analysis of six phase 2 and 3 clinical trials, Roberts *et al.*<sup>33</sup> found an SVR12 rate of 94% (316/337) in GT3-infected patients with compensated cirrhosis (with 97% [316/326] infected with GT3a among patients with available genotype data) after 12 weeks of SOF/VEL (Supplementary Fig. 1) but noted that A30K+L31M- and Y93H- carriers achieved SVR12 rates of 88% (22/25) and 60% (6/10), respectively.<sup>33</sup> These results suggest that Y93H-carrying, cirrhotic patients with GT3 infection may represent a particular patient population that do not respond optimally to 12-week SOF/VEL.<sup>33</sup> As a result, the AASLD and EASL guidelines now recommend 12 weeks of SOF/VEL for GT3-infected patients with compensated cirrhosis,<sup>2,3,29</sup> with co-administration of RBV in the presence of the Y93H RAS.<sup>2,29</sup> Likely due to the low prevalence (1.6%) of the Y93H RAS in Chinese GT3-infected patients,<sup>6,23</sup> the CMA guidelines do not recommend Y93H RAS testing in GT3-infected patients prior to treatment with SOF/VEL.

**Western GT3a-infected patients treated with GLE/PIB:** In an integrated analysis of five clinical trials of GLE/PIB including GT3-infected patients (with 99% [683/693] infected with GT3a), Flamm *et al.*<sup>34</sup> found that extending the treatment duration from 8 weeks to 12 weeks did not increase efficacy in treatment-naïve, non-cirrhotic patients, with the SVR12 rates at 95% (198/208 and 280/294) in both groups (Supplementary Fig. 1). Based on these findings, current guidelines generally recommend 8 weeks of GLE/PIB in such patients.<sup>1-4</sup> However, the treatment duration affected efficacy in treatment-experienced, non-cirrhotic patients. The rates of virological failure in those

receiving 12 and 16 weeks of treatment were 10.2% (5/49) and 4.5% (1/22), respectively.<sup>34</sup> Currently, the EASL guidelines recommend 12 weeks of treatment in this group of patients,<sup>3</sup> while the CMA and WHO guidelines recommend 16 weeks.<sup>1,4</sup> Flamm *et al.*<sup>34</sup> also reported that 97% (67/69) of treatment-naïve patients with cirrhosis achieved SVR12 following 12 weeks of GLE/PIB, and 94% (48/51) of their treatment-experienced counterparts achieved SVR12 following 16 weeks of the regimen. Overall, GLE/PIB showed high efficacy among GT3a-infected patients. However, its treatment duration is dependent on treatment history and cirrhosis status, which may complicate clinical practice and affect its use in primary care settings.

Flamm *et al.*<sup>34</sup> also explored the effect of RASs on the efficacy of GLE/PIB in GT3-infected patients that were treatment-naïve and non-cirrhotic. In patients receiving 8-week GLE/PIB, 100% (10/10) of Y93H carriers and 83% (15/18) of A30K carriers achieved SVR12 based on modified intention-to-treat (mITT) analysis.<sup>34</sup> Among those receiving 12-week GLE/PIB, Y93H carriers and A30K carriers achieved mITT SVR12 rates of 86% (12/14) and 93% (13/14), respectively;<sup>34</sup> whereas, a meta-analysis showed that both the A30K and Y93H RASs can reduce the efficacy of GLE/PIB in GT3-infected patients.<sup>35</sup> More real-world studies with larger samples are needed to verify this effect.

Although no head-to-head studies have been conducted between SOF/VEL and GLE/PIB, an analysis based on the American TRIO Network found that among cirrhotic, GT3-infected patients, GLE/PIB yielded a lower per-protocol SVR rate than SOF/VEL (88% [22/25] vs. 98% [57/58],  $p=0.044$ ).<sup>36</sup> This suggests a difference in efficacy between GLE/PIB and SOF/VEL in this patient population, but the reason for this remains to be investigated.

**Western GT3a-infected patients treated with SOF/VEL/VOX and EBR/GZR+SOF:** The phase 3 clinical trials POLARIS-2 and -3, both conducted in North America, Europe, and Oceania, found that 8 weeks of SOF/VEL/VOX achieved high SVR12 rates of 99% (91/92) and 96% (106/110) in GT3-infected patients without and with compensated cirrhosis, respectively (Supplementary Fig. 2).<sup>37</sup> Nevertheless, as experiences thus far indicate that GT3 is difficult-to-treat with DAAs, both the AASLD and EASL guidelines recommend a 12-week course for SOF/VEL/VOX for precautionary reasons.<sup>2,3</sup> The phase 2 study C-ISLE in the UK determined the use of EBR/GZR+SOF in GT3-infected patients with compensated cirrhosis (Supplementary Fig. 2).<sup>38</sup> In this trial, treatment-naïve patients receiving 8 weeks of EBR/GZR+SOF+RBV and 12 weeks of EBR/GZR+SOF achieved SVR12 rates of 91% (21/23) and 96% (23/24), respectively.<sup>38</sup> Treatment-experienced patients achieved an SVR12 rate of 100% (17/17) with 12 weeks of EBR/GZR+SOF, while addition of RBV or extension to a 16-week duration did not improve efficacy (with the SVR12 rates at 94% [17/18] for both).<sup>38</sup> Based on these findings, the AASLD recommends 12 weeks of EBR/GZR+SOF as an alternative for PegIFN+RBV-experienced, GT3-infected patients with compensated cirrhosis.<sup>2</sup>

**Western GT3a-infected patients treated with other DAA regimens:** In clinical trials for SOF+RBV, LDV/SOF+RBV, and SOF+DCV, cirrhotic and/or treatment-experienced GT3-infected patients emerged as difficult-to-treat patient populations (Supplementary Fig. 3) and achieved lower SVR12 rates compared with their counterparts in clinical trials for SOF/VEL and GLE/PIB.<sup>22,34</sup> For GT3-infected patients in the European phase 3 clinical trial VALANCE, while 24-week SOF+RBV treatment achieved an SVR12 rate of 91% (172/190) in non-cirrhotic patients, the SVR12 rates were 68% (41/60) in those with compensated cirrhosis and 62% (29/47) in treatment-experienced patients with compensated cirrhosis.<sup>39</sup> These observations align with the findings from the SOF+RBV arm in the ASTRAL-3

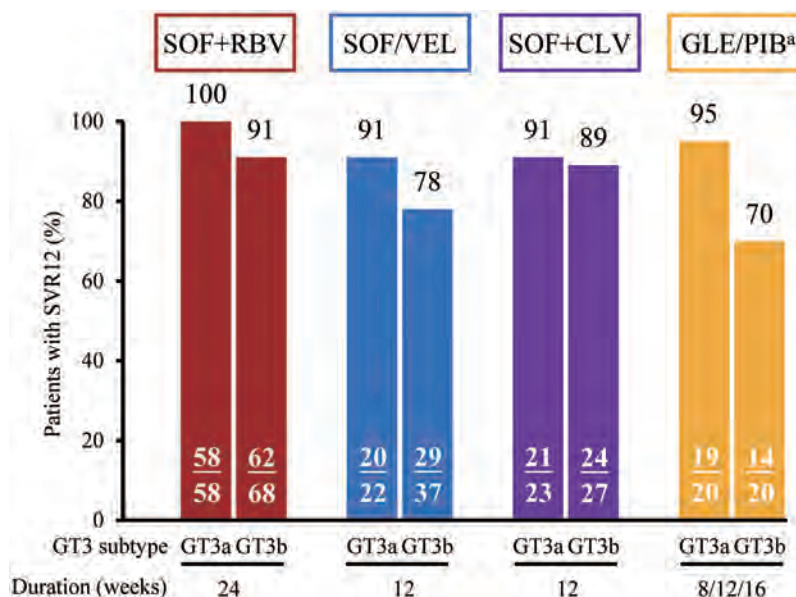


**Fig. 1. SVR12 rates of SOF+RBV,<sup>45</sup> SOF/VEL,<sup>46</sup> SOF+CLV,<sup>44</sup> and GLE/PIB<sup>30</sup> in Chinese patients with GT3 infection.** <sup>a</sup>Treatment-naïve patients without or with compensated cirrhosis received 8 or 12 weeks of treatment, respectively, while treatment-experienced patients received a 16-week treatment regardless of cirrhosis status.

study.<sup>22</sup> The Canadian phase 2 trial study 1701 evaluated the efficacy of 12-week LDV/SOF+RBV in treatment-naïve, GT3-infected patients (with 95% [105/110] infected with GT3a) and found that those with compensated cirrhosis had a lower SVR12 rate than those without cirrhosis (79% [31/39] vs. 94% [68/72]).<sup>40</sup> As for 12-week SOF+DCV, the phase 3 study ALLY-3 conducted in the USA reported that among GT3-infected patients, the SVR12 rate was 96% (105/109) in non-cirrhotic patients, but was only 63% (20/32) in those with compensated cirrhosis.<sup>21</sup> The follow-up ALLY-3+ study investigated the efficacy of RBV co-administration with SOF+DCV in GT3-infected patients with compensated cirrhosis from the USA and found that despite co-administration with RBV, suboptimal SVR12 rates of 83% (15/18) and 89% (16/18) were achieved with 12-week and 16-week treatment, respectively.<sup>41</sup> Possibly for this reason, SOF+DCV is now not recommended by the CMA, AASLD, and EASL guidelines as a first-line regimen for GT3-infected patients.<sup>1–3</sup>

**Chinese GT3a-infected patients:** Among the seven DAA regimens that have been approved for GT3-infected patients in China, phase 3 clinical data in Chinese GT3-infected patients are only available for SOF/VEL (NCT02671500), SOF+RBV (NCT02021643), SOF+CLV (NCT03995485), and GLE/PIB (NCT03222583 and NCT03235349) (Figs. 1, 2).<sup>30,42–44</sup> It should be noted that no head-to-head clinical trials between these regimens have been conducted among Chinese GT3-infected patients.

In Chinese phase 3 clinical trials, the SVR12 rates in GT3a-infected patients receiving 12 weeks of SOF/VEL and 24 weeks of SOF+RBV were 91% (20/22) (89% [17/19] and 100% [3/3] in patients without and with compensated cirrhosis, respectively) and 100% (58/58), respectively,<sup>45,46</sup> similar to those reported among Western GT3-infected patients.<sup>22,39</sup> Since the prevalence of Y93H (the predominant NS5A RAS affecting the efficacy of SOF/VEL in GT3a-infected patients) is lower in China,<sup>6,23</sup> it is reasonable to anticipate SOF/VEL to have similar or better efficacy in Chinese GT3a-infected patients. Twelve weeks of SOF+CLV achieved an SVR12 rate of 91% (21/23) in GT3a-infected patients, being 90% (19/21) and 100% (2/2) in patients without and

with compensated cirrhosis, respectively.<sup>44</sup> Thus, SOF+CLV and SOF/VEL appear to demonstrate comparable efficacy among Chinese patients with GT3a infection.

The two phase 3 studies VOYAGE-1 and -2 of GLE/PIB included Chinese GT3-infected patients without and with compensated cirrhosis, respectively.<sup>30</sup> In these two trials, treatment-naïve, GT3-infected patients without and with compensated cirrhosis received 8 or 12 weeks of treatment, respectively, while those who were GT3-infected and treatment-experienced were treated for 16 weeks regardless of cirrhosis status.<sup>30</sup> GLE/PIB achieved SVR12 rates of 93% (13/14) in non-cirrhotic, GT3a-infected patients in VOYAGE-1 and 100% (6/6) in GT3a-infected patients with compensated cirrhosis in VOYAGE-2.<sup>30</sup> The SVR12 rate in GT3a-infected patients across the two trials was 95% (19/20); similar to the efficacy of GLE/PIB in Western GT3-infected patients.<sup>34</sup> As such, recommendations that were largely based on clinical data from Western GT3-infected patients are most likely also applicable for GT3a-infected patients in China.

### GT3b-infected patients

Currently, limited data are available on the treatment of GT3b infection with DAAs. GT3b infection is under-represented in Western countries while in China only five phase 3 trials and a small number of real-world studies have reported on GT3b-infected patients treated with DAAs, revealing a gap in treatment needs that could not be sufficiently addressed based on Western experiences. More China-specific data are needed to inform guidelines for treating Chinese patients with GT3b infection and until then, preliminary strategies could be formulated for managing GT3 infection in the Chinese scenario, as discussed below.

**SOF-based regimens:** In pivotal trials of Chinese GT3b-infected patients, the SVR12 rates were 78% (29/37) for 12-week SOF/VEL, 89% (24/27) for 12-week SOF+CLV, and 91% (62/68) for 24-week SOF+RBV; these were all lower than their corresponding SVR12 rates in GT3a-infected patients in the same trials (Fig. 1).<sup>44–46</sup> The SVR12 rate for



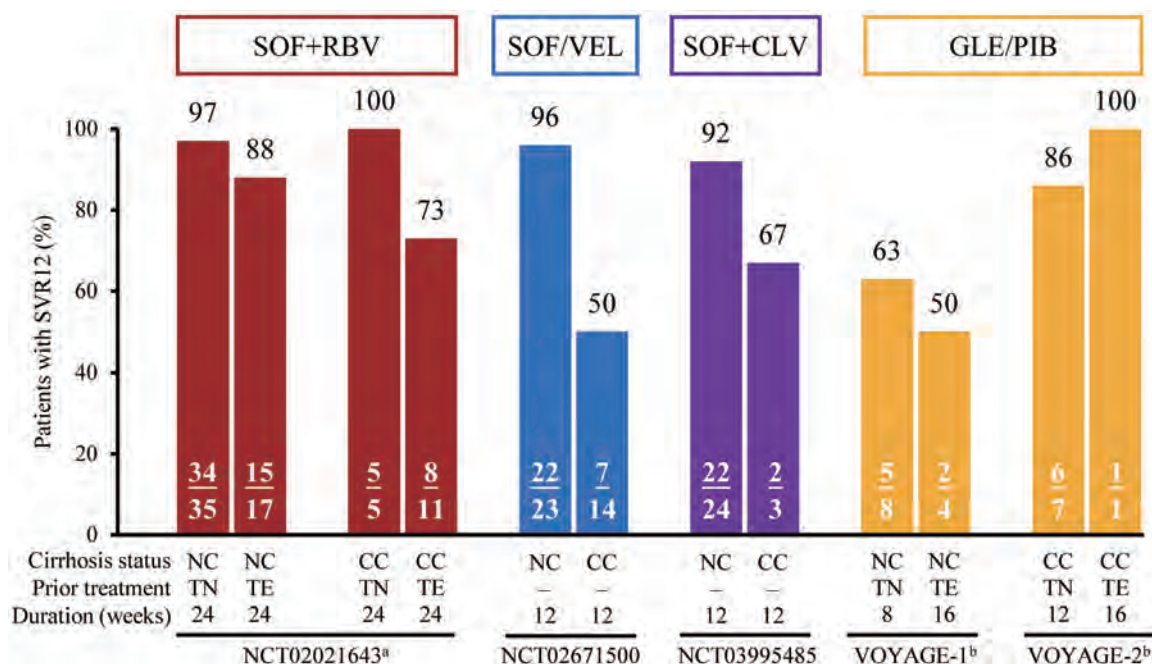


**Fig. 2. SVR12 rates of SOF+RBV,<sup>45</sup> SOF/VEL,<sup>46</sup> SOF+CLV,<sup>44</sup> and GLE/PIB<sup>30,50</sup> in Chinese patients with GT3b infection.** <sup>a</sup>TE in this study was defined as prior treatment with IFN-based therapy. <sup>b</sup>TE in these two studies was defined as prior treatment with IFN with or without RBV, and/or SOF+RBV with or without IFN. CC, compensated cirrhosis; NC, no cirrhosis; TE, treatment-experienced; TN, treatment-naïve.

SOF/VEL in GT3b-infected patients was still as high as 96% (22/23) in those without cirrhosis, but decreased to 50% (7/14) in those with compensated cirrhosis (Fig. 2).<sup>46</sup> Similarly, post hoc analysis found that the SVR12 rates of 12-week SOF+CLV were 92% (22/24) and 67% (2/3) in GT3b-infected patients without and with compensated cirrhosis, respectively (Fig. 2).<sup>44</sup>

The Chinese GT3b-infected patients with available sequencing data in the phase 3 study of SOF/VEL all carried NS5A RASs, with the A30K+L31M double RASs present in 94% (33/35) of them.<sup>46</sup> It was thus suggested that A30K+L31M, when present concurrently with cirrhosis, could reduce the efficacy of SOF/VEL in GT3b-infected patients.<sup>47</sup> It is worth noting that the clinical trial of SOF/VEL in China included only 37 GT3b-infected patients, of whom 38% (14/37) were cirrhotic. This small sample might not be representative of the real-world GT3b-infected patient population in China.<sup>43</sup> Therefore, the effectiveness of SOF/VEL in this patient population awaits further elucidation.

The above pivotal trial identified cirrhotic, GT3b-infected patients (with pervasive key NS5A RASs) as a difficult-to-treat population, specifically in China. For such patients, Chinese data are not yet available on the effect of RBV co-administration with SOF/VEL. However, a meta-analysis of studies from Western countries showed that regardless of cirrhosis status, co-administering RBV can improve the efficacy of SOF/VEL in GT3-infected patients.<sup>48</sup> A Spanish randomized, open-label trial reported that 12 weeks of SOF/VEL without and with RBV achieved high SVR12 rates of 91% (92/101) and 96% (99/103), respectively, among GT3-infected patients with cirrhosis.<sup>49</sup> In patients carrying NS5A RASs, the addition of RBV resulted in a higher SVR12 rate (95% [21/22] vs. 84% [16/19]).<sup>49</sup> The SVR12 rate of 81% (13/16) achieved by 24 weeks of SOF+RBV in GT3b-infected patients with compensated cirrhosis also indicates the potential benefit from RBV co-administration.<sup>45</sup> These data, primarily from GT3a-infected patients, point to RBV co-administration as a possible strategy for improving the

efficacy of SOF/VEL in Chinese GT3b-infected patients, likely through reducing the risk of virological relapse. It will also be interesting to know whether the addition of PegIFN to SOF/VEL could increase its SVR rates among GT3b-infected patients with compensated cirrhosis, but this needs further investigation.

In this age of treatment pathway simplification for HCV management, cirrhotic, GT3-infected patients with baseline NS5A RASs remain a patient population with special treatment needs. Even for SOF/VEL, the regimen with the fixed treatment duration across HCV genotypes, cirrhotic status, and treatment history, the above patient population remains the only sub-group requiring treatment modification in the form of RBV co-administration.<sup>1,2,29</sup> Here, we propose a hierarchical pathway for identifying this specific patient population in the Chinese context, while avoiding excessive pre-treatment testing. Firstly, patients' cirrhosis status should be evaluated. Since clinical data support SOF/VEL's efficacy in non-cirrhotic European and Asian patients with various genotypes of HCV,<sup>22,43</sup> genotyping would not be necessary when initiating 12 weeks of SOF/VEL in non-cirrhotic patients. In patients with compensated cirrhosis, the transmission route could serve as a preliminary indicator of the need for genotyping. In China, given that GT3 is particularly common among HCV-infected PWID, genotyping would be necessary for cirrhotic PWID. Once a cirrhotic patient is identified with GT3 infection, the HCV subtype can direct the treatment decision, possibly without baseline RAS testing. As the Y93H RAS has a low prevalence in China, cirrhotic, GT3a-infected patients may consider an RBV-free regimen; in contrast, the near-universal presence of A30K+L31M in Chinese GT3b-infected patients warrants RBV co-administration for cirrhotic, GT3b-infected patients.

**GLE/PIB:** Across VOYAGE-1 and -2, SVR12 was achieved by GLE/PIB in 70% (14/20) of Chinese patients with GT3b infection (Fig. 1).<sup>30</sup> In VOYAGE-1, the SVR12 rate was 58% (7/12) in non-cirrhotic, GT3b-infected patients, with 63% (5/8) in treatment-naïve patients and 50% (2/4) in treat-

ment-experienced patients (Fig. 2).<sup>50</sup> These results are inferior to the SVR12 rates that GLE/PIB achieved in Western GT3-infected patients and Chinese GT3a-infected patients, as discussed above.<sup>30,34</sup> The findings from these two trials imply that the recommended 8-week course of GLE/PIB in treatment-naïve, non-cirrhotic patients with GT3 infection is not feasible in China.<sup>1-4</sup> An extended course might be a reasonable approach to improve the efficacy in those patients but would further complicate the treatment duration of GLE/PIB, which already depends on HCV genotype, cirrhosis status, and treatment history. In contrast, 12-week SOF/VEL achieved an SVR12 rate of 96% in non-cirrhotic, GT3b-infected patients,<sup>46</sup> and thus may be a better option for this patient population. In VOVAGE-2, the SVR12 rate was 88% (7/8) in GT3b-infected patients with compensated cirrhosis; specifically, 6 out of 7 treatment-naïve patients and 1 treatment-experienced patient achieved SVR12 (Fig. 2).<sup>50</sup> However, the efficacy of GLE/PIB in cirrhotic patients with GT3b infection should be considered inconclusive given the small sample size ( $n=8$ ) of such patients in the trial.<sup>30</sup> All six GT3b-infected patients experiencing virologic failure in VOYAGE-1 and -2 carried NS5A M31 polymorphism at baseline,<sup>30</sup> indicating that the efficacy of GLE/PIB in Chinese patients with GT3b infection may be affected by the presence of NS5A M31 polymorphism.<sup>6,23</sup>

There is a small amount of real-world data for using DAAs among Chinese GT3-infected patients. A retrospective study conducted in six hospitals across provinces investigated the efficacy of different DAAs in GT3-infected patients.<sup>51</sup> The study included 12 patients (5 GT3a, 7 GT3b) receiving 12 weeks of SOF+DCV and 10 patients (5 GT3a, 5 GT3b) receiving 12 weeks of SOF/VEL.<sup>51</sup> All patients receiving SOF/VEL achieved SVR12, but only 3 (60%) GT3a- and 4 (57%) GT3b-infected patients in the SOF+DCV group achieved SVR12.<sup>51</sup> In a cohort study conducted at a tertiary hospital of Sichuan Province in treatment-naïve, GT3-infected patients, SVR24 was achieved in 86% (49/57), 92% (22/24), and 100% (21/21) of patients receiving SOF+DCV, SOF+DCV+RBV, and SOF/VEL, respectively;<sup>52</sup> all 10 patients with virologic failure were in the SOF+DCV±RBV groups.<sup>52</sup> Taken together, these data suggest that for Chinese GT3-infected patients, SOF+DCV may be a suboptimal option due to higher failure rates, while SOF/VEL tends to have better efficacy. As GLE/PIB and SOF+CLV were only recently approved in China, their real-world efficacy in Chinese GT3-infected patients remains to be determined.

## Future directions

In order to achieve the WHO 2030 HCV elimination goal, China would need effective solutions to increase the diagnosis and treatment rates and to reduce the incidence of HCV infection. Studies have shown a low treatment rate of HCV infection in China. One retrospective study in a tertiary hospital in Chongqing, southwest China showed that from 2013 to 2015, only 46% of the HCV RNA-positive patients received antiviral treatment.<sup>53</sup> The low treatment rates before the availability of DAAs could be partly due to the tedious administration method, the various contraindications, and the prevalent side effects of PegIFN+RBV, which severely limited its use in HCV treatment.

By 2020, all the DAAs recommended in the international guidelines have been approved in China, as well as some domestically produced ones (Table 1). To increase the treatment rates of HCV infection and reduce the financial burden of HCV treatment for patients, the National Healthcare Security Administration (commonly known as the NHSA) have included four regimens (SOF/VEL and SOF+CLV for non-GT1b patients; LDV/SOF and EBR/GZR for GT1b patients)

into the National Reimbursement Drug List. It should be noted that in the regimen of SOF+CLV, only CLV has been included in the list, but generic SOF is given to patients free of charge by the CLV manufacturer to form a complete regimen. The prices of the regimens included in the list have been reduced drastically as a result of drug pricing negotiations between NHSA and the manufacturers. For the treatment of GT3 infection, the total price paid by a patient and medical insurance is RMB13,104 (~\$2,019 USD) for a 12-week course of SOF/VEL and RMB10,038 (~\$1,547 USD) for a 12-week course of SOF+CLV. To fully capitalize on high efficacy and good tolerability of these versatile regimen options as well as the reduced prices, strategies should be devised to roll out DAA treatment on a large scale. These regimens would not only help existing HCV-infected patients achieve virological clearance and thereby slow down disease progression but also contribute to reducing the risk of further HCV transmission. As discussed above, data for cirrhotic, GT3b-infected patients are still insufficient to formulate treatment recommendations and thus clinical trials focusing on this subpopulation should be conducted in China to determine the optimal regimens.

In terms of HCV prevention, it is important to adopt interventions tailored to the epidemiological characteristics of HCV transmission, for different high-risk populations and in different geographical regions. Specifically, southwest China sees higher prevalence of GT3 and concentration of the GT3b subtype.<sup>9,11</sup> Considering that injection drug use is the main risk factor for contracting GT3 in China,<sup>52</sup> strategies targeting PWID, such as providing single-use injection supplies and opioid replacement rehabilitation therapy, would be critical for controlling HCV transmission in this region.<sup>54</sup> Recently, the number of patients contracting GT3 infection from unprotected sex has been rising in China.<sup>11</sup> As GT3 infection is also starting to spread beyond southwest China,<sup>13</sup> changes in the epidemiological pattern of HCV transmission may necessitate adjustments to regional or local HCV prevention strategies. Another HCV high-risk population in China are patients undergoing hemodialysis (HD), with a meta-analysis from 2009 revealing an HCV prevalence of 41.1% in this group.<sup>55</sup> With more stringent hygiene practices in hospitals in recent years, the prevalence of HCV in HD patients has decreased dramatically. Nevertheless, a 2011 cross-sectional study in Beijing showed that the prevalence of HCV antibody in patients on HD was still as high as 6.1%, and HCV RNA positivity was 4.6%, with GT3a and GT3b each taking up 1.1% of these HCV-infected patients.<sup>56</sup> The national sentinel surveillance for HCV also reported that the rate of HCV antibody positivity among Chinese patients on HD was 4.5% in 2016 and 4.4% in 2017.<sup>57</sup> These findings suggest that standard operation procedures and management guidelines in HD centers should be strictly enforced to further reduce the HCV transmission in this patient population.<sup>58</sup> Overall, the considerable geographical variation across the expanse of China calls for more systematic, region-specific investigations into the epidemiology of HCV in high-risk populations, so that treatment and intervention strategies can cater to local needs.

## Conclusions

GT3a and GT3b subtypes each account for around half of the GT3 infections in China, with the A30K and L31M double RASs universally present in GT3b-infected patients. Phase 3 clinical trials in Chinese GT3-infected patients have supported the efficacy of SOF/VEL, SOF+RBV, SOF+CLV, and GLE/PIB in GT3a-infected patients with high SVR12 rates. SOF/VEL for 12 weeks has proven to be highly efficacious in non-cirrhotic, GT3b-infected patients but achieved a

lower SVR12 rate in GT3b-infected patients with cirrhosis; hence, RBV might need to be co-administered for this latter group to improve SVR12. The clinical data of SOF+CLV in GT3b-infected patients are scarce but appear similar to those of SOF/VEL. GLE/PIB for 8 weeks produced a suboptimal SVR12 rate in treatment-naïve, non-cirrhotic patients with GT3b infection, and its efficacy is still inconclusive in cirrhotic, GT3b-infected patients. For the Chinese population, treatment strategies for GT3a-infected patients can be formulated based on recommendations in international guidelines and current clinical data, but there are insufficient data to make recommendations for GT3b-infected patients. More clinical trials with larger sample sizes are thus needed to evaluate various regimens and then to determine the optimal ones in this group. Additionally, considering the increasing number of GT3-infected patients in recent years, China needs to adopt active intervention strategies to minimize HCV transmission.

## Acknowledgments

The authors would like to thank Jinlong Guo, Ph.D. and Jingyao Han, BSc. (both employees of Costello Medical Singapore, funded by Gilead Sciences Shanghai Pharmaceutical Technology Co., Ltd.) for writing assistance and editorial support for the development of the manuscript.

## Funding

Nothing to declare.

## Conflict of interest

XW reports consulting fees for MSD and speaker fees for Gilead Sciences and GlaxoSmithKline. The other author has no conflict of interests related to this publication.

## Author contributions

Study concept and design (XW, LW), drafting of the manuscript (XW, LW), and critical revision of the manuscript (XW, LW).

## References

- Guidelines for the prevention and treatment of hepatitis C (2019 version). *Zhonghua Gan Zang Bing Za Zhi* 2019;27(12):962–979. doi: 10.3760/cma.j.issn.1007-3418.2019.12.008.
- HCV guidance: Recommendations for testing, managing, and treating hepatitis C. Available from: <https://www.hcvguidelines.org/>.
- EASL recommendations on treatment of hepatitis C 2018. *J Hepatol* 2018;69(2):461–511. doi: 10.1016/j.jhep.2018.03.026.
- World Health Organization. Guidelines for the care and treatment of persons diagnosed with chronic hepatitis C virus infection. Available from: <https://apps.who.int/iris/bitstream/handle/10665/273174/9789241550345-eng.pdf?ua=1>.
- Tapper EB, Afdhal NH. Is 3 the new 1: perspectives on virology, natural history and treatment for hepatitis C genotype 3. *J Viral Hepat* 2013;20(10):669–677. doi: 10.1111/jvh.12168.
- Wei L, Omata M, Lim YS, Xie Q, Hou JL, Jia J, *et al*. HCV phylogenetic signature and prevalence of pretreatment NS5A and NS5B NI-Resistance associated substitutions in HCV-infected patients in Mainland China. *Antiviral Res* 2018;158:178–184. doi: 10.1016/j.antiviral.2018.08.001.
- Global prevalence and genotype distribution of hepatitis C virus infection in 2015: a modelling study. *Lancet Gastroenterol Hepatol* 2017;2(3):161–176. doi: 10.1016/S2468-1253(16)30181-9.
- Messina JP, Humphreys I, Flaxman A, Brown A, Cooke GS, Pybus OG, *et al*. Global distribution and prevalence of hepatitis C virus genotypes. *Hepatology* 2015;61(1):77–87. doi: 10.1002/hep.27259.
- Chen Y, Yu C, Yin X, Guo X, Wu S, Hou J. Hepatitis C virus genotypes and subtypes circulating in Mainland China. *Emerg Microbes Infect* 2017;6(11):e95. doi: 10.1038/emmi.2017.77.
- Zhang Y, Chen LM, He M. Hepatitis C virus in mainland China with an emphasis on genotype and subtype distribution. *Viral J* 2017;14(1):41. doi: 10.1186/s12985-017-0710-z.
- Du G, Li X, Musa TH, Ji Y, Wu B, He Y, *et al*. The nationwide distribution and trends of hepatitis C virus genotypes in mainland China. *J Med Virol* 2019;91(3):401–410. doi: 10.1002/jmv.25311.
- Lu J, Xiang X, Cao Z, Wang W, Zhao G, Tang W, *et al*. Younger trend of cirrhosis incidence in genotype 3 HCV infected patients in Eastern China. *J Med Virol* 2017;89(11):1973–1980. doi: 10.1002/jmv.24894.
- Ju W, Yang S, Feng S, Wang Q, Liu S, Xing H, *et al*. Hepatitis C virus genotype and subtype distribution in Chinese chronic hepatitis C patients: nationwide spread of HCV genotypes 3 and 6. *Viral J* 2015;12:109. doi: 10.1186/s12985-015-0341-1.
- Yu NM, Latt AZ, Kyaw MK, Hlaing NKT, Naing W. Hepatitis C genotype 3 subtypes and Y93H mutation in single center experience in Myanmar. The 30<sup>th</sup> Annual Conference for Asian Pacific Association for the Study of the Liver; 2021 Feb 4–6; Bangkok, Thailand.
- Welzel TM, Bhardwaj N, Hedskog C, Chodavarapu K, Camus G, McNally J, *et al*. Global epidemiology of HCV subtypes and resistance-associated substitutions evaluated by sequencing-based subtype analyses. *J Hepatol* 2017;67(2):224–236. doi: 10.1016/j.jhep.2017.03.014.
- Lee SS, Kim CY, Kim BR, Cha RR, Kim WS, Kim JJ, *et al*. Hepatitis C virus genotype 3 was associated with the development of hepatocellular carcinoma in Korea. *J Viral Hepat* 2019;26(4):459–465. doi: 10.1111/jvh.13047.
- Kanwal F, Kramer JR, Ilyas J, Duan Z, El-Serag HB. HCV genotype 3 is associated with an increased risk of cirrhosis and hepatocellular cancer in a national sample of U.S. Veterans with HCV. *Hepatology* 2014;60(1):98–105. doi: 10.1002/hep.27095.
- McMahon BJ, Bruden D, Townshend-Bulson L, Simons B, Spradling P, Livingston S, *et al*. Infection with hepatitis C virus genotype 3 is an independent risk factor for end-stage liver disease, hepatocellular carcinoma, and liver-related death. *Clin Gastroenterol Hepatol* 2017;15(3):431–437.e2. doi: 10.1016/j.cgh.2016.10.012.
- Wu N, Rao HY, Yang WB, Gao ZL, Yang RF, Fei R, *et al*. Impact of hepatitis C virus genotype 3 on liver disease progression in a Chinese national cohort. *Chin Med J (Engl)* 2020;133(3):253–261. doi: 10.1097/CM9.0000000000000629.
- Smith D, Magri A, Bonsall D, Ip CLC, Trebes A, Brown A, *et al*. Resistance analysis of genotype 3 hepatitis C virus indicates subtypes inherently resistant to nonstructural protein 5A inhibitors. *Hepatology* 2019;69(5):1861–1872. doi: 10.1002/hep.29837.
- Nelson DR, Cooper JN, Lalezari JP, Lawitz E, Pockros PJ, Gitlin N, *et al*. All-oral 12-week treatment with daclatasvir plus sofosbuvir in patients with hepatitis C virus genotype 3 infection: ALLY-3 phase III study. *Hepatology* 2015;61(4):1127–1135. doi: 10.1002/hep.27726.
- Foster GR, Afdhal N, Roberts SK, Brau N, Gane EJ, Planko S, *et al*. Sofosbuvir and velpatasvir for HCV genotype 2 and 3 infection. *N Engl J Med* 2015;373(27):2608–2617. doi: 10.1056/NEJMoa1512612.
- Lu J, Feng Y, Chen L, Zeng Z, Liu X, Cai W, *et al*. Subtype-specific prevalence of hepatitis C virus NS5A resistance associated substitutions in mainland China. *Front Microbiol* 2019;10:535. doi: 10.3389/fmicb.2019.00535.
- Ruta S, Cernescu C. Injecting drug use: A vector for the introduction of new hepatitis C virus genotypes. *World J Gastroenterol* 2015;21(38):10811–10823. doi: 10.3748/wjg.v21.i38.10811.
- Degenhardt L, Peacock A, Colledge S, Leung J, Grebely J, Vickerman P, *et al*. Global prevalence of injecting drug use and sociodemographic characteristics and prevalence of HIV, HBV, and HCV in people who inject drugs: a multistage systematic review. *Lancet Glob Health* 2017;5(12):e1192–e1207. doi: 10.1016/S2214-109X(17)30375-3.
- Liu CR, Li X, Chan PL, Zhuang H, Jia JD, Wang X, *et al*. Prevalence of hepatitis C virus infection among key populations in China: A systematic review. *Int J Infect Dis* 2019;80:16–27. doi: 10.1016/j.ijid.2018.11.006.
- Tao J, Liang J, Zhang H, Pei L, Qian HZ, Chambers MC, *et al*. The molecular epidemiological study of HCV subtypes among intravenous drug users and non-injection drug users in China. *PLoS One* 2015;10(10):e0140263. doi: 10.1371/journal.pone.0140263.
- Lu J, Zhang L, Xu X, Chen Y, Zhou Y, Zhang Z, *et al*. Hepatitis C virus genotype diversity and distribution among methadone maintenance treatment patients in Jiangsu, China. *Drug Alcohol Depend* 2019;194:101–106. doi: 10.1016/j.drugalcdep.2018.09.026.
- European Association for the Study of the Liver. Reply to: “Sofosbuvir/velpatasvir for patients with chronic genotype 3 HCV infection with compensated cirrhosis: Response to EASL recommendations on treatment of Hepatitis C 2018”: EASL Recommendations on Treatment of Hepatitis C 2018: Precision on the treatment of patients with genotype 3a infection and compensated cirrhosis. *J Hepatol* 2019;70(3):562–564. doi: 10.1016/j.jhep.2018.11.004.
- Wei L, Wang G, Alami NN, Xie W, Heo J, Xie Q, *et al*. Glecaprevir-pibrentasvir to treat chronic hepatitis C virus infection in Asia: two multicentre, phase 3 studies – a randomised, double-blind study (VOYAGE-1) and an open-label, single-arm study (VOYAGE-2). *Lancet Gastroenterol Hepatol* 2020;5(9):839–849. doi: 10.1016/S2468-1253(20)30086-8.
- U.S. Food & Drug Administration. FDA warns about rare occurrence of serious liver injury with use of hepatitis C medicines Mavyret, Zepatier, and Vosevi in some patients with advanced liver disease - FDA Drug Safety Communication. Available from: <https://www.fda.gov/drugs/drug-safety-and-availability/fda-warns-about-rare-occurrence-serious-liver-injury->



- use-hepatitis-c-medicines-mavyret-zepatier-and.
- [32] Hezode C, Reau N, Svarovskaia ES, Doehle BP, Shanmugam R, Dvory-Sobol H, *et al.* Resistance analysis in patients with genotype 1-6 HCV infection treated with sofosbuvir/velpatasvir in the phase III studies. *J Hepatol* 2018; 68(5):895–903. doi:10.1016/j.jhep.2017.11.032.
  - [33] Roberts SK, Buti M, Foster GR, Luis Calleja J, Sood A, Isakov VA, *et al.* Sofosbuvir/velpatasvir for patients with chronic genotype 3 HCV infection with compensated cirrhosis: An integrated analysis of phase 2 and phase 3 clinical trials. *The Liver Meeting®* 2018; 2018 Nov 9–13; San Francisco, USA.
  - [34] Flamm S, Mutimer D, Asatryan A, Wang S, Rockstroh J, Horsmans Y, *et al.* Glecaprevir/Pibrentasvir in patients with chronic HCV genotype 3 infection: An integrated phase 2/3 analysis. *J Viral Hepat* 2019; 26(3):337–349. doi:10.1111/jvh.13038.
  - [35] Singh AD, Maitra S, Singh N, Tyagi P, Ashraf A, Kumar R, *et al.* Systematic review with meta-analysis: Impact of baseline resistance-associated substitutions on the efficacy of glecaprevir/pibrentasvir among chronic hepatitis C patients. *Aliment Pharmacol Ther* 2020; 51(5):490–504. doi:10.1111/apt.15633.
  - [36] Curry M, Bacon B, Flamm S, Milligan S, Tsai N, Wick N, *et al.* THU-127-Clinical Practice experience with pan genotypic therapies glecaprevir-pibrentasvir and sofosbuvir-velpatasvir in the TRIO Network. *The International Liver Congress™* 2019; 2019 Apr 10–14; Vienna, Austria.
  - [37] Jacobson IM, Lawitz E, Gane EJ, Willems BE, Ruane PJ, Nahass RG, *et al.* Efficacy of 8 weeks of sofosbuvir, velpatasvir, and voxilaprevir in patients with chronic HCV infection: 2 phase 3 randomized trials. *Gastroenterology* 2017; 153(1):113–122. doi:10.1053/j.gastro.2017.03.047.
  - [38] Foster GR, Agarwal K, Cramp ME, Moree S, Barclay S, Collier J, *et al.* Elbasvir/grazoprevir and sofosbuvir for hepatitis C virus genotype 3 infection with compensated cirrhosis: A randomized trial. *Hepatology* 2018; 67(6):2113–2126. doi:10.1002/hep.29852.
  - [39] Zeuzem S, Dusheiko GM, Salupere R, Mangia A, Flisiak R, Hyland RH, *et al.* Sofosbuvir and ribavirin in HCV genotypes 2 and 3. *N Engl J Med* 2014; 370(21):1993–2001. doi:10.1056/NEJMoa1316145.
  - [40] Feld JJ, Ramji A, Shafraan SD, Willems B, Marotta P, Huchet E, *et al.* Ledipasvir-sofosbuvir plus ribavirin in treatment-naïve patients with hepatitis C virus genotype 3 infection: An open-label study. *Clin Infect Dis* 2017; 65(1):13–19. doi:10.1093/cid/cix289.
  - [41] Leroy V, Angus P, Bronowicki JP, Dore GJ, Hezode C, Pianko S, *et al.* Dacatasvir, sofosbuvir, and ribavirin for hepatitis C virus genotype 3 and advanced liver disease: A randomized phase III study (ALLY-3+). *Hepatology* 2016; 63(5):1430–1441. doi:10.1002/hep.28473.
  - [42] Wei L, Xie Q, Hou JL, Jia J, Li W, Xu M, *et al.* Sofosbuvir plus ribavirin with or without peginterferon for the treatment of hepatitis C virus: Results from a phase 3b study in China. *J Gastroenterol Hepatol* 2018; 33(6):1168–1176. doi:10.1111/jgh.14102.
  - [43] Wei L, Lim SG, Xie Q, Văn KN, Piratvisuth T, Huang Y, *et al.* Sofosbuvir-velpatasvir for treatment of chronic hepatitis C virus infection in Asia: a single-arm, open-label, phase 3 trial. *Lancet Gastroenterol Hepatol* 2019; 4(2):127–134. doi:10.1016/S2468-1253(18)30343-1.
  - [44] Gao Y, Kong F, Li G, Li C, Zheng S, Lin J, *et al.* Cobloprevir and sofosbuvir for treatment of chronic hepatitis C virus infection in China: A single-arm, open-label, phase 3 trial. *Liver Int* 2020; 40(11):2685–2693. doi:10.1111/liv.14633.
  - [45] Huang R, Rao H, Xie Q, Gao Z, Li W, Jiang D, *et al.* Comparison of the efficacy of sofosbuvir plus ribavirin in Chinese patients with genotype 3a or 3b HCV infection. *J Med Virol* 2019; 91(7):1313–1318. doi:10.1002/jmv.25454.
  - [46] Wei L, Xie Q, Huang Y, Wu S, Xu M, Tang H, *et al.* Safety and efficacy of sofosbuvir/velpatasvir in genotype 1-6 HCV-infected patients in China: Results from a phase 3 clinical trial. *The Liver Meeting®* 2018; 2018 Nov 9–13; San Francisco, USA.
  - [47] Al Marzooqi SH, Feld JJ. Sorting out cirrhosis: mechanisms of non-response to hepatitis C therapy. *Liver Int* 2015; 35(8):1923–1933. doi:10.1111/liv.12861.
  - [48] Berden FA, Aaldering BR, Groenewoud H, Int'Hout J, Kievit W, Drenth JP. Identification of the best direct-acting antiviral regimen for patients with hepatitis C Virus genotype 3 infection: A systematic review and network meta-analysis. *Clin Gastroenterol Hepatol* 2017; 15(3):349–359. doi:10.1016/j.cgh.2016.10.034.
  - [49] Esteban R, Pineda JA, Calleja JL, Casado M, Rodríguez M, Turnes J, *et al.* Efficacy of sofosbuvir and velpatasvir, with and without ribavirin, in patients with hepatitis C virus genotype 3 infection and cirrhosis. *Gastroenterology* 2018; 155(4):1120–1127.e4. doi:10.1053/j.gastro.2018.06.042.
  - [50] European Medicines Agency. Maviret : EPAR - Product Information. Available from: [https://www.ema.europa.eu/en/documents/product-information/maviret-epar-product-information\\_en.pdf](https://www.ema.europa.eu/en/documents/product-information/maviret-epar-product-information_en.pdf).
  - [51] Hu C, Yuan G, Liu J, Huang H, Ren Y, Li Y, *et al.* Sofosbuvir-based therapies for patients with hepatitis C virus infection: Real-world experience in China. *Can J Gastroenterol Hepatol* 2018; 2018:3908767. doi:10.1155/2018/3908767.
  - [52] Tao YC, Deng R, Wang ML, Lv DD, Yuan M, Wang YH, *et al.* Satisfactory virological response and fibrosis improvement of sofosbuvir-based regimens for Chinese patients with hepatitis C virus genotype 3 infection: results of a real-world cohort study. *Viral J* 2018; 15(1):150. doi:10.1186/s12985-018-1066-8.
  - [53] Chen ZW, Li Z, Wang QH, Wu XL, Li H, Ren H, *et al.* Large disparity between prevalence and treatment rates for hepatitis C in western China. *J Clin Transl Hepatol* 2018; 6(4):385–390. doi:10.14218/JCTH.2018.00027.
  - [54] Turner KM, Hutchinson S, Vickerman P, Hope V, Craine N, Palmateer N, *et al.* The impact of needle and syringe provision and opiate substitution therapy on the incidence of hepatitis C virus in injecting drug users: pooling of UK evidence. *Addiction* 2011; 106(11):1978–1988. doi:10.1111/j.1360-0443.2011.03515.x.
  - [55] Sun J, Yu R, Zhu B, Wu J, Larsen S, Zhao W. Hepatitis C infection and related factors in hemodialysis patients in China: systematic review and meta-analysis. *Ren Fail* 2009; 31(7):610–620. doi:10.1080/08860220903003446.
  - [56] Su Y, Yan R, Duan Z, Norris JL, Wang L, Jiang Y, *et al.* Prevalence and risk factors of hepatitis C and B virus infections in hemodialysis patients and their spouses: a multicenter study in Beijing, China. *J Med Virol* 2013; 85(3):425–432. doi:10.1002/jmv.23486.
  - [57] Ding GW, Ye SD, Hei FX, Lian QL, Pei XD, Bai JY, *et al.* Sentinel surveillance for viral hepatitis C in China, 2016–2017. *Zhonghua Liu Xing Bing Xue Za Zhi* 2019; 40(1):41–45. doi:10.3760/cma.j.issn.0254-6450.2019.01.009.
  - [58] National Health and Family Planning Commission. Notice of the National Health and Family Planning Commission on the issuance of Basic Standards and Management Practices for Hemodialysis Centers (for Trial Implementation). 2016. Available from: <http://www.nhc.gov.cn/yzygj/s3594q/201612/69a95ec0335c4a45883713094c8ef10d.shtml>.



## Review Article

# Nonalcoholic Fatty Liver Disease after Liver Transplant

Akshay Shetty<sup>1</sup> , Fanny Giron<sup>2</sup>, Mukul K. Divatia<sup>3</sup> , Muhammad I. Ahmad<sup>1</sup>, Sudha Kodali<sup>1</sup> and David Victor<sup>1\*</sup>

<sup>1</sup>Department of Medicine, Sherrie and Alan Conover Center for Liver Disease and Transplantation, Houston Methodist Hospital, Houston, TX, USA; <sup>2</sup>Department of Medicine, Houston Methodist Hospital, Houston, TX, USA; <sup>3</sup>Department of Pathology and Genomic Medicine, Weill Cornell Medical College, Houston Methodist Hospital, Houston, TX, USA

Received: 26 July 2020 | Revised: 24 February 2021 | Accepted: 28 March 2021 | Published: 17 May 2021

## Abstract

Nonalcoholic fatty liver disease (NAFLD) is one of the most common causes of chronic liver disease in the world. The rising prevalence of nonalcoholic steatohepatitis (NASH) has led to a 170% increase in NASH cirrhosis as the listing indication for liver transplantation from 2004 to 2013. As of 2018, NASH has overtaken hepatitis C as an indication for liver transplantation in the USA. After liver transplantation, the allograft often develops recurrent NAFLD among patients with known NASH cirrhosis. In addition to recurrent disease, de novo NAFLD has been reported in patients with other indications for liver transplantation. In this review, we will discuss the risk factors associated with recurrent and de novo NAFLD, natural course of the disease, and management strategies after liver transplantation.

**Citation of this article:** Shetty A, Giron F, Divatia MK, Ahmad MI, Kodali S, Victor D. Nonalcoholic fatty liver disease after liver transplant. *J Clin Transl Hepatol* 2021;9(3):428–435. doi: 10.14218/JCTH.2020.00072.

## Introduction

Nonalcoholic fatty liver disease (NAFLD) is the leading cause of chronic liver disease in the western world, and is strongly associated with metabolic syndrome, often referred to as the liver manifestation of metabolic syndrome.<sup>1</sup> NAFLD is also among the most common indications for orthotopic liver transplantation (OLT) in the USA.<sup>2</sup> The metabolic syndrome persists after liver transplant and is often further exacerbated among NAFLD patients, thereby leading to recurrence of NAFLD in the allograft.<sup>3,4</sup> Aside from recurrent NAFLD, patients transplanted for other etiologies of liver disease are also at risk of new onset metabolic syndrome

and de novo NAFLD in the allograft due to post-OLT weight gain and immunosuppression side effects.<sup>5</sup> Differentiating between recurrent versus de novo NAFLD is challenging and is currently limited to pre-OLT identification of NAFLD. In this review, we will discuss recurrent and de novo NAFLD, their associated risk factors, natural course of the disease, diagnosis, and management strategies.

## Epidemiology

NAFLD is the most common etiology of chronic liver disease, with a global prevalence of 25%. Regions with higher prevalence include the Middle East (31.8%) and South America (30.4%), while in North America, the estimated prevalence is 24.1%.<sup>6</sup> The rise in the prevalence of NAFLD over the last three decades has mirrored the global epidemic of obesity, type 2 diabetes mellitus (T2DM), and metabolic syndrome. A recent study estimated a 63% increase in the prevalence of nonalcoholic steatohepatitis (NASH) in the USA by 2030, accompanied by a 168% rise in decompensated NASH cirrhosis patients.<sup>7</sup> With such a steep increase in the incidence and prevalence of NASH and metabolic syndrome, there has been a parallel rise in NASH-related decompensated cirrhosis, recently surpassing hepatitis C (commonly referred to as HCV) as an indication for OLT in the USA.<sup>2,8</sup>

The initial studies reviewing recurrence of NAFLD post-OLT based on protocol liver biopsies demonstrated universal 100% recurrence within 5-years compared to 25% of de novo NAFLD post-OLT.<sup>3</sup> Follow up studies have shown variable results, with recurrence rates for steatosis ranging from 8% to 100% in known NASH patients, with follow-up ranging from 1 year to >5 years post-OLT; recurrent NASH rates over a similar follow up period ranged between 38–57%. In comparison, incidence of de novo NAFLD varied from 18% to up to 78% for steatosis over a similar range of follow-up, while de novo NASH ranged from 13% to 17%.<sup>3–5,9–15</sup> Recurrent NAFLD after transplant is more common compared to de novo NAFLD. It is important to note that all the above studies utilized histology to arrive at the diagnosis, with biopsies being pursued based on institutional protocols or due to abnormal liver labs. Recurrent NAFLD was reported at lower rates when imaging, specifically computed tomography (CT), was utilized, with 1-year recurrence of 12% and 5-year recurrence of 33%.<sup>16</sup>

## Histology and diagnosis

NAFLD encompasses a wide spectrum of histopathological

**Keywords:** Nonalcoholic fatty liver disease; Nonalcoholic steatohepatitis; Post-transplant; Recurrent NAFLD; De novo NAFLD; Recurrent NASH; De novo NASH.

**Abbreviations:** ALD, alcohol-related liver disease; BMI, body mass index; CNI, calcineurin inhibitor; CT, computed tomography; HCV, hepatitis C virus; MRE, magnetic resonance elastography; MRI, magnetic resonance imaging; NAFL, non-alcoholic fatty liver; NAFLD, nonalcoholic fatty liver disease; NASH, nonalcoholic steatohepatitis; OLT, orthotopic liver transplant; T2DM, type 2 diabetes mellitus.

\*Correspondence to: David Victor, Department of Medicine, Sherrie and Alan Conover Center for Liver Disease and Transplantation, Houston Methodist Hospital, Outpatient Center 22<sup>nd</sup> Floor, Houston, TX 77030, USA. ORCID: <https://orcid.org/0000-0003-1414-3128>. Tel: +1-713-790-3089, E-mail: [dwvictor@houstonmethodist.org](mailto:dwvictor@houstonmethodist.org)

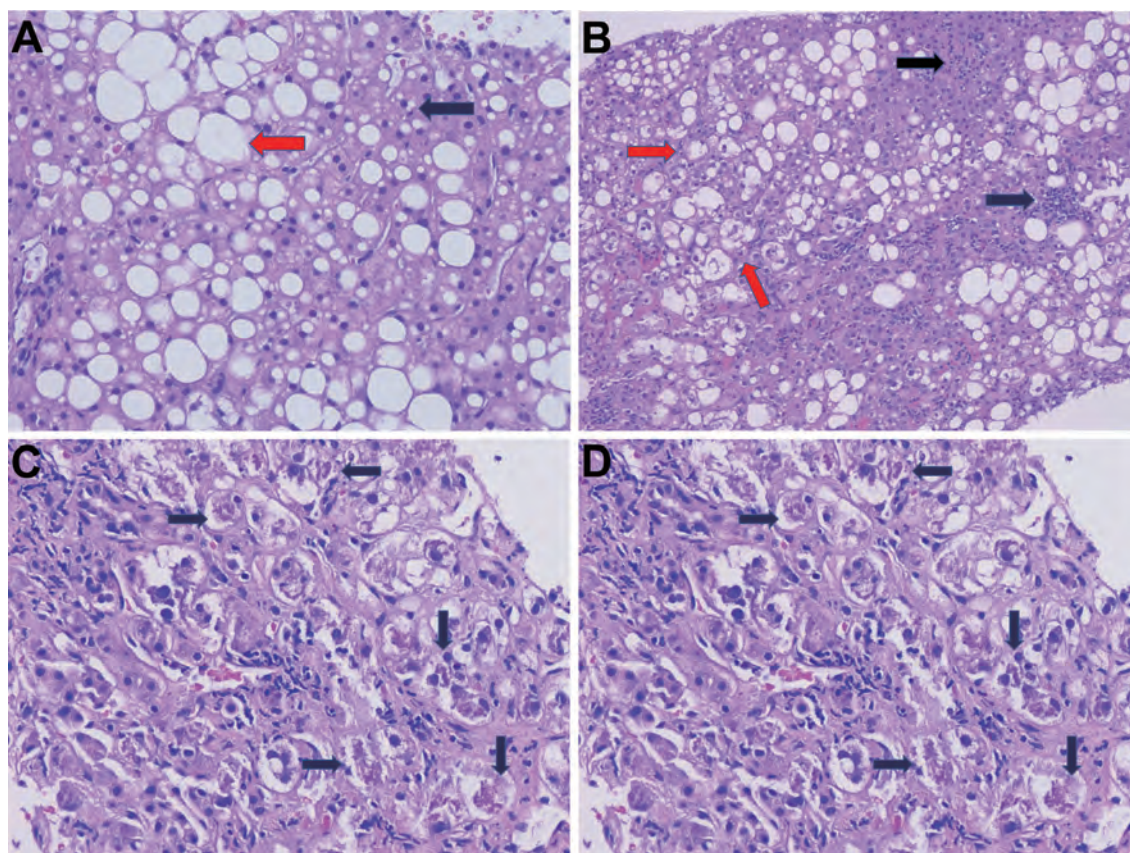


**Fig. 1. Post-liver transplant NAFLD histology findings.** (A) Macrovesicular steatosis with presence of both small droplet (black arrow) and large droplet (H&E, 200 $\times$ ). (B) Steatohepatitis with several hepatocytes exhibiting ballooning degeneration (red arrow) and chronic lobular inflammation (black arrows) (H&E, 100 $\times$ ). (C) Mallory-Denk bodies (black arrows) in ballooned hepatocytes (H&E, 200 $\times$ ). (D) Characteristic centrilobular pericellular fibrosis in steatohepatitis radiating around a terminal branch of the central vein. Note the ballooned hepatocytes (black arrows) (Masson-Trichrome stain, 100 $\times$ ). H&E, hematoxylin-eosin.

states, which includes simple hepatic steatosis or nonalcoholic fatty liver (NAFL) to NASH highlighted by hepatocyte injury and inflammation which may or may not be accompanied by fibrosis.<sup>1</sup> Quantitative histological scoring systems, like the NAFLD activity score and the Steatosis, Activity, Fibrosis assessment, have been identified and widely used to diagnose NAFLD.<sup>17,18</sup> In contrast, no histological scoring systems currently exist to assess NAFLD in the post-transplant allograft. As such, differentiating between recurrent NAFLD and de novo NAFLD is limited to its clinical diagnosis based on pre-existing disease prior to OLT.<sup>19</sup>

Liver biopsy remains the gold standard for diagnosis of post-OLT NAFLD/NASH (Fig. 1). There are multiple possible causes for elevated liver enzymes post-OLT that are not easily differentiated without a biopsy. The indications for biopsy in a post-OLT patient include confirmation of NAFLD (recurrent or de novo), fibrosis, or elevated liver enzymes that require further evaluation.<sup>20</sup> While liver biopsy is safe in the post-OLT patient with low risk of complications, it remains an invasive test.<sup>21</sup> Currently available noninvasive tests can help to direct clinic care but often lack the granularity offered by histology from a liver biopsy.

Steatosis is commonly encountered after liver transplantation. Steatosis is often noted incidentally on imaging for protocol testing or on imaging done for abnormal liver enzymes.<sup>19</sup> To identify steatosis, ultrasound requires the presence of moderate or greater degree of steatosis, defined as >30% involvement of hepatic parenchyma. Ultrasound carries a sensitivity of 65% and specificity of 75% to identify

hepatic steatosis. CT scan's ability to identify steatosis is similar to that of ultrasound. In comparison, magnetic resonance imaging (MRI) is vastly superior at identifying steatosis, with 90% sensitivity and 91% specificity.<sup>22</sup> However, imaging modalities are unable to differentiate between NAFL and NASH, as their strengths lie in identifying patients who may need more specific testing or monitoring of steatosis.

The use of noninvasive testing for fibrosis assessment in patients with chronic liver disease is increasingly common. There is a growing body of literature in post-OLT patients; however, they carry a few limitations. The allograft itself may have post-surgical preservation injury or presurgical changes of fibrosis that increase graft stiffness. Acute cellular rejection or presence of inflammation can influence liver stiffness measurements.<sup>23</sup> A meta-analysis evaluating noninvasive methods to identify fibrosis after transplant revealed that transient elastography performed better than serum biomarkers, such as the aspartate aminotransferase to platelet ratio index and FIB-4. However, most of the studies included in this analysis had evaluated recurrent HCV and none looked specifically into NAFLD recurrence, so more data is required in this population.<sup>24</sup> Magnetic resonance elastography (commonly known as MRE) has been studied in small cohorts to identify fibrosis in post-OLT patients.<sup>25</sup> However, there is a relative lack of evidence regarding MRE in NAFLD patients post-OLT. Fibrosis assessment remains helpful to the clinician in identifying patients with advanced fibrosis. Noninvasive testing has some potential advantages in post-OLT monitoring of NAFLD given



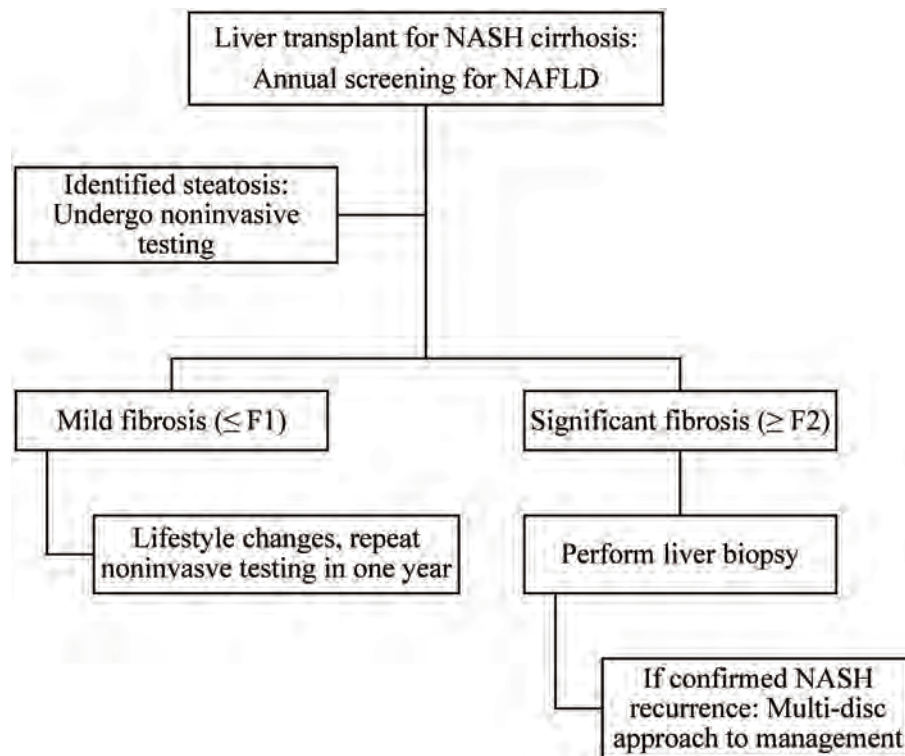


**Fig. 2. Screening algorithm for post-liver transplant patients.** Annual screening for NAFLD is recommended, with an ultrasound. If NAFLD is identified or suspected by ultrasound or elevated liver enzymes, noninvasive testing can be performed by a combination of transient elastography with serum biomarkers, such as FIB-4. If mild fibrosis ( $\leq F1$ ) is present, lifestyle changes, including diet and weight loss, are recommended. If significant fibrosis ( $\geq F2$ ) is suspected, a liver biopsy is recommended. If findings are confirmed, a multidisciplinary approach should be adopted to assist with weight loss and management of metabolic syndrome co-morbidities.

its limited side effects. Patients who have an established diagnosis of recurrent or de novo NAFLD can likely be followed with serial noninvasive testing to determine if they have advancing fibrotic disease. These changes likely need confirmation with biopsy, however, given the current lack of data regarding fibrosis monitoring and the myriad of factors that can influence these markers in transplant patients. A proposed algorithm for screening and diagnostic evaluation is included in Figure 2.

### Risk factors for NAFLD in allograft

Historically, the pathogenesis of NAFLD was postulated to be a “tale of two hits”, beginning with fat deposition in the liver and followed by inflammation; however, our current understanding suggests that NAFLD is a complex disorder with multiple pathways, all contributing to steatosis, inflammation, and fibrosis.<sup>26,27</sup> A combination of environmental factors in genetically-predisposed individuals leads to insulin resistance, altered lipid homeostasis, dysbiosis of gut microbiome leading to hepatic steatosis, and initiation of the inflammatory cascade leading to steatohepatitis and fibrosis development by activation of stellate cells.<sup>28</sup> Significant investigative effort has been put forth to understand this process in the non-transplant setting. On the other hand, the pathogenesis of recurrent or de novo NAFLD post-OLT has not been well delineated but similar processes (Fig. 3) are suspected to play a role in post-OLT NAFLD.

Post-transplant patients carry multiple risk factors for developing NAFLD in the allograft, including pre-OLT body mass index (BMI), significant weight gain after OLT, pre-existing metabolic syndrome risk factors in patients with NASH cir-

rhosis pre-OLT, and high likelihood of developing metabolic syndrome post-OLT due to immunosuppressants and donor graft characteristics. These are summarized in Table 1.

### Obesity and sarcopenia

Obesity remains a well-known risk factor for NAFLD. Among studies reviewing pre-OLT BMI, two retrospective studies reported pre-OLT BMI as an associated risk factor for post-OLT NAFLD.<sup>4,29</sup> In comparison, post-OLT BMI, often calculated at time of the liver biopsy, was noted to carry a higher risk for post-OLT NAFLD.<sup>4,5,29–31</sup> Weight gain post-OLT carried the highest odds ratio (19.38 [95%CI: 3.5–107.4]) in a small retrospective study of 68 patients, with weight gain defined as an increase in BMI by greater than 10%.<sup>13</sup> This risk of post-OLT NAFLD needs to be balanced against the expected weight gain early after liver transplantation in the majority of patients who are sarcopenic and against studies supporting survival and graft benefit with post-OLT weight gain.<sup>32</sup> Worsening sarcopenia post-OLT was associated with increased risk of new onset diabetes mellitus in a single small study;<sup>33</sup> however, studies associating sarcopenia to post-OLT NAFLD are lacking. Future studies should consider focusing on assessing the ratio between gain in skeletal muscle mass versus overall weight gain in order to improve our understanding of obesity and post-OLT NAFLD.

### Insulin resistance and diabetes mellitus

Insulin resistance is often viewed as the defining feature of

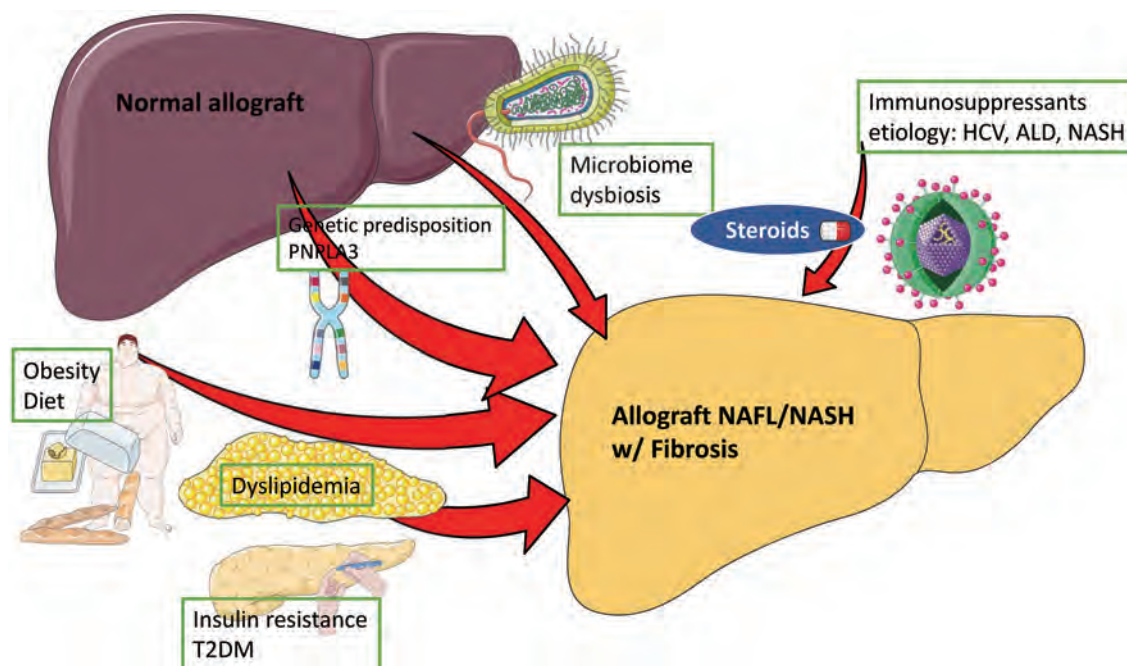


**Fig. 3. Factors involved in the pathogenesis of post-liver transplant NAFLD.** Factors similar to non-transplant NAFLD are suspected to play a role in post-liver transplant NAFLD. In addition, some post-transplant factors have also been shown to be associated with post-transplant NAFLD.

metabolic syndrome and is strongly associated with NAFLD.<sup>1</sup> While multiple studies looking at pre-existing T2DM and post-OLT NAFLD have failed to show a significant association,<sup>3,4,12,13,15,29,31</sup> some have shown an increased risk of post-OLT NAFLD among known diabetic patients.<sup>30,34,35</sup> New onset T2DM after liver transplantation, in particular poorly controlled T2DM, was associated with a higher risk of post-OLT NAFLD.<sup>5,29,30,36</sup> Tight glucose control, sparing using of corticosteroids, and early referrals to endocrinology should be considered to decrease the risk of NAFLD disease progression in this patient population.<sup>19,37</sup>

### Hypertension

While pre-OLT hypertension remains a key part of metabolic syndrome and strongly associated with NAFLD, it lacks any significant association to post-OLT NAFLD.<sup>4,9,12,13,15,29,31</sup> Onset of post-OLT hypertension is common, but has not shown any significant association on multivariate analysis across multiple studies to date,<sup>4,12,15,16,29,30,38</sup> except for a single study by Dumortier *et al.*<sup>5</sup> that showed a positive association. A potential reason for a surprising lack of association could be related to the duration of follow-up in the above studies.

### Hyperlipidemia

Pre-OLT hyperlipidemia was not associated with an increased risk of post-OLT NAFLD despite its known association to NAFLD.<sup>4,9,13,15,29,31</sup> In contrast, post-OLT hyperlipidemia had mixed results in multivariate analysis, with a few studies supporting a positive association to post-OLT NAFLD,<sup>4,5,29</sup> while others failed to show a significant association.<sup>15,16,30,31</sup>

### Immunosuppression

Immunosuppressants are linked to multiple aspects of metabolic syndrome, with post-OLT corticosteroid treatment known to increase risk of obesity, worsening existing T2DM, increasing the risk of new onset diabetes mellitus, hypertension, and hyperlipidemia.<sup>20</sup> Studies directly linking post-OLT NAFLD to corticosteroids use and duration are limited to two small retrospective studies.<sup>3,39</sup> Despite limited data, use of corticosteroids should be minimized with early tapers.

Insulin resistance, hypertension, and hyperlipidemia are well recognized side effects of calcineurin inhibitors (CNIs), with tacrolimus more strongly associated with insulin re-

**Table 1. Summary of factors associated with post-liver transplant NAFLD**

Increased risk	Possible risk	Possible protection
Obesity	Sarcopenia	Everolimus
T2DM	CNI therapy	
Hyperlipidemia	Donor graft steatosis	
PNPLA3 polymorphism		
Corticosteroid therapy		
Indications: NASH, ALD, HCV		

sistance, while cyclosporine is known to worsen hypertension.<sup>19,20</sup> Studies linking CNI therapy to NAFLD are few, with a single retrospective study associating tacrolimus use with increased risk of post-OLT NAFLD on multivariate analysis,<sup>5</sup> while other studies' findings have failed to support this association.<sup>4,15,29,30</sup>

Retrospective studies reviewing mammalian target of rapamycin (i.e. mTOR) inhibitors are limited in size and have not shown any significant association to post-OLT NAFLD.<sup>5,13,29,30</sup> In a randomized multicenter study, decreasing exposures to tacrolimus by adding everolimus was associated with less weight gain over 2-year follow up, suggesting potential protective effects against onset of metabolic syndrome and post-OLT NAFLD.<sup>40</sup>

### Other factors

NASH is a well-known, strong risk factor for recurrent NAFLD in the allograft. In addition to NASH, alcohol-related liver disease (ALD) cirrhosis and HCV cirrhosis (as primary etiologies of liver disease) were noted to carry a higher risk for de novo NASH in small retrospective studies, while auto-immune etiologies seemed to carry the lowest risk of de novo NAFLD.<sup>5,29,30</sup> Finkenstedt *et al.*<sup>16</sup> highlighted the role of recipient genetics, showing that the presence of G-allele in rs738409 of *PNPLA3*, a known risk factor for NASH, among OLT recipients increased their risk for graft steatosis based on CT imaging. Donor graft steatosis led to mixed results from small studies, with two studies<sup>5,31</sup> suggesting increased risk of post-OLT NAFLD, while multiple studies failed to show any significant association.<sup>11,12,29,30</sup> Factors associated with the liver transplantation, such as the model for end-stage liver disease score at transplant<sup>4,12,29,38</sup> and cold or warm ischemia time, did not carry any significant risk.<sup>10,12</sup>

### Natural history and outcomes

Long-term follow-up studies of NAFLD in the nontransplant setting have found a slowly progressive disease, with time to progression between stages of fibrosis approximated as ~7 years per stage for NASH patients.<sup>41</sup> As noted above, allograft NAFL and NASH was more common in the recurrent NAFLD group when compared to de novo NAFLD. Despite recurrent steatosis and inflammation in both groups, risk of progression to advanced fibrosis ( $\geq$ F3 stage) and cirrhosis was overall low in both groups, with a few exceptions; decompensated cirrhosis or graft loss due to post-OLT NAFLD was uncommon.

Studies reviewing patients transplanted for NASH or cryptogenic cirrhosis presumed to be NASH, demonstrated the prevalence of advanced fibrosis to be 2–5% at 5 years, 5–10% at 10 years, and up to 24% in one of the studies that followed patients up to 15 years.<sup>3,4,9,15</sup> The single exception to this was the French study by Vallin *et al.*,<sup>42</sup> which reported the prevalence of advanced fibrosis at 71.4% in its recurrent NAFLD group at 5 years. Progression to advanced fibrosis was mixed in the de novo group, with a 10-year prevalence rate of 2.3% for advanced fibrosis reported by Dumortier *et al.*<sup>5</sup> compared against the significantly higher prevalence of 20% for advanced fibrosis reported by Galvin *et al.*<sup>30</sup> A possible explanation for such discrepancy between the two studies could be due to a difference in patient characteristics, with the latter group having a higher BMI and higher prevalence of T2DM. In studies comparing progression of fibrosis between recurrent and de novo NAFLD groups, mixed results were noted with higher rates of advanced fibrosis at 5 years in the recurrent NAFLD group

compared to the de novo NAFLD group.<sup>42</sup> These findings were not supported by two larger studies, which showed no significant difference in fibrosis progression between recurrent and de novo NAFLD.<sup>29,38</sup> As such, we suspect that the risk of progressive fibrosis is not statistically different between recurrent and de novo NAFLD, but further studies with a closer assessment of individual risk factors to fibrosis accompanied with protocolized liver biopsies are needed.

Post-OLT NAFL or NASH, either recurrent or de novo, were not associated with decreased survival or graft loss across retrospective studies, with up to 15 years follow-up data.<sup>29,30,38</sup> Similarly, post-OLT NAFLD was not associated with a higher risk of cardiovascular events or cardiovascular mortality.<sup>29,38</sup> While these findings are re-assuring, further studies are needed to support these results. The reported 1-, 3-, and 5-year survival rates are similar in patients transplanted for NASH compared to ALD, viral hepatitis, or autoimmune diseases, with the exception of lower survival in patients with NASH and concomitant hepatocellular carcinoma compared to other indications.<sup>43,44</sup>

### Prevention and management

Currently, there are no Food and Drug Administration approved treatment options available for NAFLD in the pre-transplant setting, and no drugs have been studied or approved for post-transplant NAFLD. Management for post-OLT NAFLD is extrapolated from non-transplant NAFLD management and relies heavily on lifestyle modification and optimization of their metabolic and medical comorbidities, as summarized in Figure 4.

### Prevention

Pre-transplant identification of risk factors, such as obesity, sarcopenia, and uncontrolled T2DM, should be optimized aggressively prior to transplant. Bariatric surgery has been studied among NAFLD patients, with excellent improvement in steatosis, steatohepatitis, and fibrosis, while laparoscopic bariatric surgery approaches have been shown to be safe in compensated cirrhosis patients.<sup>45–47</sup> In the transplant setting, simultaneous sleeve gastrectomy during OLT has been compared to weight loss pre-OLT, with lower rates of graft loss and new onset T2DM reported in the sleeve gastrectomy group.<sup>48</sup> These approaches require a multidisciplinary effort at large volume transplant centers with clinical experience and expertise, and further studies are required to optimize patient selection and timing of bariatric surgery in the pre-transplant setting. Sarcopenia, while not directly associated with post-OLT NAFLD, is an important predictor of OLT outcomes and hence requires aggressive management with early intervention, optimization of nutrition in combination with muscle toning and strengthening exercise programs that would improve post-OLT outcomes.<sup>49</sup>

Aside from recipient optimization, donor graft allocation has been an area of contention among NASH recipients, as steatosis and *PNPLA3* polymorphism in donor graft may potentially add to the risk of post-OLT NAFLD. In the era of donor shortage accompanied by a surge in prevalence of NAFLD within the potential donor pool, optimization strategies and prospective studies are needed to decrease ischemia/reperfusion injury and to better understand the long-term effects of these on the natural course and risk of post-OLT NAFLD.<sup>50</sup>

Prevention of post-OLT NAFLD requires a multidisciplinary approach to avoid excess weight gain post-liver transplant, treatment of metabolic comorbidities as discussed below, and among patients without metabolic syndrome,



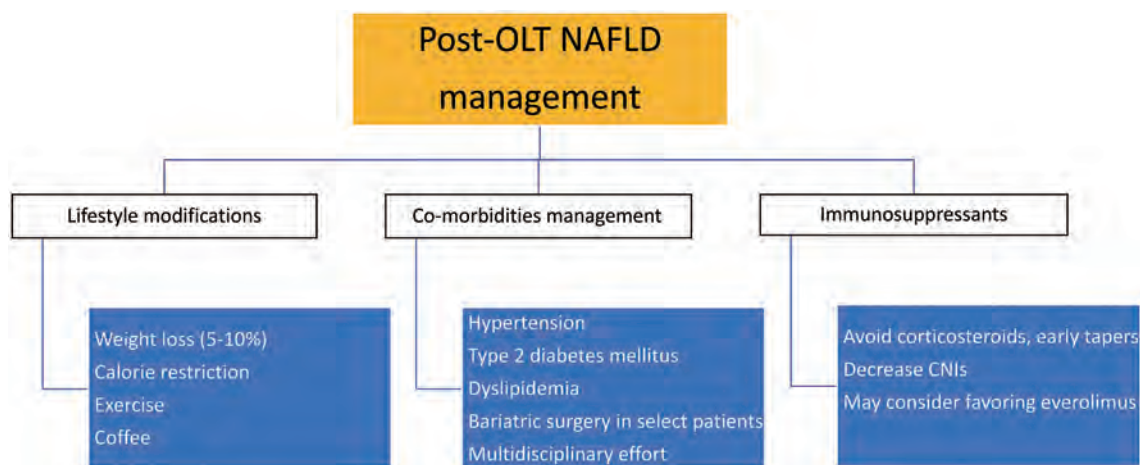


**Fig. 4. Management for post-liver transplant NAFLD.** The cornerstone for management of post-OLT NAFLD is weight loss by lifestyle modifications. When present, metabolic comorbidities should be tightly controlled, with early involvement of consultants for a multidisciplinary approach. Bariatric surgery may be an option for a select few patients. Immunosuppression optimization should focus on protecting the graft but, when feasible, these corrections should be pursued to decrease their side effects.

implementing routine screening for glucose intolerance, hypertension, and hyperlipidemia.<sup>19,20</sup>

### Lifestyle modification

The management for all NAFLD patients, whether pre- or post-OLT, should start with lifestyle modification, with the goal of gradual but sustained weight loss. However, in the initial few weeks to months after liver transplantation, patients are still recovering from their sarcopenic and debilitated state and often need to gain weight and muscle mass. The data discussed below are from studies in non-transplant NAFLD patients, and the optimal time of initiating these recommendations should be tailored to individual patients based on their recovery and risk factors.

Weight loss has been shown to improve all histological features of NAFLD, with 5% of weight loss required for improvement in steatosis, 7% required for steatohepatitis reduction, and 10% over 12 months for fibrosis regression.<sup>51</sup> While longitudinal studies to confirm similar changes in post-OLT NAFLD are lacking, we would suggest similar goals for these patients. Weight loss is best achieved through a calorie deficit, and the daily deficit goal should be adjusted based on the patient's basal metabolic rate. The Mediterranean diet, often higher in monounsaturated fatty acids, has been shown to reduce steatosis. In general, despite multiple options for macronutrient-specific diets studied, when choosing isocaloric diets, no significant difference in weight loss has been noted in patients choosing low-fat, low-carbohydrate, or high-protein diets; we would still recommend a diet low in carbohydrate for improving insulin resistance. Lastly, weight loss is challenging and diet modifications often require expert guidance; hence, choosing a multidisciplinary approach with the assistance of a nutritionist is recommended.<sup>52</sup>

Exercise offers a synergistic effect in hepatic fat mobilization when paired with calorie restriction, and either aerobic or resistance exercises, or both, may be pursued based on the patient's cardiopulmonary fitness, as both exercises lead to similar improvement in hepatic steatosis.<sup>53</sup> Drinking coffee confers a protective effect against multiple chronic liver diseases, including NAFLD, ALD, and viral hepatitis.<sup>54</sup> Patients should, therefore, be encouraged to drink 1–2 cups of unsweetened filtered coffee daily. The association

of prebiotics, probiotics, and the gut microbiome to metabolic syndrome and NAFLD are areas of great interest with emerging data, but their benefits in the post-OLT NAFLD population needs to be explored further. Similarly, circadian rhythm, the importance of good sleep hygiene, and optimal sleep duration of 7–8 h/night have been shown to be associated with NAFLD, but further studies are needed to study their association to post-OLT NAFLD patients.

### Management of comorbidities

Management of the majority of comorbidities among post-OLT patients is comparable to the general population, but the increased risk of renal insufficiency in post-OLT patients from their immunosuppressive therapy needs to be remembered. Drug-to-drug interactions with immunosuppressants should be evaluated when initiating newer therapies. Initial hypertension management should begin with sodium restriction, weight loss, and exercise, followed by first-line therapy with dihydropyridine calcium channel blockers, such as amlodipine or nifedipine, as they counteract the vasoconstrictive effect of CNIs.<sup>55</sup> Second-line therapy options include beta-blockers in patients without proteinuria, while an angiotensin converting enzyme inhibitor or angiotensin receptor blocker should be used in patients with T2DM and proteinuria.<sup>20</sup> Statin therapy should be initiated for dyslipidemia if lifestyle modification fails to correct elevated low-density lipoprotein cholesterol levels (>100 mg/dL when fasting), while closely monitoring for hepatotoxicity and drug-to-drug interaction with CNIs. Initial therapy for hypertriglyceridemia includes fish oil, up to 4 g per day, followed by fibrate therapy if persistently elevated.<sup>19,20</sup>

Diabetes management often requires endocrine consultation, as patients routinely need insulin therapy among both pre-existing T2DM and new onset diabetes patients, especially when corticosteroids are a part of their immunosuppression regimen. Oral hypoglycemic agents, thiazolidinediones, glucagon-like peptide-1 analogues, and dipeptidyl peptidase-4 inhibitors have been studied in non-transplant NAFLD patients, yielding promising results, and may be considered as the preferred therapeutic options post-OLT as well.<sup>19,52</sup> Bariatric surgery after liver transplant can lead to significant weight loss and decreased insulin requirement, as shown in a small study of select patients.<sup>56</sup>

## Immunosuppression

Immunosuppressant therapy is vital in improving allograft survival and outcomes but, unfortunately, they are accompanied by multiple side effects, including altered metabolic homeostasis. Among the immunosuppressants, corticosteroids carry the highest risk of diabetes, hypertension, obesity, and hyperlipidemia, and as such early tapering regimens are recommended.<sup>20</sup> CNIs are linked to hypertension, diabetes, and hyperlipidemia, as discussed previously and dose reduction should be considered in patients with these comorbidities, especially when they remain refractory to medical therapy.<sup>19,20</sup> The mTOR inhibitors are associated with significant hyperlipidemia, and an alternate immunosuppressant should be considered when hyperlipidemia remains uncontrolled.<sup>57</sup> Among the mTOR inhibitors, everolimus has been associated with decreased weight gain in a small study, but longitudinal studies are needed to extend this benefit to post-NAFLD population.<sup>40</sup>

## Conclusions

The epidemic of NAFLD, in parallel with obesity and metabolic syndrome, is expected to worsen and add to the growing burden of the post-liver transplant population. After liver transplantation, both recurrent and de novo NAFLD are common, and their prevalence will likely rise in the upcoming decades. Future basic science studies should help identify any differences between the pathogenesis of non-transplant versus post-OLT NAFLD. Clinically, longitudinal studies are needed to characterize the natural disease course of post-OLT NAFLD, using protocolized follow-up with noninvasive studies ideally paired with liver biopsies. Among the noninvasive tests, fibrosis assessment tools such as transient elastography and MRE, are of interest to assess disease progression. Additionally, management strategies and their effects on post-OLT NAFLD require long-term studies, with a focus on cardiovascular complications in addition to allograft and survival outcomes. As our post-liver transplant population continues to age, filling the aforementioned knowledge gaps will help to improve the transplant community's ability to better serve them.

## Acknowledgments

Some figures were created with "Biological illustration" (<http://smart.servier.com>) by Servier, used under the Creative Commons Attributions 3.0 Unported License, and modified by Akshay Shetty.

## Funding

None to declare.

## Conflict of interest

The authors have no conflict of interests related to this publication.

## Author contributions

Conception and design of the review (AS, FG, DV), drafting of the manuscript (AS, FG, MA, DV), critical revision of the

manuscript for important intellectual content (AS, SK, DV), administrative, technical, or material support (DK, DV), and study supervision (AS, DV).

## References

- [1] Chalasani N, Younossi Z, Lavine JE, Charlton M, Cusi K, Rinella M, *et al*. The diagnosis and management of nonalcoholic fatty liver disease: Practice guidance from the American Association for the Study of Liver Diseases. *Hepatology* 2018; 67(1): 328–357. doi:10.1002/hep.29367.
- [2] Kwong A, Kim WR, Lake JR, Smith JM, Schladt DP, Skeans MA, *et al*. OPTN/SRTR 2018 annual data report: Liver. *Am J Transplant* 2020; 20(Suppl s1): 193–299. doi:10.1111/ajt.15674.
- [3] Contos MJ, Cales W, Sterling RK, Luketic VA, Shiffman ML, Mills AS, *et al*. Development of nonalcoholic fatty liver disease after orthotopic liver transplantation for cryptogenic cirrhosis. *Liver Transpl* 2001; 7(4): 363–373. doi:10.1053/jlts.2001.23011.
- [4] Dureja P, Mellinger J, Agni R, Chang F, Avey G, Lucey M, *et al*. NAFLD recurrence in liver transplant recipients. *Transplantation* 2011; 91(6): 684–689. doi:10.1097/TP.0b013e31820b6b84.
- [5] Dumortier J, Giotra E, Belbouab S, Morard I, Guillaud O, Spahr L, *et al*. Non-alcoholic fatty liver disease in liver transplant recipients: another story of "seed and soil". *Am J Gastroenterol* 2010; 105(3): 613–620. doi:10.1038/ajg.2009.717.
- [6] Younossi ZM, Koenig AB, Abdelatif D, Fazel Y, Henry L, Wymer M. Global epidemiology of nonalcoholic fatty liver disease-Meta-analytic assessment of prevalence, incidence, and outcomes. *Hepatology* 2016; 64(1): 73–84. doi:10.1002/hep.28431.
- [7] Estes C, Razavi H, Loomba R, Younossi Z, Sanyal AJ. Modeling the epidemic of nonalcoholic fatty liver disease demonstrates an exponential increase in burden of disease. *Hepatology* 2018; 67(1): 123–133. doi:10.1002/hep.29466.
- [8] Goldberg D, Ditah IC, Saelan K, Lalehzari M, Aronsohn A, Gorospe EC, *et al*. Changes in the prevalence of hepatitis C virus infection, nonalcoholic steatohepatitis, and alcoholic liver disease among patients with cirrhosis or liver failure on the waitlist for liver transplantation. *Gastroenterology* 2017; 152(5): 1090–1099.e1. doi:10.1053/j.gastro.2017.01.003.
- [9] Bhati C, Idowu MO, Sanyal AJ, Rivera M, Driscoll C, Stravitz RT, *et al*. Long-term outcomes in patients undergoing liver transplantation for nonalcoholic steatohepatitis-related cirrhosis. *Transplantation* 2017; 101(8): 1867–1874. doi:10.1097/TP.0000000000001709.
- [10] El Atrache MM, Abouljoud MS, Divine G, Yoshida A, Kim DY, Kazimi MM, *et al*. Recurrence of non-alcoholic steatohepatitis and cryptogenic cirrhosis following orthotopic liver transplantation in the context of the metabolic syndrome. *Clin Transplant* 2012; 26(5): E505–E512. doi:10.1111/ctr.12014.
- [11] Lim LG, Cheng CL, Wee A, Lim SG, Lee YM, Sutedja DS, *et al*. Prevalence and clinical associations of posttransplant fatty liver disease. *Liver Int* 2007; 27(1): 76–80. doi:10.1111/j.1478-3231.2006.01396.x.
- [12] Malik SM, Devera ME, Fontes P, Shaikh O, Sasatomi E, Ahmad J. Recurrent disease following liver transplantation for nonalcoholic steatohepatitis cirrhosis. *Liver Transpl* 2009; 15(12): 1843–1851. doi:10.1002/lt.21943.
- [13] Seo S, Maganti K, Khehra M, Ramsamooj R, Tsodikov A, Bowlus C, *et al*. De novo nonalcoholic fatty liver disease after liver transplantation. *Liver Transpl* 2007; 13(6): 844–847. doi:10.1002/lt.20932.
- [14] Sourianarayanan A, Arikapudi S, McCullough AJ, Humar A. Nonalcoholic steatohepatitis recurrence and rate of fibrosis progression following liver transplantation. *Eur J Gastroenterol Hepatol* 2017; 29(4): 481–487. doi:10.1097/MEG.0000000000000820.
- [15] Yalamanchili K, Saadeh S, Klintmalm GB, Jennings LW, Davis GL. Nonalcoholic fatty liver disease after liver transplantation for cryptogenic cirrhosis or nonalcoholic fatty liver disease. *Liver Transpl* 2010; 16(4): 431–439. doi:10.1002/lt.22004.
- [16] Finkenstedt A, Auer C, Glodny B, Posch U, Steitzer H, Lanzer G, *et al*. Patain-like phospholipase domain-containing protein 3 rs738409-G in recipients of liver transplants is a risk factor for graft steatosis. *Clin Gastroenterol Hepatol* 2013; 11(12): 1667–1672. doi:10.1016/j.cgh.2013.06.025.
- [17] Bedossa P, Poltoui C, Veyrie N, Bouillot JL, Basdevant A, Paradis V, *et al*. Histopathological algorithm and scoring system for evaluation of liver lesions in morbidly obese patients. *Hepatology* 2012; 56(5): 1751–1759. doi:10.1002/hep.25889.
- [18] Kleiner DE, Brunt EM, Van Natta M, Behling C, Contos MJ, Cummings OW, *et al*. Design and validation of a histological scoring system for nonalcoholic fatty liver disease. *Hepatology* 2005; 41(6): 1313–1321. doi:10.1002/hep.20701.
- [19] Germani G, Laryea M, Rubbia-Brandt L, Egawa H, Burra P, O'Grady J, *et al*. Management of recurrent and de novo NAFLD/NASH after liver transplantation. *Transplantation* 2019; 103(1): 57–67. doi:10.1097/TP.0000000000002485.
- [20] Lucey MR, Terrault N, Ojo L, Hay JE, Neuberger J, Blumberg E, *et al*. Long-term management of the successful adult liver transplant: 2012 practice guideline by the American Association for the Study of Liver Diseases and the American Society of Transplantation. *Liver Transpl* 2013; 19(1): 3–26. doi:10.1002/lt.23566.
- [21] Alten TA, Negm AA, Voigtlander T, Jaeckel E, Lehner F, Brauner C, *et al*. Safety and performance of liver biopsies in liver transplant recipients. *Clin Transplant* 2014; 28(5): 585–589. doi:10.1111/ctr.12352.
- [22] van Werven Jr, Marsman HA, Nederveen AJ, Smits NJ, ten Kate FJ, van

- Gulik TM, *et al*. Assessment of hepatic steatosis in patients undergoing liver resection: comparison of US, CT, T1-weighted dual-echo MR imaging, and point-resolved 1H MR spectroscopy. *Radiology* 2010;256(1):159–168. doi: 10.1148/radiol.10091790.
- [23] Crespo G, Castro-Narro G, García-Juárez I, Benítez C, Ruiz P, Sastre L, *et al*. Usefulness of liver stiffness measurement during acute cellular rejection in liver transplantation. *Liver Transpl* 2016;22(3):298–304. doi: 10.1002/lt.24376.
- [24] Bhat M, Tazari M, Sebastiani G. Performance of transient elastography and serum fibrosis biomarkers for non-invasive evaluation of recurrent fibrosis after liver transplantation: A meta-analysis. *PLoS One* 2017;12(9):e0185192. doi: 10.1371/journal.pone.0185192.
- [25] Singh S, Venkatesh SK, Keaveny A, Adam S, Miller FH, Asbach P, *et al*. Diagnostic accuracy of magnetic resonance elastography in liver transplant recipients: A pooled analysis. *Ann Hepatol* 2016;15(3):363–376. doi: 10.5604/16652681.1198808.
- [26] Buzzetti E, Pinzani M, Tsochatzis EA. The multiple-hit pathogenesis of non-alcoholic fatty liver disease (NAFLD). *Metabolism* 2016;65(8):1038–1048. doi: 10.1016/j.metabol.2015.12.012.
- [27] Day CP, James OF. Steatohepatitis: a tale of two “hits”? *Gastroenterology* 1998;114(4):842–845. doi: 10.1016/s0016-5085(98)70599-2.
- [28] Manne V, Handa P, Kowdley KV. Pathophysiology of nonalcoholic fatty liver disease/nonalcoholic steatohepatitis. *Clin Liver Dis* 2018;22(1):23–37. doi: 10.1016/j.cld.2017.08.007.
- [29] Hejlova I, Honsova E, Sticova E, Lanska V, Hucl T, Spicak J, *et al*. Prevalence and risk factors of steatosis after liver transplantation and patient outcomes. *Liver Transpl* 2016;22(5):644–655. doi: 10.1002/lt.24393.
- [30] Galvin Z, Rajakumar R, Chen E, Adeyi O, Selzner M, Grant D, *et al*. Predictors of de novo nonalcoholic fatty liver disease after liver transplantation and associated fibrosis. *Liver Transpl* 2019;25(1):56–67. doi: 10.1002/lt.25338.
- [31] Kim H, Lee K, Lee KW, Yi NJ, Lee HW, Hong G, *et al*. Histologically proven non-alcoholic fatty liver disease and clinically related factors in recipients after liver transplantation. *Clin Transplant* 2014;28(5):521–529. doi: 10.1111/ctr.12343.
- [32] Martínez-Camacho A, Fortune BE, Gralla J, Bambha K. Early weight changes after liver transplantation significantly impact patient and graft survival. *Eur J Gastroenterol Hepatol* 2016;28(1):107–115. doi: 10.1097/MEG.0000000000000490.
- [33] Tsen C, Garber A, Narayanan A, Shah SN, Barnes D, Eghtesad B, *et al*. Post-liver transplantation sarcopenia in cirrhosis: a prospective evaluation. *J Gastroenterol Hepatol* 2014;29(6):1250–1257. doi: 10.1111/jgh.12524.
- [34] Noureddin M, Sanyal AJ. Pathogenesis of NASH: The impact of multiple pathways. *Curr Hepatol Rep* 2018;17(4):350–360. doi: 10.1007/s11901-018-0425-7.
- [35] Saeed N, Glass L, Sharma P, Shannon C, Sonnenday CJ, Tincopa MA. Incidence and risks for nonalcoholic fatty liver disease and steatohepatitis post-liver transplant: systematic review and meta-analysis. *Transplantation* 2019;103(11):e345–e354. doi: 10.1097/TP.00000000000002916.
- [36] Sprinzl MF, Weinmann A, Lohse N, Tönissen H, Koch S, Schattenberg J, *et al*. Metabolic syndrome and its association with fatty liver disease after orthotopic liver transplantation. *Transpl Int* 2013;26(1):67–74. doi: 10.1111/j.1432-2277.2012.01576.x.
- [37] Alvarez-Sotomayor D, Satorres C, Rodríguez-Medina B, Herrero I, de la Mata M, Serrano T, *et al*. Controlling diabetes after liver transplantation: Room for improvement. *Transplantation* 2016;100(10):e66–e73. doi: 10.1097/TP.0000000000001399.
- [38] Narayanan P, Mara K, Izzy M, Dierkhising R, Heimbach J, Allen AM, *et al*. Recurrent or de novo allograft steatosis and long-term outcomes after liver transplantation. *Transplantation* 2019;103(1):e14–e21. doi: 10.1097/TP.0000000000002317.
- [39] Hanouneh IA, Macaron C, Lopez R, Feldstein AE, Yerian L, Eghtesad B, *et al*. Recurrence of disease following liver transplantation: Nonalcoholic steatohepatitis vs hepatitis C virus infection. *Int J Organ Transplant Med* 2011;2(2):57–65.
- [40] Charlton M, Rinella M, Patel D, McCague K, Heimbach J, Watt K. Everolimus is associated with less weight gain than tacrolimus 2 years after liver transplantation: Results of a randomized multicenter study. *Transplantation* 2017;101(12):2873–2882. doi: 10.1097/TP.0000000000001913.
- [41] Satapathy SK, Sanyal AJ. Epidemiology and natural history of nonalcoholic fatty liver disease. *Semin Liver Dis* 2015;35(3):221–235. doi: 10.1055/s-0035-1562943.
- [42] Vallin M, Guillaud O, Boillot O, Hervieu V, Scoazec JY, Dumortier J. Recurrent or de novo nonalcoholic fatty liver disease after liver transplantation: natural history based on liver biopsy analysis. *Liver Transpl* 2014;20(9):1064–1071. doi: 10.1002/lt.23936.
- [43] Pais R, Barritt AS, Calmus Y, Scatton O, Runge T, Lebray P, *et al*. NAFLD and liver transplantation: Current burden and expected challenges. *J Hepatol* 2016;65(6):1245–1257. doi: 10.1016/j.jhep.2016.07.033.
- [44] Wang X, Li J, Riaz DR, Shi G, Liu C, Dai Y. Outcomes of liver transplantation for nonalcoholic steatohepatitis: a systematic review and meta-analysis. *Clin Gastroenterol Hepatol* 2014;12(3):394–402.e1. doi: 10.1016/j.cgh.2013.09.023.
- [45] Mummadi RR, Kasturi KS, Chennareddygar S, Sood GK. Effect of bariatric surgery on nonalcoholic fatty liver disease: systematic review and meta-analysis. *Clin Gastroenterol Hepatol* 2008;6(12):1396–1402. doi: 10.1016/j.cgh.2008.08.012.
- [46] Nickel F, Tapking C, Benner L, Sollors J, Billeter AT, Kenngott HG, *et al*. Bariatric surgery as an efficient treatment for non-alcoholic fatty liver disease in a prospective study with 1-year follow-up: BariScan study. *Obes Surg* 2018;28(5):1342–1350. doi: 10.1007/s11695-017-3012-z.
- [47] Cobb WS, Heniford BT, Burns JM, Carbonell AM, Matthews BD, Kercher KW. Cirrhosis is not a contraindication to laparoscopic surgery. *Surg Endosc* 2005;19(3):418–423. doi: 10.1007/s00464-004-8722-3.
- [48] Zamora-Valdes D, Watt KD, Kellogg TA, Poterucha JJ, Di Cecco SR, Francisco-Ziller NM, *et al*. Long-term outcomes of patients undergoing simultaneous liver transplantation and sleeve gastrectomy. *Hepatology* 2018;68(2):485–495. doi: 10.1002/hep.29848.
- [49] Carey EJ, Lai JC, Sonnenday C, Tapper EB, Tandon P, Duarte-Rojo A, *et al*. A North American expert opinion statement on sarcopenia in liver transplantation. *Hepatology* 2019;70(5):1816–1829. doi: 10.1002/hep.30828.
- [50] Pezzati D, Ghinolfi D, De Simone P, Balzano E, Filippini F. Strategies to optimize the use of marginal donors in liver transplantation. *World J Hepatol* 2015;7(26):2636–2647. doi: 10.4254/wjh.v7.i26.2636.
- [51] Vilar-Gomez E, Martinez-Perez Y, Calzadilla-Bertot L, Torres-Gonzalez A, Gra-Olamos B, Gonzalez-Fabian L, *et al*. Weight loss through lifestyle modification significantly reduces features of nonalcoholic steatohepatitis. *Gastroenterology* 2015;149(2):367–378.e5; quiz e14-5. doi: 10.1053/j.gastro.2015.04.005.
- [52] Shetty A, Syn WK. Current treatment options for nonalcoholic fatty liver disease. *Curr Opin Gastroenterol* 2019;35(3):168–176. doi: 10.1097/MOG.0000000000000528.
- [53] Golabi P, Locklear CT, Austin P, Afdhal S, Byrns M, Gerber L, *et al*. Effectiveness of exercise in hepatic fat mobilization in non-alcoholic fatty liver disease: Systematic review. *World J Gastroenterol* 2016;22(27):6318–6327. doi: 10.3748/wjg.v22.i27.6318.
- [54] Hodge A, Lim S, Goh E, Wong O, Marsh P, Knight V, *et al*. Coffee intake is associated with a lower liver stiffness in patients with non-alcoholic fatty liver disease, hepatitis C, and hepatitis B. *Nutrients* 2017;9(1):56. doi: 10.3390/nu9010056.
- [55] Textor SC, Taler SJ, Canzanella VJ, Schwartz L, Augustine JE. Posttransplantation hypertension related to calcineurin inhibitors. *Liver Transpl* 2000;6(5):521–530. doi: 10.1053/jlts.2000.9737.
- [56] Morris MC, Jung AD, Kim Y, Lee TC, Kaiser TE, Thompson JR, *et al*. Delayed sleeve gastrectomy following liver transplantation: A 5-year experience. *Liver Transpl* 2019;25(11):1673–1681. doi: 10.1002/lt.25637.
- [57] Neff GW, Montalbano M, Tzakis AG. Ten years of sirolimus therapy in orthotopic liver transplant recipients. *Transplant Proc* 2003;35(3 Suppl):209S–216S. doi: 10.1016/s0041-1345(03)00217-3.





## Review Article

# Current and New Drugs for COVID-19 Treatment and Its Effects on the Liver

Sandeep Satsangi<sup>1\*</sup>, Nitin Gupta<sup>2</sup> and Parul Kodan<sup>3</sup>

<sup>1</sup>Department of Apollo comprehensive Liver Care, Apollo Hospital, Bangalore, Karnataka, India; <sup>2</sup>Department of Infectious Diseases, Kasturba Medical College, Manipal Academy of Higher Education, Manipal, Karnataka, India; <sup>3</sup>Department of Medicine, All India Institute of Medical Sciences, New Delhi, India

Received: 21 December 2020 | Revised: 11 March 2021 | Accepted: 18 March 2021 | Published: 19 April 2021

## Abstract

Corona virus disease (COVID)-19 is caused by the novel severe acute respiratory syndrome coronavirus-2 (commonly referred to as SARS-CoV-2). In March 2020, the World Health Organization declared the COVID-19 outbreak a pandemic. Though the target organ for the virus is primarily the lungs, with the recent understanding of the pathobiology of this disease and the immune dysregulation associated with it, it is now clear that COVID-19 affects multiple organ systems. Several drugs and therapies have been tried or repurposed to combat the wrath posed by this disease. On October 22, 2020, the USA Food and Drug Administration approved remdesivir for use in adults and pediatric patients (12 years of age and older). Several of the drugs being tried against COVID-19 have hepatotoxicity as their potential side effect. This review aims to provide the latest insights on various drugs being used in the treatment of COVID-19 and their effects on the liver.

**Citation of this article:** Satsangi S, Gupta N, Kodan P. Current and new drugs for COVID-19 treatment and its effects on the liver. J Clin Transl Hepatol 2021;9(3):436–446. doi: 10.14218/JCTH.2020.00174.

## Introduction

Coronavirus disease (COVID)-19 caused by the novel severe

acute respiratory syndrome coronavirus-2 (SARS-CoV-2) has affected millions worldwide and the numbers of cases are consistently rising.<sup>1</sup> The ongoing COVID-19 caused by SARS-CoV-2 poses a serious threat to healthcare systems globally. As the virus continues to create havoc across the globe, it is eminent that the knowledge about the impact of this virus and its potential impact on different organs will evolve. Pulmonary and extra-pulmonary manifestations of COVID-19 are increasingly being recognized.<sup>2</sup>

Information on how COVID-19 affects the liver and how the drugs used for its treatment can affect the liver are slowly emerging. Although the real burden of this is currently unknown, as our understanding of the disease is constantly evolving, hepatic manifestations are being increasingly recognized. Various management strategies and research on drugs for COVID-19 are currently under study, many of which may have significant impact on liver.<sup>3</sup> In the present review we aim to provide updated information regarding interplay of liver and COVID-19 in the face of this pandemic and to promote understanding of the role of drugs used for COVID-19 treatment and their effects on the liver.

## Virology: key aspects

SARS-CoV-2 is an enveloped, positive-sense, single-stranded RNA virus classified as the newest member of the family of  $\beta$  coronaviruses.<sup>4</sup> The life cycle of this spiked virus typically involves attachment, penetration, biosynthesis, maturation, and release. Angiotensin converting enzyme 2 (ACE2) has been identified as an important functional receptor, to which the virus attaches and continues its lifecycle. The spike protein of the virus binds to the ACE2 receptors of the cell, which enables the virus to enter and subsequently replicate within the cells.<sup>5</sup> The receptor is not only present in the lungs but is also present in many extra-pulmonary sites like the kidney and gastrointestinal tract.<sup>6</sup> This may explain the extra-pulmonary symptoms associated with COVID-19. The virus, after its entry, induces an inflammatory response and virus-specific T cells are attracted to the site of infection.<sup>7</sup> The disease manifestations are primarily the result of direct viral-mediated damage and immune-mediated injury.<sup>8</sup>

## Clinical manifestations

The symptoms of patients infected with SARS-CoV-2 can range from none or minimal to severe respiratory failure

**Keywords:** COVID-19; Drugs; Liver; Drug-induced liver injury.

**Abbreviations:** AAK1, adaptor-associated protein kinase 1; ACE2, angiotensin converting enzyme 2; AKR, anakinra; ALI, acute liver injury; ALP, alkaline phosphatase; ALT, alanine aminotransferase; AST, aspartate aminotransferase; AZT, azithromycin; COVID, coronavirus disease; CP, convalescent plasma; CYP, cytochrome; DILI, drug-induced liver injury; DXA, dexamethasone; FDA, Food and Drug Administration; FPR, favipiravir; HBc, hepatitis B core; HBsAg, hepatitis B surface antigen; HBV, hepatitis B virus; HCQ, hydroxychloroquine; HCV, hepatitis C virus; HIV, human immunodeficiency virus; ICU, intensive care unit; IL, interleukin; IVN, ivermectin; JAK, Janus kinase; LPV/r, lopinavir/ritonavir; NAK, numb associated kinase; NIAID, National Institute of Allergy and Infectious Diseases; PCR, polymerase chain reaction; RdRp, RNA-dependent RNA polymerase inhibitor; RDV, remdesivir; REFHEPS, Réseau d'Étude Francophone de l'Hépatotoxicité des Produits de Santé; SARS-CoV-2, severe acute respiratory syndrome coronavirus-2; SOC, standard of care; SOFA, sequential organ failure assessment; TCZ, tocilizumab; ULN, upper limit of normal; VTE, venous thromboembolism.

\*Correspondence to: Sandeep Satsangi, Consultant Hepatologist & Liver Transplant Physician, Department of Apollo comprehensive Liver Care, Apollo Hospital, Bangalore, Karnataka 560076, India. Tel: +91-7899243962, E-mail: sandeephepatology@gmail.com

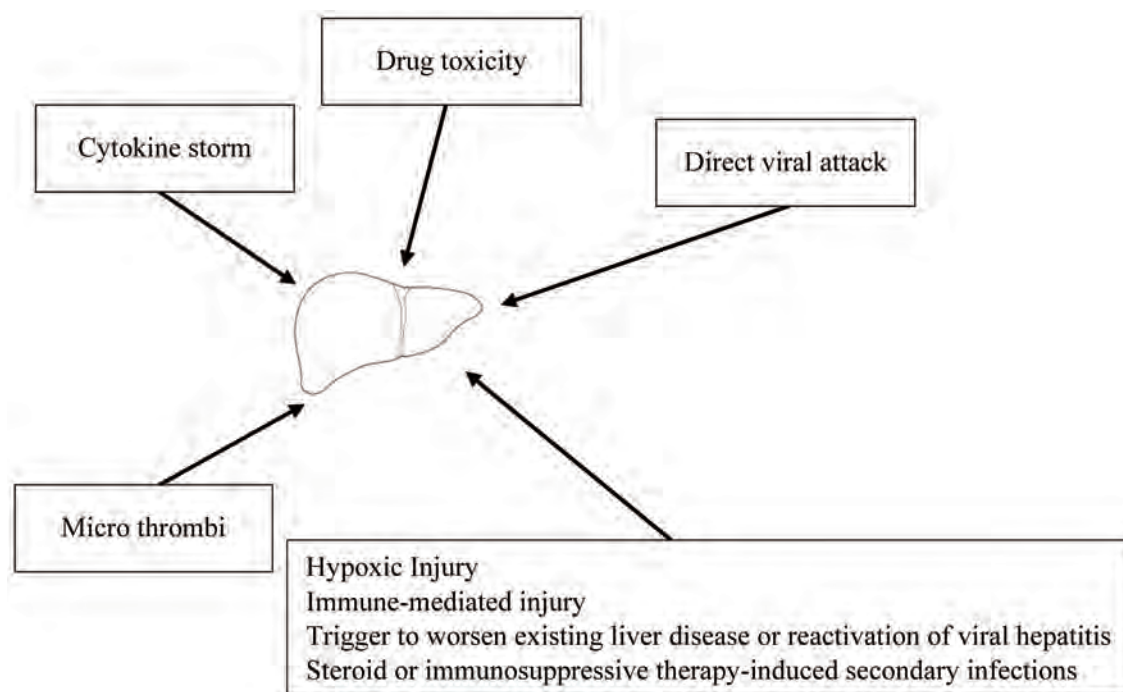


Fig. 1. Possible mechanisms of effects of SARS-CoV-2 on liver.

with multiple organ involvement.<sup>9</sup> The majority of patients experience mild symptoms, like fever, cough, myalgia, fatigue and less commonly headache, hemoptysis and diarrhea. The clinical severity in the largest published registry to date (i.e. Chinese Center for Disease Control and Prevention) reported disease being mild in 81.4%, severe in 13.9%, and critical in 4.7%.<sup>10</sup> The severe clinical manifestations have typically been described as severe pneumonia, acute respiratory distress syndrome and respiratory failure.<sup>11</sup> However, the recent literature has shed light on the extra-pulmonary manifestations of the virus. Although the major manifestations involve the respiratory system, owing to its attachment to the ACE2 receptors, the cardiac, vascular, neurological, renal, and hepatic manifestations have also been described.<sup>12</sup>

### Liver involvement in COVID-19

Liver injury in patients with COVID-19 might be due to a direct viral infection of the liver cells or due to multiple indirect pathways (Fig. 1). Given the higher expression of ACE2 receptors in cholangiocytes, the liver forms a potential target for SARS-CoV-2. Studies from biopsy of liver tissues of SARS-CoV-2-infected patients have shown liver cell apoptosis, which supports the direct hit hypothesis for this virus.<sup>13</sup> In an elegant study by Lagana SM *et al*,<sup>14</sup> histopathologic analysis of liver sections in a cohort of 40 COVID-19 autopsies was performed. Histologically, the most frequently encountered findings were macrovesicular steatosis, minimal-to-mild portal inflammation, and mild acute hepatitis. Thirty eight percent of cases had lobular cholestasis. Two cases had pale ovoid sinusoidal inclusions, which at low power resembled apoptotic hepatocytes. Vascular findings were focal in nature, with sinusoidal microthrombi being present in six cases. Polymerase chain reaction (commonly known as PCR) was performed on 20 autopsied livers and was positive in eleven (55%); however, there were no significant

correlations between PCR positivity and any histologic findings.<sup>14</sup> Other reports have described a significant cluster or scattered apoptotic hepatocytes, which are characterized by condensed nuclear or formed apoptotic bodies. There was no eosinophil infiltration, granuloma formation, centrilobular necrosis, or evidence of interface hepatitis.<sup>15</sup> The virus may bind to cholangiocytes and cause bile duct dysfunction, thereby impairing liver regeneration and immune responses.<sup>16</sup>

SARS-CoV-2 can affect the liver directly but also indirectly, via several mechanisms.<sup>17</sup> Indirect effects may be multifactorial, as depicted in Figure 1. Liver injury in patients with COVID-19 may be accounted for by a systemic inflammation induced by the cytokine storm or secondary to hypoxia or acute respiratory distress syndrome. The cytokine storm secondary to the virus infection can trigger extra-pulmonary systemic hyperinflammation syndrome. The cytokine surge (including interleukin (IL)-1, IL-6, and IL-10), inflammation and sepsis-related factors can damage the liver directly or indirectly.<sup>18</sup> The possibility of hypoxia-induced damage, microthrombi, immune dysfunction or drug toxicities are other important mechanisms which can impact the liver.<sup>19</sup>

To battle this new enigmatic virus, a plethora of drugs and therapies have been tried or repurposed. Newer drugs or drug combinations may have concerns of exacerbating liver diseases or causing drug-induced hepatotoxicity, or can interact with other drugs to exacerbate their hepatotoxic potential. Some drugs may also reactivate a latent virus, which might lead to liver damage. In patients with pre-existing liver disease, COVID-19 infection could trigger a potentially fatal acute-on chronic liver failure.<sup>20</sup>

Several case reports, series and studies have shed light on the hepatobiliary manifestations of the disease. Transaminitis has been found to be associated in up to 14% to 53% of COVID-19 cases.<sup>21,22</sup> Recent studies have reported abnormal liver function tests in as many as 76.3% of patients admitted with COVID-19. The authors also noted that liver test abnormalities became more pronounced during hospi-

talization. This can be explained in part by disease progression and super-added drug-induced liver injury (DILI). Hyperbilirubinemia has been documented in 11–18% of cases in some series.<sup>23</sup> One series from New York, USA showed 46.5% of the patients had aspartate aminotransferase (AST) >40 U/L, 32% had alanine aminotransferase (ALT) >40 U/L, and 9.1% had total bilirubin >17.1 µmol/L.<sup>24</sup> Cases of acute liver injury (ALI) have been reported and are associated with higher mortality.<sup>22</sup> Most of the transaminitis may be self-resolving; however, more studies are needed to determine the significance of mildly deranged liver enzymes with the outcome of the disease. An extensive meta-analysis including 21 studies concluded that altered liver and kidney function and increased coagulation parameters are seen in severe and fatal cases of COVID-19.<sup>25</sup>

Patients with chronic medical comorbidities have been clearly shown to have severe COVID-19 disease and worse outcomes. A systematic review including 1,527 patients reported the prevalence of hypertension, cardiac and cerebrovascular disease, and diabetes to be 17.1%, 16.4%, and 9.7%, respectively.<sup>26</sup> However, there is growing evidence to predict worse outcomes in patients with underlying liver disease.<sup>27</sup> Literature has suggested patients who have a second 'hit', that is liver injury on the background of underlying liver disease, have poor outcomes.<sup>27</sup> The first author of the manuscript has also noted a higher mortality in patients with acute-on chronic liver failure, in whom the acute precipitant was linked to COVID-19 infection.

## Drugs used in the management of COVID-19

Several drugs have been tried in the prophylaxis and treatment of COVID-19 (Fig. 2); however, only one drug (remdesivir, RDV) has recently been approved by the USA FDA. Supplementary Table 1 depicts the current treatment protocol for COVID-19. The following section describes the various drugs used for COVID-19 and their implications on liver.

## Antivirals

### Hydroxychloroquine (HCQ)

HCQ is an oral drug which has both antimalarial and anti-inflammatory properties. It is commonly used in the management of rheumatological diseases. It is increasingly being used for management of COVID-19 based on *in vitro* data and initial reports.<sup>28</sup> HCQ is supposed to act by preventing ACE2-mediated or endosomal-mediated viral entry (Fig. 2).<sup>29</sup> Although it is considered as a relatively safe drug, reports of adverse cardiac effects in patients with COVID-19 is concerning (Supplementary Table 1).<sup>30</sup> Despite retrospective observational studies showing mixed results, randomized controlled trials have not shown any benefit in COVID-19 patients irrespective of severity (Supplementary Table 2).<sup>31</sup> HCQ has also been tried for the prophylaxis to prevent COVID-19. In an elegant randomized, double-blind, placebo-controlled trial, HCQ was used in people within 4 days of exposure to someone with confirmed COVID-19. After a high-risk or moderate-risk exposure to COVID-19, HCQ was not found to be effective in preventing illness compatible with COVID-19 (Supplementary Table 2).<sup>32</sup> In a study by Cavalcanti *et al.*,<sup>33</sup> the use of HCQ with or without azithromycin (AZT) in patients with mild to moderate COVID-19 did not improve clinical status at 15 days, as compared with standard care. In another randomized, controlled, open-label platform trial, the investigators noted that among patients hospitalized with COVID-19, HCQ us-

age did not result in a lower incidence of death at 28 days than those who received the usual care.<sup>34</sup>

HCQ is metabolized in the liver and may alter the metabolism of other drugs. HCQ has not been associated with significant elevations of liver enzymes and is not usually incriminated as a cause of DILI. ALI with jaundice due to usage of HCQ is very rare, with only few reports in the literature.<sup>35</sup> An exception to this is when HCQ is used in patients with porphyria cutanea tarda. Its usage in high doses can trigger ALI, which is associated with sudden onset of fever and marked serum enzyme elevations. This reaction appears to be caused by the sudden mobilization of porphyrins and can be avoided when HCQ is started at lower doses.<sup>36</sup> There have been scattered case reports in literature regarding DILI with the usage of HCQ in patients with COVID-19; however, it is to be noted that this is extremely rare.<sup>37</sup>

With recent data pointing at ineffectiveness of HCQ in altering the course of COVID-19 infection, the authors of this manuscript are not in favor of its clinical usage in patients with COVID-19.

### Azithromycin (AZT)

AZT is commonly used in the treatment of bacterial infections and might also have antiviral activity against certain RNA viruses.<sup>38</sup> AZT has also been shown to be effective *in vitro* against viruses such as Zika and rhinovirus, in addition to SARS-CoV-2,<sup>39</sup> depicts immunomodulatory properties and can reduce exacerbations in chronic airway diseases.<sup>40</sup> The COALITION II is an open-label randomized trial evaluating AZT in addition to standard of care (SOC), which included HCQ, compared with SOC alone in patients admitted to hospital with severe COVID-19. The investigators however found no benefit of AZT on clinical outcomes, including clinical status or mortality when added to SOC (odds ratio 1.36 [95% confidence interval: 0.94–1.97]; *p*=0.11).<sup>41</sup>

AZT may lead to idiosyncratic ALI. The clinical presentation of AZT-related DILI is usually of a cholestatic hepatitis arising within 1–3 weeks after start of treatment. It occasionally arises after AZT is stopped, and can occur even after a short 2 to 3 day course. This form of DILI due to AZT usually follows a benign course, but in some instances is associated with a prolonged jaundice and persistence of liver test abnormalities for 6 months or more.<sup>42</sup> Case reports of vanishing bile duct syndrome with AZT usage have also been reported.<sup>43</sup> AZT can occasionally be associated with hepatocellular injury as well. In these instances, the period of latency is typically short. Serum aminotransferase levels are markedly elevated and alkaline phosphatase (ALP) and gamma glutamyl transpeptidase is usually less than twice the upper limit of normal (ULN). The hepatocellular forms of DILI can be severe and lead to acute liver failure, mandating the need for an urgent liver transplant (LT) in certain patients. AZT has also been linked to the development of cutaneous reactions, such as erythema multiforme, Stevens Johnson syndrome and toxic epidermal necrosis. These cutaneous reactions are often associated with a certain degree of liver injury.<sup>44</sup> HCQ and AZT are known to induce QT prolongation via a human Ether-à-go-go-related gene potassium channel blockade.<sup>45</sup> In certain instances, this can trigger ventricular arrhythmias.

### Lopinavir/ritonavir (LPV/r)

LPV/r is a protease inhibitor used in the treatment of human immunodeficiency virus (commonly known as HIV) infection. In the initial part of the COVID-19 pandemic, LPV/r was one of the first antivirals to be used in an attempt to



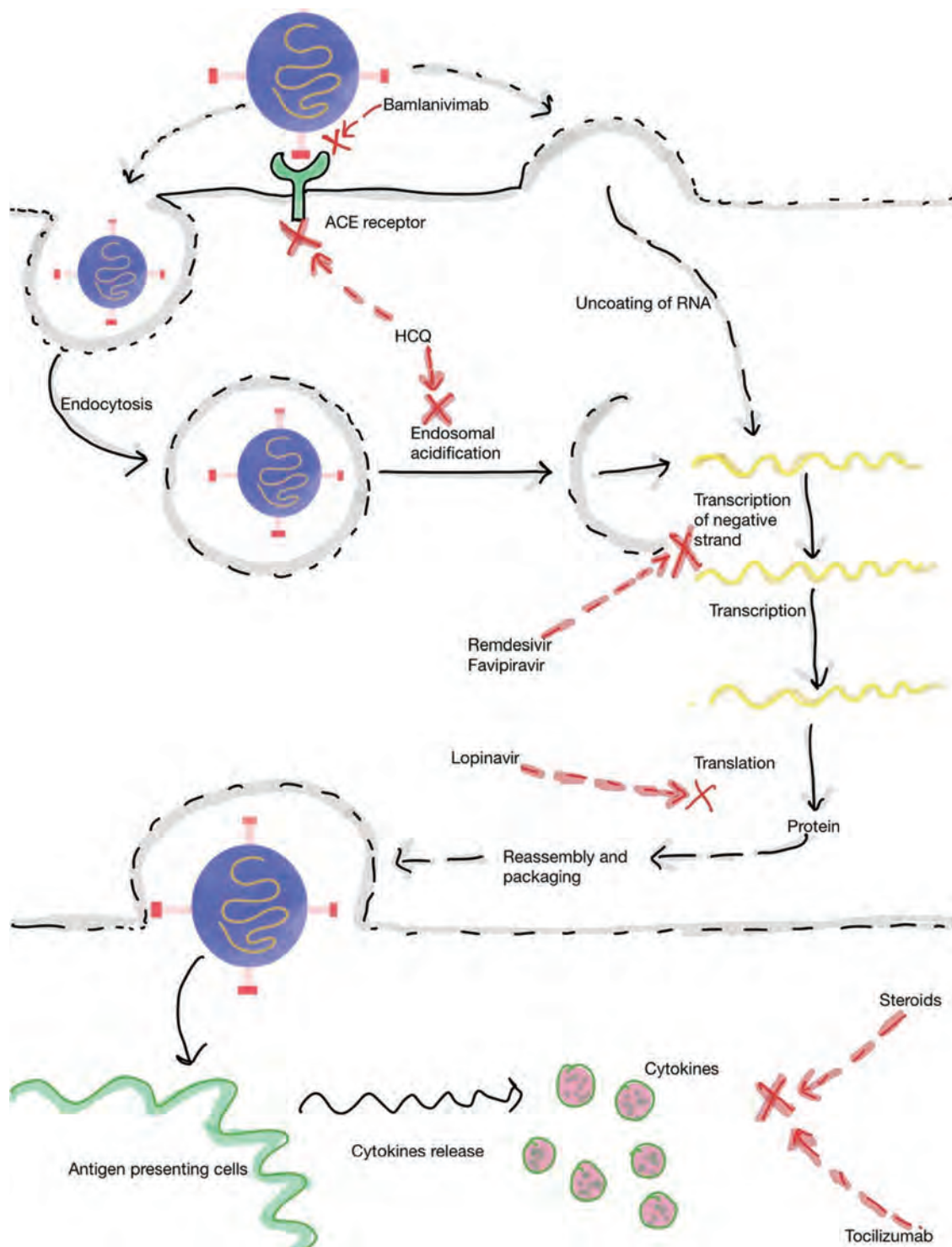


Fig. 2. Mechanism of action of drugs used in the treatment for COVID-19.

improve clinical outcomes. Except for minor gastrointestinal disturbances and potential for drug interactions, the short-term use of this drug is not associated with major side effects (Supplementary Table 1).<sup>46</sup> Although retrospective observational studies showed faster clearance with LPV/r, it was not associated with significantly better outcomes in

randomized trials. In one of the pivotal randomized, controlled, open-label, platform trials of LPV/r conducted in patients admitted to the hospital with COVID-19, the investigators noted LPV/r not to be associated with reductions in 28-day mortality, duration of hospital stay, or risk of progressing to invasive mechanical ventilation or death.<sup>47</sup> In

another key study in patients with severe COVID-19, no benefit was noted with LPV/r treatment beyond standard care.<sup>48</sup>

LPV/r is primarily metabolized in the liver, largely via the cytochrome (CYP) P450 pathway. This pathway can lead to the formation of a toxic intermediate, which can cause DILI.<sup>49</sup> Though mild elevation of liver enzymes can happen with LPV/r therapy, clinically apparent hepatotoxicities appear to be rare. The rate of DILI is higher in patients having underlying hepatitis B virus (HBV) and hepatitis C virus (HCV) infection.<sup>50</sup> The latency to the onset of symptoms is usually 1 to 8 weeks, and the pattern of serum enzyme elevations varies from cholestatic to hepatocellular or mixed.<sup>51</sup> The injury is usually self-limited; however, fatal cases have been reported. Using LPV/r in patients with underlying HBV and HCV infection can also lead to exacerbation of underlying chronic liver disease, with associated rise in HBV DNA or HCV RNA levels.<sup>52</sup> In the context of LPV/r, the Réseau d'Étude Francophone de l'Hépatotoxicité des Produits de Santé (also known as REFHEPS), which is a European French-speaking study network, reported that within 2 weeks, four cases of LPV/r combination discontinuation occurred in patients with COVID-19 who were being treated with this drug.<sup>53</sup> As the LPV/r combination is falling out of practice to treat COVID-19, its potential to cause DILI in patients with COVID remains more of a theoretical problem.

### Remdesivir (RDV)

RDV is an adenosine analogue that is an RNA-dependent RNA polymerase (RdRp) inhibitor. It was developed by Gilead Sciences and was initially used for the treatment of Ebola virus disease. It is a broad spectrum antiviral drug that has shown to inhibit SARS-CoV-2, *in vitro* and *in vivo*.<sup>54,55</sup> RDV has recently been approved by the USA FDA for use in patients who are older than 12 years of age and weighing at least 40 kg for the treatment of COVID-19 requiring hospitalization. In a recent double-blind, randomized, placebo-controlled trial of using intravenous RDV in patients who were hospitalized with COVID-19 and had evidence of lower respiratory tract infection; the investigators noted that RDV was superior to placebo in shortening the time to recovery in adults who were hospitalized with COVID-19 (Supplementary Table 2).<sup>56</sup> There have also been reports suggesting the use of RDV to not be associated with a difference in time to clinical improvement; however, it has been suggested that RDV is to be used early in the clinical course of COVID-19 infection, before the peak viral replication occurs.<sup>57,58</sup> The duration of therapy in most cases is 5 days.<sup>59</sup>

RDV is a prodrug and is metabolized in the cells into an alanine metabolite which is processed further into the monophosphate derivative and ultimately into the active nucleoside triphosphate.<sup>60</sup> Studies have shown RDV usage to be associated with elevations of AST and ALT.<sup>61</sup> In most instances, the enzyme elevations did not progress to severe liver damage, but cases of acute liver failure suspected as due to RDV usage have been reported.<sup>62</sup> In the report describing two patients with RDV-induced acute liver failure, significant increases in transaminases occurred between day 3 and day 10 of RDV usage. This was also associated with coagulopathy and hepatic encephalopathy. The authors utilized the Naranjo algorithm to determine the possibility of a drug-induced effect and both the cases scored as a 'probable' adverse drug reaction, with a score of 6 each. After discontinuing the drug and treatment with N-acetyl cysteine infusion, there was a marked improvement in transaminases and liver functions.<sup>62</sup> RDV is suggested to be stopped if the ALT >5-times ULN or ALP >2-times ULN, and

total bilirubin >2-times ULN or in the presence of coagulopathy or clinical decompensation.<sup>63</sup> In view of its potential for hepatotoxicity, the authors of this manuscript have not used RDV in patients with decompensated cirrhosis who have COVID-19 infection.

### Favipiravir (FPR)

FPR is a prodrug with excellent bioavailability and has been approved in Japan for the treatment of influenza. FPR undergoes phosphoribosylation to favipiravir-RTP, which is the active form of this drug. It acts via inhibition of RdRp and also gets incorporated into the viral RNA strand, preventing its further extension.<sup>64</sup> As the SARS-CoV-2-RdRp complex is at least 10-fold more active than any other viral RdRp known, the adequate dose of FPR for COVID-19 needs to be ascertained.<sup>65</sup> The dose usually used in clinical practice is 1,800 mg twice a day on day 1, followed by 800 mg twice a day on days 2–14. An open-label, nonrandomized study conducted in China compared the effect of FPR vs. LPV/r in the treatment of COVID-19. Both groups had also received interferon-alpha (5 million units twice daily) by nasal inhalation. Compared with the LPV/r arm, patients in the FPR arm showed a statistically significant shorter median length of time to viral clearance (4 days vs. 11 days,  $p < 0.001$ ), improvement in chest computed tomography findings at day 14 (91.4% vs. 62.2%,  $p = 0.004$ ) and lower incidence of adverse effects (11.43% vs. 55.56%  $p < 0.001$ ).<sup>66</sup> A phase 3 Russian trial (COVIDFPR 01) using FPR (ClinicalTrials.gov Identifier: NCT04434248) is currently ongoing and includes 330 patients from 30 medical centers across 9 Russian regions. A randomized, multicenter, open-labeled clinical trial in Indian patients has just been completed and the results are expected to be published soon.<sup>64</sup>

Though FPR usage can lead to increases in AST, ALP, ALT and total bilirubin, clinically apparent DILI seems rare. Less than 10% of patients with COVID-19 might experience ALT elevation with the use of FPR.<sup>63</sup> Patients with severe liver dysfunction (Child-Pugh C) showed an increase in area under curve (6.3-fold) and  $C_{max}$  (2.1-fold). It is thus suggested that FPR dosage should be reduced in patients with COVID-19 who have severe liver function impairment.<sup>67</sup>

### Ivermectin (IVN)

IVN is well known for its antiparasitic activity. This drug has shown an *in vitro* reduction of viral RNA in Vero-hSLAM cells at 2 h post-infection with the SARS-CoV-2 clinical isolate Australia/VIC01/2020.<sup>68</sup> IVN has demonstrated a broad spectrum of antiviral properties and acts as an inhibitor of the nuclear transport, which is mediated by the importin  $\alpha/\beta 1$  heterodimer, itself which is pivotal for the translocation of viral species proteins (i.e. HIV-1 and SV40).<sup>69</sup> The Ivermectin in COVID-19 trial is a retrospective cohort study ( $n = 280$ ) which enrolled patients with COVID-19 infection admitted at four Florida hospitals. This study documented a significantly lower mortality rate in the IVN ( $n = 173$ ) arm compared with the usual care ( $n = 107$ ) arm (15% vs. 25.2%;  $p = 0.03$ ).<sup>70</sup> More data are needed to assess pulmonary tissue levels in humans and to assess its efficacy in the prophylaxis and treatment of COVID-19.

IVN is usually considered a safe drug and reports of IVN-related DILI are rare. In a case report where IVN was used for the treatment of Loa loa, IVN resulted in DILI that manifested 1 month later with aminotransferase elevation, showing a hepatocellular type of DILI. Liver biopsy depicted acute hepatocellular necrosis, lymphocytic lobular infiltrates and no fibrosis. The patient improved clinically within days

and serum aminotransferase levels fell rapidly, becoming normal 3 months later.<sup>71</sup>

## Immunomodulators

### Steroids

In patients with severe COVID-19, the pathogenesis has been described in two phases, namely the viremic phase and the hyper-inflammatory phase. The use of steroids has been proposed in the hyper-inflammatory phase based on the observations of trials, including the RECOVERY trial (Supplementary Table 2). In the UK-based RECOVERY trial, 6,425 patients [2,104 randomized to receive dexamethasone (DXA) and 4,321 randomized to receive SOC], treatment with DXA lead to a reduction in mortality by one-third in patients receiving mechanical ventilation and by one-fifth in patients receiving supplemental oxygen compared to usual care alone.<sup>72</sup> The recommended dose of DXA was 6 mg for a duration of 10 days. The CoDEX multicenter, open-label trial enrolled 299 patients in Brazil with COVID-19 and moderate to severe acute respiratory distress syndrome to 20 mg DXA daily (intravenous) treatment for 5 days, then 10 mg daily for 5 days or until intensive care unit (ICU) discharge atop SOC, or to SOC alone. DXA increased days alive and days free from mechanical ventilation during the first 28 days to a mean of 6.6 vs. 4.0 among controls ( $p=0.04$ ) and also reduced the acute morbidity of the disease, with lower mean sequential organ failure assessment (commonly referred to as SOFA) scores at day 7 than with usual care (6.1 vs. 7.5,  $p=0.004$ ).<sup>73</sup> In a recent meta-analysis by the World Health Organization's Rapid Evidence Appraisal for COVID-19 Therapies (otherwise known as REACT) working group, a total of 1,703 critically ill patients with COVID-19 were analyzed. The studies analyzed in the meta-analysis enrolled patients who were randomized to receive systemic DXA, hydrocortisone, or methylprednisolone, or to receive usual care or placebo. The use of steroids reduced 28-day mortality by a relative 34% compared with controls and the mortality effect size appeared similar between drugs used.<sup>74</sup>

Studies have also evaluated pulse steroid therapy in the treatment of COVID-19. In a single-blind, randomized, controlled, clinical trial involving hospitalized patients with severe COVID-19 who were in the early pulmonary phase of the illness were enrolled. Patients were randomized to either the steroid arm or the SOC arm. Methylprednisolone pulse was given as an intravenous injection of 250 mg daily for 3 days in the steroid arm. Patients with clinical improvement were higher in the methylprednisolone group than in the SOC group (94.1% vs. 57.1%), and the mortality rate was numerically lower in the methylprednisolone group (5.9% vs. 42.9%;  $p<0.001$ ).<sup>75</sup>

Though steroids are generally considered safe, they can lead to worsening of liver functions in certain specific clinical conditions. Of special interest is HBV reactivation and consequent liver involvement. It is well known that steroid treatment can lead to viral flare and HBV reactivation, and there exist specific guidelines to address this issue.<sup>76</sup> In hepatitis B surface antigen (HBsAg)-positive patients, HBV reactivation is defined as a sudden and rapid increase in HBV DNA levels in patients with previously detectable DNA or reappearance of HBV DNA viremia in individuals who did not have viremia before the initiation of immunosuppressive therapy. In individuals who are initially negative for HBsAg and are hepatitis B core antibody (anti-HBc)-positive, HBV reactivation is defined by appearance of HBsAg and/or HBV DNA. In patients who are HBsAg-positive or patients who are HBsAg-negative but positive for anti-HBc, the doses of steroids which place the patient at risk of reactivation are

reported as follows below.<sup>76</sup>

**High risk (>10% risk):** Prednisone therapy at either medium dose (10–20 mg orally daily) or high dose (>20 mg orally daily) for more than 4-week duration increases the reactivation in patients who are HBsAg-positive.

**Moderate risk (1–10% risk):** Low-dose steroid therapy equivalent to prednisone 10 mg administered orally daily over 4 weeks may increase the risk of reactivation up to 10% in HBsAg-positive individuals, and medium-dose steroids such as prednisone 10–20 mg administered orally (or equivalent) daily may increase the risk of seroconversion in HBsAg-negative and anti-HBc-positive individuals.

**Low risk (<1% risk):** Patients are administered intra-articular steroid injections or a low dose of prednisone < 10 mg orally daily.

Recently, a pivotal study was published which analyzed the risk of HBsAg seroconversion in 12,997 patients exposed to at least one dose of systemic corticosteroids in the period between 2001 and 2010. Among the patients analyzed, 1,800 were positive for anti-HBc. Among those, 830 were positive for anti-HBs, which served as a protective factor. It was noted that in the remaining group of 970 anti-HBc-positive/anti-HBs-negative patients, the annual risk of presenting with a hepatitis flare was 16.2%, independent of the time of corticosteroid treatment. Patients who were anti-HBc-positive only had a higher risk of HBsAg Seroreversion (1-year incidence was 1.8%) as well.<sup>77</sup>

Drugs used to treat the disproportionate immune response after SARS-CoV-2 infection (mainly IL-6 receptor antagonists or high dose corticosteroids) were considered to be associated with moderate risk for HBV reactivation in HBsAg-negative/anti-HBc-positive individuals. However, a recent study enrolling 600 patients with severe COVID-19, who were treated with immune-modulator therapy, demonstrated that the risk of HBV reactivation while undergoing immunosuppressive treatment was low.<sup>78</sup> This study was not randomized and had a small sample size, which is why more data is needed in this area to make strong recommendations.

In patients who merit HBV prophylaxis (HBV is otherwise inactive, but antiviral therapy is started to prevent HBV reactivation), it should ideally be started 2–4 weeks before the initiation of immunosuppressive therapy and maintained for at least 6 months after the last dose of immunosuppressive therapy. In patients where a decision to monitor (antiviral therapy not being initiated) has been made, the strategy should be monitoring of viral reactivation with determination of aminotransferases and HBV DNA levels conducted every 3 months.<sup>76</sup>

Figure 3 describes an algorithm for COVID-19-positive patients who are candidates for treatment with steroid therapy according to serological findings of an HBV screening.<sup>76,79</sup>

### IL-6 receptor antagonists

**Tocilizumab (TCZ):** TCZ is a humanized IgG1 recombinant monoclonal antibody used for the treatment of cytokine release syndrome associated with rheumatological conditions. It inhibits the inflammatory action of IL-6 by inhibiting the IL-6 receptor (Fig. 2). Since IL-6 is one of the prominent cytokines responsible for the hyper-inflammatory phase of COVID-19, it was postulated to have some role in patients with a severe or life-threatening disease. In a recent randomized, double-blind, placebo-controlled trial involving patients with confirmed SARS-CoV-2 infection having features of hyperinflammation, patients were randomized to receive a single dose of either TCZ (8 mg/kg of body weight) or placebo. The hazard ratio for intubation or death in the TCZ



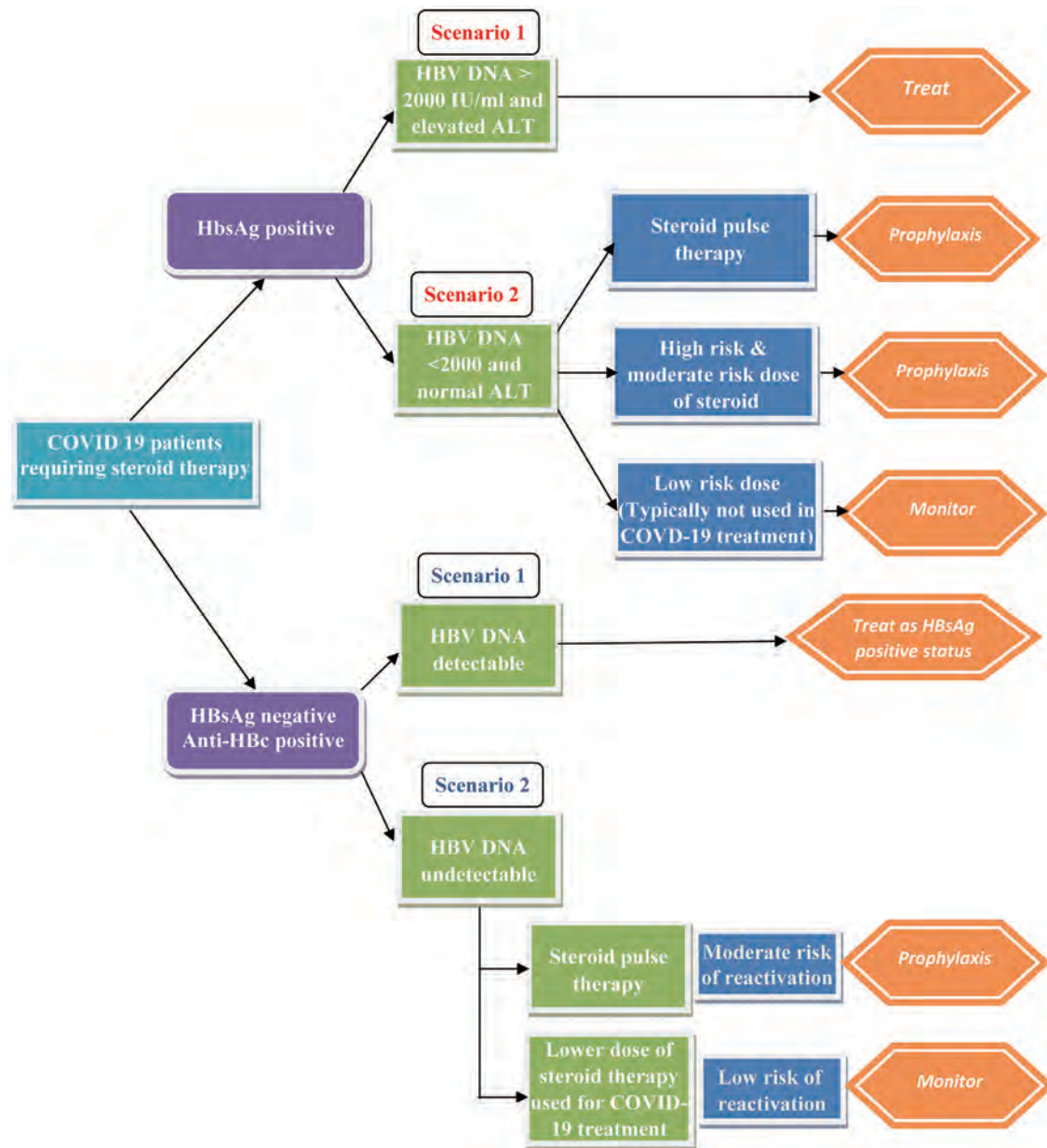


Fig. 3. Antiviral treatment strategy in patients with COVID-19 at risk for HBV reactivation receiving steroid therapy.

group, as compared with the placebo group, was 0.83 (95% confidence interval: 0.38–1.81;  $p=0.64$ ), and the hazard ratio for disease worsening was 1.11 (95% confidence interval: 0.59–2.10;  $p=0.73$ ). It was thus inferred that TCZ was not effective for preventing intubation or death in moderately ill hospitalized patients with COVID-19.<sup>80</sup> The EMPACTA trial is the first global phase III trial to demonstrate patients with COVID-19 pneumonia who received TCZ in the first 2 days of ICU admission to have a lower risk of in-hospital mortality compared with those not treated with TCZ. Patients randomized to the TCZ group were 44% less likely to progress to mechanical ventilation or death compared to patients who received placebo plus SOC.<sup>81</sup>

The most common side effects of TCZ are headache, upper respiratory symptoms and hypertension. TCZ has minimal hepatic metabolism, and early registration trials of the

usage of TCZ in rheumatologic conditions have shown mild serum aminotransferase elevations to occur in a high proportion (10% to 50%) of patients receiving TCZ. In a minority of patients (1–2%) levels rose above 5-times the ULN, which triggered discontinuation of treatment. The liver injury with TCZ is predominantly hepatocellular in nature, with no immunoallergic or autoimmune features. While the liver injury was severe, it was usually self-limited, with complete recovery occurring in 2 to 3 months. The mechanism by which it causes DILI is unknown, but may be the result of its effects on the immune system or on the IL-6 pathway, which is important in liver regeneration. TCZ being an immunosuppressive medication might also cause liver injury indirectly by reactivation of HBV.

Data of TCZ-related DILI when being used in the management of COVID-19 is scarce and limited to case reports.

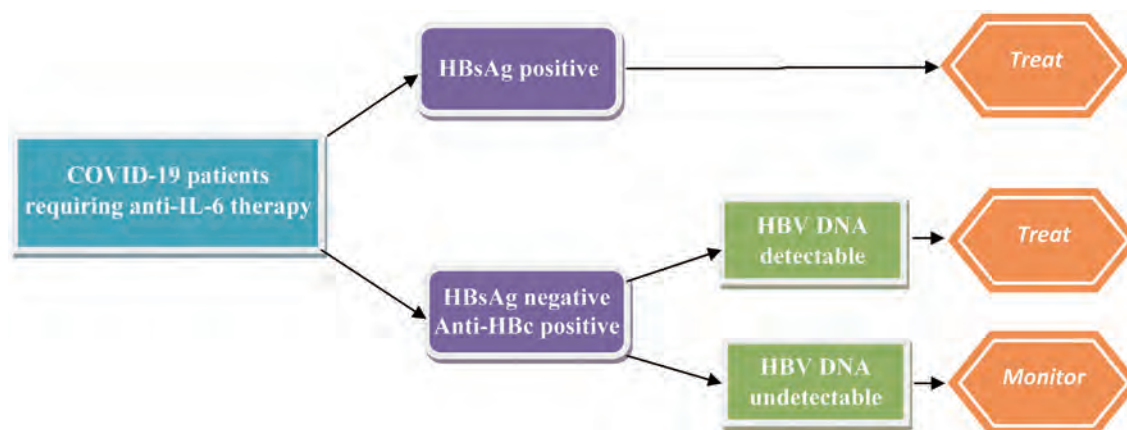


Fig. 4. Antiviral treatment strategy in patients with COVID-19 at risk for HBV reactivation receiving anti-IL-6 therapy.

Case reports also exist on the usage of TCZ in patients with elevated liver enzymes. In one of the case series using TCZ for patients with severe COVID-19 and having elevated liver enzymes (up to 5-times the ULN), it was noted that after TCZ administration, the clinical condition of patients rapidly improved and liver function test normalized within 3 weeks of treatment.<sup>82</sup>

TCZ, being an immunosuppressive agent, is associated with the risk of hepatitis B reactivation. There have been reports of HBV reactivation and flare in patients with rheumatoid arthritis who have chronic hepatitis B and receive a short course of TCZ therapy, which in severe cases has also led to liver failure.<sup>83</sup>

In patients with past resolved infection, the risk of HBV reactivation seems low with the use of TCZ therapy. In a key study, which enrolled 152 patients with resolved hepatitis B infection managed with disease-modifying anti-rheumatic drugs (including 25 patients with TCZ), the risk of HBV reactivation was very low (<5%).<sup>84</sup> In a study enrolling patients with COVID-19 who received TCZ, the risk of HBV reactivation was reported to be low in patients with markers of past HBV infection.<sup>78</sup> Though concrete guidelines on using antiviral prophylaxis to prevent HBV reactivation in patients with COVID-19 being treated with TCZ are lacking, we suggest using antiviral prophylaxis in patients with chronic hepatitis B infection and serial monitoring in patients with past HBV infection with undetectable HBV DNA levels (Fig. 4).

Other IL-6 receptor antagonists being tried for COVID-19-related cytokine release syndrome are siltuximab and sarilumab.

### IL-1 receptor antagonists

Endogenous IL-1 levels are elevated in patients with COVID-19 and high levels are associated with cytokine release syndrome.<sup>85</sup> Anakinra (AKR) is the prototype drug being studied for COVID-19. A study conducted in Paris, France compared the outcomes of 52 patients with COVID-19 who were given AKR with 44 historical cohort patients. Admission to the ICU for invasive mechanical ventilation or death occurred for 13 (25%) patients in the AKR group and 32 (73%) patients in the historical group [hazard ratio of 0.22 (95% confidence interval: 0.11–0.41;  $p < 0.0001$ ).<sup>86</sup> An increase in liver aminotransferases (>3-times the ULN) occurred in seven (13%) patients in the AKR group and four (9%) patients in the historical group.

In large registration trials enrolling patients with rheumatologic conditions, ALT elevations occurred in <1% of pa-

tients taking AKR, a rate not different from that in placebo recipients, and no cases of clinically apparent liver injury with jaundice were reported. AKR-related DILI usually follows a hepatocellular pattern. Liver biopsies have demonstrated an acute hepatocellular injury with prominence of eosinophils. Most patients with AKR-related DILI recovered within 2 to 8 weeks of stopping the drug, without evidence of residual injury. There have been cases reported where the DILI is severe, protracted and associated with transient features of hepatic failure.<sup>87</sup>

In patients with COVID-19 being treated with AKR, Cavalli *et al.*<sup>88</sup> discuss the observations of elevated liver aminotransferases in some patients receiving the drug. Three of the 29 patients with COVID-19 who received AKR had derangement of liver enzymes, while 5 of 16 similar patients who did not receive AKR also showed increased enzymes. The authors, however, chose to taper AKR in those with elevated liver enzymes and observed that the LFTs did respond to the reduction in the dose of AKR. AKR has not been linked to reactivation of hepatitis B or exacerbation of chronic hepatitis C.<sup>89</sup>

### Janus kinase (i.e. JAK) and numb associated kinase (i.e. NAK) inhibitors

ACE2 receptors are a point of cellular entry for the COVID-19 virus, which is expressed in lung alveolar epithelial type 2 cells. A known regulator of endocytosis is the adaptor-associated protein kinase 1 (i.e. AAK1). Disruption of AAK1 may interrupt intracellular entry of the virus. Baricitinib is a JAK inhibitor and has been identified as a NAK inhibitor, with a particularly high affinity for AAK1.<sup>90</sup> Drugs which target NAK are likely mitigate alveolar and systemic inflammation in patients with COVID-19 pneumonia by inhibiting cytokine signaling.<sup>91</sup> The National Institute of Allergy and Infectious Diseases (commonly referred to as the NIAID) Adaptive COVID-19 Treatment Trial evaluated the combination of RDV (100 mg administered intravenously daily, up to 10 days) along with baricitinib (4 mg per once daily, up to 14 days) compared with RDV alone. In September 2020, the investigators reported a 1-day reduction in the median time to recovery for the overall population treated with RDV plus baricitinib compared with RDV alone.<sup>92</sup>

In the large prelicensure clinical trials evaluating baricitinib in patients with rheumatoid arthritis, serum aminotransferase derangements occurred in up to 17% of subjects treated with baricitinib compared to 11% in placebo recipients. The aminotransferase elevations were typically

mild and only in <1% of patients, and the values rose above 5-times the ULN. Less than 10% of the drug undergoes hepatic metabolism, which is primarily via the CYP 3A4 pathway. Serum aminotransferase elevations above 5-times the ULN should lead to temporary cessation of the drug. If liver enzyme elevations do not completely normalize or improve within a few weeks of drug cessation, or if symptoms of DILI worsen, baricitinib should be permanently discontinued.<sup>93</sup>

### Convalescent plasma (CP)

Plasma from an individual who has recovered from COVID-19 with high titers of neutralizing antibodies has been proposed as a novel therapy for COVID-19. Although there is a theoretical risk of antibody enhancement and transfusion-related reactions, this therapy is otherwise considered safe. The FDA granted emergency use authorization on August 23, 2020 for use of CP in patients who are hospitalized with COVID-19. Early data indicated that the use of CP seemed to be effective for a better course of COVID-19 in critically ill patients.<sup>94</sup> However, the multicenter, randomized, controlled PLACID trial, published recently and which enrolled 464 adults (≥18 years) admitted to the hospital with confirmed moderate COVID-19, demonstrated that the use of CP was not associated with a reduction in progression to severe COVID-19 or all-cause mortality.<sup>95</sup> No serious adverse effects have been reported with use of CP; however, there exists a theoretical risk of transmission of infections like HBV and HCV.

Several other drugs being tried in the treatment of COVID-19 are mentioned in Supplementary Table 3.

### Anticoagulants

The risk of venous thromboembolism (VTE) is increased in critically ill patients with COVID-19. A recent meta-analysis which analyzed 86 studies (33,970 patients) reported that VTE occurs in 22.7% of patients with COVID-19 who are admitted to the ICU. VTE risk was reported to be higher in non-ICU hospitalized patients as well.<sup>96</sup> Reports have shown that there is a substantial microthrombosis, or immunothrombosis, related to hypoxemia, endothelial injury, and inflammation.<sup>97</sup> Data is emerging on the discrepancy between the rate of pulmonary embolism and deep-vein thrombosis in patients with COVID-19 infection, and several cases are being reported where pulmonary embolism is occurring in the absence of deep-vein thrombosis and are located in the more peripheral pulmonary arteries. This leads to the hypothesis that immunothrombosis is probably much more prominent in patients with COVID-19 than originally recognized.<sup>97,98</sup> Most current guidelines thus recommend that standard doses of anticoagulants be used for thromboprophylaxis in patients hospitalized with COVID-19. VTE prophylaxis is also to be administered post-discharge in patients with known additional risk factors for VTE, such as thrombophilia, obesity, advanced age, and a prior history of VTE.<sup>97</sup>

The potential effects of anticoagulants on liver are displayed in Supplementary Table 4.

### Conclusions

COVID-19 is a disease which causes multisystem involvement. The immune dysregulation and the cytokine release syndrome associated with the disease are primarily responsible for the worse outcomes in those affected with it. Several drugs have been tried and several others remain in the

pipeline to combat the deadly effects of this virus. Hepatotoxicity, reactivation of underlying viral hepatitis and potential to cause DILI remains with several of the drugs being used to treat COVID-19. However, as the involvement of liver can be the result of various pathobiologic pathways, in many instances it becomes difficult to discern the accurate etiology of the same.

### Funding

None to declare.

### Conflict of interest

The authors have no conflict of interests related to this publication.

### Author contributions

Manuscript writing and critical revision (SS, NG, PK), administration (SS).

### References

- [1] Ge H, Wang X, Yuan X, Xiao G, Wang C, Deng T, *et al*. The epidemiology and clinical information about COVID-19. *Eur J Clin Microbiol Infect Dis* 2020; 39(6): 1011–1019. doi:10.1007/s10096-020-03874-z.
- [2] Gupta A, Madhavan MV, Sehgal K, Nair N, Mahajan S, Sehrawat TS, *et al*. Extrapulmonary manifestations of COVID-19. *Nat Med* 2020; 26(7): 1017–1032. doi:10.1038/s41591-020-0968-3.
- [3] Wu J, Song S, Cao HC, Li LJ. Liver diseases in COVID-19: Etiology, treatment and prognosis. *World J Gastroenterol* 2020; 26(19): 2286–2293. doi:10.3748/wjg.v26.i19.2286.
- [4] Zheng J. SARS-CoV-2: an Emerging Coronavirus that Causes a Global Threat. *Int J Biol Sci* 2020; 16(10): 1678–1685. doi:10.7150/ijbs.45053.
- [5] Ni W, Yang X, Yang D, Bao J, Li R, Xiao Y, *et al*. Role of angiotensin-converting enzyme 2 (ACE2) in COVID-19. *Crit Care* 2020; 24(1): 422. doi:10.1186/s13054-020-03120-0.
- [6] Grace JA, Casey S, Burrell LM, Angus PW. Proposed mechanism for increased COVID-19 mortality in patients with decompensated cirrhosis. *Hepatol Int* 2020; 14(5): 884–885. doi:10.1007/s12072-020-10084-4.
- [7] Parasher A. COVID-19: Current understanding of its pathophysiology, clinical presentation and treatment. *Postgrad Med J* 2020. doi:10.1136/postgradmedj-2020-138577.
- [8] Xu Z, Shi L, Wang Y, Zhang J, Huang L, Zhang C, *et al*. Pathological findings of COVID-19 associated with acute respiratory distress syndrome. *Lancet Respir Med* 2020; 8(4): 420–422. doi:10.1016/S2213-2600(20)30076-X.
- [9] Manabe T, Akatsu H, Kotani K, Kudo K. Trends in clinical features of novel coronavirus disease (COVID-19): A systematic review and meta-analysis of studies published from December 2019 to February 2020. *Respir Investig* 2020; 58(5): 409–418. doi:10.1016/j.resinv.2020.05.005.
- [10] Wu Z, McGoogan JM. Characteristics of and important lessons from the coronavirus disease 2019 (COVID-19) outbreak in China: Summary of a report of 72 314 cases from the Chinese Center for Disease Control and Prevention. *JAMA* 2020; 323(13): 1239–1242. doi:10.1001/jama.2020.2648.
- [11] Tahvildari A, Arbabi M, Farsi Y, Jamshidi P, Hasanzadeh S, Calcagno TM, *et al*. Clinical features, diagnosis, and treatment of COVID-19 in hospitalized patients: A systematic review of case reports and case series. *Front Med (Lausanne)* 2020; 7: 231. doi:10.3389/fmed.2020.00231.
- [12] Elhence A, Shalimar. COVID-19: Beyond respiratory tract. *J Digest Endosc* 2020; 11(1): 24–26. doi:10.1055/s-0040-1712550.
- [13] Jothimani D, Venugopal R, Abedin MF, Kaliamoorthy I, Rela M. COVID-19 and the liver. *J Hepatol* 2020; 73(5): 1231–1240. doi:10.1016/j.jhep.2020.06.006.
- [14] Lagana SM, Kudose S, Iuga AC, Lee MJ, Fazlollahi L, Remotti HE, *et al*. Hepatic pathology in patients dying of COVID-19: a series of 40 cases including clinical, histologic, and virologic data. *Mod Pathol* 2020; 33(11): 2147–2155. doi:10.1038/s41379-020-00649-x.
- [15] Wang Y, Liu S, Liu H, Li W, Lin F, Jiang L, *et al*. SARS-CoV-2 infection of the liver directly contributes to hepatic impairment in patients with COVID-19. *J Hepatol* 2020; 73(4): 807–816. doi:10.1016/j.jhep.2020.05.002.
- [16] Zou X, Chen K, Zou J, Han P, Hao J, Han Z. Single-cell RNA-seq data analysis on the receptor ACE2 expression reveals the potential risk of different human organs vulnerable to 2019-nCoV infection. *Front Med* 2020; 14(2): 185–192. doi:10.1007/s11684-020-0754-0.
- [17] Pedersen SF, Ho YC. SARS-CoV-2: a storm is raging. *J Clin Invest* 2020; 130(5): 2202–2205. doi:10.1172/JCI1137647.
- [18] Tang Y, Liu J, Zhang D, Xu Z, Ji J, Wen C. Cytokine storm in COVID-19: The



- current evidence and treatment strategies. *Front Immunol* 2020; 11:1708. doi: 10.3389/fimmu.2020.01708.
- [19] Yuki K, Fujitani M, Koutsoglannaki S. COVID-19 pathophysiology: A review. *Clin Immunol* 2020; 215: 108427. doi: 10.1016/j.clim.2020.108427.
- [20] Ji D, Zhang D, Yang T, Mu J, Zhao P, Xu J, *et al*. Effect of COVID-19 on patients with compensated chronic liver diseases. *Hepatol Int* 2020; 14(5): 701–710. doi: 10.1007/s12072-020-10058-6.
- [21] Chen N, Zhou M, Dong X, Qu J, Gong F, Han Y, *et al*. Epidemiological and clinical characteristics of 99 cases of 2019 novel coronavirus pneumonia in Wuhan, China: a descriptive study. *Lancet* 2020; 395(10223): 507–513. doi: 10.1016/S0140-6736(20)30211-7.
- [22] Phipps MM, Barraza LH, LaSota ED, Sobieszczek ME, Pereira MR, Zheng EX, *et al*. Acute liver injury in COVID-19: Prevalence and association with clinical outcomes in a large U.S. cohort. *Hepatology* 2020; 72(3): 807–817. doi: 10.1002/hep.31404.
- [23] Paliogiannis P, Zinellu A. Bilirubin levels in patients with mild and severe Covid-19: A pooled analysis. *Liver Int* 2020; 40(7): 1787–1788. doi: 10.1111/liv.14477.
- [24] Goyal P, Choi JJ, Pinheiro LC, Schenck EJ, Chen R, Jabri A, *et al*. Clinical characteristics of Covid-19 in New York city. *N Engl J Med* 2020; 382(24): 2372–2374. doi: 10.1056/NEJMc2010419.
- [25] Henry BM, de Oliveira MHS, Benoit S, Plebani M, Lippi G. Hematologic, biochemical and immune biomarker abnormalities associated with severe illness and mortality in coronavirus disease 2019 (COVID-19): a meta-analysis. *Clin Chem Lab Med* 2020; 58(7): 1021–1028. doi: 10.1515/cclm-2020-0369.
- [26] Li B, Yang J, Zhao F, Zhi L, Wang X, Liu L, *et al*. Prevalence and impact of cardiovascular metabolic diseases on COVID-19 in China. *Clin Res Cardiol* 2020; 109(5): 531–538. doi: 10.1007/s00392-020-01626-9.
- [27] Shalimar, Elhence A, Vaishnav M, Kumar R, Pathak P, Soni KD, *et al*. Poor outcomes in patients with cirrhosis and Corona Virus Disease-19. *Indian J Gastroenterol* 2020; 39(3): 285–291. doi: 10.1007/s12664-020-01074-3.
- [28] Meo SA, Klonoff DC, Akram J. Efficacy of chloroquine and hydroxychloroquine in the treatment of COVID-19. *Eur Rev Med Pharmacol Sci* 2020; 24(8): 4539–4547. doi: 10.26355/eurrev\_202004\_21038.
- [29] Satarcker S, Ahuja T, Banerjee M, Vignesh Balaji E, Dogra S, Agarwal T, *et al*. Hydroxychloroquine in COVID-19: Potential Mechanism of Action Against SARS-CoV-2. *Curr Pharmacol Rep* 2020; 6: 203–211. doi: 10.1007/s40495-020-00231-8.
- [30] Uzelac I, Irvanian S, Ashikaga H, Bhatia NK, Herndon C, Kaboudian A, *et al*. Fatal arrhythmias: Another reason why doctors remain cautious about chloroquine/hydroxychloroquine for treating COVID-19. *Heart Rhythm* 2020; 17(9): 1445–1451. doi: 10.1016/j.hrthm.2020.05.030.
- [31] Pathak SK, Salunke AA, Thivari P, Pandey A, Nandy K, Ratna HVK, *et al*. No benefit of hydroxychloroquine in COVID-19: Results of Systematic Review and Meta-Analysis of Randomized Controlled Trials. *Diabetes Metab Syndr* 2020; 14(6): 1673–1680. doi: 10.1016/j.dsx.2020.08.033.
- [32] Boulware DR, Pullen MF, Bangdiwala AS, Pastick KA, Lofgren SM, Okafor EC, *et al*. A randomized trial of hydroxychloroquine as postexposure prophylaxis for Covid-19. *N Engl J Med* 2020; 383(6): 517–525. doi: 10.1056/NEJMoa2016638.
- [33] Cavalcanti AB, Zampieri FG, Rosa RG, Azevedo LCP, Veiga VC, Avezum A, *et al*. Hydroxychloroquine with or without azithromycin in mild-to-moderate Covid-19. *N Engl J Med* 2020; 383(21): 2041–2052. doi: 10.1056/NEJMoa2019014.
- [34] Horby P, Mafham M, Linsell L, Bell JL, Staplin N, Emberson JR, *et al*. Effect of hydroxychloroquine in hospitalized patients with Covid-19. *N Engl J Med* 2020; 383(21): 2030–2040. doi: 10.1056/NEJMoa2022926.
- [35] Giner Galvañ V, Oltra MR, Rueda D, Esteban MJ, Redón J. Severe acute hepatitis related to hydroxychloroquine in a woman with mixed connective tissue disease. *Clin Rheumatol* 2007; 26(6): 971–972. doi: 10.1007/s10067-006-0218-1.
- [36] Hydroxychloroquine. In: *LiverTox: Clinical and Research Information on Drug-Induced Liver Injury* [Internet]. Bethesda (MD): National Institute of Diabetes and Digestive and Kidney Diseases. Available from: <https://www.ncbi.nlm.nih.gov/books/NBK548738/>.
- [37] Falcão MB, Pamplona de Góes Cavalcanti L, Filgueiras Filho NM, Antunes de Brito CA. Case report: Hepatotoxicity associated with the use of hydroxychloroquine in a patient with COVID-19. *Am J Trop Med Hyg* 2020; 102: 1214–1216. doi: 10.4269/ajtmh.20-0276.
- [38] Schögl A, Kopf BS, Edwards MR, Johnston SL, Casaulta C, Kieninger E, *et al*. Novel antiviral properties of azithromycin in cystic fibrosis airway epithelial cells. *Eur Respir J* 2015; 45(2): 428–439. doi: 10.1183/09031936.00102014.
- [39] Oldenburg CE, Doan T. Azithromycin for severe COVID-19. *Lancet* 2020; 396(10256): 936–937. doi: 10.1016/S0140-6736(20)31863-8.
- [40] Gibson PG, Yang IA, Upham JW, Reynolds PN, Hodge S, James AL, *et al*. Effect of azithromycin on asthma exacerbations and quality of life in adults with persistent uncontrolled asthma (AMAZES): a randomised, double-blind, placebo-controlled trial. *Lancet* 2017; 390(10095): 659–668. doi: 10.1016/S0140-6736(17)31281-3.
- [41] Furtado RHM, Berwanger O, Fonseca HA, Corrêa TD, Ferraz LR, Lapa MG, *et al*. Azithromycin in addition to standard of care versus standard of care alone in the treatment of patients admitted to the hospital with severe COVID-19 in Brazil (COALITION II): a randomised clinical trial. *Lancet* 2020; 396(10256): 959–967. doi: 10.1016/S0140-6736(20)31862-6.
- [42] Maggiori C, Santi L, Zaccarini G, Bevilacqua V, Giunchi F, Caraceni P. A case of prolonged cholestatic hepatitis induced by azithromycin in a young woman. *Case Reports Hepatol* 2011; 2011: 314231. doi: 10.1155/2011/314231.
- [43] Juricic D, Hrstic I, Radic D, Skegro M, Coric M, Vucelic B, *et al*. Vanishing bile duct syndrome associated with azithromycin in a 62-year-old man. *Basic Clin Pharmacol Toxicol* 2010; 106(1): 62–65. doi: 10.1111/j.1742-7843.2009.00474.x.
- [44] Brkljacic N, Gracin S, Prkacin I, Sabljari-Matovinovic M, Mrzljak A, Nemet Z. Stevens-Johnson syndrome as an unusual adverse effect of azithromycin. *Acta Dermatovenereol Croat* 2006; 14(1): 40–45.
- [45] Lopez-Medina AI, Campos-Staffico AM, Luzum JA. QT prolongation with hydroxychloroquine and azithromycin for the treatment of COVID-19: The need for pharmacogenetic insights. *J Cardiovasc Electrophysiol* 2020; 31(10): 2793–2794. doi: 10.1111/jce.14722.
- [46] Sulkowski MS, Mehta SH, Chaisson RE, Thomas DL, Moore RD. Hepatotoxicity associated with protease inhibitor-based antiretroviral regimens with or without concurrent ritonavir. *AIDS* 2004; 18(17): 2277–2284. doi: 10.1097/00002030-200411190-00008.
- [47] Lopinavir-ritonavir in patients admitted to hospital with COVID-19 (RECOVERY): a randomised, controlled, open-label, platform trial. *Lancet*. 2020; 396(10259): 1345–1352. doi: 10.1016/S0140-6736(20)32013-4.
- [48] Cao B, Wang Y, Wen D, Liu W, Wang J, Fan G, *et al*. A trial of lopinavir-ritonavir in adults hospitalized with severe Covid-19. *N Engl J Med* 2020; 382(19): 1787–1799. doi: 10.1056/NEJMoa2001282.
- [49] Yeh RF, Gaver VE, Patterson KB, Rezk NL, Baxter-Meheux F, Blake MJ, *et al*. Lopinavir/ritonavir induces the hepatic activity of cytochrome P450 enzymes CYP2C9, CYP2C19, and CYP1A2 but inhibits the hepatic and intestinal activity of CYP3A as measured by a phenotyping drug cocktail in healthy volunteers. *J Acquir Immune Defic Syndr* 2006; 42(1): 52–60. doi: 10.1097/01.qai.0000219774.20174.64.
- [50] Kottitil S, Polis MA, Kovacs JA. HIV Infection, hepatitis C infection, and HAART: hard clinical choices. *JAMA* 2004; 292(2): 243–250. doi: 10.1001/jama.292.2.243.
- [51] Zell SC. Clinical vignette in antiretroviral therapy: jaundice. *J Int Assoc Physicians AIDS Care (Chic)* 2003; 2(4): 133–139. doi: 10.1177/154510970300200402.
- [52] Canta F, Marrone R, Bonora S, D'Avolio A, Scialandra M, Sinicco A, *et al*. Pharmacokinetics and hepatotoxicity of lopinavir/ritonavir in non-cirrhotic HIV and hepatitis C virus (HCV) co-infected patients. *J Antimicrob Chemother* 2005; 55(2): 280–281. doi: 10.1093/jac/dkh516.
- [53] Olry A, Meunier L, Delire B, Larrey D, Horsmans Y, Le Louët H. Drug-induced liver injury and COVID-19 infection: The rules remain the same. *Drug Saf* 2020; 43(7): 615–617. doi: 10.1007/s40264-020-00954-z.
- [54] Wang M, Cao R, Zhang L, Yang X, Liu J, Xu M, *et al*. Remdesivir and chloroquine effectively inhibit the recently emerged novel coronavirus (2019-nCoV) in vitro. *Cell Res* 2020; 30(3): 269–271. doi: 10.1038/s41422-020-0282-0.
- [55] Williamson BN, Feldmann F, Schwarz B, Meade-White K, Porter DP, Schulz J, *et al*. Clinical benefit of remdesivir in rhesus macaques infected with SARS-CoV-2. *Nature* 2020; 585(7824): 273–276. doi: 10.1038/s41586-020-2423-5.
- [56] Beigel JH, Tomashek KM, Dodd LE, Mehta AK, Zingman BS, Kalil AC, *et al*. Remdesivir for the treatment of Covid-19 - Final report. *N Engl J Med* 2020; 383(19): 1813–1826. doi: 10.1056/NEJMoa2007764.
- [57] Wang Y, Zhang D, Du G, Du R, Zhao J, Jin Y, *et al*. Remdesivir in adults with severe COVID-19: a randomised, double-blind, placebo-controlled, multicentre trial. *Lancet* 2020; 395(10236): 1569–1578. doi: 10.1016/S0140-6736(20)31022-9.
- [58] Glaus MJ, VonRuden S. Remdesivir and COVID-19. *Lancet* 2020; 396(10256): 952. doi: 10.1016/S0140-6736(20)32021-3.
- [59] Goldman JD, Lye DCB, Hui DS, Marks KM, Bruno R, Montejano R, *et al*. Remdesivir for 5 or 10 days in patients with severe Covid-19. *N Engl J Med* 2020; 383(19): 1827–1837. doi: 10.1056/NEJMoa2015301.
- [60] Eastman RT, Roth JS, Brimacombe KR, Simeonov A, Shen M, Patnaik S, *et al*. Remdesivir: A review of its discovery and development leading to emergency use authorization for treatment of COVID-19. *ACS Cent Sci* 2020; 6(5): 672–683. doi: 10.1021/acscentsci.0c00489.
- [61] Zampino R, Mele F, Florio LL, Bertolino L, Andini R, Galdo M, *et al*. Liver injury in remdesivir-treated COVID-19 patients. *Hepatol Int* 2020; 14(5): 881–883. doi: 10.1007/s12072-020-10077-3.
- [62] Carothers C, Birrer K, Vo M. Acetylcysteine for the treatment of suspected remdesivir-associated acute liver failure in COVID-19: A case series. *Pharmacotherapy* 2020; 40(11): 1166–1171. doi: 10.1002/phar.2464.
- [63] Wong GL, Wong VW, Thompson A, Jia J, Hou J, Lesmana CRA, *et al*. Management of patients with liver derangement during the COVID-19 pandemic: an Asia-Pacific position statement. *Lancet Gastroenterol Hepatol* 2020; 5(8): 776–787. doi: 10.1016/S2468-1253(20)30190-4.
- [64] Agrawal U, Raju R, Udawadia ZF. Favipiravir: A new and emerging antiviral option in COVID-19. *Med J Armed Forces India* 2020; 76(4): 370–376. doi: 10.1016/j.mjafi.2020.08.004.
- [65] Shannon A, Sellisko B, Le N, Huchting J, Touret F, Piorkowski G, *et al*. Favipiravir strikes the SARS-CoV-2 at its Achilles heel, the RNA polymerase. *bioRxiv* 2020: 2020.05.15.098731. doi: 10.1101/2020.05.15.098731.
- [66] Cai Q, Yang M, Liu D, Chen J, Shu D, Xia J, *et al*. Experimental treatment with favipiravir for COVID-19: An open-label control study. *Engineering (Beijing)* 2020; 6(10): 1192–1198. doi: 10.1016/j.eng.2020.03.007.
- [67] Li L, Wang X, Wang R, Hu Y, Jiang S, Lu X. Antiviral agent therapy optimization in special populations of COVID-19 patients. *Drug Des Devel Ther* 2020; 14: 3001–3013. doi: 10.2147/DDDT.S259058.
- [68] Caly L, Druce JD, Catton MG, Jans DA, Wagstaff KM. The FDA-approved drug ivermectin inhibits the replication of SARS-CoV-2 in vitro. *Antiviral Res* 2020; 178: 104787. doi: 10.1016/j.antiviral.2020.104787.
- [69] Rizzo E. Ivermectin, antiviral properties and COVID-19: a possible new mechanism of action. *Naunyn-Schmiedeberg Arch Pharmacol* 2020; 393(7): 1153–1156. doi: 10.1007/s00210-020-01902-5.
- [70] Rajter JC, Sherman MS, Fatteh N, Vogel F, Sacks J, Rajter JJ. Use of Iver-

- mectin is associated with lower mortality in hospitalized patients with coronavirus disease 2019: The ivermectin in COVID nineteen study. *Chest* 2021; 159(1):85–92. doi: 10.1016/j.chest.2020.10.009.
- [71] Veit O, Beck B, Steuerwald M, Hatz C. First case of ivermectin-induced severe hepatitis. *Trans R Soc Trop Med Hyg* 2006; 100(8):795–797. doi: 10.1016/j.trstmh.2006.02.003.
- [72] Horby P, Lim WS, Emberson JR, Mafham M, Bell JL, Linsell L, *et al*. Dexamethasone in hospitalized patients with Covid-19. *N Engl J Med* 2021; 384(8):693–704. doi: 10.1056/NEJMoa2021436.
- [73] Tomazini BM, Maia IS, Cavalcanti AB, Berwanger O, Rosa RG, Veiga VC, *et al*. Effect of dexamethasone on days alive and ventilator-free in patients with moderate or severe acute respiratory distress syndrome and COVID-19: The CoDEX randomized clinical trial. *JAMA* 2020; 324(13):1307–1316. doi: 10.1001/jama.2020.17021.
- [74] Sterne JAC, Murthy S, Diaz JV, Slutsky AS, Villar J, Angus DC, *et al*. Association between administration of systemic corticosteroids and mortality among critically ill patients with COVID-19: A meta-analysis. *JAMA* 2020; 324(13):1330–1341. doi: 10.1001/jama.2020.17023.
- [75] Edalatfard M, Akhtari M, Salehi M, Naderi Z, Jamshidi A, Mostafaei S, *et al*. Intravenous methylprednisolone pulse as a treatment for hospitalised severe COVID-19 patients: results from a randomised controlled clinical trial. *Eur Respir J* 2020; 56(6):2002808. doi: 10.1183/13993003.02808-2020.
- [76] Loomba R, Liang TJ. Hepatitis B reactivation associated with immune suppressive and biological modifier therapies: Current concepts, management strategies, and future directions. *Gastroenterology* 2017; 152(6):1297–1309. doi: 10.1053/j.gastro.2017.02.009.
- [77] Wong GL, Wong VW, Yuen BW, Tse YK, Yip TC, Luk HW, *et al*. Risk of hepatitis B surface antigen seroreversion after corticosteroid treatment in patients with previous hepatitis B virus exposure. *J Hepatol* 2020; 72(1):57–66. doi: 10.1016/j.jhep.2019.08.023.
- [78] Rodríguez-Tajes S, Miralpeix A, Costa J, López-Suñé E, Laguno M, Pocurull A, *et al*. Low risk of hepatitis B reactivation in patients with severe COVID-19 who receive immunosuppressive therapy. *J Viral Hepat* 2021; 28(1):89–94. doi: 10.1111/jvh.13410.
- [79] Varona Pérez J, Rodríguez Chinesta JM. Risk of hepatitis B reactivation associated with treatment against SARS-CoV-2 (COVID-19) with corticosteroids. *Rev Clin Esp* 2020; 220(8):534–536. doi: 10.1016/j.rce.2020.04.012.
- [80] Stone JH, Frigault MJ, Serling-Boyd NJ, Fernandes AD, Harvey L, Foulkes AS, *et al*. Efficacy of tocilizumab in patients hospitalized with Covid-19. *N Engl J Med* 2020; 383(24):2333–2344. doi: 10.1056/NEJMoa2028836.
- [81] Parr JB. Time to reassess tocilizumab's role in COVID-19 pneumonia. *JAMA Intern Med* 2021; 181(1):12–15. doi: 10.1001/jamainternmed.2020.6557.
- [82] Serviddio G, Villani R, Stallone G, Scioscia G, Foschino-Barbaro MP, Lacedonia D. Tocilizumab and liver injury in patients with COVID-19. *Therap Adv Gastroenterol* 2020; 13:doi: 10.1177/1756284820959183.
- [83] Sonneveld MJ, Murad SD, van der Eijk AA, de Man RA. Fulminant liver failure due to hepatitis B reactivation during treatment with tocilizumab. *ACG Case Rep J* 2019; 6(12):e00243. doi: 10.14309/crj.0000000000000243.
- [84] Watanabe T, Fukae J, Fukaya S, Sawamukai N, Isobe M, Matsushashi M, *et al*. Incidence and risk factors for reactivation from resolved hepatitis B virus in rheumatoid arthritis patients treated with biological disease-modifying antirheumatic drugs. *Int J Rheum Dis* 2019; 22(4):574–582. doi: 10.1111/1756-185X.13401.
- [85] Costela-Ruiz VJ, Illescas-Montes R, Puerta-Puerta JM, Ruiz C, Melguizo-Rodríguez L. SARS-CoV-2 infection: The role of cytokines in COVID-19 disease. *Cytokine Growth Factor Rev* 2020; 54:62–75. doi: 10.1016/j.cytogr.2020.06.001.
- [86] Huet T, Beaussier H, Voisin O, Jouvesshomme S, Dauriat G, Lazareth I, *et al*. Anakinra for severe forms of COVID-19: a cohort study. *Lancet Rheumatol* 2020; 2(7):e393–e400. doi: 10.1016/S2665-9913(20)30164-8.
- [87] Taylor SA, Vittorio JM, Martinez M, Fester KA, Lagana SM, Lobritto SJ, *et al*. Anakinra-induced acute liver failure in an adolescent patient with still's disease. *Pharmacotherapy* 2016; 36(1):e1–e4. doi: 10.1002/phar.1677.
- [88] Cavalli G, De Luca G, Campochiaro C, Della-Torre E, Ripa M, Canetti D, *et al*. Interleukin-1 blockade with high-dose anakinra in patients with COVID-19, acute respiratory distress syndrome, and hyperinflammation: a retrospective cohort study. *Lancet Rheumatol* 2020; 2(6):e325–e331. doi: 10.1016/S2665-9913(20)30127-2.
- [89] Anakinra in: LiverTox: Clinical and research information on drug-induced liver injury. Available from: <https://www.ncbi.nlm.nih.gov/books/NBK548615/>.
- [90] Richardson P, Griffin I, Tucker C, Smith D, Oechsle O, Phelan A, *et al*. Baricitinib as potential treatment for 2019-nCoV acute respiratory disease. *Lancet* 2020; 395(10223):e30–e31. doi: 10.1016/S0140-6736(20)30304-4.
- [91] Stebbing J, Phelan A, Griffin I, Tucker C, Oechsle O, Smith D, *et al*. COVID-19: combining antiviral and anti-inflammatory treatments. *Lancet Infect Dis* 2020; 20(4):400–402. doi: 10.1016/S1473-3099(20)30132-8.
- [92] Adaptive COVID-19 treatment trial 2 (ACTT-2). Available from: <https://clinicaltrials.gov/ct2/show/NCT04401579>.
- [93] Jorgensen SCJ, Tse CLY, Burry L, Dresser LD. Baricitinib: A review of pharmacology, safety, and emerging clinical experience in COVID-19. *Pharmacotherapy* 2020; 40(8):843–856. doi: 10.1002/phar.2438.
- [94] Altuntas F, Ata N, Yigenoglu TN, Basci S, Dal MS, Korkmaz S, *et al*. Convalescent plasma therapy in patients with COVID-19. *Transfus Apher Sci* 2021; 60(1):102955. doi: 10.1016/j.transci.2020.102955.
- [95] Agarwal A, Mukherjee A, Kumar G, Chatterjee P, Bhatnagar T, Malhotra P. Convalescent plasma in the management of moderate covid-19 in adults in India: open label phase II multicentre randomised controlled trial (PLACID Trial). *BMJ* 2020; 371:m3939. doi: 10.1136/bmj.m3939.
- [96] Nopp S, Moik F, Jilma B, Pabinger I, Ay C. Risk of venous thromboembolism in patients with COVID-19: A systematic review and meta-analysis. *Res Pract Thromb Haemost* 2020; 4(7):1178–1191. doi: 10.1002/rth2.12439.
- [97] Chowdhury JF, Moores LK, Connors JM. Anticoagulation in hospitalized patients with Covid-19. *N Engl J Med* 2020; 383(17):1675–1678. doi: 10.1056/NEJMcide2028217.
- [98] Desborough MJR, Doyle AJ, Griffiths A, Retter A, Breen KA, Hunt BJ. Image-proven thromboembolism in patients with severe COVID-19 in a tertiary critical care unit in the United Kingdom. *Thromb Res* 2020; 193:1–4. doi: 10.1016/j.thromres.2020.05.049.



## Case Report

# Acute-on-chronic Liver Failure in a Patient with *Candida Endophthalmitis*: A Case Report

Ying Cao<sup>1</sup> , Ying Fan<sup>1</sup> , Yanbin Wang<sup>1</sup> , Xiyao Liu<sup>2</sup> and Wen Xie<sup>1\*</sup>

<sup>1</sup>Center of Liver Diseases, Capital Medical University Affiliated to Beijing Ditan Hospital, Beijing, China; <sup>2</sup>Department of Ophthalmology, Capital Medical University Affiliated to Beijing Ditan Hospital, Beijing, China

Received: 11 October 2020 | Revised: 19 February 2021 | Accepted: 1 March 2021 | Published: 30 March 2021

## Abstract

Acute-on-chronic liver failure (ACLF) is a risk factor for fungal infection. Endogenous fungal endophthalmitis is a serious, sight-threatening disease. Common causes include immunocompromised state and intravenous drug use, permitting opportunistic pathogens to reach the eye through the blood stream. We report a case of *Candida endophthalmitis* in a 47-year-old woman who was admitted to our hospital with ACLF and poorly controlled diabetes. In addition, she was treated with glucocorticoids due to severe jaundice. After treatment for ACLF, the patient experienced fever with blurred vision in the left eye and was diagnosed with candidemia, endogenous *Candida endophthalmitis* in the left eye, and chorioretinitis in the right eye. Systemic and topical antifungal treatment was administered based on the positive *Candida albicans* test in intraocular fluid using second-generation sequencing. The patient underwent vitrectomy in the left eye and *C. albicans* was confirmed in vitreous cultures. Follow-up visit, at 6 weeks after the operation, showed only light perception in the left eye and stable visual acuity in the right eye. Physicians should be aware of endogenous fungal endophthalmitis in patients with ACLF, especially those with *Candida* infection, a history of glucocorticoid use, and diabetes. A dilated retinal examination should be performed by an ophthalmologist if ACLF patients develop fever and fungal infection.

**Citation of this article:** Cao Y, Fan Y, Wang Y, Liu X, Xie W. Acute-on-chronic liver failure patient with *Candida endophthalmitis*: A Case Report. J Clin Transl Hepatol 2021;9(3): 447–451. doi: 10.14218/JCTH.2020.00092.

## Introduction

Acute-on-chronic liver failure (ACLF) is associated with a

poor outcome. Invasive fungal infections (IFIs) are common in patients with ACLF due to defects in the host immune system, complications, widespread antibiotic use, and invasive procedures.<sup>1</sup> IFI indicates patients with a high mortality risk in the long term.<sup>2</sup> Many studies have reported that the common sites of fungal infection in ACLF are the respiratory tract, kidneys, skin/soft tissue, esophagus, oropharynx, and peritoneum.<sup>3–5</sup> There are few reports of endogenous fungal endophthalmitis (EFE) in patients with liver failure.<sup>6,7</sup>

In this case report, a 47-year-old woman with diabetes developed endogenous *Candida endophthalmitis* in the clinical course of ACLF. We suggest that endogenous *C. endophthalmitis* should be considered in patients with ACLF who have fever and *Candida* infection. In addition, it is important to perform ophthalmologic examinations and implement appropriate approaches to eliminate fungal infection.

## Case report

A 47-year-old woman was hospitalized with acute onset of marked jaundice at a local hospital in April 2019. The most disturbing symptoms were asthenia, anorexia, and dark urine. The patient received supportive liver protection and glucocorticoid therapy for jaundice at a local hospital, while liver function became progressively worse. The patient was diagnosed with ACLF and transferred to our hospital on May 24, 2019. Her past medical history suggested that she had been a carrier of hepatitis B surface antigen for the past 10 years, in addition to having poorly controlled sugar levels. A physical examination, conducted after admission to our hospital, revealed the following findings: body temperature, 36.3 °C; blood pressure, 114/67 mmHg; heart rate, 87 beats/m; and respiratory rate, 17 breaths/m. There were small ecchymoses in the skin, serious yellow sclera and skin, suspicious abdominal shifting dullness, and lower limb edema. Heart and lung examinations were without remarkable findings. The abdomen was not distended. The liver and spleen were not palpable. There was no presence of ascites. Clinical examination revealed normal mental status and vital signs.

The laboratory data were as follows: increased white blood cell count ( $11.30 \times 10^9/L$ ), neutrophil granulocyte (89.60%), red blood cells ( $3.29 \times 10^{12}/L$ ), hemoglobin (104.0 g/L), platelets ( $143.0 \times 10^9/L$ ); prothrombin time activity 58%; international normalized ratio 1.50; severe liver function damage (alanine aminotransferase 252.5 U/L, aspartate transaminase 182.0 U/L, total bilirubin 477.2 μmol/L, direct bilirubin 384.4 μmol/L, gamma-gluta-

**Keywords:** Acute-on-chronic liver failure; *Candida endophthalmitis*; *Candida albicans*; Glucocorticoid; Case report.

**Abbreviations:** ACLF, acute-on-chronic liver failure; BCVA, best-corrected visual acuity; IFI, invasive fungal infections; EFE, endogenous fungal endophthalmitis; IDSA, Infectious Diseases Society of America; MELD, model for end-stage liver disease; T-SPOT, T cell enzyme-linked immuno-spot.

\*Correspondence to: Wen Xie, Center of Liver Diseases, Capital Medical University Affiliated to Beijing Ditan Hospital, No. 8, Jingshun East Street, Chaoyang District, Beijing 100015, China. ORCID: <https://orcid.org/0000-0002-7314-8175>. Tel: +86-10-84322816, Fax: +86-10-84322818, E-mail: [xiewen6218@163.com](mailto:xiewen6218@163.com)



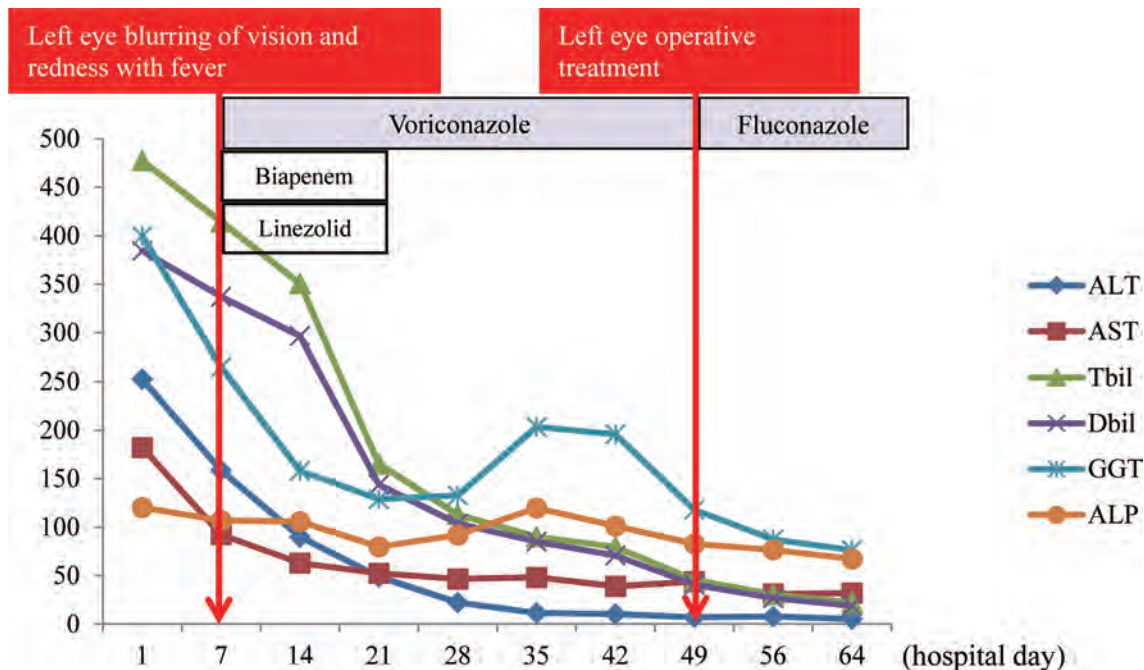


**Fig. 1.** Clinical course and changes of biochemistry parameters after the patient was admitted to our hospital. The levels of hyperbilirubinemia slowly trended downward, from over 470  $\mu\text{mol/L}$  to 30  $\mu\text{mol/L}$ . ALP, alkaline phosphatase (U/L); ALT, alanine aminotransferase (U/L); AST, aspartate transaminase (U/L); Dbil, direct bilirubin ( $\mu\text{mol/L}$ ); GGT: gamma-glutamyltransferase (U/L); Tbil, total bilirubin ( $\mu\text{mol/L}$ ).

myl transpeptidase 399.6 U/L, alkaline phosphatase 120.2 U/L, and albumin 39.0 g/L; elevated HbA1c level (7.2%). The hepatitis B virus DNA viral load was 292 IU/mL. Tests for hepatitis B surface antigen, hepatitis B surface antibody, and hepatitis B core antibody were positive. Magnetic resonance cholangiopancreatography revealed small stones in the gallbladder, without intrahepatic or extrahepatic bile duct dilatation; computed tomography enhancement scanning revealed a low enhancement area around the portal vein and little intraperitoneal free fluid but no vascular abnormalities. On the basis of clinical manifestations, she was diagnosed with ACLF, having an ACLF model for end-stage liver disease (commonly referred to as MELD) score of 24, chronic hepatitis B, and type II diabetes mellitus. She was administered entecavir (0.5 mg/day) antiviral therapy, oral methylprednisolone (gradually decreased by reduction of 5 mg/week and then ceased), which protected the liver, reduced enzyme activity, and eliminated jaundice, and insulin subcutaneous injection to control blood glucose. Her liver function improved. The changes in biochemistry parameters are shown in Figure 1.

However, the patient developed a high fever, blurred vision, and redness in the left eye at 7 days after hospitalization. Ophthalmologic examinations were performed immediately. The best-corrected visual acuity (commonly referred to as BCVA) was 8/20 in the left eye and 8/20 in the right eye. The intraocular pressure was 12 mmHg in both eyes. Slit lamp examination revealed ciliary hyperemia, hypopyon, and Tyn (2+) in the left eye, but no significant abnormality in the right eye. Funduscopy examination revealed severe vitreous opacity, invisible fundus in the left eye, and the presence of a well-demarcated yellowish-white round exudate below the macula in the right eye (Fig. 2A, B). Optical coherence tomography revealed a small, highly reflective clump in the sub-retina of the right eye, and a highly reflective clump above the retina of the left eye in the first examination (Fig. 3A, B). Laboratory tests showed decreased lymphocyte count ( $0.74 \times 10^9/\text{L}$ ) and CD4-positive

T lymphocyte count (124 cells/ $\mu\text{L}$ ). The results of the blood levels of white blood cell count ( $12.98 \times 10^9/\text{L}$ ), C-reactive protein (39 mg/dL), procalcitonin (0.60 ng/mL) and 1, and 3- $\beta$ -D glucan (240 pg/mL) were increased on the same day. Interferon- $\gamma$  release assays were performed using T cell enzyme-linked immuno-spot (commonly known as T-SPOT) tuberculosis assay, and the results were positive (the number of spot-forming cells was  $100/2.5 \times 10^5$  peripheral blood mononuclear cells).

The microbial DNA amplification of the aqueous humor using second-generation sequencing technology showed positive results for fungal 26S ribosomal RNA, strongly suggestive of *Candida albicans* infection. The urine culture showed *C. albicans* infection. Blood cultures were positive for *Staphylococcus aureus* infection. Chest computed tomography images showed nodules in the upper and lower lobes of the right lung, considered to be newly infectious nodules. Thus, we suspected candidemia, endogenous *C. endophthalmitis* in the left eye, chorioretinitis in the right eye, and sepsis. The patient was immediately started on systemic intravenous administration of antibiotics (biapenem 300 mg twice daily and linezolid 600 mg/day) and antifungal agent (voriconazole, loading dose 400 mg twice daily for 2 doses, followed by 200 mg twice daily), plus binocular intravitreal injection of amphotericin B deoxycholate for 6 weeks. Intravitreal injections were administered based on the response to treatment. The patient received a dose of 10  $\mu\text{g}$  in 0.1 mL of intravitreal amphotericin-B, every 3 days in the left eye and one injection in the right eye for the first week, and every week thereafter in both eyes for the next 5 weeks. Oral methylprednisolone was discontinued. The patient became afebrile 48 h after starting the systemic antifungal therapy. The results of white blood cell count, C-reactive protein, and procalcitonin were normal, and blood and urine cultures were negative after 2 weeks of antibiotic therapy, and antibiotics were stopped.

After 6 weeks of systemic antibiotics and intravitreal injections, the anterior chamber reaction improved in both

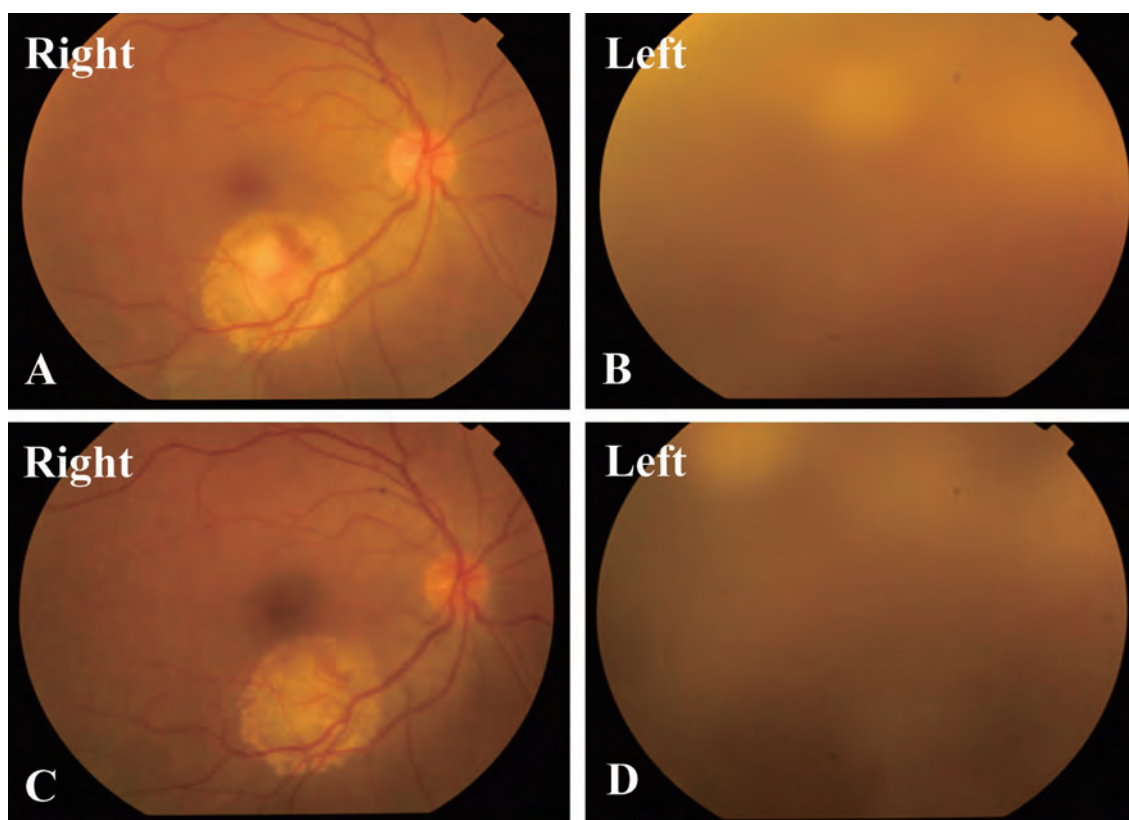


**Fig. 2. Funduscopy images.** (A–B) First funduscopy examination. (A) A yellowish-white round lesion was seen in the right eye. (B) Vitreous opacity was observed in the left eye. (C–D) After 6 weeks antifungal treatment. (C) The lesion in the right eye became thin and localized at this site. (D) Vitreous opacity still existed as before in the left eye.

eyes. The routine blood count and liver function test results were almost normal. The broad-range real-time PCR and cultures of the vitreous fluid, blood, and urine cultures were all negative. However, the blood level of 1, 3- $\beta$  D glucan was still positive (171 pg/mL). Before the vitrectomy, slit lamp examination revealed ciliary hyperemia, corneal edema, and Tyn (2+) in the left eye. The fundus of the left eye remained invisible. The lesion in the right eye became thinner and localized, but the lesion in the left eye showed no improvement (Fig. 2C, D and Fig. 3C, D). The BCVA of the left eye was reduced to light perception only. Before the vitrectomy, slit lamp examination revealed ciliary hyperemia, corneal edema, and Tyn (2+) in her left eye. The fundus was invisible in her left eye as Binocular B-scan was performed in the first examination and before the vitrectomy. The images were shown in Figure S1.

We performed a complete lensectomy, pars plana vitrectomy, and silicone oil tamponade. During vitrectomy, the dense yellowish-white opacity in the vitreous adhered closely to the retina, the proliferating membrane shrank and the retina completely detached. There was no hole in the retina. The patient received intravitreal amphotericin B injections (10  $\mu$ g/0.1 mL). After vitrectomy, the vitreous cavity was filled with silicone oil and the retina was reattached.

A culture of the vitreous tissue revealed *C. albicans* growth. Based on the bacterial culture test results, fluconazole (loading dose 800 mg, then 400 daily) was administered with intravenous fluids for 2 weeks, and a 200 mg oral fluconazole was administered daily for 2 weeks (Table 1). Finally, 1 month after surgery, the lesions in the right eye disappeared by funduscopy examination; the BCVA was still 16/20 in the right eye and light perception only in the left eye.

## Discussion

In the present study, we report a female patient with a history of ACLF and diabetes who developed sudden decrease in both eyes' vision due to endophthalmitis caused by *C. albicans*. ACLF patients usually have immune disorders, hypoalbuminemia, ascites, dysregulation of intestinal flora, impaired gastrointestinal barrier function, susceptibility to flora migration, and reduced body defense. On the other hand, such patients also often have prolonged antibiotic therapy, various kinds of complications, or severe endocrine and metabolic disorders (such as diabetes), systemic corticosteroid use, the use of central venous catheters, and receipt of liver replacement therapy. Therefore, ACLF patients with IFI are not uncommon.<sup>8</sup>

In the Asian Pacific Association for the Study of Liver ACLF consensus of 2019, it is recommended that hospitalized patients with ACLF are closely monitored for the presence of infections in order to enable early diagnosis and treatment. Prophylactic administration of antifungal agents in ACLF patients with high-risk factors can be performed using echinocandins.<sup>9,10</sup> In the former reports, the most common site of IFI infection in liver failure patients is the lung, followed by the intestinal tract, urinary tract, abdominal cavity, bloodstream, and others; intra-ocular infections are rare. Toshikuni *et al.*<sup>6</sup> reported the case of a 69 year-old man who developed fungemia due to *C. albicans* and bilateral endogenous endophthalmitis associated with liver failure due to decompensated liver cirrhosis during hospitalization. Kaburaki *et al.*<sup>7</sup> reported a case of *C. albicans* endophthalmitis with subretinal abscess formation in a patient who under-

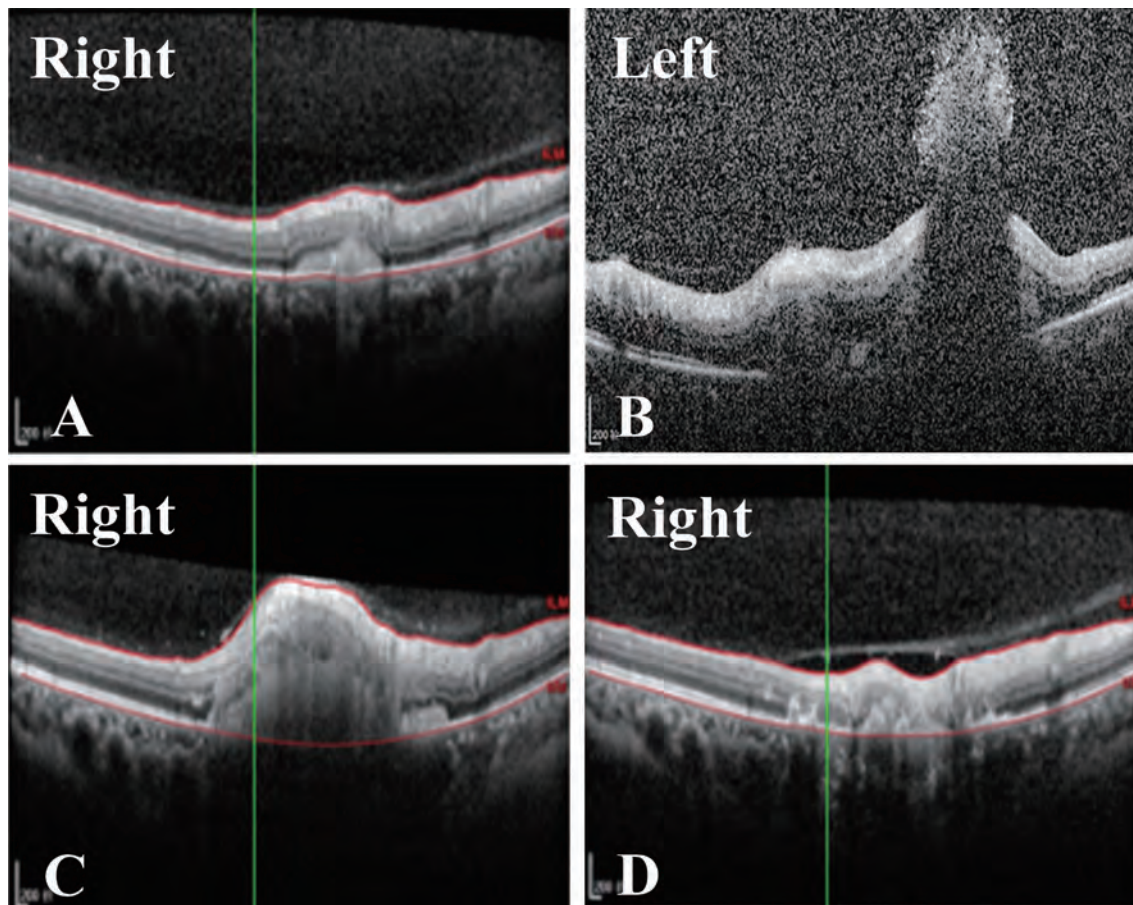


**Fig. 3. Eye optical coherence tomography images.** (A–B) First optical coherence tomography examination. (A) Small high-reflection was observed in the sub-retina. (B) Clumps of high reflection were found in front of the retina. (C) After 2 weeks anti-infective therapy. The sub-retina high-reflection was significantly thicker than before. (D) After 6 weeks antifungal therapy. The lesion was significantly thinner.

went liver transplantation for cirrhosis caused by hepatitis C. To our knowledge, there have been no reports of ACLF with endogenous *C. endophthalmitis*. EFE is a rare but sight-threatening condition that requires immediate diagnosis and appropriate treatment. EFE is derived from systemic fungal infections outside the eye, which are usually caused by candidemia. *Candida* is the most common EFE organism.<sup>11</sup> Once candida enters the bloodstream, it can access the eyes via the short posterior ciliary artery. Infection typically progresses vertically, via chorioretinal infiltration, and the vitreous is a primary site of localization. It has been suggested that higher glucose concentrations support the growth of *Candida* in the vitreous.<sup>12</sup> Our patient had a history of diabetes and poor blood glucose control, therefore at higher risk for

development of endogenous *C. endophthalmitis*. One unilateral case of *C. endophthalmitis* after liver transplantation has been reported.<sup>7</sup> The incidence of *C. endophthalmitis* is rare in patients with candidemia, ranging from 0% to 1.6%.<sup>13</sup> In contrast, Ueda *et al.*<sup>14</sup> reported that the overall incidence of endogenous *C. endophthalmitis* was 21.2%.

The most common symptom of endophthalmitis is decreased vision. Eye pain or discomfort and a red eye are also common. Systemic symptoms, such as fever, are often present in cases of endogenous endophthalmitis. Diagnosis of EFE is based on eye findings rather than vitreous cultures in most cases of documented candidemia. Risk factors for EFE, such as central venous catheters, total parenteral nutrition, broad-spectrum antibiotics, recent abdominal surgery, neutropenia, glucocorticoid therapy and intravenous drug use, have been identified.<sup>11</sup> In this case, the patient had high-risk factors of diabetes and a history of glucocorticoid therapy. Unfortunately, there is a lack of understanding for factors that could predict EFE. Therefore, early diagnosis, timely identification of pathogens, and appropriate treatment are particularly important.

All patients with candidemia are recommended to undergo funduscopic examination at the time of diagnosis and should be closely monitored within 2 weeks of candidemia onset, as ocular involvement sometimes appears later.<sup>15,16</sup> Our patient received systemic antifungal treatment for at least 6 weeks, intravitreal amphotericin B injections, and had left eye vitrectomy. Both procedures were deemed ef-

**Table 1. Bacterial culture test results for *C. albicans***

	Cut-off	MIC, mg/L	
5-Fluorouracil		<= 4	
Fluconazole	≥8≤2	4	SDD
Voriconazole	≥1≤0.125	0.5	I
Amphotericin B		<=0.5	
Itraconazole	≥1≤0.25	0.25	S

I, intermediate; MIC, minimum inhibitory concentration; S, sensitive; SDD, susceptible dose-dependent.



fective in controlling endophthalmitis. Voriconazole is an oral antifungal agent valued for its broad spectrum of activity, favorable side-effect profile, and relatively good ocular penetration. In the Infectious Diseases Society of America (commonly known as IDSA) guidelines, fluconazole or voriconazole are strongly recommended as the first-line systemic medication for *C. endophthalmitis* due to their broad spectrum of activity and superior ocular penetration. The IDSA 2016 guidelines suggest that systemic treatment be administered for at least 4–6 weeks, as determined by repeated ophthalmological examinations to verify the resolution.<sup>16</sup> The IDSA 2016 guidelines strongly recommend that *Candida* chorioretinitis without vitritis be treated with a systemic antifungal agent for at least 4–6 weeks, while the treatment for *Candida* chorioretinitis with vitritis requires systemic therapy plus intravitreal antifungal injections; the final duration of treatment should be based on the resolution of the lesions, as determined by repeated ophthalmological examinations. The guidelines also strongly suggest that vitrectomy should be considered in patients with significant vitritis. The literature demonstrates that vitrectomy plays an important role in the diagnosis of EFE, enhancing the treatment of infection and the management of vision-threatening post-infectious sequelae.<sup>17,18</sup> While the role and timing of vitrectomy for EFE is still unclear, randomized controlled trials are needed to measure its effect.

## Conclusions

In conclusion, patients with liver failure, especially those with high risk factors such as long-term hospitalization, corticosteroid uptake, and diabetes, should be wary of the occurrence of EFE. It is recommended that patients with candidemia have routine funduscopic examinations. Appropriate systemic and topical antifungal treatment combined with surgical intervention can lead to a beneficial clinical outcome.

## Acknowledgments

We thank the patient and participants from our department for their cooperation.

## Funding

This study was supported by grants from the Beijing Municipal Science and Technology Commission (D171100003117005) and the National Science and Technology Major Project (2018ZX10302204). The sponsors only provided the funds.

## Conflict of interest

The authors have no conflict of interests related to this publication.

## Author contributions

Study concept and design (WX, YC), acquisition of data (YC,

YF, XL), analysis and interpretation of data (YC, YF, XL, YW, WX), drafting of the manuscript (YC), critical revision of the manuscript for important intellectual content (YC, YF, XL, YW).

## Data sharing statement

All data are available upon request.

## References

- [1] Fernández J, Acevedo J, Wiest R, Gustot T, Amoros A, Deulofeu C, et al. Bacterial and fungal infections in acute-on-chronic liver failure: prevalence, characteristics and impact on prognosis. *Gut* 2018;67(10):1870–1880. doi: 10.1136/gutjnl-2017-314240.
- [2] Bajaj JS, Reddy RK, Tandon P, Wong F, Kamath PS, Biggins SW, et al. Prediction of fungal infection development and their impact on survival using the NACSELD cohort. *Am J Gastroenterol* 2018;113(4):556–563. doi: 10.1038/ajg.2017.471.
- [3] Verma N, Singh S, Taneja S, Duseja A, Singh V, Dhiman RK, et al. Invasive fungal infections amongst patients with acute-on-chronic liver failure at high risk for fungal infections. *Liver Int* 2019;39(3):503–513. doi: 10.1111/liv.13981.
- [4] Hassan EA, Abd El-Rehim AS, Hassany SM, Ahmed AO, Elsherbiny NM, Mohammed MH. Fungal infection in patients with end-stage liver disease: low frequency or low index of suspicion. *Int J Infect Dis* 2014;23:69–74. doi: 10.1016/j.ijid.2013.12.014.
- [5] Lahmer T, Brandl A, Rasch S, Schmid RM, Huber W. Fungal peritonitis: Underestimated disease in critically ill patients with liver cirrhosis and spontaneous peritonitis. *PLoS One* 2016;11(7):e0158389. doi: 10.1371/journal.pone.0158389.
- [6] Toshikuni N, Ujike K, Yanagawa T, Suga T, Shimizu T, Kusuda Y, et al. *Candida albicans* endophthalmitis after extracorporeal shock wave lithotripsy in a patient with liver cirrhosis. *Intern Med* 2006;45(22):1327–1332. doi: 10.2169/internalmedicine.45.1761.
- [7] Kaburaki T, Takamoto M, Araki F, Fujino Y, Nagahara M, Kawashima H, et al. Endogenous *Candida albicans* infection causing subretinal abscess. *Int Ophthalmol* 2010;30(2):203–206. doi: 10.1007/s10792-009-9304-0.
- [8] Pappas PG, Kauffman CA, Andes D, Benjamin DK Jr, Calandra TF, Edwards JE Jr, et al. Clinical practice guidelines for the management of candidiasis: 2009 update by the Infectious Diseases Society of America. *Clin Infect Dis* 2009;48(5):503–535. doi: 10.1086/596757.
- [9] Sarin SK, Choudhury A, Sharma MK, Maiwall R, Al Mahtab M, Rahman S, et al. Acute-on-chronic liver failure: consensus recommendations of the Asian Pacific association for the study of the liver (APASL): an update. *Hepatol Int* 2019;13(4):353–390. doi: 10.1007/s12072-019-09946-3.
- [10] Sarin SK, Choudhury A. Management of acute-on-chronic liver failure: an algorithmic approach. *Hepatol Int* 2018;12(5):402–416. doi: 10.1007/s12072-018-9887-5.
- [11] Durand ML. Bacterial and fungal endophthalmitis. *Clin Microbiol Rev* 2017;30(3):597–613. doi: 10.1128/CMR.00113-16.
- [12] Rao NA, Hidayat AA. Endogenous mycotic endophthalmitis: variations in clinical and histopathologic changes in candidiasis compared with aspergillosis. *Am J Ophthalmol* 2001;132(2):244–251. doi: 10.1016/s0002-9394(01)00968-0.
- [13] Oude Lashof AM, Rothova A, Sobel JD, Ruhnke M, Pappas PG, Viscogli C, et al. Ocular manifestations of candidemia. *Clin Infect Dis* 2011;53(3):262–268. doi: 10.1093/cid/cir355.
- [14] Ueda T, Takesue Y, Tokimatsu I, Miyazaki T, Nakada-Motokawa N, Nagao M, et al. The incidence of endophthalmitis or macular involvement and the necessity of a routine ophthalmic examination in patients with candidemia. *PLoS One* 2019;14(5):e0216956. doi: 10.1371/journal.pone.0216956.
- [15] Krishna R, Amuh D, Lowder CY, Gordon SM, Adal KA, Hall G. Should all patients with candidaemia have an ophthalmic examination to rule out ocular candidiasis? *Eye (Lond)* 2000;14(Pt 1):30–34. doi: 10.1038/eye.2000.7.
- [16] Pappas PG, Kauffman CA, Andes DR, Clancy CJ, Marr KA, Ostrosky-Zeichner L, et al. Clinical practice guideline for the management of Candidiasis: 2016 update by the Infectious Diseases Society of America. *Clin Infect Dis* 2016;62(4):e1–e50. doi: 10.1093/cid/civ933.
- [17] Celiker H, Kazokoglu H. The role of pars plana vitrectomy in the management of fungal endogenous endophthalmitis. *Eur J Ophthalmol* 2020;30(1):88–93. doi: 10.1177/1120672118815105.
- [18] Chee YE, Elliott D. The role of vitrectomy in the management of fungal endophthalmitis. *Semin Ophthalmol* 2017;32(1):29–35. doi: 10.1080/08820538.2016.1228396.

## Biographies of the Editors-in-Chief

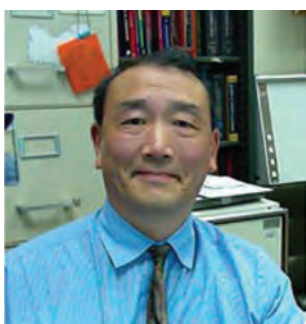
### Prof. Hong Ren (General Editor-in-Chief)



Prof. Ren, is the President, Director [Key Laboratory of Molecular Biology of Infectious Diseases (Ministry of Education of China), Medical Imaging Department, Liver and Viral Hepatitis Research Institute], Leader and Distinguished Super Specialist Consultant [Division of Infectious Diseases (one of the

national key discipline in China), Department of Internal Medicine] of the Second Affiliated Hospital of Chongqing Medical University. In addition, he is also the Vice-Chairman and Group Head of the Chinese Society of Hepatology, Chinese Medical Association.

### Prof. George Y. Wu (Comprehensive Editor-in-Chief)



Prof. Wu obtained his MD and PhD degree at Albert Einstein College of Medicine in 1976. He was a resident at Harlem Hospital Center from 1976 to 1979. He worked as a post-doctoral fellow at Albert Einstein College of Medicine from 1979 to 1982. From 1983, he worked as Assistant Professor and then Professor at

University of Connecticut School of Medicine. He is now the Director of Hepatology Section, Division of Gastroenterology-Hepatology. Dr. Wu's awards include the following: Research Prize awarded by the American Liver Foundation in 1982; Industry Research Scholar Award from the American Gastroenterological Association for 1985 to 1988; Gastroenterology Research Group Young Scientist Award from the American Gastroenterological Association in 1990; Herman Lopata Chair in Hepa-

titis Research from 1992 to date; Scientific Award from the Chinese American Medical Society in 1992; He was elected to membership in exclusive societies: American Society for Clinical Investigation in 1989; Association of American Physicians in 1995; and Top Doctor in the U.S. awarded by U.S. News and World Report in 2011. He has published about 180 peer-reviewed academic articles, 11 books, and is series editor for Clinical Gastroenterology book series by Springer-Nature, and is Senior Associate editor of J. Digestive Diseases.

### Prof. Harry Hua-Xiang Xia (Editor-in-Chief)



Prof. Xia obtained his PhD in 1994 and worked as a postdoctoral fellow at Trinity College, Dublin University, Ireland. He spent 5 years as a senior Research Officer at Nepean Hospital, University of Sydney, Australia, and 6 years as an Assistant Professor at Queen Mary Hospital, University of Hong Kong to

continue his research on *Helicobacter pylori* and associated diseases. He has achieved an academic reputation worldwide in the field. He was elected as a fellow of the American College of Gastroenterology in 2008. He joined Novartis Pharmaceuticals Corporation, USA, in 2006 for clinical development of new investigational drugs in different therapeutic areas. He is currently an Adjunct Professor of Beijing Friendship Hospital, Capital Medical University, Beijing; Municipal Hospital, Qingdao University, Qingdao; and First Affiliated Hospital, Guangdong Pharmaceutical University, Guangdong, China. He has published about 180 peer-reviewed academic articles. He has published two books, namely, "Helicobacter pylori infection: Basic Principles and Clinical Practice" (1997), and A Comprehensive Guide to English Medical Manuscript Writing and Publication (2017).



# Xia & He Publishing

Published by Xia & He Publishing Inc.

14090 Southwest Freeway, Suite 300, Sugar Land, Texas, 77478, USA

Telephone: +1 281-980-0553

E-mail: [service@xiahepublishing.com](mailto:service@xiahepublishing.com)

Website: [www.xiahepublishing.com](http://www.xiahepublishing.com)

